INSIGHTS OF CONTEMPORARY DIFFUSION WEIGHTED IMAGING SIGNAL MODELING TECHNIQUES ON WHITE MATTER MICROSTRUCTURAL CHANGES FOLLOWING MILD TRAUMATIC BRAIN INJURY

By

Joshua H. Baker

A DISSERTATION

Submitted to
Michigan State University
in partial fulfillment of the requirements
for the degree of

Neuroscience-Doctor of Philosophy

2024

ABSTRACT

Mild traumatic brain injury, which accounts for up to 90% of traumatic brain injuries, is currently diagnosed and monitored with a thorough history and physical exam. There is growing consensus in the literature that pathophysiologic changes in white matter extend past symptomatic recovery, and that these biological changes should be the target of diagnosis and monitoring. This would replace the current clinical consensus that symptom resolution and a level of functioning that allows return to work/play indicates recovery. Diffusion magnetic resonance imaging has been a critical tool for studying white matter change, and the diffusion tensor model developed in the 1990s has been the cornerstone of studying white matter in human subjects with mild traumatic brain injury. This model has several limitations, however, which in part may contribute to inconsistencies observed in the localization and direction of changes in diffusion tensor metrics such as fractional anisotropy. The past decade has brought forth scanner advancements, including stronger gradients, high angular-resolution imaging, and modeling strategies specific to these imaging data. Here, we review these contemporary techniques and apply them in a secondary analysis of data collected during the Transforming Research and Clinical Knowledge in Traumatic Brain Injury Study. Constrained spherical deconvolution and fixed-based analysis were applied to diffusion magnetic resonance imaging data collected during the study, revealing significant differences in tract-specific and global fiber-density and fiber-density cross-section measures between patient and control groups. However, results remained relatively stable over time, indicating that in this population-based sample of patients, not much change occurred in the white matter from 2 weeks to 6-months post-injury. This would seem to suggest there is a drastically different timeline for white matter recovery than was previously thought, even in injuries categorized as mild in the general population. Additionally, this reinforces the notion that multimodal tools for diagnosis and monitoring need further evaluation to create gold-standard objective classifiers of injury severity. In the short-term,

future work should focus on the development of an imaging technique that when collected in the acute period following injury can predict prolonged recovery in individual patients with reasonable accuracy. Finally, characteristics which convey resiliency to poor outcomes should be investigated to facilitate development of interventions that hasten biological recovery.

This dissertation is dedicated to my loving family.
Mom & Dad thank you for your sacrifice and love.
Mimi, Granduke & Gary, this wouldn't have been possible.
without your support.
Finally, to my partner Sarah. Because of you, I live.
I'll always be by your side, loving you.

ACKNOWLEDGEMENTS

First, I want to acknowledge the DO/PhD program that has funded my work and education. Also, Drs. Brian Schutte and John Goudreau who helped me form ideas and think critically as a scientist. Of course, endless thanks to the amazing Michelle Volker she took care of so many things behind the scenes so I could focus on the science. Additionally, I would like to thank Dr. AJ Robison and Eleri Thomas for their guidance and cheerful attitudes in the Neuroscience program. I want to acknowledge my lab mates and colleagues Dr. Zac Fernandez and Joshua Hubert for always being there with the boost I needed. Your collaboration and support on projects helped me grow into the scientist I am today. When I first came to MSU, I was set to work on a high school concussion study for my dissertation, and would like to thank the MSU/Sparrow Concussion clinic staff especially Jill Leavitt who coordinated recruitment from the side of the concussion clinic and Dr. Matthew Saffarian who trained me to administer the SCAT5. I want to acknowledge Dr. Kan Ding, who provided feedback on the TRACK-TBI proposal. The TRACK-TBI investigators are the only reason the data for this project exists and allowed me to reap the benefits of their insight into addressing the great need for open TBI research; a special thank you to Dr. Pratik Mukhurjee. Thank you to the employees, administrators, and scientists at FITBIR who facilitated the simple acquisition of the data from their revolutionary repository. Finally, I am eternally grateful to the members of my guidance committee who mentored me, listened to my ideas and gave invaluable feedback to improve me work. I want to specifically thank Dr. Rebecca Knickmeyer who was always available for discussions, and gave feedback regularly on the work at poster presentations and other neuroscience events during my training. Also, Dr. Norman Scheel, the world's most metal computational neuroscientist, made this project possible with his insights and as my computer programming mentor. A profound thank you to Dr. Andrew Bender, who has been a kind, nurturing mentor and challenged me to learn and do more. His expertise in diffusion, and as an

endless source of MRTrix3 metadata was invaluable during the preparation of this document. Finally, I would like to thank Dr. David Zhu, who gave me the opportunity to start down a new path of discovery in my research career in his laboratory and taught me everything I know about magnetic resonance imaging.

PREFACE

The field of neuroimaging is unique in that it requires a working base of knowledge in MRI physics, computer science, statistics, and software development, in addition to expertise in the disease area in which you study. This massive amount of information is difficult to maintain in a single person, and all fields are rapidly advancing with novelty giving way to antiquity with singular publications. Neuroimaging, therefore, is a highly collaborative team-based science discipline. It is easy to overestimate one's knowledge in any one of the areas as a neuroimaging researcher, and blind spots are abundant in the literature including this dissertation. Therefore, a critical piece of advice for the neuroimaging practitioner is a piece of wisdom from Clint Eastwood's character "Dirty" Harry Callahan in Magnum Force, "A mans got to know his limitations". Obviously, this is partially in jest. However, this phrase could be updated for more inclusive modern times and made specific to neuroimaging with the phrase "for a person using neuroimaging in research knowing what you don't know is almost more important than what you do, consult colleagues with more knowledge in these intersecting fields often."

With the recent advances and decreasing cost of computers, this incredible field has become accessible to more individuals than ever. A challenge in the neuroimaging of mild traumatic brain injury is the ever-changing set of tools and evolving technologies with which the disease is studied. Nonetheless, diffusion MRI and other quantitative imaging techniques have been a mainstay in human subjects' research on this traumatic event for decades. During the 21st century, these neuroimaging research tools will likely translate from keyboard to bedside and be used in numerous applications to classify historically ambiguous neuropsychiatric diseases with the precision of in vivo imaging. Indeed, a major area of research will focus on delineating the numerous factors that drive resiliency to injury and that underlie various phenotypes of recovery in the general population. Devising model systems to test novel therapeutics to intervene in cases of poor recovery will be

informed by ongoing large population-based studies. It is critical in my opinion to first fully describe the phenomenology of brain trauma in humans. Much of this hinges on the ability to localize and characterize changes in the brain accurately and predict who is likely to have a poor outcome. This will allow researchers to focus on these individuals for a more detailed understanding of what drives this phenomenon. Quantitative MRI is likely one of the best tools we currently have available to accomplish this. As a physician-scientist in training aspiring towards a career in Diagnostic Radiology, the knowledge, and skills developed in the preparation of this dissertation could be applied widely in numerous disease processes whose pathophysiology affect white matter. In addition, much of our knowledge on the embryology of the developing human brain come from animal studies, and advanced imaging techniques hold promise to unlock the intricate processes of the developing human brain by scanning the fetus while still in the womb. Finally, as a classically trained anatomist, my perspective is that structural brain imaging is the modern scalpel with which advances in our understanding of white matter morphology will continue to evolve. Presently, the anatomical record of white matter is a wild west of tracts and fibers organized by function, location, and cell type. As a classically trained anatomist with expertise in structural neuroimaging, I hope to contribute to classification of white matter and add to our understanding of the relationship between white matter lesion locations and brain function during my career. Needless to say, there is much work yet to be done, or as the great character Sherlock Holmes from the writings of Sir Arthur Conan Doyle said, "The game is afoot".

TABLE OF CONTENTS

CHAPTER 1: INTRODUCTION

Mild traumatic brain injury (mTBI) is a classification currently used by clinicians and researchers to describe a limited range of brain injuries resulting from a traumatic event. Currently, designating a traumatic brain injury as "mild" often refers to injuries causing heterogeneous clinical sequelae considered to be modest and that typically resolve entirely within weeks.[1] However, the lack of prognostic value of the current nosology of traumatic brain injury poses a major challenge for clinicians and scientists. In the current framework, categorizing an injury as 'mild' has little clinical significance and fails to predict the clinical course of recovery; therefore, the mTBI classification provides clinicians little guidance regarding patient counseling and treatment options. Notably, there is currently no treatment targeting the biological underpinnings of mTBI.[2] In addition, despite considerable extant research efforts, there are neither reliable objective prognostic biomarkers, nor a clear understanding of the dynamic brain changes occurring during recovery.[3,4] Early studies often focused on predominantly white male populations engaged in contact sports or military personnel, limiting the generalizability of the findings to date.[5] One promising source of potential diagnostic and prognostic biomarkers is in vivo magnetic resonance imaging (MRI), including diffusion magnetic resonance imaging (DWI).[3,17] Neuroimaging methods sensitive to neurophysiologic changes from the traumatic injury could provide new valuable prognostic approaches for these patients.

Currently, there is no validated prognostic biomarker for patients with brain injuries classified as mild. Recent studies report that up to 50% of mTBI patients report persisting symptoms at one-year post-injury that are significantly worse than baseline pre-injury symptoms. [6–8] This length of symptom persistence represents a significant divergence from current frameworks which underestimate the time course and severity of prolonged symptoms following mTBI.[9] Clinical

trials to develop targeted treatments for individuals who develop prolonged symptoms will be challenging without a prognostic biomarker, as enrollment weighting to capture those who are at the most significant risk of developing prolonged symptoms cannot be accomplished without one. Several potential candidates exist, including various neuroimaging techniques[10,11], serum biomarkers[12,13], and clinical assessment scores. Combining these measures in a multivariate prognostic model will likely have the highest accuracy due to the dynamic and heterogeneous nature of this injury.[14]

Evidence from neuroimaging studies have identified differences in white matter (WM) and brain function that occur during mTBI recovery. Neuroimaging studies have correlated observed changes during recovery with poor outcomes on the Glasgow outcome scale-extended (GOSE) and Rivermead post-concussion symptoms questionnaire (RPQ).[15] DWI, specifically, assesses the diffusion/random movement of water molecules to infer changes in WM microanatomy indirectly. Diffusion Tensor Imaging (DTI) is a modeling technique for estimating parameters such as Fractional Anisotropy (FA), an inference of microstructural coherence of WM fibers, which is often considered a proxy for WM integrity and the capacity to carry signals between brain regions.[16] An early examination of the Transforming Research and Clinical Knowledge in Traumatic Brain Injury (TRACK-TBI) Study demonstrated that DTI regions of interest (ROI) with FA 2.2 standard deviations below controls were predictive of poor recovery, having >2-3 symptoms worse than pre-injury, at 3- and 6-month follow-up.[15] Several systematic reviews of DWI studies in mTBI add further strong evidence that these measures can identify differences that current clinical MRI sequences and CT cannot.[3,5,17]

DWI studies of the acute and subacute phases following injury, defined as the first 7 days and between 1 week and 3 months following injury, respectively, demonstrated a pattern of reduced FA and increased mean diffusivity (MD)/radial diffusivity (RD) in frontal and deep white matter

regions.[3,17] It is postulated that this reflects demyelination and inflammation related to diffuse axonal injury. However, in this same review, conflicting patterns of FA and MD were consistently observed, casting uncertainty onto the true pattern of DWI metric change following mTBI and how to interpret it. More consistent injury to scan time, acquisition parameters and modeling techniques will help translate this body of literature into clinical practice. However, there are significant limitations of DTI that cannot be ignored, which will be covered in this dissertation. Therefore, analysis with novel and complimentary DWI modeling techniques may reveal more about the pattern of post-injury brain changes with greater interpretability regarding the underlying pathophysiology observed following a mTBI.

This dissertation details our application of constrained spherical deconvolution (CSD), a higher-order DWI modeling technique developed by the creators of the diffusion analysis software package MRTrix3.[18] We concatenate two separate DWI sequences with b-values of 1300 mm/s^2 and 3000 mm/s^2 collected during the same scanning session to create a pseudo-multi-shell dataset. Using this process, we used legacy data for a more specific secondary analysis of the diffusion data from the open-access Federal Interagency Traumatic Brain Injury Repository (FITBIR). We then compared control and mTBI patients using an analysis method developed for MRTrix3 termed "fixed-based analysis (FBA)."[19] As will be subsequently expanded upon, a 'fixel' refers to a specific fiber population within a voxel. Unlike traditional voxel-based techniques like DTI, FBA defines a novel volume element for inference with DWI data and utilizes a more biologically plausible modeling technique with potentially greater specificity for underlying WM microstructural change.[20] A fixel can represent more than a single distinct fiber bundle within a voxel, allowing inference of effects beyond simply within voxel microstructure. FBA addresses some of the significant limitations of the DTI model and analysis with Tract-Based Spatial Statistics (TBSS) by addressing

the crossing fibers issue and allowing comprehensive analysis of WM tracts by addressing partial volume effects at the interface of tissue types.[20–22]

This exciting area of research falls at the intersection of many rapidly changing fields, including the clinical research of traumatic brain injury, the advancement of DWI pulse sequences, and the development of new neuroimaging modeling and analysis techniques.

MILD TRAUMATIC BRAIN INJURY

A concussion, or interchangeably mTBI, is damage to the brain caused by a transfer of mechanical force to neuronal tissue [23,24]. The molecular and cellular changes secondary to this impact result in a metabolic deficit, inflammation, and damage to the blood-brain barrier (BBB), which are incompatible with normal brain homeostasis. Here, the current knowledge of the epidemiology, pathophysiology, and management of mTBI will be discussed. Additionally, there will be a translational emphasis on studies that attempt to link cellular and molecular changes in the brain to the diverse symptoms of this injury.

The epidemiology of traumatic brain injury, especially those that are categorized as mild, is a challenging area of literature to summarize. This is mainly due to the historical heterogeneity of classification and siloed consensus statements from specific professional societies that were slow to gain exposure in the mainstream research community.[25] This is further complicated by the two areas of literature, concussion, and mTBI, being in largely separate disciplines, which likely contributed to the slow adoption of this classification.[26] For example, concussion research, especially with a sports etiology, has generally been housed within fields such as sports medicine and kinesiology. In contrast, mild traumatic brain injury work is often conducted by groups composed of emergency medicine, neurology, psychiatry, and neurosurgery researchers.

Mild TBI represents the dominant type of TBI, comprising 70-90% of injuries and creating an estimated worldwide financial burden of $400 billion annually.[9,27] In the US, the CDC reported

traumatic brain injury accounted for 2.5 million emergency department visits in 2010.[28] Epidemiologic studies have demonstrated a roughly 2:1 ratio of male to female traumatic brain injuries when including all severity levels; however, it is important to note that these studies were conducted on data collected before 2015. At the time of writing, more recent nationwide estimates are not available. The primary precipitating events in mTBI vary by age, with motor vehicle accidents being the leading cause in younger individuals and falls being most common in older individuals. In pediatric populations, the most common mechanism of mild TBI is falls (~50%), followed by impact injuries such as patient vs vehicle (~25%).[29] Importantly, 30% of individuals over the age of 65 fall each year, and since 1999, the incidence of death from falls has more than doubled.[30] It is likely that these statistics foreshadow a similar increase in traumatic brain injury morbidity and mortality among the aging US population, with fall prevention a major potential mechanism for healthcare professionals to intervene.

During a traumatic impact, mechanical forces are transferred to neural tissue, which are hypothesized to transiently disrupt the lipid bilayer by a mechanism called mechanoporation.[1] Ultimately, mechanoporation leads to the precipitating events for the pathophysiologic cascade of mTBI. It causes an efflux of potassium exacerbated in part by the mechanical opening of voltage-gated potassium channels and also a subsequent opening of ligand-gated ion channels after the indiscriminate release of glutamate [31,32]. As a result, a cascade of events is triggered by the opening of ligand-gated ion channels and the cells' attempt to restore ionic equilibrium. Potassium flux and release of glutamate return to baseline levels within 24 hours of injury [33]. Despite this, a series of events triggered by the imbalance of ions plague the cells for days, weeks, and sometimes months post-injury. Most of our knowledge of the timeline of these pathophysiologic processes is extrapolated from animal studies or early human studies utilizing serum biomarkers with small sample sizes.

To restore ionic equilibrium, there is increased activity of the sodium-potassium ATPase.[34] Animal models have shown that increased ATPase activity is reflected in a biphasic change within cerebral metabolism. In the hours following the mTBI injury, there is a significant increase in glucose metabolism followed by a depression which lasts up to 10 days in adult rats [35,36]. The depression in glucose metabolism is linked in part to mitochondrial dysfunction.[37] Another significant contributor to the pathophysiology of mTBI is calcium flux into the neuron cell body, contributing to mitochondrial dysfunction.

Neuronal calcium concentration is maintained at low concentrations compared to extracellular levels due to its cytotoxic effects. As a result of the indiscriminate release of glutamate after impact, there is an acute increased activation of the N-methyl-D-aspartate receptor (NMDAR) through which calcium enters the cell. Interestingly, it has been shown that molecular changes to the NMDAR occur following mTBI, and that these changes directly affect the conduction of calcium across the neuronal membrane. As a result, following mTBI, there is increased sensitivity to glutamatergic activity and increased intracellular calcium concentrations.[38,39] These changes to the NMDAR have been shown to persist for as long as 10 days following injury in animal models.[37] Neurons can buffer calcium with intracellular binding proteins and sequestration in organelles. Mitochondria also play a role in sequestering calcium; however, it results in the dissipation of the chemical gradient necessary for energy production via the electron transport chain.[40] The burden of calcium sequestration on mitochondria further exacerbates the mismatch between energy demands after mTBI and energy production.

In mTBI, mitochondria in damaged neurons ultimately fail to sequester calcium. This leads to increased intracellular calcium concentration and mitochondrial dysfunction, bringing into focus an increasing energy deficit for damaged neuronal cells. This situation is made worse by a mismatch in cerebral blood flow (CBF) and metabolic demand following mTBI injury, termed flow-

metabolism uncoupling. [41] The brain is unique in that it has no capacity to store energy, and therefore, it needs a consistent supply of glucose and oxygen-rich blood. Experimental studies in rats have shown that following mTBI, there is a decrease in CBF by as much as 71% in injured areas.[42] Importantly, this study also demonstrated a relationship between the degree of CBF reduction and the degree of delayed axotomy, a form of axonal injury that is another critical aspect of mTBI pathophysiology.

Traumatic axonal injury (TAI) is a description to delineate a developing area of research into secondary axonal injuries following TBI.[43] The exact mechanism of axonal injury has long been debated. The cause of morphological changes to axons observed after injury, such as neurofilament disorganization and blebbing, a bulging of the cell membrane, was a point of contention.[44]Kandel

It was debated whether this was the product of primary physical damage or a result of secondary injury. Classical feline studies demonstrate that injections of horseradish peroxidase do not indicate a change in axonal membrane permeability to macromolecules following mTBI.[44] The same study demonstrated that mTBI caused neurofilament misalignment and axonal blebbing or swelling. This was hypothesized to be due to the influx of calcium and activation of $Ca2^{+}$-induced proteolytic pathways, as opposed to the physical forces of the injury. Indeed, unbound intracellular calcium above a threshold concentration can activate phospholipases, proteases, and nucleases.[45] More recent work in vitro has demonstrated that, in fact, intracellular calcium does play an important role in axonal injury in mTBI. Interestingly, however, it seems the release of intracellular stores of calcium is the initial perturbation leading to calcium-dependent cytoskeletal damage and morphologic changes.[46]

Experimental animal models of mTBI have demonstrated that the hours and days after mTBI hold incredible challenges to neuronal cell homeostasis. Upon impact, potassium flux, excitatory neurotransmitter release, and subsequent depolarization disturb ionic equilibrium. In an

attempt to restore ionic equilibrium, ATP-dependent ion pumps consume energy, moving ions out of the cell This leads to an increased demand for glucose metabolism in the mitochondria. Mitochondria are attempting to both sequester cytotoxic calcium and generate ATP, and cannot meet the cell's energy needs. These challenges at the cellular level, seem to last 7-10 days after injury in animal models.[33] They represent a molecular and cellular explanation for the window of cerebral vulnerability (WoCV), a description recently coined in the human literature.[47] The major peril during this window is a risk of reinjury due to the fragile metabolic state of the cell and accumulating cytoskeletal damage. In the weeks and months following mTBI, further cellular damage occurs through inflammation, intensified due to damage sustained to the blood-brain barrier.

A major cause of secondary injury post-mTBI is damage accumulated due to the activity of the innate immune system. The brain has its own immune cells, microglia, which have been implicated in initiating deleterious immune responses following mTBI.[48] Following mTBI injury, microglia are attracted to sites of neuronal cell damage by chemokines released by astrocytes. Notably, this process is a normal physiologic process to quarantine damaged tissue. There appears to be differential activation of microglia, with some aiding in tissue repair and others contributing to its damage.[49] Nonetheless, there is evidence of astrogliosis and subsequent microglia recruitment after TBI, as demonstrated by glial fibrillary acidic protein staining (GFAP) and staining with monoclonal antibodies ED1 and OX42.[50] These data should be interpreted cautiously, as these monoclonal antibodies do not stain specifically for microglia and will also demonstrate other monocyte/macrophage-like cells. Indeed, other cell types, indistinguishable from microglia, are present in the injured tissue following mTBI. This is proposed to result from an inflammatory-mediated breakdown of the BBB following mTBI. Leukocyte invasion of brain tissue appears to be an essential event in perpetuating adverse effects of the post-TBI immune response.[51]

The BBB is a highly selective physical barrier between the bloodstream and neural tissue. It is maintained to prevent the entrance of immune cells and neurotoxic substances. Additionally, it allows for the transfer of toxic byproducts of neuronal cell function to re-enter the bloodstream for excretion.[40] In mTBI, byproducts of the inflammatory response, including reactive oxygen species (ROS) and Interleukin-1β (IL-1β), result in upregulation in matrix metalloproteinases (MMPs).[51] MMPs are endopeptidases and are essential for extracellular matrix turnover. It has been demonstrated in rats that MMP-9 expression, as measured by gelatin zymography and reverse transcription polymerase chain reaction, is upregulated by a ROS-dependent mechanism.[52] In addition, it was demonstrated in a rat model of cerebral ischemia that MMPs alter the structure of occludin and claudin, tight junction proteins essential for BBB integrity.[53] Taken together, it appears that inflammation, as a result of neuronal cell damage, has the potential to cause damage to the BBB through disruption of its microstructure. This breakdown of the BBB allows leukocyte infiltration of brain tissue and further perpetuates inflammation. Interestingly, it is known that MMPs activate pro-interleukins or cleave pro-interleukins, potentially igniting a vicious cycle of inflammation and BBB damage.[54]

Post-concussion syndrome or persistent post-concussive symptoms are interchangeable classifications for individuals with a mTBI who have symptoms for a period longer than what is considered a normal time for recovery. Arbitrarily, this is usually thought to be two to three symptoms that are worse than before the mTBI injury, and lasting greater than 3 months post-injury. Commonly, patients experience migraine-like symptoms, disruptions in learning and memory, and slower reaction time. It is theorized that headache following mTBI reflects altered cerebral excitability due to the ionic flux discussed previously.[55] A human study in severe TBI has demonstrated depressed cortical electrical activity, as measured by electrocorticogram, a pattern similar to that observed in migraine.[56] A study in mice demonstrated a single mTBI resulted in

learning impairments, and mice subjected to multiple impacts exhibited cognitive, learning, and behavioral deficits.[57] Additionally, MRI studies in rats provide strong evidence that these changes are due to altered neurotransmission. For example, administration of antagonists of the NMDA and α-amino-3-hydroxy-5-methyl-4-isoxazolepropionic acid receptor (AMPA) were shown to alter electrical and hemodynamic activity in rats significantly.[58] This may also be responsible for changes in reaction time identified in humans. It has been shown using a novel device to measure reaction time in humans; reaction time is significantly slower in individuals suffering from mTBI.[59]

Other major post-concussive symptoms are behavioral disturbances such as sleep disturbance, anxiety, and depression. In a population-based sample of mTBI patients, 65% experienced sleep difficulties in the 2-weeks following injury, and 41% had clinically significant sleep disturbances one year after injury. [60] It is hypothesized that sleep disturbances have a synergistic effect on the negative inflammatory response, potentially increasing the time to recovery in mTBI patients. [61,62]

The main observations in animal models of TBI are shorter wake periods and increased sleep bouts. [63] The evidence for a synergistic effect of sleep and damaging inflammation is extrapolated from work done outside of the TBI literature; nonetheless, it is a major complaint following mTBI and warrants further investigation. Finally, changes in neurotransmission in the basolateral amygdala and hippocampus, important limbic structures in fear conditioning, are hypothesized to be responsible for an increased incidence of anxiety following mTBI. Animal studies have demonstrated increased NMDAR expression in these limbic structures and decreased γ-aminobutyric acid-mediated inhibition. These changes were associated with increased fear conditioning and anxiety-like behaviors in multiple fear conditioning paradigms [64,65]. Management of the underlying causes of these symptoms are important targets of ongoing research to improve the clinical management of mTBI.

For most, the symptoms of mTBI fade after approximately 6-months. More recently, there has been growing concern that the resolution of symptoms is not the end of this story. In fact, it has been demonstrated in humans that inflammation following mTBI can persist for years after the initial injury.[66] It is hypothesized that J2-prostaglandins (PGJ2) might mediate the transition from an acute and beneficial inflammatory response to a chronic and damaging one. After injury, PGJ2 is released by astrocytes and microglia, exhibiting both anti- and pro-inflammatory effects. A review of the experimental literature depicts PGJ2-mediated disruption of mitochondria and the ubiquitin-proteasome pathway as a potential mechanism for this switch.[67]

More recent experimental work has advanced the PGJ2 hypothesis. An in vivo study demonstrated that a particularly reactive 15-deoxy-PGJ2 caused activation of the integrated stress response (ISR) via phosphorylation of eukaryotic translation initiation factor 2 alpha.[68] The ISR is an adaptive cellular pathway activated in precarious situations to restore cellular equilibrium.[69] However, long-term activation can lead to cellular damage and even programmed cell death.[69] Interestingly, animal models of mTBI have demonstrated increased cyclooxygenase (COX) concentration, the rate-limiting enzyme in prostaglandin production, in injured neurons.[70,71] Chronic inflammation and resultant BBB breakdown are thought of as a potential link to what is arguably the most detrimental long-term effect of repetitive mTBI, chronic traumatic encephalopathy (CTE).[72]

The molecular and cellular events following mTBI are complex, and any treatment must consider the multiple perturbations to neuronal homeostasis that occur following mTBI. This challenge is particularly evident given the numerous clinical trials (over 30) that have failed to produce meaningful patient results.[51] Additionally, the cellular and animal literature itself is challenging to translate due to a variety of experimental models of mTBI, e.g. fluid percussion, weight drop, etc., and no objective criteria to delineate how to produce a ground truth for the severity of simulated mTBI.[73,74] Therefore, great effort is being placed into defining the in vivo

pathophysiology of mTBI in humans fully, using current experimental knowledge as a guide and in vivo methods such as neuroimaging before attempting to develop more specific model systems.

Currently, mTBI patients are diagnosed and monitored clinically with neuropsychological tests, but primarily by patient reports of symptoms.[75] Close medical observation and intervention are only used if more severe pathology is suspected, e.g., cerebral hemorrhage. However, many patients, including those with mild injuries, often receive neuroimaging in the form of a routine computed tomography (CT) scan of the head. The treatment for a sports-related mTBI consists of rest and a gradual return to mental and physical activity. When symptoms disappear, patients are considered "recovered" from a mTBI, which may or may not coincide with neuropsychological measures returning to baseline values. However, based on the combined human and animal literature presented, recovery cannot be definitively determined by symptom resolution alone. There is a great need for objective criteria to monitor true biological recovery from mTBI.

A clinically useful objective marker for diagnosis of mTBI will reflect cellular damage to neurons or related aspects of mTBI pathophysiology. The quest for a measurable prognostic blood biomarker of mTBI is an ongoing search. A recent review points towards numerous blood biomarkers that have shown promise.[4] For example, neurofilament light chain (NfL), a marker of neurofilament damage due to axonal injury, and glial fibrillary acidic protein (GFAP), a marker of astrogliosis, both were found to be elevated in patients suffering mTBI compared to controls.[13,76] Of particular interest, given rising concerns about CTE following mTBI, are biomarkers that would link mTBI pathophysiology to the tauopathy's characteristic of CTE. In a recent animal model of tauopathy, it was demonstrated that NfL is not only elevated in CSF and plasma, but it also appears to be a good marker of response to treatment with β-site amyloid precursor protein cleaving enzyme-inhibitor.[77]

A recent study developed a new highly sensitive immunoassay for NfL and examined its efficacy as a biomarker for mTBI in a sample of professional hockey players. They demonstrated that NfL was correlated with a standard of care neuropsychological test and was effective in predicting return to play time.[78] NfL outperformed other biomarkers, such as S100 calcium binding protein B, neuron-specific enolase, and plasma tau, in predicting return to play time, a newer criteria for severity grading in sports-related mTBI. Several other studies in athletic populations have demonstrated increases in plasma NfL following even sub-concussive hits.[79–81] Ideally, in future studies, serial and longitudinal sampling would be conducted to determine if there is any circadian fluctuation and begin to gain an understanding of how plasma levels of NfL change after injury. The culmination of years of blood biomarker work more recently resulted in the FDA approval of GFAP and UCH-L1 for plasma detection of intracranial injury following mTBI.[76,82] However, there still remains a need for a biomarker of true biological recovery, and an understanding of the longitudinal changes in these markers in recovery. For these reasons, it is important that a paradigm shift take place. mTBI should not be thought of as an accident with a swift resolution, but as a potential trigger for a long-standing cascade of pathophysiology that ultimately can lead to neurodegeneration. Some even feel that 'mild' is a designation that should be entirely done away with, and that we should focus efforts on outcome measurement instead of imprecise classification systems.[83]

Presently, mTBI is a clinical diagnosis guided by a thorough history and physical exam conducted by a physician, with imaging and clinical assessment scores as supplements. A traumatic brain injury is classified as mild based on the widely accepted American Congress of Rehabilitation Medicine diagnostic criteria for mTBI, which was recently updated in 2023.[84] To be considered a mild injury, the patient must have a plausible mechanism of injury likely to cause trauma, and meet one to two of the following criteria: 1) have one or more signs attributable to the injury; 2) at least

two symptoms and at least one clinical laboratory finding attributable to the injury; and 3) CT or MRI intracranial abnormalities attributable to the injury. Patient diagnosis is elevated to a higher severity if they meet the following criteria: 1) loss of consciousness greater than 30 minutes; 2) Glasgow Coma Scale less than 13, 30 minutes after the injury; and 3) post-traumatic amnesia greater than 24 hours. Signs of injury are considered observable acute changes in the physiological functioning of the brain attributable to the injury, including loss of consciousness, altered mental status, amnesia for events, and other neurologic signs such as seizure or motor incoordination. Symptoms, on the other hand, are divided explicitly into somatic, such as dizziness or headache, as well as neuropsychiatric, such as anxiety or difficulty focusing. Ultimately, in the office, the resolution of clinical symptoms and an individual's ability to return to work, play, or learning environments drive the clinical resolution of the injury.

Although an injury may be classified as mild, clearly, this is an imprecise description.[83] In the future, the clinical and basic research communities will need to focus on understanding what drives differences in outcomes among individuals who are considered to have a mild injury. Recent work from the TRACK-TBI study demonstrated that up to 54% of patients following one year of injury were experiencing functional limitations, and many reported greater than one or more symptoms that were worse before their injury. Patients experiencing this type of outcome are far from mildly injured.

DIFFUSION MAGNETIC RESONANCE IMAGING

The following section will give a foundational overview of how the DWI signal is created. This information will be given using a conceptual framework aimed at a neuroscientific and clinical audience, with few underlying mathematical equations included. An understanding of fundamental magnetic resonance physics and spin magnetic resonance is assumed. For a more mathematically based explanation, I suggest the first four chapters of the text *Diffusion MRI* or the third chapter of

Introduction to Diffusion Tensor Imaging for a more abridged explanation.[85,86] Notably, the underlying physics principles are complex, and some simplifications has been utilized to aid in understanding. In addition, the data collection process and different vendor equipment are nuanced; a clinician or basic scientist should not undertake an MRI experiment without the direct involvement of an MRI physicist to facilitate data quality and harmonization. George Fueschel coined the phrase, "Garbage in, Garbage out", which most certainly applies here.

MRI allows for the observation of signals from nuclei; when discussing DWI, the nuclei in question are the proton (^{1}H) of water molecules in the human body. The experiment begins by putting energy into the subject tissue (in this document, the brain) and listening for the signal emitted after the excitation, referred to as an echo. The signal itself is caused by a current induced by magnetic flux due to the precession of spins around a static magnetic field and detected as a voltage by a receiver coil. The information in the signal has a frequency, intensity, and phase produced by the magnetic field oscillations. This data is collected at a particular time after the excitation. The composite data, called k space is then transformed to become an image via Fourier Transform.[87]

The opening of the MRI, or bore of the magnet, has a continuously active magnetic field oriented through the bore or along its z-axis, referred to as B_0. The x-axis is in the left-right direction, and the y-axis is in the up-down direction. When a subject's brain enters the magnet's bore, all of the spins of the protons hydrogen nuclei of water molecules are oriented along this B_0. The signal of interest during experiments is not generated with by B_0 magnetic field, but rather as a result of secondary magnetic field gradients applied in transverse planes to B_0.[88] By linearly modulating the B_0 field strength along any of these axes or a combination of them, the spins can be tipped out of alignment with B_0. Using combinations of gradients with different orientations and strengths, we can observe signals where certain relaxation times, for example, T1 or longitudinal

relaxation time, are emphasized. Relaxation times are specific to different tissues, so depending on the scientific question, there is great variability in the actual makeup of an MRI experiment.

Using the frequency, intensity, and phase of the emitted signal, scientists and clinicians can observe the underlying anatomy of the brain, its function, and its physical connections. Collectively, the program of changing magnetic gradients that produce the signal are referred to as "pulse sequences," of which DWI (diffusion weighted imaging) is a specific type.[89] These pulse sequences have various parameters that an MRI Physicist can manipulate to produce a particular tissue contrast. Pulse sequences can be made sensitive to specific tissue-dependent characteristics in the case of T1 or T2 weighted images. Alternatively, they can be used to measure signals sensitive to an underlying phenomenon, for example, diffusion or blood oxygen-dependent signal of functional MRI. What is unique about DWI is that it is not necessarily the underlying tissue characteristics we are measuring directly but rather the alterations in the random motion of water in the human brain caused by the organized tissue structure of white and grey matter. [90]

The diffusion of water molecules we are interested in measuring is averaged within the confines of the approximately 2mm isotropic "voxel", a three-dimensional volume from which we are measuring data, and is also referred to as intravoxel incoherent motion or, more commonly, Brownian motion.[91] This is distinctly different than bulk flow of a fluid, for example, the movement of blood within the internal carotid artery. Typically, the motion of a single water molecule during the time of a single diffusion-weighted pulse sequence is around 1-20 μm, significantly smaller than the voxel from which we measure, and, therefore, it is essential to reiterate that we are observing the averaged motion of large quantities of water molecules.[90] We use gradients that make the signal sensitive to the diffusion of water molecules. In DWI, multiple gradients with varying orientations are used to acquire information about the underlying diffusion directionality of water molecules.

All molecules, at temperatures above absolute zero, possess thermal energy that results in motion, commonly called molecular diffusion.[91] Work by Albert Einstein (1.1) proposed that the conditional probability distribution of a group of particles after a diffusion time (t) is proportional to the diffusion coefficient (D) where (x^2) is the mean squared displacement in one dimension.[92]

$$x^2 = 2Dt \tag{1.1}$$

The diffusion coefficient (D) can be thought of as an innate property of the tissue being measured that depends on the size of the diffusing molecules (in this dissertation, water or H_2O), the temperature, and the microstructural environment in which it is being measured.

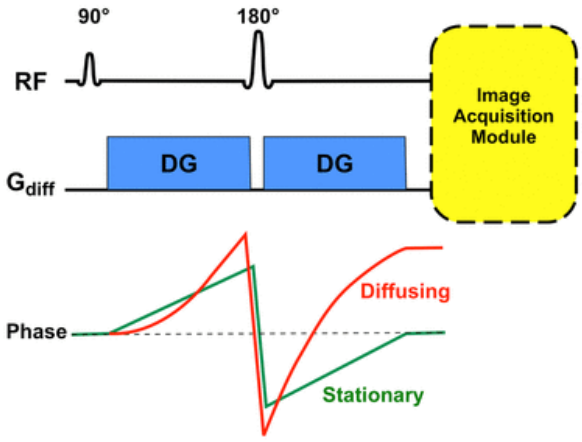

Figure 1.1 – A vector magnetization diagram or pulse sequence diagram representative of the spin-echo sequence described by Stejskal & Tanner in 1965. Diffusion Gradients (DG) are applied to "label" protons of water molecules. Those molecules that move from their original position will fall out of phase (red line), resulting in signal loss. Courtesy of Allen D. Elster, MRIquestions.com

A typical DWI pulse sequence shown in Figure 1.1 builds on a spin-echo sequence, which gives a T2-weighted contrast.[93] Following the 90° radiofrequency pulse, the first diffusion-sensitizing gradient (DG), is applied, causing different protons to experience different magnetic field strengths and resonate at different frequencies depending on their location. This can be thought of as effectively labeling all protons in a single brain slice. Then, after the second 180° radiofrequency

(RF) pulse, a second diffusion-sensitizing gradient, is applied.[93] The approach was adapted from a body of work on characterizing diffusion with nuclear magnetic resonance and is called Stejskal-Tanner diffusion encoding.[94] Figure 1.1 represents a single repetition of the acquisition of data in k-space. This can be thought of as acquiring data in a single three-dimensional slice of brain tissue and is repeated many times to acquire DWI data in slices that cover the entire brain.

Protons that have not moved or diffused since the initial dephasing gradient will regain the same phase and emit a signal as indicated by the green line in Figure 1.1. However, protons that have diffused or moved from their original position will fall out of phase, resulting in overall signal loss when combining the effect of all protons in a voxel. Recalling (Equation 1.1), water molecules allowed to diffuse in an unrestricted environment for a certain time will diffuse equally in all directions; this is termed "isotropic" diffusion.[91] The greater the diffusion distance, the greater the signal loss. The tissue type in the brain with the greatest diffusion distances is the CSF, and therefore experiences the greatest signal loss and appears dark on DWI images.

Most, if not all, molecules in the brain have moved away from their original position, resulting in a spread of phases and attenuation of the signal. However, in the highly organized WM, diffusion distances are far greater along the "grain" of the WM, as opposed to across bundles of axons.[95] This is due to the tightly packed nature of the WM pathways and the negligible diffusion across myelin sheaths or axon cell membranes. Therefore, the diffusion is said to be "anisotropic" in WM or not the same in all directions.[91] This process of applying gradients is repeated multiple times along many directions to capture the complex fiber architecture of the brain's WM pathways.[93] Each additional gradient direction helps to detect the direction of diffusion and improve the accuracy of diffusivity quantification, which infers changes in the microanatomy and organization of connections of WM pathways.

Another important concept when discussing DWI is the concept of a "b-value" and how it relates to the diffusion-weighted signal. Mathematically, the two are related with (Equation 1.2):

$$S = S_0 e^{-bD} \tag{1.2}$$

The signal without diffusion weighting (S_0) is related to the signal with diffusion weighting (S) by the term (e^{-bD}) in which (D) represents the diffusion coefficient and (b) represents the b-factor or b-value.[91] At this point, a clinician will appreciate noting that the equation term (e^{-bD}) when no diffusion gradient is utilized, would leave only T2-weighting ($e^{-TE/T2}$) of the signal, as mentioned previously. DWI sequences have a long echo time (TE), and, for this reason, are heavily T2-weighted. Therefore, the first few images in a DWI dataset without the diffusion-weighted gradients applied, referred to as b=0 images (pronounced b-zero), look very similar to a typical T2-weighted image where CSF appears bright.[96]

Quite simply, the b-value represents how sensitive the pulse sequence is to diffusion. The b-value is proportional to the square of the gradient strength; stronger gradients (higher b-values) are sensitive to smaller diffusion distances.[93] Equation (1.3) represents the b-value for a rectangular gradient where (G) is the strength of the diffusion gradient, (δ) is the length of the gradient, and (Δ) is the length of time between the onset of the first gradient and the onset of the second gradient.

$$b = (\gamma G \Delta)^2 (\Delta - \frac{\delta}{3}) \tag{1.3}$$

The b-value has units of seconds per millimeter squared. Gradient strength, length of the gradient, and length of time between gradients are parameters that an MRI physicist can manipulate to alter the diffusion weighting of a specific pulse sequence.[93] This is at the expense of signal-to-noise ratio (SNR), with higher b-values having lower SNR, as evident by the relationship between equations 1.2 and 1.3.

In the present dissertation, data with two separate b-values, or shells, will be utilized. This is important to mention because these two shells were collected separately at the time of data collection. From a practical standpoint, when a b-value is chosen for a study, the diffusion time is typically not set purposefully. Instead, it reflects the shortest duration of gradient application that is possible to achieve the desired diffusion weighting. This means diffusion times may vary between b-values, and as a result, two separate acquisitions at different b-values may have slightly different repetition times (TR). Ultimately, this results in slight differences in signal intensity, which can be problematic when processing concatenated data with different b-values. This is only an issue when using modern modeling techniques that use both shells instead of one to estimate diffusion metrics. We address these slight differences in signal intensity between shells using a data harmonization approach described in Chapter 3 of this dissertation.

Finally, we would like to briefly touch on the strengths and limitations of the specific pulse sequence used for the TRACK-TBI data acquisition. Understanding the specific pulse sequence used to collect DWI data is crucial for clinicians designing studies as it will dictate the type and severity of artifacts and noise present in the data. TRACK-TBI utilized a cutting-edge acquisition at the time of the study's inception, known generally as a multislice single-shot spin-echo echo planar pulse sequence.[15] The data were collected on a General Electric (GE) MRI scanner, for which the proprietary name of the sequence is single-shot fast spin echo echo planar imaging (EPI). Early in the clinical use of DWI, data was collected using single-shot echo-planar imaging (EPI) methods, which are faster due to the use of EPI echo train.[97] However, data acquisition with EPI echo train is prone to susceptibility field distortions, especially in regions close to an air-tissue interface.[98] A strength of the diffusion EPI methods was their resilience to patient motion. This lays the foundation for the rigorous preprocessing necessary before analysis of DWI data outlined in Chapters 3 and 4.

DIFFUSION TENSOR IMAGING IN MILD TRAUMATIC BRAIN INJURY

DTI is a modeling technique developed at the NIH largely due to the work of Dr. Peter Basser and colleagues.[100,101] Interestingly, a pork loin was initially utilized to develop this technique, and it was not initially conceived for studying the WM.[102,103] This subtlety, although seemingly trivial, is actually quite important, as a major weakness of this technique when applied to human WM is an inability to model the complex architecture of certain WM regions, which is noted in the original manuscripts published in 1994. Despite the excitement at the time in the neuroscience community, this limitation makes the technique ill-suited for studying the brain's WM comprehensively. Additionally, fiber tracking based on the DTI model is problematic, as any voxels containing signal contributions from more than one distinct fiber population could result in inaccurate connections.[20,104] Nonetheless, due to its ease of use and sensitivity to pathologic changes in many disease states, the neuroimaging community widely adopted it with success, albeit the interpretation of findings was questionable.[105] Some have argued its simplification of the complex information collected with DWI is, in fact, a strength as opposed to a weakness.[20] I propose it is an emerging scientific controversy whether or not DTI should continue to be used as the sole modelling technique in mTBI studies due to well documented limitations of the model.[1–4] This section will overview the diffusion tensor model, the localization of effects, and patterns of changes observed in DTI metrics in the WM of mTBI patients.

The diffusion tensor model is represented by equation (1.4) and is applied to each voxel of diffusion MRI data collected to fit numerous tensors throughout the brain.[100] This equation relates the signal (S_0) from the b_0 image without a diffusion gradient applied to the signal (S_j) with a diffusion gradient (*j*) applied.[106] The signal with a gradient applied is equal to the signal without a diffusion gradient applied multiplied by the exponential value of the known b-value (b), a unit vector

(x_j) representing the direction of the applied gradient, and the unknown value of the diffusion tensor D.

$$S_j = S_0 exp\left(-b x_j^T D x_j\right) \quad (1.4)$$

The diffusion tensor is a matrix with dimensions equal to the number of gradient directions applied, with the lowest possible being six unique directions and, therefore, a three-by-three matrix.[100]

The diagonal elements of the tensor along the x, y, and z-directions are in scanner space. These are what a diagnostic radiologist may be familiar with seeing when discussing diffusion-weighted MRI and are used to calculate the Apparent Diffusion Coefficient (ADC). These diagonal elements are averaged to create the trace image or diffusion-weighted image commonly used with the ADC image in diagnostic imaging of stroke patients.[107,108] The ADC map is generated by dividing the signal in each voxel of the trace image by the signal in each voxel of the b0-image and taking the logarithm of that result. Therefore, the ADC and trace images are inversely related, with restricted diffusion, as in the region of an infarct, appearing dark on the ADC image and bright on the Trace image.[107]

For DTI, more commonly used in research applications, the tensor information in scanner space is diagonalized using an eigendecomposition where the direction of principal diffusion, or eigenvector (v_1), corresponds to the direction of greatest diffusivity, which theoretically should be along the "grain" of the WM.[95] The shape of the diffusion tensor is described as either isotropic, with diffusivity equal in all directions, and therefore, all eigenvalues are similar, or anisotropic diffusivity, i.e., not equal in all directions.[91] The diffusion tensor is anisotropic in WM, owing to the coherent organization of tightly packed myelinated axons. Likewise, in the less organized grey matter, the diffusion tensor is isotropic; however, it is obviously less so when compared to CSF.

The eigenvalues can then be used to calculate quantitative diffusion maps or diffusion tensor metrics/scalars, such as the summary measures fractional anisotropy (FA) and mean diffusivity (MD), two commonly published metrics. FA is the variance across the eigenvalues with a value of 0 to 1, with one representing completely anisotropic diffusion and 0 representing isotropic diffusion.[109] MD is the average of the eigenvalues, with WM generally having lower MD when compared to grey matter and CSF.[105] Less commonly reported DTI metrics include Axial diffusivity (AD), which is the diffusivity along the principal direction of diffusion and is equal to the first eigenvalue (λ_1). Finally, radial diffusivity (RD) is the average of the second (λ_2) and third eigenvalues (λ_3), perpendicular to the first, representing the diffusivity across the grain of WM.

Commonly in mTBI, DTI metrics are interpreted as reflecting changes in WM microstructure, with the most common pattern observed in the acute period following injury being decreased FA and increased MD.[3,5,17] This change after mTBI is interpreted as being related to diffuse axonal injury, associated edema, and increases in cellularity during the ensuing inflammatory process. These claims have been confirmed in ROI analyses with coinciding histopathology in animal studies examining colocalized voxels with DTI metrics and histologic staining.[110,111]

The TRACK-TBI Study, the main source of data for this dissertation, collected various MRI pulse sequences in over 300 mTBI patients recruited from level 1 trauma centers across the U.S., specifically collecting DWI data at 2-weeks and 6-months post-injury.[112] The study was originally designed to create a set of common data elements related to outcome measurement for traumatic brain injury in a population-based sample recruited across the US. Therefore, a comprehensive battery of 21 unique outcome measures was collected, including commonly used measures like the GOSE and the RPQ. The study also collected various combinations of single-shell, multi-shell/high angular resolution diffusion imaging (or HARDI data) at various b-values.[113]

An early study on DWI data collected during the TRACK-TBI pilot study built on previous strong evidence and demonstrated that DWI is sensitive to WM changes following mTBI, even in a population-based sample.[15] Compared to control subjects this voxel-wise tract-based spatial statistics (TBSS) analysis of DTI metrics revealed regions of decreased FA in the internal and external capsules, genu of the corpus callosum, uncinate fasciculi, and anterior corona radiata bilaterally. The analysis identified no other differences between the control and mTBI subjects. The sample of mTBI patients was subsequently divided into CT/MRI negative (n=44) and positive (n = 32), and comparisons of DTI metrics in these two groups did not differ significantly.[15] DTI metrics also did not differ when comparing the upper and lower halves of the control group dichotomized by years of education. DTI metrics have been shown to covary with factors like age and years of education in other samples.[120, 178]

In the same study, a post-hoc ROI analysis was conducted using the intersection of regions in the Johns Hopkins University WM atlas and clusters of significance from the analysis of the FA skeleton generated during the TBSS analysis.[114] If a voxel fell 2.2 standard deviations above or below the mean of the control group ROIs it was considered abnormal.[15] Interestingly, a subgroup of mTBI patients with a negative CT/MRI on the day of injury had a trend-level difference between the proportion of abnormal ROIs (25%) compared to controls (10%). The proportion of abnormal ROIs in the CT/MRI positive group (43.8%) did not significantly differ from that of the CT/MRI negative group (25%). This nicely highlights that even amongst a group of patients categorized as mild, there is heterogeneity in the proportion of injured tissue, which, importantly, is not detectable by the current standard-of-care imaging techniques. Also, in this early study, a point not made by the author was a lack of observed difference in the GOSE scores of the CT/MRI-negative group and CT/MRI-positive group at 6-months post-injury, with 56% and 59% reporting a GOSE <8 in the

CT/MRI-negative vs positive groups respectively. This suggests there is an additional mechanism driving recovery beyond resolution of what matter damage localized with DTI.

Subsequently, another DTI analysis was conducted on the whole TRACK-TBI sample using single shell DWI data at b = 1300 mm/s^2, with 367 mTBI patients included in the final analysis.[115] The study observed significantly decreased FA at the 2-week point in the external capsule, superior fronto-occipital fasciculus, and genu of the corpus callosum when comparing mTBI patients to (n=148) friend controls. Conversely, the mTBI group had higher AD, MD, and RD in the cerebral hemispheres at the 2-week time point compared to controls. Post-hoc tract-wise analysis utilizing the JHU atlas revealed large effect sizes, with the largest approaching and exceeding 1 for AD in the body of the corpus callosum, the superior longitudinal fasciculus, the external capsule, the anterior limb of the internal capsule and the superior corona radiata.

Longitudinal change was also examined in this second TRACK-TBI study of DWI data, although it needs to be clarified how this was done. This analysis noted no significant changes in FA or RD between the 2-week and 6-month time points.[115] The stability in metrics from the subacute to the chronic stage is a novel and interesting finding that is difficult to explain. A possible explanation is the significant proportion of patients with prolonged recovery in this sample, suggested by work examining outcome variables from the sample.[8] In a comprehensive analysis of outcomes collected in the TRACK-TBI Study, 53% of the mTBI sample reported functional impairment at 12 months post-injury. CT/MRI negative mTBI patients at the 12-month timepoint had over two times increased risk of reporting headache (RR: 2.87), irritability/anger (2.39), frustration (2.67), forgetfulness (2.76), and slowed cognition (2.42) compared to controls.[7] Additionally, the CT/MRI negative group had a slightly increased risk of reporting functional impairment at work 6 months following injury compared to controls and reporting mental/behavioral changes that affect their close relationships at 12 months post-injury. It is important to note here that these are symptoms

commonly reported in the general public, and can be due to factors other than TBI as noted in a response to the original article.[116] However, the instrument used (GOSE) was specifically modified for this study to specifically ask about symptoms related to the mTBI, and the RPQ asks patients to rate symptoms based on pre-injury levels.[83] Nonetheless, data collection at a level 1 trauma center may have contributed to this sample being more severe on the imprecise spectrum categorized as mild. This would seem to suggest that damaged white matter has only a marginal capacity to heal following mTBI and does not return to a normal defined by the control subject mean.

Studies utilizing DTI in the extant literature observe heterogenous patterns when compared to the TRACK-TBI study result, and some studies that report similar patterns of change in DTI metrics have failed to correlate these findings to outcome measures.[3,17] The design of DWI studies can be challenging and interpretation of DTI results must be done cautiously. Many changes to the environment in which water molecules are diffusing can alter DTI metrics.[105,117] For example, observations of higher FA in the acute/subacute period following mTBI are often made in pediatric populations.[17] This could be due to heterogeneity in scan timing following injury, analysis methods, and DWI acquisition differences.[118,119] Alternatively, there could be a heterogenous response in WM within mTBI patients that we have failed to quantify adequately. Beyond that, differential effects as a result of heterogeneity in force distribution from the injury and varying degrees of the post-injury pathophysiologic cascade in individuals may also be at play. This is all complicated by the field actively moving from simpler DWI acquisitions and DTI analysis to the use of HARDI techniques and novel higher-order modeling techniques developed to take advantage of this DWI acquisition, which is not necessarily comparable to classical diffusion studies in mTBI.[104,120]

The diffusion tensor model to date has been useful, and clearly, DWI data modeled with DTI can detect WM changes following mTBI that conventional imaging methods cannot. There are limitations, however, to the interpretability of the results inherent to the way in which the DTI

scalars are calculated. For example, reduced FA reported in the TRACK-TBI Study could arise from several mathematical scenarios. FA could be changing due to a reduction in diffusivity along the principal diffusion direction aligned with the grain of the WM or, equivalently, a reduction in the first eigenvalue.[121] Similarly, an increase in diffusivity across the grain of the WM (increased RD) could decrease FA, and finally, a combination of these two could occur.[122] These alterations in the DWI signal represented by the DTI scalars calculated in this fashion could be caused by many combinations of underlying changes to axons and their environment. Early animal studies utilizing DTI demonstrated increased diffusivity across the grain of WM (increased RD) in shiverer rats who have mutated myelin basic protein, resulting in malformed or absent myelin sheaths.[123] Later work demonstrated that axonal degeneration preceding demyelination in mice fed cuprizone was associated with a decrease in diffusivity along the grain of WM (decreased FA) with no change in diffusivity perpendicularly.[124] Nonetheless, in mTBI, a combination of multiple pathophysiologic mechanisms with different time courses makes interpretability a challenge for DTI metrics.

In our own lab, past work has also demonstrated that other quantitative MRI sequences may be sensitive to the effects of mTBI on the brain. In a sample of sport-related concussion/mTBI athletes at MSU, a significant drop in default mode network connectivity was observed in the subacute recovery phase following concussion, which was correlated with various composite scores of the Immediate Post-Concussion Assessment and Cognitive Testing (ImPACT) neuropsychological test battery.[125] Therefore, combinations of structural and functional quantitative MRI techniques, so-called multimodal techniques, will likely aid in a comprehensive understanding of brain changes following mTBI.[3] After decades of research using DTI, questions remain about the time course of observable changes in DTI metrics and, importantly, how they relate to the underlying pathophysiology and WM microstructure. This has largely led to denouncement of interpreting DTI changes as relating to changes in "WM integrity" as the measure does not offer

specific information to extract such conclusions.[20,104,105,121] Therefore, fundamental questions about the localization and extent of damage from mild injury and subsequent development of downstream sequelae remain unclear in humans. The largest outstanding question is how locations and extent of damage in the brain detectable with DWI relate to alterations in cognitive functioning and symptoms.

CHAPTER 2: A RAPID REVIEW OF MILD TRAUMATIC BRAIN INJURY STUDIES UTILIZING CONTEMPORARY TECHNIQUES FOR DIFFUSION IMAGING ANALYSIS

Joshua H. Baker, Andrew Bender, Sarah E. Tilden, Norman Scheel, David C. Zhu[1]

[1]Chapter 2 contains an invited rapid review manuscript that is currently under final review before submission to the *Journal of Neurotrauma*. Its use within the current dissertation was approved by the doctoral committee. Joshua H. Baker conceived the original idea, conducted the search for manuscripts, reviewed the manuscripts, and drafted this manuscript independently. The manuscript has been edited to fit the format of this dissertation.

INTRODUCTION

Diffusion-weighted magnetic resonance imaging (DWI) has been used extensively to study the brain following mild traumatic brain injury (mTBI). However, several recent comprehensive reviews, which have looked at over 100 studies collectively, concluded that a consistent pattern of change measurable with this pulse sequence/modality was not observed.[3,5,17] This lack of consensus may be due in part to individual differences in injury mechanism, components of resilience to injury, and even heterogenous phenotypes of WM recovery following injury. However, these inconsistent findings may also be partly due to the widespread use of the diffusion tensor imaging (DTI) model.

DTI is the most common method for modeling the DWI signal in neuroimaging studies of mTBI. There is no debate about DTI's sensitivity to microstructural changes in the WM following mTBI, even in patients with negative findings on conventional neuroimaging. However, this technique has several limitations, and newer complementary higher-order signal representation and modeling methods such as diffusion kurtosis imaging (DKI), neurite orientation dispersion and density imaging (NODDI), and Fixel-Based Analysis (FBA) may provide greater specificity in studies collecting DWI data in mTBI patients. The present review will introduce the foundational

principles of these modeling techniques, summarize the metrics estimated with them, and review the current findings in studies that utilized each technique in mTBI patients.

A recent comprehensive review of DTI studies in mTBI concluded the most common observed findings are decreased fractional anisotropy (FA) and increased mean diffusivity (MD) in WM tracts such as the corpus callosum, internal capsule, and corona radiata.[1] This injury pattern is thought to reflect the secondary injury cascade related to diffuse axonal injury, inflammatory cellular reactivity, and vasogenic and cytotoxic edema following the primary insult. However, there are other studies that report higher FA with lower MD and/or radial diffusivity (RD) in the acute/subacute period.[1] This lack of a reproducible pattern and specificity for secondary injury mechanisms has limited DTI's clinical translation. It is increasingly difficult to ignore the possibility that major limitations of the DTI model may be contributing to this ambiguity. The underlying assumption of DTI is a Gaussian approximation to the probability distribution governing the random displacement of water molecules. Additionally, DTI is a voxel-based technique and has difficulties modelling voxels containing anything other than a singular coherent bundle of axons. This limits the sensitivity and specificity of DTI in mTBI.[126,127]

HIGHER ORDER SIGNAL REPRESENTATION AND BIOPHYSICAL MODELLING TECHNIQUES

Diffusion Kurtosis Imaging

Diffusion kurtosis imaging (DKI), developed in the early 2000s, characterizes non-gaussian diffusion, leading to improved performance in regions with crossing fibers compared to DTI. DKI is categorized as a signal model. This is in contrast to biophysical models, which quantify microstructural characteristics of the underlying tissues and their change in pathology. The term kurtosis refers to the variation in the Gaussian shape of the distribution. The apparent diffusion kurtosis is based on the premise that deviations from a Gaussian diffusion probability distribution or

a sample of data-tailedness in the brain are a measure of underlying tissue microstructural organization.[128] Mathematically, DKI introduces a quadratic term to the linear relationship between the logarithm of the DWI signal and the b-value. Jensen and colleagues reported higher WM apparent kurtosis coefficients of 1.41±0.11 compared to grey matter 0.82±0.03, indicating the greater organization of structures that will impede free diffusion of water in WM compared to gray matter.[1]

DKI data can be characterized by fitting a 3 x 3 tensor matrix with three principal eigenvectors and eigenvalues like DTI. The most reported scalar diffusion kurtosis tensor imaging (DKTI) metrics are mean kurtosis (MK), which represents the average of the kurtosis along all directions; axial kurtosis (AK), the kurtosis along the axial direction of the diffusion tensor; and radial kurtosis (RK), the kurtosis along the radial direction of the diffusion ellipsoid (Table 1). DKI requires two non-zero b-values and at least 15 diffusion encoding directions.[1] The acquisition can take 7-10 minutes to use DKTI, or a faster protocol can be acquired in 1-2 minutes to estimate only MK.[129,129–131] An early study utilizing DKI demonstrated that MK and not MD or FA was sensitive to reactive astrogliosis, indicating the method is complementary to DTI.[132]

Neurite Orientation Dispersion and Density Imaging (NODDI)

The neurite orientation dispersion and density imaging (NODDI) compartment model of diffusion signal builds on the analytical neurite model developed by Jespersen and colleagues, 2007.[133] This method models the diffusion signal in grey and WM, with the summary term neurite referring collectively to axons in WM and dendrites in grey matter. NODDI models the signal from three microanatomical locations: the intra- and extracellular compartments and the cerebrospinal fluid (CSF); therefore, it is categorized as a multi-compartment model.[134] By quantifying the contributions from these three compartments and modeling a relationship between them, NODDI allows further interpretability of the diffusion signal in addition to DTI and DKI.

The intraaxonal compartment, a unique environment of diffusivity within axons in a voxel, is modeled as lines, or cylinders with zero radius. The orientation distribution function is estimated using a Watson distribution, which is in contrast to the spherical harmonic series used in the original work by Jespersen.[133,135] Using a Watson distribution, accurate estimation of scattering dendrites and fanning axons (referred to as dispersion), or coherent axon bundles, is possible.

Notably, compared to previous models, the parallel and perpendicular diffusivities are mathematically related. In this framework, increased dispersion and a reduction in intracellular anisotropy will also be reflected as a decrease in extracellular anisotropy due to the increased perpendicular diffusivity. In the original work by Zhang and colleagues, when the two NODDI-derived metrics, neurite density index (NDI) and orientation dispersion index (ODI), were plotted against stratified FA values, it was shown that different combinations of density and orientation in a voxel can result in the same FA value. This additional specificity is likely to aid in untangling the inconsistent findings of FA in the acute/subacute recovery period following mTBI.

NODDI requires a high angular resolution diffusing imaging (HARDI) protocol, with the ideal protocol requiring 30 diffusion directions at a low b-value of around 700 mm/s2 and 60 diffusion directions at a high b-value of around 2000 mm/s^2 . The optimized protocol is about 25 minutes long, while a reduced angular resolution protocol can be acquired in under 10 minutes.[134] The shorter protocol only decreases the certainty in the estimation of the ODI and has little effect on the other parameters. The most reported metrics estimated from the NODDI model are referred to by many names throughout the literature. They are more commonly the orientation dispersion index (ODI), neurite density index (NDI), or isotropic volume fraction (FISO) (Table 1). NDI in the original work by Zhang and colleagues was referred to as the volume of the intracellular compartment, abbreviated V_{IC}, and may also be seen in various publications as intraneurite fraction

(f_i) or intracellular volume fraction (ICVF). FISO, originally, volume of the isotropic compartment V_{iso}, is equivalent to free water fraction (FWF/ISO/f_{fw}).

ODI quantifies how uniform the organization of axons within a voxel is on a scale from zero to one. Zero indicates more anisotropic/parallel organization, whereas one represents isotropic/dispersing organization. NDI is an estimate of the volume of the intraneurite compartment and, therefore, reflects an approximation of axon density. FISO measures the contribution of isotropic diffusion present in a voxel, which is normally attributed to CSF. The isotropic compartment serves to adjust ODI and NDI, and as a measure of the extent of isotropic diffusion where it does not belong in WM. This can be useful in examining the extent to which edema following mTBI may be present in WM regions.

Constrained Spherical Deconvolution and Fixel-Based Analysis

Constrained spherical deconvolution (CSD) allows for the comparison of multiple metrics within a single voxel.[18] Importantly, these metrics are specific to distinct fiber populations within a single voxel. This new volume element, a single fiber population within a voxel, is referred to as a "fixel" (fiber in a voxel). It should be noted that this analysis technique can resolve multiple fixels in a voxel.

CSD extends earlier multi-tensor fitting models by expanding the number of fiber populations fit to infinity and neglecting the negative orientations of the fiber orientation distribution function.[136] Therefore, CSD estimates the fiber orientation distribution function without the need for prior knowledge and, importantly, assumes the diffusion characteristics of all fiber populations are identical. CSD assumes that variations in WM microstructure have a negligible effect on the measured DWI signal and that, instead, partial volume effects are responsible for variations. This underlying assumption is what allows CSD to account for crossing fiber architecture. Any variations in the diffusion anisotropy are understood to be entirely due to partial volume effects

from other tissue types or from multiple fiber bundles with varying orientations, including fanning, crossing, or divergence, collectively referred to as crossing fibers. In a way, it is model-free because no underlying assumptions about microstructure are made, and the information about fiber orientation is entirely extracted from the response function estimated directly from the DWI signal.

The major difference between previous CSD approaches and the algorithm implemented in MRtrix3's software is a lack of normalization of the DWI signal, meaning the apparent fiber density metric is directly proportional to the measured signal.[121] The metrics estimated in a fixel-based analysis (FBA) are the fiber density (FD), fiber cross-section (FC), and their product, the fiber density-cross section (FDC) (Table 1). FC compares the cross-sectional area perpendicular to a particular fiber orientation based on a subject's warp to a study-specific template space. The multiplication of FD and FC to yield FDC creates a third and vital contrast for comparison in situations when a changing diameter accompanies a change in a fiber bundle's axon quantity. Using these three measures, a group comparison of the degree to which a fiber population has had a decrease in density, a decrease in cross-section, or a simultaneous decrease in cross-sectional area and apparent number of axons is possible.

A challenge uniquely addressed by FBA when modeling multiple fiber populations within a voxel is the reorientation of data for accurate spatial normalization before group comparison.[137] The higher-order crossing fiber information has been shown to improve image registration between subjects, allowing for more accurate spatial alignment compared to FA registration.[137] This allows for a comprehensive comparison of all WM fixels compared to traditional skeletonization techniques such as FSL's Tract-based Spatial Statistics (TBSS) which reduces the analysis to a subset of WM voxels.[138] Additionally, the estimation of fiber orientation distributions (FODs) using three tissue response functions and the associated reorientation techniques also help to address partial volume effects that skeletonization techniques like TBSS were developed to address.[1]

Finally, the associated group analysis technique for FBA takes advantage of the improved tractography results using CSD estimated FODs to perform connectivity-based fixel enhancement.[126,139] This builds on the threshold-free cluster enhancement proposed by Smith and colleagues, which focused on voxel enhancement based on their connection.[140] The unique difference of the cluster-based fixel enhancement employed in FBA is the use of tractography from a study-specific template to inform the boosting of t-values. In this framework, a fixel that is connected via the tractography in a different location along a given tract is taken into account when boosting t-values. Thus, enhancement depends on membership to a tract as opposed to a local relationship in voxel space, which may not specifically define membership to a coherent WM tract and, by proxy, the projections of a specific cell population.

Ultimately, NODDI and CSD are similar in that they both quantify the signal from the intraaxonal compartment to estimate the proportion of signal from inside axons and infer the density of axons in a volume. Additionally, all three methods, DKI, NODDI, and CSD, are capable of resolving aspects of crossing fiber architecture, increasing the specificity of these measures in brain regions containing complex microstructure.[141] Each of these methods has been utilized in studying mTBI subjects, and fortunately, most studies also include DTI metrics. Moving forward, a thorough understanding of these techniques will be critical for mTBI researchers as they choose acquisition protocols and interpret the results of their diffusion studies using each technique. The robustness to crossing fibers of these methods and their increased specificity to the underlying pathophysiology in the WM will make them indispensable to traumatic brain injury researchers moving forward.

Table 2.1 Common Diffusion Magnetic Resonance Imaging Metrics for DKI, NODDI, and FBA

Metric (Abbr.)	Description
Mean Kurtosis (MK)	A scalar summary measure calculated from the diffusion kurtosis tensor which is the average amount that the diffusion displacement probability distribution deviates from a normal or gaussian distribution.
Axial Kurtosis (AK)	The average apparent diffusion kurtosis parallel to the principal diffusion direction/eigenvector.
Radial Kurtosis (RK)	The average apparent diffusion kurtosis perpendicular to the principal diffusion direction/eigenvector.
Free Water Fraction (FWF/V_{iso})	A measure of the contribution of the CSF signal within a voxel.
Neurite Density Index (NDI/V_{ic})	A measure of the proportion of the intracellular signal within a voxel, which infers the density of axons within a voxel.
Orientation Dispersion Index (ODI)	Assesses the degree to which axons are traveling in a uniformly parallel orientation or dispersing away from one another in a fanning or scattering organization with a value close to 0 reflecting a uniformly parallel organization and 1 representing neurites dispersing in many directions.
Fiber Density (FD)	For a specific orientation of a fiber orientation distribution, FD represents an estimate of the amount of underlying axons.
Fiber Cross Section (FC)	An estimate of the diameter of a fiber population represented by a fixel based upon the warps calculated from registering a subject to a study-specific template image.
Fiber Density Cross Section (FDC)	The multiplication of the Fiber Cross Section and Fiber Density of a fixel which provides sensitivity to the situation where a fiber population is losing the number of axons within it in addition to shrinking in cross sectional areas.

MATERIALS & METHODS

PubMed was searched on June 12, 2023, and a second time on February 12, 2024. Three searches were conducted to compile studies that had utilized DKI, NODDI, or CSD and FBA. Keywords searched for mTBI were mild traumatic brain injury, concussion, mild brain trauma, or mild head injury, and for DKI were kurtosis, diffusion kurtosis imaging, DKI, or mean kurtosis

tensor. The search was limited to papers published in the last 10 years. The DKI search yielded 22 manuscripts abstracts which were reviewed for inclusion. One additional study outside this range was included due to its continuity with the publication by the same authors in 2013.[142] Another DKI study was excluded because it was not available in English. Review articles, animal studies, interventional clinical trials, and manuscripts focused on methodologic development were excluded, leaving a total of 17 DKI manuscripts that are reviewed here. Keywords for NODDI were neurite orientation dispersion and density imaging, NODDI, water fractions, FISO, ODI, NDI, neurite density, and orientation dispersion. The NODDI search yielded 28 manuscripts whose abstracts were reviewed with the same criteria applied as in the DKI search, yielding 15 manuscripts. Keywords for CSD/FBA were constrained spherical deconvolution, fixel-based analysis, fixel, MRTrix3, CSD, and FBA. This search yielded 12 manuscripts whose abstracts were reviewed, with 7 manuscripts included in this review.

During the review of each article, key information about each sample's characteristics, when available, was extracted, including injury mechanism (sports-related or general mechanisms from a population-based sample), data sample size, DWI data collection time points, neuroimaging software used for analysis and diffusion metrics estimated for each method DKI, NODDI, and FBA. In addition, the main findings of each manuscript, including the finding, comparison, timepoint, and localization of effects, were extracted.

RESULTS & DISCUSSION

Summary information from each reviewed manuscript is available by modeling technique for DKI (Table 4.2), NODDI (Table 4.3), and CSD/FBA (Table 4.4).

Diffusion Kurtosis Imaging in mTBI

One of the first studies to utilize DKI in a sample of mTBI patients during the acute period of recovery was by Karlsen & colleagues 2019. In this population-based sample from a Level 1

trauma center and emergency clinic in Norway, decreased kurtosis fractional anisotropy (KFA) in mTBI patients compared to controls was observed. However, there were no other significant differences in kurtosis metrics. Interestingly, when comparing with DTI metrics, a greater number of significant voxels were observed with FA compared to KFA when comparing mTBI patients and controls. In contrast, later studies in similar populations in Norway by Stenberg & colleagues 2021 observed the opposite relationship between FA and KFA in mTBI patients and controls. The work by Stenberg and colleagues found more significant voxels with lower KFA than FA between mTBI and controls. In this larger sample, a widespread decrease in all kurtosis metrics was seen at a 72-hour time point during the acute phase of recovery (Table 2).[143,144] In numerous comparisons between subgroups of mTBI patients, including participants with persistent post-concussive symptoms (PPCS) based on the British Columbia Post-concussion Symptom Inventory, reduced KFA was observed. Notably, significant differences were observed even when comparing mTBI patients with persistent symptoms at three months post-injury with mTBI patients who did not report PPCS. However, at the acute time point when analyses were controlled for cognitive reserve, no significant differences in any diffusion metrics remained.

Contrasting patterns of DKI metrics have been observed, however, in contact sport athletes with sports-related mTBI. Two studies of male football players by Lancaster and colleagues 2016 & 2018 demonstrated acute increases in axial kurtosis in widespread brain regions at 24-hour and 8-day time points following injury.[145,146] No differences were observed for mean kurtosis or radial kurtosis. This study observed significant differences between groups at the 6-month time point in DTI metrics, including decreased MD, axonal diffusivity (AD), and RD. In more recent studies, elevated axial kurtosis was observed at 24-48 hours post-injury in two samples of male American football players.[147,148] Radial kurtosis significantly decreased in the subacute phase at the 15-day timepoint in work by Muftler & colleagues and at a timepoint seven days after return to play following a sport-

related mTBI in work by Chung & colleagues.[147,148] Increased KFA was observed in participants in frontal WM regions 15 days post-injury in both TBSS and voxel-based analysis (VBA) analyses. This finding was more pronounced at 45 days post-injury. However, a pattern of divergent KFA values in the control and mTBI groups was noted, indicating that observed differences may have been driven by decreasing KFA in the control group rather than changes in the mTBI group alone. Notably, these studies observed no between or within-group differences in DTI metrics in any comparisons, including VBA, TBSS, and ROI analyses.

A later study from the same group conducted generalized linear mixed effects models to examine the relationship between prior concussion, years of contact sport participation, and DTI/DKI metrics.[149] Interestingly, injury history was not associated with microstructural change, but years of contact sport exposure had a significant relationship with elevated RK. In the past, mTBI with a sports-related etiology was often discussed separately from other mTBI studies. However, this distinct divergence in DKI metrics in the acute phase of recovery between early population-based samples and contact sport samples highlights an opportunity to extract insight from these once separate areas of investigation.

Many studies have been conducted in the sub-acute period following injury, with an early population-based sample recruited from a Maryland ED finding decreased mean and radial kurtosis in the internal capsule one month after injury.[150] Although decreases in MK and RK at the 10-day post-injury time point were also observed in this study, this difference was not significant in the early subacute period. More recently, a population-based sample recruited from a neurosurgery clinic in China calculated MK between 2-weeks and 2-months of injury.[151] This study found decreased MK in mTBI patients compared to controls in multiple regions of association fibers and projection fibers, and this was associated with lower digit span scores on a Digit Span Forward task. Still, another study observed decreased MK in thalamic, hippocampal, and callosal ROIs at 14-days and 3-months

post-injury.[152] The difference was significant only in the thalamic ROI from the first to second time point in this study of the subacute period following injury. A subsequent analysis of the same sample observed no differences when comparing ROI averaged DKI metrics between subsamples of patients with extensive symptoms on the Rivermead post-concussion questionnaire, and those with little to no symptoms.

In the chronic period, sports-related mTBI studies far outnumber population-based samples. Early work by Grossman and colleagues 2012 examined MK in a small population-based sample of 15 patients up to three years post-mTBI and found decreased MK in several brain regions when compared to sex, age, and education-matched controls (Table 2).[142] A later study by the same group in 2013 found decreased MK in similar regions, including the thalamus and corpus callosum, over 9 months following injury.[153] Finally, strong evidence from a large population-based sample of mTBI found sustained decreases in MK at a 12-month timepoint in widespread brain regions.[144] This suggests that decreases in MK that are observed in the acute and subacute time periods persist well beyond the typical recovery period for mTBI.

Similarly, in the chronic period of recovery following injury, a decrease in MK is commonly reported at 6 months post-injury[150] and was even observed in two samples at post-season scans after a season of high school football in players without mTBI.[154,155] Still, other studies have observed no significant differences in some or all DKI metrics at 6 months post-injury in football players.[145,148] Nonetheless, it is clear that in some populations, an incompletely understood process of change in WM may persist for months to years following a traumatic brain injury, even those presently categorized as mild.

The question of what differences exist in repetitive head injury, and subconcussive blows have also been investigated with DKI. An interesting study by Gong & colleagues compared pre and post-season scans in high school athletes who were monitored during practice and games with head

impact telemetry during a football season.[154] They found significant decreases in MK in cortical and deep WM, including the thalamus, over the course of the season. They also found that, although also significant, the DTI summary metric MD had a smaller effect size in the thalamus when compared to MK. Another similar study of high school football players without mTBI by Davenport & colleagues utilized DKI in pre and post-season scans.[155] They found a significant association of risk-weighted cumulative exposure combined probability, a summary measure of risk associated with linear and rotational acceleration experienced during head blows, with voxels >2 standard deviations below the mean in DKI metrics MK, AK, and RK. These studies provide early evidence that caution must be exercised in interpreting WM changes in the context of sports-related mTBI. These differences may not necessarily be due to a singular impact that causes a diagnosed mTBI, but rather demonstrate the unique aspects of this mTBI etiology in the study of WM response to repeated traumatic insults in contact sport athletes.

Overall, studies of mTBI utilizing DKI observed mixed patterns of WM change with kurtosis metrics in the acute period following injury. In the acute period, populations of athletes, mostly football players, had increased MK[148,156], RK[156], and AK[146–148] compared to controls. In contrast, population-based studies observed decreases in MK[143,144], RK[143], and AK[143]. In population-based samples in the subacute period, the majority of studies reported decreased MK[150,151,153] , with some observing continued decreases in KFA[157], and RK[150]. One study reported an increase in MK[152], and one reported no differences in DKI metrics during the subacute period.[144] Only one study of sport-related mTBI examined group differences in DKI metrics in the subacute period and noted increased MK, decreased RK, and increased KFA.[147] In the chronic period following injury, sport-related and population-based studies most commonly observed decreased MK.[142,144,150,153] Most interestingly, studies collecting pre & post-season scans in otherwise healthy athletes observed decreased MK at post-season scans.[154,155]

Table 2.2 Summary of DKI in mTBI Studies

Article	Comparison group demographics	Post-injury measurement timepoints	Neuroimaging software & metrics	Significant metrics and localization of effects
Goubran et al., 2023	Football Players: *n* = 63 (0F, 63M) Age: mean ± SD (19.11±1.57) Volleyball Players: *n* = 34 (0F, 34M) Age: (19.57±0.91)	Timepoint 1: Annual pre-season scan. Timepoint 2: Within 24-48 hours of injury mean ± SD (1.83d±1.26) Timepoint 3: 6 mo followup scan (165d ± 77) Timepoint 4: After final athletic season	DESIGNER software for DKI analysis. MRTrix3 and automated fiber quantification (AFQ) for tractometry. Metrics: MK, AK, RK	Increased MK and RK in the L UF and R cing when comparing preseason scans with 24-48 hr scans. Increased MK in the R cing cingulate in football players who had a prior concussion or sustained an injury in the study when compared with volleyball players.

Table 2.2 (cont'd)

Article	Comparison group demographics	Post-injury measurement timepoints	Neuroimaging software & metrics	Significant metrics and localization of effects
Stenberg et al., 2023	Population Sample mTBI: *n* = 193 (70F, 123M) Age: median, range (27, 16-59) mTBI Subsample Complicated mTBI: *n* = 22 Age, gender, and education-matched community controls: *n* = 83 (33F, 50M) Age: (27.7, 16-58)	Timepoint 1: 72h mean ± SD (52h±19h) Timepoint 2: 3mo (95d±7d) Timepoint 3: 12mo (370d±17d)	Diffusional Kurtosis Estimator, TBSS-based voxel-wise analysis (FSL) Metrics: KFA, MK, AK and RK	A longitudinal analysis of diffusion metrics revealed that mean kurtosis was relatively stable over time in the mTBI group. Fluctuations in the control group drove interaction effects. Decreased MK in the CR, CC, cing, IC, Fx, TR, CST, sagittal stratum, cerebellar peduncle, and medial lemniscus at 72h time point. Decreased MK in the CR, CC, cing, IC and EC, Fx, TR, SLF, and sagittal stratum at 12 mo time point.

Table 2.2 (cont'd)

Article	Comparison group demographics	Post-injury measurement timepoints	Neuroimaging software & metrics	Significant metrics and localization of effects
Chung et al., 2022	Collegiate athletes mTBI: mTBI subsample: football players 48 hr post *n* = 24 (0F, 24M) Age: mean ± SD (19.7 ± 1.1) mTBI Subsample: Repeat head injury (RHI) with no mTBI during study: *n* = 26 (0F, 26M) Age: (19.3 ± 1.2) Non-contact sport controls w/out head injury: *n* = 28 (0F, 28M) Age: (19.7 ± 1.4)	Timepoint 1: 24-48h post injury Timepoint 2: Asymptomatic period after return to play clearance mean ± SD (8.1d±5.6d) Timepoint 3: 7 days after return to play (27d ± 12.5d) Timepoint 4: 6-months post injury (182d ± 14d)	In-house MATLAB scripts to estimate DKI metrics, TBSS-based voxelwise analysis . Post-hoc ROI analysis using ICBM-DTI-81. Metrics: MK, AK, RK	Increased AK in mTBI group compared to controls. The extent of significantly different voxels for AK decreased by the 6-month timepoint when comparing mTBI and controls. Increased MK in mTBI compared to controls in the EC, posterior limb and retrolenticular part IC, cerebral peduncle, UF, ILF, posterior TR and splenium of the CC. Differences in MK did not persist at the 6 mo time point. Decreased RK in mTBI compared to controls 7 days after return to play I the posterior CC. Increased AK and MK in the RHI group compared to controls in the CC, CR. SLF, posterior limb and reticulolenticular part of IC, posterior TR and cerebral peduncle. No significant differences between mTBI and RHI groups.

Table 2.2 (cont'd)

Article	Comparison group demographics	Post-injury measurement timepoints	Neuroimaging software & metrics	Significant metrics and localization of effects
Wang et al., 2022	Population Sample mTBI: *n*= 23 (11F, 12M) Age: mean ± SD (47± 9.9) Controls: *n* = 24 (12F, 12M) Age: (49± 13.5)	Timepoint: 2wk – 2mo mean (39d)	Diffusional Kurtosis Estimator, TBSS-based voxel-wise analysis (FSL) Metrics: MK	Decreased MK in mTBI patients compared to controls, with no differences in FA or MD in the bilateral SLF, cing, R ILF, IFF, UF, inter-hemispheric fibers of body of CC, projection fibers of CST, ATR, and bilateral IC and EC. Attention deficit as measured by lower digit span forward score was significantly associated with decreased MK in the mTBI group in the SLF, ILF, IFF, UF, body of the CC, CST, ATR, bilateral IC and EC. Decreased MK in mTBI patients in the right hippocampus, left thalamus, left caudate, right putamen, and right pallidum.
Brett et al., 2021	Football Players & Non-contact sport players: *n* = 121 (0F, 121M) Age: mean ± SD (18.52±1.74) Years of contact sport exposure (5.01y ± 4.49y)	Timepoint 1: 48h Timepoint 2: 8d Timepoint 3: 15d Timepoint 4: 45d	Diffusional Kurtosis Estimator, TBSS-based voxel-wise analysis (FSL). Generalized linear mixed effects models examining relationship of prior concussion, years of contact-sport participation and WM microstructure. Metrics: KFA, MK, AK and RK	History of concussion was not independently associated with microstructural or macrostructural WM changes. Significant associatons between years of self-reported contact sport exposure and WM microstructural abnormalities.

Table 2.2 (cont'd)

Article	Comparison group demographics	Post-injury measurement timepoints	Neuroimaging software & metrics	Significant metrics and localization of effects
Stenberg et al., 2021	Population Sample mTBI: *n*= 176 (65F, 111M) Age: median, IQR (28.1, 22) mTBI Subsample Complicated mTBI: *n* = 18 Age, gender, and education-matched community controls: *n* = 78 (30F, 48M) Age: (27.6, 20)	Timepoint 1: 72h mean ± SD (52h±19h)	Diffusional Kurtosis Estimator, TBSS-based voxel-wise analysis (FSL) Metrics: KFA, MK, AK and RK	Decreased KFA and higher RD in PPCS patients in the CC, CR, IC, and TR than patients without PPCS. No significant differences remained in any diffusion metrics between patients with and without PPCS when controlling for cognitive reserve. Decreased KFA, MK, AK, RK in the CC, CR, IC, SLF, and TR. Decreased MK was also present in the cerebellum and brainstem. These differences remained when examining only the uncomplicated mTBI patients. Decreased MK, AK and RK in mTBI patients without PPCS compared to controls in the IC, cerebellum, brainstem, and thalamus.

Table 2.2 (cont'd)

Article	Comparison group demographics	Post-injury measurement timepoints	Neuroimaging software & metrics	Significant metrics and localization of effects
Muftler et al., 2020	Football Players: *n*= 96 (0F, 96M) Age: mean± SD (18.06 ± 1.5) Controls: *n* = 82 (0F, 82M) Age: (18.37 ± 1.7)	Timepoint 1: 48h mean ± SD (32.47h ± 14.19) Timepoint 2: 8d (8.20d ± 0.98) Timepoint 3: 15d (15.42d ± 1.35) Timepoint 4: 45d (45.56d ± 3.77)	Diffusional Kurtosis Estimator, TBSS-based voxel-wise analysis (FSL), Whole-brain Voxel Based Analysis, Longitudinal ROI analysis based on significant clusters from 1st level TBSS analysis. Metrics: KFA, MK, AK and RK	Increased AK in mTBI compared to controls with increasing number of significant voxels from 48h to 15d timepoint with no significant differences at the 45d timepoint. Decreased RK in mTBI compard to controls at the 15d timepoint with both the whole brain voxel-wise and TBSS analysis, and at the 45d timepoint for the whole brain voxelwise analysis only. Increased KFA in mTBI compared to controls in frontal WM regions at th 15d and 45d timepoint.
Karlsen et al., 2019	Population Sample mTBI: *n* = 25 (13F, 12M) Age: mean ± SD (32.7 ± 13.0) Controls: *n* = 22 (12F, 10M) Age: (34.5 ± 8.7)	Timepoint 1: 72h mean, range (69h, 261h) Timepoint 2: 3mo (82d, 43d)	TBSS-based voxel-wise analysis (FSL) 5 WM ROIs created with intersection of ICBM-DTI-81 and the TBSS WM skeleton Hand drawn thalamic ROIs Metrics: KFA, MK, AK and RK	Decreased KFA in mTBI compared to controls in the genu of the CC, cerebellar peduncle, IC, CR, and SFF at the 72h timepoint. Five times the voxels of decreased FA and KFA were observed at the 3mo timepoint in the same regions with the addition of the posterior TR bilaterally. No significant differences for MK, AK or RK.

Table 2.2 (cont'd)

Article	Comparison group demographics	Post-injury measurement timepoints	Neuroimaging software & metrics	Significant metrics and localization of effects
Gong et al., 2018	Football Players w/out mTBI: *n* = 16 (0F, 16M) Age: median, range (16y, 15-17) Years of contact sport exposure (7y, 5-12)	Timepoint 1: Pre-season before first contact practice Mean, range (2d, 2-6d) Timepoint 2: Post-season (10d, 2-6d)	In-house MATLAB scripts to estimate DKI metrics. Metrics: MK	Decrease in MK in the thalamus, left paracentral, right pars triangularis, right inferior parietal, right cuneus, and right rostral middle frontal cortices from the pre- to post-season scan. A larger effect size was observed for pre to post-season differences in MK in the thalamus suggesting it may be more sensitive than MD.
Lancaster et al., 2018	Football Players: mTBI: *n*=17 (0F, 17M) Age: mean±SD (17.5± 1.7) Age, gender, sport, premorbid level of verbal intellectual functioning, and GPA matched controls: *n* = 20 (0F, 20M) Age: (17.9±1.7)	Timepoint 1: 24hr mean, range (19.69hr, 14-24hr) Timepoint 2: 8d (8.3d, 7-11d) Timepoint 3: 6mo (168.56d, 151-204d)	TBSS-based voxel-wise analysis (FSL) DTI tensors and DKTI tensors were estimated using in house software. ROI based analysis of WM tracts based on the ICBM-DTI-81 WM atlas at the 6mo timepoint. Metrics: MK, AK, RK	No differences in DKI metrics at the six mo timepoint or in longitudinal analyses when comparing controls and mTBI patients.

Table 2.2 (cont'd)

Article	Comparison group demographics	Post-injury measurement timepoints	Neuroimaging software & metrics	Significant metrics and localization of effects
Naess-Schmidt et al, 2018	Population Sample: mTBI w/ RPQ ≥ 20 *n*= 25 (16F, 9M,) Age: mean± SD (24± 3.9) mTBI w/ RPQ = 0 *n*= 25 (11F, 14M) Age: mean± SD (22.7± 3.5) Controls: *n* = 27 (16F, 11M) Age: (27 ± 6.2)	Timepoint 1: 2-5mo post mTBI	Combination of FSL and inhouse MATLAB scripts to estimate MKT. Automatic segmentation of ROIs. Metrics: MKT	No significant differences in diffusion metrics in any ROIs between patients with extensive symptoms on RPQ vs. those with minimal symptoms.
Naess-Schmidt et al., 2017	Population Sample mTBI: *n*= 27 (16F, 11M) Age: mean± SD (27.6± 6.4) Controls: *n* = 27 (16F, 11M) Age: (27.4 ± 6.2)	Timepoint 1: 14d mean± SD (10.3d ± 3) Timepoint 1: 3mo (100.1d ± 7)	Combination of FSL and inhouse MATLAB scripts were used to co-register auto-segmented thalamic, hippocampal and callosal ROIs from MP2PRAGE images with corresponding regional mean images. Metrics: MK	Increased MK in mTBI compared to controls in the thalamus at the 14d. Decreasing MK in mTBI thalamic ROIs when comparing within group between the 14d and 3 mo timepoint.

Table 2.2 (cont'd)

Article	Comparison group demographics	Post-injury measurement timepoints	Neuroimaging software & metrics	Significant metrics and localization of effects
Davenport et al., 2016	Football Players w/no mTBI: *n*=24 (0F, 24M) Age: mean± SD (16.9 ± 0.6)	Timepoint 1: Baseline Timepoint 2: Pre-season Timepoint 3: Post-season Interval between pre & post season scans: mean± SD (4.9mo ± 0.6)	Diffusional Kurtosis Estimator, FSL & SPM Metrics: MK, AK, RK	A significant association between risk weighted cumulative exposure combined probability and voxels >2 standard deviations below the mean for MK, AK and RK.
Lancaster et al., 2016	Football Players: mTBI: *n*=26 (0F, 26M) Age: mean± SD (17.6 ± 1.5) Age, gender, sport, premorbid level of verbal intellectual functioning, and GPA matched controls: *n*= 26 (0F, 26M) Age: (18 ± 1.5)	Timepoint 1: 24hr Timepoint 2: 8d	TBSS-based voxel-wise analysis (FSL) DTI tensors and DKTI tensors were estimated using in house software. Metrics: MK, AK, RK	Increased AK in the IC, UF, cerebral peduncle, CST, IFF, and ILF when comparing controls and mTBI at 24hr time point. There were more widespread regions with increased AK at the 8d time point. No observed differences for MK or RK.

Table 2.2 (cont'd)

Article	Comparison group demographics	Post-injury measurement timepoints	Neuroimaging software & metrics	Significant metrics and localization of effects
Stokum et al., 2015	Population Sample mTBI: *n*= 24 (6F, 18M) Age: mean± SD (37.4± 14.1) Controls: *n* = 24 (11F , 13M) Age: (33.9 ± 14.7)	Timepoint 1: 10d mean± SD (6 ± 3d) Timepoint 2: 1mo (33 ± 7d) Timepoint 3: 6mo (196 ± 33d)	Custom hand drawn ROIs and in house MATLAB scripts utilized to analyze mean and standard deviation of diffusion metrics in each ROI. Metrics: MK, RK, λ_r	Decreased RK and MK were observed in the anterior limb of the IC at the 1mo and 6mo timepoint. No differences in λ_r when comparing mTBI patients and controls at each timepoint.
Grossman et al., 2013	Population Sample mTBI: *n*= 20 (4F, 16M) Age: mean± SD (34.8± 10.7) Sex, age, and education matched controls: *n*= 16 (3F, 13M) Age: (35.1 ± 11.9)	Timepoint 1: 1mo mean± SD (22.1d ± 15.4) Timepoint 2: >9mo (369.6d ± 112.1)	In-house MATLAB scripts, TBSS-based voxel-wise analysis (FSL) Metrics: MK	Decreased MK in mTBI compared to controls in the thalamus, IC, EC, CC, cing, optic radiations, centrum semiovale, total deep gray matter, and total WM at the 1mo time point. In the thalamus DTI, DKI and ASL metrics were significantly associated. Decreased MK in mTBI patients in the thalamus, CC, cing, optic radiations, centrum semiovale, total deep gray matter, and total WM at the >9 month timepoint.

Table 2.2 (cont'd)

Article	Comparison group demographics	Post-injury measurement timepoints	Neuroimaging software & metrics	Significant metrics and localization of effects
Grossman et al., 2012	Population Sample mTBI: *n*= 22 (8F, 14M) Age: mean± SD (38.2± 11.7) Sex, age, and education matched controls: *n*= 14 (5F, 9M) Age: (36.5 ± 12.3)	Follow up varied by group: Group 1 (7 mTBI patients) Timepoint 1: Within 1 year of injury Mean, range (65.7d, 14.6-215.35d) Group 2 (15 mTBI patients) Timepoint 1: >1 year after injury (3.9y, 1.33-9.58y)	In-house MATLAB scripts, SPM, and ImageJ. Hand-drawn ROIs with average diffusion metrics were compared for the thalamus, IC, CC, and centrum semiovale.	Decreased MK in mTBI patients compared to controls. Decreased MK in Group 1 patients compared to controls in the thalamus. Decreased MK in Group 2 patients compared to controls in the thalamus, IC, splenium of the CC and centrum semiovale.

NODDI in mTBI

Early work with NODDI by Churchill and colleagues in a sample of athletes with sports-related concussions revealed correspondence between acute increases in RD and decreases in V_{IC}.[158] No difference in V_{ISO} or ODI was observed, suggesting that these findings were not related to increases in free water or a change in the organization of fibers within colocalized regions of significant RD and V_{IC} in this sample. Only sparse areas of longitudinal change were observed in ODI, and other DTI metrics preceding participants' return to play, seemingly suggesting that during the recovery period in some mTBI patients, significant changes in WM microstructure may not coincide with symptomatic recovery and current clinical definitions of recovery.

Although not a purely mTBI sample, a study of repetitive mTBI in mixed-martial arts athletes scanned during a professional competition season similarly demonstrates the relationship between NODDI and DTI.[159] In this sample, decreases in FA were colocalized with increases in ODI, demonstrating the inverse relationship between these two metrics. Similarly, decreased MD was related to decreased $V_{ISO,}$ while V_{IC} did not demonstrate significant overlap with either FA or MD. Estimates of variance were calculated for the relationship between NODDI metrics as explanatory variables and DTI metrics as dependent variables, and it was demonstrated that only moderate relationships exist between V_{ic}, V_{iso}, and DTI metrics. Taken together, this study supports the notion that although complementary, the biophysical model NODDI offers increased specificity for pathologic microstructural change beyond DTI.

In a study of (n =32) CT/MRI negative mTBI patients, patients' DTI, DKI, and NODDI metrics from a multi-shell DWI were compared in the acute phase of injury with a median scan time of 29 hours.[160] TBSS whole-brain VBA revealed numerous regions of significant difference between mTBI patients and controls. The largest areas of difference by significant voxel number were with AD in the right posterior thalamic radiation, external capsule, and internal capsule. Similarly, for NODDI metrics, large effects for ODI were observed bilaterally in the posterior thalamic radiation, posterior limb of the internal capsule, and external capsule. In ROC analysis of whole brain WM averages ODI had the best performance differentiating mTBI and control patients compared to all other metrics (AUC = 0.73).

Some studies utilize hybrid analysis methods, such as the work by Oehr and colleagues 2021, in which an ROI analysis was conducted using average DWI metrics calculated using hand-drawn tractography masks.[161] In this study, the NODDI metrics ODI, ICVF, and ISO were compared between mTBI patients and orthopedic trauma controls between 6 to 12 weeks following injury. The NODDI metric ODI was significantly higher in this sample of mTBI patients when compared

with controls in the left uncinate fasciculus. ISO also demonstrated significant group-level differences, with the measure being lower in the mTBI group in the corpus callosum, and bilaterally in the superior longitudinal fasciculus direct and indirect segments. Interestingly, no differences were observed between mTBI patients and controls for the NODDI metric ICVF or the DTI metrics MD, AD, and RD. This suggests that edema related to the injury is resolved 6-12 weeks post-injury in this sample. The observation of reduced FA without concurrent changes in other DTI metrics is difficult to explain; however, it may be due to the smaller sample size of this study. Also, averaging metrics across entire WM tracts can be problematic, as the analysis technique can mask effects in certain more susceptible regions along the tract. Nonetheless, from a clinical perspective, this is likely a step closer to an approach that could be useful in single patients to gain a rough idea of these metrics in comparison to population averages in specific WM tracts.

An analysis of DWI data collected in pediatric mTBI patients in the Advancing Concussion Assessment in Pediatrics (A-CAP), revealed no difference in any diffusion metrics.[162] A possible explanation for these results could be the low number of directions collected for the b=2000 direction, as the optimized protocol for NODDI calls for 60 directions at b=2000. Recent work by Seider and colleagues suggests that the number of directions needed to fit diffusion models accurately could be significantly greater than was previously thought.[163] Additionally and similar to other studies, due to the heterogeneous and mild nature of the injury, tract averaging may obscure the ability to localize individual differences in specific locations along a tract.

In contrast, results from the PLAYGAME trial found decreased free water fraction in grey matter regions often colocalized with reduced MD, while differences between groups with mTBI having increased intracellular water fraction were generally more widespread and did not overlap with DTI metrics.[164] This study used a modified approach to calculate NODDI metrics without the fixed rates of intra and extracellular diffusivity in the original model for a more biologically informed

multicompartmental diffusion model with tissue-specific rates of diffusivity.[165] They noted that there were different statistical relationships between traditional NODDI metrics and those calculated with a more biologically plausible tissue-dependent diffusivity value.

Further evidence for NODDI metrics' sensitivity in pediatric mTBI comes from another study that sought to test NODDI metrics in outcome prediction models with multiple logistic regression.[166] In this study, they found that the model incorporating global WM ROI ODI at 1-month post-injury had the greatest performance in predicting the 2-3 month outcome with 81.82% and 87.18% negative and positive predictive power, respectively. This significantly outperformed the null clinical predictor model, with 58.8% and 70.5% negative and positive predictive power, respectively. Interestingly, models including FISO did not outperform the null models.

Currently, there are no interventions to improve outcomes following mTBI, so an understanding of factors following injury that may affect recovery is important. In a recent study examining the interaction of self-reported sleep quality in the first week following injury, it was noted that adolescent mTBI patients with poor sleep quality had decreased NDI in almost all tracts investigated when compared to those with good sleep quality and healthy controls.[167]

Another development in the field is the use of novel acquisition sequences, such as Hybrid diffusion imaging (HYDI), that would allow the application of numerous signal modeling techniques. A recent study of mTBI patients with chronic symptoms 3 months post-injury utilizing a HYDI acquisition found significant differences in numerous WM regions in the NODDI metrics ODI and V_{ic}.[168] No differences in DTI metrics were observed in this study. In another study using HYDI acquisition, mTBI patients had lower V_{ic} compared to controls in the corpus callosum and corona radiata.[122] This study also correlated diffusion metrics with neuropsychological performance on the Delis–Kaplan Executive Function System and found that increasing V_{ic} was associated with decreased performance in the form of increased reaction time and decreased recall on short and

long-delayed recall tasks. This would seem to suggest these higher-order modeling techniques are more sensitive to acute and chronic WM change, even using a clinically feasible acquisition that takes only 8 minutes to acquire. More recently, work by Anderson and colleagues demonstrated a lack of relationship between NODDI metrics and measures of cognitive performance that was present in mTBI patients but not control subjects.[169] Taken together, these studies demonstrate that not only is this higher-order modeling technique sensitive to changes in WM but also specific for differences in neuropsychological tests. This will be important in understanding how these WM changes relate to altered function.

Additional strong evidence that NODDI is more sensitive in detecting changes in WM microstructure than DTI comes from the analysis of data in the TRACK-TBI study.[112] A comprehensive analysis of patients, friend controls, and orthopedic injury controls was collected during the initial study, and a second replication sample of mTBI patients was conducted on multi-shell DWI data at b=1300 mm/s^2 and 3000 mm/s^2. Higher FISO was observed in the mTBI group compared to controls at the 2-week timepoint in widespread brain regions, including the genu and body of the corpus callosum, anterior and posterior limbs of the internal capsule, anterior corona radiata, anterior thalamic radiation, external capsule, cingulum, superior longitudinal fasciculi, posterior corona radiata, and inferior frontal-occipital fasciculus. Conversely, lower NDI in mTBI patients compared to controls was observed at two weeks post-injury in the external capsule, anterior thalamic radiation, inferior longitudinal fasciculi, fornix, and stria terminalis. Significant longitudinal decreases in NDI were observed between the 2-week and 6-month timepoints in the anterior corona radiata, posterior corona radiata, posterior thalamic radiation, inferior longitudinal fasciculi, inferior frontal-occipital fasciculus, anterior thalamic radiation, external capsule, and uncinate fasciculi. Interestingly, increases in FISO among mTBI patients was associated with membership to a cluster with greater improvement on a composite score for recovery in an

unsupervised machine learning analysis. These observations were made in the context of either no difference or less extensive voxel-wise differences in DTI metrics. This would seem to support the notion that higher-order models are more sensitive and, therefore, more useful in characterizing the subtle WM changes thought to be driving symptoms following mTBI.

Finally, another study examined the association between peripheral blood biomarkers commonly associated with aspects of neurotrauma (tau, neurofilament light (NfL), and glial fibrillary acidic protein (GFAP)), and NODDI metrics.[170] In this study, healthy high school football players with a history of a prior football season in the past 12 months had serum collection and DWI scans at a preseason baseline timepoint. Modest associations were observed including a negative association between serum tau and NDI, and a negative association between NfL and NDI. Notably, MD had widespread positive associations with plasma tau in this analysis.
Contemporary studies will benefit from utilizing multiple signal representation and higher-order modeling techniques. For example, Goubran & colleagues compared DTI, NODDI, and DKI metrics in a longitudinal sample of male college football and volleyball athletes (Tables 2 & 3). The longitudinal comparison of time and sport, which excluded post-injury scans, demonstrated a pattern of increasing FA in volleyball players and decreasing MD/RD and ODI throughout the season when compared to football players. This adds further strong evidence that changes observed in non-injured subjects may drive the statistical differences in diffusion metrics via disruption of healthy WM remodeling. However, a subsequent analysis demonstrated an increase over time in ODI mediated by player position, casting uncertainty on the possibility of altered WM dynamics as a possible mechanism. This increase in WM dispersion and lack of change in other NODDI metrics demonstrate the real possibility that dynamic partial volume effects in mTBI are a source of unaccounted variance in DKI and DTI studies. Additionally, in contact sport samples, the degree and type of impact may play more of a role in observed changes than previously understood.

Table 2.3 Summary of Studies Utilizing NODDI in mTBI Patients

Article	Comparison group demographics	Post-injury Measurement Timepoints	Neuroimaging software & metrics	Significant metrics and localization of effects
Anderson et al., 2023	Hospitalized mTBI: *n* = 26 (4F,22M) Age: mean ± SD (34.81 ± 13.76) Trauma controls: *n* = 20 (2F, 18M) (38.75± 12.59)	Timepoint 1: 6-12 wks post injury mTBI mean ± SD (63.269 ± 12.127) Controls: (49.95 ± 9.185)	MRTrix3, FSL, NODDI MATLAB toolbox Metrics: ODI, ICVF	ICVF was positively predictive of processing speed ability and memory index performance for the control group in numerous WM tracts. ICVF was negatively predictive of executive function index in the SLF only.
Goubran et al., 2023	Football Players: *n* = 63 (0F, 63M) Age: mean ± SD (19.11±1.57) Volleyball Players: *n* = 34 (0F, 34M) Age: (19.57±0.91)	Timepoint 1: Annual pre-season scan. Timepoint 2: Within 24-48 hours of injury mean ± SD (1.83d± 1.26) Timepoint 3: 6 month followup scan (65d ± 77) Timepoint 4: After final athletic season	DESIGNER software for DKI analysis. MRTrix3 and automated fiber quantification (AFQ) for tractometry. Metrics: F_{iso}, ODI and F_{icvf}	ODI decreased longitudinally in volleyball players but not football players in the forceps minor of CC, L superior SLF, L TR, R cing ODI decreased longitudinally in non-injured football players compared to injured. ODI increased in players with high position based impact risk over the course of the season.

Table 2.3 (cont'd)

Article	Comparison group demographics	Post-injury Measurement Timepoints	Neuroimaging software & metrics	Significant metrics and localization of effects
Stein et al., 2023	Pediatric population sample mTBI: Symptomatic group *n* = 80 (46F, 34M) Age: median, IQR (14.6y, 3.2) Asymptomatic group: *n* = 32 (12F, 20M) Age: (14.5y, 3.1) Controls: *n* = 21 (12F, 9M) Age: (14.7y, 6.8)	Timepoint 1: 1-month post injury mean ± SD (37.9d± 5.7) Timepoint 2: 2-3 months post injury (69.3± 6.3)	Voxel-wise analysis with the Multivariate and Repeated Measures (MRM) toolbox. ROI analysis based on significant voxel-wise statistical map. Metrics: ODI, FISO	Increased ODI in symptomatic mTBI compared to all other groups in the global WM, bilateral UF and bilateral IFF at both 1 mo and 2-3mo time points.
Huang et al., 2022	Patients: mTBI: *n*= 32 (15F, 17M) Age: mean ± SD (32 ± 13) Controls: *n* = 31 (17F, 14M) Age: (37 ± 9)	Timepoint 1: Median: 29 hours post-injury	TBSS-based voxel-wise analysis (FSL) ROC analysis to discriminate mTBI from controls with whole brain WM averages Metrics: ODI, V_{ic} and V_{iso}	Decreased ODI, Vic and Viso were significantly lower throughout the brain, especially in long-association fiber and commissural fiber tracts.

Table 2.3 (cont'd)

Article	Comparison group demographics	Post-injury Measurement Timepoints	Neuroimaging software & metrics	Significant metrics and localization of effects
Mayer et al, 2022	Pediatric population sample mTBI: *n*= 204 (83F, 121M) Age: mean ± SD (14.5y ± 2.9) Controls: *n* = 173 (73F, 100M) Age: (14.2y ± 2.8)	Timepoint 1: 1-11 days mean ± SD (7.4d± 2.2) Timepoint 2: ~4 months (130.9d±14.5)	AFNI, FSL, SPM, MATLAB NODDI toolbox Metrics: ODI, V_{ic} and V_{iso}	Decreased V_{iso} in mTBI compared to controls in the right post-central gyrus, right superior parietal lobule, right precuneus and left superior parietal lobule. Increased V_{ic} in mTBI compared to controls in the right temporal pole, right inferior temporal gyrus, ILF, right interior temporal/fusiform gyrus, left fusiform gyrus, left middle occipital gyrus and bilateral precuneus. No differences observed for ODI. Use of a biologically informed microstructure diffusion toolbox algorithim yielded different statistical relationships compared to standard NODDI analysis.

Table 2.3 (cont'd)

Article	Comparison group demographics	Post-injury Measurement Timepoints	Neuroimaging software & metrics	Significant metrics and localization of effects
Lima Santos et al., 2022	Adolescent population sample mTBI: *n*= 57 (23F, 34M) Age: mean ± SD (15.3y ± 1.5) Controls: *n* = 33 (15F, 18M) Age: (15.3y ± 1.6)	Timepoint 1: Post-injury scan mean ± SD (6.9d± 2.5)	FSL, and MATLAB NODDI toolbox, TractSeg for ROI generation Metrics: NDI, ODI, FISO	Decreased NDI in self-report poor sleeping mTBI patients compared to other groups in the first week following injury in the anterior TR, arcuate fasciculus, cing, CC, corticospinal tract, fronto-pontine tract, IFF, ILF, optic radiation, parieto-occipital pontine, striatofronto-orbital, striato-premotor, SLF, thalamic-parietal, thalamo-premotor tracts and UF. Decreased NDI in poor sleeping mTBI patients compared to other groups including good sleeping mTBI in the cing, optic radiation, striato-fronto-orbital tract and SLF were associated with more symptoms on the post-concussion symptom scale.
Oehr et al., 2021	Population sample mTBI: *n*= 26 (2F, 22M) Age: mean ± SD (34.81 ± 13.76) Tramua Controls: *n* = 20 (2F, 18M) Age: (38.75 ± 12.59)	Timepoint 1: 6-12wk post injury: mTBI: mean ± SD (73.31d ± 32.68) Control: (49.95d ± 9.19)	MRtrix3, FSL Comparison of WM tract averaged metrics with hand-drawn ROIs Metrics: ODI, ICVF, ISO	Increased ODI in mTBI compared to controls in the left uncinate fasciculus. Decreased ISO in mTBI compared to controls in the CC, bilateral SLF direct and indirect segments.

Table 2.3 (cont'd)

Article	Comparison group demographics	Post-injury Measurement Timepoints	Neuroimaging software & metrics	Significant metrics and localization of effects
Shukla et al., 2021	Pediatric population sample mTBI: *n*= 320 (121F, 199M) Age: mean ± SD (12.38 ± 2.42) Orthopedic Injury Controls: *n* = 176 (80F, 96M) Age: (12.49 ± 2.22)	Timepoint 1: mean ± SD (11.56d± 5.43)	MRIcron, ExploreDTI. MATLAB NODDI toolbox Metrics: NDI, ODI, FISO	No differences observed in any diffusion metrics.
Muller et al., 2021	Population sample mTBI: *n* = 40 (28F, 12M) Age: mean ± SD (48 ± 16.8) Controls: *n* = 17 (7F, 10M) Age: 33.2 ± 10.9	Timepoint 1: mTBI: mean ± SD (73mo± 117.8)	NODDI MATLAB toolbox, FSL TBSS-based voxel-wise analysis Metrics: ODI, V_{ic}	Decreased V_{ic} in mTBI compared to controls in the bilateral SLF, ILF, IFF, and forceps major and minor. Decreased ODI in the bilateral SLF, ILF, IFF, and forceps major.
Kawata et al, 2020	Football Players: *n* = 17 (0F, 17M) Age: mean, range (16, 16-17)	Timepoint 1: Preseason baseline assessment w/ prior history of football season in last 12 mo	MRtrix3, FSL TBSS-based voxel-wise analysis, NODDI MATLAB toolbox Metrics: NDI, ODI	Serum Tau was negatively associated with NDI in the genu of the corpus callosum. Neurofilament light was negatively associated with NDI in the superior longitudinal fasciculus.

Table 2.3 (cont'd)

Article	Comparison group demographics	Post-injury Measurement Timepoints	Neuroimaging software & metrics	Significant metrics and localization of effects
Palacios et al., 2020	Population sample mTBI: *n*= 40 (9F , 31M) Age: mean ± SD (30.35 ± 7.5) Replication sample mTBI: *n*= 40 (11F , 29M) Age: (34.38 ± 11) Orthopedic Controls: *n* = 14 (6F, 8M) Age: (31.71 ± 10.14) Friend Controls: *n* = 19 (6F, 13 M) Age: (36.33 ± 13.5)	Timepoint 1: 2 wk mean ± SD (13.30d± 2.10) Timepoint 2: 6 mo (184d± 8.86)	NODDI MATLAB toolbox, FSL TBSS-based voxel-wise analysis JHU-atlas based ROI analysis Metrics: ODI, NDI and FISO	Initial mTBI cohort: Increased FISO and decreased NDI at 2-weeks in widespread brain regions in mTBI compared to controls. Decreased NDI longitudinally from 2-week to 6-month timepoint in the anterior corona radiata, posterior corona radiata, posterior TR, ILF, and IFF, anterior TR, EC, and UF. Increased FISO was associated with membership to a cluster with greater improvement on a global improvement measurement in an unsupervised machine learning analysis.
Wu et al., 2018	Patients: mTBI: *n*= 19 (11F , 8M) Age: mean ± SD (35 ± 12) Controls: *n*= 23 (11F , 12M) Age: (35.6 ± 14.1)	Timepoint 1: mTBI: mean ± SD (15d ± 10) Control: (31d ± 20)	TBSS-based voxel-wise analysis JHU-atlas based ROI analysis Metrics: V_{ic}, OD, and P_0	Decreased V_{ic} in mTBI compared to controls in the CC, anterior and superior CR. Decreased V_{ic} and P_0 were associated with worse performance on neuropsychological tests. Increased V_{ic} and P_0 were associated with better performance in the trauma control group.

Table 2.3 (cont'd)

Article	Comparison group demographics	Post-injury Measurement Timepoints	Neuroimaging software & metrics	Significant metrics and localization of effects
Churchill et al., 2019	Patients: mTBI: *n*= 33 (17F, 16M) Age: mean ± SD (20.5 ± 1.7) Controls: *n* = 33 (17F, 16M) Age: (20.3 ± 2.0)	Timepoint 1: symptomatic phase 1-7 days post injury Timepoint 2: following medical clearance for return to play mean, IQR (19d, 13d-58)	TBSS-based voxel-wise comparison, in-house N-way partial least squares testing of the six diffusion metrics. Metrics: FA, AD, RD, ODI, V_{ISO}, V_{IC}	Decreased V_{IC} in mTBI compared to controls in the CR and longitudinal fasciculus at the first timepoint. These differences remained significant at the second timepoint, but were not significant when comparing longitudinal change between timepoints. Increased ODI between the first and second timepoint in the UF.
Churchill et al., 2017	Athletes with prior history of concussion: *n* = 31 (16F, 15M) Age: mean ± SD (21 ± 1.7) Athletes without prior history of concussion: *n* = 37 (20F, 17M) Age: (20.1 ± 1.7)	Timepoint 1: Preseason assessments	FSL, NODDI MATLAB Toolbox Metrics: V_{IC}, ODI	Decreased ODI in athletes with history of concussion compared to those without in the genu body and splenium of CC, Fx, anterior and posterior limb of IC, left CR. Increased V_{IC} in athletes with history of concussion compared to those without in the genu body and splenium of CC, Fx, anterior and posterior limb of IC, left CR. V_{IC} increased and ODI decreased with increasing time since last concussion between subjects with a history of concussion.

Table 2.3 (cont'd)

Article	Comparison group demographics	Post-injury Measurement Timepoints	Neuroimaging software & metrics	Significant metrics and localization of effects
Mayer et al., 2017	Mixed Martial Arts professional athletes rmTBI: *n* = 13 (11M, 2F) Age: mean ± SD (28.2± 4.9) Sex, age and education matched Controls: *n* = 14 (12M, 2F) Age: (28.1± 5.1)	Timepoint 1: Scanned during a competition season	SPM, FSL, Voxel-wise comparison with AFNI Metrics: V_{ISO}, V_{IC} and ODI	Increased ODI in rmTBI compared to controls in grey matter regions including the caudate and cerebellum, and WM regions including the splenium of the CC, cing and posterior CR. Decreased V_{ISO} in rmTBI compared to controls in grey matter regions including the diencephalon, and WM regions including the brain stem and cerebellar peduncles. Increased V_{ISO} in rmTBI compared to controls in WM regions including the IC, EC, CR, saggital striatum, posterior TR and SLF. Increased V_{IC} in the cerebellar peduncles, IC and SLF.

Constrained Spherical Deconvolution and Fixel-Based Analysis in mTBI

Early studies that utilized CSD mainly took advantage of the improved tractography results produced by tracking with CSD-estimated FODs.[171] For example, CSD was used to analyze the TBICare study, a prospective study of mTBI in Europe that collected a single timepoint in the subacute period following injury.[172] This early study highlights the utility of CSD as a method for improved tractography and improved sensitivity and specificity by accounting for voxels with crossing fibers. In this analysis, DTI metrics in an FA WM skeleton generated using TBSS were compared between groups, in addition to a skeleton with only voxels that contained a single fiber population as determined by CSD. The global average of metrics in the whole brain tractogram

generated with probabilistic tractography was also compared. Interestingly, using CSD, it was determined that only 29.13% of voxels in the FA WM skeleton contained a single fiber population. This would suggest that even methods like TBSS aimed at reducing partial volume effects are still likely to contain significant confounds from crossing fibers. The mean FA in voxels of the whole WM skeleton was 0.412 in mTBI patients vs. 0.576 in voxels containing only a single fiber population, demonstrating the impact of crossing fibers on summary measures like FA.

Another study employed CSD-based whole-brain tractography to conduct graph theory analysis in a sample of mTBI patients based on the number of post-traumatic symptoms in the subacute stage of recovery.[173] Whole brain structural connectivity was similar between mTBI subjects and controls. However, mTBI subjects had a trend relationship between lower network clustering and higher processing speed, which was associated with reporting >3 symptoms post-injury and at least one cognitive and/or affective complaint. The improved performance of tractography algorithms on DWI signal modeling with CSD may facilitate the use of more sophisticated graph analysis techniques in future studies. More recently, a study compared CSD-based tractography with the automated probabilistic segmentation tool TractSeg with DTI-based deterministic tractography methods conducted by board-certified neuroradiologists. They found that when comparing tract-averaged FA values in tracts generated with each method, there were significantly lower FA values in the mTBI group compared to controls for tract averages created using TractSeg-generated FA values. No significant differences were observed for DTI-based tract averages. They also conducted this study on low b-value data, collecting only 15 gradient encoding directions at b= 800 mm/s^2, a more clinically feasible acquisition.

The first study to employ a FBA in mTBI patients was conducted by Wallace and colleagues in 2020. This study examined WM changes at roughly 7 months post-injury.[174] No differences between mTBI patients and controls were identified. A possible explanation for this result is the

highly variable scanning time and length of scanning time employed in this study (Table 4). Additionally, the majority (63%) of the mTBI sample had a Glasgow coma scale score of 15, meaning this mTBI sample may have sustained very minor injuries.

Two more recent analyses of sports-related mTBI in samples of Australian football players found significant differences in fixel-based metrics in widespread brain regions. The first study by Wright and colleagues compared football athletes with mTBI and athlete controls in addition to conducting within-group sex comparisons.[175] They observed a pattern of increased FD that improved between the first timepoint within 24-48 hours of injury and a second timepoint at 2 weeks post-injury. The whole brain fixel-wise analysis revealed male athletes had increased FD in the cingulum compared to female athletes sustaining a mTBI. The cause of sex differences needs further exploration to determine if morphological differences between sexes or some combination of factors lead to increased susceptibility of one sex over another. DTI metrics were also compared in this study; interestingly, differences were detected in more widespread regions than with the FBA metrics.

A second study compared subgroups of mTBI patients scanned ≤ 12 days following injury, >12 days, and controls. Interestingly, acute mTBI patients had increased FD, FC, and FDC compared to subacute mTBI patients.[176] The authors posit this could be related to cytotoxic edema following injury in the acute period, resulting in axonal swelling, which resolves in the subacute period. There was also a preponderance of left-sided changes observed, which may reflect differential hemispheric susceptibility via a mechanism that is currently unclear. The findings of this study also seem to suggest a decrease in FBA metrics that occurred in the subacute period, which could indicate either recovery following injury or axonal loss following injury. Future studies will benefit from larger sample sizes, more frequent and standard data collection following injury, and

complimentary signal modeling techniques to build a complete picture of WM changes following mTBI.

Table 2.4 Summary of Studies Utilizing FBA and/or CSD in mTBI Patients

Author	Sample Characteristics	Post-injury Measurement Time	DWI Image Analysis Method	Location of Significant Effects
Tallus et al., 2023	Population sample mTBI: *n* = 37 (15F, 22M) Age: mean ± SD (37.2 ± 11.4) Age and Sex matched Controls: *n*= 41 (17F, 24M) Age: (36.4 ± 11.9)	Timepoint 1: Mean, range (1.2y, 2.2wk – 9.9y)	MRTrix3 standard preprocessing. FOD peaks for Tract-Seg analysis. Metrics: FA, MD	Fixel-based analysis metrics not calculated in this manuscript. CSD probabilistic tractography was able to differentiate mTBI from controls using tract-wise averages of FA, while DTI deterministic tractography was not.

Table 2.4 (cont'd)

Author	Sample Characteristics	Post-injury Measurement Time	DWI Image Analysis Method	Location of Significant Effects
Mito et al., 2022	Patients: mTBI scanned ≤ 12 days: *n* = 14 (0F, 14M) Age: mean ± SD (24.07 ± 3.82) mTBI scanned >12 days: *n*=15 (0F, 15M) Age: (25.18 ± 3.45) Age matched Controls: *n*=29 (0F, 29M) Age: (24.1 ± 4.8)	Timepoint 1: mTBI scanned ≤ 12 days mean ± SD (7.6d ± 3.3) Timepoint 2: mTBI scanned >12 days: (34.3d ± 19.4)	MRTrix3 standard preprocessing and fixel-based analysis. Dhollander and multi-shell multi-tissue algorithms used. Metrics: FD, FC and FDC	Increased FD in the acute group (scanned ≤ 12 days post injury) compared to the subacute (>12 days) and control groups in the left posterior parahippocampal WM extending into the isthmus. Increased FD in acute compared to subacute specifically in the splenium of the CC, and left posterior parahippocampal WM. Increased FC in the acute group compared to subacute group in the splenium and left frontal aspect of the SLF. Increased FDC was observed in the acute group compared to the subacute and control groups predominantly in the CC and prominently in the forceps minor.

Table 2.4 (cont'd)

Author	Sample Characteristics	Post-injury Measurement Time	DWI Image Analysis Method	Location of Significant Effects
Roine et al., 2022	Population sample mTBI: *n* = 85 (26F, 59M) Age: mean ± SD (47 ± 20) Age and Sex matched Controls: *n*= 41 (22F, 18M) Age: (50 ± 20)	Timepoint 1: 3wks post-injury mean ± SD (21.14 ± 14.91) Timepoint 2: 8mos (251.8 ± 86.87)	MRtrix3, FSL, FreeSurfer. MATLAB connectivity toolbox Metrics: Average betweenness centrality, Normalized clustering coefficient, normalized global efficiency, Normalized characteristic path length, Small-worldness, Average degree, Average strength	No differences in global network properties between patients with mTBI and control subjects at the either timepoint. Increased betweenness centrality in mTBI compared to controls in the R pars opercularis at the second timepoint. This did not remain significant when comparing CT-negative patients and controls. Decreased normalized global efficiency and increased small worldness in mTBI patients with GOSE of 7 or 8 when compared to GOSE <7.
Wright et al., 2021	Patients: mTBI *n*=14 (6F, 8M) Male Age: mean ± SD (22.1 ± 2.4) Female Age: (24.2 ± 4.1) Athlete healthy controls: *n*= 16 (7F, 9M) Male Age: (24.7 ± 2.4) Female Age: (24.3 ± 4.3)	Timepoint 1: 24-48h post injury Timepoint 2: 2 weeks post injury	MRTrix3 standard preprocessing and fixel-based analysis. Tract based ROI analysis. Dhollander and MSMT algorithms used. Metrics: FD, FC and FDC	Increased FD in mTBI compared to controls in the splenium of the CC with number of significant fixels observed decreasing from the 24-48h to the 2 week timepoint. No significant differences observed for FC or FDC at either timepoint when comparing mTBI and controls. Increased FD in the cing of male compared to female mTBI patients at both timepoints.

Table 2.4 (cont'd)

Author	Sample Characteristics	Post-injury Measurement Time	DWI Image Analysis Method	Location of Significant Effects
Wallace et al., 2020	Patients: mTBI: *n*=133 (30F, 103M) Age: mean ± SD (43.6 ± 16.9) Overall Controls: *n*=107 (47F, 60M) Age: (39.3 ± 16.6) Healthy Controls *n*=60 Orthopedic Controls: *n*=47	Timepoint 1: mean ± SD (194.4d± 38.3)	MRTrix3 standard preprocessing and fixel-based analysis. Tournier and CSD algorithms used Metrics: FD, FC and FDC	No significant differences in FD, FC and FDC when comparing mTBI and controls
van der Horn et al., 2017	Patients: 3+ Posttraumatic symptoms mTBI: *n*= 33 (16F, 17M) Age: median, range (33, 19-63) ≤ 2 Posttraumatic symptoms mTBI: *n*=34 (3F , 30M) Age: (34, 20-64) Age, Sex and Education matched Controls: *n*= 20 (6F, 14M) Age: (30, 18-61)	Timepoint 1: 3+ Posttraumatic symptoms mTBI: Median, range (32d, 22-56) ≤ 2 Posttraumatic symptoms mTBI: (33d, 22-69)	Graph Theory Analysis with Explore DTI and MATLAB brain connectivity toolbox. Metrics: Eglob, C_i, C, γ, $Eloc_i$, Eloc, Q, K_i, BC_i. EC_i	Fixel-based analysis metrics not calculated in this manuscript. Lower eigenvector centrality within the left temporal pole in mTBI compared to controls. Whole brain structural connectivity was similar for controls and mTBI

Table 2.4 (cont'd)

Author	Sample Characteristics	Post-injury Measurement Time	DWI Image Analysis Method	Location of Significant Effects
Mohammadian et al., 2017	Patients: mTBI: *n*= 102 (32F, 70M) Age: mean ± SD (47 ± 20) Orthopedic Controls: *n*= 30 (16F, 14M) Age: (50 ± 20)	Timepoint 1: mTBI: mean ± SD (21d± 15)	Bespoke analysis with MATLAB and ExploreDTI. Voxel-wise comparison of TBSS FA skeleton, voxels with a single fiber population as determined with CSD CSD tractogram based ROI analysis Metrics: FA, MD, AD, RD	Fixel-based analysis metrics not calculated in this manuscript. ICC values demonstrated limiting comparisons to single fiber population voxels in the WM skeleton was superior to comparisons in the whole brain tractogram and FA WM skeleton

General Discussion

Taken together, these DWI studies of mTBI with various modelling techniques demonstrate WM differences compared to healthy controls throughout the recovery period following mTBI. Interpreting these changes is complex, as observed differences could be attributed to various phenomena at the microstructural level and to numerous sources of variance, including post-injury measurement time, acquisition parameters, scanner differences, and statistical methods. Nonetheless, many studies report differences in DKI and NODDI while observing no differences in DTI metrics, demonstrating the increased sensitivity of these measures in mTBI. Many studies had relatively small sample sizes and differing methodologies, highlighting that the field would benefit from more consistency in analysis techniques and study design. Still, an early look at this developing body of literature that utilizes these contemporary DWI analysis techniques has revealed promising and exciting findings.

DKI studies focused on athletes with sports-related mTBI were, on average, younger than the general population. Sports-related mTBI and mTBI from other etiologies are two areas of literature that can inform one another and may unlock new questions as more details about WM change from these two distinct populations and injury mechanisms emerge. This review noted that uniformly, studies in sports-related mTBI observe an acute decrease in the DKI metrics MK, RK , and AK, while the opposite is observed in population-based samples. A decrease in MK results from a more uniform environment of diffusion, which could be related to degenerative changes in WM and axonal shrinkage, whereas the increase could be due to tighter packing of fiber bundles due to edema. Results from several studies suggest changes in DWI metrics in sport-related mTBI may relate to accumulated damage or altered homeostatic WM changes from cumulative contact-sport participation as opposed to the single traumatic event resulting in diagnosis with mTBI.[154–156]

A major critique of DKI is that despite its increased sensitivity to underlying tissue microstructural complexity, it still has limitations in interpretability. It is also susceptible to partial volume effects, which limits its reliability in whole-brain VBA, especially at tissue interfaces like the grey-white matter junction. Techniques developed for DTI to address similar limitations, such as TBSS, may further obscure findings and complicate interpretation. By design, TBSS only questions part of the data collected in WM, resulting in loss of information, computing artificially lower FA values, and making it difficult to colocalize effects in multimodal studies.[105,138,172,177] Future work will benefit from reporting multiple diffusion metrics and employing multi-level statistical comparison schemes, as shown in the work of Goubran et al., 2023 and Huang et al., 2022. Goubran and colleagues' work on male football players showed ODI, but not DKI metrics was sensitive to player position. This work similarly highlights the importance of repeated sampling within subjects, as dynamic temporal WM changes even in adulthood may obscure true patterns of pathologic change in experimental comparison groups.[178]

NODDI's increased sensitivity and specificity come at the cost of the highly computationally intensive analysis process, with reported computation times greater than 65 hours without using a high-powered computing cluster.[179] This is partly due to its dependence on multi-shell data with many diffusion encoding directions. An ongoing body of work is actively attempting to create analysis schemes that would allow the NODDI model to fit low b-value or single shell acquisitions.[180] Additionally, axon tracing in animal studies has brought into question the degree to which WM regions have a coherent morphology that would facilitate Gaussian modeling in any significant part of the brain. In animal work with electron microscopy, the corpus callosum, a region commonly thought to have a uniform orientation of axons, had significant dispersion in a mouse brain.[181] Ground truth work in human brains to better understand the extent of crossing fibers is still needed and will inform future modeling techniques.[182,183] Despite the increased complexity of this biophysical model, the extracellular compartment is still modeled using a Gaussian distribution, which may only be an accurate representation in small regions of the brain's WM. Finally, as discussed previously, the use of fixed intra- and extra-axonal diffusivity values may bias this model in certain regions. However, novel optimization methods have been developed for a more biologically accurate representation.[165]

Few studies have been published using CSD, and only 3 have conducted FBA in mTBI patients. This may be partly due to it being a relatively recently released software package, or the computational skill to implement this method.[18] A critique of CSD is the assumption of a single fiber response, which, similarly to the above, means this method is only an approximation of the brain's WM.[105] Additionally, to be clinically useful, large standard population-based studies would need to be conducted to establish population average tissue response functions for normative comparisons of single patients. Nonetheless, these early studies seem to support an acute pattern of edema

resulting in increases in FD and FDC, followed by axonal degeneration in the subacute period as indicated by decreases in FD, FC and FDC. These changes need to be confirmed in future studies.[176]

Recent animal studies provide strong evidence that the interpretation of microstructural change in human studies utilizing biophysical models is accurate. For example, a recent study collected 7T DWI data of ex vivo fixed brain tissue in a mouse model of closed head injury.[184] This study observed increased ODI in mTBI animals in the optic tract only, compared to sham, with no significant differences observed for FA.[184] Interestingly, behavioral impairment resolved after a 6-week timepoint, whereas alterations in ODI and pathologic staining with GFAP persisted to an 18-week timepoint post-injury. Similar results were observed in a smaller animal study of the acute period following injury, in which increased NDI and ODI compared to control animals were observed at 1- to 4-hour post-injury timepoints. Similarly, this study observed no differences in any DTI metrics.[185]

The strongest evidence from animal studies has been work by Chary and colleagues.[111] In this study, colocalized DWI maps of DTI, NODDI, and FBA metrics at 11.7T and photomicrographs of nissl and gold chloride stained histologic sections were compared.[111] In this ex vivo study, more significant voxels were observed between mTBI and sham mice with decreased FD and FDC when compared to FA in the WM. Most importantly, no differences were observed for FWF or NDI in this data collected in the subacute stage 35 days post-injury. In fact, the only significant NODDI metric in this animal study was ODI, which was observed in regions near the fluid percussion injury. This may indicate that for longitudinal studies, FBA metrics are more sensitive than NODDI metrics in identifying changes in the subacute stage, whereas the FWF of NODDI is more useful in the acute period following injury.

Finally, a clear observation in this review is the underrepresentation of females. Among the reviewed manuscripts, 11 samples included no females, and of the 28 studies that did include

females, 15 had a greater proportion of males than females. This pattern of underrepresentation is in line with the recent consensus of a national work group and represents an additional emerging gap in our understanding of sex differences in WM change following mTBI.[186] The work by Wright and colleagues suggests that in a sample of biologically female Australian football athletes, less detectable WM changes were observed compared to males.[175] Larger comprehensive studies like TRACK-TBI have concluded females experience more symptoms, including insomnia, with greater severity and are more susceptible to persistent symptoms following mTBI.[187,188] Taken together, there may be a lower threshold of damage for symptom generation in females and more pronounced differences in adult females as compared to young females that need further investigation. Many of the included studies utilized age, sex and education matched controls, which seems to be an ideal practice, and even large studies have shown success collecting friend controls (Tables 4.2-4.4).[112,142–145,151–153,159,189–191]

Conclusion

The overall results of these studies suggest there may be unique trajectories of WM recovery that have yet to be fully described by Tensor based methods. The improved sensitivity and specificity of higher-order modeling methods, paired with the widespread adoption of high angular resolution data collection, will help to delineate these individual differences in recovery trajectory. The increased understanding of WM changes in healthy individuals will also improve our understanding of neurotrauma. FBA is unique in that it offers a novel volume element for the analysis of diffusion data, which may help to further our understanding of differential effects on non-dominant fiber tracts in a voxel and how they are affected by trauma. Similarly, NODDI moves away from modeling the diffusion signal as a single Gaussian compartment and adds increased detail that brings this representation closer to biological reality. DKI is clearly a distinct improvement over the original DTI model. However, the growing body of literature suggests that, like DTI, DKI is still

unable to provide the clear picture of WM change following mTBI that is necessary to translate the modality into clinical use. Future work will benefit from utilizing a combination of several models and analysis techniques to characterize WM change in mTBI. Additionally, legacy datasets could be revisited and analyzed with contemporary techniques if made available via data-sharing initiatives such as the Federal Interagency Traumatic Brain Injury Research (FITBIR) Informatics System.[192]

CHAPTER 3: FIXEL-BASED ANALYSIS PIPELINE TESTING IN A TRACK-TBI SUBSAMPLE

INTRODUCTION

In the present study, a subsample of the TRACK-TBI comprehensive assessment plus MRI (CA+MRI) group was randomly selected from a single recruitment site as an initial test of the standard FBA pipeline preprocessing and analysis steps. Diffusion MRI data that was collected on the same scanner was analyzed with the standard FBA pipeline to determine the feasibility of its use with concatenated data from two shells. The original acquisition recommended for single tissue constrained spherical deconvolution (CSD) was a single high b-value of 3000 mm/s^2 or greater; however, the ideal data acquisition protocol is debated.[193–195] The present study is a secondary analysis of participants with two separate acquisitions of b=1300 mm/s^2 and b=3000 mm/s^2 obtained in the same scanning session, which, if concatenated, could represent a pseudo-multi-shell acquisition. Recently, a multi-shell, multi-tissue (MSMT) CSD pipeline was proposed that allows deconvolution with three separate tissue response functions for white matter (WM), grey matter (GM), and cerebrospinal fluid (CSF).[193] This model has shown good reliability across multiple timescales with varying acquisitions, including an interclass correlation coefficient larger than 0.8 for all tissue compartments for data collected >100 days apart.[196] Therefore, we sought to apply the MSMT-CSD pipeline to the pseudo-multi-shell TRACK-TBI data and apply the recently described longitudinal FBA approach to the 2-week and 6-month time points.

Few studies have used CSD and FBA to analyze single-shell DWI data in mTBI.[79,176,214] In addition, to our knowledge, no studies have applied MSMT-CSD to multi-shell DWI data in mTBI patients and analyzed it following the standard FBA pipeline outlined by the developers of MRtrix3. In the present study, we seek to apply the standard pipeline for MSMT-CSD and FBA to DWI data collected at a single site on a single scanner during the TRACK-TBI study. We also sought to

examine change in WM tracts using a longitudinal FBA approach recently outlined in the literature.[197] Finally, we apply a novel deep learning algorithm, Synthesized b0 for diffusion distortion correction (Synb0-DisCo), which facilitates susceptibility field distortion of diffusion MRI data that was collected without reverse phase-encoded images, as is the case in the legacy TRACK-TBI data.[113,198] Data used for the present study are available publicly through the FITBIR registry (https://fitbir.nih.gov/) from the TRACK-TBI U01 Study [FITBIR-DATA0012173].[192]

MATERIALS & METHODS

Transforming Research and Clinical Knowledge in Traumatic Brain Injury Overview

The TRACK-TBI Study is a multi-site clinical cohort study that collected patient data across the spectrum of TBI, including mild, moderate, and severe.[15,112] The present study will focus on the neuroimaging data collected from participants in the CA+MRI sub-cohort, which includes 600 participants.[112] The CA+MRI group had anatomical MRI and DWI collected at 2-weeks and 6-months post-injury.[113]

TRACK-TBI: Participants

Participants diagnosed with a TBI based on the American College of Rehabilitation Medicine[1] <24 hours before presenting at an emergency department were included if they met the following criteria: received a brain MRI/CT, had adequate visual acuity and hearing for testing, and were fluent in English or Spanish in order to provide consent. Patients were excluded if they met one or more of the following criteria: polytrauma present, penetrating injury to the skull, spinal cord injury with American Spinal Injury criteria C or worse, low likelihood of follow-up, an existing debilitating mental health or neurologic disorder, notable preexisting health conditions, contraindications to MRI or were incarcerated, pregnant, awaiting psychiatric evaluation.[112] For the present study, patients were considered to have a mTBI if their Glasgow coma scale (GCS) was 13-15 in the CA+MRI group (N= 554). Of the 554 who met the mTBI GCS metric, 86 had two-shells

of diffusion-weighted magnetic resonance imaging data collected (N= 86). We used all available control multi-shell data which was only collected at the Zuckerberg San Francisco General Hospital and Trauma Center recruitment site for cases and controls. 20 mTBI patients with available multi-shell data were randomly selected for pipeline testing. Image quality and model fit was assessed at intervening steps throughout the analysis pipeline to determine successful application of the preprocessing and analysis steps.

TRACK-TBI: Neuroimaging Acquisition

Neuroimaging data were collected at 2-weeks and 6-months post-injury at the same clinical site on the same 3T MRI scanner. Whole-brain high-definition fiber tracking DWI data was collected (64 directions at b = 1300 and 3000 s/mm2), eight acquisitions at b = 0 s/mm2 for each set of 64 directions.

Neuroimaging Preprocessing and Analysis

The imaging preprocessing and analysis pipeline utilized in this pilot analysis is summarized in Figure 3.1 adapted from a figure in Genc et al., 2018, to signify our modified preprocessing. All developer recommendation for default parameters were followed, and detailed command-line analysis step descriptions are available online at (https://mrtrix.readthedocs.io/en/latest/fixel_based_analysis/mt_fibre_density_cross-section.html, Accessed Nov 2022). The standard preprocessing for MSMT-CSD included denoising, Gibb's ringing artifact removal, eddy current, and susceptibility field distortion correction. Since reverse-phase encoded images were not collected during the initial study, Synb0-DisCo[183] was utilized to generate synthetic undistorted b0 images for input to FSL's topup option in eddy. Finally, individual subject images were corrected for bias field distortion to improve mask estimation directly from the DWI data with *dwi2mask*.

Tissue response functions for WM, GM and CSF were estimated from preprocessed DWI data with *dwi2response* using the Dhollander algorithm option.[199,200] With the voxels option of *dwi2response*, the voxel.mif file was overlayed on the DWI data and visually inspected to ensure the automatically selected voxels were true single tissue voxels. All subject tissue response functions were then averaged for the whole sample to create average tissue response functions for the WM, GM, and CSF. DWI images were then upsampled with *mrgrid* to the recommended isotropic voxel size of 1.25 mm^3. Brain masks were estimated directly from the subject DWI data using *dwi2mask*. Fiber orientation distribution (FODs) functions were estimated with *dwi2fod* using the single set of averaged response functions with the MSMT-CSD algorithm (msmt_csd) option.[193] A colorized image based upon the three tissue types was then generated, and subject FODs were overlayed on this image to ensure WM fixels were only fit in WM regions and that regions containing crossing fibers had multiple fixels fit per voxel (Figure 3.1). A second bias field correction and intensity normalization was conducted on the FODs to approximate signal amplitude across subjects and correct for sample-wide intensity differences not corrected in previous individual bias field correction preprocessing steps.

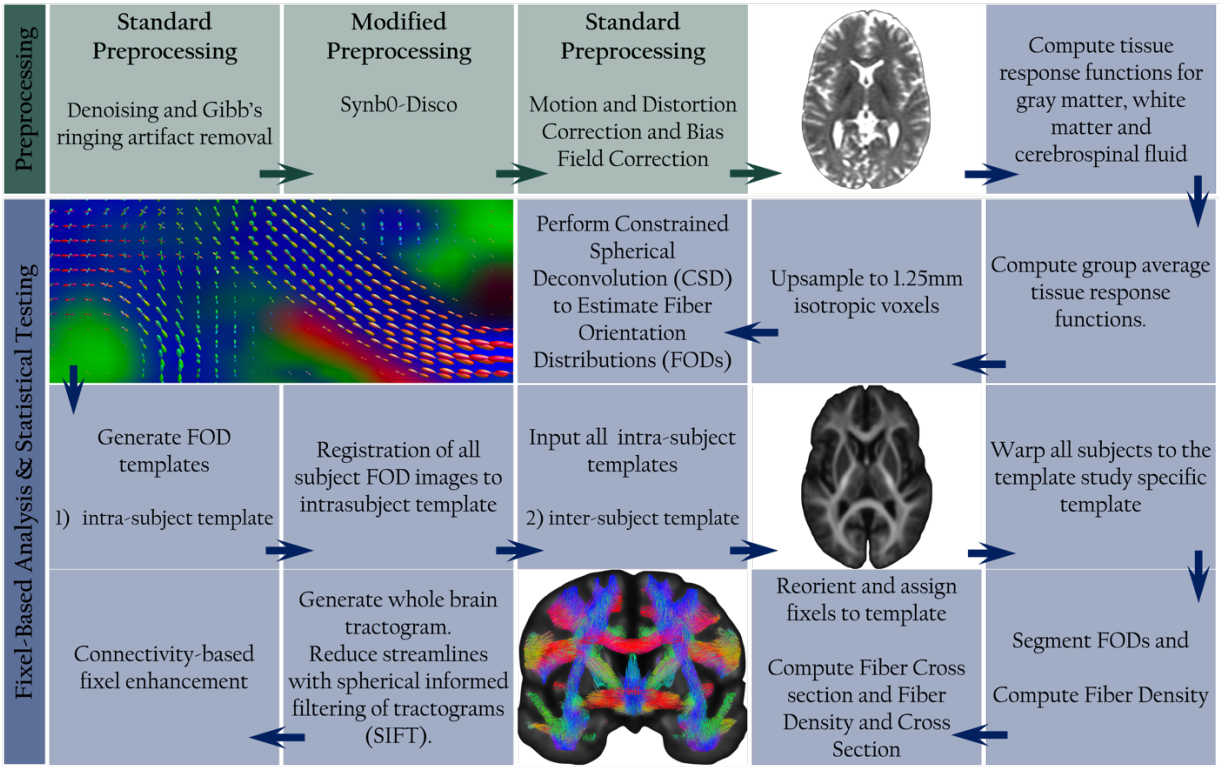

Figure 3.1- Schematic representation of standard preprocessing and analysis pipeline for fixel-based analysis adapted from Genc et al., 2018. This schematic includes the modified preprocessing for images without reverse phase encoded b0 images collected with the use of Synb0-DISCO, and representative intermediate images throughout the processing pipeline. (Top Row Fourth Column)- axial view of preprocessed DWI b0 image after eddy current and motion correction, (Second Row First Column)- Average b0 image for a single subject colorized by voxels selected for three tissue response function estimation with white matter (WM) FODs overlayed for quality assessment of fit in region with crossing fibers, and minimal fitting in the CSF and grey matter, (Third Row Fourth column)- axial view of the whole sample WM FOD template generated from the linear and non-linear registration of all intra-timepoint subject templates, (bottom row third column)- coronal view of whole sample WM FOD template overlayed with tractography generated from this image.

The procedure described by Genc and colleagues, 2018 to create a whole sample unbiased template for longitudinal FBA was implemented.[197] First, each individual subject's first and second timepoint FODs were brought into an intra-template space using the *population_template* script. These intra-subject templates were used as input a second time to the *population_template* script to generate a whole sample template unbiased towards either timepoint.[201]

Subject warps into template space for all FOD images were calculated with *mrregister*.[202] Warps were applied to all subject masks with *mrtransform* and averaged to create a whole sample template mask. The whole sample mask in template space was visually inspected to ensure minimal extra-brain regions were included and no holes or fissures would exclude WM regions from subsequent analysis. A whole sample fixel mask was generated from the whole sample template FOD image, thereby defining the fixels that would be included in subsequent analysis steps with *fod2fixel*. Subject fixels were then segmented from their warped FOD images in the whole sample template space, and FD was calculated per fixel in each voxel with *fod2fixel*. Subject fixels were then reoriented in whole sample template space with *fixelreorient* and assigned to template fixels with *fixelcorrespondence*, specifying which fixels across subjects' match fixels in template space. FC was computed from each subject's calculated warp to template space with *warp2metric*, and this metric was normalized by applying a logarithmic transformation to each image.[203,204] The FDC measure was then calculated as the product of the fiber density and cross-section.

Whole brain tractography was then conducted on the whole sample population template FOD image using *tckgen* with 20 million streamlines. Spherical-deconvolution informed filtering of tractograms was then performed on the 20 million streamline image with *tcksift* to generate a filtered tractogram with 2 million streamlines. This tractogram was used to generate a fixel-fixel connectivity matrix with *fixelconnectivity*.

Statistical Analysis

As this is a population-based sample and WM is known to change as adults age, demeaned age was included as a nuisance covariate in our statistical model. Sex was also included as a potential confound in statistical models. We tested the hypotheses that the mTBI subjects would have decreased FD, FC, and FDC at the 2-week and 6-month timepoint. We also calculated the difference between

the second and first timepoints and divided by the amount of time in years between each participant's two scans to get a change image representative of longitudinal change in FBA metric (Equation 3.1).

$$\Delta FBA\ Metric = \frac{metric_{P2} - metric_{P1}}{Date\ 1 - Date\ 2\ (y)} \quad (3.1)$$

We tested the hypothesis that change in FBA metrics would be greater in mTBI patients compared to controls. Permutation testing with 5000 repetitions was utilized for the reported results of the FBA, and family-wise error-corrected p-values were computed for each comparison.

RESULTS

On the whole brain tractogram (Figure 3.2), differences in effect size (Cohen's D) at ($p<0.01$) before family-wise error correction between controls and mTBI patients are displayed. Differences are highlighted in yellow, representing a positive effect in which the metric is higher in the mTBI group compared to the controls. Differences highlighted in blue represent the opposite effect where the metric is lower in the mTBI group compared to controls. Differences representing decreased FD, FC, and FDC are apparent peripherally in the cortical WM, primarily in the frontal WM regions. Most interestingly, there are large effects in deep WM, specifically in the anterior limb of the internal capsule, external capsule, and the forceps minor. No effects remained significant after family-wise error correction for FD, FC or FDC at either timepoint or in change images.

Table 3.1 Summary of Findings in Chapter 3

Main Finding 1	No significant differences between mTBI and control groups for any fixel based metrics. Uncorrected differences between mTBI and control groups revealed a typical pattern of regional differences with lower white matter microstructural metrics in the mTBI group in the frontal and deep white matter regions. This is an expected pattern of injury due to the contact of the brain with the frontal parts of the skull, and the torsional forces of impact which are greatest in the regions closest to the axis of rotation about the brainstem.
Main Finding 2	Synb0-DisCo was not successful in all participants and introduced geometric distortions, it was removed from the analysis pipeline in Chapter 4 after quality check of the raw images revealed only modest susceptibility field distortions were present in some participants.

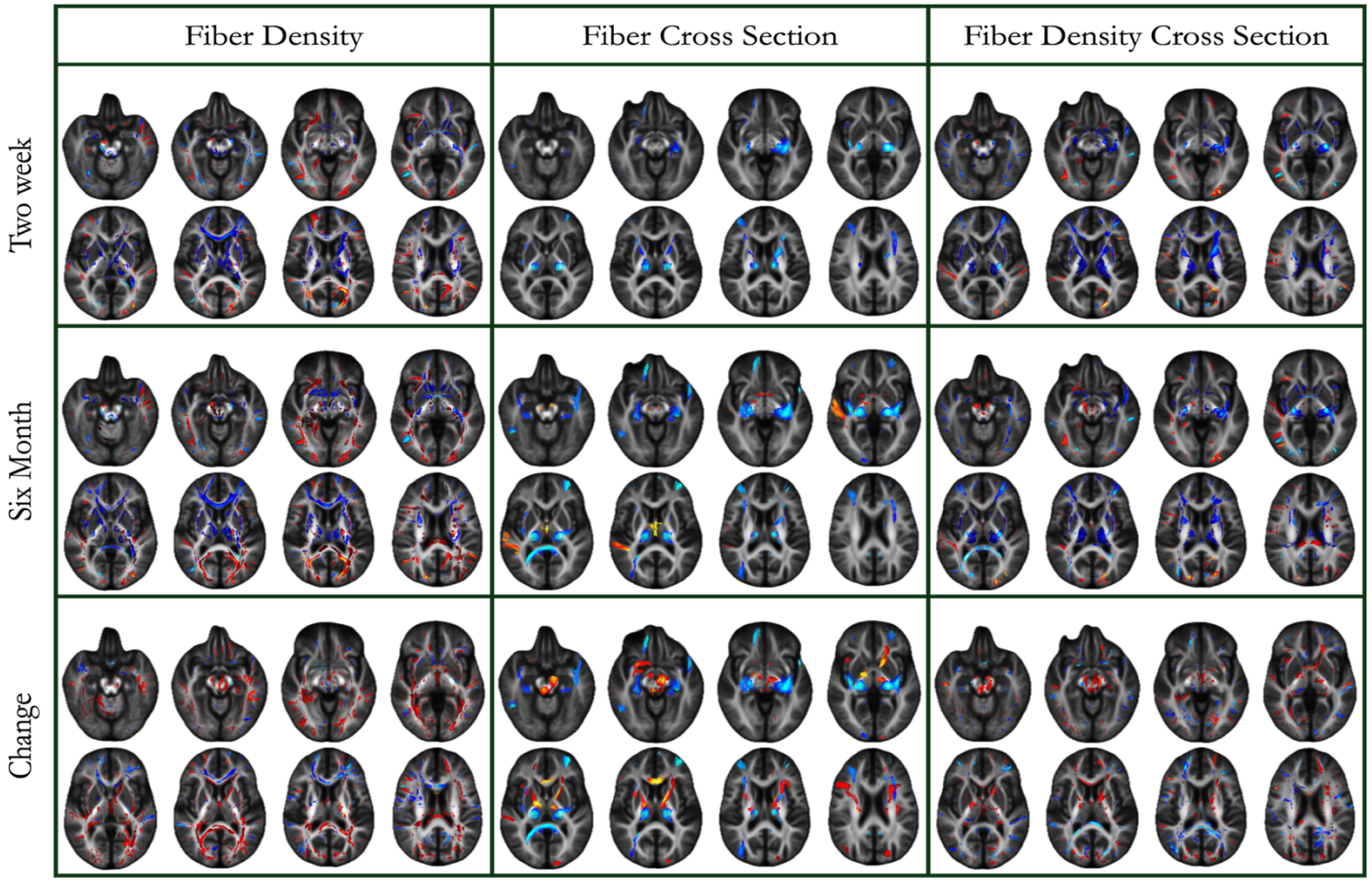

Figure 3.2.- Results of MRtrix3 *fixelcfestats* command comparing mTBI patients and controls are displayed for the FBA metrics fiber density, fiber cross-section and fiber density cross section at the 2-week and 6-month timepoint as well as the calculate change images. Significant fixels colorized by Cohens D and thresholded to a p-value of $p<0.05$ are displayed on the whole brain tractogram and displayed in an axial lightbox view with 5mm seperation between slices. Yellow-red designates regions where the mean of the mTBI group is higher than controls and light to dark blue indicates regions where the mean for mTBi is lower than controls. Scaling for ease of visualization is from 0 to the maximum Cohen's D with red and dark blue representing regions with maximum Cohen's D. No Cohen's D was greater than 0.2. For change images blue represents significant regions where mean change was lower in mTBI compared to controls and vice versa for red. Images are presented in typical radiologic convention with the left side of the brain on the right.

CHAPTER 4: A POPULATION-BASED SAMPLE OF MILD TRAUMATIC BRAIN INJURY REVEALS ABNORMAL WHITE MATTER STRUCTURE 6-MONTHS POST-INJURY WITH FIXEL-BASED ANALYSIS: A TRACK-TBI STUDY

After attempting the initial FBA in the sample in Chapter 3, the analysis was conducted with the whole sample to maximize power to detect differences between groups. All subjects included in the analysis in Chapter 3 were reanalyzed from their raw data with the rest of the sample that had multi-shell data using the adjusted analysis pipeline presented in this chapter. The FBA extends the work that has been done to date with the TRACK-TBI diffusion data by applying a model that not only account for crossing fibers like High Angular Resolution Diffusion Imaging (HARDI), but additionally allows a comprehensive analysis of WM regions without the need for skeletonization with FSL's TBSS. This should allow more precise localization of effects compared to the NODDI analysis conducted previously. Additionally, we sought to replicate the previous findings by the TRACK-TBI investigators in post hoc analyses with tensor models and NODDI to add important context to the FBA findings.

INTRODUCTION

Traumatic brain injuries categorized as mild account for the majority, up to 90%, of injuries worldwide, and are a major source of disability in a subset of patients with persistent symptoms.[9,28,205,206] A bimodal distribution of prevalence exists, as well as trauma etiology, in which older individuals sustain TBI in falls, while younger individuals experience accidents, including motor vehicle accidents and sports-related mTBI. Of particular concern are the rising rates of death and disability from falls resulting in TBI in the aging US population, which is likely to increase based on current demographic and injury trends.[30] Additionally, clinicians still rely on a thorough history and physical exam to categorize injuries, and recovery is defined based on the subjective resolution of symptoms and a return to "normal" functioning.[1] There is a great need to develop neuroimaging

biomarkers that can help clinicians prognosticate outcomes and allow the development of interventions that target the underlying pathophysiologic changes of mTBI as opposed to the symptoms.

Conventional neuroimaging is not required to diagnose mTBI, and most often reveals no intracranial pathology.[1,207,208] Despite that, persistent WM changes have been detected in the chronic stages of recovery following mTBI with DWI even beyond one-year post-injury, and changes in DTI metrics have been correlated to symptoms and functioning throughout the recovery period in the majority of studies.[17,160,209,210] Still, however, several recent reviews have concluded that inconsistent patterns of change following mTBI are frequently observed with DTI, and weaknesses of DTI, the most widely used technique to date, have limited interpretation.[3,17]

Contemporary DWI modelling techniques such as fixel-based analysis(FBA) have yielded interesting insights into pathologic conditions[211,212] and WM development in children[194,213], but only a few studies have applied it in mTBI.[176,214,215] The largest study by Wallace and colleagues did not find any differences in the FBA metrics FD, FC, or FDC in comparisons of mTBI patients and controls; however, the wide range of injury to scan time may have contributed to this null finding (mean: 194.4d± 38.3, range 98-338 days).[215] A smaller study in amateur Australian football players that measured WM change in the acute (48hr) and subacute period (2 weeks) following injury found a greater number of symptoms and symptom severity in male athletes which is contrary to previous work. This occurred in the setting of significant sex differences in fixel-based metrics with males having increased FD in the cingulum and corticospinal tract compared to females.[214] The most recent study in Australian football players that compared mTBI patients scanned in acute with those scanned in the subacute period found acute increases in FD, FC, and FDC.[176] A review of these early studies shows that fixel-based metrics may be sensitive to a transient increase in axonal

diameter due to post-injury cytotoxic edema in the acute period, that is followed by axonal degeneration in subacute and chronic periods reflected as decreased FD, FC and FDC.

We demonstrate that contemporary methods can be applied to legacy datasets that reproduce original findings and extend our understanding of previously collected data. These data represent innumerable research hours and public research funds. The present study reinforces the importance of open data sharing in neuroimaging studies. To date TRACK-TBI studies have utilized the analysis technique TBSS. TBSS improves subject registration and avoids partial volume effects; however, by design, it limits the analysis to a subset of WM voxels with relatively high FA representing only a fraction of all white matter regions.[138,172,177] Additionally, recent calls that future studies should focus on multimodal methodology further limit analyses with TBSS, as the results in the skeletonized WM are not easily compatible with registration to other modalities.[3] Additionally, in the present study, we conduct a comprehensive post hoc tract of interest analysis utilizing the highly reproducible deep-learning tracking algorithm TractSeg, which is trained on Human Connectome Project data and verified in several external samples.[216] This approach is an improvement over traditional atlas-based approaches which involve an additional interpolation step.[216,217] Within these tracts we present the relationship of tract averaged diffusion metrics estimated with DTI, DKI and NODDI between mTBI patients and controls for comparison with the findings of TRACK-TBI with these same techniques.[120]

MATERIALS & METHODS

Overview

The TRACK-TBI Study is a multi-site clinical cohort study that involved 18 clinical sites and collected patient data across the spectrum of TBI, including mild, moderate, and severe.[15,83,112] Patients were enrolled on three paths: 1) evaluated and discharged from the emergency department (ED), 2) admitted to the hospital but not the ICU, or 3) patients admitted to the ICU. Additionally,

300 extracranial trauma controls (orthopedic controls) were collected, 100 each from each enrollment path. The present study will focus on the CA+MRI sub-cohort, which includes 600 participants.[112] In addition, the CA+MRI group had anatomical MRI and DWI collected at 2-weeks and 6-months post-injury.[113]

TRACK-TBI: Participants

Participants had 1) a documented TBI based on the American College of Rehabilitation Medicine <24 hours before presenting to a site, 2) received a brain MRI/CT, 3) adequate visual acuity and hearing for testing, and 4) to be fluent in English or Spanish and provide consent. Excluded participants were those that met at least one of the following criteria: 1) had significant polytrauma present, 2) were prisoners, 3) were pregnant, 4) were on a psychiatric hold, 5) had a major baseline debilitating mental health disorder, 6) had a major debilitating neurologic disease, 7) had a significant history of preexisting health conditions, 8) had contraindications to MRI, 9) had a low-likelihood of follow up, 10) had a penetrating TBI, or 11) had spinal cord injury with ASIA score of C or worse. For the present study, we will focus on the mTBI patients with a presenting Glasgow coma scale (GCS) of 13-15 in the CA+MRI group (N= 554) who had multi-shell diffusion-weighted magnetic resonance imaging data collected (N= 86).

TRACK-TBI: Neuroimaging

Neuroimaging data were collected at 2-weeks and 6-months post-injury. Each participant underwent a scanning protocol that consisted of the following standard 3T MRI sequences: axial three-dimensional (3D) MPRAGE or IRFSPGR T1-weighted images (echo time [TE] = 1.5 ms; repetition time [TR]= 6.3 ms; inversion time = 400 ms; flip angle, 15 degrees) with 230 mm, field of view [FOV], 156 continuous slices (1.0 mm) with a 256 × 256 matrix size. Whole-brain DWI was performed ([TE] = 81 ms; [TR] = 9 s) using 64 diffusion-encoding directions, acquired at b = 1300 s/mm2 and for the high definition fiber tracking (HDFT) group multi-shell data was collected (64

directions at b = 1300 and 64 directions at 3000 s/mm2), eight acquisitions at b = 0 s/mm2 for each set of 64 directions, slices of 2.7-mm thickness each with no gap between slices, a 128 x128 matrix, and FOV of 350 x 350 mm.[15,120] Ten participants did not pass quality check at several stages of the neuroimaging processing pipeline resulting in a final sample of (N=76).

Image Preprocessing & Analysis

All participant images were preprocessed using a combination of commands from FSL version 6.0 and MRtrix3 64-bit release version 3.0.3, and the analysis is schematically represented in Figure 4.1. Raw DWI images downloaded from FITBIR underwent denoising, Gibb's ringing artifact removal, motion, and eddy current correction, and bias field correction. No susceptibility field distortion correction was conducted due to the lack of reverse-phase encoded b0 images for input to FSL's topup tool. Quality assessment of all preprocessed images was conducted, and it was determined that data quality was reasonable without this correction. To facilitate the concatenation of the two separate acquisitions for use with MSMT- CSD, diffusion-weighted images were normalized by the mean of the b = 0 s/mm2 images to offset slight differences in signal intensity due to small differences in TE between the b=1300 and 3000 acquisitions. This was done in a way previously described by Chang & colleagues 2015.[218] Participant masks for subsequent analysis steps were generated using the deep-learning optimized automated segmentation software FastSurfer and those generated with the *dwi2mask* were then coregistered to the mean b0 images of the DWI data.[219] Masks with the best fit were selected, and all subject masks were visually inspected as an overlay on the preprocessed DWI data. When necessary, masks were eroded by one to two voxels to exclude any extra-axial voxels from subsequent analysis steps. A visual summary of the neuroimaging pipeline is presented in (Figure 4.1).

Diffusion Tensor and Kurtosis Analysis

Tensor models were fit with the functional magnetic imaging of the brain (FMRIB)'s diffusion toolbox, and the following tensor metrics were computed: FA, MD, AD, RD, KFA, MK, AK, and RK.[220–222]

NODDI

A multicompartment model was fit to the preprocessed DWI data with the NODDI toolbox (www.nitrc.org/projects/noddi_toolbox, Accessed Jun 2023) for MATLAB.[134] The NODDI metrics computed were the ODI, NDI, and FWF.

Fixel-Based Analysis

Three tissue response functions were estimated from preprocessed DWI data using the Dhollander algorithm.[199,200] A subset of control response functions was then averaged for the whole sample to create average tissue response functions for the WM, CSF, and GM. DWI images were then upsampled to an isotropic voxel size of 1.25 mm. Anatomical brain masks derived from Fastsurfer were registered to the DWI data and visually checked before the subsequent analysis steps. FODs functions were estimated using the single set of averaged response functions with the MSMT-CSD algorithm.[193] Joint bias field correction and intensity normalization were then conducted on the FODs to approximate signal amplitude across subjects and correct for sample-wide intensity differences not corrected in previous individual bias field correction preprocessing steps.

A whole sample unbiased template was generated as described in Chapter 3. First, each individual subject's first and second timepoint FODs were brought into an intra-template space. All subject brain masks were then registered to this intra-subject template, and the intra-subject FODs and masks were used as input to the population template script a second time to generate a whole sample template.

All subject FOD images from time points one and two were warped into the whole sample template space.[202] All subject masks were then warped to the whole sample template using those same transformations and then averaged to create a whole sample mask. The whole sample mask in template space was visually inspected to ensure minimal extra-axial regions were included for subsequent analysis steps. A fixel mask was generated from the whole sample template FODs within the whole sample mask, defining the fixels that would be included in subsequent analysis steps. Subject fixels were then segmented from their warped FODs in whole sample template space. These subject fixels were then reoriented in whole sample template space and assigned to template fixels, specifying which fixels across subjects match fixels in the template space. FD, FC, and the product FDC were computed.[203,204] The FC measure was log-transformed for statistical comparison. Change images calculated in a manner identical to that in Chapter 3 were computed. Briefly, longitudinal change images were calculated by subtracting the 2-week image from the 6-month image and dividing by time in years between scan dates as in Equation 3.1.

Probabilistic tractography was conducted on the whole sample template FODs using MRtrix's *tckgen* command.[139] The resultant twenty million streamline tractogram was thinned to two million streamlines using SIFT filtering to account for false positive connections.[223] This tractogram was then used to generate a fixel-fixel connectivity matrix to facilitate the connectivity-based fixel enhancement aspect of the statistical analysis.[126] The fixel maps for FD, FC, and FDC were then smoothed using this matrix.

Statistical Analyses

Demographics

Means and standard deviations for demographic variables were calculated. Normality was tested for all demographic variables. Due to the presence of outliers, non-normal distribution of the

variable age, and the presence of low counts in some cells of contingency tables for categorical variables, non-parametric tests for independence were utilized.

Whole Brain Fixel-Based Analysis

General linear models (GLM) comparing FD, logFC, and FDC across the groups were conducted cross-sectionally for the 2-week and 6-month timepoint images, and for the longitudinal change images. In addition to the family-wise error correction done implicitly a Bonferroni corrected alpha value of 0.0083 was used to designate significance. This alpha value reflects an additional correction for the multiple comparisons of the three metrics FD, logFC, and FDC, and the two directions tested in each comparison.[224] The model was run with demeaned age, sex and handedness as potential confounding variables. Similarly, the log transformed intracranial volume was controlled for in the FC and FDC models.[225]

Post-hoc Tract-wise Analysis

Spherical harmonic peaks were extracted from the whole sample WM FOD template for input to TractSeg, an automatic WM segmentation algorithm that utilizes a convolutional neural network.[216] The default 72 WM tracts created by TractSeg were calculated using the default 2000 streamlines per tract. As these tracts were generated in template space, they were subsequently used to create binarized fixel and voxel masks for post-hoc tract-wise analysis with a method similar to as previously described at (https://github.com/smeisler/Meisler_Reading_FBA: Accessed Dec 2023).[213] Mean and standard deviation for FBA, NODDI, DKI, and DTI metrics were calculated within these masks for images from the 2-week and 6-month timepoints and compared between and within mTBI and controls groups with unpaired and paired two-sample t-tests respectively in MATLAB Version: 9.13.0.2126072 (R2022b) using the Statistical and Machine Learning Toolbox Version 12.4.[226] Multiple comparison correction was conducted by applying false discovery rate

(FDR) correction with the MATLAB Bioinformatics Toolbox Version 4.16.1 using the default Storey (2002) procedure, setting the threshold for significance to $q < 0.05$.[227]

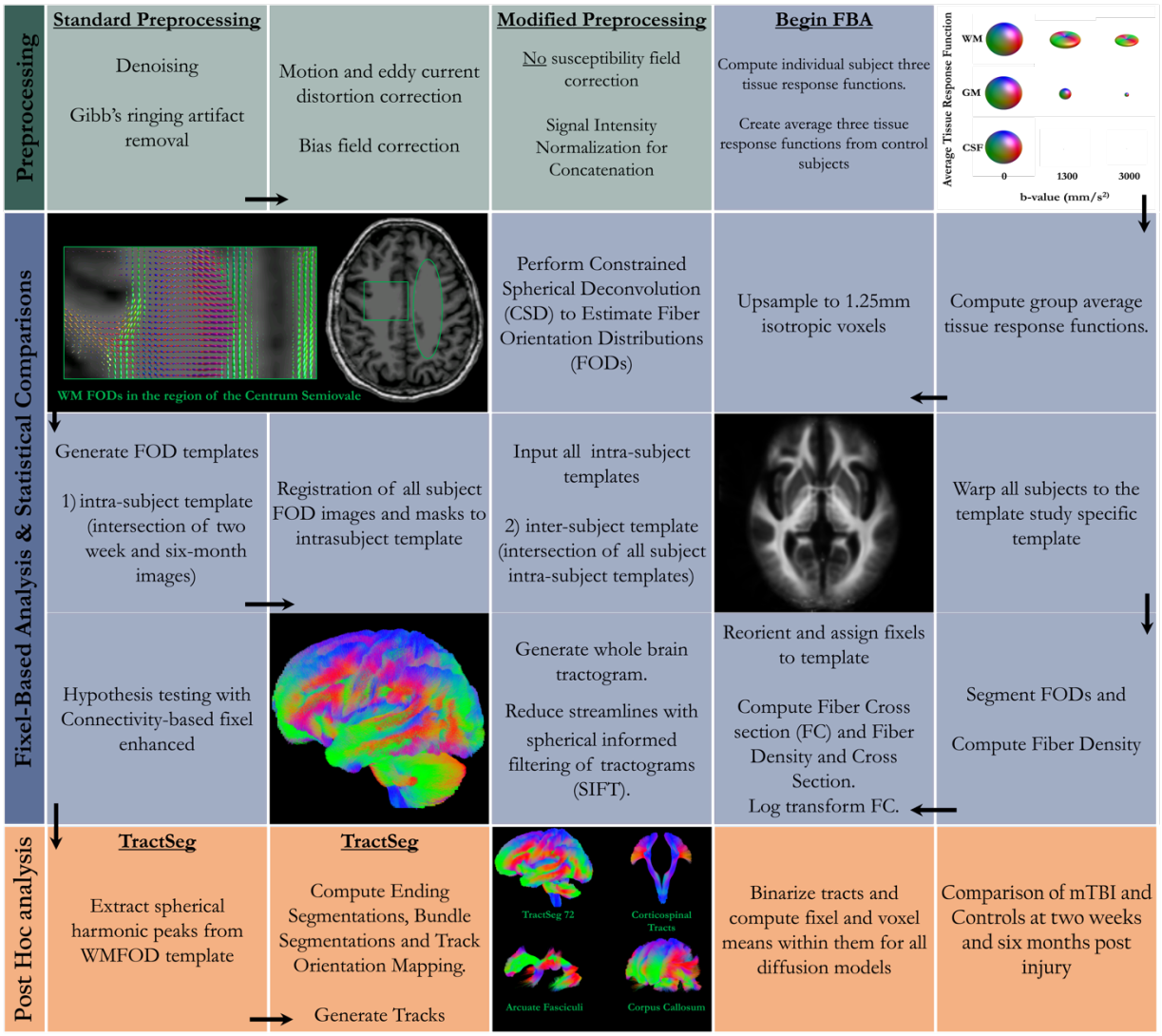

Figure 4.1- Schematic representation of standard preprocessing and analysis pipeline for fixel-based analysis adapted from Genc et al., 2018. This schematic includes the modified preprocessing in which we omitted correction for susceptibility field distortions and representative images generated throughout processing as examples. (Top Row Fifth Column)- average tissue response functions at each b-value for white matter (WM), grey matter (GM) and cerebrospinal fluid (CSF), (Second Row First Column)- green oval represents the left centrum semiovale a region known to contain crossing fibers, green box represents region of interest displayed to the left with WM FODs displayed, (Third Row Fourth column)- axial view of the whole sample WM FOD template generated from the linear and non-linear registration of all intra-timepoint subject templates, (fourth row second column)- whole brain tractogram with two-hundred thousand streamlines after processing with SIFT, (bottom row third column)- 72 tracts generated with TractSeg with isolated example tracts including the right and left corticospinal tracts and arcuate fasciculi and all streamlines traversing various the corpus callosum.

RESULTS

Sample Demographics

No significant differences were observed between mTBI and controls for any demographic variables. Means and standard deviations for the whole sample, mTBI patient and control groups, and the associated p-values from the Wilcox rank sum and Fischer's exact tests are reported in Table 4.1.

Table 4.1. Demographic Characteristics of Whole Sample, mTBI patients, and Controls

	Whole Sample	**mTBI**	**Controls**	
	N = 76	N = 60	N = 16	p-value
Age (years)	37 ± 14	36 ± 14	39 ± 14	0.418
Gender				0.226
Female	23 (30%)	16 (27%)	7 (44%)	
Male	53 (70%)	44 (73%)	9 (56%)	
Race				0.145
Asian	13 (17%)	9 (15%)	4 (25%)	
Black or African American	5 (6.6%)	2 (3.3%)	3 (19%)	
Native Hawaiian or Other Pacific Islander	1 (1.3%)	1 (1.7%)		
Unknown	2 (2.6%)	2 (3.3%)		
White	55 (72%)	46 (77%)	9 (56%)	
Ethnicity				1
Hispanic or Latino	15 (20%)	12 (20%)	3 (19%)	
Not Hispanic or Latino	61 (80%)	48 (80%)	13 (81%)	
Right-Handed				0.122
Both hands	3 (3.9%)	1 (1.7%)	2 (13%)	
Left hand	5 (6.6%)	5 (8.3%)		
Right hand	68 (89%)	54 (90%)	14 (88%)	
Years of Education				0.967
10th Grade	1 (1.3%)	1 (1.7%)		
Associate's degree	4 (5.3%)	3 (5.0%)	1 (6.3%)	
Bachelor's degree	29 (38%)	23 (38%)	6 (38%)	
Doctoral degree	3 (3.9%)	2 (3.3%)	1 (6.3%)	
GED or equivalent	1 (1.3%)	1 (1.7%)		
High school graduate	4 (5.3%)	4 (6.7%)		
Master's degree	13 (17%)	9 (15%)	4 (25%)	
Professional school degree	2 (2.6%)	2 (3.3%)		
Some college, no degree	17 (22%)	13 (22%)	4 (25%)	
Unknown	2 (2.6%)	2 (3.3%)		
School Dropout				0.704
Missing	2 (2.6%)	2 (3.3%)		
No	71 (93%)	56 (93%)	15 (93.7%)	
Yes	3 (3.9%)	2 (3.3%)	1 (6.3%)	
Expelled from School				1
Missing	2 (2.6%)	2 (3.3%)		

Table 4.1. (cont'd)

	Whole Sample	mTBI	Controls	
	N = 76	N = 60	N = 16	p-value
No	69 (91%)	54 (90%)	15 (93.7%)	
Yes	5 (6.6%)	4 (6.7%)	1 (6.3%)	
Employed in Last 12 Months				0.735
Missing	2 (2.6%)	2 (3.3%)		
1 Month	1 (1.3%)	1 (1.7%)		
10 Months	3 (3.9%)	2 (3.3%)	1 (6.3%)	
11 Months	3 (3.9%)	3 (5.0%)		
12 Months	50 (66%)	37 (62%)	13 (81%)	
3 Months	2 (2.6%)	1 (1.7%)	1 (6.3%)	
4 Months	3 (3.9%)	3 (5.0%)		
5 Months	1 (1.3%)	1 (1.7%)		
6 Months	2 (2.6%)	2 (3.3%)		
8 Months	2 (2.6%)	1 (1.7%)	1 (6.3%)	
9 Months	1 (1.3%)	1 (1.7%)		
N/A	6 (7.9%)	6 (10%)		
Insurance Status				0.488
Missing	2 (2.6%)	2 (3.3%)		
Other	4 (5.3%)	2 (3.3%)	2 (13%)	
Insurance purchased directly from an insurance company or on the health insurance exchange (this person or family member)	6 (7.9%)	6 (10%)		
Insurance through a current or former employer (of this person or another family member)	47 (62%)	35 (58%)	12 (75%)	
Medicaid, Medical Assistance	3 (3.9%)	2 (3.3%)	1 (6.3%)	
Medicare,	2 (2.6%)	2 (3.3%)		
Self-pay (Uninsured)	11 (14%)	10 (17%)	1 (6.3%)	
TRICARE, VA or other military health care	1 (1.3%)	1 (1.7%)		

Table 4.1- Means with standard deviations and frequencies with percentages for demographic variables collected from mTBI participants and controls with multi-shell DWI data in the CA+MRI cohort of the TRACK-TBI study. P-values represent the Wilcox rank-sum test for independence and Fisher's exact test for independence, calculated using the 'rstatix' package in R Studio v2023.09.1+494.

Whole Brain FBA Results

Compared to controls lower FDC in mTBI patients at the 2-week timepoint was primarily driven by differences in FD. Lower LogFC in the mTBI group in small regions of the posterior limb of the internal capsule at the 2-week timepoint remained at the 6-month timepoint and included frontal white matter regions in the later comparison Figures 4.6 and 4.7. Figure 4.2 shows fixels that had significantly decreased FDC in mTBI patients compared to controls at the 2-week timepoint; fixels are colored by Z-statistic and thresholded with family-wise error corrected p-values of $p < 0.0083$. Significant differences were primarily localized to the anterior commissure, projection fibers including the left thalamo-prefrontal tract, internal capsule and genu of the corpus callosum. Figure 4.3 shows fixels that had significantly decreased FDC in mTBI patients compared to controls at 6-months post injury, fixels are colored by Z-statistic. Differences were observed in similar brain regions as the 2-week timepoint, with a greater number of significant fixels at 6-months. Primarily, differences were observed in the forceps minor fibers traversing the genu of the corpus callosum and projection fibers of the left thalamo-prefrontal tract. Smaller significant regions were also observed in the internal capsule, external capsule, and anterior commissure. No regions of increased FDC were observed at either timepoint, and no regions had significant differences in comparisons of change images.

Significant differences in FD were observed throughout the WM especially in the deep WM at the 2-week timepoint as shown in Figure 4.4. These differences remained fairly stable over time with the majority of regions falling about 10-15% below the control mean at both timepoints. There were some regions of greater difference around 30%, including the anterior commissure and internal capsule, appearing at the 6-month timepoint (Figure 4.5). No regions with increased FD were observed, and no differences in FD change images survived family-wise error correction.

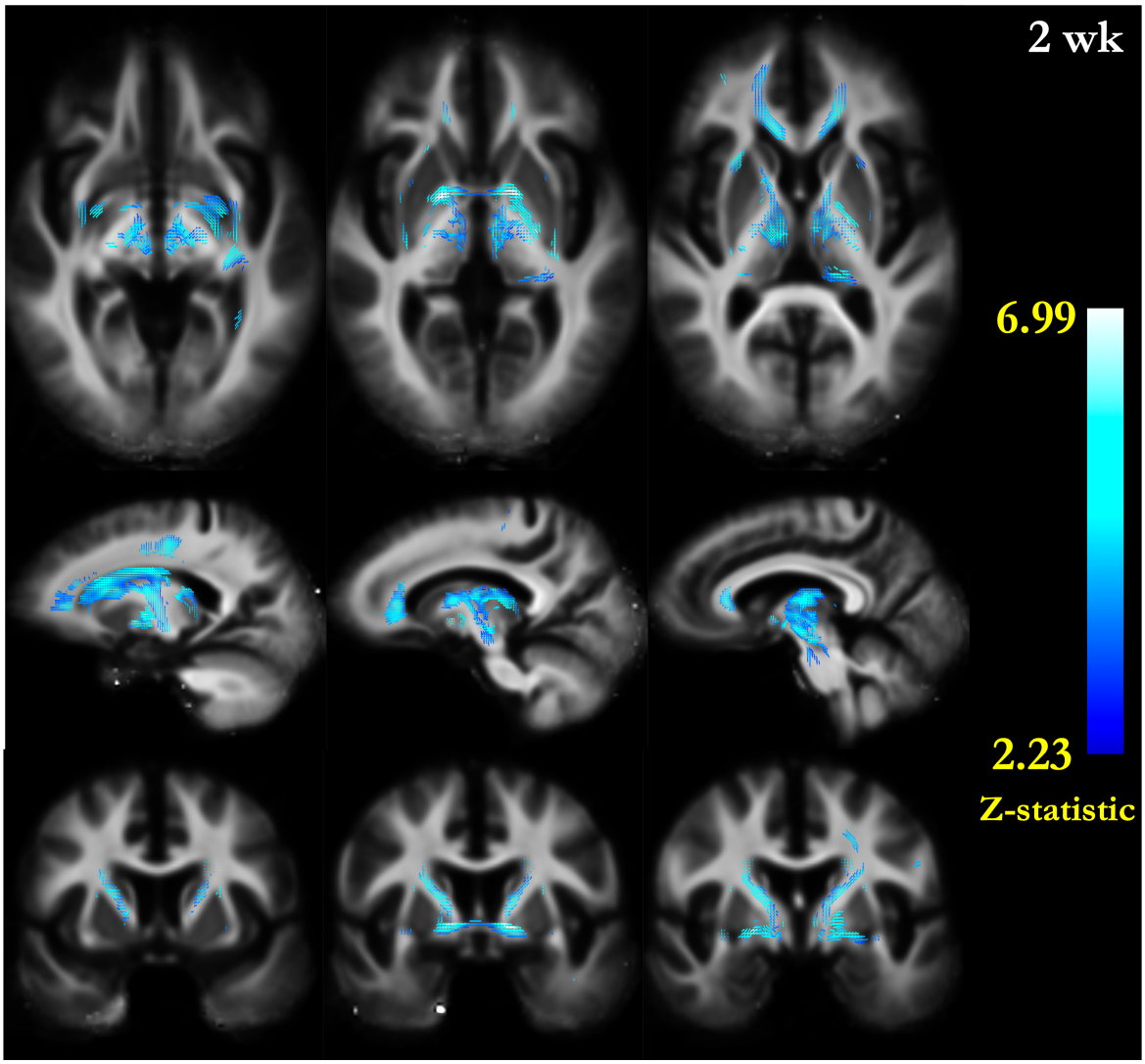

Figure 4.2 – Axial, sagittal and coronal view of the white matter template with fixels from the fixel mask colorized by the GLM Z-statistic from comparisons of FDC at the 2-week timepoint post injury and thresholded with a family wise error corrected p-value of <0.0083.

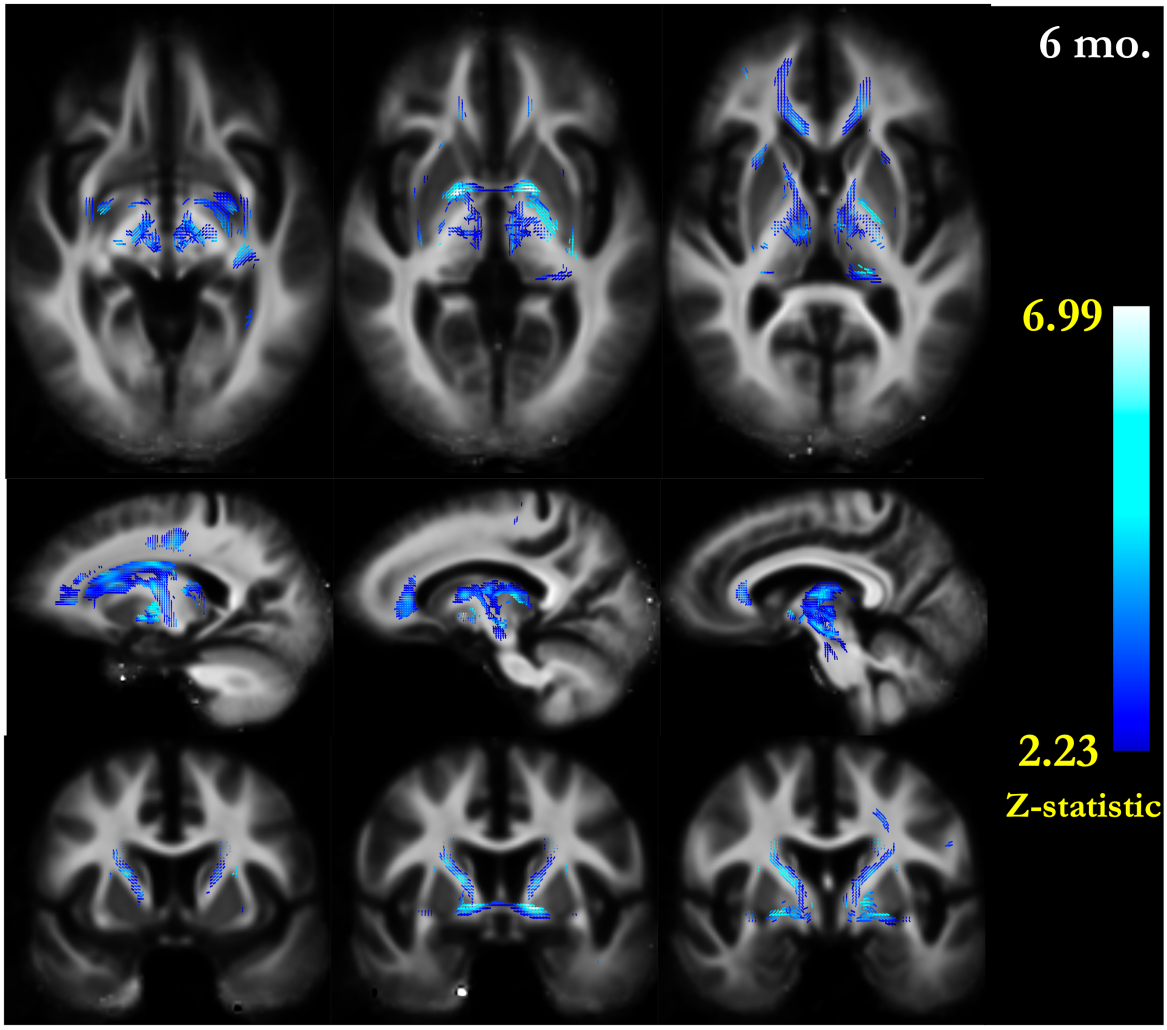

Figure 4.3 - Axial, sagittal and coronal view of the white matter template with fixels from the fixel mask colorized by the GLM Z-statistic from comparisons of FDC at the 6-month timepoint post injury and thresholded with a family wise error corrected p-value of <0.0083

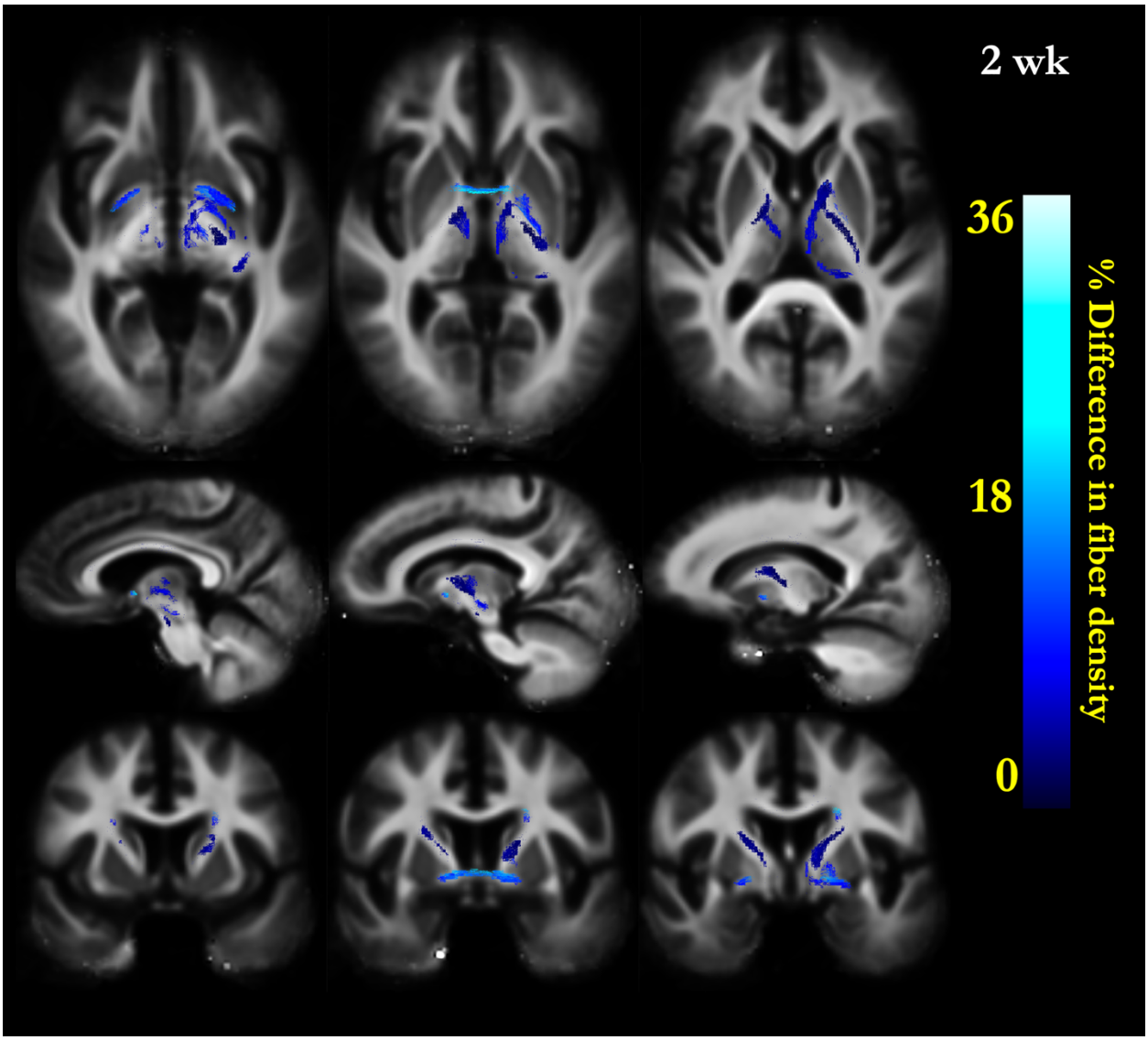

Figure 4.4 – Axial, sagittal and coronal view of the white matter template with fixels from the fixel mask colorized by the percent difference in mTBI compared to controls from comparisons of FD at the 2-week timepoint post injury and thresholded with a family wise error corrected p-value of <0.0083.

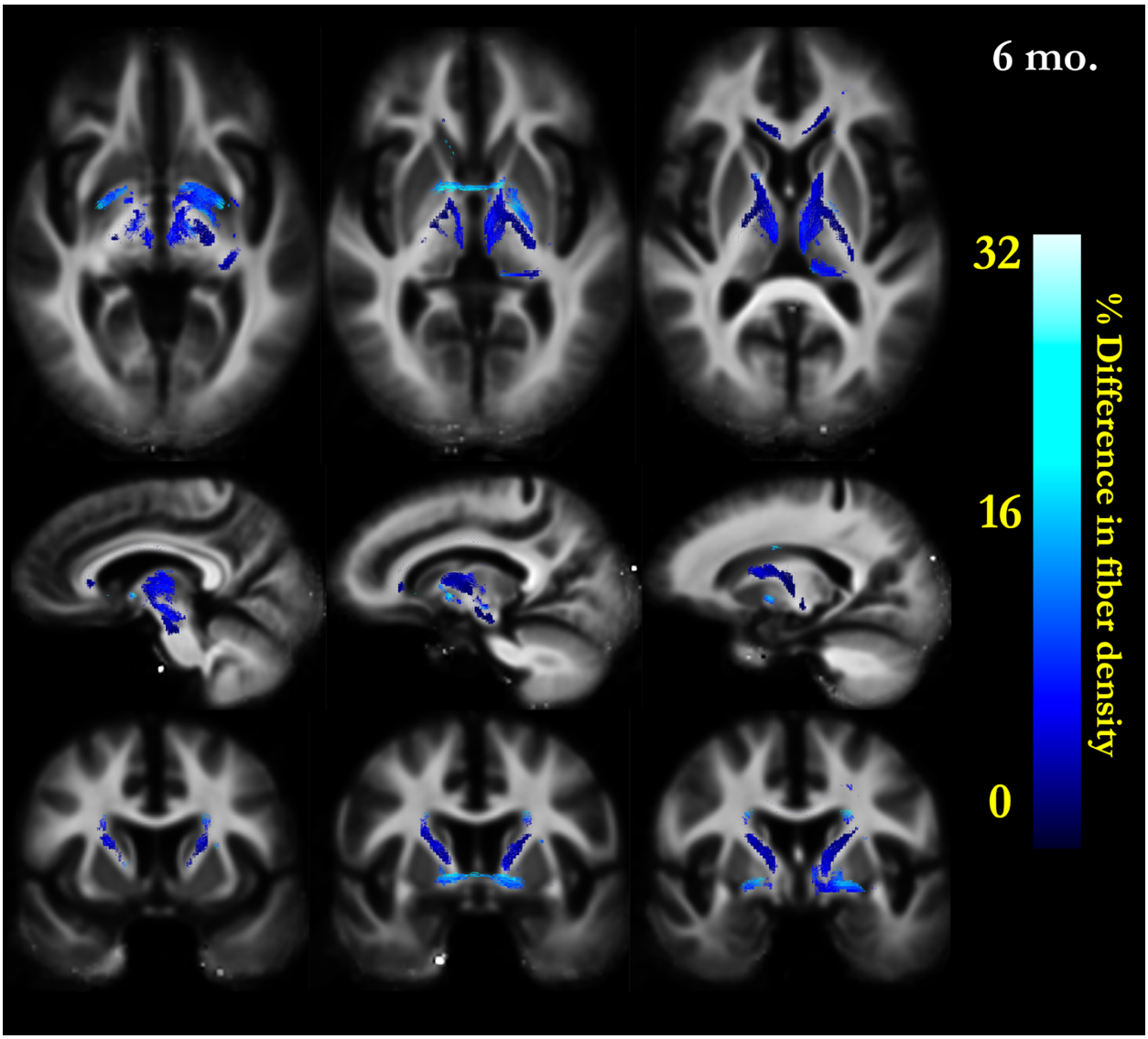

Figure 4.5 – Axial, sagittal and coronal view of the white matter template with fixels from the fixel mask colorized by the percent difference in mTBI compared to controls from comparisons of FD at the 6-month timepoint post injury and thresholded with a family wise error corrected p-value of <0.0083

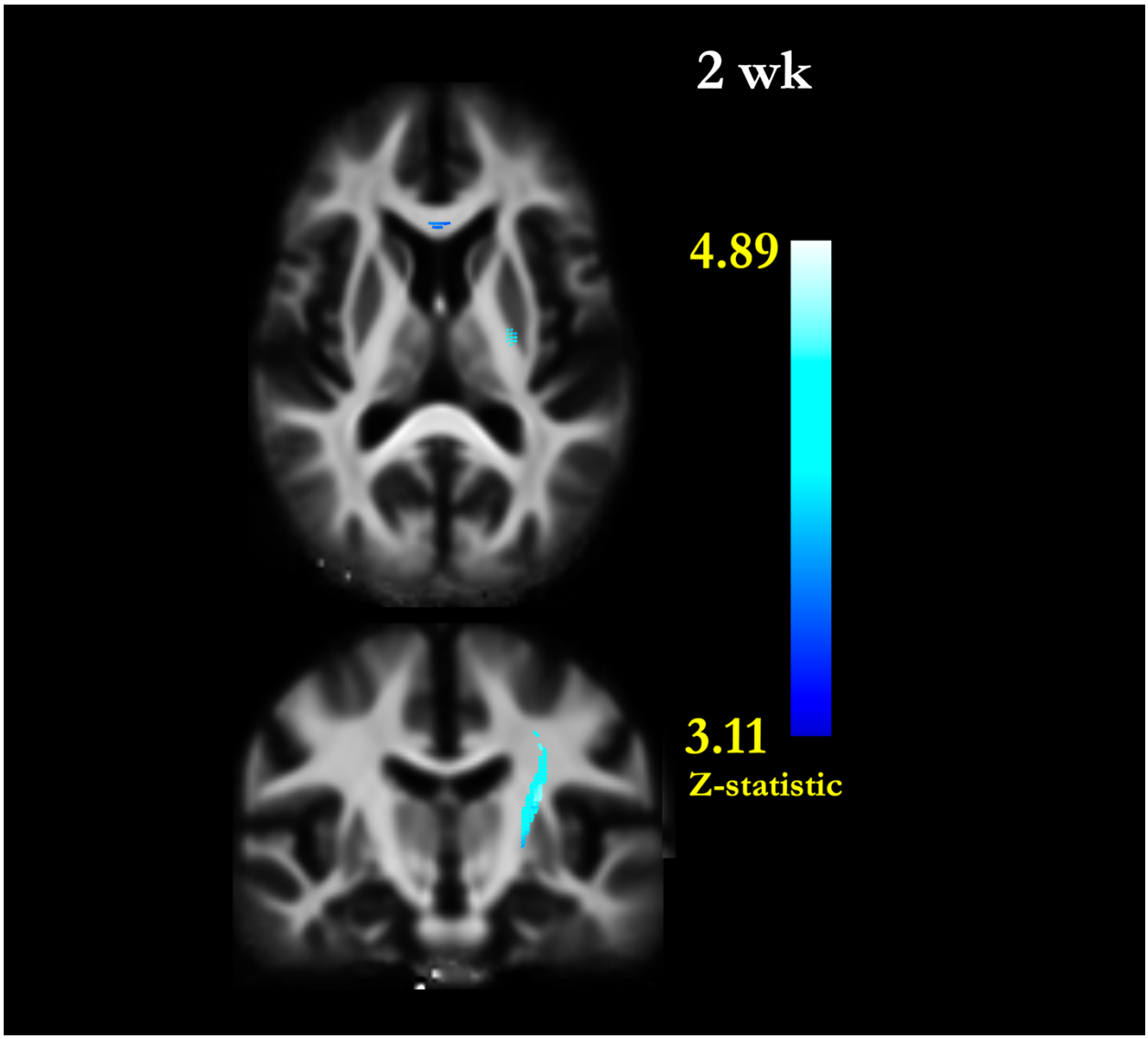

Figure 4.6 – Axial, sagittal and coronal view of the white matter template with fixels from the fixel mask colorized by the GLM Z-statistic from comparisons of FC at the 2-week timepoint post injury and thresholded with a family wise error corrected p-value of <0.0083.

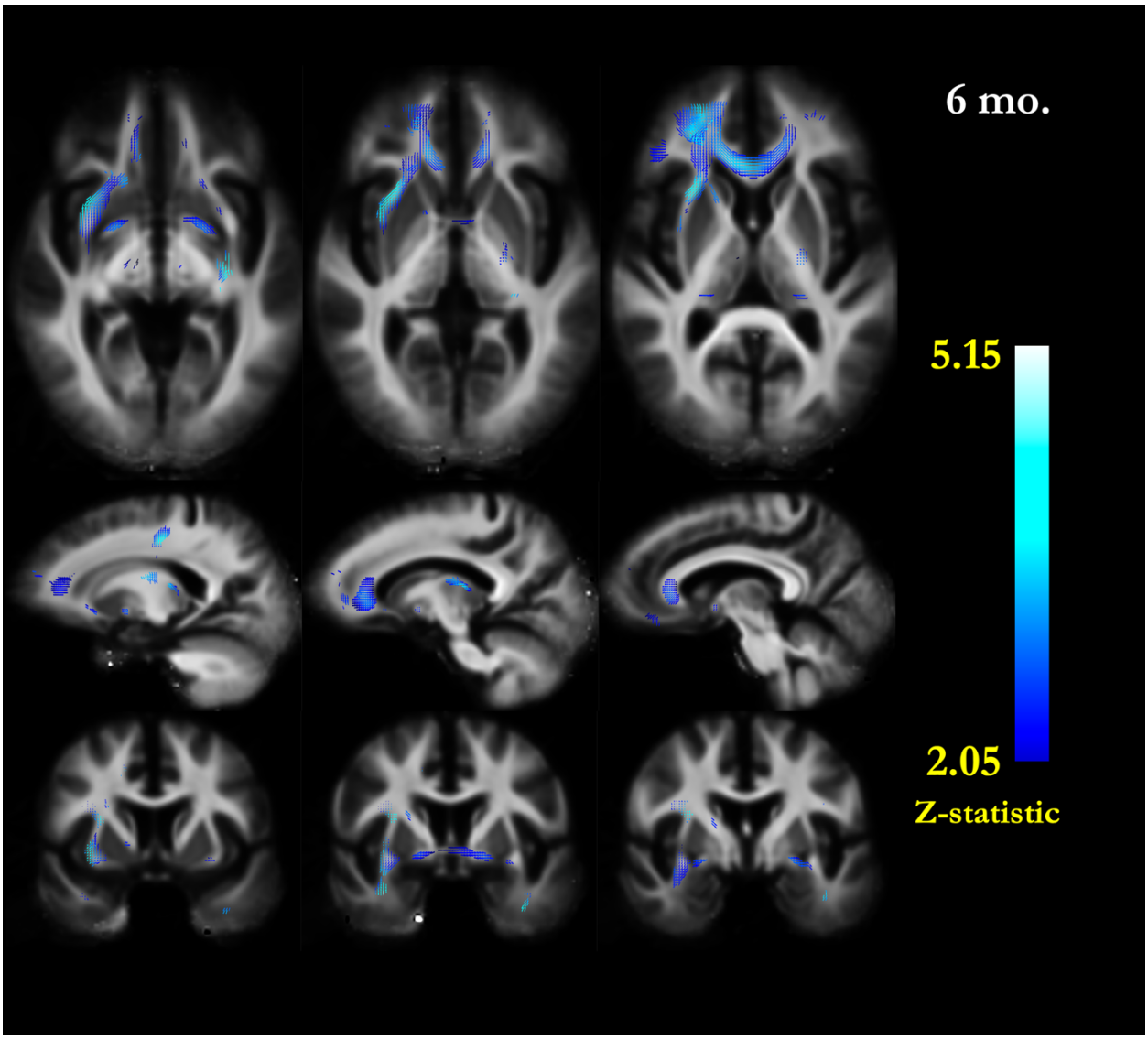

Figure 4.7 – Axial, sagittal and coronal view of the white matter template with fixels from the fixel mask colorized by the GLM Z-statistic from comparisons of FDC at the 6-month timepoint post injury and thresholded with a family wise error corrected p-value of <0.0083.

Post Hoc Tract-wise Results

All post hoc comparison results from two-sample t-tests including the group mean, standard deviation at each timepoint, percent change, t-statistic and FDR corrected q-values are presented in Appendix Tables 1-14. Means, standard deviations and outliers are displayed as boxplots for tracts with significant comparisons at either the 2-week or 6-month timepoint are presented in Appendix Figures 1-94. Tract-wise results for significant metrics with direction of effect relative to controls for DTI, DKI, NODDI, and FBA are summarized for left and right projection and long association

fibers, and commissural fibers in Figures 4.6-4.8.

Tensor Tract-wise Results

At the first timepoint mTBI patients had significantly higher tensor metrics AD, and AK throughout the brain in all projection fibers, long association fibers excluding the inferior longitudinal fasciculus, and commissural fibers. These differences remained at the second timepoint almost uniformly. Similarly, MD and MK were also elevated in widespread tracts throughout the brain in mTBI patients compared to controls at both timepoints. Far fewer tracts additionally exhibited increased RD and RK. No significant differences were observed in any tracts at either timepoint for the tensor metrics FA or KFA. No significant differences in within group comparisons between the first and second timepoint were observed for any tensor metrics Appendix Tables 15-22.

NODDI and FBA Post Hoc Tract-wise Results

A pattern of increased FWF, and decreased FDC, FD, ODI and NDI was observed in almost all WM tracts tested. Differences in FD, FDC, ODI and NDI were more commonly observed in left sided association fiber and projection fiber tracts Appendix Tables 1-14. The pattern of difference held uniformly throughout the brain at both timepoints. No tensor metrics compared within groups between the 2-week and 6-month timepoints were significant. The mTBI group had increased ODI and decreased FWF, NDI, FC and FDC at the second timepoint compared to the first Appendix Tables 23-28. The control group differed only in the FDC metric between the first and second timepoint with increased FDC at the second timepoint compared to the first.

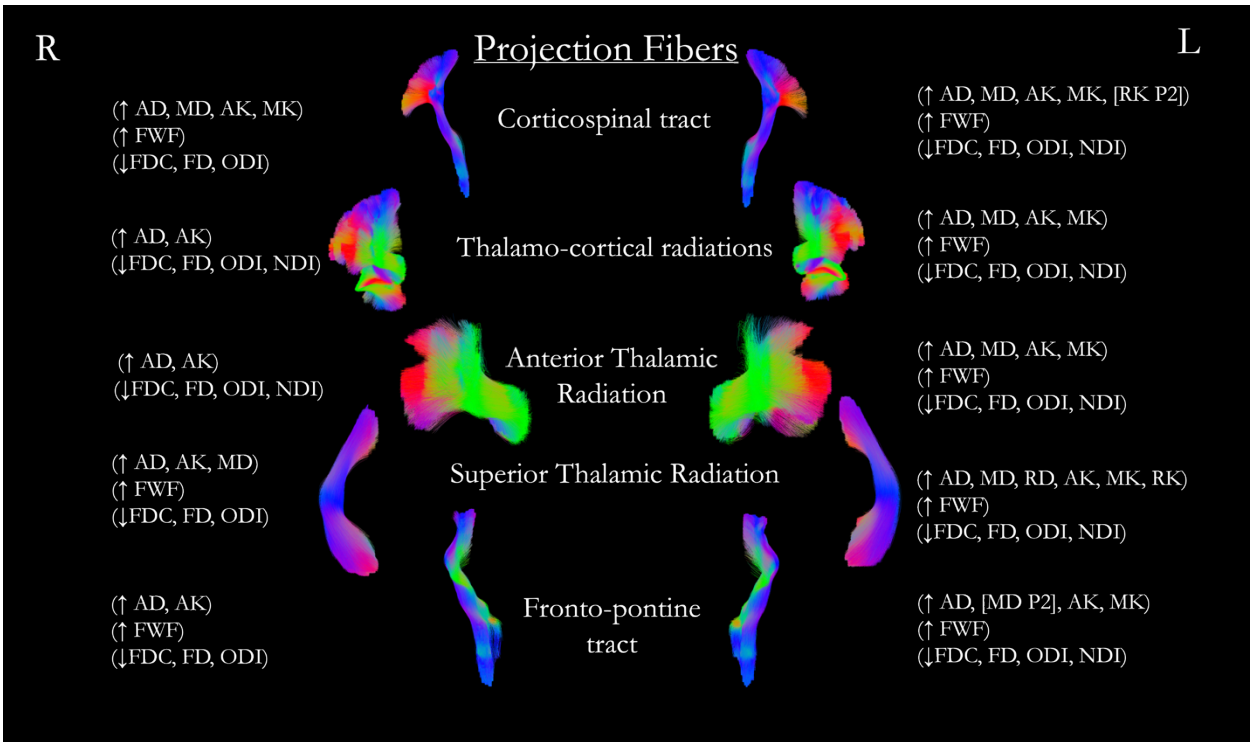

Figure 4.8-Summary of results from post hoc two-sample t-tests for DTI, DKI, NODDI, and FBA analyses for metrics estimated within projection fiber tracks with a significant q-value of $q<0.05$. The center of the image are the tract names with corresponding TractSeg generated tractograms. To the left and right are the significant metrics with the direction of the difference displayed with respect to controls. Metrics abbreviations: DTI: axial diffusivity (AD), mean diffusivity (MD), radial diffusivity (RD); DKI: axial kurtosis (AK), mean kurtosis (MK), radial kurtosis (RK); FBA: fiber density (FD), fiber density cross-section (FDC); NODDI: free water fraction (FWF), neurite density index (NDI), orientation dispersion index (ODI). All metrics were significant at both timepoint unless otherwise indicated in brackets with the significant timepoint designated with P1 (2-week) or P2 (6-month).

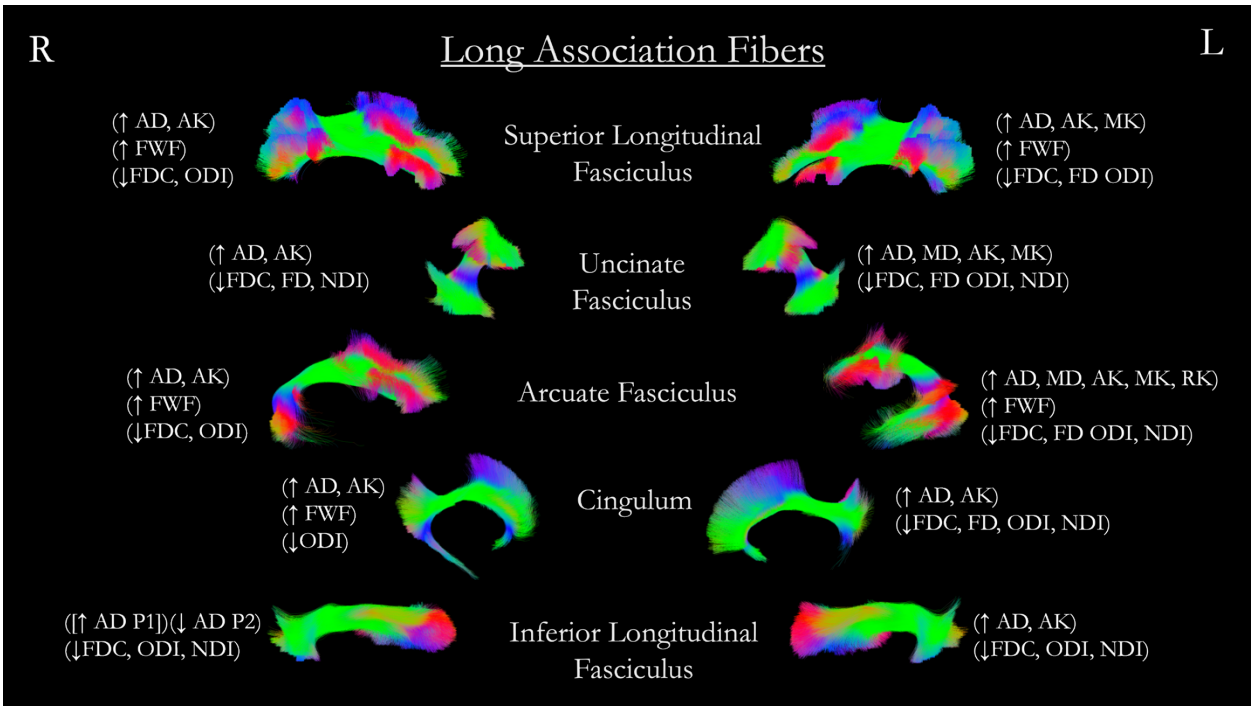

Figure 4.9-Summary of results from post hoc two-sample t-tests for DTI, DKI, NODDI and FBA analyses for metrics estimated within association fiber tracts with a significant q-value of $q<0.05$. The center of the image are the tract names with corresponding TractSeg generated tractograms to the left and right. Also on the left and right are the significant metrics with the direction of the difference displayed with respect to controls. Metrics abbreviations: DTI: axial diffusivity (AD), mean diffusivity (MD), radial diffusivity (RD); DKI: axial kurtosis (AK), mean kurtosis (MK), radial kurtosis (RK); FBA: fiber density (FD), fiber density cross-section (FDC); NODDI: free water fraction (FWF), neurite density index (NDI), orientation dispersion index (ODI). All metrics were significant at both timepoint unless otherwise indicated in brackets with the significant timepoint designated with P1 (2-week) or P2 (6-month).

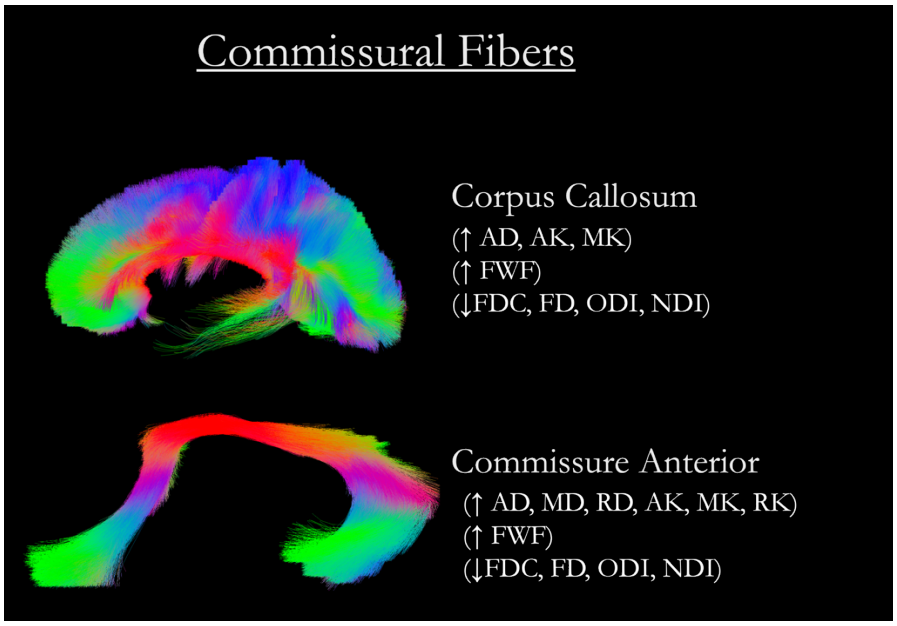

Figure 4.10-Summary of results from post hoc two-sample t-tests for DTI, DKI, NODDI and FBA analyses for metrics estimated within commissural fiber tracts with a significant q-value of $q<0.05$. The center of the image are the tract names with corresponding TractSeg generated tractograms to the left and right. Also, on the left and right are the significant metrics with the direction of the difference displayed with respect to controls. Metrics abbreviations: DTI: axial diffusivity (AD), mean diffusivity (MD), radial diffusivity (RD); DKI: axial kurtosis (AK), mean kurtosis (MK), radial kurtosis (RK); FBA: fiber density (FD), fiber density cross-section (FDC); NODDI: free water fraction (FWF), neurite density index (NDI), orientation dispersion index (ODI).

Table 4.2 Summary of Findings in Chapter 4

Main Finding 1	Compared to controls mTBI subjects had significantly lower fiber density, fiber cross-section and fiber density cross-section metrics from the fixel-based analysis at the two-week and six-month timepoints. Although difficult to know because no baseline or acute DWI images were collected my interpretation of the result is initially at the two-week timepoint lower FDC was driven by lower FD in the mTBI group compared to controls. In the context of the animal literature covered in Chapter 1 this finding reflects the axonal degeneration characteristic of the subacute period following injury. FC on the other hand is not significantly lower at this two-week subacute period likely due to the presence of microglia and astrocytes which play a significant role in the post-injury inflammatory response. At the six-month timepoint FC is likely now significantly lower in mTBI compared to controls due to the resolution of inflammation and consolidation of white matter tracts with fewer axons.
Main Finding 2	No comparisons of change images for the FBA were significant when comparing mTBI and control subjects. This demonstrates that there was not a significant difference in direction or rate of change in white matter characteristics between mTBI and controls. In the context of the animal and human literature covered in Chapter 1, this would seem to suggest that the mechanism of symptom resolution in mTBI patients during the subacute and chronic stages of recovery is unlikely to relate to a return of white matter microstructure towards control means which we consider normal or healthy in the present study.
Main Finding 3	Post Hoc Comparisons revealed significant differences in tensor based metrics and metrics computed with higher order modeling techniques when comparing mTBI and controls. No differences for FA or KFA were observed for any white matter tracts, demonstrating the decreased sensitivity of these metrics in the presence of crossing fibers when averaged across an entire white matter tract mask. The observed pattern of differences reflects the same underlying pathophysiology described in Main Finding 1 above. mTBI patients had increased MD, MK, AD, AK, RD and RK in numerous white matter tracts reflecting greater isotropic diffusion throughout the brain due to the loss of tightly packed axons impeding water diffusion. This was reflected in higher order modelling metrics like increased FWF indicating greater isotropic diffusion, and decreased NDI and FD demonstrating decreased density of axons.
Main Finding 4	Paired sample t-tests comparing group means within the mTBI group and control group between timepoints revealed no significant differences for any tensor metrics or fiber density. Increased ODI and decreased NDI and FWF were observed at the second timepoint compared to the first for the mTBI but not controls. Significantly increased FDC was observed for controls when comparing the first and second timepoint. In the absence of significant difference in FD or FC in controls, this is likely a false positive finding. This may be driven by outliers which could be further explored by either rerunning the comparisons with outliers removed or bootstrapping to estimate variance and assessing the stability of the t-statistic.

CHAPTER 5: FIXEL-BASED ANALYSIS IN A SAMPLE OF HIGH SCHOOL ATHLETES WITH SPORTS-RELATED MILD TRAUMATIC BRAIN INJURY

INTRODUCTION

The latest study to examine epidemiologic factors of traumatic brain injury in the United States was published in 2013. This study reported 640,000 emergency department visits for traumatic brain injury in children and adolescents under 14 years of age.[228,229] In the context that the majority of traumatic brain injuries are categorized as mild, up to 90%, the report that 14% of children with mTBI will experience lifelong disability is alarming.[229] A prominent etiology of traumatic brain injury among children and adolescents is sports-related concussion/mTBI. Similar to traumatic brain injury of other etiologies, diagnosis and return to play are based on resolution of symptoms and history/physical exam findings of phyicians.[84] Accumulating evidence has demonstrated that the resolution of these physical signs and symptoms do not correspond to a return toward healthy control means of objective markers such as serum biomarkers and neuroimaging.[24,125,170,230] Additionally, there is evidence that even the stress and strain on the brain from a season of participation in contact sports can alter imaging markers including metrics of WM microstructure measured with DWI.[156,231]

DTI has been the predominant tool utilized to study sport-related mTBI to date. However, a recent consensus has been reached that multimodal imaging studies are needed to fully understand the phenomena of resolving symptoms without resolution of observed changes in metrics like FA.[3] MSMT-CSD and FBA address the crossing fibers issue and account for partial volume effects at tissue interfaces, eliminating the need to skeletonize the diffusion metric images.[193] Ultimately, the fiber-specific results are highly sensitive metrics that can be applied uniformly to the brain's WM, which will facilitate the anatomical specificity needed to localize effects in the diffuse injuries characteristic of mTBI.

During its initial development, the developers of MRtrix3 recommended a HARDI acquisition with high b-values of at least 2000 mm/s^2 with at least 45 unique diffusion encoding directions. Later methodologic work in simulated and participant DWI data in childhood and adolescence showed increased sensitivity of higher b-value acquisitions when associating apparent fiber density and participant age.[194] Still, other work has shown that even at low b-values (b=1000 mm/s^2) with fewer diffusion encoding directions (30), FD can be accurately quantified, albeit with an expected decrease in angular resolution.[195] In this work, a comparison of CSD and DTI based deterministic and probabilistic tractography was compared in the corticospinal tract and arcuate fasciculus, along with comparisons of the precision of FD and FA estimation along the tract. It was shown that CSD improves on DTI-based tractography and provided more consistent estimation of FD along the tract. This work is important as it demonstrates that CSD is a clinically feasible technique that could be applied to estimate parameters with widely available acquisitions that require less data, a commonly cited strength of DTI.

In the present study we sought to conduct an exploratory analysis of DWI data collected from adolescent athletes with mTBI. We used the contemporary analysis technique fixel-based analysis to do so. In this study, single shell data with a b-value of 1000 mm/s^2 and 40 directions was collected without reverse phase-encoded images. We sought to explore the model fit on this data acquired in under 10 minutes with conventional preprocessing that would be applied in a typical DTI analysis. In the pursuit of study designs that are adequately powered factors such as sample size and scan time relate to cost per participant, and are important to consider to optimize use of public funds.[232] In addition, when assessing the translational potential of a technique, the minimum necessary clinically feasible acquisition parameters that still allow adequate differentiation of lesions should be explored.[233,234]

MATERIALS & METHODS

Participants

Participants were recruited from an affiliated concussion clinic at Michigan State University Health Care. Inclusion criteria for participants included: participation in high school athletics, age 14-18 years, concussion in the last 8 days, and no metallic objects (such as dental braces) in the head and neck region. Ten participants completed all three timepoints, one participant completed only the first and second time points and one participant only completed the first timepoint. This study was approved by the Michigan State University Institutional Review Board.

Sport Concussion Assessment Tool

Participant data was collected with a retrospective chart review in EPIC at Sparrow Health System. Responses from the administration of the Sport Concussion Assessment Tool 5th edition (SCAT-5) were compiled from their first visit to the concussion clinic and then again each subsequent visit they had until they were cleared to return to play.[235] All available administrations of the SCAT-5 were plotted to examine the time from injury until the SCAT-5 symptom inventory was zero Figure 5.1. Creating these plots revealed three of eleven participants still had symptoms 30 days post-injury.

Neuroimaging

Twelve high school athletes completed MRI scans at an acute timepoint 5-8 days, subacute timepoint 1-month, and chronic timepoint 6-months post-injury on a GE 3T Signa® HDx MR scanner with an 8-channel head coil. T_1-weighted images were collected for assessment of intracranial pathology with the following acquisition parameters: 184 1-mm sagittal slices, echo time [TE] = 3.8ms, repetition time [TR] of acquisition = 8.6ms, inversion time [TI] = 831ms, TR of inversion = 2332ms, flip angle = 8°, FOV = 250 mm ×250 mm, matrix size = 256×256, and

receiver bandwidth = ± 20.8kHz. Whole-brain DWI was conducted employing a multislice single-shot spin-echo EPI sequence. Key parameters included a [TE] set to minimum, repetition time [TR] = 12.8s, and 40 diffusion-encoding directions, acquired with a b-value of b= 1000 mm/s^2, and four b= 0 s/mm^2. Slices had a thickness of 2.4 mm with no inter-slice spacing and utilized a 128 × 128 matrix with a field of view (FOV) of 220 mm. The patient was positioned supine with head-first entry with a total scan time of approximately 10 minutes. One incidental meningioma was discovered during the present study and the participant was ultimately included due to the extra-axial location of the pathology and a low likely hood of interference with WM.

Image Preprocessing and Fixel-based Analysis

Image preprocessing and analysis were identical to that described in Chapter 4, with a few notable exceptions. No susceptibility field distortion correction was conducted due to the lack of reverse-phase encoded b0 images. Similarly, due to this data being single-shell, the MSMT-CSD approach was applied in a similar fashion to that in Chapter 4; however, only the WM and CSF response functions were estimated, given that only one shell is available (b=1000). Finally, an additional template-building step was taken. First, WM FOD images from the 3-8 day and 1-month timepoint as well as the 1-month and 6-month were linearly and non-linearly coregistered. These resultant images were similarly linearly and non-linearly coregistered. These final intra-subject template images were coregistered for an unbiased whole sample population template.

Statistical Analysis

GLM were fit comparing FD, logFC, and FDC between the 3-8 day and 1-month timepoints, the 1-month and 6-month timepoints, and cross-sectionally comparing participants recovered within one month to those who took longer than one month. In addition to the family-wise error correction done implicitly by the MRtrix3 *fixelcfestats* command, a Bonferroni corrected alpha value of 0.0083 was used to designate significance. This alpha value reflects correction for the

multiple comparisons of the FD, logFC, and FDC, and the two directions tested in each comparison.

RESULTS

On the whole brain tractogram (Figure 5.1), significant differences at ($p<0.01$) before family-wise error correction for multiple comparisons are displayed. The overlay is the whole brain tractogram colorized by effect size (Cohen's D) from zero to the maximum effect size. The differences highlighted in yellow represent a positive effect in which the metric is higher in subjects with symptoms 30-days post-injury, and the differences highlighted in blue represent the opposite negative effect. Differences representing decreased FD, FC, and FDC are apparent peripherally in the cortical WM, and genu and body of the corpus callosum. Regions of increased FD, FC, and FDC are also present in the bilateral fornices and left inferior fronto-occipital fasciculus. The largest effects are in the deep WM, specifically in the anterior limb of the internal capsule, external capsule, and the forceps minor that persist to the 6-month timepoint when comparing participants symptoms after 30-days with the rest of the sample. No effects remained significant after family-wise error correction.

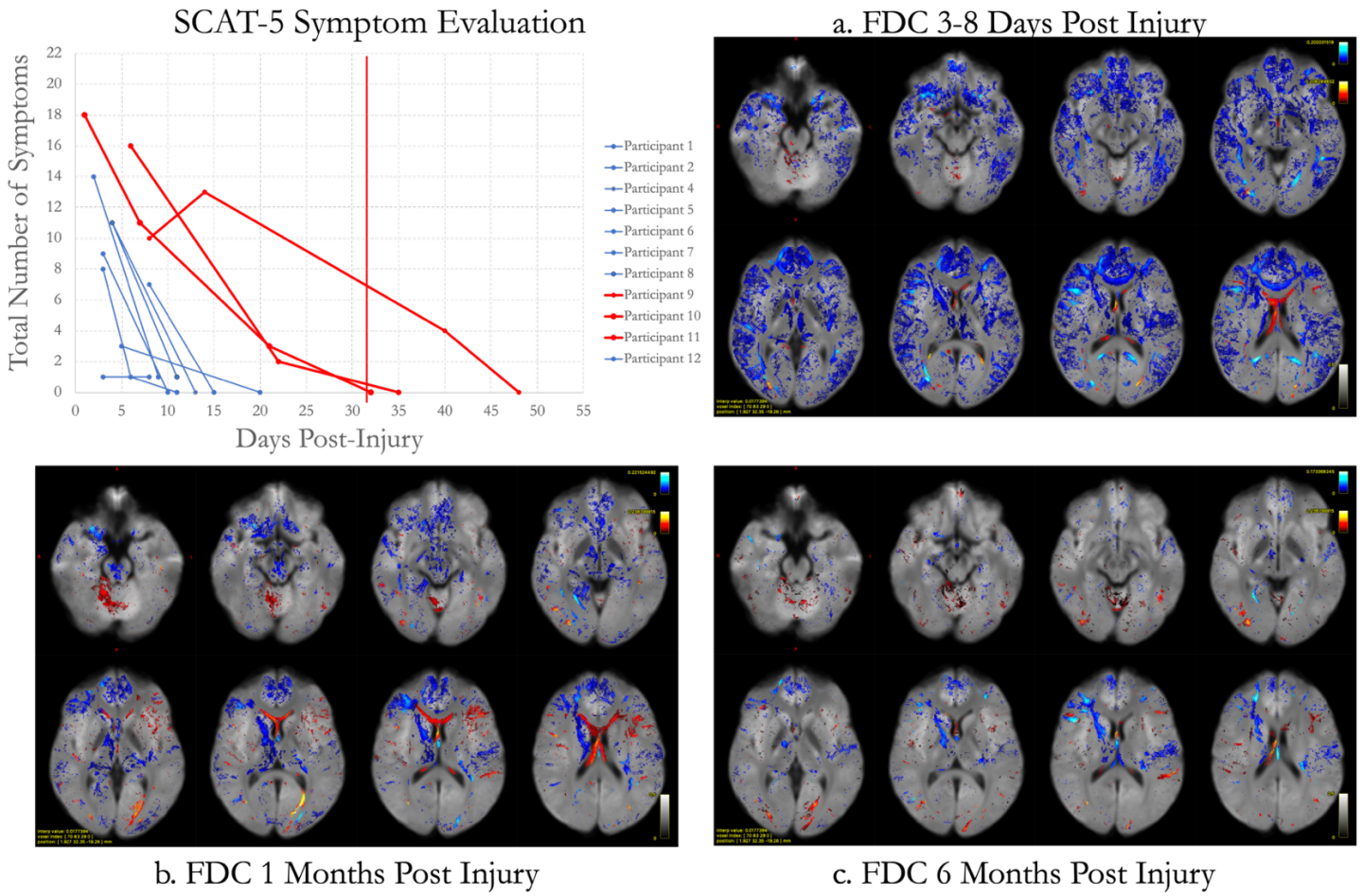

Figure 5.1- Results of the fixel-based analysis comparing a subsample of patients with a prolonged time-course for symptom resolution (red lines in top-left figure) compared to those with complete symptom resolution within one month post-injury. Results are displayed in an axial lightbox view with 5mm spacing between slices, the whole sample population white matter FOD template as an underlay, and SIFT corrected whole brain tractogram with two hundred thousand streamlines colorized by Cohens D and thresholded with an image containing tract-wise uncorrected p-values of $p<0.05$. Panels are arranged in order of timepoint from the acute to chronic period (a-c).

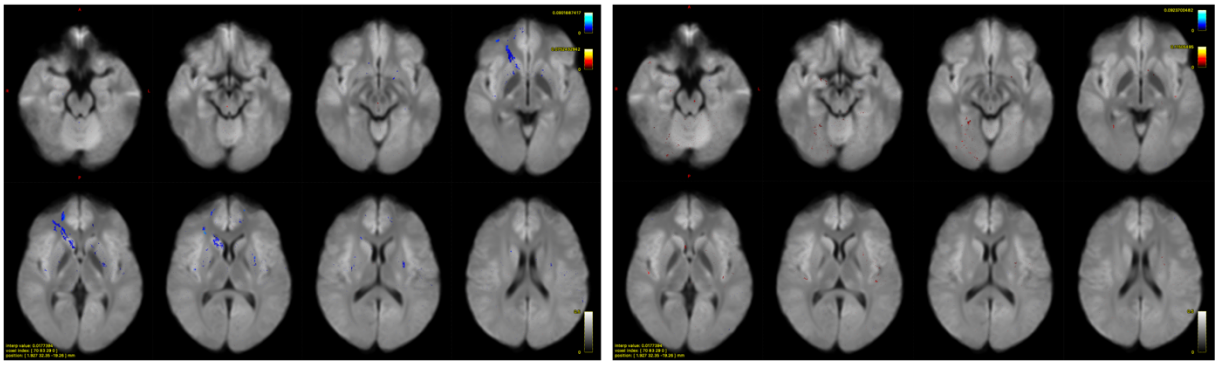

a. FDC 3-8 Day v 1 Month Timepoint

b. FDC 1 Month v 6 Month Timepoint

Figure 5.2- Results of the fixel-based analysis comparing group means between timepoints. Results are displayed in an axial lightbox view with 5mm spacing between slices, the whole sample population white matter FOD template as an underlay, and SIFT corrected whole brain tractogram with two hundred thousand streamlines colorized by Cohen's D and thresholded with an image containing tract-wise uncorrected p-values of $p<0.05$. Panels are a comparison of the acute and subacute timepoints (left) and the subacute and chronic timepoint (right).

Table 5.1 Summary of Findings in Chapter 5

Main Finding 1	No significant differences between mTBI subjects when comparing within group between the first and second timepoints and second and third timepoints. Additionally, a cluster of subjects with symptoms one month post injury did not differ significantly in any fixel based metrics when comparing acute, subacute and chronic DWI scans.
Main Finding 2	This data had significant susceptibility field distortions in the frontal and temporal regions in several subjects. This is evident in the frontal regions of the group average template. A reasonable next step would be application of Synb0 to each subject, segmentation of each individual subjects data from the acute, subacute and chronic timepoints with TractSeg and comparison of tract averaged metrics estimated in subject space with a less conservative correction for multiple comparisons like false discovery rate.

CHAPTER 6: GENERAL DISCUSSION & FUTURE DIRECTIONS

GENERAL DISCUSSION OF EXPERIMENTAL CHAPTERS

Here, the findings from experimental Chapters 3-5 will be discussed in the context of the TRACK-TBI diffusion literature and the articles covered in Chapter 2. We also cover some of the pitfalls encountered in working with the open-access TRACK-TBI data from FITBIR. Finally, future directions for this work are outlined with short-term and long-term plans to accomplish them.

The lack of significance in any FBA metrics in Chapter 3 is likely due to lack of power from the small sample size; the effect size of the diffuse injuries that occur in mTBI is small. The motivation for the small sample size in this initial analysis was to reserve the remaining participants with multi-shell data to facilitate replication of the analysis in a second subgroup of the mTBI participants with multi-shell data similar to the analysis by Palacios and colleagues.[120] Although we cannot know with complete confidence that it was a lack of power that led to our non-significant results in the pilot study, an interesting future direction would be to test with methods similar to that used in Genc et al., 2018 to see if the analysis was underpowered to detect differences with this sample size.[197,236] Numerous small studies and large studies that have utilized DTI and contemporary modeling techniques have reported similarly negative results for some or all DTI metrics.[17,122,161,174,191] However, Mito and colleagues noted significant increased in FDC and FD in their study of 29 Australian football players.[176] Nonetheless, the results observed before family-wise error correction in the whole brain fixel-wise analysis follow a pattern that we would expect, with widespread diffuse difference, especially in the deep WM, like the internal and external capsule, and frontal WM regions, like the forceps minor fibers traversing the genu of the corpus callosum. It is well described that the effect size of mTBI injuries is quite small and requires adequate power to detect, especially for DTI metrics like FA.[112] It remains to be seen if the added specificity from accounting for crossing fibers increases power in analyses with mTBI DWI data.

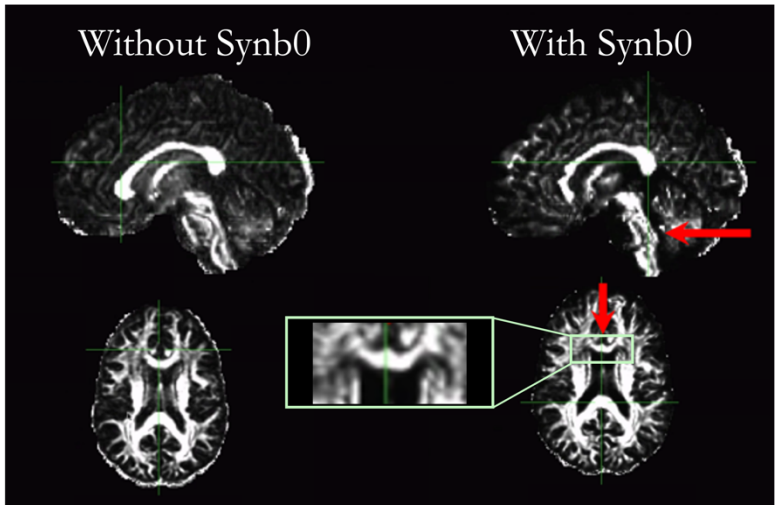

Figure 6.1- Fractional anisotropy images from a single subject demonstrating the geometric distortions introduced with the use of Synb0-DISCO to generate undistorted b0 images for input to FSL's topup. The top images are a sagittal view with the distorted image on the right, particularly evident in the brainstem region of this view. The bottom image is an axial view with emphasis on the genu of the corpus callosum where the geometric distortions are evident in this view.

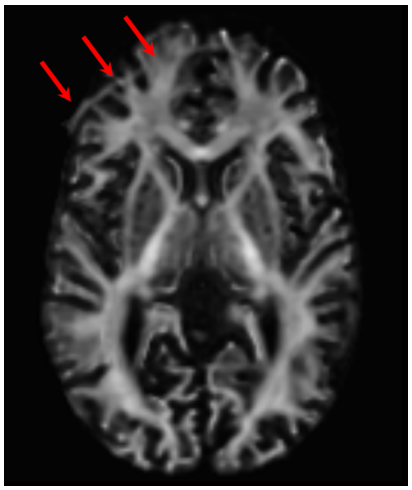

Figure 6.2- An MRI artifact, likely ghosting of the skull or less likely Gibbs ringing artifact, that was not removed in preprocessing. In subjects with this artifact, Synb0-DISCO attempted to interpolate data proximal to this arc and within the brain resulting in an anterior-posterior compression distortion of the data as in (Figure 6.1).

We ultimately did not proceed with the initial pilot processing pipeline, as the use of Synb0-Disco introduced severe geometric distortions in some patient data (Figure 6.1). Although CSD is an ill-posed problem and, therefore, highly susceptible to noise, after a quality check of the DWI data, it was deemed that the improvement in data quality would be only incremental for the subjects on which it was successfully implemented.[22] After consulting with the originator of Synb0-Disco, Dr. Kurt Schilling, it was discovered that a scanner artifact present in some of the datasets was likely the culprit for the distortions introduced in the data (Figure 6.2).[198] A forthcoming GitHub issue will be created to document this occurrence for future users of the TRACK-TBI dataset or those attempting to do susceptibility field distortion correction on open-access datasets in the future. Nonetheless, it is important to include this pilot pipeline, as theoretically, it should work on other data and would be a useful method to ensure optimal data quality in legacy datasets collected before the collection of reverse phase-encoded direction b0 images was standard. Finally, an important quality check in pipelines utilizing FBA and Synb0-DISCO is the visual inspection of images after distortion correction to detect potential artificial distortions.

In Chapter 4 we demonstrate that FBA metrics of WM microstructure differ between mTBI and controls in the subacute and chronic periods following mTBI. The most prominent areas of difference in whole brain FBA were in the internal capsule, anterior regions of the corpus callosum, and projection fibers from the thalamus to anterior brain regions. Differences included more fixels and greater percent differences on the left side of the brain in both the whole brain FBA and post hoc analyses in this sample. Most interestingly, from the 2-week to 6-month timepoint there was not much resolution of injured tissue, which would have been indicated by a return of the mTBI mean towards the control mean and significant differences in the comparisons of longitudinal change images. This would seem to suggest that in this general population sample, the injured tissue characteristics did not change much in the subacute and chronic periods following injury.

The TRACK-TBI investigators have previously applied the higher-order multicompartment modeling technique NODDI. In their analysis, they observed more widespread differences compared to the present analysis, however, a similar pattern of lower NDI was observed in both. NDI a measure of neurite density, which is similar to the fiber density metric of FBA. A possible explanation for this difference in localization could be their use of TBSS in the analysis which has been shown to generate artificially lower values of FA in prior studies.[172] This highlights a major strength of the FBA method to comprehensively question all WM voxels while taking into account tract-specific changes with the connectivity-based fixel enhancement.[19] Additionally, the NODDI TRACK-TBI study used false-discovery rate for correction of multiple comparisons which is a less conservative approach for correction compared to family-wise error correction. This is further supported by the widespread significant differences observed in the post hoc tract averaged comparisons of DTI, DKI and NODDI metrics in which we also utilized false discovery rate correction for multiple comparisons. Again, this highlights the challenge of multiple comparison correction in the field of neuroimaging. Given the current need to establish a consistent pattern of WM change as measured by DWI following injury, the field may have a higher tolerance for more false positives associated with false discovery rate. On the other hand, given the numerous factors that can result in DWI signal change at the microstructural level, such as extent of myelination, presence of other cell, and intra-axonal organelles to name a few, the more conservative family-wise error correction may in fact be preferred.[105,237]

Prior findings with FBA in the literature have also been mixed largely due to variations in study design, which was part of the genesis of the TRACK-TBI study. For example, Wallace and colleagues 2020 were the first to conduct a FBA in a mTBI cohort, and found no differences in fiber-specific metrics.[174] These findings are likely due to the high variability in scan time between subjects as discussed in Chapter 2, meaning WM at various stages of recovery were averaged,

emphasizing the importance of consistent scan time in mTBI studies. In the TRACK-TBI NODDI study, for example, an injury to scan time standard deviation of 2-days and 8-days for the 2-week and 6-month timepoints respectively, was reported.[112]

Only two other studies have utilized FBA in populations of sport-related mTBI patients. They both observed increased FDC primarily driven by increases in FD. These findings are in contrast to the analysis in this dissertation, which could be due to differences in WM reactivity to injury in athletes vs the general population. For example, it has been proposed that observations of WM change in contact sports athletes may reflect a synergistic effect of repetitive subconcussive blows accumulated during the season amplified in the setting of the trauma that resulted in the singular mTBI diagnosis.[112,154,155,231] Similarly, in healthy athletic young populations the time course of pathophysiologic change as described in Chapter 1 may be different compared to the general population; this is an open question. It is likely, however, as the authors propose, this pattern reflects cytotoxic edema following injury, which may be in contrast to a predominant pattern of vasogenic edema and diffuse axonal injury followed by axonal degeneration in the general population.[112,176,214]

It is unusual that the tensor metrics AD and AK were significantly different throughout the brain with no differences in FA or KFA. All of these metrics are related to the principal diffusion direction, which should be aligned along the principal fiber population in voxel. A possible explanation is that averaging across tracts with a large number of included crossing fiber regions may have artificially lowered FA and KFA values, however a comparable effect would occur in averaging AD and AK. Particularly in the context of concurrent observed decreases in NDI, FDC and FD which would suggest decreases in intraaxonal compartment signal and axonal loss, higher AD and AK in the mTBI group seems unlikely. Finally, increased FWF in numerous tracts at the six month timepoint is similarly difficult to explain as it is commonly observed to be increased in the acute phase of injury indicative of edema. This should be resolved in more chronic stages of recovery. It is

more likely that this finding in conjunction with decreased FD, FDC and NDI reflect an increase in extracellular fluid space due to chronic axonal degeneration. This further demonstrates how multicompartment models offer improved interpretability of DWI results compared to traditional tensor metrics.

There are several important limitations to the present study that should be considered in the interpretation of the results. First, the cohort was smaller than the entire TRACK-TBI CA+MRI cohort, owing to the availability of multi-shell data in only a small proportion of the TRACK-TBI sample. Multiband MRI technology, which accelerates the acquisition of data, was used widely in research in the early 2010s but was not widely available on clinical scanners until later. This may have motivated the primarily single shell acquisitions used for the TRACK-TBI study.[238] Furthermore, a goal of the TRACK-TBI study was to produce standardized and widely reproducible outcome measures for the study of TBI, and the novelty of multi-shell data and advanced modeling techniques may not have aligned with that goal. This is also a relative strength of this study, as all participants were collected at the same study site on the same scanner. There was also a difference between the number of participants in the control and mTBI groups. Therefore, the group means for WM from mTBI patients may have been estimated more precisely in this sample compared to the control group. In light of this small control group sample size, the t-test results in particular should be interpreted with caution.

We observed no differences in FC in this study at both timepoints. This could be due in part to the lack of susceptibility field distortion correction. The construction of the population template and individual subject warps used to calculate FC are sensitive to distortions. Therefore, the lack of susceptibility field distortions was likely to have affected the quality of the metric estimation Chapter 4 & 5. The work around is correction with Synb0-Disco, which was unsuccessful for the TRACK-TBI data and visual inspection showed susceptibility field distortions were minor in subjects

included in this analysis. However, this may be an important future direction for the data presented in Chapter 5.

Although the two samples were well matched on demographic variables, WM is known to change with age, as well as other factors which were not controlled for in the present analysis.[178] An important future direction will be fitting additional models that include demeaned age, sex, and handedness as covariates to confirm the present findings. Even then, there could be additional factors driving the differences between groups, including components of resilience to WM injury that have yet to be fully described. For example, in the TRACK-TBI NODDI analysis two clusters of mTBI patients differing on performance on neuropsychological test of processing speed and verbal memory were identified.[112] These lower performing patients had, on average, lower years of education and had lower ODI in the central WM. These patients reported fewer symptoms than the higher performing group, suggesting components of resilience to injury may be contributing to differences in recovery.[112]

As an emerging technique, FBA is continuing to evolve. Recently, the developers released guidelines on the correction of metrics for intracranial volume, and an additional next step will be adjusting for this with the results of a Freesurfer segmentation per the developer's recommendations.[225] Finally, multiple comparisons are inherent to the high dimensional data in the field of neuroimaging and the biological significance of findings in this context can be challenging.[239] In this analysis, we perform conservative "strong" family-wise error correction by additionally correcting the alpha value for multiple comparisons to assign significance. However, this is not the method recommended by the MRtrix3 developers and may have reduced our sensitivity in this analysis.[224]

Finally, with relation to CSD a potential limitation is the assumption of a single tissue response function for all WM. This is a core assumption of CSD and may simply be an inaccurate

way to model WM. However, this issue is inherent to any modeling approach. In fact, in mild traumatic brain injury research, it could potentially be seen as a strength, as any fixel-wise deviations in WM could be attributed to partial volume effects as a result of the injury or the presence of multiple fiber orientations. Computing the average tissue response functions from the control group facilitates this, however, it is not currently a specific recommendation of the developers. A potential future analysis with an average response function from the whole sample or the mTBI patients alone could help add context to these findings. Along these lines, the test-retest reliability of MSMT-CSD has only been tested in data up to 3-months past a baseline scan.[196] In the 3-month cohort of this study, the interclass correlation coefficient was good (ICC>0.8). However, the sample size was small, and more work is needed to understand the agreement of this measure over time, especially at longitudinal time points like the 6-month collection in TRACK-TBI.

The animal literature covered in Chapter 1 lends important context to the findings in Chapter 5. We know based on the work in animals that the energy crisis as a result of the injury lasts well into the subacute period following injury, and contributes to cell death due to calcium toxicity.[33,35,36] This would seem to support the observation that higher order modeling techniques that infer density of axons in a voxel were lower in mTBI patients compared to controls at the two-week timepoint due to continued cell death and degeneration of axons during the subacute period. Similarly, fiber cross-section was not lower at this timepoint as the damaged tissue is likely undergoing astrogliosis and has an increased presence of microglia and non-resident inflammatory cells extravasated from the damaged BBB maintaining the cross sectional area of the tracts.[48, 49, 50, 52, 53] Along the same lines this increased cellularity would impede diffusion and is reflected by reduced MD, MK, AD, AK, RD, and RK in numerous tracts. These processes have likely resolved by the 6-month timepoint as reflected by the increased regions of lower ODI and FC at this chronic stage of recovery.

In Chapter 5 we take an exploratory look at the Michigan State University (MSU) Health Care concussion clinic participants with data collected before the COVID-19 pandemic. In this experiment, the general gestalt of Figure 5.1 is an expected pattern of decreasing differences in group means between participants with prolonged symptom recovery and those with a more typical course of symptom recovery. Notably, in the group mean comparisons between the acute and subacute periods post-injury shown in Figure 5.2, there is only a single right-sided frontal WM region where FDC was observed to be lower in the acute period following injury. This could indicate that a similar pattern of only modest changes occurs in WM during the acute to subacute recovery period. This is an imperfect interpretation however, and the true comparison will come with calculation and comparison of change images using the same approach as described in Chapters 3 & 4. Similarly, the small sample size in comparisons and uncorrected results are likely heavily influenced by type-I errors. Further, these images were not corrected for susceptibility distortions, which may have affected the quality of the population template and, therefore, the subjects' warps and fiber-cross section measure. An important next step will be attempting to apply the Synb0-DISCO distortion correction to these data as in Chapter 3 and repeating the analysis with the recommended additional distortion corrections.[18] This would allow application of TractSeg to each individual subject for direct estimation of metrics in subject native space.

In the MSU Health Care study, more information about the remainder of the athletic seasons of participants were not collected. In an ideal study design, given the literature reviewed in Chapter 2, it is necessary to understand the impact exposure of high school athletes, and the length of time they have been exposed to contact practice pre-injury and after return to play that coincides with data collection periods.[176,214] Additionally, this sample was entirely male, and highlights the underrepresentation of female mTBI participants in studies of sport-related concussion as identified in Chapter 2. We almost recruited a single female participant soccer player; however, she was

scheduled to have dental braces installed during the course of the study. In future work, increased effort should be placed to recruit female participants, which should include targeted community engagement in the sports in which females experience increased head impact exposure such as soccer and basketball.[25] This underscores the importance of future work to take into consideration the early descriptions in the literature of disparities in outcome, referral for clinical care, and follow-up care adherence.[240–242]

With respect to the single shell low b-value acquisition, Genc and colleagues 2020 demonstrated that high b-value single-shell acquisitions applied with the single-shell multi-tissue CSD approach were more sensitive than multi-shell acquisitions.[194] The interpretation being that isolating signal from the intracellular compartment with high-b value acquisitions in studies that are solely interested in observing differences in FD could be a viable strategy in mTBI. This underscores the importance of close collaboration with an MR Physicist who can guide researchers when selecting acquisitions that are specifically tuned to their research question.

FUTURE DIRECTIONS

In the future, it will be important to assess if metrics derived from DWI can be used to train predictive models of patient outcome following mTBI. For example, a support vector machine algorithm to classify DWI data in mTBI patients who did not recover by 6-months would be an interesting next step. Support vector machines (SVM) are supervised machine learning algorithms that learn a linear discriminant function.[243] The goal of applying a SVM classification is to find a hyperplane in high-dimensional space between groups of neuroimaging data that predict a discrete class, in this case, recovery status at 6-months as indicated by GOSE total score. A similar approach, logistic regression, was successfully applied in the TRACK-TBI NODDI analysis.[112] These methods are an improvement over the univariate methods in the present dissertation, as it allows the identification of regional patterns of pathology in disease, which lends itself to the current problem of poor localization

in mTBI. Injured WM following an mTBI is not necessarily constrained to a specific ROI or single pattern of change; therefore, more data-driven modeling approaches may have greater success in predicting which patients will not recover. Compared to unsupervised approaches which may produce superior classifiers, SVM would allow examination of the factors that uphold the support vectors for increased understanding of what features the model is using for classification.

We would expect SVM to identify patterns of regional change in DWI metrics that predict recovery with high sensitivity and specificity. A predictive DWI model would likely include WM features of decreased FA and increased MD in the corpus callosum, longitudinal fasciculi, internal capsule, and corona radiata as previously described in the literature.[5,17] It would be interesting to compare if AD alone is more predictive than FA and MD, as this metric was more sensitive to differences in the post hoc tract-wise analysis conducted in this dissertation. We would expect that in comparisons of models, including, tensor models and higher order modelling techniques such as FBA and NODDI, higher order modelling techniques would outperform tensor models. Additionally, it would be interesting to compare the performance of a model containing only clinical variables and FD, which seems to be the most sensitive metrics requiring the least data for estimation compared to all other metrics.[194,195] We could use the tract-wise averages for the seventy-two tracts from TractSeg to train a SVM. Nevertheless, a superior approach would be to apply TractSeg to each individual participant and estimate the diffusion parameters in native subject space. This would entail re-running TractSeg on each subject's three primary spherical harmonic peaks extracted from their WM FODs. This would facilitate calculation of tract-wise metrics in native subject space for training the model as opposed to the current data analysis scheme which includes an additional interpolation step to estimate metrics in the study specific WM FOD template space.

To add clinical context to the neuroimaging findings presented in this dissertation, we plan to explore subgroup differences in mTBI participants on the GOSE. In the absence of gold standard

objective biological markers of outcome, clinical assessment tools such as the GOSE, are essential for understanding how observed group differences in WM relate to patient functioning and clinical outcomes. As a part of our collaborative agreement with TRACK-TBI, the present results from the FBA and post hoc tract-wise analysis will be shared with the TRACK-TBI biostatistics core to examine how metrics derived with this technique relate to outcome on the GOSE, symptoms on the RPQ, and verbal memory and processing speed on the Rey-Auditory verbal learning test.[244] We will also request more detailed demographic information be computed on mechanism of injury. This important future direction will add context to the reductions in FD is related to differences in functioning in this sample. This is particularly important as many of the lasting effects of mTBI are related to post-injury deficits in function at work, in school, and in patients personal relationships.[7,8,112]

An emerging objective marker of mTBI pathophysiology in human samples is alterations in cerebral blood flow and functional connectivity. Early work by Zhu and colleagues demonstrated a transient decrease in default mode network connectivity at 1-month post-injury. The authors proposed this distributed network is likely to be affected in a large proportion of diffuse mTBI injuries.[125] These findings must be re-examined in the context of other modalities that quantify perfusion to confirm if the effect is related to disconnection or dysfunction on the neuronal side or changes in blood flow on the vascular side. ASL is an MRI technique that magnetically "marks" protons in arterial blood.[245] When these protons reach a new vascular bed, they can be measured because of their unique magnetic signal. Early MRI studies in rats with induced TBI demonstrated that cerebral blood flow as measured by ASL was reduced acutely seven days after injury and even one year after injury compared to sham group.[246,247] It is known that a biphasic change in nitric oxide, a potent vasodilator, and nitric oxide synthase, an enzyme that catalyzes the synthesis of nitric oxide, are in part responsible for the observed changes in cerebral blood flow.[248] However, animal

studies have demonstrated that in most cases, nitric oxide production and nitric oxide synthase expression return to pre-injury levels after approximately 7-10 days.

Following mTBI, ASL studies in humans have revealed that there is a similar pattern of changes in cerebral blood flow as observed in animal studies. A recent study demonstrated a significant decrease in cerebral blood flow from 24-hours to 8-days post-injury in a human sample.[47] Importantly, scores on neuropsychological tests had returned to baseline levels at 8 days. The authors proposed this transient alteration in perfusion represents a window of cerebral vulnerability that current clinical management cannot assess. This is of particular importance when considering the diagnosis and return to play considerations around sports-related concussion. Work by Meier and colleagues, 2015 demonstrated similarly depressed cerebral blood flow at 1-day and 1-week post-mTBI when compared to age and fitness matched controls.[249] This study also demonstrated a region-specific decrease in cerebral blood flow between participants who returned to play before 2-weeks vs. after 2-weeks. As is common in early studies in the mTBI literature, a major limitation of sample size and variations in measurement timing temper the strength of this evidence. However, these early works demonstrate the potential detrimental effects of TBI classification that is not biologically performed with objective markers of neurophysiology. These early studies are compelling and demonstrate the importance of considering the time course of disturbed perfusion when utilizing imaging modalities dependent on the blood-oxygen-level-dependent signal in mTBI. A very unique study recently demonstrated that a wearable brain vibration device that may mimic forces experienced in sport or operation of machinery caused localized decreases in cerebral blood flow in the region of the posterior cingulate cortex and precuneus, both of which are hubs of the default mode network.[250]

Given this early evidence, there is a great need to better understand the natural history of cerebral blood flow changes following mTBI. The TRACK-TBI study collected ASL data in a subset

of patients, and it would be an interesting future direction to examine the localization of decreased perfusion with changes in resting-state fMRI functional connectivity at the subacute 2-week timepoint. Additionally, the high quality tractography results demonstrated in this dissertation would facilitate comparisons of structural and functional connectivity in participants with multi-shell data and resting-state fMRI data that could be colocalized with alterations in perfusion found with ASL. ASL findings from the department of defense concussion research and education (CARE) study demonstrated alterations in cerebral blood flow acutely following injury in sports-related mTBI.[251] Most recently, studies of cerebral blood flow alterations in non-injured contact sport athletes demonstrated alterations in pre and post-season ASL scans lending increased strong evidence to this line of investigation.[252] Finally a recent review of ASL findings in 23 mTBI studies concluded there is strong evidence for a relationship between alterations in ASL measured cerebral blood flow and clinical recovery.[253]

In the pursuit of discriminative technologies that will not overly burden the already high healthcare costs in the US, it is important to consider cost-effectiveness in clinical research.[254] Magnetic resonance imaging is an expensive technology, and requires in person appointments for the patients, personnel to run the scanner, and physicians to interpret the images. Functional near infrared spectroscopy (fNIRs), measures alterations in cerebral blood flow in peripheral brain regions using light which can penetrate the skull and detect alterations in oxygenated and deoxygenated hemoglobin based on light absorption.[255] Although less sensitive than MRI, fNIRs is a simple wearable technology. A recent study demonstrated a functioning device can be constructed for as low as $215.[256] An intriguing early study in mTBI, demonstrated decreased brain oxygenation, as measured by fNIRs, in patients suffering from persistent post-concussive symptoms.[257] More recently, acute alterations in cerebral blood flow and oxygenation have been observed with fNIRs in mixed martial arts athletes between pre to post contact training session scans but not non-contact

training sessions.[258] These findings were significantly associated with cumulative angular accelerations as measured by kinematic mouth pieces. Future studies could benefit from using this technology to study the natural history of cerebral blood flow in an emergent setting and longitudinally with serial measurement at regular intervals during the recovery period. Presumably, patients could even be trained to take a device home for real time monitoring of alterations by a physician, which further necessitate greater investigation with this device.

Conclusion

Taken together, DWI is sensitive to even the diffuse minor WM changes in patients with mTBI of varying location and mechanism in the general population. Contemporary modelling techniques facilitate better interpretability of results by assigning effects to specific fiber populations within a voxel in the case of FBA, or to specific pathophysiologic mechanisms such as edema as in the NODDI metric FWF. Additionally, the use of reproducible tracking algorithms such as TractSeg are an improvement over atlas-based methods, allowing comprehensive localization of effects as measured by DWI in the whole brain. Albeit not ideal, tract averaging of metrics is more reliable when used in conjunction with methods that account for crossing fibers. Ultimately, such methods will allow the colocalization of effects observed with other modalities to fully describe the natural history of brain change following mTBI.

REFERENCES

1. Silverberg ND, Iverson GL, Cogan A, et al. The American Congress of Rehabilitation Medicine Diagnostic Criteria for Mild Traumatic Brain Injury. *Arch Phys Med Rehabil*. 2023;104(8):1343-1355. doi:10.1016/j.apmr.2023.03.036

2. Georges A, M Das J. Traumatic Brain Injury. In: *StatPearls*. StatPearls Publishing; 2024. Accessed February 29, 2024. http://www.ncbi.nlm.nih.gov/books/NBK459300/

3. Puig J, Ellis MJ, Kornelsen J, et al. Magnetic Resonance Imaging Biomarkers of Brain Connectivity in Predicting Outcome after Mild Traumatic Brain Injury: A Systematic Review. *J Neurotrauma*. 2020;37(16):1761-1776. doi:10.1089/neu.2019.6623

4. Kim HJ, Tsao JW, Stanfill AG. The current state of biomarkers of mild traumatic brain injury. *JCI Insight*. 3(1):e97105. doi:10.1172/jci.insight.97105

5. Asken BM, DeKosky ST, Clugston JR, Jaffee MS, Bauer RM. Diffusion tensor imaging (DTI) findings in adult civilian, military, and sport-related mild traumatic brain injury (mTBI): a systematic critical review. *Brain Imaging Behav*. 2018;12(2):585-612. doi:10.1007/s11682-017-9708-9

6. McMahon PJ, Hricik A, Yue JK, et al. Symptomatology and Functional Outcome in Mild Traumatic Brain Injury: Results from the Prospective TRACK-TBI Study. *J Neurotrauma*. 2014;31(1):26-33. doi:10.1089/neu.2013.2984

7. Nelson LD, Temkin NR, Dikmen S, et al. Recovery After Mild Traumatic Brain Injury in Patients Presenting to US Level I Trauma Centers: A Transforming Research and Clinical Knowledge in Traumatic Brain Injury (TRACK-TBI) Study. *JAMA Neurol*. 2019;76(9):1049. doi:10.1001/jamaneurol.2019.1313

8. Machamer J, Temkin N, Dikmen S, et al. Symptom Frequency and Persistence in the First Year after Traumatic Brain Injury: A TRACK-TBI Study. *J Neurotrauma*. 2022;39(5-6):358-370. doi:10.1089/neu.2021.0348

9. Cassidy JD, Carroll L, Peloso P, et al. Incidence, risk factors and prevention of mild traumatic brain injury: results of the who collaborating centre task force on mild traumatic brain injury. *J Rehabil Med*. 2004;36(0):28-60. doi:10.1080/16501960410023732

10. Wilde EA, Wanner IB, Kenney K, et al. A Framework to Advance Biomarker Development in the Diagnosis, Outcome Prediction, and Treatment of Traumatic Brain Injury. *J Neurotrauma*. 2022;39(7-8):436-457. doi:10.1089/neu.2021.0099

11. Bigler ED. Neuroimaging Biomarkers in Mild Traumatic Brain Injury (mTBI). *Neuropsychol Rev*. 2013;23(3):169-209. doi:10.1007/s11065-013-9237-2

12. Gan ZS, Stein SC, Swanson R, et al. Blood Biomarkers for Traumatic Brain Injury: A Quantitative Assessment of Diagnostic and Prognostic Accuracy. *Front Neurol*. 2019;10:446. doi:10.3389/fneur.2019.00446

13. Visser K, Koggel M, Blaauw J, Van Der Horn HJ, Jacobs B, Van Der Naalt J. Blood-based biomarkers of inflammation in mild traumatic brain injury: A systematic review. *Neurosci Biobehav Rev*. 2022;132:154-168. doi:10.1016/j.neubiorev.2021.11.036

14. Silverberg ND, Gardner AJ, Brubacher JR, Panenka WJ, Li JJ, Iverson GL. Systematic Review of Multivariable Prognostic Models for Mild Traumatic Brain Injury. *J Neurotrauma*. 2015;32(8):517-526. doi:10.1089/neu.2014.3600

15. Yuh EL, Cooper SR, Mukherjee P, et al. Diffusion Tensor Imaging for Outcome Prediction in Mild Traumatic Brain Injury: A TRACK-TBI Study. *J Neurotrauma*. 2014;31(17):1457-1477. doi:10.1089/neu.2013.3171

16. O'Donnell LJ, Westin CF. An Introduction to Diffusion Tensor Image Analysis. *Neurosurg Clin N Am*. 2011;22(2):185-196. doi:10.1016/j.nec.2010.12.004

17. Lindsey HM, Hodges CB, Greer KM, Wilde EA, Merkley TL. Diffusion-Weighted Imaging in Mild Traumatic Brain Injury: A Systematic Review of the Literature. *Neuropsychol Rev*. 2023;33(1):42-121. doi:10.1007/s11065-021-09485-5

18. Tournier JD, Smith R, Raffelt D, et al. MRtrix3: A fast, flexible and open software framework for medical image processing and visualisation. *NeuroImage*. 2019;202:116137. doi:10.1016/j.neuroimage.2019.116137

19. Raffelt DA, Smith RE, Ridgway GR, et al. Connectivity-based fixel enhancement: Whole-brain statistical analysis of diffusion MRI measures in the presence of crossing fibres. *NeuroImage*. 2015;117:40-55. doi:10.1016/j.neuroimage.2015.05.039

20. Tournier J, Mori S, Leemans A. Diffusion tensor imaging and beyond. *Magn Reson Med*. 2011;65(6):1532-1556. doi:10.1002/mrm.22924

21. Farquharson S, Tournier JD, Calamante F, et al. White matter fiber tractography: why we need to move beyond DTI: Clinical article. *J Neurosurg*. 2013;118(6):1367-1377. doi:10.3171/2013.2.JNS121294

22. Tournier JD, Calamante F, Gadian DG, Connelly A. Direct estimation of the fiber orientation density function from diffusion-weighted MRI data using spherical deconvolution. *NeuroImage*. 2004;23(3):1176-1185. doi:10.1016/j.neuroimage.2004.07.037

23. Mccrory P, Meeuwisse W, Dvorak J, et al. Consensus statement on concussion in sport-the 5 th international conference on concussion in sport held in Berlin, October 2016 Consensus statement. *Br J Sports Med*. 2018;51:838-847. doi:10.1136/bjsports-2017-097699

24. Giza C, Greco T, Prins ML. Concussion: pathophysiology and clinical translation. *Handb Clin Neurol*. 2018;158:51-61. doi:10.1016/B978-0-444-63954-7.00006-9

25. Harmon KG, Drezner JA, Gammons M, et al. American Medical Society for Sports Medicine position statement: concussion in sport. *Br J Sports Med*. 2013;47(1):15-26. doi:10.1136/bjsports-2012-091941

26. Sussman ES, Pendharkar AV, Ho AL, Ghajar J. Mild traumatic brain injury and concussion: terminology and classification. In: *Handbook of Clinical Neurology*. Vol 158. Elsevier; 2018:21-24. doi:10.1016/B978-0-444-63954-7.00003-3

27. Maas AIR, Menon DK, Steyerberg EW, et al. Collaborative European NeuroTrauma Effectiveness Research in Traumatic Brain Injury (CENTER-TBI): A Prospective Longitudinal Observational Study. *Neurosurgery*. 2015;76(1):67-79. doi:10.3174/ajnr.A1051

28. Frieden TR, Houry D, Baldwin G. The Report to Congress on Traumatic Brain Injury in the United States: Epidemiology and Rehabilitation. https://www.cdc.gov/traumaticbraininjury/pdf/tbi_report_to_congress_epi_and_rehab-a.pdf

29. Faul M, Coronado V. Epidemiology of traumatic brain injury. In: *Handbook of Clinical Neurology*. Vol 127. Elsevier; 2015:3-13. doi:10.1016/B978-0-444-52892-6.00001-5

30. Santos-Lozada AR. Trends in Deaths From Falls Among Adults Aged 65 Years or Older in the US, 1999-2020. *JAMA*. 2023;329(18):1605. doi:10.1001/jama.2023.3054

31. Katayama Y, Becker DP, Tamura T, Hovda DA. Massive increases in extracellular potassium and the indiscriminate release of glutamate following concussive brain injury. *J Neurosurg*. 2009;73(6):889-900. doi:10.3171/jns.1990.73.6.0889

32. Takahashi H, Manaka S, Sano K. Changes in extracellular potassium concentration in cortex and brain stem during the acute phase of experimental closed head injury. *J Neurosurg*. 2009;55(5):708-717. doi:10.3171/jns.1981.55.5.0708

33. Giza CC, Hovda DA. The new neurometabolic cascade of concussion. *Neurosurgery*. Published online 2014. doi:10.1227/NEU.0000000000000505

34. Hovda DA, Yoshino A, Kawamata T, Katayama Y, Fineman I, Becker DP. The increase in local cerebral glucose utilization following fluid percussion brain injury is prevented with kynurenic acid and is associated with an increase in calcium. *Acta Neurochir Suppl (Wien)*. 1990;51:331-333.

35. Thomas S, Prins ML, Samii M, Hovda DA. Cerebral Metabolic Response to Traumatic Brain Injury Sustained Early in Development: A 2-Deoxy-D-Glucose Autoradiographic Study. *J Neurotrauma*. 2002;17(8):649-665. doi:10.1089/089771500415409

36. Yoshino A, Hovda DA, Kawamata T, Katayama Y, Becker DP. Dynamic changes in local cerebral glucose utilization following cerebral concussion in rats: evidence of a hyper- and subsequent hypometabolic state. *Brain Res*. 1991;561(1):106-119. doi:10.1016/0006-8993(91)90755-K

37. Giza CC, Hovda DA. The New Neurometabolic Cascade of Concussion. *Neurosurgery*. 2014;75(Supplement 4):S24-S33. doi:10.1227/NEU.0000000000000505

38. Giza CC, Maria NSS, Hovda DA. *N* -Methyl-D-Aspartate Receptor Subunit Changes after Traumatic Injury to the Developing Brain. *J Neurotrauma*. 2006;23(6):950-961. doi:10.1089/neu.2006.23.950

39. Osteen CL, Giza CC, Hovda DA. Injury-induced alterations in N-methyl-d-aspartate receptor subunit composition contribute to prolonged 45calcium accumulation following lateral fluid percussion. *Neuroscience*. 2004;128(2):305-322. doi:10.1016/j.neuroscience.2004.06.034

40. Kandel E, Schwartz J, Jessell T, Siegelbaum S, Hudspeth A, Mack S. Membrane Potential and the Passive Electrical Properties of the Neuron. In: *Principles of Neuroscience*. 6th ed. McGraw HIll. Accessed December 1, 2019. https://neurology.mhmedical.com/content.aspx?bookid=1049&sectionid=59138628

41. Fehily B, Fitzgerald M. Repeated Mild Traumatic Brain Injury. *Cell Transplant*. 2017;26(7):1131-1155. doi:10.1177/0963689717714092

42. Chen SF, Richards HK, Smielewski P, et al. Relationship Between Flow-Metabolism Uncoupling and Evolving Axonal Injury After Experimental Traumatic Brain Injury. Published online 2004. doi:10.1097/01.WCB.0000129415.34520.47

43. Hill CS, Coleman MP, Menon DK. Traumatic Axonal Injury: Mechanisms and Translational Opportunities. *Trends Neurosci*. 2016;39(5):311-324. doi:10.1016/j.tins.2016.03.002

44. Pettus EH, Christman CW, Giebel ML, Povlishock JT. Traumatically Induced Altered Membrane Permeability: Its Relationship to Traumatically Induced Reactive Axonal Change. *J Neurotrauma*. 1994;11(5):507-522. doi:10.1089/neu.1994.11.507

45. Oakes S. Cell Injury, Cell Death, and Adaptations. In: *Robbins & Cotran Pathologic Basis of Disease*. 10th ed. Elsevier. Accessed December 29, 2023. https://www-clinicalkey-com.proxy1.cl.msu.edu/#!/content/book/3-s2.0-B9780323531139000029

46. Staal J, Dickson T, Gasperini R, Liu Y, Foa L, Vickers J. Initial calcium release from intracellular stores followed by calcium dysregulation is linked to secondary axotomy following transient axonal stretch injury. Accessed December 29, 2023. https://onlinelibrary.wiley.com/doi/10.1111/j.1471-4159.2009.06531.x

47. Wang Y, Nelson LD, LaRoche AA, et al. Cerebral Blood Flow Alterations in Acute Sport-Related Concussion. *J Neurotrauma*. 2016;33(13):1227-1236. doi:10.1089/neu.2015.4072

48. Loane DJ, Byrnes KR. Role of microglia in neurotrauma. *Neurotherapeutics*. 2010;7(4):366-377. doi:10.1016/j.nurt.2010.07.002

49. Donat CK, Scott G, Gentleman SM, Sastre M. Microglial Activation in Traumatic Brain Injury. *Front Aging Neurosci*. 2017;9:208. doi:10.3389/fnagi.2017.00208

50. Csuka E, Hans VHJ, Ammann E, Trentz O, Kossmann T, Morganti-Kossmann MC. Cell activation and in¯ammatory response following traumatic axonal injury in the rat.

51. Sulhan S, Lyon KA, Shapiro LA, Huang JH. Neuroinflammation and Blood-Brain Barrier Disruption Following Traumatic Brain Injury: Pathophysiology and Potential Therapeutic Targets. *J Neurosci Res*. 2020;98(1):19-28. doi:10.1002/jnr.24331

52. Hsieh HL, Wang HH, Wu WB, Chu PJ, Yang CM. Transforming growth factor-b1 induces matrix metalloproteinase-9 and cell migration in astrocytes: roles of ROS-dependent ERK- and JNK- NF- B pathways. Published online 2010.

53. Yang Y, Estrada EY, Thompson JF, Liu W, Rosenberg GA. Matrix Metalloproteinase-Mediated Disruption of Tight Junction Proteins in Cerebral Vessels is Reversed by Synthetic Matrix Metalloproteinase Inhibitor in Focal Ischemia in Rat. *J Cereb Blood Flow Metab*. 2007;27(4):697-709. doi:10.1038/sj.jcbfm.9600375

54. Abdul-Muneer PM, Pfister BJ, Haorah J, Chandra N. Role of Matrix Metalloproteinases in the Pathogenesis of Traumatic Brain Injury. *Mol Neurobiol*. 2016;53(9):6106-6123. doi:10.1007/s12035-015-9520-8

55. Giza C, Greco T, Prins ML. Concussion: pathophysiology and clinical translation. In: *Handbook of Clinical Neurology*. Vol 158. Elsevier; 2018:51-61. doi:10.1016/B978-0-444-63954-7.00006-9

56. Strong AJ, Fabricius M, Boutelle MG, et al. Spreading and Synchronous Depressions of Cortical Activity in Acutely Injured Human Brain. *Stroke*. 2002;33(12):2738-2743. doi:10.1161/01.STR.0000043073.69602.09

57. Mouzon BC, Bachmeier C, Ferro A, et al. Chronic neuropathological and neurobehavioral changes in a repetitive mild traumatic brain injury model. *Ann Neurol*. 2014;75(2):241-254. doi:10.1002/ana.24064

58. Gsell W, Burke M, Wiedermann D, et al. Differential Effects of NMDA and AMPA Glutamate Receptors on Functional Magnetic Resonance Imaging Signals and Evoked Neuronal Activity during Forepaw Stimulation of the Rat. *J Neurosci*. 2006;26(33):8409-8416. doi:10.1523/JNEUROSCI.4615-05.2006

59. Eckner JT, Kutcher JS, Broglio SP, Richardson JK. Effect of sport-related concussion on clinically measured simple reaction time. *Br J Sports Med*. 2014;48(2):112-118. doi:10.1136/bjsports-2012-091579

60. Theadom A, Cropley M, Parmar P, et al. Sleep difficulties one year following mild traumatic brain injury in a population-based study. *Sleep Med*. 2015;16(8):926-932. doi:10.1016/j.sleep.2015.04.013

61. Wickwire EM, Williams SG, Roth T, et al. Sleep, Sleep Disorders, and Mild Traumatic Brain Injury. What We Know and What We Need to Know: Findings from a National Working Group. *Neurotherapeutics*. 2016;13(2):403-417. doi:10.1007/s13311-016-0429-3

62. Wickwire EM, Schnyer DM, Germain A, et al. Sleep, Sleep Disorders, and Circadian Health following Mild Traumatic Brain Injury in Adults: Review and Research Agenda. *J Neurotrauma*. 2018;35(22):2615-2631. doi:10.1089/neu.2017.5243

63. Sandsmark DK, Elliott JE, Lim MM. Sleep-wake disturbances after traumatic brain injury: Synthesis of human and animal studies. *Sleep*. 2017;40(5). doi:10.1093/sleep/zsx044

64. Popovitz J, Mysore SP, Adwanikar H. Long-Term Effects of Traumatic Brain Injury on Anxiety-Like Behaviors in Mice: Behavioral and Neural Correlates. *Front Behav Neurosci*. 2019;13(January):1-12. doi:10.3389/fnbeh.2019.00006

65. Reger ML, Poulos AM, Buen F, Giza CC, Hovda DA, Fanselow MS. Concussive brain injury enhances fear learning and excitatory processes in the amygdala. *Biol Psychiatry*. 2012;71(4):335-343. doi:10.1016/j.biopsych.2011.11.007

66. Gentleman SM, Leclercq PD, Moyes L, et al. Long-term intracerebral inflammatory response after traumatic brain injury. *Forensic Sci Int*. 2004;146(2-3):97-104. doi:10.1016/j.forsciint.2004.06.027

67. Figueiredo-Pereira ME, Rockwell P, Schmidt-Glenewinkel T, Serrano P. Neuroinflammation and J2 prostaglandins: linking impairment of the ubiquitin-proteasome pathway and mitochondria to neurodegeneration. *Front Mol Neurosci*. 2015;7. doi:10.3389/fnmol.2014.00104

68. Tauber D, Parker R. 15-Deoxy-Δ12,14-prostaglandin J2 promotes phosphorylation of eukaryotic initiation factor 2α and activates the integrated stress response. *J Biol Chem*. 2019;294(16):6344-6352. doi:10.1074/jbc.RA118.007138

69. Pakos-Zebrucka K, Koryga I, Mnich K, Ljujic M, Samali A, Gorman AM. The integrated stress response. *EMBO Rep*. 2016;17(10):1374-1395. doi:10.15252/embr.201642195

70. Hickey RW, Adelson PD, Johnnides MJ, et al. Cyclooxygenase-2 Activity Following Traumatic Brain Injury in the Developing Rat. *Pediatr Res*. 2007;62(3):271-276. doi:10.1203/PDR.0b013e3180db2902

71. Kunz T, Marklund N, Hillered L, Oliw EH. Cyclooxygenase-2, Prostaglandin Synthases, and Prostaglandin H $_2$ Metabolism in Traumatic Brain Injury in the Rat. *J Neurotrauma*. 2002;19(9):1051-1064. doi:10.1089/089771502760341965

72. Chung D eun C, Roemer S, Petrucelli L, Dickson DW. Cellular and pathological heterogeneity of primary tauopathies. *Mol Neurodegener*. 2021;16(1):57. doi:10.1186/s13024-021-00476-x

73. Smith DH, Hicks RR, Johnson VE, et al. Pre-Clinical Traumatic Brain Injury Common Data Elements: Toward a Common Language Across Laboratories. *J Neurotrauma*. 2015;32(22):1725-1735. doi:10.1089/neu.2014.3861

74. Wojnarowicz MW, Fisher AM, Minaeva O, Goldstein LE. Considerations for Experimental Animal Models of Concussion, Traumatic Brain Injury, and Chronic Traumatic Encephalopathy—These Matters Matter. *Front Neurol*. 2017;8:240. doi:10.3389/fneur.2017.00240

75. Mullally WJ. Concussion. *Am J Med*. 2017;130(8):885-892. doi:10.1016/j.amjmed.2017.04.016

76. Diaz-Arrastia R, Wang KKW, Papa L, et al. Acute Biomarkers of Traumatic Brain Injury: Relationship between Plasma Levels of Ubiquitin C-Terminal Hydrolase-L1 and Glial Fibrillary Acidic Protein. *J Neurotrauma*. 2014;31(1):19-25. doi:10.1089/neu.2013.3040

77. Bacioglu M, Maia LF, Preische O, et al. Neurofilament Light Chain in Blood and CSF as Marker of Disease Progression in Mouse Models and in Neurodegenerative Diseases. *Neuron*. 2016;91(1):56-66. doi:10.1016/j.neuron.2016.05.018

78. Shahim P, Tegner Y, Marklund N, Blennow K, Zetterberg H. Neurofilament light and tau as blood biomarkers for sports-related concussion. *Neurology*. 2018;90(20):e1780-e1788. doi:10.1212/WNL.0000000000005518

79. Wallace C, Smirl JD, Zetterberg H, et al. Heading in soccer increases serum neurofilament light protein and SCAT3 symptom metrics. *BMJ Open Sport Exerc Med*. 2018;4(1):e000433. doi:10.1136/bmjsem-2018-000433

80. Wirsching A, Chen Z, Bevilacqua ZW, Huibregtse ME, Kawata K. Association of Acute Increase in Plasma Neurofilament Light with Repetitive Subconcussive Head Impacts: A Pilot Randomized Control Trial. *J Neurotrauma*. 2019;36(4):548-553. doi:10.1089/neu.2018.5836

81. Rubin LH, Tierney R, Kawata K, et al. NFL blood levels are moderated by subconcussive impacts in a cohort of college football players. *Brain Inj*. 2019;33(4):456-462. doi:10.1080/02699052.2019.1565895

82. Korley FK, Datwyler SA, Jain S, et al. Comparison of GFAP and UCH-L1 Measurements from Two Prototype Assays: The Abbott i-STAT and ARCHITECT Assays. *Neurotrauma Rep*. 2021;2(1):193-199. doi:10.1089/neur.2020.0037

83. Manley G. TRACK-TBI: Study Design, Early Deliverables, and Future Directions with Geoffrey Manley, MD, PhD. Presented at: 2020; University of Michigan Concussion Center. https://www.youtube.com/watch?v=bZEhRhE_PqM

84. Patricios JS, Schneider KJ, Dvorak J, et al. Consensus statement on concussion in sport: the 6th International Conference on Concussion in Sport–Amsterdam, October 2022. *Br J Sports Med*. 2023;57(11):695-711. doi:10.1136/bjsports-2023-106898

85. *Diffusion MRI from Quantitative Measurement to In-Vivo Neuroanatomy*. 2nd ed. Elsevier/Academic Press,; 2014.

86. *Introduction to Diffusion Tensor Imaging and Higher Order Models*. 2nd edition /. Elsevier/Academic Press,; 2014.

87. Cooley JW, Tukey JW. An Algorithm for the Machine Calculation of Complex Fourier Series.

88. Bammer R. Basic principles of diffusion-weighted imaging. *Eur J Radiol*. 2003;45(3):169-184. doi:10.1016/S0720-048X(02)00303-0

89. Pipe J. Pulse Sequences for Diffusion-Weighted MRI. In: *Diffusion MRI*. Elsevier; 2014:11-34. doi:10.1016/B978-0-12-396460-1.00002-0

90. Novikov DS, Fieremans E, Jespersen SN, Kiselev VG. Quantifying brain microstructure with diffusion MRI: Theory and parameter estimation. *NMR Biomed*. 2019;32(4):e3998. doi:10.1002/nbm.3998

91. Basser PJ, Özarslan E. Introduction to Diffusion MR. In: *Diffusion MRI*. Elsevier; 2014:3-9. doi:10.1016/B978-0-12-396460-1.00001-9

92. Einstein A. Investigations on the Theory of the Brownian Movement.

93. Anatomy of Diffusion Measurement. In: *Introduction to Diffusion Tensor Imaging*. Elsevier; 2014:11-15. doi:10.1016/B978-0-12-398398-5.00002-3

94. Stejskal EO, Tanner JE. Spin Diffusion Measurements: Spin Echoes in the Presence of a Time-Dependent Field Gradient. *J Chem Phys*. 1965;42(1):288-292. doi:10.1063/1.1695690

95. Principle of Diffusion Tensor Imaging. In: *Introduction to Diffusion Tensor Imaging*. Elsevier; 2014:27-32. doi:10.1016/B978-0-12-398398-5.00004-7

96. Learning Radiology - 9780323878173 | Elsevier Health. MEA Elsevier Health. Accessed March 3, 2024. https://www.mea.elsevierhealth.com/learning-radiology-9780323878173.html

97. Bastin ME, Le Roux P. On the application of a non-CPMG single-shot fast spin-echo sequence to diffusion tensor MRI of the human brain. *Magn Reson Med*. 2002;48(1):6-14. doi:10.1002/mrm.10214

98. Elster AD. Gradient-Echo MR Imaging: Techniques and Acronyms. *Radiology*. 1993;186(1):1-8. doi:10.1148/radiology.186.1.8416546.

99. Xu D, Henry RG, Mukherjee P, et al. Single-shot fast spin-echo diffusion tensor imaging of the brain and spine with head and phased array coils at 1.5 T and 3.0 T. *Magn Reson Imaging*. 2004;22(6):751-759. doi:10.1016/j.mri.2004.01.075

100. Basser PJ, Mattiello J, LeBihan D. MR diffusion tensor spectroscopy and imaging. *Biophys J*. 1994;66(1):259-267. doi:10.1016/S0006-3495(94)80775-1

101. Basser PJ, Mattiello J, LeBihan D. Estimation of the Effective Self-Diffusion Tensor from the NMR Spin Echo. *J Magn Reson B*. 1994;103(4):247-254. doi:doi: 10.1006/jmrb.1994.1037.

102. Basser PJ, LeBihant D. Fiber orientation mapping in an anisotropic medium with NMR diffusion spectroscopy.

103. Basser PJ, Zierler D. *Oral History Interview with Peter Basser*.

104. Moving Beyond DTI. In: *Introduction to Diffusion Tensor Imaging*. Elsevier; 2014:65-78. doi:10.1016/B978-0-12-398398-5.00008-4

105. Jones DK, Knösche TR, Turner R. White matter integrity, fiber count, and other fallacies: the do's and don'ts of diffusion MRI. *NeuroImage*. 2013;73:239-254. doi:10.1016/j.neuroimage.2012.06.081

106. Mathematics of Diffusion Tensor Imaging. In: *Introduction to Diffusion Tensor Imaging*. Elsevier; 2014:33-37. doi:10.1016/B978-0-12-398398-5.00005-9

107. Beauchamp N, Ulug A, Passe T, van Zijl P. MR Diffusion Imaging in Stroke: Review and Controversies. *Radiographics*. 1998;18:1269-1283.

108. Apparent Diffusion. Questions and Answers in MRI. Accessed March 3, 2024. http://mriquestions.com/apparent-diffusion.html

109. DTI. Questions and Answers in MRI. Accessed March 3, 2024. http://mriquestions.com/dti-tensor-imaging.html

110. Chary K, Manninen E, Claessens J, Ramirez-Manzanares A, Gröhn O, Sierra A. Diffusion MRI approaches for investigating microstructural complexity in a rat model of traumatic brain injury. *Sci Rep*. 2023;13(1):2219. doi:10.1038/s41598-023-29010-3

111. Chary K, Narvaez O, Salo RA, et al. Microstructural Tissue Changes in a Rat Model of Mild Traumatic Brain Injury. *Front Neurosci*. 2021;15:746214. doi:10.3389/fnins.2021.746214

112. TRACK-TBI Investigators. Transforming Research and Clinical Knowledge in Traumatic Brain Injury Clinical Protocol. Published online 18 2018. Accessed June 16, 2023. https://tracktbi.ucsf.edu/sites/tracktbi.ucsf.edu/files/TRACKTBI%20U01%20Clinical%20Protocol%20V18-January%2018%202019.pdf

113. TRACK-TBI Precision Medicine Neuroimaging MOP v1.1. Published online March 10, 2021.

114. Oishi K, ed. *MRI Atlas of Human White Matter*. 2. ed. Academic Press; 2011.

115. Palacios EM, Yuh EL, Mac Donald CL, et al. Diffusion Tensor Imaging Reveals Elevated Diffusivity of White Matter Microstructure that Is Independently Associated with Long-Term Outcome after Mild Traumatic Brain Injury: A TRACK-TBI Study. *J Neurotrauma*. 2022;39(19-20):1318-1328. doi:10.1089/neu.2021.0408

116. Zhang B, Daneshvar DH, Polich G, Glenn MB. Response to Machamer et al., "Symptom Frequency and Persistence in the First Year after Traumatic Brain Injury: A TRACK-TBI Study" (doi: 10.1089/neu.2021.0348). *J Neurotrauma*. 2023;40(5-6):595-596. doi:10.1089/neu.2022.0292

117. Chiang CW, Wang Y, Sun P, et al. Quantifying white matter tract diffusion parameters in the presence of increased extra-fiber cellularity and vasogenic edema. *NeuroImage*. 2014;101:310-319. doi:10.1016/j.neuroimage.2014.06.064

118. Chu Z, Wilde EA, Hunter JV, et al. Voxel-Based Analysis of Diffusion Tensor Imaging in Mild Traumatic Brain Injury in Adolescents. *Am J Neuroradiol*. 2010;31(2):340-346. doi:10.3174/ajnr.A1806

119. Wilde EA, McCauley SR, Hunter JV, et al. Diffusion tensor imaging of acute mild traumatic brain injury in adolescents. *Neurology*. 2008;70(12):948-955. doi:10.1212/01.wnl.0000305961.68029.54

120. Palacios EM, Owen JP, Yuh EL, et al. The evolution of white matter microstructural changes after mild traumatic brain injury: A longitudinal DTI and NODDI study. *Sci Adv*. 2020;6(32):eaaz6892. doi:10.1126/sciadv.aaz6892

121. Raffelt D, Crozier S, Connelly A, Salvado O, Tournier JD. Apparent Fibre Density: A New Measure for High Angular Resolution Diffusion-Weighted Image Analysis.

122. Wu YC, Mustafi SM, Harezlak J, Kodiweera C, Flashman LA, McAllister TW. Hybrid Diffusion Imaging in Mild Traumatic Brain Injury. *J Neurotrauma*. 2018;35(20):2377-2390. doi:10.1089/neu.2017.5566

123. Song SK, Sun SW, Ramsbottom MJ, Chang C, Russell J, Cross AH. Dysmyelination Revealed through MRI as Increased Radial (but Unchanged Axial) Diffusion of Water. *NeuroImage*. 2002;17(3):1429-1436. doi:10.1006/nimg.2002.1267

124. Song SK, Yoshino J, Le TQ, et al. Demyelination increases radial diffusivity in corpus callosum of mouse brain. *NeuroImage*. 2005;26(1):132-140. doi:10.1016/j.neuroimage.2005.01.028

125. Zhu DC, Covassin T, Nogle S, et al. A Potential Biomarker in Sports-Related Concussion: Brain Functional Connectivity Alteration of the Default-Mode Network Measured with Longitudinal Resting-State fMRI over Thirty Days. *J Neurotrauma*. 2015;32(5):327-341. doi:10.1089/neu.2014.3413

126. Raffelt DA, Smith RE, Ridgway GR, et al. Connectivity-based fixel enhancement: Whole-brain statistical analysis of diffusion MRI measures in the presence of crossing fibres. *NeuroImage*. 2015;117:40-55. doi:10.1016/j.neuroimage.2015.05.039

127. Winston GP. The physical and biological basis of quantitative parameters derived from diffusion MRI. *Quant Imaging Med Surg*. 2012;2(4). doi:10.3978/j.issn.2223-4292.2012.12.05

128. Jensen JH, Helpern JA, Ramani A, Lu H, Kaczynski K. Diffusional kurtosis imaging: The quantification of non-gaussian water diffusion by means of magnetic resonance imaging. *Magn Reson Med*. 2005;53(6):1432-1440. doi:10.1002/mrm.20508

129. Hansen B, Lund TE, Sangill R, Jespersen SN. Experimentally and computationally fast method for estimation of a mean kurtosis. *Magn Reson Med*. 2013;69(6):1754-1760. doi:10.1002/mrm.24743

130. Yan X, Zhou M, Ying L, et al. Evaluation of optimized b-value sampling schemas for diffusion kurtosis imaging with an application to stroke patient data. *Comput Med Imaging Graph*. 2013;37(4):272-280. doi:10.1016/j.compmedimag.2013.04.007

131. Steven AJ, Zhuo J, Melhem ER. Diffusion Kurtosis Imaging: An Emerging Technique for Evaluating the Microstructural Environment of the Brain. *Am J Roentgenol*. 2014;202(1):W26-W33. doi:10.2214/AJR.13.11365

132. Zhuo J, Xu S, Proctor JL, et al. Diffusion kurtosis as an in vivo imaging marker for reactive astrogliosis in traumatic brain injury. *NeuroImage*. 2012;59(1):467-477. doi:10.1016/j.neuroimage.2011.07.050

133. Jespersen SN, Kroenke CD, Østergaard L, Ackerman JJH, Yablonskiy DA. Modeling dendrite density from magnetic resonance diffusion measurements. *NeuroImage*. 2007;34(4):1473-1486. doi:10.1016/j.neuroimage.2006.10.037

134. Zhang H, Schneider T, Wheeler-Kingshott CA, Alexander DC. NODDI: Practical in vivo neurite orientation dispersion and density imaging of the human brain. *NeuroImage*. 2012;61(4):1000-1016. doi:10.1016/j.neuroimage.2012.03.072

135. Zhang H, Hubbard PL, Parker GJM, Alexander DC. Axon diameter mapping in the presence of orientation dispersion with diffusion MRI. *NeuroImage*. 2011;56(3):1301-1315. doi:10.1016/j.neuroimage.2011.01.084

136. Tournier JD, Calamante F, Connelly A. Robust determination of the fibre orientation distribution in diffusion MRI: Non-negativity constrained super-resolved spherical deconvolution. *NeuroImage*. 2007;35(4):1459-1472. doi:10.1016/j.neuroimage.2007.02.016

137. Raffelt D, Tournier JD, Fripp J, Crozier S, Connelly A, Salvado O. Symmetric diffeomorphic registration of fibre orientation distributions. *NeuroImage*. 2011;56(3):1171-1180. doi:10.1016/j.neuroimage.2011.02.014

138. Smith SM, Jenkinson M, Johansen-Berg H, et al. Tract-based spatial statistics: Voxelwise analysis of multi-subject diffusion data. *NeuroImage*. 2006;31(4):1487-1505. doi:10.1016/j.neuroimage.2006.02.024

139. Tournier JD, Calamante F, Connelly A. Improved probabilistic streamlines tractography by 2nd order integration over fibre orientation distributions.

140. Smith S, Nichols T. Threshold-free cluster enhancement: Addressing problems of smoothing, threshold dependence and localisation in cluster inference. *NeuroImage*. 2009;44(1):83-98. doi:10.1016/j.neuroimage.2008.03.061

141. Glenn GR, Kuo LW, Chao YP, Lee CY, Helpern JA, Jensen JH. Mapping the Orientation of White Matter Fiber Bundles: A Comparative Study of Diffusion Tensor Imaging, Diffusional Kurtosis Imaging, and Diffusion Spectrum Imaging. *Am J Neuroradiol*. 2016;37(7):1216-1222. doi:10.3174/ajnr.A4714

142. Grossman EJ, Ge Y, Jensen JH, et al. Thalamus and Cognitive Impairment in Mild Traumatic Brain Injury: A Diffusional Kurtosis Imaging Study. *J Neurotrauma*. 2012;29(13):2318-2327. doi:10.1089/neu.2011.1763

143. Stenberg J, Eikenes L, Moen KG, Vik A, Håberg AK, Skandsen T. Acute Diffusion Tensor and Kurtosis Imaging and Outcome following Mild Traumatic Brain Injury. *J Neurotrauma*. 2021;38(18):2560-2571. doi:10.1089/neu.2021.0074

144. Stenberg J, Skandsen T, Gøran Moen K, Vik A, Eikenes L, Håberg AK. Diffusion Tensor and Kurtosis Imaging Findings the First Year following Mild Traumatic Brain Injury. *J Neurotrauma*. 2023;40(5-6):457-471. doi:10.1089/neu.2022.0206

145. Lancaster MA, Meier TB, Olson DV, McCrea MA, Nelson LD, Muftuler LT. Chronic differences in white matter integrity following sport-related concussion as measured by diffusion MRI: 6-Month follow-up. *Hum Brain Mapp*. 2018;39(11):4276-4289. doi:10.1002/hbm.24245

146. Lancaster MA, Olson DV, McCrea MA, Nelson LD, LaRoche AA, Muftuler LT. Acute white matter changes following sport-related concussion: A serial diffusion tensor and diffusion kurtosis tensor imaging study. *Hum Brain Mapp*. 2016;37(11):3821-3834. doi:10.1002/hbm.23278

147. Muftuler LT, Meier TB, Keith M, Budde MD, Huber DL, McCrea MA. Serial Diffusion Kurtosis Magnetic Resonance Imaging Study during Acute, Subacute, and Recovery Periods after Sport-Related Concussion. *J Neurotrauma*. 2020;37(19):2081-2092. doi:10.1089/neu.2020.6993

148. Chung S, Chen J, Li T, Wang Y, Lui YW. Investigating Brain White Matter in Football Players with and without Concussion Using a Biophysical Model from Multishell Diffusion MRI. *Am J Neuroradiol*. 2022;43(6):823-828. doi:10.3174/ajnr.A7522

149. Brett BL, Koch KM, Muftuler LT, Budde M, McCrea MA, Meier TB. Association of Head Impact Exposure with White Matter Macrostructure and Microstructure Metrics. *J Neurotrauma*. 2021;38(4):474-484. doi:10.1089/neu.2020.7376

150. Stokum JA, Sours C, Zhuo J, Kane R, Shanmuganathan K, Gullapalli RP. A longitudinal evaluation of diffusion kurtosis imaging in patients with mild traumatic brain injury. *Brain Inj*. 2015;29(1):47-57. doi:10.3109/02699052.2014.947628

151. Wang ML, Wei XE, Yu MM, Li WB. Cognitive impairment in mild traumatic brain injury: a diffusion kurtosis imaging and volumetric study. *Acta Radiol*. 2022;63(4):504-512. doi:10.1177/0284185121998317

152. Næss-Schmidt ET, Blicher JU, Eskildsen SF, et al. Microstructural changes in the thalamus after mild traumatic brain injury: A longitudinal diffusion and mean kurtosis tensor MRI study. *Brain Inj*. 2017;31(2):230-236. doi:10.1080/02699052.2016.1229034

153. Grossman EJ, Jensen JH, Babb JS, et al. Cognitive Impairment in Mild Traumatic Brain Injury: A Longitudinal Diffusional Kurtosis and Perfusion Imaging Study. *AJNR Am J Neuroradiol*. 2013;34(5):951-957. doi:10.3174/ajnr.A3358

154. Gong NJ, Kuzminski S, Clark M, et al. Microstructural alterations of cortical and deep gray matter over a season of high school football revealed by diffusion kurtosis imaging. *Neurobiol Dis*. 2018;119:79-87. doi:10.1016/j.nbd.2018.07.020

155. Davenport EM, Apkarian K, Whitlow CT, et al. Abnormalities in Diffusional Kurtosis Metrics Related to Head Impact Exposure in a Season of High School Varsity Football. *J Neurotrauma*. 2016;33(23):2133-2146. doi:10.1089/neu.2015.4267

156. Goubran M, Mills BD, Georgiadis M, et al. Microstructural Alterations in Tract Development in College Football and Volleyball Players: A Longitudinal Diffusion MRI Study. *Neurology*. 2023;101(9). doi:10.1212/WNL.0000000000207543

157. Karlsen RH, Einarsen C, Moe HK, et al. Diffusion kurtosis imaging in mild traumatic brain injury and postconcussional syndrome. *J Neurosci Res*. 2019;97(5):568-581. doi:10.1002/jnr.24383

158. Churchill NW, Caverzasi E, Graham SJ, Hutchison MG, Schweizer TA. White matter during concussion recovery: Comparing diffusion tensor imaging (DTI) and neurite orientation dispersion and density imaging (NODDI). *Hum Brain Mapp*. 2019;40(6):1908-1918. doi:10.1002/hbm.24500

159. Mayer AR, Ling JM, Dodd AB, Meier TB, Hanlon FM, Klimaj SD. A prospective microstructure imaging study in mixed-martial artists using geometric measures and diffusion tensor imaging: methods and findings. *Brain Imaging Behav*. 2017;11(3):698-711. doi:10.1007/s11682-016-9546-1

160. Huang S, Huang C, Li M, Zhang H, Liu J. White Matter Abnormalities and Cognitive Deficit After Mild Traumatic Brain Injury: Comparing DTI, DKI, and NODDI. *Front Neurol*. 2022;13:803066. doi:10.3389/fneur.2022.803066

161. Oehr LE, Yang JYM, Chen J, Maller JJ, Seal ML, Anderson JFI. Investigating White Matter Tract Microstructural Changes at Six–Twelve Weeks following Mild Traumatic Brain Injury: A Combined Diffusion Tensor Imaging and Neurite Orientation Dispersion and Density Imaging Study. *J Neurotrauma*. 2021;38(16):2255-2263. doi:10.1089/neu.2020.7310

162. Shukla A, Ware AL, Guo S, et al. Examining brain white matter after pediatric mild traumatic brain injury using neurite orientation dispersion and density imaging: An A-CAP study. *NeuroImage Clin*. 2021;32:102887. doi:10.1016/j.nicl.2021.102887

163. Seider NA, Adeyemo B, Miller R, et al. Accuracy and reliability of diffusion imaging models. *NeuroImage*. 2022;254:119138. doi:10.1016/j.neuroimage.2022.119138

164. Mayer AR, Ling JM, Dodd AB, et al. Multicompartmental models and diffusion abnormalities in paediatric mild traumatic brain injury. *Brain*. 2022;145(11):4124-4137. doi:10.1093/brain/awac221

165. Harms RL, Fritz FJ, Tobisch A, Goebel R, Roebroeck A. Robust and fast nonlinear optimization of diffusion MRI microstructure models. *NeuroImage*. 2017;155:82-96. doi:10.1016/j.neuroimage.2017.04.064

166. Stein A, Vinh To X, Nasrallah FA, Barlow KM. Evidence of Ongoing Cerebral Microstructural Reorganization in Children With Persisting Symptoms Following Mild Traumatic Brain Injury: A NODDI DTI Analysis. *J Neurotrauma*. 2024;41(1-2):41-58. doi:10.1089/neu.2023.0196

167. Lima Santos JP, Kontos AP, Holland CL, et al. The role of sleep quality on white matter integrity and concussion symptom severity in adolescents. *NeuroImage Clin*. 2022;35:103130. doi:10.1016/j.nicl.2022.103130

168. Muller J, Middleton D, Alizadeh M, et al. Hybrid diffusion imaging reveals altered white matter tract integrity and associations with symptoms and cognitive dysfunction in chronic traumatic brain injury. *NeuroImage Clin*. 2021;30:102681. doi:10.1016/j.nicl.2021.102681

169. Anderson JFI, Oehr LE, Chen J, Maller JJ, Seal ML, Yang JYM. The relationship between cognition and white matter tract damage after mild traumatic brain injury in a premorbidly healthy, hospitalised adult cohort during the post-acute period. *Front Neurol*. 2023;14:1278908. doi:10.3389/fneur.2023.1278908

170. Kawata K, Steinfeldt JA, Huibregtse ME, et al. Association Between Proteomic Blood Biomarkers and DTI/NODDI Metrics in Adolescent Football Players: A Pilot Study. *Front Neurol*. 2020;11:581781. doi:10.3389/fneur.2020.581781

171. Farquharson S, Tournier JD, Calamante F, et al. White matter fiber tractography: why we need to move beyond DTI: Clinical article. *J Neurosurg*. 2013;118(6):1367-1377. doi:10.3171/2013.2.JNS121294

172. Mohammadian M, Roine T, Hirvonen J, et al. High angular resolution diffusion-weighted imaging in mild traumatic brain injury. *NeuroImage Clin*. 2016;13:174-180. doi:10.1016/j.nicl.2016.11.016

173. Van Der Horn HJ, Kok JG, De Koning ME, et al. Altered Wiring of the Human Structural Connectome in Adults with Mild Traumatic Brain Injury. *J Neurotrauma*. 2017;34(5):1035-1044. doi:10.1089/neu.2016.4659

174. Wallace EJ, Mathias JL, Ward L, Fripp J, Rose S, Pannek K. A fixel-based analysis of micro- and macro-structural changes to white matter following adult traumatic brain injury. *Hum Brain Mapp*. 2020;41(8):2187-2197. doi:10.1002/hbm.24939

175. Winston GP. The physical and biological basis of quantitative parameters derived from diffusion MRI. *Quant Imaging Med Surg*. 2012;2(4):254-265. doi:10.1093/cercor/bhab095

176. Mito R, Parker DM, Abbott DF, Makdissi M, Pedersen M, Jackson GD. White matter abnormalities characterize the acute stage of sports-related mild traumatic brain injury. *Brain Commun*. 2022;4(4):fcac208. doi:10.1093/braincomms/fcac208

177. Bach M, Laun FB, Leemans A, et al. Methodological considerations on tract-based spatial statistics (TBSS). *NeuroImage*. 2014;100:358-369. doi:10.1016/j.neuroimage.2014.06.021

178. Kelley S, Plass J, Bender AR, Polk TA. Age-Related Differences in White Matter: Understanding Tensor-Based Results Using Fixel-Based Analysis. *Cereb Cortex N Y NY*. 2021;31(8):3881-3898. doi:10.1093/cercor/bhab056

179. Daducci A, Canales-Rodríguez EJ, Zhang H, Dyrby TB, Alexander DC, Thiran JP. Accelerated Microstructure Imaging via Convex Optimization (AMICO) from diffusion MRI data. *NeuroImage*. 2015;105:32-44. doi:10.1016/j.neuroimage.2014.10.026

180. Faiyaz A, Doyley M, Schifitto G, Zhong J, Uddin MN. Single-shell NODDI using dictionary-learner-estimated isotropic volume fraction. *NMR Biomed*. 2022;35(2):e4628. doi:10.1002/nbm.4628

181. Mikula S, Binding J, Denk W. Staining and embedding the whole mouse brain for electron microscopy. *Nat Methods*. 2012;9(12):1198-1201. doi:10.1038/nmeth.2213

182. Jeurissen B, Leemans A, Tournier J, Jones DK, Sijbers J. Investigating the prevalence of complex fiber configurations in white matter tissue with diffusion magnetic resonance imaging. *Hum Brain Mapp*. 2013;34(11):2747-2766. doi:10.1002/hbm.22099

183. Schilling KG, Tax CMW, Rheault F, et al. Prevalence of white matter pathways coming into a single white matter voxel orientation: The bottleneck issue in tractography. *Hum Brain Mapp*. 2022;43(4):1196-1213. doi:10.1002/hbm.25697

184. Gazdzinski LM, Mellerup M, Wang T, et al. White Matter Changes Caused by Mild Traumatic Brain Injury in Mice Evaluated Using Neurite Orientation Dispersion and Density Imaging. *J Neurotrauma*. 2020;37(16):1818-1828. doi:10.1089/neu.2020.6992

185. McCunn P, Xu X, Moszczynski A, Li A, Brown A, Bartha R. Neurite orientation dispersion and density imaging in a rodent model of acute mild traumatic brain injury. *J Neuroimaging*. 2021;31(5):879-892. doi:10.1111/jon.12917

186. Valera EM, Joseph ALC, Snedaker K, et al. Understanding Traumatic Brain Injury in Females: A State-of-the-Art Summary and Future Directions. *J Head Trauma Rehabil*. 2021;36(1):E1-E17. doi:10.1097/HTR.0000000000000652

187. Levin HS, Temkin NR, Barber J, et al. Association of Sex and Age With Mild Traumatic Brain Injury–Related Symptoms: A TRACK-TBI Study. *JAMA Netw Open*. 2021;4(4):e213046. doi:10.1001/jamanetworkopen.2021.3046

188. Wickwire EM, Albrecht JS, Capaldi VF, et al. Trajectories of Insomnia in Adults After Traumatic Brain Injury. *JAMA Netw Open*. 2022;5(1):e2145310. doi:10.1001/jamanetworkopen.2021.45310

189. Næss-Schmidt ET, Blicher JU, Tietze A, et al. Diffusion MRI findings in patients with extensive and minimal post-concussion symptoms after mTBI and healthy controls: a cross sectional study. *Brain Inj*. 2018;32(1):91-98. doi:10.1080/02699052.2017.1377352

190. Tallus J, Mohammadian M, Kurki T, Roine T, Posti JP, Tenovuo O. A comparison of diffusion tensor imaging tractography and constrained spherical deconvolution with automatic segmentation in traumatic brain injury. *NeuroImage Clin*. 2023;37:103284. doi:10.1016/j.nicl.2022.103284

191. Roine T, Mohammadian M, Hirvonen J, et al. Structural Brain Connectivity Correlates with Outcome in Mild Traumatic Brain Injury. *J Neurotrauma*. 2022;39(5-6):336-347. doi:10.1089/neu.2021.0093

192. Thompson HJ, Vavilala MS, Rivara FP. Common Data Elements and Federal Interagency Traumatic Brain Injury Research Informatics System for TBI Research. *Annu Rev Nurs Res*. 2015;33(1):1-11. doi:10.1891/0739-6686.33.1

193. Jeurissen B, Tournier JD, Dhollander T, Connelly A, Sijbers J. Multi-tissue constrained spherical deconvolution for improved analysis of multi-shell diffusion MRI data. *NeuroImage*. 2014;103:411-426. doi:10.1016/j.neuroimage.2014.07.061

194. Genc S, Tax CMW, Raven EP, Chamberland M, Parker GD, Jones DK. Impact of b-value on estimates of apparent fibre density. *Hum Brain Mapp*. 2020;41(10):2583-2595. doi:10.1002/hbm.24964

195. Calamuneri A, Arrigo A, Mormina E, et al. White Matter Tissue Quantification at Low b-Values Within Constrained Spherical Deconvolution Framework. *Front Neurol*. 2018;9. Accessed November 16, 2023. https://www.frontiersin.org/articles/10.3389/fneur.2018.00716

196. Newman BT, Dhollander T, Reynier KA, Panzer MB, Druzgal TJ. Test-retest reliability and long-term stability of 3-tissue constrained spherical deconvolution methods for analyzing diffusion MRI data. *Magn Reson Med*. 2020;84(4):2161-2173. doi:10.1002/mrm.28242

197. Genc S, Smith RE, Malpas CB, et al. Development of white matter fibre density and morphology over childhood: A longitudinal fixel-based analysis. *NeuroImage*. 2018;183:666-676. doi:10.1016/j.neuroimage.2018.08.043

198. Schilling KG, Blaber J, Huo Y, et al. Synthesized b0 for diffusion distortion correction (Synb0-DisCo). *Magn Reson Imaging*. 2019;64:62-70. doi:10.1016/j.mri.2019.05.008

199. Dhollander T, Mito R, Raffelt D, Connelly A. Improved white matter response function estimation for 3-tissue constrained spherical deconvolution. Published online 2019.

200. Dhollander T, Raffelt D, Connelly A. Unsupervised 3-tissue response function estimation from single-shell or multi-shell diffusion MR data without a co-registered T1 image. Published online 2016.

201. Raffelt D, Tournier JD, Fripp J, Crozier S, Connelly A, Salvado O. Symmetric diffeomorphic registration of fibre orientation distributions. Neuroimage. 2011 Jun 1;56(3):1171-80. doi: 10.1016/j.neuroimage.2011.02.014. Epub 2011 Feb 18. PMID: 21316463.

202. Raffelt D, Tournier J, Crozier S, Connelly A, Salvado O. Reorientation of fiber orientation distributions using apodized point spread functions. *Magn Reson Med*. 2012;67(3):844-855. doi:10.1002/mrm.23058

203. Raffelt D, Tournier JD, Rose S, et al. Apparent Fibre Density: A novel measure for the analysis of diffusion-weighted magnetic resonance images. *NeuroImage*. 2012;59(4):3976-3994. doi:10.1016/j.neuroimage.2011.10.045

204. Raffelt DA, Tournier JD, Smith RE, et al. Investigating white matter fibre density and morphology using fixel-based analysis. *NeuroImage*. 2017;144:58-73. doi:10.1016/j.neuroimage.2016.09.029

205. Gardner RC, Yaffe K. Epidemiology of mild traumatic brain injury and neurodegenerative disease. *Mol Cell Neurosci*. 2015;66:75-80. doi:10.1016/j.mcn.2015.03.001

206. Rao DP, McFaull S, Thompson W, Jayaraman GC. Trends in self-reported traumatic brain injury among Canadians, 2005-2014: a repeated cross-sectional analysis. *CMAJ Open*. 2017;5(2):E301-E307. doi:10.9778/cmajo.20160115

207. Panwar J, Hsu CCT, Tator CH, Mikulis D. Magnetic Resonance Imaging Criteria for Post-Concussion Syndrome: A Study of 127 Post-Concussion Syndrome Patients. *J Neurotrauma*. 2020;37(10):1190-1196. doi:10.1089/neu.2019.6809

208. Isokuortti H, Iverson GL, Silverberg ND, et al. Characterizing the type and location of intracranial abnormalities in mild traumatic brain injury. *J Neurosurg*. 2018;129(6):1588-1597. doi:10.3171/2017.7.JNS17615

209. Huang W, Hu W, Zhang P, et al. Early Changes in the White Matter Microstructure and Connectome Underlie Cognitive Deficit and Depression Symptoms After Mild Traumatic Brain Injury. *Front Neurol*. 2022;13:880902. doi:10.3389/fneur.2022.880902

210. Dean PJA, Sato JR, Vieira G, McNamara A, Sterr A. Long-term structural changes after mTBI and their relation to post-concussion symptoms. *Brain Inj*. 2015;29(10):1211-1218. doi:10.3109/02699052.2015.1035334

211. Boonstra FM, Clough M, Strik M, et al. Longitudinal tracking of axonal loss using diffusion magnetic resonance imaging in multiple sclerosis. *Brain Commun*. 2022;4(2):fcac065. doi:10.1093/braincomms/fcac065

212. Petersen M, Frey BM, Mayer C, et al. Fixel based analysis of white matter alterations in early stage cerebral small vessel disease. *Sci Rep*. 2022;12(1):1581. doi:10.1038/s41598-022-05665-2

213. Meisler SL, Gabrieli JD. Fiber-specific structural properties relate to reading skills in children and adolescents. *eLife*. 2022;11:e82088. doi:10.7554/eLife.82088

214. Wright DK, Symons GF, O'Brien WT, et al. Diffusion Imaging Reveals Sex Differences in the White Matter Following Sports-Related Concussion. *Cereb Cortex*. 2021;31(10):4411-4419. doi:10.1093/cercor/bhab095

215. Wallace EJ, Mathias JL, Ward L, Fripp J, Rose S, Pannek K. A fixel-based analysis of micro- and macro-structural changes to white matter following adult traumatic brain injury. *Hum Brain Mapp*. 2020;41(8):2187-2197. doi:10.1002/hbm.24939

216. Wasserthal J, Neher P, Maier-Hein KH. TractSeg - Fast and accurate white matter tract segmentation. *NeuroImage*. 2018;183:239-253. doi:10.1016/j.neuroimage.2018.07.070

217. Rohlfing T. Incorrect ICBM-DTI-81 atlas orientation and white matter labels. *Front Neurosci*. 2013;7. doi:10.3389/fnins.2013.00004

218. Chang YS, Owen JP, Pojman NJ, et al. White Matter Changes of Neurite Density and Fiber Orientation Dispersion during Human Brain Maturation. Gong G, ed. *PLOS ONE*. 2015;10(6):e0123656. doi:10.1371/journal.pone.0123656

219. Henschel L, Conjeti S, Estrada S, Diers K, Fischl B, Reuter M. FastSurfer - A fast and accurate deep learning based neuroimaging pipeline. *NeuroImage*. 2020;219:117012. doi:10.1016/j.neuroimage.2020.117012

220. Behrens TEJ, Woolrich MW, Jenkinson M, et al. Characterization and propagation of uncertainty in diffusion-weighted MR imaging. *Magn Reson Med*. 2003;50(5):1077-1088. doi:10.1002/mrm.10609

221. Behrens TEJ, Berg HJ, Jbabdi S, Rushworth MFS, Woolrich MW. Probabilistic diffusion tractography with multiple fibre orientations: What can we gain? *NeuroImage*. 2007;34(1):144-155. doi:10.1016/j.neuroimage.2006.09.018

222. Jbabdi S, Sotiropoulos SN, Savio AM, Graña M, Behrens TEJ. Model-based analysis of multishell diffusion MR data for tractography: How to get over fitting problems. *Magn Reson Med*. 2012;68(6):1846-1855. doi:10.1002/mrm.24204

223. Smith RE, Tournier JD, Calamante F, Connelly A. SIFT: Spherical-deconvolution informed filtering of tractograms. *NeuroImage*. 2013;67:298-312. doi:10.1016/j.neuroimage.2012.11.049

224. Smith R, Christiaens D, Jeurissen B, et al. On false positive control in Fixel-Based Analysis. *Proc Intl Soc Mag Reson Med*. Published online 2021.

225. Smith RE, Dhollander T, Connelly A. On the regression of intracranial volume in Fixel-Based Analysis.

226. MATLAB 2022b, The MathWorks, Inc., Natick, Massachusetts, United States.

227. Storey JD. A Direct Approach to False Discovery Rates. *J R Stat Soc Ser B Stat Methodol*. 2002;64(3):479-498. doi:10.1111/1467-9868.00346

228. Taylor CA, Bell JM, Breiding MJ, Xu L. Traumatic Brain Injury–Related Emergency Department Visits, Hospitalizations, and Deaths — United States, 2007 and 2013. *MMWR Surveill Summ*. 2017;66(9):1-16. doi:10.15585/mmwr.ss6609a1

229. Centers for Disease Control and Prevention. (2018). Report to Congress: The Management of Traumatic Brain Injury in Children, National Center for Injury Prevention and Control; Division of Unintentional Injury Prevention. Atlanta, GA.

230. Muftuler LT, Meier TB, Keith M, Budde MD, Huber DL, McCrea MA. Serial Diffusion Kurtosis Magnetic Resonance Imaging Study during Acute, Subacute, and Recovery Periods after Sport-Related Concussion. *J Neurotrauma*. 2020;37(19):2081-2092. doi:10.1089/neu.2020.6993

231. Slobounov SM, Walter A, Breiter HC, et al. The effect of repetitive subconcussive collisions on brain integrity in collegiate football players over a single football season: A multi-modal neuroimaging study. *NeuroImage Clin*. 2017;14:708-718. doi:10.1016/j.nicl.2017.03.006

232. Ooi LQR, Orban C, Nichols T, et al. *MRI Economics: Balancing Sample Size and Scan Duration in Brain Wide Association Studies*. Neuroscience; 2024. doi:10.1101/2024.02.16.580448

233. Scarpazza C, Ha M, Baecker L, et al. Translating research findings into clinical practice: a systematic and critical review of neuroimaging-based clinical tools for brain disorders. *Transl Psychiatry*. 2020;10(1):107. doi:10.1038/s41398-020-0798-6

234. Wintermark M, Colen R, Whitlow CT, Zaharchuk G. The vast potential and bright future of neuroimaging. *Br J Radiol*. Published online June 6, 2018:20170505. doi:10.1259/bjr.20170505

235. Echemendia RJ, Meeuwisse W, McCrory P, et al. The Sport Concussion Assessment Tool 5th Edition (SCAT5). *Br J Sports Med*. Published online April 26, 2017:bjsports-2017-097506. doi:10.1136/bjsports-2017-097506

236. Dienes Z. Bayesian Versus Orthodox Statistics: Which Side Are You On? *Perspect Psychol Sci*. 2011;6(3):274-290. doi:10.1177/1745691611406920

237. Afzali M, Pieciak T, Newman S, et al. The sensitivity of diffusion MRI to microstructural properties and experimental factors. *J Neurosci Methods*. 2021;347:108951. doi:10.1016/j.jneumeth.2020.108951

238. Setsompop K, Kimmlingen R, Eberlein E, et al. Pushing the limits of in vivo diffusion MRI for the Human Connectome Project. *NeuroImage*. 2013;80:220-233. doi:10.1016/j.neuroimage.2013.05.078

239. Bennett CM, Wolford GL, Miller MB. The principled control of false positives in neuroimaging. *Soc Cogn Affect Neurosci*. 2009;4(4):417-422. doi:10.1093/scan/nsp053

240. Mohammed FN, Master CL, Arbogast KB, et al. Disparities in Adherence to Concussion Clinical Care Recommendations in a Pediatric Population. *J Head Trauma Rehabil*. 2023;38(2):147-155. doi:10.1097/HTR.0000000000000823

241. Seabury SA, Gaudette É, Goldman DP, et al. Assessment of Follow-up Care After Emergency Department Presentation for Mild Traumatic Brain Injury and Concussion: Results From the TRACK-TBI Study. *JAMA Netw Open*. 2018;1(1):e180210. doi:10.1001/jamanetworkopen.2018.0210

242. Merritt VC, Padgett CR, Jak AJ. A systematic review of sex differences in concussion outcome: What do we know? *Clin Neuropsychol*. 2019;33(6):1016-1043. doi:10.1080/13854046.2018.1508616

243. Wiederschain GYa. Data mining techniques for the life sciences: (Olivero Carugo and Frank Eisenhaber (eds.), in Series "Springer Protocols. Methods in Molecular Biology", Vol. 609, Humana Press, 2010, 407 p., $110). *Biochem Mosc*. 2011;76(4):494-494. doi:10.1134/S0006297911040158

244. Vakil E, Blachstein H. Rey auditory-verbal learning test: Structure analysis. *J Clin Psychol*. 1993;49(6):883-890. doi:10.1002/1097-4679(199311)49:6<883::AID-JCLP2270490616>3.0.CO;2-6

245. Huettel SA, Song AW, McCarthy G. *Functional Magnetic Resonance Imaging*. Sinauer Associates, Publishers; 2009.

246. Kochanek PM, Hendrich KS, Dixon CE, Schiding JK, Williams DS, Ho C. Cerebral Blood Flow at One Year after Controlled Cortical Impact in Rats: Assessment by Magnetic Resonance Imaging. *J Neurotrauma*. 2002;19(9):1029-1037. doi:10.1089/089771502760341947

247. Hendrich KS, Kochanek PM, Williams DS, Schiding JK, Marion DW, Ho C. Early perfusion after controlled cortical impact in rats: Quantification by arterial spin-labeled MRI and the influence of spin-lattice relaxation time heterogeneity. *Magn Reson Med*. 1999;42(4):673-681. doi:10.1002/(SICI)1522-2594(199910)42:4<673::AID-MRM8>3.0.CO;2-B

248. DeWitt DS, Prough DS. Traumatic Cerebral Vascular Injury: The Effects of Concussive Brain Injury on the Cerebral Vasculature. *J Neurotrauma*. 2003;20(9):795-825. doi:10.1089/089771503322385755

249. Meier TB, Bellgowan PSF, Singh R, Kuplicki R, Polanski DW, Mayer AR. Recovery of Cerebral Blood Flow Following Sports-Related Concussion. *JAMA Neurol*. 2015;72(5):530. doi:10.1001/jamaneurol.2014.4778

250. Kong L, Qiu S, Chen Y, et al. Assessment of vibration modulated regional cerebral blood flow with MRI. *NeuroImage*. 2023;269:119934. doi:10.1016/j.neuroimage.2023.119934

251. Wang Y, Nencka AS, Meier TB, et al. Cerebral blood flow in acute concussion: preliminary ASL findings from the NCAA-DoD CARE consortium. *Brain Imaging Behav*. 2019;13(5):1375-1385. doi:10.1007/s11682-018-9946-5

252. Brett BL, Cohen AD, McCrea MA, Wang Y. Longitudinal alterations in cerebral perfusion following a season of adolescent contact sport participation compared to non-contact athletes. *NeuroImage Clin*. 2023;40:103538. doi:10.1016/j.nicl.2023.103538

253. Wang Y, Bartels HM, Nelson LD. A Systematic Review of ASL Perfusion MRI in Mild TBI. *Neuropsychol Rev*. 2023;33(1):160-191. doi:10.1007/s11065-020-09451-7

254. Ramsey S, Willke R, Briggs A, et al. Good Research Practices for Cost-Effectiveness Analysis Alongside Clinical Trials: The ISPOR RCT-CEA Task Force Report. *Value Health*. 2005;8(5):521-533. doi:10.1111/j.1524-4733.2005.00045.x

255. Chen WL, Wagner J, Heugel N, et al. Functional Near-Infrared Spectroscopy and Its Clinical Application in the Field of Neuroscience: Advances and Future Directions. *Front Neurosci*. 2020;14:724. doi:10.3389/fnins.2020.00724

256. Tsow F, Kumar A, Hosseini SH, Bowden A. A low-cost, wearable, do-it-yourself functional near-infrared spectroscopy (DIY-fNIRS) headband. *HardwareX*. 2021;10:e00204. doi:10.1016/j.ohx.2021.e00204

257. Helmich I, Saluja RS, Lausberg H, et al. Persistent Postconcussive Symptoms Are Accompanied by Decreased Functional Brain Oxygenation. *J Neuropsychiatry Clin Neurosci*. 2015;27(4):287-298. doi:10.1176/appi.neuropsych.14100276

258. Grijalva C, Mullins VA, Michael BR, et al. Neuroimaging, wearable sensors, and blood-based biomarkers reveal hyperacute changes in the brain after sub-concussive impacts. *Brain Multiphysics*. 2023;5:100086. doi:10.1016/j.brain.2023.100086

APPENDIX

Joint Caption for Appendix Tables A.1-14- All tables are t-test results for comparisons of the automatically segmented tracts from TractSeg between mTBI and control subjects.

Joint Caption for Appendix Figures A.1-94 – All figures are boxplots representing significant comparisons from appendix tables 1-14. Boxplots are colored green if the false discovery rate corrected q-value was $q<0.05$, and otherwise appear black. Titles are the matching abbreviated TractSeg labels from Tables 1-14, with the abbreviated metric being compared. Y-labels indicate the signal representation or modelling technique used to derive the metric and the full name of the metric as in the abbreviated title. The results from 2-week timepoint (P1), 6-month timepoint (P2) are arranged with P1 on the left and P2 on the right.

Joint Caption for Appendix Tables A.15-25- All tables are t-test results for comparisons of the automatically segmented tracts from TractSeg between timepoints within mTBI and control subject groups.

Table A.1 Results of Post Hoc Tract Specific Comparisons of Diffusion Tensor Imaging Fractional Anisotropy

	mTBI		Controls		Percent Change					
TractSeg Abbv.	P1	P2	P1	P2	mTBI	Controls	t-score P1	q-value P1′	t-score P2	q-value P2′
AF_left	0.256 ± 0.013	0.256 ± 0.011	0.259 ± 0.019	0.260 ± 0.016	-0.12 %	0.41 %	-0.716	0.875	-1.238	0.472
AF_right	0.267 ± 0.011	0.266 ± 0.013	0.263 ± 0.016	0.261 ± 0.026	-0.45 %	-0.64 %	1.248	0.875	1.053	0.472
ATR_left	0.271 ± 0.011	0.271 ± 0.012	0.278 ± 0.020	0.280 ± 0.019	-0.03 %	0.74 %	-1.926	0.494	-2.521	0.271
ATR_right	0.263 ± 0.010	0.264 ± 0.012	0.266 ± 0.016	0.269 ± 0.018	0.3 %	1.3 %	-0.844	0.875	-1.418	0.472
CA	0.270 ± 0.017	0.267 ± 0.022	0.287 ± 0.024	0.286 ± 0.030	-1.11 %	-0.4 %	-3.227	0.119	-2.827	0.237
CC_1	0.343 ± 0.023	0.336 ± 0.032	0.351 ± 0.023	0.343 ± 0.056	-1.88 %	-2.17 %	-1.195	0.875	-0.613	0.472
CC_2	0.296 ± 0.014	0.295 ± 0.013	0.298 ± 0.023	0.298 ± 0.025	-0.27 %	-0.03 %	-0.411	0.917	-0.560	0.472
CC_3	0.291 ± 0.017	0.290 ± 0.021	0.295 ± 0.035	0.295 ± 0.034	-0.47 %	0.16 %	-0.615	0.916	-0.831	0.472
CC_4	0.307 ± 0.018	0.305 ± 0.019	0.305 ± 0.032	0.307 ± 0.031	-0.63 %	0.83 %	0.386	0.917	-0.341	0.478
CC_5	0.318 ± 0.017	0.314 ± 0.020	0.313 ± 0.033	0.315 ± 0.035	-1.12 %	0.6 %	0.742	0.875	-0.128	0.525
CC_6	0.301 ± 0.016	0.300 ± 0.015	0.295 ± 0.023	0.293 ± 0.026	-0.25 %	-0.57 %	1.234	0.875	1.435	0.472
CC_7	0.308 ± 0.015	0.306 ± 0.016	0.304 ± 0.014	0.297 ± 0.037	-0.57 %	-2.3 %	0.797	0.875	1.401	0.472
CC	0.298 ± 0.013	0.297 ± 0.013	0.296 ± 0.022	0.294 ± 0.025	-0.27 %	-0.43 %	0.429	0.917	0.522	0.472
CG_left	0.278 ± 0.017	0.281 ± 0.021	0.279 ± 0.023	0.277 ± 0.027	1.02 %	-0.92 %	-0.180	0.922	0.704	0.472
CG_right	0.282 ± 0.019	0.283 ± 0.016	0.280 ± 0.025	0.277 ± 0.025	0.27 %	-1 %	0.457	0.917	1.241	0.472
CST_left	0.344 ± 0.014	0.345 ± 0.016	0.347 ± 0.025	0.351 ± 0.024	0.46 %	1.16 %	-0.557	0.916	-1.022	0.472
CST_right	0.352 ± 0.013	0.351 ± 0.017	0.350 ± 0.025	0.350 ± 0.031	-0.08 %	-0.01 %	0.385	0.917	0.262	0.485
FPT_left	0.333 ± 0.014	0.335 ± 0.015	0.334 ± 0.027	0.336 ± 0.027	0.52 %	0.65 %	-0.263	0.921	-0.345	0.478
FPT_right	0.333 ± 0.013	0.333 ± 0.014	0.331 ± 0.023	0.335 ± 0.025	0 %	1.01 %	0.250	0.921	-0.472	0.472
FX_left	0.288 ± 0.046	0.281 ± 0.045	0.295 ± 0.047	0.291 ± 0.055	-2.34 %	-1.51 %	-0.510	0.917	-0.683	0.472
FX_right	0.294 ± 0.045	0.289 ± 0.049	0.294 ± 0.048	0.300 ± 0.052	-1.54 %	1.95 %	-0.051	0.924	-0.784	0.472
ICP_left	0.275 ± 0.025	0.273 ± 0.030	0.260 ± 0.029	0.263 ± 0.044	-0.62 %	1.02 %	1.956	0.494	1.079	0.472
ICP_right	0.258 ± 0.016	0.255 ± 0.017	0.242 ± 0.025	0.248 ± 0.031	-1.4 %	2.42 %	3.021	0.119	1.155	0.472
IFO_left	0.283 ± 0.011	0.281 ± 0.011	0.285 ± 0.013	0.279 ± 0.029	-0.51 %	-1.94 %	-0.652	0.9	0.417	0.473
IFO_right	0.281 ± 0.010	0.279 ± 0.012	0.281 ± 0.011	0.279 ± 0.027	-0.47 %	-0.63 %	-0.005	0.94	0.094	0.532
ILF_left	0.277 ± 0.011	0.275 ± 0.017	0.283 ± 0.012	0.274 ± 0.032	-0.7 %	-3.15 %	-1.777	0.603	0.213	0.493
ILF_right	0.273 ± 0.011	0.272 ± 0.019	0.278 ± 0.013	0.272 ± 0.033	-0.66 %	-2.31 %	-1.376	0.875	0.005	0.541
MCP	0.301 ± 0.015	0.299 ± 0.016	0.291 ± 0.029	0.291 ± 0.037	-0.87 %	0.02 %	1.934	0.494	1.242	0.472

Table A.1 (cont'd)

	mTBI		Controls		Percent Change					
TractSeg Abbv	P1	P2	P1	P2	mTBI	Controls	t-score P1	q-value P1	t-score P2	q-value P2
MLF_left	0.265 ± 0.014	0.266 ± 0.014	0.262 ± 0.018	0.264 ± 0.016	0.39 %	0.57 %	0.585	0.916	0.512	0.472
MLF_right	0.272 ± 0.013	0.271 ± 0.014	0.266 ± 0.020	0.264 ± 0.023	-0.35 %	-0.71 %	1.480	0.875	1.569	0.472
OR_left	0.293 ± 0.014	0.292 ± 0.014	0.294 ± 0.009	0.289 ± 0.035	-0.43 %	-1.73 %	-0.221	0.921	0.525	0.472
OR_right	0.300 ± 0.013	0.300 ± 0.015	0.300 ± 0.015	0.297 ± 0.026	-0.26 %	-0.99 %	0.225	0.921	0.623	0.472
POPT_left	0.313 ± 0.013	0.313 ± 0.015	0.309 ± 0.022	0.311 ± 0.022	0.14 %	0.84 %	0.988	0.875	0.436	0.472
POPT_right	0.327 ± 0.012	0.326 ± 0.016	0.323 ± 0.023	0.325 ± 0.024	-0.16 %	0.52 %	0.767	0.875	0.228	0.493
SCP_left	0.313 ± 0.019	0.313 ± 0.023	0.308 ± 0.026	0.315 ± 0.034	-0.01 %	2.26 %	0.778	0.875	-0.323	0.478
SCP_right	0.313 ± 0.013	0.311 ± 0.015	0.302 ± 0.029	0.310 ± 0.028	-0.66 %	2.62 %	2.078	0.494	0.077	0.532
SLF_III_left	0.264 ± 0.015	0.262 ± 0.016	0.263 ± 0.028	0.266 ± 0.022	-0.76 %	1.03 %	0.183	0.922	-0.774	0.472
SLF_III_right	0.273 ± 0.012	0.270 ± 0.020	0.263 ± 0.020	0.259 ± 0.038	-1.15 %	-1.43 %	2.566	0.281	1.587	0.472
SLF_II_left	0.250 ± 0.015	0.253 ± 0.016	0.249 ± 0.022	0.255 ± 0.027	1.16 %	2.16 %	0.107	0.922	-0.371	0.478
SLF_II_right	0.252 ± 0.014	0.253 ± 0.016	0.247 ± 0.021	0.249 ± 0.018	0.5 %	0.96 %	1.145	0.875	0.873	0.472
SLF_I_left	0.243 ± 0.014	0.245 ± 0.018	0.238 ± 0.028	0.239 ± 0.023	1 %	0.68 %	0.990	0.875	1.093	0.472
SLF_I_right	0.257 ± 0.014	0.259 ± 0.019	0.252 ± 0.027	0.256 ± 0.022	0.97 %	1.65 %	0.913	0.875	0.556	0.472
STR_left	0.335 ± 0.017	0.336 ± 0.019	0.338 ± 0.024	0.338 ± 0.035	0.47 %	0.18 %	-0.568	0.916	-0.303	0.478
STR_right	0.339 ± 0.016	0.339 ± 0.020	0.339 ± 0.027	0.344 ± 0.023	-0.13 %	1.42 %	0.098	0.922	-0.825	0.472
ST_FO_left	0.285 ± 0.017	0.281 ± 0.018	0.295 ± 0.016	0.295 ± 0.033	-1.41 %	0.09 %	-2.075	0.494	-2.306	0.313
ST_FO_right	0.290 ± 0.017	0.288 ± 0.020	0.294 ± 0.016	0.293 ± 0.037	-0.75 %	-0.36 %	-0.852	0.875	-0.743	0.472
ST_OCC_left	0.294 ± 0.014	0.293 ± 0.013	0.294 ± 0.013	0.289 ± 0.036	-0.33 %	-1.62 %	0.050	0.924	0.702	0.472

Table A.1 (cont'd)

	mTBI		Controls		Percent Change					
TractSeg Abbv	P1	P2	P1	P2	mTBI	Controls	t-score P1	q-value P1	t-score P2	q-value P2
ST_PAR_left	0.280 ± 0.012	0.282 ± 0.016	0.278 ± 0.019	0.279 ± 0.018	0.46 %	0.68 %	0.668	0.9	0.462	0.472
ST_PAR_right	0.296 ± 0.012	0.295 ± 0.015	0.292 ± 0.019	0.293 ± 0.020	-0.22 %	0.21 %	0.938	0.875	0.540	0.472
ST_POSTC_left	0.291 ± 0.014	0.292 ± 0.018	0.292 ± 0.019	0.296 ± 0.015	0.42 %	1.2 %	-0.305	0.921	-0.744	0.472
ST_POSTC_right	0.308 ± 0.014	0.306 ± 0.020	0.307 ± 0.022	0.308 ± 0.023	-0.5 %	0.62 %	0.245	0.921	-0.402	0.473
ST_PREC_left	0.295 ± 0.012	0.296 ± 0.015	0.300 ± 0.019	0.301 ± 0.017	0.59 %	0.61 %	-1.189	0.875	-1.106	0.472
ST_PREC_right	0.305 ± 0.012	0.305 ± 0.017	0.305 ± 0.019	0.307 ± 0.019	-0.07 %	0.81 %	0.132	0.922	-0.447	0.472
ST_PREF_left	0.285 ± 0.012	0.286 ± 0.011	0.289 ± 0.020	0.288 ± 0.020	0.38 %	-0.36 %	-1.111	0.875	-0.597	0.472
ST_PREF_right	0.283 ± 0.010	0.283 ± 0.011	0.284 ± 0.014	0.286 ± 0.019	-0.05 %	0.68 %	-0.292	0.921	-0.814	0.472
ST_PREM_left	0.272 ± 0.011	0.274 ± 0.011	0.275 ± 0.022	0.277 ± 0.018	0.65 %	0.5 %	-0.736	0.875	-0.697	0.472
ST_PREM_right	0.285 ± 0.011	0.285 ± 0.013	0.285 ± 0.021	0.285 ± 0.024	0.24 %	0.16 %	-0.044	0.924	0.012	0.541
T_OCC_left	0.289 ± 0.013	0.288 ± 0.014	0.291 ± 0.009	0.285 ± 0.034	-0.4 %	-1.79 %	-0.405	0.917	0.466	0.472
T_OCC_right	0.295 ± 0.013	0.294 ± 0.014	0.294 ± 0.014	0.291 ± 0.025	-0.18 %	-0.98 %	0.155	0.922	0.628	0.472
T_PAR_left	0.280 ± 0.012	0.282 ± 0.016	0.277 ± 0.019	0.279 ± 0.020	0.45 %	0.71 %	0.754	0.875	0.486	0.472
T_PAR_right	0.296 ± 0.013	0.296 ± 0.016	0.292 ± 0.020	0.294 ± 0.020	0.13 %	0.5 %	0.887	0.875	0.568	0.472
T_POSTC_left	0.296 ± 0.014	0.297 ± 0.018	0.293 ± 0.025	0.299 ± 0.022	0.22 %	2.07 %	0.795	0.875	-0.294	0.478
T_POSTC_right	0.311 ± 0.016	0.310 ± 0.023	0.305 ± 0.033	0.307 ± 0.029	-0.27 %	0.64 %	0.993	0.875	0.468	0.472
T_PREC_left	0.300 ± 0.013	0.302 ± 0.017	0.304 ± 0.023	0.307 ± 0.022	0.66 %	1.05 %	-0.969	0.875	-1.101	0.472
T_PREC_right	0.304 ± 0.013	0.305 ± 0.018	0.302 ± 0.024	0.305 ± 0.020	0.47 %	0.96 %	0.263	0.921	-0.057	0.533
T_PREF_left	0.287 ± 0.012	0.289 ± 0.013	0.292 ± 0.022	0.292 ± 0.022	0.55 %	0.11 %	-1.199	0.875	-0.885	0.472
T_PREF_right	0.277 ± 0.011	0.278 ± 0.013	0.278 ± 0.017	0.282 ± 0.016	0.4 %	1.23 %	-0.360	0.921	-0.945	0.472
T_PREM_left	0.283 ± 0.013	0.284 ± 0.015	0.287 ± 0.023	0.292 ± 0.021	0.48 %	1.63 %	-0.980	0.875	-1.675	0.472
T_PREM_right	0.286 ± 0.014	0.289 ± 0.016	0.288 ± 0.027	0.291 ± 0.023	0.92 %	1.01 %	-0.442	0.917	-0.505	0.472
UF_left	0.277 ± 0.014	0.273 ± 0.017	0.281 ± 0.019	0.277 ± 0.029	-1.6 %	-1.17 %	-0.744	0.875	-0.784	0.472
UF_right	0.275 ± 0.013	0.271 ± 0.018	0.277 ± 0.014	0.276 ± 0.033	-1.45 %	-0.37 %	-0.470	0.917	-0.760	0.472

Tables A.1- T-test results for comparisons of the automatically segmented tracts from TractSeg between mTBI and control subjects.

[1]Significant values are marked with an asterisk (*) or <0.001

Table A.2 Results of Post Hoc Tract Specific Comparisons of Diffusion Tensor Imaging Mean Diffusivity

	mTBI		Controls		Percent Change					
TractSeg Abbv.	P1	P2	P1	P2	mTBI	Controls	t-score P1	q-value P1[f]	t-score P2	q-value P2[f]
AF_left	7.999e-04 ± 2.322e-05	7.943e-04 ± 2.429e-05	7.756e-04 ± 3.105e-05	7.686e-04 ± 3.164e-05	-0.7 %	-0.91 %	3.362	0.007*	3.522	0.001*
AF_right	7.868e-04 ± 2.222e-05	7.837e-04 ± 1.881e-05	7.764e-04 ± 2.585e-05	7.686e-04 ± 2.719e-05	-0.4 %	-1.01 %	1.560	0.138	2.567	0.009*
ATR_left	8.409e-04 ± 3.346e-05	8.358e-04 ± 3.916e-05	8.161e-04 ± 4.401e-05	8.005e-04 ± 4.388e-05	-0.61 %	-1.91 %	2.397	0.043*	3.114	0.004*
ATR_right	8.461e-04 ± 3.803e-05	8.380e-04 ± 3.574e-05	8.330e-04 ± 5.677e-05	8.175e-04 ± 5.208e-05	-0.95 %	-1.86 %	1.068	0.241	1.837	0.028*
CA	8.916e-04 ± 2.541e-05	8.887e-04 ± 4.040e-05	8.460e-04 ± 3.763e-05	8.296e-04 ± 3.660e-05	-0.33 %	-1.95 %	5.569	<0.001	5.289	<0.001
CC_1	8.586e-04 ± 4.152e-05	8.545e-04 ± 4.578e-05	8.494e-04 ± 6.718e-05	8.243e-04 ± 4.685e-05	-0.48 %	-2.96 %	0.668	0.336	2.335	0.012*
CC_2	8.375e-04 ± 2.624e-05	8.373e-04 ± 2.961e-05	8.216e-04 ± 3.730e-05	8.096e-04 ± 4.104e-05	-0.02 %	-1.45 %	1.909	0.09	3.036	0.004*
CC_3	8.569e-04 ± 3.301e-05	8.594e-04 ± 4.634e-05	8.383e-04 ± 4.583e-05	8.302e-04 ± 6.241e-05	0.29 %	-0.97 %	1.789	0.107	2.066	0.02*
CC_4	8.417e-04 ± 2.701e-05	8.466e-04 ± 3.477e-05	8.317e-04 ± 4.394e-05	8.367e-04 ± 8.721e-05	0.58 %	0.61 %	1.115	0.241	0.700	0.109
CC_5	8.335e-04 ± 2.607e-05	8.422e-04 ± 3.891e-05	8.266e-04 ± 4.895e-05	8.317e-04 ± 9.654e-05	1.04 %	0.61 %	0.744	0.316	0.668	0.109
CC_6	8.171e-04 ± 3.205e-05	8.205e-04 ± 2.704e-05	8.113e-04 ± 3.214e-05	8.161e-04 ± 6.004e-05	0.41 %	0.59 %	0.627	0.338	0.428	0.133
CC_7	8.307e-04 ± 5.528e-05	8.309e-04 ± 3.870e-05	8.254e-04 ± 3.388e-05	8.321e-04 ± 6.310e-05	0.02 %	0.81 %	0.353	0.422	-0.096	0.164
CC	8.297e-04 ± 2.690e-05	8.312e-04 ± 2.563e-05	8.208e-04 ± 3.323e-05	8.188e-04 ± 5.572e-05	0.19 %	-0.25 %	1.079	0.241	1.293	0.06
CG_left	7.949e-04 ± 2.359e-05	7.935e-04 ± 2.323e-05	7.818e-04 ± 4.112e-05	7.856e-04 ± 7.225e-05	-0.17 %	0.49 %	1.622	0.126	0.721	0.109
CG_right	7.884e-04 ± 2.595e-05	7.859e-04 ± 2.197e-05	7.774e-04 ± 4.034e-05	7.734e-04 ± 5.455e-05	-0.32 %	-0.52 %	1.299	0.197	1.414	0.051
CST_left	8.246e-04 ± 2.229e-05	8.226e-04 ± 3.099e-05	7.999e-04 ± 4.135e-05	7.953e-04 ± 6.590e-05	-0.25 %	-0.58 %	3.140	0.011*	2.377	0.011*
CST_right	7.904e-04 ± 2.320e-05	7.882e-04 ± 2.337e-05	7.718e-04 ± 3.429e-05	7.795e-04 ± 6.850e-05	-0.27 %	0.99 %	2.492	0.043*	0.831	0.103
FPT_left	8.283e-04 ± 2.218e-05	8.271e-04 ± 3.052e-05	8.068e-04 ± 5.824e-05	7.937e-04 ± 6.377e-05	-0.14 %	-1.61 %	2.278	0.05	2.986	0.004*
FPT_right	8.233e-04 ± 2.398e-05	8.223e-04 ± 2.555e-05	8.074e-04 ± 5.361e-05	7.924e-04 ± 5.552e-05	-0.13 %	-1.85 %	1.721	0.11	3.122	0.004*
FX_left	1.609e-03 ± 2.432e-04	1.590e-03 ± 2.420e-04	1.597e-03 ± 2.552e-04	1.580e-03 ± 2.864e-04	-1.21 %	-1.03 %	0.181	0.48	0.137	0.162
FX_right	1.594e-03 ± 2.327e-04	1.579e-03 ± 2.466e-04	1.585e-03 ± 2.478e-04	1.529e-03 ± 3.021e-04	-0.9 %	-3.5 %	0.129	0.48	0.684	0.109
ICP_left	7.459e-04 ± 5.752e-05	7.398e-04 ± 3.820e-05	7.409e-04 ± 5.451e-05	7.325e-04 ± 5.920e-05	-0.81 %	-1.14 %	0.298	0.436	0.596	0.116
ICP_right	7.377e-04 ± 4.462e-05	7.329e-04 ± 2.946e-05	7.393e-04 ± 5.818e-05	7.150e-04 ± 6.579e-05	-0.64 %	-3.28 %	-0.117	0.48	1.600	0.039*
IFO_left	8.088e-04 ± 2.674e-05	8.078e-04 ± 2.595e-05	7.904e-04 ± 2.080e-05	7.875e-04 ± 3.704e-05	-0.12 %	-0.37 %	2.476	0.043*	2.524	0.009*
IFO_right	8.034e-04 ± 3.017e-05	8.009e-04 ± 2.404e-05	7.924e-04 ± 2.364e-05	7.865e-04 ± 2.874e-05	-0.32 %	-0.74 %	1.317	0.197	2.027	0.02*
ILF_left	8.232e-04 ± 3.840e-05	8.165e-04 ± 3.108e-05	8.006e-04 ± 2.704e-05	7.935e-04 ± 4.082e-05	-0.8 %	-0.89 %	2.136	0.062	2.457	0.01*
ILF_right	8.137e-04 ± 3.955e-05	8.085e-04 ± 2.961e-05	8.014e-04 ± 3.538e-05	7.931e-04 ± 4.544e-05	-0.64 %	-1.04 %	1.096	0.241	1.635	0.037*

Table A.2 (cont'd)

	mTBI		Controls		Percent Change					
TractSeg Abbv.	P1	P2	P1	P2	mTBI	Controls	t-score P1	q-value P1′	t-score P2	q-value P2′
MCP	7.251e-04 ± 4.452e-05	7.239e-04 ± 3.381e-05	7.178e-04 ± 5.040e-05	7.300e-04 ± 6.087e-05	-0.17 %	1.7 %	0.551	0.36	-0.528	0.121
MLF_left	8.097e-04 ± 2.705e-05	8.088e-04 ± 2.591e-05	8.013e-04 ± 3.068e-05	7.968e-04 ± 4.225e-05	-0.1 %	-0.56 %	1.041	0.246	1.427	0.051
MLF_right	8.024e-04 ± 2.876e-05	8.033e-04 ± 2.571e-05	7.993e-04 ± 3.606e-05	7.949e-04 ± 4.326e-05	0.12 %	-0.55 %	0.346	0.422	0.984	0.086
OR_left	8.340e-04 ± 3.934e-05	8.315e-04 ± 3.878e-05	8.193e-04 ± 3.161e-05	8.179e-04 ± 6.352e-05	-0.3 %	-0.17 %	1.342	0.197	1.075	0.078
OR_right	8.257e-04 ± 4.445e-05	8.239e-04 ± 3.876e-05	8.261e-04 ± 3.738e-05	8.206e-04 ± 5.220e-05	-0.22 %	-0.66 %	-0.034	0.491	0.273	0.149
POPT_left	8.315e-04 ± 2.473e-05	8.350e-04 ± 2.884e-05	8.286e-04 ± 4.189e-05	8.256e-04 ± 7.224e-05	0.41 %	-0.36 %	0.351	0.422	0.801	0.105
POPT_right	8.162e-04 ± 2.751e-05	8.184e-04 ± 2.682e-05	8.094e-04 ± 3.952e-05	8.114e-04 ± 6.759e-05	0.28 %	0.24 %	0.770	0.312	0.644	0.111
SCP_left	7.868e-04 ± 2.581e-05	7.823e-04 ± 3.232e-05	7.625e-04 ± 4.451e-05	7.543e-04 ± 5.961e-05	-0.58 %	-1.08 %	2.762	0.029*	2.515	0.009*
SCP_right	7.779e-04 ± 2.147e-05	7.733e-04 ± 2.205e-05	7.682e-04 ± 5.620e-05	7.523e-04 ± 3.878e-05	-0.6 %	-2.06 %	1.070	0.241	2.821	0.005*
SLF_III_left	7.962e-04 ± 2.382e-05	7.944e-04 ± 2.694e-05	7.806e-04 ± 5.033e-05	7.732e-04 ± 5.376e-05	-0.23 %	-0.95 %	1.736	0.11	2.192	0.015*
SLF_III_right	7.828e-04 ± 2.264e-05	7.829e-04 ± 2.113e-05	7.793e-04 ± 3.347e-05	7.740e-04 ± 4.087e-05	0.01 %	-0.68 %	0.477	0.386	1.187	0.07
SLF_II_left	8.100e-04 ± 2.939e-05	8.057e-04 ± 3.014e-05	7.989e-04 ± 4.336e-05	7.891e-04 ± 5.031e-05	-0.54 %	-1.22 %	1.176	0.229	1.661	0.037*
SLF_II_right	8.013e-04 ± 2.816e-05	7.979e-04 ± 2.601e-05	7.935e-04 ± 4.066e-05	7.839e-04 ± 4.224e-05	-0.43 %	-1.22 %	0.869	0.284	1.654	0.037*
SLF_I_left	8.457e-04 ± 3.854e-05	8.478e-04 ± 4.422e-05	8.576e-04 ± 8.340e-05	8.492e-04 ± 9.782e-05	0.25 %	-0.98 %	-0.815	0.299	-0.088	0.164
SLF_I_right	8.284e-04 ± 3.527e-05	8.267e-04 ± 3.849e-05	8.296e-04 ± 6.358e-05	8.219e-04 ± 8.344e-05	-0.21 %	-0.93 %	-0.094	0.48	0.336	0.145
STR_left	7.828e-04 ± 2.238e-05	7.788e-04 ± 3.467e-05	7.458e-04 ± 4.054e-05	7.504e-04 ± 9.970e-05	-0.52 %	0.62 %	4.747	<0.001	1.839	0.028*
STR_right	7.658e-04 ± 2.186e-05	7.614e-04 ± 2.653e-05	7.499e-04 ± 4.676e-05	7.410e-04 ± 6.010e-05	-0.58 %	-1.19 %	1.924	0.09	2.006	0.02*
ST_FO_left	8.061e-04 ± 3.489e-05	8.052e-04 ± 3.935e-05	7.719e-04 ± 3.447e-05	7.685e-04 ± 5.548e-05	-0.11 %	-0.44 %	3.386	0.007*	3.015	0.004*
ST_FO_right	8.106e-04 ± 3.320e-05	8.071e-04 ± 3.231e-05	7.906e-04 ± 4.002e-05	7.746e-04 ± 2.859e-05	-0.44 %	-2.03 %	1.991	0.082	3.648	0.001*
ST_OCC_left	8.169e-04 ± 3.222e-05	8.147e-04 ± 3.153e-05	7.958e-04 ± 1.883e-05	7.951e-04 ± 4.364e-05	-0.27 %	-0.1 %	2.416	0.043*	2.019	0.02*
ST_OCC_right	8.034e-04 ± 3.557e-05	8.012e-04 ± 3.058e-05	7.937e-04 ± 2.386e-05	7.912e-04 ± 3.384e-05	-0.28 %	-0.31 %	1.001	0.249	1.127	0.075
ST_PAR_left	8.232e-04 ± 2.826e-05	8.248e-04 ± 2.954e-05	8.176e-04 ± 3.713e-05	8.152e-04 ± 6.397e-05	0.19 %	-0.3 %	0.635	0.338	0.869	0.099
ST_PAR_right	8.055e-04 ± 2.877e-05	8.060e-04 ± 2.623e-05	7.978e-04 ± 3.132e-05	7.990e-04 ± 5.421e-05	0.07 %	0.15 %	0.900	0.277	0.735	0.109
ST_POSTC_left	8.273e-04 ± 2.845e-05	8.256e-04 ± 3.665e-05	8.107e-04 ± 4.887e-05	8.032e-04 ± 7.729e-05	-0.21 %	-0.93 %	1.709	0.11	1.659	0.037*
ST_POSTC_right	7.981e-04 ± 2.772e-05	7.965e-04 ± 2.909e-05	7.923e-04 ± 4.763e-05	7.963e-04 ± 7.827e-05	-0.2 %	0.5 %	0.619	0.338	0.020	0.171
ST_PREC_left	8.188e-04 ± 2.658e-05	8.139e-04 ± 3.580e-05	7.880e-04 ± 4.243e-05	7.863e-04 ± 6.738e-05	-0.6 %	-0.22 %	3.498	0.007*	2.217	0.015*
ST_PREC_right	7.950e-04 ± 2.800e-05	7.895e-04 ± 2.563e-05	7.793e-04 ± 3.716e-05	7.789e-04 ± 5.685e-05	-0.69 %	-0.05 %	1.805	0.107	1.092	0.078

Table A.2 (cont'd)

	mTBI		Controls		Percent Change					
TractSeg Abbv.	P1	P2	P1	P2	mTBI	Controls	t-score P1	q-value P1[1]	t-score P2	q-value P2[1]
ST_PREF_left	8.095e-04 ± 2.509e-05	8.057e-04 ± 2.998e-05	7.828e-04 ± 4.072e-05	7.759e-04 ± 4.752e-05	-0.47 %	-0.88 %	3.193	0.011*	3.073	0.004*
ST_PREF_right	8.088e-04 ± 2.644e-05	8.044e-04 ± 2.507e-05	7.893e-04 ± 4.033e-05	7.747e-04 ± 3.372e-05	-0.55 %	-1.86 %	2.265	0.05	3.891	<0.001
ST_PREM_left	8.177e-04 ± 2.850e-05	8.119e-04 ± 3.848e-05	7.848e-04 ± 4.277e-05	7.662e-04 ± 3.664e-05	-0.71 %	-2.38 %	3.571	0.007*	4.261	<0.001
ST_PREM_right	8.010e-04 ± 2.579e-05	7.946e-04 ± 2.784e-05	7.778e-04 ± 4.761e-05	7.692e-04 ± 4.500e-05	-0.8 %	-1.11 %	2.562	0.043*	2.804	0.005*
T_OCC_left	8.390e-04 ± 4.054e-05	8.360e-04 ± 3.969e-05	8.243e-04 ± 3.169e-05	8.229e-04 ± 6.250e-05	-0.35 %	-0.17 %	1.301	0.197	1.026	0.082
T_OCC_right	8.269e-04 ± 4.470e-05	8.247e-04 ± 3.885e-05	8.267e-04 ± 3.792e-05	8.218e-04 ± 5.292e-05	-0.26 %	-0.6 %	0.009	0.494	0.247	0.151
T_PAR_left	8.334e-04 ± 3.315e-05	8.354e-04 ± 3.495e-05	8.344e-04 ± 4.703e-05	8.312e-04 ± 7.984e-05	0.24 %	-0.39 %	-0.098	0.48	0.311	0.146
T_PAR_right	8.233e-04 ± 3.552e-05	8.233e-04 ± 3.270e-05	8.221e-04 ± 4.550e-05	8.210e-04 ± 7.266e-05	0.01 %	-0.13 %	0.106	0.48	0.185	0.157
T_POSTC_left	8.257e-04 ± 2.980e-05	8.265e-04 ± 3.850e-05	8.250e-04 ± 6.229e-05	8.151e-04 ± 9.048e-05	0.09 %	-1.2 %	0.065	0.485	0.753	0.109
T_POSTC_right	7.981e-04 ± 3.203e-05	7.993e-04 ± 3.469e-05	8.069e-04 ± 6.816e-05	8.105e-04 ± 1.036e-04	0.15 %	0.45 %	-0.727	0.317	-0.708	0.109
T_PREC_left	8.208e-04 ± 2.865e-05	8.160e-04 ± 3.953e-05	7.968e-04 ± 5.194e-05	7.935e-04 ± 8.025e-05	-0.58 %	-0.41 %	2.400	0.043*	1.575	0.039*
T_PREC_right	7.933e-04 ± 3.078e-05	7.874e-04 ± 2.872e-05	7.833e-04 ± 4.619e-05	7.813e-04 ± 6.742e-05	-0.74 %	-0.25 %	1.005	0.249	0.536	0.121
T_PREF_left	8.255e-04 ± 2.786e-05	8.209e-04 ± 3.525e-05	8.027e-04 ± 5.094e-05	7.926e-04 ± 5.755e-05	-0.55 %	-1.27 %	2.329	0.048*	2.464	0.01*
T_PREF_right	8.317e-04 ± 3.290e-05	8.253e-04 ± 3.271e-05	8.185e-04 ± 5.609e-05	8.013e-04 ± 5.377e-05	-0.77 %	-2.1 %	1.181	0.229	2.239	0.015*
T_PREM_left	8.370e-04 ± 3.299e-05	8.305e-04 ± 4.623e-05	8.121e-04 ± 5.641e-05	7.900e-04 ± 6.052e-05	-0.78 %	-2.72 %	2.219	0.053	2.900	0.004*
T_PREM_right	8.186e-04 ± 3.557e-05	8.100e-04 ± 3.750e-05	8.064e-04 ± 7.571e-05	7.926e-04 ± 6.976e-05	-1.05 %	-1.71 %	0.905	0.277	1.338	0.057
UF_left	8.116e-04 ± 2.571e-05	8.142e-04 ± 2.716e-05	7.926e-04 ± 3.163e-05	7.837e-04 ± 2.922e-05	0.33 %	-1.12 %	2.430	0.043*	3.921	<0.001
UF_right	8.327e-04 ± 2.444e-05	8.318e-04 ± 2.798e-05	8.186e-04 ± 4.089e-05	8.018e-04 ± 3.281e-05	-0.11 %	-2.05 %	1.709	0.11	3.666	0.001*

Tables A.2- T-test results for comparisons of the automatically segmented tracts from TractSeg between mTBI and control subjects.

[1]Significant values are marked with an asterisk (*) or <0.001

Table A.3 Results of Post Hoc Tract Specific Comparisons of Diffusion Tensor Imaging Axial Diffusivity

	mTBI		Controls		Percent Change					
TractSeg Abbv.	P1	P2	P1	P2	mTBI	Controls	t-score P1	q-value P1[f]	t-score P2	q-value P2[f]
AF_left	1.015e-03 ± 2.342e-05	1.007e-03 ± 2.573e-05	9.847e-04 ± 2.329e-05	9.765e-04 ± 2.670e-05	-0.74 %	-0.83 %	4.394	<0.001	4.168	<0.001
AF_right	1.005e-03 ± 2.231e-05	1.000e-03 ± 2.132e-05	9.878e-04 ± 2.429e-05	9.759e-04 ± 1.501e-05	-0.5 %	-1.2 %	2.662	<0.001	4.269	<0.001
ATR_left	1.079e-03 ± 3.541e-05	1.073e-03 ± 4.054e-05	1.053e-03 ± 3.877e-05	1.035e-03 ± 3.740e-05	-0.61 %	-1.74 %	2.537	<0.001	3.395	<0.001
ATR_right	1.077e-03 ± 4.010e-05	1.068e-03 ± 3.867e-05	1.061e-03 ± 5.729e-05	1.044e-03 ± 4.945e-05	-0.85 %	-1.58 %	1.269	0.005*	2.053	0.005*
CA	1.153e-03 ± 3.106e-05	1.146e-03 ± 3.747e-05	1.113e-03 ± 3.338e-05	1.089e-03 ± 2.505e-05	-0.65 %	-2.19 %	4.402	<0.001	5.742	<0.001
CC_1	1.198e-03 ± 5.031e-05	1.187e-03 ± 6.398e-05	1.192e-03 ± 7.785e-05	1.152e-03 ± 7.825e-05	-0.95 %	-3.37 %	0.382	0.013*	1.853	0.007*
CC_2	1.109e-03 ± 2.756e-05	1.107e-03 ± 3.109e-05	1.087e-03 ± 3.036e-05	1.070e-03 ± 2.602e-05	-0.19 %	-1.54 %	2.726	<0.001	4.337	<0.001
CC_3	1.129e-03 ± 3.908e-05	1.129e-03 ± 4.402e-05	1.105e-03 ± 3.968e-05	1.092e-03 ± 4.430e-05	-0.06 %	-1.16 %	2.187	0.001*	2.981	<0.001
CC_4	1.121e-03 ± 2.533e-05	1.122e-03 ± 3.542e-05	1.097e-03 ± 3.661e-05	1.101e-03 ± 6.714e-05	0.16 %	0.33 %	2.925	<0.001	1.763	0.008*
CC_5	1.121e-03 ± 2.864e-05	1.126e-03 ± 4.085e-05	1.099e-03 ± 4.358e-05	1.103e-03 ± 7.685e-05	0.47 %	0.36 %	2.358	<0.001	1.631	0.009*
CC_6	1.083e-03 ± 2.908e-05	1.086e-03 ± 3.002e-05	1.068e-03 ± 2.105e-05	1.070e-03 ± 4.447e-05	0.25 %	0.19 %	1.945	0.002*	1.724	0.008*
CC_7	1.116e-03 ± 5.499e-05	1.114e-03 ± 4.317e-05	1.105e-03 ± 4.256e-05	1.104e-03 ± 5.584e-05	-0.15 %	-0.08 %	0.727	0.009*	0.799	0.031*
CC	1.097e-03 ± 2.436e-05	1.097e-03 ± 2.547e-05	1.080e-03 ± 2.395e-05	1.074e-03 ± 3.965e-05	0.02 %	-0.58 %	2.342	<0.001	2.817	<0.001
CG_left	1.031e-03 ± 2.378e-05	1.032e-03 ± 2.771e-05	1.013e-03 ± 3.399e-05	1.013e-03 ± 6.512e-05	0.11 %	0.05 %	2.335	<0.001	1.693	0.008*

Table A.3 (cont'd)

	mTBI		Controls		Percent Change					
TractSeg Abbv.	P1	P2	P1	P2	mTBI	Controls	t-score P1	q-value P1[f]	t-score P2	q-value P2[f]
CG_right	1.027e-03 ± 2.690e-05	1.024e-03 ± 2.496e-05	1.009e-03 ± 2.887e-05	9.993e-04 ± 4.918e-05	-0.2 %	-0.98 %	2.201	0.001*	2.837	<0.001
CST_left	1.139e-03 ± 2.442e-05	1.136e-03 ± 3.320e-05	1.098e-03 ± 3.481e-05	1.092e-03 ± 5.409e-05	-0.26 %	-0.57 %	5.193	<0.001	4.021	<0.001
CST_right	1.100e-03 ± 2.556e-05	1.095e-03 ± 2.623e-05	1.068e-03 ± 3.136e-05	1.072e-03 ± 5.302e-05	-0.4 %	0.41 %	4.071	<0.001	2.424	0.002*
FPT_left	1.131e-03 ± 2.590e-05	1.129e-03 ± 3.320e-05	1.095e-03 ± 4.753e-05	1.078e-03 ± 5.047e-05	-0.12 %	-1.49 %	3.961	<0.001	4.826	<0.001
FPT_right	1.124e-03 ± 2.818e-05	1.121e-03 ± 2.925e-05	1.095e-03 ± 4.575e-05	1.078e-03 ± 4.495e-05	-0.24 %	-1.55 %	3.083	<0.001	4.644	<0.001
FX_left	2.085e-03 ± 2.114e-04	2.046e-03 ± 2.231e-04	2.066e-03 ± 2.208e-04	2.028e-03 ± 2.725e-04	-1.89 %	-1.85 %	0.309	0.014*	0.271	0.053
FX_right	2.077e-03 ± 2.037e-04	2.048e-03 ± 2.239e-04	2.052e-03 ± 2.155e-04	1.990e-03 ± 3.089e-04	-1.4 %	-3.03 %	0.426	0.013*	0.852	0.029*
ICP_left	9.628e-04 ± 5.867e-05	9.534e-04 ± 3.663e-05	9.448e-04 ± 4.185e-05	9.368e-04 ± 3.789e-05	-0.97 %	-0.84 %	1.114	0.006*	1.598	0.009*
ICP_right	9.386e-04 ± 4.624e-05	9.298e-04 ± 3.252e-05	9.265e-04 ± 4.801e-05	9.044e-04 ± 7.191e-05	-0.93 %	-2.38 %	0.898	0.008*	2.070	0.005*
IFO_left	1.056e-03 ± 2.808e-05	1.053e-03 ± 2.968e-05	1.035e-03 ± 2.153e-05	1.024e-03 ± 2.312e-05	-0.26 %	-0.99 %	2.736	<0.001	3.603	<0.001
IFO_right	1.047e-03 ± 3.094e-05	1.043e-03 ± 2.640e-05	1.033e-03 ± 3.013e-05	1.023e-03 ± 3.073e-05	-0.39 %	-0.98 %	1.511	0.003*	2.536	0.002*
ILF_left	1.072e-03 ± 4.333e-05	1.061e-03 ± 4.141e-05	1.049e-03 ± 3.176e-05	1.030e-03 ± 3.628e-05	-0.99 %	-1.85 %	1.881	0.002*	2.753	0.001*
ILF_right	1.053e-03 ± 4.591e-05	1.045e-03 ± 3.940e-05	1.043e-03 ± 4.700e-05	1.025e-03 ± 6.098e-05	-0.75 %	-1.68 %	0.750	0.009*	1.562	0.01*

Table A.3 (cont'd)

	mTBI		Controls		Percent Change					
TractSeg Abbv.	mTBI P1	mTBI P2	Controls P1	Controls P2	mTBI	Controls	t-score P1	q-value P1[f]	t-score P2	q-value P2[f]
MCP	9.671e-04 ± 4.922e-05	9.626e-04 ± 3.853e-05	9.479e-04 ± 3.816e-05	9.606e-04 ± 4.000e-05	-0.47 %	1.33 %	1.399	0.004*	0.184	0.057
MLF_left	1.033e-03 ± 2.652e-05	1.033e-03 ± 2.832e-05	1.020e-03 ± 2.389e-05	1.015e-03 ± 3.585e-05	-0.05 %	-0.51 %	1.818	0.002*	2.177	0.004*
MLF_right	1.029e-03 ± 2.723e-05	1.029e-03 ± 2.783e-05	1.019e-03 ± 2.749e-05	1.011e-03 ± 3.368e-05	0.01 %	-0.8 %	1.235	0.005*	2.194	0.004*
OR_left	1.102e-03 ± 3.927e-05	1.097e-03 ± 4.030e-05	1.084e-03 ± 3.617e-05	1.074e-03 ± 4.706e-05	-0.45 %	-0.9 %	1.600	0.003*	1.939	0.006*
OR_right	1.094e-03 ± 4.333e-05	1.091e-03 ± 3.987e-05	1.093e-03 ± 4.489e-05	1.081e-03 ± 6.077e-05	-0.28 %	-1.09 %	0.061	0.017*	0.758	0.032*
POPT_left	1.109e-03 ± 2.802e-05	1.112e-03 ± 3.210e-05	1.094e-03 ± 3.411e-05	1.090e-03 ± 6.348e-05	0.28 %	-0.34 %	1.755	0.002*	1.903	0.006*
POPT_right	1.100e-03 ± 2.963e-05	1.101e-03 ± 3.086e-05	1.084e-03 ± 3.327e-05	1.085e-03 ± 5.636e-05	0.11 %	0.08 %	1.808	0.002*	1.533	0.01*
SCP_left	1.057e-03 ± 2.989e-05	1.050e-03 ± 3.242e-05	1.016e-03 ± 3.352e-05	1.010e-03 ± 3.981e-05	-0.61 %	-0.58 %	4.535	<0.001	4.136	<0.001
SCP_right	1.044e-03 ± 2.503e-05	1.035e-03 ± 2.552e-05	1.018e-03 ± 4.347e-05	1.006e-03 ± 2.895e-05	-0.79 %	-1.18 %	3.009	<0.001	3.991	<0.001
SLF_III_left	1.013e-03 ± 2.510e-05	1.008e-03 ± 2.923e-05	9.897e-04 ± 3.604e-05	9.819e-04 ± 4.455e-05	-0.47 %	-0.79 %	2.957	<0.001	2.866	<0.001
SLF_III_right	1.006e-03 ± 2.348e-05	1.003e-03 ± 2.646e-05	9.898e-04 ± 2.919e-05	9.790e-04 ± 2.266e-05	-0.31 %	-1.09 %	2.229	0.001*	3.263	<0.001
SLF_II_left	1.017e-03 ± 2.591e-05	1.014e-03 ± 2.883e-05	1.001e-03 ± 3.330e-05	9.931e-04 ± 4.407e-05	-0.29 %	-0.74 %	2.021	0.002*	2.245	0.003*
SLF_II_right	1.007e-03 ± 2.589e-05	1.004e-03 ± 2.526e-05	9.925e-04 ± 3.316e-05	9.820e-04 ± 3.410e-05	-0.29 %	-1.06 %	1.842	0.002*	2.892	<0.001
SLF_I_left	1.051e-03 ± 3.764e-05	1.054e-03 ± 4.073e-05	1.056e-03 ± 7.126e-05	1.045e-03 ± 8.891e-05	0.32 %	-1.01 %	-0.353	0.013*	0.606	0.038*
SLF_I_right	1.041e-03 ± 3.308e-05	1.041e-03 ± 3.473e-05	1.036e-03 ± 5.265e-05	1.029e-03 ± 7.461e-05	-0.01 %	-0.73 %	0.445	0.013*	0.955	0.026*
STR_left	1.071e-03 ± 2.795e-05	1.067e-03 ± 3.761e-05	1.018e-03 ± 3.962e-05	1.019e-03 ± 8.800e-05	-0.42 %	0.09 %	5.964	<0.001	3.229	<0.001
STR_right	1.052e-03 ± 2.962e-05	1.045e-03 ± 3.229e-05	1.025e-03 ± 4.226e-05	1.014e-03 ± 5.503e-05	-0.64 %	-1.03 %	2.922	<0.001	2.912	<0.001
ST_FO_left	1.059e-03 ± 4.021e-05	1.054e-03 ± 4.817e-05	1.025e-03 ± 4.049e-05	1.018e-03 ± 3.978e-05	-0.47 %	-0.7 %	2.957	<0.001	2.790	<0.001
ST_FO_right	1.073e-03 ± 3.768e-05	1.067e-03 ± 3.943e-05	1.051e-03 ± 4.138e-05	1.029e-03 ± 2.899e-05	-0.6 %	-2.05 %	1.986	0.002*	3.522	<0.001

Table A.3 (cont'd)

	mTBI		Controls		Percent Change					
TractSeg Abbv.	mTBI P1	mTBI P2	Controls P1	Controls P2	mTBI	Controls	t-score P1	q-value P1[f]	t-score P2	q-value P2[f]
ST_OCC_left	1.082e-03 ± 3.268e-05	1.078e-03 ± 3.508e-05	1.055e-03 ± 2.302e-05	1.047e-03 ± 2.724e-05	-0.36 %	-0.73 %	2.965	<0.001	3.212	<0.001
ST_OCC_right	1.062e-03 ± 3.557e-05	1.058e-03 ± 3.316e-05	1.049e-03 ± 3.533e-05	1.042e-03 ± 3.978e-05	-0.32 %	-0.69 %	1.188	0.005*	1.644	0.009*
ST_PAR_left	1.064e-03 ± 2.882e-05	1.066e-03 ± 3.255e-05	1.050e-03 ± 2.912e-05	1.047e-03 ± 5.636e-05	0.2 %	-0.31 %	1.660	0.003*	1.768	0.008*
ST_PAR_right	1.055e-03 ± 2.873e-05	1.055e-03 ± 2.928e-05	1.040e-03 ± 2.724e-05	1.040e-03 ± 4.490e-05	-0.05 %	-0.05 %	1.810	0.002*	1.600	0.009*
ST_POSTC_left	1.081e-03 ± 3.349e-05	1.078e-03 ± 4.209e-05	1.052e-03 ± 4.335e-05	1.043e-03 ± 7.582e-05	-0.23 %	-0.78 %	2.818	<0.001	2.426	0.002*
ST_POSTC_right	1.058e-03 ± 3.114e-05	1.053e-03 ± 3.115e-05	1.044e-03 ± 4.490e-05	1.046e-03 ± 7.164e-05	-0.43 %	0.22 %	1.395	0.004*	0.584	0.038*
ST_PREC_left	1.076e-03 ± 2.947e-05	1.070e-03 ± 3.950e-05	1.033e-03 ± 3.791e-05	1.029e-03 ± 6.310e-05	-0.51 %	-0.4 %	4.681	<0.001	3.214	<0.001
ST_PREC_right	1.053e-03 ± 3.045e-05	1.046e-03 ± 2.879e-05	1.029e-03 ± 3.861e-05	1.026e-03 ± 5.209e-05	-0.72 %	-0.23 %	2.633	<0.001	1.975	0.006*
ST_PREF_left	1.056e-03 ± 2.776e-05	1.052e-03 ± 3.464e-05	1.022e-03 ± 3.595e-05	1.011e-03 ± 4.110e-05	-0.4 %	-1.1 %	3.951	<0.001	4.013	<0.001
ST_PREF_right	1.054e-03 ± 3.014e-05	1.048e-03 ± 3.014e-05	1.028e-03 ± 4.096e-05	1.010e-03 ± 3.036e-05	-0.55 %	-1.72 %	2.805	<0.001	4.510	<0.001
ST_PREM_left	1.053e-03 ± 3.357e-05	1.047e-03 ± 4.465e-05	1.010e-03 ± 3.695e-05	9.868e-04 ± 2.854e-05	-0.57 %	-2.27 %	4.323	<0.001	5.080	<0.001
ST_PREM_right	1.044e-03 ± 3.148e-05	1.036e-03 ± 3.357e-05	1.011e-03 ± 4.473e-05	9.990e-04 ± 4.066e-05	-0.71 %	-1.21 %	3.238	<0.001	3.756	<0.001
T_OCC_left	1.103e-03 ± 4.013e-05	1.097e-03 ± 4.116e-05	1.085e-03 ± 3.587e-05	1.076e-03 ± 4.708e-05	-0.48 %	-0.9 %	1.499	0.003*	1.798	0.008*
T_OCC_right	1.090e-03 ± 4.353e-05	1.086e-03 ± 3.999e-05	1.088e-03 ± 4.596e-05	1.077e-03 ± 6.103e-05	-0.3 %	-1.03 %	0.086	0.017*	0.709	0.034*
T_PAR_left	1.075e-03 ± 3.197e-05	1.078e-03 ± 3.489e-05	1.069e-03 ± 3.948e-05	1.064e-03 ± 7.090e-05	0.24 %	-0.44 %	0.621	0.011*	1.053	0.023*
T_PAR_right	1.076e-03 ± 3.398e-05	1.076e-03 ± 3.320e-05	1.068e-03 ± 3.920e-05	1.066e-03 ± 6.324e-05	-0.02 %	-0.25 %	0.747	0.009*	0.866	0.029*
T_POSTC_left	1.083e-03 ± 3.168e-05	1.083e-03 ± 3.916e-05	1.067e-03 ± 5.405e-05	1.058e-03 ± 8.290e-05	-0.02 %	-0.85 %	1.464	0.004*	1.705	0.008*
T_POSTC_right	1.059e-03 ± 3.156e-05	1.059e-03 ± 3.222e-05	1.057e-03 ± 5.480e-05	1.059e-03 ± 9.134e-05	-0.04 %	0.14 %	0.151	0.016*	-0.026	0.064
T_PREC_left	1.083e-03 ± 2.815e-05	1.078e-03 ± 3.880e-05	1.047e-03 ± 4.469e-05	1.042e-03 ± 7.164e-05	-0.49 %	-0.55 %	3.804	<0.001	2.679	0.001*

Table A.3 (cont'd)

	mTBI		Controls		Percent Change					
TractSeg Abbv.	mTBI P1	mTBI P2	Controls P1	Controls P2	mTBI	Controls	t-score P1	q-value P1[1]	t-score P2	q-value P2[1]
T_PREC_right	1.049e-03 ± 3.081e-05	1.042e-03 ± 2.871e-05	1.031e-03 ± 4.103e-05	1.026e-03 ± 6.015e-05	-0.62 %	-0.39 %	1.915	0.002*	1.514	0.011*
T_PREF_left	1.076e-03 ± 2.889e-05	1.071e-03 ± 3.634e-05	1.047e-03 ± 4.445e-05	1.033e-03 ± 4.993e-05	-0.45 %	-1.37 %	3.101	<0.001	3.479	<0.001
T_PREF_right	1.074e-03 ± 3.428e-05	1.067e-03 ± 3.426e-05	1.055e-03 ± 5.484e-05	1.035e-03 ± 4.852e-05	-0.67 %	-1.85 %	1.677	0.003*	2.957	<0.001
T_PREM_left	1.087e-03 ± 3.444e-05	1.079e-03 ± 4.639e-05	1.054e-03 ± 5.017e-05	1.029e-03 ± 5.125e-05	-0.69 %	-2.4 %	2.989	<0.001	3.796	<0.001
T_PREM_right	1.065e-03 ± 3.573e-05	1.057e-03 ± 3.830e-05	1.047e-03 ± 6.767e-05	1.030e-03 ± 6.163e-05	-0.79 %	-1.6 %	1.414	0.004*	2.115	0.004*
UF_left	1.057e-03 ± 2.840e-05	1.056e-03 ± 2.995e-05	1.036e-03 ± 3.224e-05	1.020e-03 ± 1.933e-05	-0.12 %	-1.52 %	2.553	<0.001	4.554	<0.001
UF_right	1.085e-03 ± 2.861e-05	1.080e-03 ± 2.984e-05	1.067e-03 ± 4.207e-05	1.045e-03 ± 1.620e-05	-0.49 %	-2.11 %	1.962	0.002*	4.528	<0.001

Tables A.3- T-test results for comparisons of the automatically segmented tracts from TractSeg between mTBI and control subjects.

[1]Significant values are marked with an asterisk (*) or <0.001

Table A.4 Results of Post Hoc Tract Specific Comparisons of Diffusion Tensor Imaging Radial Diffusivity

	mTBI		Controls		Percent Change					
TractSeg Abbv	P1	P2	P1	P2	mTBI	Control	t-score P1	q-value P1ᶠ	t-score P2	q-value P2ᶠ
AF_left	6.926e-04 ± 2.510e-05	6.880e-04 ± 2.491e-05	6.710e-04 ± 3.590e-05	6.646e-04 ± 3.528e-05	-0.66 %	-0.96 %	2.703	0.077	3.039	0.027*
AF_right	6.776e-04 ± 2.346e-05	6.754e-04 ± 1.976e-05	6.708e-04 ± 2.842e-05	6.650e-04 ± 3.511e-05	-0.32 %	-0.87 %	0.960	0.47	1.559	0.217
ATR_left	7.217e-04 ± 3.371e-05	7.173e-04 ± 3.941e-05	6.977e-04 ± 4.747e-05	6.835e-04 ± 4.824e-05	-0.61 %	-2.03 %	2.250	0.158	2.899	0.03*
ATR_right	7.305e-04 ± 3.776e-05	7.230e-04 ± 3.543e-05	7.189e-04 ± 5.714e-05	7.041e-04 ± 5.440e-05	-1.02 %	-2.06 %	0.945	0.47	1.674	0.202
CA	7.607e-04 ± 2.680e-05	7.601e-04 ± 4.472e-05	7.125e-04 ± 4.266e-05	7.000e-04 ± 4.786e-05	-0.08 %	-1.75 %	5.445	<0.001	4.699	<0.001
CC_1	6.890e-04 ± 4.217e-05	6.885e-04 ± 4.672e-05	6.783e-04 ± 6.571e-05	6.606e-04 ± 5.164e-05	-0.07 %	-2.6 %	0.774	0.529	2.071	0.138
CC_2	7.017e-04 ± 2.825e-05	7.024e-04 ± 3.106e-05	6.889e-04 ± 4.400e-05	6.794e-04 ± 5.003e-05	0.11 %	-1.39 %	1.376	0.374	2.285	0.104
CC_3	7.207e-04 ± 3.389e-05	7.247e-04 ± 5.072e-05	7.052e-04 ± 5.606e-05	6.995e-04 ± 7.412e-05	0.55 %	-0.81 %	1.362	0.374	1.588	0.217
CC_4	7.022e-04 ± 3.236e-05	7.087e-04 ± 3.842e-05	6.990e-04 ± 5.347e-05	7.047e-04 ± 9.832e-05	0.93 %	0.82 %	0.298	0.709	0.251	0.674
CC_5	6.899e-04 ± 3.043e-05	7.003e-04 ± 4.238e-05	6.906e-04 ± 5.817e-05	6.961e-04 ± 1.081e-04	1.51 %	0.81 %	-0.061	0.725	0.240	0.674
CC_6	6.840e-04 ± 3.575e-05	6.876e-04 ± 2.890e-05	6.831e-04 ± 4.045e-05	6.892e-04 ± 6.888e-05	0.53 %	0.89 %	0.089	0.725	-0.137	0.674
CC_7	6.882e-04 ± 5.660e-05	6.893e-04 ± 3.900e-05	6.858e-04 ± 3.193e-05	6.963e-04 ± 7.274e-05	0.16 %	1.53 %	0.156	0.725	-0.519	0.597
CC	6.962e-04 ± 3.001e-05	6.984e-04 ± 2.789e-05	6.912e-04 ± 4.055e-05	6.913e-04 ± 6.451e-05	0.31 %	0.01 %	0.535	0.626	0.658	0.546
CG_left	6.770e-04 ± 2.722e-05	6.744e-04 ± 2.774e-05	6.662e-04 ± 4.741e-05	6.717e-04 ± 7.710e-05	-0.4 %	0.83 %	1.163	0.414	0.217	0.674
CG_right	6.694e-04 ± 2.930e-05	6.667e-04 ± 2.393e-05	6.615e-04 ± 4.739e-05	6.604e-04 ± 5.967e-05	-0.4 %	-0.17 %	0.807	0.517	0.645	0.546
CST_left	6.676e-04 ± 2.487e-05	6.660e-04 ± 3.272e-05	6.507e-04 ± 4.765e-05	6.469e-04 ± 7.265e-05	-0.24 %	-0.6 %	1.895	0.204	1.541	0.217
CST_right	6.358e-04 ± 2.449e-05	6.347e-04 ± 2.548e-05	6.237e-04 ± 3.943e-05	6.331e-04 ± 7.721e-05	-0.17 %	1.5 %	1.489	0.354	0.143	0.674
FPT_left	6.770e-04 ± 2.380e-05	6.760e-04 ± 3.174e-05	6.628e-04 ± 6.547e-05	6.514e-04 ± 7.116e-05	-0.15 %	-1.72 %	1.369	0.374	2.040	0.139
FPT_right	6.729e-04 ± 2.448e-05	6.726e-04 ± 2.664e-05	6.634e-04 ± 5.898e-05	6.495e-04 ± 6.193e-05	-0.04 %	-2.1 %	0.961	0.47	2.233	0.108
FX_left	1.372e-03 ± 2.615e-04	1.362e-03 ± 2.560e-04	1.362e-03 ± 2.757e-04	1.356e-03 ± 3.019e-04	-0.7 %	-0.4 %	0.128	0.725	0.076	0.674
FX_right	1.352e-03 ± 2.505e-04	1.345e-03 ± 2.628e-04	1.351e-03 ± 2.675e-04	1.299e-03 ± 3.085e-04	-0.51 %	-3.85 %	0.006	0.728	0.593	0.558
ICP_left	6.374e-04 ± 5.814e-05	6.330e-04 ± 4.076e-05	6.390e-04 ± 6.150e-05	6.304e-04 ± 7.152e-05	-0.69 %	-1.35 %	-0.096	0.725	0.191	0.674
ICP_right	6.372e-04 ± 4.490e-05	6.344e-04 ± 2.976e-05	6.457e-04 ± 6.380e-05	6.203e-04 ± 6.577e-05	-0.43 %	-3.93 %	-0.594	0.621	1.258	0.308
IFO_left	6.853e-04 ± 2.739e-05	6.851e-04 ± 2.548e-05	6.683e-04 ± 2.269e-05	6.691e-04 ± 4.612e-05	-0.02 %	0.11 %	2.207	0.158	1.844	0.167
IFO_right	6.818e-04 ± 3.044e-05	6.800e-04 ± 2.425e-05	6.720e-04 ± 2.238e-05	6.683e-04 ± 3.391e-05	-0.26 %	-0.54 %	1.173	0.414	1.567	0.217
ILF_left	6.988e-04 ± 3.708e-05	6.941e-04 ± 2.885e-05	6.762e-04 ± 2.638e-05	6.752e-04 ± 4.890e-05	-0.66 %	-0.15 %	2.211	0.158	1.978	0.142
ILF_right	6.943e-04 ± 3.747e-05	6.904e-04 ± 2.834e-05	6.808e-04 ± 3.137e-05	6.771e-04 ± 4.371e-05	-0.56 %	-0.55 %	1.277	0.408	1.470	0.24

Table A.4 (cont'd)

	mTBI		Controls		Percent Change					
TractSeg Abbv	P1	P2	P1	P2	mTBI	Control	t-score P1	q-value P1′	t-score P2	q-value P2′
MCP	6.041e-04 ± 4.311e-05	6.046e-04 ± 3.286e-05	6.028e-04 ± 5.747e-05	6.147e-04 ± 7.219e-05	0.08 %	1.98 %	0.102	0.725	-0.818	0.488
MLF_left	6.978e-04 ± 2.931e-05	6.968e-04 ± 2.710e-05	6.920e-04 ± 3.567e-05	6.879e-04 ± 4.632e-05	-0.14 %	-0.6 %	0.643	0.598	0.986	0.414
MLF_right	6.892e-04 ± 3.101e-05	6.905e-04 ± 2.741e-05	6.895e-04 ± 4.188e-05	6.870e-04 ± 4.959e-05	0.19 %	-0.36 %	-0.032	0.725	0.378	0.657
OR_left	7.003e-04 ± 4.076e-05	6.990e-04 ± 3.968e-05	6.871e-04 ± 3.076e-05	6.899e-04 ± 7.430e-05	-0.19 %	0.41 %	1.165	0.414	0.657	0.546
OR_right	6.915e-04 ± 4.588e-05	6.903e-04 ± 3.964e-05	6.925e-04 ± 3.584e-05	6.903e-04 ± 5.206e-05	-0.18 %	-0.33 %	-0.080	0.725	0.002	0.683
POPT_left	6.928e-04 ± 2.568e-05	6.964e-04 ± 3.043e-05	6.958e-04 ± 4.768e-05	6.931e-04 ± 7.727e-05	0.52 %	-0.38 %	-0.336	0.707	0.258	0.674
POPT_right	6.742e-04 ± 2.835e-05	6.769e-04 ± 2.844e-05	6.720e-04 ± 4.540e-05	6.745e-04 ± 7.402e-05	0.41 %	0.37 %	0.231	0.725	0.209	0.674
SCP_left	6.519e-04 ± 2.732e-05	6.483e-04 ± 3.494e-05	6.356e-04 ± 5.143e-05	6.262e-04 ± 7.020e-05	-0.55 %	-1.47 %	1.689	0.253	1.763	0.176
SCP_right	6.451e-04 ± 2.198e-05	6.422e-04 ± 2.353e-05	6.433e-04 ± 6.362e-05	6.256e-04 ± 4.642e-05	-0.44 %	-2.76 %	0.177	0.725	1.992	0.142
SLF_III_left	6.876e-04 ± 2.547e-05	6.873e-04 ± 2.821e-05	6.761e-04 ± 5.829e-05	6.689e-04 ± 5.911e-05	-0.05 %	-1.07 %	1.149	0.414	1.776	0.176
SLF_III_right	6.713e-04 ± 2.392e-05	6.730e-04 ± 2.385e-05	6.741e-04 ± 3.759e-05	6.716e-04 ± 5.256e-05	0.25 %	-0.38 %	-0.352	0.707	0.159	0.674
SLF_II_left	7.067e-04 ± 3.277e-05	7.016e-04 ± 3.297e-05	6.981e-04 ± 4.919e-05	6.871e-04 ± 5.678e-05	-0.72 %	-1.56 %	0.813	0.517	1.313	0.289
SLF_II_right	6.984e-04 ± 3.077e-05	6.947e-04 ± 2.901e-05	6.940e-04 ± 4.574e-05	6.848e-04 ± 4.679e-05	-0.53 %	-1.33 %	0.442	0.67	1.049	0.388
SLF_I_left	7.430e-04 ± 4.054e-05	7.445e-04 ± 4.786e-05	7.586e-04 ± 9.004e-05	7.513e-04 ± 1.027e-04	0.19 %	-0.96 %	-0.995	0.47	-0.385	0.657
SLF_I_right	7.220e-04 ± 3.788e-05	7.195e-04 ± 4.255e-05	7.262e-04 ± 7.028e-05	7.184e-04 ± 8.837e-05	-0.35 %	-1.07 %	-0.312	0.709	0.070	0.674
STR_left	6.387e-04 ± 2.448e-05	6.349e-04 ± 3.693e-05	6.095e-04 ± 4.429e-05	6.160e-04 ± 1.065e-04	-0.6 %	1.07 %	3.417	0.019 *	1.144	0.351
STR_right	6.227e-04 ± 2.252e-05	6.193e-04 ± 2.865e-05	6.126e-04 ± 5.202e-05	6.044e-04 ± 6.454e-05	-0.53 %	-1.33 %	1.137	0.414	1.367	0.279
ST_FO_left	6.794e-04 ± 3.460e-05	6.807e-04 ± 3.755e-05	6.454e-04 ± 3.381e-05	6.439e-04 ± 6.515e-05	0.18 %	-0.23 %	3.405	0.019 *	2.918	0.03 *
ST_FO_right	6.794e-04 ± 3.338e-05	6.773e-04 ± 3.279e-05	6.604e-04 ± 4.087e-05	6.472e-04 ± 3.854e-05	-0.31 %	-2.01 %	1.868	0.204	3.135	0.024*
ST_OCC_left	6.844e-04 ± 3.375e-05	6.831e-04 ± 3.157e-05	6.662e-04 ± 2.020e-05	6.689e-04 ± 5.584e-05	-0.2 %	0.41 %	1.996	0.202	1.324	0.289
ST_OCC_right	6.743e-04 ± 3.673e-05	6.726e-04 ± 3.110e-05	6.658e-04 ± 2.164e-05	6.658e-04 ± 3.611e-05	-0.25 %	-0.01 %	0.856	0.508	0.759	0.516
ST_PAR_left	7.027e-04 ± 2.979e-05	7.040e-04 ± 3.110e-05	7.013e-04 ± 4.253e-05	6.992e-04 ± 6.829e-05	0.18 %	-0.3 %	0.147	0.725	0.406	0.657
ST_PAR_right	6.805e-04 ± 3.013e-05	6.816e-04 ± 2.781e-05	6.765e-04 ± 3.588e-05	6.785e-04 ± 5.953e-05	0.16 %	0.3 %	0.440	0.67	0.298	0.674
ST_POSTC_left	7.006e-04 ± 2.844e-05	6.993e-04 ± 3.708e-05	6.903e-04 ± 5.255e-05	6.831e-04 ± 7.874e-05	-0.19 %	-1.05 %	1.030	0.461	1.182	0.339
ST_POSTC_right	6.683e-04 ± 2.854e-05	6.682e-04 ± 3.251e-05	6.665e-04 ± 5.109e-05	6.713e-04 ± 8.250e-05	-0.03 %	0.72 %	0.186	0.725	-0.236	0.674
ST_PREC_left	6.905e-04 ± 2.735e-05	6.859e-04 ± 3.627e-05	6.655e-04 ± 4.600e-05	6.650e-04 ± 7.016e-05	-0.66 %	-0.07 %	2.697	0.077	1.631	0.211
ST_PREC_right	6.658e-04 ± 2.834e-05	6.613e-04 ± 2.734e-05	6.546e-04 ± 3.867e-05	6.551e-04 ± 6.024e-05	-0.68 %	0.08 %	1.268	0.408	0.601	0.558

Table A.4 (cont'd)

	mTBI		Controls		Percent Change					
TractSeg Abbv	P1	P2	P1	P2	mTBI	Control	t-score P1	q-value P1[1]	t-score P2	q-value P2[1]
ST_PREF_left	6.862e-04 ± 2.550e-05	6.826e-04 ± 2.901e-05	6.631e-04 ± 4.479e-05	6.584e-04 ± 5.170e-05	-0.53 %	-0.71 %	2.633	0.078	2.461	0.079
ST_PREF_right	6.861e-04 ± 2.578e-05	6.823e-04 ± 2.420e-05	6.701e-04 ± 4.125e-05	6.570e-04 ± 3.744e-05	-0.55 %	-1.96 %	1.873	0.204	3.277	0.024*
ST_PREM_left	7.003e-04 ± 2.757e-05	6.946e-04 ± 3.653e-05	6.724e-04 ± 4.717e-05	6.559e-04 ± 4.144e-05	-0.81 %	-2.45 %	2.975	0.053	3.652	0.012*
ST_PREM_right	6.798e-04 ± 2.468e-05	6.738e-04 ± 2.700e-05	6.611e-04 ± 5.068e-05	6.543e-04 ± 4.936e-05	-0.88 %	-1.02 %	2.045	0.195	2.104	0.137
T_OCC_left	7.072e-04 ± 4.198e-05	7.054e-04 ± 4.044e-05	6.937e-04 ± 3.080e-05	6.965e-04 ± 7.268e-05	-0.25 %	0.4 %	1.162	0.414	0.648	0.546
T_OCC_right	6.955e-04 ± 4.611e-05	6.939e-04 ± 3.958e-05	6.959e-04 ± 3.580e-05	6.940e-04 ± 5.270e-05	-0.23 %	-0.27 %	-0.029	0.725	-0.010	0.683
T_PAR_left	7.125e-04 ± 3.498e-05	7.142e-04 ± 3.744e-05	7.171e-04 ± 5.163e-05	7.146e-04 ± 8.467e-05	0.24 %	-0.35 %	-0.406	0.682	-0.025	0.683
T_PAR_right	6.970e-04 ± 3.743e-05	6.972e-04 ± 3.505e-05	6.990e-04 ± 4.984e-05	6.988e-04 ± 7.777e-05	0.03 %	-0.04 %	-0.177	0.725	-0.120	0.674
T_POSTC_left	6.971e-04 ± 3.117e-05	6.983e-04 ± 4.104e-05	7.039e-04 ± 6.754e-05	6.936e-04 ± 9.480e-05	0.18 %	-1.46 %	-0.572	0.625	0.295	0.674
T_POSTC_right	6.677e-04 ± 3.483e-05	6.697e-04 ± 3.996e-05	6.816e-04 ± 7.665e-05	6.863e-04 ± 1.103e-04	0.3 %	0.68 %	-1.046	0.461	-0.962	0.416
T_PREC_left	6.898e-04 ± 3.095e-05	6.852e-04 ± 4.194e-05	6.714e-04 ± 5.676e-05	6.694e-04 ± 8.506e-05	-0.66 %	-0.31 %	1.687	0.253	1.045	0.388
T_PREC_right	6.655e-04 ± 3.227e-05	6.598e-04 ± 3.168e-05	6.596e-04 ± 5.046e-05	6.588e-04 ± 7.162e-05	-0.84 %	-0.13 %	0.550	0.626	0.087	0.674
T_PREF_left	7.001e-04 ± 2.893e-05	6.957e-04 ± 3.602e-05	6.806e-04 ± 5.524e-05	6.725e-04 ± 6.216e-05	-0.63 %	-1.19 %	1.884	0.204	1.925	0.151
T_PREF_right	7.107e-04 ± 3.313e-05	7.047e-04 ± 3.333e-05	7.004e-04 ± 5.745e-05	6.844e-04 ± 5.691e-05	-0.85 %	-2.29 %	0.907	0.484	1.830	0.167
T_PREM_left	7.121e-04 ± 3.405e-05	7.060e-04 ± 4.735e-05	6.912e-04 ± 6.029e-05	6.707e-04 ± 6.564e-05	-0.85 %	-2.97 %	1.776	0.234	2.427	0.079
T_PREM_right	6.954e-04 ± 3.690e-05	6.867e-04 ± 3.860e-05	6.861e-04 ± 8.031e-05	6.738e-04 ± 7.435e-05	-1.25 %	-1.8 %	0.654	0.598	0.949	0.416
UF_left	6.887e-04 ± 2.637e-05	6.933e-04 ± 2.901e-05	6.710e-04 ± 3.417e-05	6.656e-04 ± 3.905e-05	0.67 %	-0.81 %	2.174	0.158	3.138	0.024*
UF_right	7.064e-04 ± 2.464e-05	7.077e-04 ± 3.061e-05	6.943e-04 ± 4.186e-05	6.804e-04 ± 4.518e-05	0.19 %	-2.01 %	1.448	0.364	2.848	0.031*

Tables A.4- T-test results for comparisons of the automatically segmented tracts from TractSeg between mTBI and control subjects.

[1]Significant values are marked with an asterisk (*) or <0.001

Table A.5 Results of Post Hoc Tract Specific Comparisons of Diffusion Kurtosis Imaging Fractional Anisotropy

	mTBI		Controls		Percent Change					
TractSeg Abbv.	P1	P2	P1	P2	mTBI	Controls	t-score P1	q-value P1[1]	t-score P2	q-value P21
AF_left	0.200 ± 0.010	0.200 ± 0.008	0.202 ± 0.014	0.204 ± 0.013	0.02 %	0.77 %	-0.689	0.638	-1.403	0.383
AF_right	0.204 ± 0.008	0.203 ± 0.008	0.202 ± 0.011	0.201 ± 0.020	-0.53 %	-0.71 %	0.654	0.638	0.605	0.665
ATR_left	0.204 ± 0.008	0.204 ± 0.009	0.210 ± 0.015	0.213 ± 0.014	0.26 %	1.53 %	-2.185	0.365	-3.155	0.125
ATR_right	0.199 ± 0.008	0.200 ± 0.009	0.203 ± 0.013	0.204 ± 0.016	0.27 %	0.77 %	-1.386	0.525	-1.555	0.383
CA	0.208 ± 0.013	0.207 ± 0.018	0.220 ± 0.016	0.219 ± 0.027	-0.34 %	-0.44 %	-3.209	0.111	-2.250	0.245
CC_1	0.258 ± 0.016	0.255 ± 0.023	0.264 ± 0.017	0.257 ± 0.041	-0.98 %	-2.65 %	-1.265	0.615	-0.188	0.738
CC_2	0.224 ± 0.010	0.223 ± 0.010	0.227 ± 0.016	0.228 ± 0.021	-0.34 %	0.43 %	-0.810	0.638	-1.203	0.402
CC_3	0.224 ± 0.012	0.223 ± 0.017	0.229 ± 0.025	0.231 ± 0.028	-0.67 %	1.07 %	-0.953	0.638	-1.491	0.383
CC_4	0.234 ± 0.013	0.232 ± 0.014	0.235 ± 0.024	0.238 ± 0.025	-0.64 %	1.09 %	-0.235	0.722	-1.075	0.457
CC_5	0.243 ± 0.013	0.241 ± 0.015	0.243 ± 0.025	0.245 ± 0.029	-0.98 %	1.06 %	0.086	0.752	-0.879	0.551
CC_6	0.234 ± 0.013	0.234 ± 0.010	0.230 ± 0.017	0.229 ± 0.021	-0.27 %	-0.14 %	1.209	0.638	1.262	0.383
CC_7	0.236 ± 0.012	0.235 ± 0.012	0.233 ± 0.009	0.229 ± 0.030	-0.33 %	-1.92 %	0.855	0.638	1.373	0.383
CC	0.228 ± 0.010	0.228 ± 0.009	0.228 ± 0.016	0.228 ± 0.021	-0.3 %	0.06 %	0.182	0.722	-0.065	0.738
CG_left	0.215 ± 0.012	0.217 ± 0.014	0.217 ± 0.018	0.216 ± 0.022	0.95 %	-0.37 %	-0.410	0.722	0.273	0.738
CG_right	0.219 ± 0.013	0.219 ± 0.012	0.218 ± 0.017	0.217 ± 0.019	0.21 %	-0.16 %	0.308	0.722	0.542	0.671
CST_left	0.255 ± 0.010	0.257 ± 0.011	0.260 ± 0.019	0.264 ± 0.018	0.45 %	1.47 %	-1.391	0.525	-2.030	0.308
CST_right	0.262 ± 0.010	0.262 ± 0.011	0.263 ± 0.018	0.263 ± 0.024	0.07 %	0.09 %	-0.231	0.722	-0.206	0.738
FPT_left	0.246 ± 0.010	0.247 ± 0.011	0.249 ± 0.020	0.252 ± 0.020	0.44 %	1.2 %	-1.067	0.638	-1.490	0.383
FPT_right	0.248 ± 0.010	0.248 ± 0.010	0.249 ± 0.017	0.251 ± 0.020	0.15 %	1 %	-0.244	0.722	-0.823	0.566
FX_left	0.185 ± 0.037	0.186 ± 0.039	0.192 ± 0.038	0.191 ± 0.046	0.55 %	-0.54 %	-0.669	0.638	-0.453	0.684
FX_right	0.189 ± 0.037	0.190 ± 0.042	0.193 ± 0.039	0.198 ± 0.042	0.56 %	2.1 %	-0.378	0.722	-0.602	0.665
ICP_left	0.200 ± 0.020	0.200 ± 0.022	0.189 ± 0.023	0.189 ± 0.031	-0.15 %	-0.38 %	1.800	0.375	1.643	0.383
ICP_right	0.189 ± 0.013	0.187 ± 0.014	0.178 ± 0.019	0.181 ± 0.024	-1.15 %	1.79 %	2.748	0.211	1.356	0.383
IFO_left	0.217 ± 0.009	0.216 ± 0.009	0.218 ± 0.010	0.215 ± 0.023	-0.26 %	-1.35 %	-0.416	0.722	0.359	0.727
IFO_right	0.216 ± 0.008	0.215 ± 0.009	0.216 ± 0.008	0.215 ± 0.021	-0.37 %	-0.7 %	-0.049	0.752	0.174	0.738
ILF_left	0.214 ± 0.009	0.213 ± 0.011	0.217 ± 0.007	0.212 ± 0.027	-0.45 %	-2.37 %	-1.156	0.638	0.302	0.738
ILF_right	0.214 ± 0.009	0.213 ± 0.013	0.216 ± 0.009	0.212 ± 0.028	-0.29 %	-1.6 %	-0.850	0.638	0.153	0.738
MCP	0.218 ± 0.012	0.217 ± 0.012	0.212 ± 0.023	0.209 ± 0.026	-0.53 %	-1.08 %	1.495	0.485	1.632	0.383
MLF_left	0.207 ± 0.011	0.208 ± 0.008	0.204 ± 0.014	0.206 ± 0.013	0.33 %	0.85 %	0.860	0.638	0.692	0.656
MLF_right	0.214 ± 0.010	0.213 ± 0.009	0.209 ± 0.015	0.208 ± 0.019	-0.46 %	-0.05 %	1.560	0.457	1.251	0.383
OR_left	0.223 ± 0.011	0.223 ± 0.011	0.223 ± 0.007	0.220 ± 0.028	-0.08 %	-1.31 %	-0.034	0.752	0.587	0.665
OR_right	0.231 ± 0.011	0.231 ± 0.011	0.230 ± 0.009	0.228 ± 0.020	-0.09 %	-0.66 %	0.352	0.722	0.628	0.665
POPT_left	0.238 ± 0.009	0.238 ± 0.010	0.236 ± 0.017	0.239 ± 0.017	0.12 %	1.2 %	0.627	0.645	-0.143	0.738
POPT_right	0.249 ± 0.010	0.249 ± 0.010	0.248 ± 0.017	0.250 ± 0.020	-0.06 %	0.78 %	0.375	0.722	-0.226	0.738
SCP_left	0.230 ± 0.013	0.231 ± 0.017	0.229 ± 0.019	0.233 ± 0.023	0.4 %	1.81 %	0.302	0.722	-0.384	0.722
SCP_right	0.232 ± 0.009	0.231 ± 0.012	0.226 ± 0.020	0.231 ± 0.021	-0.32 %	2.19 %	1.696	0.375	0.095	0.738
SLF_III_left	0.205 ± 0.011	0.204 ± 0.010	0.205 ± 0.021	0.208 ± 0.017	-0.62 %	1.43 %	0.048	0.752	-1.184	0.402
SLF_III_right	0.209 ± 0.009	0.206 ± 0.011	0.203 ± 0.014	0.200 ± 0.028	-1.33 %	-1.53 %	2.040	0.365	1.363	0.383
SLF_II_left	0.193 ± 0.011	0.194 ± 0.011	0.192 ± 0.015	0.198 ± 0.018	0.69 %	2.71 %	0.067	0.752	-1.045	0.457
SLF_II_right	0.194 ± 0.010	0.194 ± 0.010	0.191 ± 0.014	0.194 ± 0.015	0.08 %	1.46 %	0.909	0.638	0.058	0.738
SLF_I_left	0.193 ± 0.010	0.194 ± 0.012	0.190 ± 0.022	0.193 ± 0.018	0.44 %	1.79 %	0.788	0.638	0.128	0.738
SLF_I_right	0.201 ± 0.011	0.203 ± 0.012	0.199 ± 0.019	0.203 ± 0.017	0.58 %	2.23 %	0.737	0.638	-0.156	0.738
STR_left	0.247 ± 0.011	0.249 ± 0.014	0.254 ± 0.019	0.256 ± 0.026	0.53 %	1.05 %	-1.720	0.375	-1.624	0.383
STR_right	0.255 ± 0.012	0.255 ± 0.012	0.257 ± 0.020	0.261 ± 0.018	0.01 %	1.7 %	-0.474	0.709	-1.622	0.383
ST_FO_left	0.225 ± 0.012	0.223 ± 0.013	0.233 ± 0.013	0.231 ± 0.026	-0.77 %	-0.72 %	-2.225	0.365	-1.721	0.383
ST_FO_right	0.228 ± 0.013	0.227 ± 0.016	0.232 ± 0.014	0.229 ± 0.028	-0.52 %	-1.02 %	-0.991	0.638	-0.503	0.679
ST_OCC_left	0.225 ± 0.011	0.225 ± 0.011	0.225 ± 0.010	0.221 ± 0.028	0 %	-1.4 %	0.241	0.722	0.873	0.551

Table A.5 (cont'd)

	mTBI		Controls		Percent Change					
TractSeg Abbv.	P1	P2	P1	P2	mTBI	Controls	t-score P1	q-value P1[1]	t-score P2	q-value P21
ST_OCC_right	0.229 ± 0.011	0.228 ± 0.011	0.227 ± 0.010	0.226 ± 0.020	-0.34 %	-0.46 %	0.496	0.706	0.476	0.679
ST_PAR_left	0.217 ± 0.010	0.218 ± 0.009	0.215 ± 0.016	0.217 ± 0.015	0.42 %	1.09 %	0.555	0.688	0.126	0.738
ST_PAR_right	0.228 ± 0.010	0.228 ± 0.009	0.226 ± 0.014	0.228 ± 0.016	-0.25 %	0.76 %	0.760	0.638	0.026	0.738
ST_POSTC_left	0.222 ± 0.010	0.223 ± 0.011	0.226 ± 0.017	0.230 ± 0.015	0.57 %	1.82 %	-1.133	0.638	-1.970	0.313
ST_POSTC_right	0.234 ± 0.011	0.233 ± 0.012	0.235 ± 0.017	0.238 ± 0.019	-0.22 %	1.24 %	-0.199	0.722	-1.058	0.457
ST_PREC_left	0.222 ± 0.009	0.223 ± 0.011	0.229 ± 0.016	0.231 ± 0.014	0.53 %	1.18 %	-2.122	0.365	-2.506	0.245
ST_PREC_right	0.230 ± 0.009	0.230 ± 0.009	0.231 ± 0.015	0.234 ± 0.016	0.18 %	1.25 %	-0.515	0.706	-1.305	0.383
ST_PREF_left	0.215 ± 0.009	0.216 ± 0.008	0.220 ± 0.015	0.221 ± 0.016	0.29 %	0.41 %	-1.718	0.375	-1.817	0.383
ST_PREF_right	0.214 ± 0.008	0.214 ± 0.008	0.217 ± 0.012	0.218 ± 0.016	0.03 %	0.69 %	-1.011	0.638	-1.445	0.383
ST_PREM_left	0.207 ± 0.009	0.208 ± 0.009	0.213 ± 0.017	0.215 ± 0.015	0.46 %	1.27 %	-1.720	0.375	-2.409	0.245
ST_PREM_right	0.216 ± 0.008	0.216 ± 0.009	0.218 ± 0.016	0.221 ± 0.018	0.26 %	1.1 %	-0.803	0.638	-1.298	0.383
T_OCC_left	0.220 ± 0.011	0.220 ± 0.011	0.221 ± 0.006	0.218 ± 0.027	-0.02 %	-1.35 %	-0.193	0.722	0.548	0.671
T_OCC_right	0.227 ± 0.011	0.227 ± 0.011	0.226 ± 0.009	0.224 ± 0.019	-0.04 %	-0.68 %	0.299	0.722	0.638	0.665
T_PAR_left	0.216 ± 0.010	0.217 ± 0.009	0.214 ± 0.016	0.217 ± 0.017	0.36 %	1.36 %	0.657	0.638	-0.006	0.739
T_PAR_right	0.228 ± 0.011	0.228 ± 0.010	0.226 ± 0.015	0.228 ± 0.016	0.08 %	1.05 %	0.695	0.638	0.042	0.738
T_POSTC_left	0.227 ± 0.010	0.228 ± 0.012	0.226 ± 0.021	0.233 ± 0.019	0.32 %	2.76 %	0.141	0.738	-1.270	0.383
T_POSTC_right	0.239 ± 0.013	0.238 ± 0.015	0.235 ± 0.025	0.238 ± 0.024	-0.28 %	1.38 %	0.756	0.638	-0.077	0.738
T_PREC_left	0.225 ± 0.009	0.226 ± 0.012	0.231 ± 0.019	0.235 ± 0.017	0.56 %	1.79 %	-1.735	0.375	-2.291	0.245
T_PREC_right	0.230 ± 0.010	0.231 ± 0.011	0.231 ± 0.018	0.234 ± 0.016	0.45 %	1.47 %	-0.190	0.722	-0.862	0.551
T_PREF_left	0.215 ± 0.009	0.216 ± 0.010	0.220 ± 0.016	0.223 ± 0.017	0.49 %	1.05 %	-1.813	0.375	-2.121	0.285
T_PREF_right	0.209 ± 0.008	0.210 ± 0.009	0.212 ± 0.013	0.214 ± 0.015	0.39 %	1.22 %	-0.985	0.638	-1.527	0.383
T_PREM_left	0.212 ± 0.009	0.214 ± 0.011	0.219 ± 0.017	0.224 ± 0.016	0.66 %	2.24 %	-2.032	0.365	-2.885	0.138
T_PREM_right	0.217 ± 0.010	0.219 ± 0.011	0.220 ± 0.020	0.224 ± 0.019	0.72 %	1.63 %	-0.818	0.638	-1.332	0.383
UF_left	0.221 ± 0.012	0.219 ± 0.014	0.224 ± 0.014	0.220 ± 0.026	-1.12 %	-1.77 %	-0.787	0.638	-0.292	0.738
UF_right	0.215 ± 0.010	0.214 ± 0.015	0.218 ± 0.011	0.216 ± 0.028	-0.82 %	-0.92 %	-0.913	0.638	-0.479	0.679

Tables A.5- T-test results for comparisons of the automatically segmented tracts from TractSeg between mTBI and control subjects.

[1]Significant values are marked with an asterisk (*) or <0.001

Table A.6 Results of Post Hoc Tract Specific Comparisons of Diffusion Kurtosis Imaging Mean Diffusivity

	mTBI		Controls		Percent Change					
TractSeg Abbv.	P1	P2	P1	P2	mTBI	Controls	t-score P1	q-value P1′	t-score P2	q-value P2′
AF_left	9.405e-04 ± 2.940e-05	9.323e-04 ± 3.288e-05	9.049e-04 ± 3.749e-05	8.943e-04 ± 4.150e-05	-0.87 %	-1.18 %	3.941	0.002*	3.874	<0.001
AF_right	9.296e-04 ± 2.842e-05	9.242e-04 ± 2.501e-05	9.134e-04 ± 3.055e-05	9.025e-04 ± 3.455e-05	-0.58 %	-1.19 %	1.948	0.066	2.831	0.004*
ATR_left	9.992e-04 ± 4.547e-05	9.917e-04 ± 5.552e-05	9.651e-04 ± 5.828e-05	9.416e-04 ± 6.102e-05	-0.75 %	-2.43 %	2.438	0.031*	3.133	0.002*
ATR_right	1.011e-03 ± 5.214e-05	9.990e-04 ± 5.000e-05	9.922e-04 ± 7.752e-05	9.710e-04 ± 7.387e-05	-1.2 %	-2.13 %	1.126	0.197	1.780	0.025*
CA	1.051e-03 ± 3.639e-05	1.045e-03 ± 5.522e-05	9.882e-04 ± 4.902e-05	9.673e-04 ± 5.410e-05	-0.58 %	-2.11 %	5.509	<0.001	4.988	<0.001
CC_1	1.027e-03 ± 5.777e-05	1.019e-03 ± 6.614e-05	1.018e-03 ± 9.343e-05	9.792e-04 ± 6.515e-05	-0.81 %	-3.77 %	0.484	0.348	2.118	0.015*
CC_2	9.983e-04 ± 3.397e-05	9.973e-04 ± 4.112e-05	9.747e-04 ± 4.772e-05	9.563e-04 ± 5.529e-05	-0.1 %	-1.89 %	2.194	0.047*	3.272	0.002*
CC_3	1.023e-03 ± 4.521e-05	1.026e-03 ± 6.617e-05	9.953e-04 ± 6.128e-05	9.825e-04 ± 8.887e-05	0.35 %	-1.29 %	1.934	0.066	2.174	0.013*
CC_4	1.015e-03 ± 3.549e-05	1.021e-03 ± 4.994e-05	9.975e-04 ± 5.900e-05	1.003e-03 ± 1.205e-04	0.61 %	0.6 %	1.475	0.139	0.895	0.076
CC_5	1.004e-03 ± 3.478e-05	1.015e-03 ± 5.405e-05	9.915e-04 ± 6.630e-05	9.959e-04 ± 1.314e-04	1.13 %	0.44 %	0.973	0.229	0.881	0.076
CC_6	9.667e-04 ± 4.284e-05	9.703e-04 ± 3.623e-05	9.569e-04 ± 3.907e-05	9.626e-04 ± 7.973e-05	0.37 %	0.59 %	0.797	0.275	0.563	0.102
CC_7	9.930e-04 ± 7.692e-05	9.924e-04 ± 5.292e-05	9.851e-04 ± 4.702e-05	9.946e-04 ± 8.659e-05	-0.06 %	0.96 %	0.378	0.377	-0.127	0.141
CC	9.882e-04 ± 3.531e-05	9.895e-04 ± 3.479e-05	9.744e-04 ± 4.187e-05	9.700e-04 ± 7.486e-05	0.13 %	-0.45 %	1.303	0.17	1.503	0.037*
CG_left	9.343e-04 ± 2.881e-05	9.320e-04 ± 2.868e-05	9.146e-04 ± 5.173e-05	9.169e-04 ± 9.080e-05	-0.25 %	0.24 %	1.966	0.066	1.107	0.065
CG_right	9.228e-04 ± 3.196e-05	9.186e-04 ± 2.781e-05	9.050e-04 ± 4.795e-05	8.982e-04 ± 7.526e-05	-0.46 %	-0.75 %	1.720	0.091	1.716	0.027*
CST_left	1.005e-03 ± 3.049e-05	1.002e-03 ± 4.362e-05	9.677e-04 ± 5.499e-05	9.620e-04 ± 9.214e-05	-0.34 %	-0.59 %	3.510	0.004*	2.458	0.008*
CST_right	9.612e-04 ± 3.090e-05	9.573e-04 ± 3.144e-05	9.326e-04 ± 4.490e-05	9.427e-04 ± 9.243e-05	-0.4 %	1.08 %	2.888	0.017*	1.031	0.071
FPT_left	1.005e-03 ± 2.968e-05	1.003e-03 ± 4.230e-05	9.738e-04 ± 7.679e-05	9.531e-04 ± 8.568e-05	-0.18 %	-2.13 %	2.504	0.03*	3.292	0.002*
FPT_right	9.983e-04 ± 3.213e-05	9.962e-04 ± 3.487e-05	9.747e-04 ± 7.129e-05	9.528e-04 ± 7.834e-05	-0.21 %	-2.25 %	1.900	0.069	3.263	0.002*
FX_left	2.084e-03 ± 3.622e-04	2.053e-03 ± 3.602e-04	2.071e-03 ± 3.822e-04	2.052e-03 ± 4.225e-04	-1.49 %	-0.92 %	0.119	0.461	0.006	0.151
FX_right	2.055e-03 ± 3.465e-04	2.035e-03 ± 3.660e-04	2.050e-03 ± 3.706e-04	1.971e-03 ± 4.431e-04	-1.01 %	-3.89 %	0.049	0.461	0.594	0.1
ICP_left	8.986e-04 ± 8.235e-05	8.888e-04 ± 5.192e-05	8.881e-04 ± 6.794e-05	8.751e-04 ± 8.569e-05	-1.08 %	-1.47 %	0.453	0.354	0.809	0.081
ICP_right	8.806e-04 ± 6.453e-05	8.727e-04 ± 4.092e-05	8.802e-04 ± 7.328e-05	8.455e-04 ± 9.221e-05	-0.9 %	-3.94 %	0.018	0.461	1.735	0.026*
IFO_left	9.595e-04 ± 3.503e-05	9.568e-04 ± 3.508e-05	9.338e-04 ± 2.693e-05	9.277e-04 ± 4.550e-05	-0.28 %	-0.66 %	2.635	0.027*	2.761	0.004*
IFO_right	9.506e-04 ± 4.005e-05	9.457e-04 ± 3.215e-05	9.348e-04 ± 3.207e-05	9.272e-04 ± 3.808e-05	-0.51 %	-0.82 %	1.407	0.153	1.964	0.018*
ILF_left	9.724e-04 ± 5.191e-05	9.619e-04 ± 4.314e-05	9.423e-04 ± 3.590e-05	9.315e-04 ± 5.478e-05	-1.07 %	-1.15 %	2.108	0.054	2.357	0.01*
ILF_right	9.614e-04 ± 5.392e-05	9.529e-04 ± 4.118e-05	9.451e-04 ± 4.685e-05	9.341e-04 ± 6.133e-05	-0.88 %	-1.16 %	1.069	0.211	1.451	0.038*

Table A.6 (cont'd)

	mTBI		Controls		Percent Change					
TractSeg Abbv.	P1	P2	P1	P2	mTBI	Controls	t-score P1	q-value P1[f]	t-score P2	q-value P2[f]
MCP	8.708e-04 ± 6.393e-05	8.685e-04 ± 4.820e-05	8.572e-04 ± 6.320e-05	8.784e-04 ± 8.677e-05	-0.27 %	2.47 %	0.735	0.284	-0.608	0.099
MLF_left	9.510e-04 ± 3.528e-05	9.494e-04 ± 3.444e-05	9.384e-04 ± 3.773e-05	9.319e-04 ± 5.611e-05	-0.18 %	-0.69 %	1.220	0.174	1.550	0.035*
MLF_right	9.415e-04 ± 3.877e-05	9.415e-04 ± 3.484e-05	9.359e-04 ± 4.410e-05	9.289e-04 ± 5.616e-05	0 %	-0.75 %	0.483	0.348	1.111	0.065
OR_left	9.945e-04 ± 5.449e-05	9.898e-04 ± 5.405e-05	9.744e-04 ± 4.405e-05	9.733e-04 ± 8.667e-05	-0.47 %	-0.12 %	1.315	0.17	0.943	0.076
OR_right	9.831e-04 ± 6.108e-05	9.795e-04 ± 5.414e-05	9.841e-04 ± 5.234e-05	9.772e-04 ± 7.327e-05	-0.37 %	-0.7 %	-0.058	0.461	0.138	0.141
POPT_left	9.991e-04 ± 3.297e-05	1.003e-03 ± 3.879e-05	9.932e-04 ± 5.520e-05	9.883e-04 ± 9.957e-05	0.39 %	-0.49 %	0.528	0.342	0.912	0.076
POPT_right	9.794e-04 ± 3.744e-05	9.816e-04 ± 3.672e-05	9.688e-04 ± 5.193e-05	9.708e-04 ± 9.200e-05	0.22 %	0.2 %	0.898	0.246	0.725	0.088
SCP_left	9.493e-04 ± 3.634e-05	9.421e-04 ± 4.372e-05	9.138e-04 ± 5.534e-05	9.047e-04 ± 7.949e-05	-0.75 %	-0.99 %	3.000	0.014*	2.499	0.008*
SCP_right	9.361e-04 ± 2.950e-05	9.290e-04 ± 3.024e-05	9.207e-04 ± 7.218e-05	9.000e-04 ± 5.096e-05	-0.75 %	-2.25 %	1.273	0.174	2.899	0.003*
SLF_III_left	9.434e-04 ± 3.034e-05	9.396e-04 ± 3.632e-05	9.186e-04 ± 6.050e-05	9.067e-04 ± 6.975e-05	-0.4 %	-1.29 %	2.241	0.045*	2.579	0.007*
SLF_III_right	9.267e-04 ± 2.895e-05	9.254e-04 ± 2.677e-05	9.196e-04 ± 3.960e-05	9.110e-04 ± 5.053e-05	-0.15 %	-0.94 %	0.784	0.275	1.544	0.035*
SLF_II_left	9.559e-04 ± 3.748e-05	9.506e-04 ± 3.974e-05	9.367e-04 ± 5.163e-05	9.242e-04 ± 6.602e-05	-0.56 %	-1.33 %	1.630	0.106	2.013	0.017*
SLF_II_right	9.449e-04 ± 3.611e-05	9.399e-04 ± 3.350e-05	9.310e-04 ± 4.893e-05	9.181e-04 ± 5.575e-05	-0.54 %	-1.39 %	1.237	0.174	1.979	0.018*
SLF_I_left	9.992e-04 ± 5.026e-05	1.002e-03 ± 5.790e-05	1.011e-03 ± 1.104e-04	9.988e-04 ± 1.340e-04	0.29 %	-1.24 %	-0.630	0.313	0.147	0.141
SLF_I_right	9.798e-04 ± 4.602e-05	9.771e-04 ± 5.018e-05	9.788e-04 ± 8.196e-05	9.684e-04 ± 1.147e-04	-0.27 %	-1.06 %	0.064	0.461	0.450	0.112
STR_left	9.481e-04 ± 2.894e-05	9.418e-04 ± 4.814e-05	8.943e-04 ± 5.409e-05	9.001e-04 ± 1.305e-04	-0.66 %	0.65 %	5.250	<0.001	2.022	0.017*
STR_right	9.235e-04 ± 2.917e-05	9.162e-04 ± 3.585e-05	8.993e-04 ± 6.302e-05	8.863e-04 ± 8.140e-05	-0.8 %	-1.45 %	2.186	0.047*	2.173	0.013*
ST_FO_left	9.471e-04 ± 4.708e-05	9.451e-04 ± 5.533e-05	9.020e-04 ± 4.637e-05	8.959e-04 ± 6.989e-05	-0.21 %	-0.67 %	3.320	0.006*	2.980	0.003*
ST_FO_right	9.540e-04 ± 4.446e-05	9.478e-04 ± 4.387e-05	9.270e-04 ± 5.471e-05	9.033e-04 ± 3.635e-05	-0.65 %	-2.56 %	2.002	0.066	3.723	<0.001
ST_OCC_left	9.709e-04 ± 4.304e-05	9.666e-04 ± 4.266e-05	9.416e-04 ± 2.495e-05	9.403e-04 ± 5.582e-05	-0.44 %	-0.14 %	2.514	0.03*	2.046	0.017*
ST_OCC_right	9.519e-04 ± 4.755e-05	9.476e-04 ± 4.183e-05	9.384e-04 ± 3.310e-05	9.355e-04 ± 4.555e-05	-0.45 %	-0.3 %	1.034	0.218	1.006	0.073
ST_PAR_left	9.781e-04 ± 3.716e-05	9.795e-04 ± 3.927e-05	9.692e-04 ± 4.808e-05	9.649e-04 ± 8.628e-05	0.14 %	-0.45 %	0.775	0.275	0.991	0.073
ST_PAR_right	9.555e-04 ± 3.860e-05	9.552e-04 ± 3.533e-05	9.441e-04 ± 4.045e-05	9.445e-04 ± 7.279e-05	-0.03 %	0.04 %	1.009	0.222	0.835	0.079
ST_POSTC_left	9.937e-04 ± 3.872e-05	9.907e-04 ± 5.073e-05	9.698e-04 ± 6.816e-05	9.574e-04 ± 1.078e-04	-0.3 %	-1.27 %	1.795	0.082	1.771	0.025*
ST_POSTC_right	9.563e-04 ± 3.757e-05	9.534e-04 ± 3.951e-05	9.484e-04 ± 6.615e-05	9.513e-04 ± 1.081e-04	-0.31 %	0.31 %	0.617	0.313	0.125	0.141
ST_PREC_left	9.860e-04 ± 3.607e-05	9.786e-04 ± 5.040e-05	9.413e-04 ± 5.738e-05	9.381e-04 ± 9.289e-05	-0.75 %	-0.34 %	3.749	0.002*	2.337	0.01*
ST_PREC_right	9.556e-04 ± 3.735e-05	9.469e-04 ± 3.475e-05	9.327e-04 ± 5.116e-05	9.306e-04 ± 7.729e-05	-0.91 %	-0.22 %	1.958	0.066	1.234	0.055

Table A.6 (cont'd)

	mTBI		Controls		Percent Change					
TractSeg Abbv.	P1	P2	P1	P2	mTBI	Controls	t-score P1	q-value P1[1]	t-score P2	q-value P2[1]
ST_PREF_left	9.640e-04 ± 3.279e-05	9.582e-04 ± 4.179e-05	9.262e-04 ± 5.308e-05	9.136e-04 ± 6.012e-05	-0.6 %	-1.36 %	3.463	0.004*	3.428	0.001*
ST_PREF_right	9.622e-04 ± 3.418e-05	9.550e-04 ± 3.441e-05	9.342e-04 ± 5.387e-05	9.133e-04 ± 4.582e-05	-0.75 %	-2.24 %	2.490	0.03*	3.995	<0.001
ST_PREM_left	9.727e-04 ± 3.862e-05	9.648e-04 ± 5.527e-05	9.254e-04 ± 5.624e-05	8.975e-04 ± 4.967e-05	-0.81 %	-3.02 %	3.824	0.002*	4.409	<0.001
ST_PREM_right	9.570e-04 ± 3.336e-05	9.475e-04 ± 3.796e-05	9.252e-04 ± 6.306e-05	9.101e-04 ± 5.958e-05	-0.99 %	-1.64 %	2.682	0.026*	3.071	0.003*
T_OCC_left	1.001e-03 ± 5.633e-05	9.958e-04 ± 5.548e-05	9.813e-04 ± 4.437e-05	9.800e-04 ± 8.538e-05	-0.53 %	-0.14 %	1.259	0.174	0.896	0.076
T_OCC_right	9.842e-04 ± 6.157e-05	9.801e-04 ± 5.434e-05	9.846e-04 ± 5.332e-05	9.783e-04 ± 7.429e-05	-0.41 %	-0.63 %	-0.023	0.461	0.110	0.141
T_PAR_left	9.924e-04 ± 4.415e-05	9.945e-04 ± 4.689e-05	9.928e-04 ± 6.218e-05	9.876e-04 ± 1.092e-04	0.21 %	-0.53 %	-0.031	0.461	0.376	0.119
T_PAR_right	9.798e-04 ± 4.823e-05	9.789e-04 ± 4.424e-05	9.773e-04 ± 6.115e-05	9.748e-04 ± 9.990e-05	-0.1 %	-0.26 %	0.170	0.448	0.242	0.134
T_POSTC_left	9.904e-04 ± 3.971e-05	9.908e-04 ± 5.222e-05	9.876e-04 ± 8.681e-05	9.722e-04 ± 1.256e-04	0.04 %	-1.56 %	0.183	0.448	0.894	0.076
T_POSTC_right	9.554e-04 ± 4.229e-05	9.565e-04 ± 4.577e-05	9.661e-04 ± 9.372e-05	9.680e-04 ± 1.417e-04	0.12 %	0.19 %	-0.659	0.308	-0.536	0.103
T_PREC_left	9.895e-04 ± 3.827e-05	9.824e-04 ± 5.481e-05	9.537e-04 ± 6.981e-05	9.490e-04 ± 1.109e-04	-0.72 %	-0.49 %	2.674	0.026*	1.689	0.028*
T_PREC_right	9.530e-04 ± 4.062e-05	9.440e-04 ± 3.812e-05	9.369e-04 ± 6.181e-05	9.331e-04 ± 9.125e-05	-0.94 %	-0.41 %	1.216	0.174	0.723	0.088
T_PREF_left	9.875e-04 ± 3.675e-05	9.809e-04 ± 4.894e-05	9.550e-04 ± 6.698e-05	9.383e-04 ± 7.597e-05	-0.67 %	-1.76 %	2.525	0.03*	2.720	0.005*
T_PREF_right	9.944e-04 ± 4.383e-05	9.846e-04 ± 4.471e-05	9.749e-04 ± 7.562e-05	9.510e-04 ± 7.470e-05	-0.98 %	-2.44 %	1.303	0.17	2.276	0.011*
T_PREM_left	9.990e-04 ± 4.493e-05	9.901e-04 ± 6.565e-05	9.630e-04 ± 7.541e-05	9.316e-04 ± 8.453e-05	-0.9 %	-3.26 %	2.378	0.034*	2.965	0.003*
T_PREM_right	9.810e-04 ± 4.743e-05	9.687e-04 ± 5.084e-05	9.640e-04 ± 1.017e-04	9.429e-04 ± 9.568e-05	-1.26 %	-2.19 %	0.947	0.233	1.462	0.038*
UF_left	9.459e-04 ± 3.425e-05	9.485e-04 ± 3.537e-05	9.204e-04 ± 4.060e-05	9.080e-04 ± 4.121e-05	0.28 %	-1.35 %	2.471	0.03*	3.918	<0.001
UF_right	9.729e-04 ± 3.170e-05	9.701e-04 ± 3.521e-05	9.535e-04 ± 5.527e-05	9.301e-04 ± 4.556e-05	-0.29 %	-2.46 %	1.786	0.082	3.777	<0.001

Tables A.6- T-test results for comparisons of the automatically segmented tracts from TractSeg between mTBI and control subjects.

[1]Significant values are marked with an asterisk (*) or <0.001

Table A.7 Results of Post Hoc Tract Specific Comparisons of Diffusion Kurtosis Imaging Axial Diffusivity

	mTBI		Controls		Percent Change					
TractSeg Abbv.	P1	P2	P1	P2	mTBI	Controls	t-score P1	q-value P1′	t-score P2	q-value P2
AF_left	1.137e-03 ± 2.870e-05	1.127e-03 ± 3.362e-05	1.095e-03 ± 3.274e-05	1.082e-03 ± 3.656e-05	-0.86 %	-1.15 %	4.927	<0.001	4.659	<0.001
AF_right	1.126e-03 ± 2.878e-05	1.119e-03 ± 2.558e-05	1.105e-03 ± 3.145e-05	1.089e-03 ± 2.307e-05	-0.68 %	-1.42 %	2.574	0.008*	4.230	<0.001
ATR_left	1.207e-03 ± 4.550e-05	1.199e-03 ± 5.503e-05	1.169e-03 ± 5.415e-05	1.143e-03 ± 5.492e-05	-0.7 %	-2.24 %	2.755	0.006*	3.578	<0.001
ATR_right	1.216e-03 ± 5.206e-05	1.203e-03 ± 4.988e-05	1.193e-03 ± 7.617e-05	1.168e-03 ± 6.844e-05	-1.1 %	-2.09 %	1.395	0.057	2.279	0.005*
CA	1.285e-03 ± 3.787e-05	1.276e-03 ± 5.025e-05	1.223e-03 ± 4.878e-05	1.194e-03 ± 3.581e-05	-0.69 %	-2.44 %	5.236	<0.001	6.108	<0.001
CC_1	1.318e-03 ± 6.172e-05	1.306e-03 ± 7.864e-05	1.310e-03 ± 9.903e-05	1.255e-03 ± 8.869e-05	-0.85 %	-4.21 %	0.371	0.196	2.264	0.005*
CC_2	1.238e-03 ± 3.436e-05	1.235e-03 ± 4.059e-05	1.207e-03 ± 4.365e-05	1.184e-03 ± 4.207e-05	-0.25 %	-1.97 %	2.868	0.004*	4.425	<0.001
CC_3	1.267e-03 ± 4.850e-05	1.267e-03 ± 6.164e-05	1.232e-03 ± 5.686e-05	1.214e-03 ± 7.173e-05	0.02 %	-1.48 %	2.387	0.011*	2.958	0.001*
CC_4	1.264e-03 ± 3.244e-05	1.267e-03 ± 4.850e-05	1.234e-03 ± 5.206e-05	1.237e-03 ± 1.013e-04	0.23 %	0.19 %	2.770	0.006*	1.702	0.014*
CC_5	1.260e-03 ± 3.440e-05	1.268e-03 ± 5.256e-05	1.235e-03 ± 5.934e-05	1.236e-03 ± 1.116e-04	0.63 %	0.08 %	2.117	0.019*	1.634	0.015*
CC_6	1.204e-03 ± 3.913e-05	1.207e-03 ± 3.687e-05	1.185e-03 ± 3.034e-05	1.188e-03 ± 6.570e-05	0.22 %	0.21 %	1.733	0.036*	1.526	0.017*
CC_7	1.240e-03 ± 7.382e-05	1.239e-03 ± 5.439e-05	1.227e-03 ± 5.163e-05	1.229e-03 ± 7.370e-05	-0.13 %	0.18 %	0.655	0.15	0.575	0.06
CC	1.225e-03 ± 3.237e-05	1.225e-03 ± 3.325e-05	1.204e-03 ± 3.478e-05	1.195e-03 ± 6.046e-05	-0.02 %	-0.75 %	2.240	0.015*	2.644	0.002*
CG_left	1.148e-03 ± 3.020e-05	1.147e-03 ± 2.997e-05	1.123e-03 ± 4.682e-05	1.121e-03 ± 8.185e-05	-0.06 %	-0.15 %	2.516	0.009*	2.012	0.008*
CG_right	1.136e-03 ± 3.228e-05	1.132e-03 ± 2.951e-05	1.112e-03 ± 3.971e-05	1.100e-03 ± 6.918e-05	-0.39 %	-1.08 %	2.479	0.009*	2.772	0.002*
CST_left	1.278e-03 ± 3.066e-05	1.272e-03 ± 4.403e-05	1.226e-03 ± 4.775e-05	1.218e-03 ± 8.127e-05	-0.4 %	-0.69 %	5.110	<0.001	3.610	<0.001
CST_right	1.232e-03 ± 3.136e-05	1.226e-03 ± 3.289e-05	1.192e-03 ± 4.279e-05	1.197e-03 ± 7.733e-05	-0.48 %	0.46 %	4.096	<0.001	2.246	0.005*
FPT_left	1.265e-03 ± 3.123e-05	1.263e-03 ± 4.285e-05	1.221e-03 ± 6.699e-05	1.197e-03 ± 7.479e-05	-0.23 %	-1.98 %	3.733	<0.001	4.548	<0.001
FPT_right	1.260e-03 ± 3.421e-05	1.256e-03 ± 3.649e-05	1.224e-03 ± 6.438e-05	1.199e-03 ± 6.964e-05	-0.29 %	-2.09 %	2.951	0.004*	4.517	<0.001
FX_left	2.431e-03 ± 3.183e-04	2.393e-03 ± 3.217e-04	2.407e-03 ± 3.339e-04	2.369e-03 ± 3.880e-04	-1.57 %	-1.56 %	0.261	0.215	0.252	0.083
FX_right	2.408e-03 ± 3.038e-04	2.381e-03 ± 3.238e-04	2.386e-03 ± 3.260e-04	2.295e-03 ± 4.230e-04	-1.11 %	-3.82 %	0.241	0.216	0.878	0.045*
ICP_left	1.081e-03 ± 8.088e-05	1.069e-03 ± 5.278e-05	1.059e-03 ± 5.528e-05	1.043e-03 ± 6.917e-05	-1.1 %	-1.47 %	1.017	0.096	1.641	0.015*
ICP_right	1.051e-03 ± 6.341e-05	1.040e-03 ± 4.193e-05	1.039e-03 ± 6.510e-05	1.004e-03 ± 9.658e-05	-1.08 %	-3.33 %	0.647	0.15	2.171	0.006*
IFO_left	1.181e-03 ± 3.524e-05	1.177e-03 ± 3.770e-05	1.152e-03 ± 2.899e-05	1.139e-03 ± 3.157e-05	-0.31 %	-1.11 %	2.968	0.004*	3.738	<0.001
IFO_right	1.168e-03 ± 4.034e-05	1.162e-03 ± 3.385e-05	1.150e-03 ± 3.763e-05	1.137e-03 ± 3.810e-05	-0.54 %	-1.11 %	1.593	0.043*	2.526	0.003*
ILF_left	1.195e-03 ± 5.468e-05	1.181e-03 ± 5.091e-05	1.163e-03 ± 4.061e-05	1.142e-03 ± 4.550e-05	-1.1 %	-1.82 %	2.110	0.019*	2.837	0.001*
ILF_right	1.179e-03 ± 5.903e-05	1.169e-03 ± 4.907e-05	1.163e-03 ± 5.609e-05	1.143e-03 ± 7.127e-05	-0.88 %	-1.66 %	0.966	0.102	1.647	0.015*

Table A.7 (cont'd)

	mTBI		Controls		Percent Change					
TractSeg Abbv.	P1	P2	P1	P2	mTBI	Controls	t-score P1	q-value P1[f]	t-score P2	q-value P2
MCP	1.071e-03 ± 6.466e-05	1.066e-03 ± 5.086e-05	1.047e-03 ± 5.328e-05	1.066e-03 ± 6.899e-05	-0.44 %	1.75 %	1.289	0.067	0.022	0.099
MLF_left	1.155e-03 ± 3.379e-05	1.153e-03 ± 3.526e-05	1.136e-03 ± 3.268e-05	1.128e-03 ± 5.063e-05	-0.15 %	-0.69 %	1.943	0.025*	2.276	0.005*
MLF_right	1.148e-03 ± 3.761e-05	1.146e-03 ± 3.513e-05	1.136e-03 ± 3.777e-05	1.125e-03 ± 4.764e-05	-0.14 %	-0.91 %	1.138	0.082	1.965	0.009*
OR_left	1.229e-03 ± 5.251e-05	1.223e-03 ± 5.395e-05	1.205e-03 ± 4.734e-05	1.196e-03 ± 6.880e-05	-0.5 %	-0.72 %	1.651	0.04*	1.686	0.014*
OR_right	1.221e-03 ± 5.889e-05	1.216e-03 ± 5.357e-05	1.219e-03 ± 5.695e-05	1.206e-03 ± 7.741e-05	-0.36 %	-1.06 %	0.093	0.237	0.600	0.06
POPT_left	1.244e-03 ± 3.416e-05	1.247e-03 ± 3.929e-05	1.227e-03 ± 4.715e-05	1.220e-03 ± 9.075e-05	0.23 %	-0.55 %	1.582	0.043*	1.745	0.013*
POPT_right	1.231e-03 ± 3.839e-05	1.231e-03 ± 3.888e-05	1.212e-03 ± 4.598e-05	1.212e-03 ± 8.075e-05	0.07 %	0 %	1.645	0.04*	1.401	0.02*
SCP_left	1.179e-03 ± 3.726e-05	1.170e-03 ± 4.364e-05	1.130e-03 ± 4.542e-05	1.120e-03 ± 6.357e-05	-0.75 %	-0.85 %	4.365	<0.001	3.674	<0.001
SCP_right	1.164e-03 ± 3.064e-05	1.154e-03 ± 3.182e-05	1.134e-03 ± 6.193e-05	1.115e-03 ± 4.157e-05	-0.85 %	-1.74 %	2.622	0.007*	4.094	<0.001
SLF_III_left	1.143e-03 ± 3.106e-05	1.136e-03 ± 3.644e-05	1.110e-03 ± 4.811e-05	1.097e-03 ± 6.196e-05	-0.58 %	-1.18 %	3.262	0.003*	3.264	<0.001
SLF_III_right	1.128e-03 ± 2.968e-05	1.123e-03 ± 2.680e-05	1.111e-03 ± 3.722e-05	1.096e-03 ± 3.389e-05	-0.43 %	-1.37 %	1.812	0.032*	3.354	<0.001
SLF_II_left	1.143e-03 ± 3.460e-05	1.138e-03 ± 3.768e-05	1.118e-03 ± 4.439e-05	1.107e-03 ± 6.121e-05	-0.44 %	-0.95 %	2.354	0.012*	2.496	0.003*
SLF_II_right	1.131e-03 ± 3.491e-05	1.126e-03 ± 3.241e-05	1.111e-03 ± 4.475e-05	1.098e-03 ± 4.853e-05	-0.5 %	-1.22 %	1.882	0.028*	2.750	0.002*
SLF_I_left	1.190e-03 ± 4.919e-05	1.192e-03 ± 5.473e-05	1.194e-03 ± 9.878e-05	1.180e-03 ± 1.248e-04	0.23 %	-1.18 %	-0.229	0.216	0.600	0.06
SLF_I_right	1.176e-03 ± 4.418e-05	1.173e-03 ± 4.698e-05	1.168e-03 ± 7.384e-05	1.158e-03 ± 1.053e-04	-0.23 %	-0.89 %	0.500	0.173	0.845	0.046*
STR_left	1.201e-03 ± 3.187e-05	1.194e-03 ± 4.787e-05	1.135e-03 ± 5.223e-05	1.137e-03 ± 1.172e-04	-0.63 %	0.16 %	6.210	<0.001	2.956	0.001*
STR_right	1.177e-03 ± 3.361e-05	1.168e-03 ± 3.931e-05	1.142e-03 ± 5.843e-05	1.127e-03 ± 7.560e-05	-0.83 %	-1.34 %	3.051	0.003*	2.937	0.001*
ST_FO_left	1.179e-03 ± 5.018e-05	1.175e-03 ± 6.145e-05	1.132e-03 ± 5.240e-05	1.118e-03 ± 5.352e-05	-0.35 %	-1.2 %	3.211	0.003*	3.350	<0.001
ST_FO_right	1.192e-03 ± 4.641e-05	1.184e-03 ± 5.045e-05	1.162e-03 ± 5.716e-05	1.130e-03 ± 3.634e-05	-0.69 %	-2.8 %	2.120	0.019*	4.018	<0.001
ST_OCC_left	1.206e-03 ± 4.186e-05	1.201e-03 ± 4.476e-05	1.171e-03 ± 2.893e-05	1.163e-03 ± 3.766e-05	-0.41 %	-0.71 %	3.062	0.003*	3.150	<0.001
ST_OCC_right	1.184e-03 ± 4.732e-05	1.179e-03 ± 4.336e-05	1.167e-03 ± 4.299e-05	1.160e-03 ± 4.903e-05	-0.48 %	-0.62 %	1.293	0.067	1.511	0.017*
ST_PAR_left	1.196e-03 ± 3.686e-05	1.197e-03 ± 3.992e-05	1.179e-03 ± 3.994e-05	1.173e-03 ± 7.820e-05	0.12 %	-0.51 %	1.586	0.043*	1.740	0.013*
ST_PAR_right	1.180e-03 ± 3.836e-05	1.178e-03 ± 3.605e-05	1.161e-03 ± 3.700e-05	1.160e-03 ± 6.385e-05	-0.15 %	-0.1 %	1.676	0.04*	1.468	0.018*
ST_POSTC_left	1.221e-03 ± 4.183e-05	1.217e-03 ± 5.251e-05	1.186e-03 ± 6.182e-05	1.172e-03 ± 1.026e-04	-0.33 %	-1.19 %	2.598	0.008*	2.424	0.003*
ST_POSTC_right	1.188e-03 ± 3.885e-05	1.183e-03 ± 3.930e-05	1.172e-03 ± 6.255e-05	1.173e-03 ± 9.963e-05	-0.43 %	0.1 %	1.201	0.076	0.575	0.06
ST_PREC_left	1.214e-03 ± 3.774e-05	1.206e-03 ± 5.141e-05	1.159e-03 ± 5.239e-05	1.153e-03 ± 8.677e-05	-0.72 %	-0.55 %	4.642	<0.001	3.100	<0.001
ST_PREC_right	1.185e-03 ± 3.839e-05	1.175e-03 ± 3.579e-05	1.155e-03 ± 5.168e-05	1.150e-03 ± 7.155e-05	-0.87 %	-0.37 %	2.581	0.008*	1.938	0.009*

Table A.7 (cont'd)

	mTBI		Controls		Percent Change					
TractSeg Abbv.	P1	P2	P1	P2	mTBI	Controls	t-score P1	q-value P1[1]	t-score P2	q-value P2
ST_PREF_left	1.183e-03 ± 3.438e-05	1.176e-03 ± 4.390e-05	1.138e-03 ± 4.938e-05	1.122e-03 ± 5.255e-05	-0.56 %	-1.46 %	4.070	<0.001	4.228	<0.001
ST_PREF_right	1.180e-03 ± 3.657e-05	1.172e-03 ± 3.706e-05	1.146e-03 ± 5.420e-05	1.121e-03 ± 4.259e-05	-0.73 %	-2.19 %	2.903	0.004*	4.699	<0.001
ST_PREM_left	1.182e-03 ± 4.221e-05	1.173e-03 ± 5.867e-05	1.126e-03 ± 5.127e-05	1.094e-03 ± 4.357e-05	-0.75 %	-2.84 %	4.344	<0.001	4.994	<0.001
ST_PREM_right	1.175e-03 ± 3.808e-05	1.164e-03 ± 4.155e-05	1.135e-03 ± 6.074e-05	1.117e-03 ± 5.415e-05	-0.9 %	-1.59 %	3.133	0.003*	3.748	<0.001
T_OCC_left	1.233e-03 ± 5.412e-05	1.226e-03 ± 5.529e-05	1.209e-03 ± 4.722e-05	1.200e-03 ± 6.843e-05	-0.54 %	-0.73 %	1.548	0.045*	1.575	0.016*
T_OCC_right	1.217e-03 ± 5.928e-05	1.212e-03 ± 5.384e-05	1.215e-03 ± 5.855e-05	1.203e-03 ± 7.828e-05	-0.39 %	-0.99 %	0.119	0.235	0.554	0.061
T_PAR_left	1.210e-03 ± 4.214e-05	1.211e-03 ± 4.516e-05	1.202e-03 ± 5.434e-05	1.195e-03 ± 9.944e-05	0.15 %	-0.58 %	0.552	0.165	0.936	0.042*
T_PAR_right	1.205e-03 ± 4.604e-05	1.203e-03 ± 4.326e-05	1.196e-03 ± 5.554e-05	1.192e-03 ± 8.996e-05	-0.16 %	-0.33 %	0.677	0.149	0.729	0.053
T_POSTC_left	1.222e-03 ± 4.028e-05	1.221e-03 ± 5.075e-05	1.205e-03 ± 7.790e-05	1.189e-03 ± 1.154e-04	-0.08 %	-1.33 %	1.133	0.082	1.612	0.015*
T_POSTC_right	1.190e-03 ± 4.058e-05	1.189e-03 ± 4.220e-05	1.190e-03 ± 8.110e-05	1.190e-03 ± 1.282e-04	-0.07 %	0.01 %	0.013	0.25	-0.041	0.098
T_PREC_left	1.221e-03 ± 3.738e-05	1.213e-03 ± 5.310e-05	1.175e-03 ± 6.239e-05	1.167e-03 ± 1.014e-04	-0.7 %	-0.65 %	3.710	<0.001	2.461	0.003*
T_PREC_right	1.182e-03 ± 3.977e-05	1.172e-03 ± 3.713e-05	1.157e-03 ± 5.724e-05	1.151e-03 ± 8.315e-05	-0.86 %	-0.51 %	1.955	0.025*	1.457	0.018*
T_PREF_left	1.208e-03 ± 3.669e-05	1.200e-03 ± 4.826e-05	1.168e-03 ± 6.137e-05	1.148e-03 ± 6.800e-05	-0.61 %	-1.74 %	3.179	0.003*	3.502	<0.001
T_PREF_right	1.209e-03 ± 4.391e-05	1.198e-03 ± 4.404e-05	1.183e-03 ± 7.357e-05	1.156e-03 ± 6.869e-05	-0.9 %	-2.3 %	1.739	0.036*	2.981	0.001*
T_PREM_left	1.217e-03 ± 4.501e-05	1.207e-03 ± 6.484e-05	1.173e-03 ± 6.971e-05	1.139e-03 ± 7.681e-05	-0.82 %	-2.97 %	2.968	0.004*	3.603	<0.001
T_PREM_right	1.202e-03 ± 4.657e-05	1.189e-03 ± 5.014e-05	1.177e-03 ± 9.451e-05	1.153e-03 ± 8.559e-05	-1.08 %	-2.04 %	1.426	0.055	2.129	0.006*
UF_left	1.173e-03 ± 3.496e-05	1.173e-03 ± 3.626e-05	1.144e-03 ± 4.304e-05	1.123e-03 ± 2.854e-05	0.02 %	-1.9 %	2.686	0.007*	5.150	<0.001
UF_right	1.201e-03 ± 3.376e-05	1.196e-03 ± 3.558e-05	1.178e-03 ± 5.722e-05	1.147e-03 ± 2.801e-05	-0.47 %	-2.66 %	2.006	0.023*	5.050	<0.001

Tables A.7- T-test results for comparisons of the automatically segmented tracts from TractSeg between mTBI and control subjects.

[1]Significant values are marked with an asterisk (*) or <0.001

Table A.8 Results of Post Hoc Tract Specific Comparisons of Diffusion Kurtosis Imaging Radial Diffusivity

	mTBI		Controls		Percent Change					
TractSeg Abbv.	P1	P2	P1	P2	mTBI	Controls	t-score P1	q-value P1ᶠ	t-score P2	q-value P2ᶠ
AF_left	8.422e-04 ± 3.098e-05	8.348e-04 ± 3.313e-05	8.099e-04 ± 4.067e-05	8.002e-04 ± 4.466e-05	-0.88 %	-1.19 %	3.364	0.013*	3.423	0.008*
AF_right	8.312e-04 ± 2.900e-05	8.269e-04 ± 2.550e-05	8.177e-04 ± 3.143e-05	8.092e-04 ± 4.166e-05	-0.52 %	-1.04 %	1.578	0.172	2.120	0.057
ATR_left	8.952e-04 ± 4.606e-05	8.882e-04 ± 5.615e-05	8.629e-04 ± 6.084e-05	8.408e-04 ± 6.470e-05	-0.78 %	-2.56 %	2.257	0.082	2.897	0.017*
ATR_right	9.084e-04 ± 5.261e-05	8.970e-04 ± 5.055e-05	8.917e-04 ± 7.865e-05	8.724e-04 ± 7.740e-05	-1.26 %	-2.16 %	0.985	0.355	1.524	0.122
CA	9.338e-04 ± 3.814e-05	9.291e-04 ± 5.964e-05	8.705e-04 ± 5.066e-05	8.542e-04 ± 6.646e-05	-0.5 %	-1.88 %	5.342	<0.001	4.354	0.001*
CC_1	8.816e-04 ± 5.782e-05	8.747e-04 ± 6.486e-05	8.714e-04 ± 9.258e-05	8.414e-04 ± 6.471e-05	-0.78 %	-3.44 %	0.530	0.495	1.821	0.085
CC_2	8.787e-04 ± 3.511e-05	8.786e-04 ± 4.244e-05	8.584e-04 ± 5.187e-05	8.427e-04 ± 6.318e-05	0 %	-1.83 %	1.792	0.146	2.686	0.022*
CC_3	9.005e-04 ± 4.544e-05	9.058e-04 ± 6.995e-05	8.769e-04 ± 6.721e-05	8.668e-04 ± 9.904e-05	0.59 %	-1.15 %	1.617	0.172	1.803	0.085
CC_4	8.905e-04 ± 3.930e-05	8.983e-04 ± 5.244e-05	8.790e-04 ± 6.563e-05	8.868e-04 ± 1.308e-04	0.88 %	0.89 %	0.869	0.366	0.541	0.323
CC_5	8.753e-04 ± 3.782e-05	8.883e-04 ± 5.664e-05	8.696e-04 ± 7.291e-05	8.757e-04 ± 1.424e-04	1.49 %	0.69 %	0.419	0.531	0.548	0.323
CC_6	8.480e-04 ± 4.596e-05	8.520e-04 ± 3.726e-05	8.428e-04 ± 4.536e-05	8.500e-04 ± 8.756e-05	0.48 %	0.85 %	0.388	0.531	0.137	0.407
CC_7	8.694e-04 ± 7.903e-05	8.693e-04 ± 5.339e-05	8.642e-04 ± 4.553e-05	8.773e-04 ± 9.609e-05	-0.01 %	1.52 %	0.244	0.555	-0.443	0.334
CC	8.698e-04 ± 3.778e-05	8.719e-04 ± 3.652e-05	8.597e-04 ± 4.716e-05	8.577e-04 ± 8.279e-05	0.24 %	-0.23 %	0.877	0.366	1.012	0.228
CG_left	8.276e-04 ± 3.046e-05	8.245e-04 ± 3.115e-05	8.105e-04 ± 5.637e-05	8.148e-04 ± 9.633e-05	-0.38 %	0.52 %	1.593	0.172	0.666	0.315
CG_right	8.160e-04 ± 3.399e-05	8.119e-04 ± 2.911e-05	8.015e-04 ± 5.317e-05	7.973e-04 ± 7.958e-05	-0.5 %	-0.52 %	1.300	0.249	1.167	0.188
CST_left	8.687e-04 ± 3.196e-05	8.661e-04 ± 4.453e-05	8.385e-04 ± 6.011e-05	8.342e-04 ± 9.824e-05	-0.3 %	-0.52 %	2.663	0.052	1.897	0.075
CST_right	8.258e-04 ± 3.205e-05	8.229e-04 ± 3.218e-05	8.031e-04 ± 4.801e-05	8.154e-04 ± 1.009e-04	-0.34 %	1.54 %	2.190	0.082	0.493	0.327
FPT_left	8.750e-04 ± 3.036e-05	8.736e-04 ± 4.320e-05	8.500e-04 ± 8.280e-05	8.310e-04 ± 9.193e-05	-0.15 %	-2.23 %	1.884	0.125	2.664	0.022*
FPT_right	8.673e-04 ± 3.241e-05	8.661e-04 ± 3.546e-05	8.499e-04 ± 7.568e-05	8.298e-04 ± 8.381e-05	-0.14 %	-2.37 %	1.352	0.244	2.602	0.023*
FX_left	1.910e-03 ± 3.849e-04	1.883e-03 ± 3.814e-04	1.903e-03 ± 4.074e-04	1.894e-03 ± 4.438e-04	-1.44 %	-0.51 %	0.060	0.589	-0.099	0.407
FX_right	1.879e-03 ± 3.690e-04	1.862e-03 ± 3.889e-04	1.882e-03 ± 3.939e-04	1.808e-03 ± 4.573e-04	-0.94 %	-3.94 %	-0.029	0.589	0.468	0.331
ICP_left	8.072e-04 ± 8.363e-05	7.985e-04 ± 5.271e-05	8.028e-04 ± 7.506e-05	7.909e-04 ± 9.539e-05	-1.07 %	-1.48 %	0.186	0.572	0.423	0.336
ICP_right	7.954e-04 ± 6.566e-05	7.892e-04 ± 4.163e-05	8.009e-04 ± 7.779e-05	7.661e-04 ± 9.179e-05	-0.78 %	-4.34 %	-0.277	0.555	1.469	0.127
IFO_left	8.488e-04 ± 3.565e-05	8.466e-04 ± 3.460e-05	8.250e-04 ± 2.747e-05	8.222e-04 ± 5.424e-05	-0.25 %	-0.35 %	2.402	0.082	2.203	0.049*
IFO_right	8.417e-04 ± 4.028e-05	8.375e-04 ± 3.205e-05	8.273e-04 ± 3.026e-05	8.221e-04 ± 4.221e-05	-0.49 %	-0.62 %	1.293	0.249	1.589	0.112
ILF_left	8.612e-04 ± 5.113e-05	8.522e-04 ± 4.061e-05	8.321e-04 ± 3.420e-05	8.265e-04 ± 6.365e-05	-1.05 %	-0.68 %	2.080	0.091	1.969	0.074
ILF_right	8.526e-04 ± 5.201e-05	8.451e-04 ± 3.895e-05	8.363e-04 ± 4.308e-05	8.295e-04 ± 6.147e-05	-0.88 %	-0.82 %	1.114	0.31	1.246	0.174

Table A.8 (cont'd)

	mTBI		Controls		Percent Change					
TractSeg Abbv.	P1	P2	P1	P2	mTBI	Controls	t-score P1	q-value P1[f]	t-score P2	q-value P2[f]
MCP	7.709e-04 ± 6.400e-05	7.697e-04 ± 4.772e-05	7.622e-04 ± 6.892e-05	7.848e-04 ± 9.616e-05	-0.16 %	2.97 %	0.461	0.518	-0.882	0.264
MLF_left	8.491e-04 ± 3.718e-05	8.474e-04 ± 3.487e-05	8.396e-04 ± 4.156e-05	8.338e-04 ± 5.953e-05	-0.19 %	-0.69 %	0.862	0.366	1.175	0.188
MLF_right	8.383e-04 ± 4.026e-05	8.390e-04 ± 3.575e-05	8.361e-04 ± 4.832e-05	8.307e-04 ± 6.177e-05	0.09 %	-0.65 %	0.178	0.572	0.697	0.309
OR_left	8.771e-04 ± 5.618e-05	8.731e-04 ± 5.497e-05	8.593e-04 ± 4.323e-05	8.620e-04 ± 9.727e-05	-0.45 %	0.31 %	1.136	0.31	0.601	0.323
OR_right	8.644e-04 ± 6.271e-05	8.611e-04 ± 5.522e-05	8.667e-04 ± 5.107e-05	8.627e-04 ± 7.361e-05	-0.38 %	-0.45 %	-0.130	0.58	-0.095	0.407
POPT_left	8.766e-04 ± 3.370e-05	8.809e-04 ± 3.966e-05	8.763e-04 ± 6.043e-05	8.723e-04 ± 1.045e-04	0.5 %	-0.45 %	0.026	0.589	0.518	0.324
POPT_right	8.538e-04 ± 3.807e-05	8.567e-04 ± 3.692e-05	8.475e-04 ± 5.643e-05	8.504e-04 ± 9.830e-05	0.34 %	0.34 %	0.518	0.495	0.404	0.338
SCP_left	8.344e-04 ± 3.701e-05	8.281e-04 ± 4.502e-05	8.059e-04 ± 6.118e-05	7.971e-04 ± 8.812e-05	-0.76 %	-1.09 %	2.296	0.082	1.943	0.074
SCP_right	8.222e-04 ± 2.993e-05	8.166e-04 ± 3.131e-05	8.140e-04 ± 7.787e-05	7.927e-04 ± 5.724e-05	-0.68 %	-2.61 %	0.649	0.44	2.221	0.049*
SLF_III_left	8.436e-04 ± 3.142e-05	8.413e-04 ± 3.709e-05	8.230e-04 ± 6.739e-05	8.117e-04 ± 7.424e-05	-0.27 %	-1.37 %	1.735	0.157	2.225	0.049*
SLF_III_right	8.262e-04 ± 2.952e-05	8.266e-04 ± 2.818e-05	8.238e-04 ± 4.219e-05	8.184e-04 ± 6.068e-05	0.04 %	-0.65 %	0.261	0.555	0.778	0.297
SLF_II_left	8.623e-04 ± 3.992e-05	8.568e-04 ± 4.166e-05	8.461e-04 ± 5.588e-05	8.326e-04 ± 7.016e-05	-0.64 %	-1.59 %	1.290	0.249	1.752	0.091
SLF_II_right	8.517e-04 ± 3.760e-05	8.470e-04 ± 3.496e-05	8.409e-04 ± 5.194e-05	8.283e-04 ± 5.991e-05	-0.56 %	-1.5 %	0.916	0.366	1.602	0.112
SLF_I_left	9.040e-04 ± 5.172e-05	9.069e-04 ± 6.034e-05	9.201e-04 ± 1.167e-04	9.083e-04 ± 1.389e-04	0.33 %	-1.29 %	-0.803	0.383	-0.059	0.409
SLF_I_right	8.819e-04 ± 4.788e-05	8.793e-04 ± 5.270e-05	8.841e-04 ± 8.675e-05	8.738e-04 ± 1.198e-04	-0.3 %	-1.17 %	-0.131	0.58	0.272	0.374
STR_left	8.215e-04 ± 2.976e-05	8.158e-04 ± 4.965e-05	7.739e-04 ± 5.671e-05	7.817e-04 ± 1.379e-04	-0.69 %	1 %	4.474	<0.001	1.581	0.112
STR_right	7.966e-04 ± 2.950e-05	7.905e-04 ± 3.606e-05	7.778e-04 ± 6.669e-05	7.659e-04 ± 8.547e-05	-0.77 %	-1.53 %	1.636	0.172	1.731	0.092
ST_FO_left	8.314e-04 ± 4.660e-05	8.305e-04 ± 5.370e-05	7.872e-04 ± 4.490e-05	7.849e-04 ± 7.971e-05	-0.11 %	-0.29 %	3.296	0.013*	2.695	0.022*
ST_FO_right	8.349e-04 ± 4.480e-05	8.297e-04 ± 4.323e-05	8.093e-04 ± 5.486e-05	7.900e-04 ± 4.325e-05	-0.62 %	-2.38 %	1.883	0.125	3.256	0.01*
ST_OCC_left	8.532e-04 ± 4.461e-05	8.493e-04 ± 4.268e-05	8.269e-04 ± 2.504e-05	8.290e-04 ± 6.754e-05	-0.46 %	0.26 %	2.184	0.082	1.471	0.127
ST_OCC_right	8.356e-04 ± 4.836e-05	8.321e-04 ± 4.202e-05	8.240e-04 ± 2.973e-05	8.235e-04 ± 4.740e-05	-0.42 %	-0.07 %	0.880	0.366	0.708	0.309
ST_PAR_left	8.693e-04 ± 3.837e-05	8.707e-04 ± 3.993e-05	8.646e-04 ± 5.316e-05	8.610e-04 ± 9.075e-05	0.16 %	-0.41 %	0.390	0.531	0.631	0.322
ST_PAR_right	8.433e-04 ± 3.958e-05	8.438e-04 ± 3.587e-05	8.355e-04 ± 4.359e-05	8.366e-04 ± 7.779e-05	0.06 %	0.14 %	0.670	0.437	0.534	0.323
ST_POSTC_left	8.801e-04 ± 3.850e-05	8.776e-04 ± 5.074e-05	8.617e-04 ± 7.188e-05	8.503e-04 ± 1.108e-04	-0.29 %	-1.32 %	1.354	0.244	1.434	0.132
ST_POSTC_right	8.407e-04 ± 3.839e-05	8.388e-04 ± 4.098e-05	8.364e-04 ± 6.896e-05	8.402e-04 ± 1.130e-04	-0.22 %	0.45 %	0.317	0.555	-0.081	0.407

Table A.8 (cont'd)

	mTBI		Controls		Percent Change					
TractSeg Abbv.	P1	P2	P1	P2	mTBI	Controls	t-score P1	q-value P1[1]	t-score P2	q-value P2[1]
ST_PREC_left	8.719e-04 ± 3.638e-05	8.652e-04 ± 5.058e-05	8.324e-04 ± 6.067e-05	8.307e-04 ± 9.639e-05	-0.77 %	-0.2 %	3.220	0.014*	1.947	0.074
ST_PREC_right	8.407e-04 ± 3.774e-05	8.328e-04 ± 3.523e-05	8.217e-04 ± 5.214e-05	8.208e-04 ± 8.085e-05	-0.94 %	-0.11 %	1.597	0.172	0.880	0.264
ST_PREF_left	8.546e-04 ± 3.296e-05	8.492e-04 ± 4.133e-05	8.202e-04 ± 5.619e-05	8.096e-04 ± 6.461e-05	-0.62 %	-1.28 %	3.071	0.019*	2.984	0.015*
ST_PREF_right	8.532e-04 ± 3.367e-05	8.467e-04 ± 3.379e-05	8.282e-04 ± 5.459e-05	8.094e-04 ± 4.894e-05	-0.76 %	-2.27 %	2.226	0.082	3.531	0.007*
ST_PREM_left	8.681e-04 ± 3.775e-05	8.606e-04 ± 5.403e-05	8.250e-04 ± 5.963e-05	7.990e-04 ± 5.342e-05	-0.86 %	-3.15 %	3.467	0.013*	4.057	0.002*
ST_PREM_right	8.483e-04 ± 3.205e-05	8.393e-04 ± 3.708e-05	8.203e-04 ± 6.524e-05	8.066e-04 ± 6.358e-05	-1.05 %	-1.67 %	2.369	0.082	2.648	0.022*
T_OCC_left	8.854e-04 ± 5.808e-05	8.808e-04 ± 5.635e-05	8.676e-04 ± 4.365e-05	8.699e-04 ± 9.549e-05	-0.52 %	0.27 %	1.107	0.31	0.582	0.323
T_OCC_right	8.678e-04 ± 6.321e-05	8.642e-04 ± 5.531e-05	8.694e-04 ± 5.158e-05	8.661e-04 ± 7.456e-05	-0.42 %	-0.38 %	-0.091	0.589	-0.113	0.407
T_PAR_left	8.839e-04 ± 4.589e-05	8.860e-04 ± 4.847e-05	8.881e-04 ± 6.674e-05	8.837e-04 ± 1.144e-04	0.25 %	-0.49 %	-0.289	0.555	0.122	0.407
T_PAR_right	8.672e-04 ± 5.007e-05	8.667e-04 ± 4.562e-05	8.681e-04 ± 6.461e-05	8.663e-04 ± 1.052e-04	-0.06 %	-0.21 %	-0.061	0.589	0.022	0.415
T_POSTC_left	8.748e-04 ± 4.064e-05	8.759e-04 ± 5.389e-05	8.789e-04 ± 9.192e-05	8.638e-04 ± 1.311e-04	0.12 %	-1.72 %	-0.255	0.555	0.562	0.323
T_POSTC_right	8.381e-04 4.468e-05	8.402e-04 ± 4.898e-05	8.543e-04 ± 1.009e-04	8.571e-04 ± 1.489e-04	0.25 %	0.32 %	-0.931	0.366	-0.743	0.304
T_PREC_left	8.735e-04 ± 3.971e-05	8.671e-04 ± 5.643e-05	8.432e-04 ± 7.421e-05	8.399e-04 ± 1.161e-04	-0.73 %	-0.38 %	2.161	0.082	1.325	0.156
T_PREC_right	8.384e-04 ± 4.199e-05	8.300e-04 ± 3.974e-05	8.268e-04 ± 6.507e-05	8.240e-04 ± 9.576e-05	-1 %	-0.34 %	0.851	0.366	0.384	0.339
T_PREF_left	8.774e-04 ± 3.761e-05	8.712e-04 ± 4.984e-05	8.484e-04 ± 7.055e-05	8.334e-04 ± 8.054e-05	-0.71 %	-1.77 %	2.178	0.082	2.333	0.043*
T_PREF_right	8.873e-04 ± 4.435e-05	8.780e-04 ± 4.565e-05	8.709e-04 ± 7.717e-05	8.488e-04 ± 7.828e-05	-1.04 %	-2.54 %	1.078	0.316	1.924	0.074
T_PREM_left	8.901e-04 ± 4.570e-05	8.816e-04 ± 6.655e-05	8.578e-04 ± 7.861e-05	8.281e-04 ± 8.883e-05	-0.95 %	-3.46 %	2.070	0.091	2.644	0.022*
T_PREM_right	8.706e-04 ± 4.872e-05	8.586e-04 ± 5.193e-05	8.573e-04 ± 1.056e-04	8.376e-04 ± 1.012e-04	-1.38 %	-2.3 %	0.717	0.421	1.144	0.19
UF_left	8.323e-04 ± 3.522e-05	8.361e-04 ± 3.717e-05	8.083e-04 ± 4.128e-05	8.006e-04 ± 5.181e-05	0.46 %	-0.95 %	2.265	0.082	3.096	0.014*
UF_right	8.588e-04 ± 3.190e-05	8.573e-04 ± 3.760e-05	8.412e-04 ± 5.533e-05	8.217e-04 ± 5.704e-05	-0.17 %	-2.32 %	1.618	0.172	2.991	0.015*

Tables A.8- T-test results for comparisons of the automatically segmented tracts from TractSeg between mTBI and control subjects.

[1]Significant values are marked with an asterisk (*) or <0.001

Table A.9 Results of Post Hoc Tract Specific Comparisons of Neurite Orientation Dispersion and Density Imaging Orientation Dispersion Index

	mTBI		Controls		Percent Change					
TractSeg Abbv.	P1	P2	P1	P2	mTBI	Controls	t-score P1	q-value P1[f]	t-score P2	q-value P2[f]
AF_left	0.351 ± 0.015	0.354 ± 0.012	0.362 ± 0.016	0.365 ± 0.017	0.9 %	0.86 %	-2.501	<0.001	-2.973	<0.001
AF_right	0.346 ± 0.010	0.350 ± 0.011	0.356 ± 0.014	0.362 ± 0.020	1.19 %	1.71 %	-3.137	<0.001	-3.167	<0.001
ATR_left	0.320 ± 0.013	0.322 ± 0.012	0.327 ± 0.012	0.331 ± 0.015	0.58 %	1.29 %	-1.939	<0.001	-2.740	<0.001
ATR_right	0.323 ± 0.011	0.326 ± 0.012	0.332 ± 0.012	0.337 ± 0.018	0.82 %	1.47 %	-2.696	<0.001	-2.840	<0.001
CA	0.283 ± 0.018	0.286 ± 0.022	0.286 ± 0.016	0.301 ± 0.042	1.28 %	5.3 %	-0.616	0.004*	-1.904	<0.001
CC_1	0.247 ± 0.017	0.252 ± 0.035	0.248 ± 0.022	0.263 ± 0.046	1.96 %	5.9 %	-0.192	0.006*	-1.027	<0.001
CC_2	0.303 ± 0.012	0.305 ± 0.012	0.313 ± 0.016	0.319 ± 0.018	0.76 %	2.09 %	-2.653	<0.001	-3.697	<0.001
CC_3	0.309 ± 0.017	0.312 ± 0.018	0.319 ± 0.026	0.327 ± 0.026	1.04 %	2.49 %	-1.809	<0.001	-2.626	<0.001
CC_4	0.299 ± 0.015	0.302 ± 0.017	0.310 ± 0.019	0.317 ± 0.023	1.16 %	2.33 %	-2.363	<0.001	-2.865	<0.001
CC_5	0.285 ± 0.015	0.290 ± 0.016	0.299 ± 0.020	0.305 ± 0.025	1.63 %	1.84 %	-2.985	<0.001	-2.866	<0.001
CC_6	0.322 ± 0.015	0.324 ± 0.015	0.333 ± 0.019	0.337 ± 0.021	0.62 %	1.22 %	-2.284	<0.001	-2.740	<0.001
CC_7	0.319 ± 0.013	0.322 ± 0.016	0.325 ± 0.015	0.333 ± 0.033	0.65 %	2.34 %	-1.561	0.001*	-2.001	<0.001
CC	0.312 ± 0.012	0.315 ± 0.012	0.322 ± 0.015	0.328 ± 0.019	0.73 %	2.03 %	-2.506	<0.001	-3.467	<0.001
CG_left	0.327 ± 0.018	0.326 ± 0.020	0.337 ± 0.022	0.344 ± 0.026	-0.28 %	2.16 %	-1.812	<0.001	-3.050	<0.001
CG_right	0.325 ± 0.021	0.326 ± 0.017	0.337 ± 0.019	0.345 ± 0.024	0.36 %	2.42 %	-2.019	<0.001	-3.646	<0.001
CST_left	0.265 ± 0.012	0.266 ± 0.012	0.277 ± 0.014	0.281 ± 0.015	0.52 %	1.67 %	-3.393	<0.001	-4.399	<0.001
CST_right	0.270 ± 0.011	0.272 ± 0.012	0.279 ± 0.013	0.287 ± 0.020	0.82 %	2.65 %	-3.044	<0.001	-3.755	<0.001
FPT_left	0.267 ± 0.012	0.268 ± 0.012	0.281 ± 0.017	0.287 ± 0.018	0.32 %	1.94 %	-3.771	<0.001	-5.007	<0.001
FPT_right	0.265 ± 0.011	0.267 ± 0.012	0.279 ± 0.013	0.283 ± 0.016	0.62 %	1.43 %	-3.976	<0.001	-4.269	<0.001
FX_left	0.140 ± 0.043	0.147 ± 0.048	0.154 ± 0.062	0.178 ± 0.079	5.17 %	15.52 %	-1.050	0.002*	-1.968	<0.001
FX_right	0.135 ± 0.041	0.142 ± 0.043	0.152 ± 0.058	0.167 ± 0.079	5.24 %	10.19 %	-1.299	0.002*	-1.692	<0.001
ICP_left	0.357 ± 0.018	0.359 ± 0.018	0.376 ± 0.023	0.374 ± 0.026	0.82 %	-0.62 %	-3.507	<0.001	-2.560	<0.001
ICP_right	0.372 ± 0.017	0.376 ± 0.018	0.390 ± 0.018	0.385 ± 0.023	1.28 %	-1.51 %	-3.804	<0.001	-1.560	<0.001
IFO_left	0.319 ± 0.011	0.321 ± 0.013	0.326 ± 0.013	0.335 ± 0.028	0.67 %	2.96 %	-2.116	<0.001	-2.950	<0.001
IFO_right	0.323 ± 0.009	0.326 ± 0.012	0.329 ± 0.014	0.334 ± 0.025	0.85 %	1.63 %	-1.874	<0.001	-1.894	<0.001
ILF_left	0.320 ± 0.012	0.324 ± 0.021	0.325 ± 0.011	0.339 ± 0.037	1.36 %	4.52 %	-1.394	0.001*	-2.133	<0.001
ILF_right	0.324 ± 0.015	0.328 ± 0.022	0.326 ± 0.018	0.336 ± 0.032	1.07 %	3.19 %	-0.328	0.005*	-1.221	<0.001
MCP	0.344 ± 0.015	0.347 ± 0.015	0.359 ± 0.020	0.359 ± 0.023	0.87 %	0.22 %	-3.277	<0.001	-2.711	<0.001
MLF_left	0.348 ± 0.015	0.349 ± 0.014	0.357 ± 0.017	0.359 ± 0.017	0.25 %	0.58 %	-2.060	<0.001	-2.587	<0.001
MLF_right	0.344 ± 0.015	0.347 ± 0.015	0.354 ± 0.018	0.359 ± 0.020	0.91 %	1.42 %	-2.245	<0.001	-2.558	<0.001
OR_left	0.309 ± 0.013	0.311 ± 0.014	0.316 ± 0.012	0.326 ± 0.032	0.56 %	3.12 %	-1.926	<0.001	-2.760	<0.001
OR_right	0.305 ± 0.012	0.306 ± 0.013	0.309 ± 0.018	0.316 ± 0.029	0.38 %	2.38 %	-1.058	0.002*	-2.050	<0.001
POPT_left	0.294 ± 0.014	0.296 ± 0.013	0.306 ± 0.015	0.308 ± 0.015	0.5 %	0.73 %	-2.877	<0.001	-3.201	<0.001
POPT_right	0.289 ± 0.013	0.291 ± 0.014	0.297 ± 0.015	0.301 ± 0.016	0.67 %	1.33 %	-1.915	<0.001	-2.306	<0.001
SCP_left	0.300 ± 0.013	0.303 ± 0.014	0.319 ± 0.016	0.319 ± 0.021	0.86 %	0.06 %	-4.760	<0.001	-3.689	<0.001
SCP_right	0.303 ± 0.010	0.307 ± 0.014	0.320 ± 0.016	0.319 ± 0.020	1.3 %	-0.5 %	-5.145	<0.001	-2.801	<0.001
SLF_III_left	0.340 ± 0.017	0.344 ± 0.015	0.353 ± 0.024	0.356 ± 0.018	1.33 %	0.91 %	-2.429	<0.001	-2.626	<0.001
SLF_III_right	0.337 ± 0.012	0.343 ± 0.017	0.352 ± 0.019	0.360 ± 0.029	1.87 %	2.05 %	-4.080	<0.001	-3.021	<0.001
SLF_II_left	0.363 ± 0.016	0.362 ± 0.016	0.372 ± 0.017	0.371 ± 0.027	-0.26 %	-0.3 %	-1.939	<0.001	-1.728	<0.001
SLF_II_right	0.364 ± 0.015	0.365 ± 0.015	0.376 ± 0.017	0.379 ± 0.017	0.35 %	0.7 %	-2.805	<0.001	-3.091	<0.001
SLF_I_left	0.360 ± 0.017	0.360 ± 0.017	0.371 ± 0.016	0.377 ± 0.017	0 %	1.51 %	-2.184	<0.001	-3.391	<0.001
SLF_I_right	0.352 ± 0.016	0.353 ± 0.018	0.362 ± 0.016	0.364 ± 0.018	0.12 %	0.66 %	-2.028	<0.001	-2.284	<0.001
STR_left	0.270 ± 0.012	0.272 ± 0.012	0.283 ± 0.013	0.292 ± 0.025	0.76 %	3.44 %	-3.328	<0.001	-4.455	<0.001
STR_right	0.272 ± 0.014	0.275 ± 0.013	0.283 ± 0.014	0.287 ± 0.016	1.04 %	1.62 %	-2.602	<0.001	-3.180	<0.001
ST_FO_left	0.295 ± 0.017	0.299 ± 0.025	0.301 ± 0.018	0.309 ± 0.035	1.52 %	2.47 %	-1.336	0.001*	-1.252	<0.001
ST_FO_right	0.287 ± 0.016	0.290 ± 0.026	0.294 ± 0.017	0.302 ± 0.028	1.19 %	2.81 %	-1.538	0.001*	-1.637	<0.001
ST_OCC_left	0.312 ± 0.013	0.313 ± 0.015	0.321 ± 0.014	0.330 ± 0.035	0.47 %	2.78 %	-2.445	<0.001	-2.895	<0.001

Table A.9 (cont'd)

	mTBI		Controls		Percent Change					
TractSeg Abbv.	P1	P2	P1	P2	mTBI	Controls	t-score P1	q-value P1[1]	t-score P2	q-value P2[1]
ST_OCC_right	0.315 ± 0.013	0.317 ± 0.014	0.321 ± 0.020	0.326 ± 0.026	0.65 %	1.83 %	-1.251	0.002*	-1.828	<0.001
ST_PAR_left	0.327 ± 0.014	0.328 ± 0.014	0.337 ± 0.015	0.341 ± 0.015	0.21 %	0.98 %	-2.450	<0.001	-3.133	<0.001
ST_PAR_right	0.319 ± 0.013	0.322 ± 0.013	0.327 ± 0.014	0.331 ± 0.016	0.86 %	1.18 %	-2.230	<0.001	-2.437	<0.001
ST_POSTC_left	0.305 ± 0.015	0.308 ± 0.014	0.319 ± 0.012	0.324 ± 0.013	0.87 %	1.51 %	-3.206	<0.001	-3.989	<0.001
ST_POSTC_right	0.301 ± 0.014	0.305 ± 0.014	0.310 ± 0.013	0.315 ± 0.018	1.29 %	1.65 %	-2.212	<0.001	-2.360	<0.001
ST_PREC_left	0.306 ± 0.013	0.309 ± 0.011	0.318 ± 0.011	0.326 ± 0.013	0.78 %	2.53 %	-3.227	<0.001	-5.235	<0.001
ST_PREC_right	0.305 ± 0.010	0.308 ± 0.012	0.314 ± 0.012	0.320 ± 0.015	0.98 %	1.94 %	-2.909	<0.001	-3.433	<0.001
ST_PREF_left	0.312 ± 0.012	0.313 ± 0.011	0.322 ± 0.015	0.330 ± 0.017	0.41 %	2.42 %	-2.927	<0.001	-4.780	<0.001
ST_PREF_right	0.312 ± 0.010	0.314 ± 0.012	0.323 ± 0.012	0.328 ± 0.016	0.76 %	1.69 %	-3.558	<0.001	-3.951	<0.001
ST_PREM_left	0.325 ± 0.015	0.327 ± 0.014	0.339 ± 0.016	0.348 ± 0.016	0.57 %	2.53 %	-3.181	<0.001	-5.007	<0.001
ST_PREM_right	0.318 ± 0.014	0.320 ± 0.014	0.330 ± 0.014	0.338 ± 0.023	0.64 %	2.42 %	-2.980	<0.001	-3.827	<0.001
T_OCC_left	0.313 ± 0.012	0.314 ± 0.014	0.319 ± 0.011	0.329 ± 0.031	0.56 %	3.07 %	-1.764	<0.001	-2.679	<0.001
T_OCC_right	0.311 ± 0.012	0.312 ± 0.013	0.314 ± 0.017	0.322 ± 0.028	0.34 %	2.31 %	-0.956	0.003*	-2.021	<0.001
T_PAR_left	0.326 ± 0.013	0.326 ± 0.013	0.335 ± 0.013	0.338 ± 0.016	0.22 %	1.02 %	-2.363	<0.001	-3.001	<0.001
T_PAR_right	0.316 ± 0.013	0.317 ± 0.014	0.323 ± 0.012	0.327 ± 0.014	0.51 %	1.19 %	-1.973	<0.001	-2.448	<0.001
T_POSTC_left	0.304 ± 0.014	0.307 ± 0.014	0.319 ± 0.015	0.322 ± 0.016	0.95 %	0.84 %	-3.600	<0.001	-3.514	<0.001
T_POSTC_right	0.301 ± 0.015	0.304 ± 0.016	0.311 ± 0.018	0.316 ± 0.020	1.13 %	1.64 %	-2.308	<0.001	-2.496	<0.001
T_PREC_left	0.303 ± 0.012	0.305 ± 0.012	0.314 ± 0.012	0.321 ± 0.015	0.65 %	2.32 %	-3.090	<0.001	-4.501	<0.001
T_PREC_right	0.308 ± 0.011	0.310 ± 0.012	0.316 ± 0.011	0.322 ± 0.014	0.6 %	2.01 %	-2.424	<0.001	-3.406	<0.001
T_PREF_left	0.307 ± 0.011	0.308 ± 0.010	0.318 ± 0.014	0.324 ± 0.017	0.32 %	2.13 %	-2.936	<0.001	-4.834	<0.001
T_PREF_right	0.314 ± 0.010	0.315 ± 0.011	0.324 ± 0.012	0.329 ± 0.014	0.56 %	1.56 %	-3.341	<0.001	-4.082	<0.001
T_PREM_left	0.312 ± 0.013	0.314 ± 0.012	0.324 ± 0.012	0.330 ± 0.015	0.54 %	1.82 %	-3.139	<0.001	-4.301	<0.001
T_PREM_right	0.309 ± 0.013	0.310 ± 0.013	0.318 ± 0.012	0.325 ± 0.018	0.28 %	2.21 %	-2.423	<0.001	-3.829	<0.001
UF_left	0.300 ± 0.014	0.303 ± 0.022	0.307 ± 0.017	0.319 ± 0.035	1.2 %	3.62 %	-1.783	<0.001	-2.126	<0.001
UF_right	0.297 ± 0.014	0.301 ± 0.021	0.305 ± 0.015	0.315 ± 0.032	1.49 %	3.28 %	-2.081	<0.001	-2.064	<0.001

Tables A.9- T-test results for comparisons of the automatically segmented tracts from TractSeg between mTBI and control subjects.

[1]Significant values are marked with an asterisk (*) or <0.001

Table A.10 Results of Post Hoc Tract Specific Comparisons of Neurite Orientation Dispersion and Density Imaging Neurite Density Index

	mTBI		Controls		Percent Change					
TractSeg Abbv.	P1	P2	P1	P2	mTBI	Controls	t-score P1	q-value P1[f]	t-score P2	q-value P2[f]
AF_left	0.482 ± 0.022	0.481 ± 0.021	0.493 ± 0.030	0.497 ± 0.025	-0.25 %	0.75 %	-1.531	0.038*	-2.550	<0.001
AF_right	0.503 ± 0.023	0.501 ± 0.019	0.507 ± 0.032	0.508 ± 0.034	-0.37 %	0.12 %	-0.547	0.087	-0.995	0.003*
ATR_left	0.478 ± 0.019	0.479 ± 0.020	0.499 ± 0.029	0.503 ± 0.024	0.13 %	0.73 %	-3.394	0.005*	-4.034	<0.001
ATR_right	0.480 ± 0.019	0.480 ± 0.018	0.495 ± 0.023	0.500 ± 0.025	0.04 %	1.03 %	-2.638	0.009*	-3.553	<0.001
CA	0.401 ± 0.026	0.396 ± 0.026	0.426 ± 0.028	0.445 ± 0.024	-1.18 %	4.44 %	-3.218	0.005*	-6.782	<0.001
CC_1	0.485 ± 0.031	0.476 ± 0.037	0.506 ± 0.031	0.496 ± 0.050	-1.73 %	-1.84 %	-2.316	0.015*	-1.790	<0.001
CC_2	0.490 ± 0.023	0.488 ± 0.023	0.502 ± 0.033	0.503 ± 0.029	-0.36 %	0.09 %	-1.669	0.033*	-2.101	<0.001
CC_3	0.493 ± 0.023	0.494 ± 0.024	0.509 ± 0.045	0.511 ± 0.034	0.1 %	0.36 %	-1.882	0.024*	-2.287	<0.001
CC_4	0.543 ± 0.026	0.544 ± 0.029	0.548 ± 0.041	0.554 ± 0.038	0.03 %	1.05 %	-0.566	0.087	-1.198	0.002*
CC_5	0.538 ± 0.024	0.537 ± 0.025	0.546 ± 0.036	0.547 ± 0.035	-0.3 %	0.27 %	-0.980	0.061	-1.395	0.002*
CC_6	0.497 ± 0.021	0.494 ± 0.020	0.498 ± 0.027	0.497 ± 0.027	-0.62 %	-0.16 %	-0.146	0.118	-0.539	0.004*
CC_7	0.514 ± 0.023	0.512 ± 0.021	0.516 ± 0.023	0.514 ± 0.033	-0.35 %	-0.27 %	-0.210	0.113	-0.271	0.006*
CC	0.501 ± 0.020	0.499 ± 0.020	0.508 ± 0.030	0.508 ± 0.028	-0.38 %	0.08 %	-1.020	0.061	-1.472	0.001*
CG_left	0.473 ± 0.025	0.473 ± 0.025	0.484 ± 0.033	0.482 ± 0.035	-0.1 %	-0.58 %	-1.425	0.042*	-1.151	0.002*
CG_right	0.482 ± 0.025	0.480 ± 0.022	0.488 ± 0.033	0.493 ± 0.030	-0.46 %	1.13 %	-0.678	0.079	-1.924	<0.001
CST_left	0.598 ± 0.021	0.597 ± 0.023	0.607 ± 0.034	0.619 ± 0.034	-0.03 %	1.96 %	-1.341	0.047*	-2.912	<0.001
CST_right	0.600 ± 0.022	0.599 ± 0.023	0.607 ± 0.033	0.610 ± 0.042	-0.18 %	0.48 %	-1.004	0.061	-1.405	0.002*
FPT_left	0.559 ± 0.022	0.559 ± 0.024	0.576 ± 0.038	0.580 ± 0.042	0.06 %	0.62 %	-2.301	0.015*	-2.552	<0.001
FPT_right	0.559 ± 0.020	0.558 ± 0.022	0.572 ± 0.034	0.579 ± 0.033	-0.21 %	1.12 %	-1.900	0.024*	-2.978	<0.001
FX_left	0.451 ± 0.053	0.451 ± 0.048	0.463 ± 0.039	0.481 ± 0.052	-0.13 %	3.88 %	-0.818	0.071	-2.227	<0.001
FX_right	0.447 ± 0.053	0.454 ± 0.056	0.467 ± 0.042	0.471 ± 0.044	1.52 %	0.69 %	-1.360	0.046*	-1.102	0.002*
ICP_left	0.591 ± 0.028	0.589 ± 0.036	0.588 ± 0.042	0.594 ± 0.060	-0.36 %	0.92 %	0.342	0.106	-0.375	0.005*
ICP_right	0.577 ± 0.021	0.573 ± 0.026	0.571 ± 0.046	0.584 ± 0.048	-0.64 %	2.26 %	0.775	0.072	-1.171	0.002*
IFO_left	0.482 ± 0.022	0.477 ± 0.020	0.491 ± 0.022	0.491 ± 0.032	-1.04 %	-0.01 %	-1.453	0.041*	-2.187	<0.001
IFO_right	0.486 ± 0.022	0.483 ± 0.020	0.493 ± 0.021	0.497 ± 0.035	-0.69 %	0.76 %	-1.019	0.061	-2.016	<0.001
ILF_left	0.467 ± 0.022	0.463 ± 0.021	0.478 ± 0.023	0.483 ± 0.029	-0.81 %	1.02 %	-1.656	0.033*	-3.025	<0.001
ILF_right	0.471 ± 0.021	0.469 ± 0.020	0.480 ± 0.026	0.486 ± 0.033	-0.51 %	1.25 %	-1.307	0.047*	-2.600	<0.001
MCP	0.617 ± 0.023	0.615 ± 0.027	0.610 ± 0.046	0.622 ± 0.046	-0.44 %	1.91 %	0.891	0.065	-0.761	0.003*
MLF_left	0.470 ± 0.021	0.467 ± 0.020	0.474 ± 0.024	0.477 ± 0.023	-0.56 %	0.79 %	-0.623	0.084	-1.804	<0.001
MLF_right	0.477 ± 0.020	0.474 ± 0.018	0.477 ± 0.028	0.479 ± 0.030	-0.65 %	0.31 %	-0.015	0.128	-0.786	0.003*
OR_left	0.487 ± 0.022	0.483 ± 0.022	0.497 ± 0.020	0.501 ± 0.033	-0.77 %	0.86 %	-1.539	0.038*	-2.530	<0.001
OR_right	0.493 ± 0.022	0.490 ± 0.022	0.499 ± 0.026	0.505 ± 0.033	-0.58 %	1.2 %	-0.903	0.065	-2.144	<0.001
POPT_left	0.531 ± 0.019	0.528 ± 0.019	0.537 ± 0.026	0.541 ± 0.028	-0.67 %	0.88 %	-0.928	0.064	-2.274	<0.001
POPT_right	0.538 ± 0.017	0.537 ± 0.019	0.545 ± 0.025	0.548 ± 0.032	-0.27 %	0.55 %	-1.261	0.049*	-1.803	<0.001
SCP_left	0.575 ± 0.021	0.575 ± 0.028	0.589 ± 0.039	0.601 ± 0.046	-0.01 %	2.01 %	-1.837	0.025*	-2.770	<0.001
SCP_right	0.572 ± 0.016	0.570 ± 0.022	0.577 ± 0.041	0.591 ± 0.039	-0.26 %	2.32 %	-0.801	0.071	-2.767	<0.001
SLF_III_left	0.513 ± 0.026	0.508 ± 0.026	0.518 ± 0.040	0.518 ± 0.034	-1.03 %	0.04 %	-0.569	0.087	-1.321	0.002*
SLF_III_right	0.517 ± 0.025	0.513 ± 0.024	0.519 ± 0.036	0.514 ± 0.048	-0.81 %	-0.99 %	-0.213	0.113	-0.081	0.007*
SLF_II_left	0.488 ± 0.023	0.490 ± 0.026	0.490 ± 0.039	0.498 ± 0.033	0.31 %	1.57 %	-0.243	0.113	-1.049	0.002*
SLF_II_right	0.488 ± 0.023	0.488 ± 0.024	0.488 ± 0.038	0.495 ± 0.026	0.02 %	1.28 %	-0.117	0.12	-1.039	0.002*
SLF_I_left	0.464 ± 0.022	0.465 ± 0.027	0.466 ± 0.036	0.472 ± 0.029	0.22 %	1.25 %	-0.268	0.112	-0.869	0.003*
SLF_I_right	0.481 ± 0.023	0.483 ± 0.026	0.485 ± 0.038	0.492 ± 0.028	0.39 %	1.46 %	-0.535	0.087	-1.258	0.002*
STR_left	0.590 ± 0.025	0.589 ± 0.025	0.605 ± 0.028	0.609 ± 0.049	-0.06 %	0.57 %	-2.137	0.018*	-2.207	<0.001
STR_right	0.598 ± 0.021	0.593 ± 0.023	0.607 ± 0.025	0.613 ± 0.030	-0.74 %	0.98 %	-1.509	0.038*	-2.933	<0.001
ST_FO_left	0.465 ± 0.026	0.462 ± 0.026	0.492 ± 0.029	0.496 ± 0.030	-0.7 %	0.93 %	-3.389	0.005*	-4.450	<0.001
ST_FO_right	0.467 ± 0.027	0.464 ± 0.029	0.486 ± 0.023	0.486 ± 0.046	-0.64 %	-0.02 %	-2.437	0.013*	-2.292	<0.001
ST_OCC_left	0.485 ± 0.022	0.481 ± 0.021	0.493 ± 0.020	0.497 ± 0.033	-0.89 %	0.78 %	-1.197	0.052	-2.324	<0.001

Table A.10 (cont'd)

	mTBI		Controls		Percent Change					
TractSeg Abbv.	P1	P2	P1	P2	mTBI	Controls	t-score P1	q-value P1[1]	t-score P2	q-value P2[1]
ST_OCC_right	0.492 ± 0.022	0.489 ± 0.021	0.497 ± 0.023	0.503 ± 0.032	-0.65 %	1.24 %	-0.720	0.076	-2.106	<0.001
ST_PAR_left	0.494 ± 0.020	0.491 ± 0.019	0.501 ± 0.023	0.504 ± 0.023	-0.61 %	0.67 %	-1.112	0.059	-2.281	<0.001
ST_PAR_right	0.509 ± 0.019	0.508 ± 0.018	0.515 ± 0.024	0.517 ± 0.029	-0.33 %	0.28 %	-1.034	0.061	-1.548	0.001*
ST_POSTC_left	0.529 ± 0.019	0.529 ± 0.021	0.547 ± 0.023	0.553 ± 0.023	-0.14 %	1.04 %	-3.006	0.007*	-3.994	<0.001
ST_POSTC_right	0.546 ± 0.021	0.547 ± 0.019	0.560 ± 0.025	0.562 ± 0.033	0.18 %	0.3 %	-2.220	0.017*	-2.323	<0.001
ST_PREC_left	0.547 ± 0.021	0.547 ± 0.023	0.563 ± 0.028	0.571 ± 0.029	0.04 %	1.52 %	-2.417	0.013*	-3.553	<0.001
ST_PREC_right	0.558 ± 0.024	0.558 ± 0.022	0.571 ± 0.029	0.573 ± 0.033	-0.04 %	0.41 %	-1.725	0.031*	-2.153	<0.001
ST_PREF_left	0.503 ± 0.022	0.502 ± 0.021	0.521 ± 0.031	0.522 ± 0.031	-0.1 %	0.09 %	-2.713	0.009*	-2.931	<0.001
ST_PREF_right	0.504 ± 0.023	0.503 ± 0.020	0.519 ± 0.026	0.524 ± 0.028	-0.28 %	0.91 %	-2.184	0.017*	-3.349	<0.001
ST_PREM_left	0.502 ± 0.021	0.503 ± 0.021	0.521 ± 0.033	0.527 ± 0.027	0.25 %	1.2 %	-2.783	0.008*	-3.871	<0.001
ST_PREM_right	0.522 ± 0.023	0.522 ± 0.021	0.542 ± 0.034	0.540 ± 0.033	0.03 %	-0.3 %	-2.627	0.009*	-2.592	<0.001
T_OCC_left	0.486 ± 0.022	0.482 ± 0.022	0.496 ± 0.020	0.499 ± 0.032	-0.71 %	0.7 %	-1.605	0.035*	-2.463	<0.001
T_OCC_right	0.492 ± 0.021	0.489 ± 0.021	0.498 ± 0.025	0.504 ± 0.033	-0.52 %	1.11 %	-0.983	0.061	-2.143	<0.001
T_PAR_left	0.497 ± 0.019	0.494 ± 0.020	0.503 ± 0.025	0.506 ± 0.025	-0.5 %	0.63 %	-1.024	0.061	-2.011	<0.001
T_PAR_right	0.510 ± 0.018	0.508 ± 0.019	0.516 ± 0.023	0.517 ± 0.027	-0.35 %	0.35 %	-1.015	0.061	-1.579	0.001*
T_POSTC_left	0.529 ± 0.020	0.528 ± 0.022	0.541 ± 0.027	0.548 ± 0.026	-0.24 %	1.23 %	-1.920	0.024*	-3.101	<0.001
T_POSTC_right	0.539 ± 0.020	0.539 ± 0.021	0.546 ± 0.027	0.549 ± 0.034	0 %	0.47 %	-1.199	0.052	-1.483	0.001*
T_PREC_left	0.555 ± 0.021	0.556 ± 0.024	0.569 ± 0.031	0.579 ± 0.031	0.2 %	1.85 %	-2.061	0.02*	-3.210	<0.001
T_PREC_right	0.559 ± 0.022	0.559 ± 0.023	0.568 ± 0.030	0.571 ± 0.033	-0.03 %	0.61 %	-1.322	0.047*	-1.770	<0.001
T_PREF_left	0.508 ± 0.021	0.509 ± 0.022	0.527 ± 0.032	0.528 ± 0.032	0.17 %	0.21 %	-2.774	0.008*	-2.802	<0.001
T_PREF_right	0.503 ± 0.020	0.503 ± 0.020	0.517 ± 0.027	0.523 ± 0.025	-0.1 %	1.27 %	-2.182	0.017*	-3.522	<0.001
T_PREM_left	0.507 ± 0.020	0.510 ± 0.022	0.529 ± 0.034	0.537 ± 0.027	0.53 %	1.61 %	-3.164	0.005*	-4.262	<0.001
T_PREM_right	0.521 ± 0.019	0.521 ± 0.022	0.539 ± 0.033	0.541 ± 0.028	0.07 %	0.37 %	-2.768	0.008*	-3.003	<0.001
UF_left	0.438 ± 0.026	0.432 ± 0.026	0.452 ± 0.025	0.458 ± 0.019	-1.24 %	1.28 %	-1.952	0.023*	-3.719	<0.001
UF_right	0.430 ± 0.024	0.426 ± 0.023	0.443 ± 0.018	0.451 ± 0.026	-0.96 %	1.74 %	-1.983	0.023*	-3.723	<0.001

Tables A.10- T-test results for comparisons of the automatically segmented tracts from TractSeg between mTBI and control subjects.

[1]Significant values are marked with an asterisk (*) or <0.001

Table A.11 Results of Post Hoc Tract Specific Comparisons of Neurite Orientation Dispersion and Density Imaging Free Water Fraction

	mTBI		Controls		Percent Change					
TractSeg Abbv.	P1	P2	P1	P2	mTBI	Controls	t-score P1	q-value P1[f]	t-score P2	q-value P2[f]
AF_left	0.071 ± 0.012	0.066 ± 0.015	0.058 ± 0.009	0.055 ± 0.014	-7.44 %	-5.23 %	3.838	<0.001	2.569	0.031*
AF_right	0.076 ± 0.013	0.072 ± 0.013	0.069 ± 0.013	0.065 ± 0.012	-4.97 %	-6.23 %	1.716	0.039*	1.903	0.081
ATR_left	0.090 ± 0.016	0.086 ± 0.022	0.082 ± 0.018	0.072 ± 0.018	-4.3 %	-11.69 %	1.623	0.039*	2.203	0.055
ATR_right	0.097 ± 0.019	0.091 ± 0.019	0.092 ± 0.024	0.084 ± 0.025	-5.92 %	-8.32 %	0.826	0.089	1.160	0.218
CA	0.069 ± 0.026	0.061 ± 0.025	0.054 ± 0.021	0.053 ± 0.029	-10.8 %	-0.49 %	2.059	0.024*	1.056	0.238
CC_1	0.100 ± 0.026	0.092 ± 0.031	0.106 ± 0.032	0.087 ± 0.023	-7.51 %	-18.55 %	-0.865	0.089	0.649	0.318
CC_2	0.099 ± 0.013	0.097 ± 0.020	0.092 ± 0.015	0.082 ± 0.018	-2.58 %	-10.93 %	1.948	0.028*	2.731	0.026*
CC_3	0.114 ± 0.021	0.113 ± 0.031	0.103 ± 0.026	0.095 ± 0.032	-0.46 %	-8.03 %	1.596	0.039*	2.077	0.064
CC_4	0.141 ± 0.019	0.142 ± 0.028	0.130 ± 0.023	0.127 ± 0.041	0.37 %	-2.04 %	2.061	0.024*	1.698	0.105
CC_5	0.131 ± 0.019	0.133 ± 0.026	0.126 ± 0.027	0.121 ± 0.044	1.86 %	-3.46 %	0.835	0.089	1.390	0.158
CC_6	0.081 ± 0.017	0.080 ± 0.015	0.078 ± 0.012	0.077 ± 0.025	-0.65 %	-0.53 %	0.597	0.104	0.540	0.318
CC_7	0.094 ± 0.027	0.093 ± 0.019	0.093 ± 0.019	0.095 ± 0.029	-1.28 %	2.33 %	0.198	0.118	-0.318	0.353
CC	0.097 ± 0.014	0.096 ± 0.016	0.093 ± 0.013	0.088 ± 0.023	-1.29 %	-5.23 %	1.035	0.078	1.526	0.13
CG_left	0.060 ± 0.012	0.059 ± 0.014	0.057 ± 0.014	0.053 ± 0.021	-2.33 %	-6.26 %	0.901	0.089	1.241	0.198
CG_right	0.060 ± 0.011	0.056 ± 0.012	0.054 ± 0.009	0.053 ± 0.025	-6.13 %	-2.81 %	1.673	0.039*	0.697	0.318
CST_left	0.168 ± 0.017	0.164 ± 0.025	0.143 ± 0.016	0.139 ± 0.027	-2.3 %	-2.3 %	5.086	<0.001	3.413	0.013*
CST_right	0.145 ± 0.015	0.142 ± 0.017	0.131 ± 0.016	0.130 ± 0.025	-2.41 %	-0.92 %	3.285	0.002*	2.230	0.055
FPT_left	0.144 ± 0.015	0.141 ± 0.022	0.128 ± 0.019	0.118 ± 0.021	-1.77 %	-7.88 %	3.472	0.002*	3.852	0.007*
FPT_right	0.140 ± 0.013	0.136 ± 0.017	0.128 ± 0.019	0.120 ± 0.022	-2.35 %	-6.47 %	2.664	0.008*	3.196	0.013*
FX_left	0.501 ± 0.108	0.490 ± 0.103	0.485 ± 0.103	0.476 ± 0.123	-2.24 %	-2 %	0.503	0.109	0.464	0.328
FX_right	0.491 ± 0.104	0.483 ± 0.108	0.482 ± 0.104	0.451 ± 0.136	-1.76 %	-6.31 %	0.313	0.113	0.966	0.265
ICP_left	0.095 ± 0.029	0.089 ± 0.016	0.089 ± 0.013	0.092 ± 0.018	-5.86 %	2.98 %	0.713	0.099	-0.551	0.318
ICP_right	0.082 ± 0.026	0.077 ± 0.017	0.081 ± 0.019	0.081 ± 0.025	-5.93 %	-0.41 %	0.183	0.118	-0.609	0.318
IFO_left	0.074 ± 0.014	0.069 ± 0.015	0.068 ± 0.012	0.065 ± 0.014	-6.55 %	-4.94 %	1.536	0.042*	1.059	0.238
IFO_right	0.072 ± 0.016	0.067 ± 0.014	0.069 ± 0.014	0.067 ± 0.020	-5.81 %	-2.47 %	0.578	0.104	0.025	0.395
ILF_left	0.070 ± 0.020	0.063 ± 0.018	0.063 ± 0.015	0.061 ± 0.019	-10.73 %	-2.8 %	1.323	0.058	0.286	0.353
ILF_right	0.067 ± 0.023	0.061 ± 0.019	0.064 ± 0.018	0.065 ± 0.026	-8.04 %	2.2 %	0.437	0.111	-0.683	0.318
MCP	0.095 ± 0.027	0.092 ± 0.019	0.085 ± 0.012	0.097 ± 0.026	-2.89 %	14.42 %	1.402	0.053	-0.871	0.276
MLF_left	0.064 ± 0.015	0.061 ± 0.014	0.061 ± 0.012	0.060 ± 0.020	-4.84 %	-2.67 %	0.648	0.104	0.286	0.353
MLF_right	0.062 ± 0.017	0.060 ± 0.015	0.061 ± 0.013	0.059 ± 0.019	-2.78 %	-2.82 %	0.315	0.113	0.333	0.353
OR_left	0.090 ± 0.024	0.085 ± 0.022	0.086 ± 0.016	0.087 ± 0.028	-5.8 %	0.89 %	0.637	0.104	-0.287	0.353
OR_right	0.086 ± 0.026	0.083 ± 0.022	0.089 ± 0.022	0.088 ± 0.030	-3.77 %	-0.46 %	-0.395	0.111	-0.849	0.276
POPT_left	0.121 ± 0.017	0.119 ± 0.019	0.117 ± 0.020	0.113 ± 0.033	-1.27 %	-3.2 %	0.721	0.099	0.922	0.275
POPT_right	0.113 ± 0.018	0.113 ± 0.018	0.111 ± 0.020	0.109 ± 0.029	-0.26 %	-1.29 %	0.410	0.111	0.573	0.318
SCP_left	0.114 ± 0.016	0.109 ± 0.015	0.100 ± 0.009	0.100 ± 0.019	-4.04 %	0.06 %	3.251	0.002*	2.017	0.069
SCP_right	0.104 ± 0.013	0.099 ± 0.014	0.097 ± 0.016	0.097 ± 0.017	-4.74 %	-0.8 %	1.708	0.039*	0.627	0.318
SLF_III_left	0.092 ± 0.015	0.086 ± 0.020	0.078 ± 0.012	0.070 ± 0.021	-6.36 %	-10.49 %	3.368	0.002*	2.913	0.02*
SLF_III_right	0.083 ± 0.015	0.080 ± 0.015	0.080 ± 0.014	0.072 ± 0.015	-3.91 %	-9.31 %	0.861	0.089	1.846	0.083
SLF_II_left	0.079 ± 0.015	0.077 ± 0.020	0.068 ± 0.011	0.066 ± 0.022	-2.78 %	-4.03 %	2.561	0.009*	1.961	0.074
SLF_II_right	0.072 ± 0.014	0.070 ± 0.015	0.065 ± 0.012	0.062 ± 0.017	-2.79 %	-5.41 %	1.708	0.039*	1.863	0.083
SLF_I_left	0.083 ± 0.022	0.085 ± 0.025	0.087 ± 0.035	0.083 ± 0.047	1.82 %	-5.55 %	-0.574	0.104	0.251	0.353
SLF_I_right	0.083 ± 0.020	0.084 ± 0.021	0.086 ± 0.027	0.082 ± 0.039	0.49 %	-4.34 %	-0.371	0.111	0.255	0.353

Table A.11 (cont'd)

TractSeg Abbv.	mTBI		Controls		Percent Change					
	P1	P2	P1	P2	mTBI	Controls	t-score P1	q-value P1[1]	t-score P2	q-value P2[1]
STR_left	0.141 ± 0.016	0.136 ± 0.026	0.117 ± 0.021	0.113 ± 0.030	-3.47 %	-4.08 %	4.787	<0.001	3.158	0.013*
STR_right	0.131 ± 0.017	0.123 ± 0.020	0.119 ± 0.025	0.111 ± 0.027	-5.49 %	-7.14 %	2.042	0.024*	2.072	0.064
ST_FO_left	0.061 ± 0.016	0.057 ± 0.023	0.056 ± 0.017	0.053 ± 0.022	-5.49 %	-5.37 %	0.927	0.089	0.644	0.318
ST_FO_right	0.066 ± 0.017	0.060 ± 0.019	0.066 ± 0.021	0.056 ± 0.018	-7.66 %	-14.49 %	-0.103	0.123	0.742	0.311
ST_OCC_left	0.080 ± 0.018	0.074 ± 0.017	0.071 ± 0.012	0.072 ± 0.020	-6.34 %	1.42 %	1.620	0.039*	0.424	0.337
ST_OCC_right	0.073 ± 0.020	0.069 ± 0.018	0.070 ± 0.014	0.071 ± 0.023	-5.05 %	1.85 %	0.440	0.111	-0.473	0.328
ST_PAR_left	0.091 ± 0.017	0.089 ± 0.018	0.090 ± 0.020	0.086 ± 0.030	-2.12 %	-4.22 %	0.285	0.114	0.557	0.318
ST_PAR_right	0.087 ± 0.018	0.086 ± 0.016	0.086 ± 0.016	0.083 ± 0.026	-1.01 %	-3.16 %	0.200	0.118	0.545	0.318
ST_POSTC_left	0.124 ± 0.019	0.121 ± 0.025	0.117 ± 0.030	0.109 ± 0.038	-2.35 %	-6.97 %	1.124	0.072	1.541	0.13
ST_POSTC_right	0.111 ± 0.019	0.111 ± 0.021	0.115 ± 0.029	0.110 ± 0.040	-0.23 %	-3.84 %	-0.543	0.106	0.111	0.378
ST_PREC_left	0.133 ± 0.019	0.128 ± 0.026	0.113 ± 0.019	0.109 ± 0.031	-3.7 %	-3.51 %	3.629	0.001*	2.478	0.032*
ST_PREC_right	0.122 ± 0.018	0.117 ± 0.018	0.115 ± 0.022	0.108 ± 0.027	-3.55 %	-5.86 %	1.166	0.069	1.519	0.13
ST_PREF_left	0.094 ± 0.013	0.091 ± 0.020	0.083 ± 0.015	0.074 ± 0.016	-4.1 %	-10.22 %	2.935	0.004*	2.925	0.02*
ST_PREF_right	0.095 ± 0.013	0.090 ± 0.016	0.088 ± 0.018	0.079 ± 0.017	-4.96 %	-10.48 %	1.681	0.039*	2.489	0.032*
ST_PREM_left	0.099 ± 0.018	0.094 ± 0.027	0.083 ± 0.017	0.071 ± 0.017	-4.37 %	-14.08 %	3.119	0.003*	3.287	0.013*
ST_PREM_right	0.104 ± 0.016	0.099 ± 0.019	0.096 ± 0.019	0.084 ± 0.023	-4.73 %	-12.23 %	1.594	0.039*	2.555	0.031*
T_OCC_left	0.092 ± 0.024	0.086 ± 0.022	0.088 ± 0.016	0.088 ± 0.028	-5.71 %	0.41 %	0.589	0.104	-0.263	0.353
T_OCC_right	0.085 ± 0.026	0.082 ± 0.022	0.088 ± 0.022	0.087 ± 0.030	-3.74 %	-0.36 %	-0.382	0.111	-0.848	0.276
T_PAR_left	0.098 ± 0.020	0.096 ± 0.021	0.100 ± 0.024	0.095 ± 0.037	-1.45 %	-4.59 %	-0.312	0.113	0.183	0.365
T_PAR_right	0.097 ± 0.021	0.095 ± 0.019	0.098 ± 0.025	0.095 ± 0.034	-1.29 %	-3.7 %	-0.261	0.115	0.118	0.378
T_POSTC_left	0.120 ± 0.019	0.119 ± 0.025	0.120 ± 0.038	0.111 ± 0.047	-1.31 %	-7.8 %	-0.026	0.13	0.877	0.276
T_POSTC_right	0.105 ± 0.019	0.106 ± 0.022	0.114 ± 0.039	0.110 ± 0.049	0.56 %	-3.25 %	-1.220	0.067	-0.510	0.323
T_PREC_left	0.139 ± 0.019	0.135 ± 0.028	0.120 ± 0.023	0.116 ± 0.037	-3.17 %	-3.68 %	3.244	0.002*	2.186	0.055
T_PREC_right	0.120 ± 0.018	0.115 ± 0.019	0.114 ± 0.025	0.108 ± 0.031	-4.04 %	-5.42 %	1.041	0.078	1.146	0.218
T_PREF_left	0.107 ± 0.014	0.103 ± 0.022	0.096 ± 0.019	0.086 ± 0.021	-3.38 %	-10.47 %	2.473	0.011*	2.804	0.023*
T_PREF_right	0.106 ± 0.016	0.101 ± 0.018	0.100 ± 0.023	0.091 ± 0.024	-5.11 %	-9.32 %	1.186	0.069	1.808	0.087
T_PREM_left	0.110 ± 0.019	0.106 ± 0.029	0.098 ± 0.022	0.086 ± 0.027	-3.74 %	-12.54 %	2.170	0.021*	2.567	0.031*
T_PREM_right	0.111 ± 0.018	0.105 ± 0.021	0.106 ± 0.029	0.094 ± 0.031	-5.76 %	-10.69 %	0.879	0.089	1.514	0.13
UF_left	0.043 ± 0.015	0.040 ± 0.016	0.041 ± 0.012	0.039 ± 0.019	-6.96 %	-5.22 %	0.448	0.111	0.218	0.359
UF_right	0.051 ± 0.014	0.046 ± 0.014	0.050 ± 0.019	0.046 ± 0.022	-8.95 %	-8.54 %	0.109	0.123	0.049	0.393

Tables A.11- T-test results for comparisons of the automatically segmented tracts from TractSeg between mTBI and control subjects.

[1]Significant values are marked with an asterisk (*) or <0.001

Table A.12 Results of Post Hoc Tract Specific Comparisons of Fixel-Based Analysis Fiber Density

	mTBI		Controls		Percent Change					
TractSeg Abbv.	P1	P2	P1	P2	mTBI	Controls	t-score P1	q-value P1[f]	t-score P2	q-value P2
AF_left	0.285 ± 0.018	0.286 ± 0.014	0.296 ± 0.014	0.296 ± 0.011	0.39 %	-0.12 %	-2.371	0.005*	-2.641	<0.001
AF_right	0.294 ± 0.015	0.293 ± 0.014	0.297 ± 0.015	0.297 ± 0.013	-0.23 %	0.28 %	-0.713	0.07	-1.145	0.003*
ATR_left	0.298 ± 0.014	0.298 ± 0.016	0.316 ± 0.016	0.318 ± 0.014	0 %	0.57 %	-4.689	<0.001	-4.699	<0.001
ATR_right	0.291 ± 0.014	0.292 ± 0.015	0.306 ± 0.014	0.310 ± 0.014	0.18 %	1.4 %	-3.629	<0.001	-4.445	<0.001
CA	0.269 ± 0.025	0.271 ± 0.024	0.295 ± 0.027	0.302 ± 0.025	0.81 %	2.26 %	-3.661	<0.001	-4.481	<0.001
CC_1	0.378 ± 0.024	0.374 ± 0.026	0.392 ± 0.024	0.393 ± 0.023	-1.04 %	0.02 %	-2.138	0.008*	-2.578	<0.001
CC_2	0.331 ± 0.018	0.330 ± 0.019	0.344 ± 0.018	0.346 ± 0.015	-0.21 %	0.55 %	-2.654	0.003*	-3.143	<0.001
CC_3	0.326 ± 0.022	0.328 ± 0.024	0.344 ± 0.029	0.346 ± 0.028	0.6 %	0.55 %	-2.776	0.002*	-2.601	<0.001
CC_4	0.366 ± 0.023	0.367 ± 0.023	0.386 ± 0.020	0.389 ± 0.019	0.14 %	0.6 %	-3.235	<0.001	-3.513	<0.001
CC_5	0.370 ± 0.021	0.370 ± 0.021	0.385 ± 0.025	0.389 ± 0.024	-0.11 %	0.8 %	-2.548	0.004*	-3.060	<0.001
CC_6	0.352 ± 0.023	0.352 ± 0.019	0.359 ± 0.015	0.357 ± 0.016	-0.15 %	-0.55 %	-1.043	0.05*	-0.967	0.003*
CC_7	0.330 ± 0.029	0.331 ± 0.020	0.333 ± 0.014	0.332 ± 0.016	0.4 %	-0.17 %	-0.466	0.088	-0.303	0.006*
CC	0.343 ± 0.018	0.343 ± 0.016	0.353 ± 0.016	0.354 ± 0.016	-0.1 %	0.2 %	-2.029	0.01*	-2.418	<0.001
CG_left	0.314 ± 0.016	0.313 ± 0.017	0.324 ± 0.016	0.326 ± 0.013	-0.24 %	0.58 %	-2.162	0.008*	-2.672	<0.001
CG_right	0.314 ± 0.017	0.313 ± 0.018	0.319 ± 0.019	0.322 ± 0.014	-0.33 %	0.95 %	-0.937	0.055	-1.808	<0.001
CST_left	0.428 ± 0.016	0.431 ± 0.016	0.449 ± 0.017	0.454 ± 0.017	0.67 %	1.04 %	-4.459	<0.001	-5.065	<0.001
CST_right	0.437 ± 0.016	0.437 ± 0.014	0.451 ± 0.015	0.455 ± 0.018	0.18 %	0.95 %	-3.180	0.001*	-4.240	<0.001
FPT_left	0.398 ± 0.015	0.400 ± 0.015	0.416 ± 0.015	0.420 ± 0.016	0.51 %	1.06 %	-4.142	<0.001	-4.532	<0.001
FPT_right	0.400 ± 0.014	0.401 ± 0.013	0.413 ± 0.016	0.418 ± 0.016	0.24 %	1.16 %	-3.315	<0.001	-4.487	<0.001
FX_left	0.210 ± 0.052	0.213 ± 0.057	0.237 ± 0.051	0.241 ± 0.056	1.45 %	1.87 %	-1.845	0.014*	-1.778	<0.001
FX_right	0.221 ± 0.054	0.224 ± 0.059	0.236 ± 0.058	0.241 ± 0.055	1.2 %	2.37 %	-0.966	0.054	-1.095	0.003*
ICP_left	0.302 ± 0.017	0.302 ± 0.012	0.302 ± 0.014	0.305 ± 0.015	0.1 %	0.95 %	-0.072	0.119	-0.833	0.004*
ICP_right	0.277 ± 0.016	0.277 ± 0.015	0.277 ± 0.010	0.278 ± 0.017	-0.2 %	0.25 %	0.082	0.119	-0.215	0.007*
IFO_left	0.313 ± 0.017	0.314 ± 0.015	0.323 ± 0.012	0.323 ± 0.013	0.15 %	0.05 %	-2.080	0.009*	-2.174	<0.001
IFO_right	0.313 ± 0.016	0.313 ± 0.014	0.319 ± 0.011	0.321 ± 0.012	0.03 %	0.57 %	-1.284	0.035*	-1.877	<0.001
ILF_left	0.288 ± 0.022	0.290 ± 0.015	0.293 ± 0.013	0.295 ± 0.013	0.84 %	0.37 %	-1.019	0.05	-1.059	0.003*
ILF_right	0.291 ± 0.019	0.291 ± 0.016	0.296 ± 0.012	0.299 ± 0.013	0.02 %	1.01 %	-0.913	0.055	-1.659	0.001*
MCP	0.315 ± 0.014	0.315 ± 0.012	0.315 ± 0.011	0.317 ± 0.010	0.1 %	0.52 %	-0.067	0.119	-0.476	0.005*
MLF_left	0.308 ± 0.022	0.308 ± 0.016	0.315 ± 0.016	0.313 ± 0.018	0.3 %	-0.57 %	-1.218	0.039*	-0.933	0.003*
MLF_right	0.325 ± 0.018	0.324 ± 0.017	0.328 ± 0.015	0.325 ± 0.017	-0.46 %	-0.75 %	-0.430	0.088	-0.241	0.007*
OR_left	0.316 ± 0.021	0.318 ± 0.021	0.325 ± 0.014	0.328 ± 0.014	0.49 %	0.92 %	-1.527	0.025*	-1.839	<0.001
OR_right	0.335 ± 0.022	0.336 ± 0.019	0.338 ± 0.012	0.340 ± 0.014	0.35 %	0.74 %	-0.438	0.088	-0.734	0.004*
POPT_left	0.379 ± 0.015	0.380 ± 0.014	0.390 ± 0.018	0.391 ± 0.019	0.2 %	0.4 %	-2.323	0.006*	-2.605	<0.001
POPT_right	0.402 ± 0.017	0.402 ± 0.016	0.411 ± 0.015	0.412 ± 0.018	0 %	0.29 %	-1.867	0.014*	-2.192	<0.001
SCP_left	0.342 ± 0.012	0.344 ± 0.012	0.351 ± 0.013	0.356 ± 0.012	0.44 %	1.66 %	-2.489	0.004*	-3.817	<0.001
SCP_right	0.339 ± 0.011	0.340 ± 0.012	0.344 ± 0.011	0.348 ± 0.013	0.15 %	1.2 %	-1.652	0.02*	-2.634	<0.001
SLF_III_left	0.304 ± 0.017	0.305 ± 0.015	0.313 ± 0.019	0.314 ± 0.019	0.1 %	0.2 %	-1.802	0.015*	-2.057	<0.001
SLF_III_right	0.300 ± 0.018	0.299 ± 0.018	0.298 ± 0.017	0.299 ± 0.017	-0.29 %	0.16 %	0.451	0.088	0.174	0.007*
SLF_II_left	0.284 ± 0.017	0.284 ± 0.017	0.288 ± 0.021	0.289 ± 0.020	0.1 %	0.37 %	-0.914	0.055	-1.056	0.003*
SLF_II_right	0.281 ± 0.017	0.281 ± 0.018	0.283 ± 0.013	0.283 ± 0.015	-0.19 %	-0.12 %	-0.476	0.088	-0.495	0.005*
SLF_I_left	0.276 ± 0.014	0.275 ± 0.014	0.278 ± 0.016	0.278 ± 0.017	-0.26 %	-0.15 %	-0.682	0.072	-0.731	0.004*
SLF_I_right	0.289 ± 0.015	0.289 ± 0.015	0.295 ± 0.014	0.294 ± 0.015	0 %	-0.39 %	-1.479	0.027*	-1.207	0.002*
STR_left	0.416 ± 0.017	0.418 ± 0.018	0.432 ± 0.022	0.439 ± 0.020	0.64 %	1.65 %	-3.115	0.001*	-3.971	<0.001
STR_right	0.434 ± 0.015	0.433 ± 0.015	0.444 ± 0.023	0.449 ± 0.023	-0.02 %	1.16 %	-2.197	0.008*	-3.287	<0.001
ST_FO_left	0.320 ± 0.019	0.319 ± 0.019	0.339 ± 0.015	0.341 ± 0.018	-0.29 %	0.64 %	-3.527	<0.001	-4.112	<0.001
ST_FO_right	0.335 ± 0.021	0.334 ± 0.019	0.350 ± 0.016	0.355 ± 0.016	-0.52 %	1.24 %	-2.617	0.003*	-4.146	<0.001
ST_OCC_left	0.326 ± 0.023	0.327 ± 0.020	0.335 ± 0.013	0.337 ± 0.015	0.46 %	0.59 %	-1.458	0.027*	-1.716	0.001*

Table A.12 (cont'd)

	mTBI		Controls		Percent Change					
TractSeg Abbv.	P1	P2	P1	P2	mTBI	Controls	t-score P1	q-value P1[1]	t-score P2	q-value P2
ST_OCC_right	0.334 ± 0.022	0.335 ± 0.018	0.339 ± 0.013	0.341 ± 0.015	0.32 %	0.45 %	-0.847	0.059	-1.068	0.003*
ST_PAR_left	0.335 ± 0.016	0.335 ± 0.015	0.345 ± 0.016	0.345 ± 0.018	0.18 %	0.08 %	-2.152	0.008*	-2.133	<0.001
ST_PAR_right	0.355 ± 0.017	0.354 ± 0.016	0.361 ± 0.013	0.361 ± 0.016	-0.23 %	0 %	-1.406	0.029*	-1.594	0.001*
ST_POSTC_left	0.338 ± 0.013	0.340 ± 0.014	0.355 ± 0.017	0.358 ± 0.018	0.54 %	0.85 %	-4.379	<0.001	-4.323	<0.001
ST_POSTC_right	0.361 ± 0.015	0.360 ± 0.014	0.374 ± 0.016	0.376 ± 0.019	-0.2 %	0.53 %	-2.958	0.002*	-3.487	<0.001
ST_PREC_left	0.346 ± 0.013	0.348 ± 0.014	0.365 ± 0.015	0.368 ± 0.016	0.57 %	0.87 %	-5.135	<0.001	-5.065	<0.001
ST_PREC_right	0.363 ± 0.014	0.363 ± 0.013	0.376 ± 0.015	0.379 ± 0.015	0.13 %	0.75 %	-3.407	<0.001	-4.122	<0.001
ST_PREF_left	0.329 ± 0.013	0.329 ± 0.015	0.344 ± 0.013	0.345 ± 0.015	0.04 %	0.51 %	-3.916	<0.001	-3.937	<0.001
ST_PREF_right	0.330 ± 0.013	0.329 ± 0.012	0.340 ± 0.013	0.344 ± 0.013	-0.12 %	1.13 %	-2.961	0.002*	-4.224	<0.001
ST_PREM_left	0.308 ± 0.014	0.309 ± 0.016	0.320 ± 0.024	0.322 ± 0.023	0.38 %	0.64 %	-2.544	0.004*	-2.576	<0.001
ST_PREM_right	0.322 ± 0.016	0.324 ± 0.016	0.335 ± 0.019	0.337 ± 0.017	0.53 %	0.61 %	-2.825	0.002*	-2.917	<0.001
T_OCC_left	0.310 ± 0.021	0.312 ± 0.020	0.319 ± 0.013	0.322 ± 0.014	0.46 %	0.96 %	-1.510	0.026*	-1.892	<0.001
T_OCC_right	0.328 ± 0.021	0.329 ± 0.019	0.331 ± 0.012	0.333 ± 0.014	0.37 %	0.61 %	-0.588	0.079	-0.824	0.004*
T_PAR_left	0.335 ± 0.015	0.335 ± 0.015	0.344 ± 0.017	0.345 ± 0.018	0.06 %	0.29 %	-2.031	0.01*	-2.227	<0.001
T_PAR_right	0.362 ± 0.017	0.361 ± 0.017	0.367 ± 0.015	0.368 ± 0.017	-0.17 %	0.24 %	-1.139	0.043*	-1.472	0.002*
T_POSTC_left	0.357 ± 0.014	0.358 ± 0.015	0.371 ± 0.021	0.374 ± 0.021	0.25 %	1.04 %	-3.056	0.001*	-3.558	<0.001
T_POSTC_right	0.372 ± 0.017	0.371 ± 0.017	0.383 ± 0.020	0.387 ± 0.021	-0.27 %	0.86 %	-2.372	0.005*	-3.213	<0.001
T_PREC_left	0.365 ± 0.015	0.367 ± 0.015	0.386 ± 0.016	0.390 ± 0.016	0.52 %	1 %	-4.968	<0.001	-5.187	<0.001
T_PREC_right	0.377 ± 0.015	0.377 ± 0.014	0.390 ± 0.016	0.393 ± 0.016	0.13 %	0.94 %	-3.046	0.001*	-3.944	<0.001
T_PREF_left	0.333 ± 0.013	0.333 ± 0.014	0.349 ± 0.013	0.352 ± 0.014	0.14 %	0.69 %	-4.522	<0.001	-4.582	<0.001
T_PREF_right	0.322 ± 0.012	0.322 ± 0.013	0.334 ± 0.013	0.338 ± 0.013	0 %	1.19 %	-3.503	<0.001	-4.490	<0.001
T_PREM_left	0.324 ± 0.013	0.326 ± 0.016	0.340 ± 0.021	0.343 ± 0.020	0.5 %	0.78 %	-3.815	<0.001	-3.674	<0.001
T_PREM_right	0.335 ± 0.015	0.337 ± 0.017	0.352 ± 0.019	0.356 ± 0.018	0.63 %	0.94 %	-3.820	<0.001	-3.839	<0.001
UF_left	0.299 ± 0.020	0.299 ± 0.017	0.313 ± 0.015	0.310 ± 0.024	-0.16 %	-0.77 %	-2.490	0.004*	-2.158	<0.001
UF_right	0.295 ± 0.016	0.293 ± 0.017	0.307 ± 0.011	0.307 ± 0.020	-0.41 %	0.27 %	-2.812	0.002*	-2.828	<0.001

Tables A.12- T-test results for comparisons of the automatically segmented tracts from TractSeg between mTBI and control subjects.

[1]Significant values are marked with an asterisk (*) or <0.001

Table A.13 Results of Post Hoc Tract Specific Comparisons of Fixel-Based Analysis Log Fiber Cross Section

	mTBI		Controls		Percent Change					
TractSeg Abbv.	P1	P2	P1	P2	mTBI	Controls	t-score P1	q-value P1ᶠ	t-score P2	q-value P2ᶠ
AF_left	0.035 ± 0.073	0.035 ± 0.070	0.056 ± 0.111	0.068 ± 0.125	-0.26 %	21.44 %	-0.908	0.269	-1.404	0.003*
AF_right	0.046 ± 0.070	0.045 ± 0.073	0.078 ± 0.101	0.087 ± 0.121	-1.42 %	11.55 %	-1.469	0.216	-1.732	0.003*
ATR_left	0.003 ± 0.082	-6.888e-03 ± 8.403e-02	0.026 ± 0.102	0.028 ± 0.121	-299.02 %	8.83 %	-0.920	0.269	-1.339	0.004*
ATR_right	0.014 ± 0.079	0.008 ± 0.080	0.052 ± 0.091	0.056 ± 0.106	-43.33 %	6.57 %	-1.679	0.216	-1.973	0.003*
CA	0.005 ± 0.083	0.010 ± 0.072	0.056 ± 0.089	0.073 ± 0.085	104.23 %	29.87 %	-2.162	0.211	-2.978	<0.001
CC_1	0.013 ± 0.089	0.003 ± 0.092	0.077 ± 0.107	0.081 ± 0.101	-75.6 %	4.94 %	-2.441	0.141	-2.950	<0.001
CC_2	0.020 ± 0.069	0.015 ± 0.071	0.054 ± 0.093	0.057 ± 0.102	-28.35 %	6.43 %	-1.593	0.216	-1.932	0.003*
CC_3	0.023 ± 0.080	0.026 ± 0.088	0.028 ± 0.103	0.039 ± 0.119	10.96 %	39.9 %	-0.193	0.419	-0.493	0.006*
CC_4	0.003 ± 0.072	0.013 ± 0.075	0.047 ± 0.078	0.064 ± 0.097	286.67 %	37.54 %	-2.110	0.211	-2.297	0.002*
CC_5	-1.106e-02 ± 6.943e-02	-2.758e-03 ± 7.171e-02	0.007 ± 0.103	0.017 ± 0.113	-75.08 %	156.28 %	-0.808	0.269	-0.845	0.004*
CC_6	8.253e-04 ± 7.889e-02	0.006 ± 0.073	0.006 ± 0.106	0.014 ± 0.110	612 %	122.82 %	-0.220	0.415	-0.336	0.007*
CC_7	0.057 ± 0.079	0.053 ± 0.080	0.043 ± 0.103	0.060 ± 0.115	-6.36 %	40.95 %	0.595	0.316	-0.276	0.007*
CC	0.013 ± 0.061	0.014 ± 0.063	0.032 ± 0.091	0.040 ± 0.099	8.12 %	25.81 %	-0.987	0.269	-1.292	0.004*
CG_left	0.008 ± 0.063	0.006 ± 0.063	0.026 ± 0.101	0.022 ± 0.092	-26.31 %	-14.76 %	-0.877	0.269	-0.822	0.004*
CG_right	0.008 ± 0.063	0.004 ± 0.064	0.024 ± 0.094	0.025 ± 0.090	-47.98 %	5.64 %	-0.836	0.269	-1.088	0.004*
CST_left	-1.905e-02 ± 7.521e-02	-8.765e-03 ± 7.238e-02	0.039 ± 0.085	0.051 ± 0.095	-53.99 %	29.98 %	-2.684	0.099	-2.750	<0.001
CST_right	-3.508e-03 ± 7.713e-02	0.003 ± 0.076	0.035 ± 0.093	0.041 ± 0.096	-174.57 %	17.98 %	-1.699	0.216	-1.714	0.003*
FPT_left	0.004 ± 0.068	0.006 ± 0.065	0.032 ± 0.073	0.039 ± 0.081	52.09 %	23.18 %	-1.432	0.216	-1.702	0.003*
FPT_right	0.001 ± 0.064	4.733e-04 ± 6.411e-02	0.030 ± 0.091	0.033 ± 0.090	-65.91 %	11.89 %	-1.435	0.216	-1.665	0.003*
FX_left	-7.329e-02 ± 1.008e-01	-7.435e-02 ± 1.209e-01	-1.159e-01 ± 1.119e-01	-1.177e-01 ± 1.174e-01	1.44 %	1.52 %	1.469	0.216	1.282	0.004*
FX_right	-7.471e-02 ± 1.073e-01	-7.727e-02 ± 1.254e-01	-1.160e-01 ± 1.090e-01	-1.159e-01 ± 1.192e-01	3.42 %	-0.08 %	1.363	0.225	1.106	0.004*
ICP_left	0.025 ± 0.091	0.024 ± 0.097	0.054 ± 0.097	0.049 ± 0.090	-4.04 %	-9.26 %	-1.107	0.269	-0.916	0.004*
ICP_right	0.023 ± 0.081	0.018 ± 0.085	0.036 ± 0.094	0.038 ± 0.103	-24.1 %	7.15 %	-0.537	0.333	-0.833	0.004*
IFO_left	0.035 ± 0.074	0.028 ± 0.074	0.044 ± 0.105	0.055 ± 0.120	-18.8 %	23 %	-0.436	0.366	-1.109	0.004*
IFO_right	0.047 ± 0.067	0.042 ± 0.068	0.066 ± 0.099	0.077 ± 0.111	-10.62 %	16.59 %	-0.882	0.269	-1.554	0.003*
ILF_left	0.069 ± 0.085	0.067 ± 0.087	0.070 ± 0.107	0.091 ± 0.113	-2.51 %	28.83 %	-0.068	0.447	-0.904	0.004*
ILF_right	0.091 ± 0.082	0.090 ± 0.082	0.091 ± 0.104	0.107 ± 0.107	-1 %	18.01 %	-0.011	0.456	-0.712	0.005*

Table A.13 (cont'd)

	mTBI		Controls		Percent Change					
TractSeg Abbv.	P1	P2	P1	P2	mTBI	Controls	t-score P1	q-value P1[f]	t-score P2	q-value P2[f]
MCP	0.028 ± 0.094	0.027 ± 0.097	0.044 ± 0.105	0.045 ± 0.107	-5.45 %	0.86 %	-0.599	0.316	-0.652	0.005*
MLF_left	0.017 ± 0.082	0.020 ± 0.075	0.026 ± 0.110	0.034 ± 0.113	18.51 %	32.39 %	-0.350	0.395	-0.587	0.005*
MLF_right	0.020 ± 0.078	0.025 ± 0.073	0.026 ± 0.102	0.032 ± 0.108	28.69 %	24.39 %	-0.270	0.408	-0.308	0.007*
OR_left	0.037 ± 0.080	0.038 ± 0.080	0.036 ± 0.098	0.052 ± 0.114	1.13 %	44.33 %	0.051	0.447	-0.574	0.005*
OR_right	0.035 ± 0.075	0.034 ± 0.074	0.042 ± 0.104	0.055 ± 0.118	-1.84 %	30.6 %	-0.324	0.399	-0.881	0.004*
POPT_left	-3.043e-02 ± 7.537e-02	-2.240e-02 ± 6.974e-02	-6.398e-03 ± 9.750e-02	-4.521e-04 ± 1.052e-01	-26.39 %	-92.93 %	-1.063	0.269	-0.997	0.004*
POPT_right	-2.630e-02 ± 7.626e-02	-1.965e-02 ± 7.247e-02	-4.322e-03 ± 1.042e-01	-9.075e-05 ± 1.045e-01	-25.31 %	-97.9 %	-0.945	0.269	-0.869	0.004*
SCP_left	0.007 ± 0.080	0.008 ± 0.085	0.032 ± 0.090	0.029 ± 0.086	28.33 %	-8.05 %	-1.093	0.269	-0.872	0.004*
SCP_right	0.017 ± 0.072	0.014 ± 0.073	0.033 ± 0.087	0.035 ± 0.093	-15.59 %	4.87 %	-0.762	0.28	-0.938	0.004*
SLF_III_left	0.036 ± 0.081	0.036 ± 0.082	0.062 ± 0.128	0.067 ± 0.134	-1 %	6.67 %	-1.021	0.269	-1.169	0.004*
SLF_III_right	0.047 ± 0.074	0.049 ± 0.078	0.089 ± 0.115	0.093 ± 0.124	5.05 %	4.68 %	-1.767	0.216	-1.739	0.003*
SLF_II_left	0.027 ± 0.072	0.028 ± 0.073	0.043 ± 0.105	0.058 ± 0.134	4.02 %	37.08 %	-0.719	0.286	-1.236	0.004*
SLF_II_right	0.035 ± 0.079	0.033 ± 0.078	0.060 ± 0.104	0.071 ± 0.120	-6.27 %	17.78 %	-1.069	0.269	-1.550	0.003*
SLF_I_left	0.007 ± 0.069	0.015 ± 0.067	0.025 ± 0.091	0.036 ± 0.099	103.82 %	45.42 %	-0.832	0.269	-0.987	0.004*
SLF_I_right	0.006 ± 0.074	0.008 ± 0.072	0.026 ± 0.110	0.035 ± 0.110	34.8 %	36.4 %	-0.849	0.269	-1.179	0.004*
STR_left	-7.186e-03 ± 7.695e-02	0.002 ± 0.075	0.029 ± 0.096	0.041 ± 0.110	-127.13 %	40.41 %	-1.598	0.216	-1.666	0.003*
STR_right	0.006 ± 0.065	0.010 ± 0.063	0.030 ± 0.108	0.035 ± 0.106	63.84 %	16.85 %	-1.112	0.269	-1.200	0.004*
ST_FO_left	0.010 ± 0.081	5.806e-06 ± 8.671e-02	0.038 ± 0.106	0.043 ± 0.114	-99.94 %	14.79 %	-1.152	0.269	-1.665	0.003*
ST_FO_right	0.033 ± 0.080	0.026 ± 0.081	0.079 ± 0.092	0.094 ± 0.094	-20.48 %	18.12 %	-1.997	0.216	-2.873	<0.001
ST_OCC_left	0.042 ± 0.078	0.042 ± 0.079	0.044 ± 0.097	0.062 ± 0.115	-0.72 %	42.71 %	-0.071	0.447	-0.835	0.004*
ST_OCC_right	0.045 ± 0.074	0.044 ± 0.074	0.050 ± 0.103	0.066 ± 0.117	-3.77 %	30.42 %	-0.221	0.415	-0.923	0.004*
ST_PAR_left	-1.348e-02 ± 7.252e-02	-6.068e-03 ± 7.133e-02	0.009 ± 0.103	0.018 ± 0.115	-54.99 %	95 %	-1.004	0.269	-1.026	0.004*
ST_PAR_right	-1.055e-02 ± 7.394e-02	-4.638e-03 ± 7.093e-02	0.010 ± 0.106	0.018 ± 0.114	-56.06 %	69.63 %	-0.912	0.269	-0.971	0.004*
ST_POSTC_left	-2.821e-02 ± 6.992e-02	-1.716e-02 ± 7.083e-02	0.012 ± 0.102	0.024 ± 0.123	-39.16 %	96.42 %	-1.852	0.216	-1.737	0.003*
ST_POSTC_right	-1.800e-02 ± 7.040e-02	-1.046e-02 ± 7.192e-02	0.016 ± 0.113	0.023 ± 0.124	-41.9 %	40.32 %	-1.514	0.216	-1.400	0.003*
ST_PREC_left	-6.573e-03 ± 6.506e-02	0.004 ± 0.066	0.049 ± 0.085	0.064 ± 0.103	-163.74 %	31.1 %	-2.844	0.095	-2.857	<0.001
ST_PREC_right	0.002 ± 0.068	0.008 ± 0.069	0.035 ± 0.096	0.044 ± 0.108	299.6 %	25.28 %	-1.583	0.216	-1.649	0.003*
ST_PREF_left	0.016 ± 0.067	0.012 ± 0.067	0.047 ± 0.085	0.054 ± 0.100	-24.73 %	14.88 %	-1.553	0.216	-1.995	0.003*
ST_PREF_right	0.020 ± 0.065	0.015 ± 0.065	0.060 ± 0.093	0.065 ± 0.102	-24.18 %	8.64 %	-1.968	0.216	-2.394	0.002*
ST_PREM_left	0.012 ± 0.074	0.015 ± 0.076	0.028 ± 0.094	0.040 ± 0.118	19.98 %	41.08 %	-0.732	0.286	-1.051	0.004*
ST_PREM_right	0.016 ± 0.070	0.018 ± 0.074	0.041 ± 0.094	0.050 ± 0.105	12.14 %	24.11 %	-1.166	0.269	-1.428	0.003*
T_OCC_left	0.038 ± 0.079	0.039 ± 0.080	0.036 ± 0.098	0.052 ± 0.115	1 %	45.46 %	0.094	0.447	-0.554	0.005*
T_OCC_right	0.037 ± 0.075	0.036 ± 0.075	0.043 ± 0.105	0.056 ± 0.119	-1.82 %	30.71 %	-0.275	0.408	-0.841	0.004*
T_PAR_left	-1.725e-02 ± 7.338e-02	-9.715e-03 ± 7.206e-02	0.003 ± 0.101	0.010 ± 0.111	-43.68 %	281.16 %	-0.883	0.269	-0.849	0.004*
T_PAR_right	-1.994e-02 ± 7.469e-02	-1.372e-02 ± 7.168e-02	-1.538e-03 ± 1.027e-01	0.005 ± 0.106	-31.2 %	-414.66 %	-0.806	0.269	-0.825	0.004*
T_POSTC_left	-3.074e-02 ± 7.699e-02	-2.048e-02 ± 7.665e-02	8.301e-04 ± 1.098e-01	0.010 ± 0.126	-33.37 %	1118.82 %	-1.325	0.232	-1.225	0.004*

Table A.13 (cont'd)

	mTBI		Controls		Percent Change					
TractSeg Abbv.	P1	P2	P1	P2	mTBI	Controls	t-score P1	q-value P1[f]	t-score P2	q-value P2[f]
T_POSTC_right	-1.552e-02 ± 7.574e-02	-7.507e-03 ± 7.689e-02	0.014 ± 0.119	0.021 ± 0.126	-51.62 %	43.72 %	-1.232	0.262	-1.123	0.004*
T_PREC_left	-9.899e-03 ± 6.619e-02	6.543e-04 ± 6.824e-02	0.049 ± 0.083	0.064 ± 0.099	-106.61 %	31.61 %	-2.970	0.095	-2.984	<0.001
T_PREC_right	0.003 ± 0.070	0.009 ± 0.072	0.037 ± 0.094	0.046 ± 0.102	196.31 %	25.4 %	-1.577	0.216	-1.650	0.003*
T_PREF_left	0.014 ± 0.067	0.010 ± 0.068	0.041 ± 0.084	0.048 ± 0.097	-25.47 %	16.15 %	-1.365	0.225	-1.772	0.003*
T_PREF_right	0.016 ± 0.066	0.011 ± 0.067	0.050 ± 0.093	0.054 ± 0.103	-29.73 %	9.28 %	-1.687	0.216	-2.038	0.003*
T_PREM_left	0.006 ± 0.071	0.008 ± 0.074	0.020 ± 0.090	0.030 ± 0.108	23.69 %	46.58 %	-0.662	0.301	-0.959	0.004*
T_PREM_right	0.012 ± 0.070	0.014 ± 0.074	0.033 ± 0.089	0.044 ± 0.096	13.12 %	32.52 %	-0.997	0.269	-1.352	0.004*
UF_left	0.025 ± 0.077	0.016 ± 0.079	0.047 ± 0.112	0.057 ± 0.116	-33.31 %	21.04 %	-0.928	0.269	-1.626	0.003*
UF_right	0.034 ± 0.071	0.033 ± 0.066	0.074 ± 0.086	0.087 ± 0.096	-3.78 %	17.82 %	-1.898	0.216	-2.634	<0.001

Tables A.13- T-test results for comparisons of the automatically segmented tracts from TractSeg between mTBI and control subjects.

[f]Significant values are marked with an asterisk (*) or <0.001

Table A.14 Results of Post Hoc Tract Specific Comparisons of Fixel-Based Analysis Fiber Density Cross Section

	mTBI		Controls		Percent Change					
TractSeg Abbv.	P1	P2	P1	P2	mTBI	Controls	t-score P1	q-value P1′	t-score P2	q-value P2′
AF_left	0.302 ± 0.033	0.302 ± 0.029	0.322 ± 0.045	0.327 ± 0.043	0.27 %	1.51 %	-2.085	0.001*	-2.690	<0.001
AF_right	0.314 ± 0.031	0.312 ± 0.031	0.327 ± 0.044	0.333 ± 0.046	-0.41 %	1.69 %	-1.382	0.004*	-2.081	<0.001
ATR_left	0.304 ± 0.032	0.301 ± 0.033	0.332 ± 0.044	0.335 ± 0.046	-0.96 %	1.09 %	-2.860	<0.001	-3.420	<0.001
ATR_right	0.300 ± 0.030	0.299 ± 0.031	0.328 ± 0.036	0.335 ± 0.042	-0.38 %	2.22 %	-3.160	<0.001	-3.855	<0.001
CA	0.274 ± 0.040	0.277 ± 0.037	0.316 ± 0.047	0.329 ± 0.040	1.14 %	4.09 %	-3.595	<0.001	-4.861	<0.001
CC_1	0.388 ± 0.051	0.380 ± 0.051	0.435 ± 0.068	0.437 ± 0.058	-2.08 %	0.44 %	-3.058	<0.001	-3.878	<0.001
CC_2	0.342 ± 0.031	0.340 ± 0.032	0.370 ± 0.045	0.375 ± 0.043	-0.68 %	1.34 %	-2.961	<0.001	-3.653	<0.001
CC_3	0.337 ± 0.032	0.340 ± 0.036	0.363 ± 0.053	0.370 ± 0.056	0.84 %	2.06 %	-2.471	<0.001	-2.668	<0.001
CC_4	0.371 ± 0.033	0.375 ± 0.034	0.408 ± 0.038	0.420 ± 0.040	1.1 %	2.77 %	-3.890	<0.001	-4.429	<0.001
CC_5	0.368 ± 0.032	0.371 ± 0.034	0.392 ± 0.044	0.400 ± 0.041	0.81 %	2.01 %	-2.509	<0.001	-2.977	<0.001
CC_6	0.360 ± 0.042	0.360 ± 0.036	0.369 ± 0.046	0.370 ± 0.042	0.12 %	0.19 %	-0.803	0.008*	-0.955	0.005*
CC_7	0.353 ± 0.046	0.353 ± 0.039	0.353 ± 0.042	0.359 ± 0.043	-0.03 %	1.61 %	-0.051	0.015*	-0.575	0.008*
CC	0.352 ± 0.030	0.352 ± 0.029	0.371 ± 0.041	0.376 ± 0.038	-0.04 %	1.25 %	-2.052	0.001*	-2.718	<0.001
CG_left	0.322 ± 0.030	0.320 ± 0.030	0.341 ± 0.051	0.340 ± 0.036	-0.63 %	-0.14 %	-1.886	0.002*	-2.264	<0.001
CG_right	0.322 ± 0.031	0.319 ± 0.032	0.333 ± 0.048	0.336 ± 0.038	-0.8 %	0.91 %	-1.159	0.005*	-1.837	0.001*
CST_left	0.424 ± 0.042	0.431 ± 0.040	0.472 ± 0.049	0.483 ± 0.047	1.66 %	2.37 %	-3.882	<0.001	-4.450	<0.001
CST_right	0.440 ± 0.041	0.443 ± 0.039	0.473 ± 0.052	0.480 ± 0.050	0.71 %	1.6 %	-2.697	<0.001	-3.201	<0.001
FPT_left	0.404 ± 0.037	0.406 ± 0.036	0.435 ± 0.042	0.443 ± 0.042	0.64 %	1.96 %	-2.872	<0.001	-3.505	<0.001
FPT_right	0.404 ± 0.034	0.405 ± 0.033	0.432 ± 0.048	0.439 ± 0.045	0.21 %	1.63 %	-2.595	<0.001	-3.290	<0.001
FX_left	0.190 ± 0.044	0.192 ± 0.049	0.207 ± 0.046	0.211 ± 0.051	0.98 %	2.17 %	-1.362	0.004*	-1.427	0.002*
FX_right	0.199 ± 0.045	0.200 ± 0.049	0.206 ± 0.050	0.211 ± 0.050	0.56 %	2.76 %	-0.513	0.01*	-0.816	0.006*
ICP_left	0.315 ± 0.040	0.315 ± 0.041	0.321 ± 0.034	0.323 ± 0.029	0.04 %	0.66 %	-0.550	0.01*	-0.731	0.006*
ICP_right	0.287 ± 0.031	0.285 ± 0.032	0.290 ± 0.031	0.291 ± 0.030	-0.65 %	0.57 %	-0.302	0.012*	-0.686	0.007*
IFO_left	0.328 ± 0.032	0.326 ± 0.032	0.342 ± 0.042	0.347 ± 0.042	-0.44 %	1.32 %	-1.560	0.003*	-2.161	<0.001
IFO_right	0.332 ± 0.030	0.330 ± 0.029	0.345 ± 0.039	0.351 ± 0.042	-0.5 %	1.75 %	-1.531	0.003*	-2.420	<0.001
ILF_left	0.311 ± 0.038	0.313 ± 0.035	0.320 ± 0.044	0.327 ± 0.040	0.64 %	2.31 %	-0.774	0.008*	-1.356	0.003*
ILF_right	0.322 ± 0.035	0.322 ± 0.035	0.329 ± 0.042	0.337 ± 0.036	-0.01 %	2.28 %	-0.686	0.009*	-1.484	0.002*
MCP	0.330 ± 0.040	0.330 ± 0.040	0.333 ± 0.039	0.336 ± 0.037	-0.03 %	0.82 %	-0.272	0.012*	-0.535	0.008*
MLF_left	0.319 ± 0.037	0.320 ± 0.031	0.330 ± 0.044	0.330 ± 0.037	0.37 %	0.15 %	-1.014	0.006*	-1.125	0.004*
MLF_right	0.337 ± 0.036	0.337 ± 0.033	0.342 ± 0.040	0.342 ± 0.037	-0.06 %	-0.06 %	-0.453	0.01*	-0.500	0.008*
OR_left	0.330 ± 0.037	0.332 ± 0.038	0.340 ± 0.037	0.350 ± 0.040	0.59 %	2.85 %	-0.982	0.006*	-1.663	0.002*
OR_right	0.350 ± 0.037	0.351 ± 0.035	0.356 ± 0.040	0.364 ± 0.045	0.26 %	2.17 %	-0.604	0.009*	-1.268	0.003*
POPT_left	0.373 ± 0.036	0.376 ± 0.033	0.394 ± 0.046	0.398 ± 0.042	0.95 %	1 %	-2.006	0.001*	-2.228	<0.001
POPT_right	0.398 ± 0.039	0.400 ± 0.036	0.418 ± 0.051	0.421 ± 0.050	0.58 %	0.76 %	-1.669	0.003*	-1.861	0.001*
SCP_left	0.348 ± 0.039	0.350 ± 0.041	0.364 ± 0.038	0.370 ± 0.033	0.71 %	1.61 %	-1.516	0.003*	-1.767	0.002*
SCP_right	0.349 ± 0.032	0.349 ± 0.032	0.360 ± 0.039	0.365 ± 0.035	0.02 %	1.44 %	-1.155	0.005*	-1.745	0.002*
SLF_III_left	0.322 ± 0.037	0.322 ± 0.035	0.344 ± 0.063	0.348 ± 0.061	0.03 %	1.08 %	-1.814	0.002*	-2.169	<0.001
SLF_III_right	0.321 ± 0.038	0.320 ± 0.038	0.334 ± 0.055	0.337 ± 0.054	-0.2 %	1.05 %	-1.097	0.006*	-1.456	0.002*
SLF_II_left	0.298 ± 0.032	0.299 ± 0.032	0.309 ± 0.045	0.316 ± 0.052	0.13 %	2.52 %	-1.050	0.006*	-1.714	0.002*
SLF_II_right	0.298 ± 0.036	0.297 ± 0.035	0.309 ± 0.042	0.314 ± 0.045	-0.54 %	1.47 %	-1.024	0.006*	-1.599	0.002*
SLF_I_left	0.283 ± 0.030	0.284 ± 0.029	0.291 ± 0.036	0.294 ± 0.032	0.45 %	1.04 %	-0.905	0.007*	-1.152	0.004*
SLF_I_right	0.297 ± 0.033	0.297 ± 0.031	0.309 ± 0.043	0.311 ± 0.040	0.12 %	0.82 %	-1.242	0.005*	-1.545	0.002*
STR_left	0.416 ± 0.041	0.423 ± 0.044	0.453 ± 0.052	0.467 ± 0.055	1.72 %	3.07 %	-3.069	<0.001	-3.411	<0.001
STR_right	0.439 ± 0.034	0.441 ± 0.036	0.466 ± 0.057	0.474 ± 0.056	0.45 %	1.69 %	-2.394	<0.001	-2.872	<0.001
ST_FO_left	0.327 ± 0.039	0.323 ± 0.039	0.358 ± 0.053	0.362 ± 0.050	-1.24 %	1.27 %	-2.621	<0.001	-3.373	<0.001
ST_FO_right	0.351 ± 0.040	0.347 ± 0.038	0.387 ± 0.048	0.397 ± 0.048	-1.32 %	2.76 %	-3.002	<0.001	-4.414	<0.001
ST_OCC_left	0.341 ± 0.037	0.343 ± 0.037	0.353 ± 0.036	0.363 ± 0.039	0.48 %	2.75 %	-1.114	0.006*	-1.857	0.001*

Table A.14 (cont'd)

	mTBI		Controls		Percent Change					
TractSeg Abbv.	P1	P2	P1	P2	mTBI	Controls	t-score P1	q-value P1[1]	t-score P2	q-value P2[1]
ST_OCC_right	0.351 ± 0.036	0.352 ± 0.033	0.360 ± 0.041	0.367 ± 0.045	0.19 %	2 %	-0.841	0.007*	-1.523	0.002*
ST_PAR_left	0.334 ± 0.032	0.337 ± 0.031	0.354 ± 0.043	0.358 ± 0.040	0.84 %	1.01 %	-2.068	0.001*	-2.224	<0.001
ST_PAR_right	0.357 ± 0.035	0.357 ± 0.032	0.372 ± 0.045	0.375 ± 0.045	0.25 %	0.86 %	-1.467	0.004*	-1.784	0.002*
ST_POSTC_left	0.330 ± 0.030	0.336 ± 0.033	0.364 ± 0.043	0.372 ± 0.041	1.88 %	2.18 %	-3.780	<0.001	-3.753	<0.001
ST_POSTC_right	0.357 ± 0.031	0.359 ± 0.031	0.385 ± 0.047	0.390 ± 0.047	0.67 %	1.27 %	-2.878	<0.001	-3.151	<0.001
ST_PREC_left	0.346 ± 0.029	0.352 ± 0.031	0.388 ± 0.039	0.399 ± 0.038	1.79 %	2.66 %	-4.821	<0.001	-5.047	<0.001
ST_PREC_right	0.367 ± 0.030	0.370 ± 0.030	0.395 ± 0.043	0.402 ± 0.044	0.73 %	1.82 %	-3.022	<0.001	-3.478	<0.001
ST_PREF_left	0.339 ± 0.030	0.338 ± 0.031	0.367 ± 0.039	0.372 ± 0.040	-0.25 %	1.53 %	-3.085	<0.001	-3.699	<0.001
ST_PREF_right	0.340 ± 0.029	0.339 ± 0.028	0.367 ± 0.041	0.374 ± 0.043	-0.56 %	1.96 %	-2.970	<0.001	-3.968	<0.001
ST_PREM_left	0.316 ± 0.030	0.318 ± 0.030	0.336 ± 0.044	0.344 ± 0.048	0.5 %	2.17 %	-2.173	0.001*	-2.665	<0.001
ST_PREM_right	0.331 ± 0.031	0.334 ± 0.032	0.357 ± 0.041	0.363 ± 0.040	0.78 %	1.85 %	-2.718	<0.001	-3.133	<0.001
T_OCC_left	0.324 ± 0.036	0.326 ± 0.037	0.334 ± 0.035	0.344 ± 0.039	0.54 %	2.92 %	-0.940	0.007*	-1.674	0.002*
T_OCC_right	0.342 ± 0.037	0.343 ± 0.034	0.349 ± 0.040	0.356 ± 0.045	0.28 %	2.03 %	-0.665	0.009*	-1.282	0.003*
T_PAR_left	0.334 ± 0.032	0.336 ± 0.031	0.352 ± 0.042	0.356 ± 0.041	0.75 %	1.06 %	-1.881	0.002*	-2.084	<0.001
T_PAR_right	0.361 ± 0.036	0.362 ± 0.033	0.374 ± 0.044	0.378 ± 0.045	0.34 %	0.98 %	-1.294	0.005*	-1.610	0.002*
T_POSTC_left	0.347 ± 0.034	0.353 ± 0.036	0.377 ± 0.047	0.385 ± 0.048	1.52 %	2.14 %	-2.816	<0.001	-2.964	<0.001
T_POSTC_right	0.368 ± 0.034	0.371 ± 0.034	0.395 ± 0.052	0.401 ± 0.052	0.64 %	1.47 %	-2.469	<0.001	-2.811	<0.001
T_PREC_left	0.365 ± 0.033	0.371 ± 0.034	0.411 ± 0.041	0.422 ± 0.043	1.71 %	2.83 %	-4.691	<0.001	-4.997	<0.001
T_PREC_right	0.382 ± 0.032	0.385 ± 0.032	0.411 ± 0.045	0.419 ± 0.046	0.75 %	2.02 %	-2.916	<0.001	-3.423	<0.001
T_PREF_left	0.342 ± 0.031	0.342 ± 0.031	0.371 ± 0.039	0.377 ± 0.041	-0.08 %	1.71 %	-3.189	<0.001	-3.783	<0.001
T_PREF_right	0.331 ± 0.028	0.330 ± 0.028	0.357 ± 0.039	0.364 ± 0.042	-0.37 %	1.97 %	-3.038	<0.001	-3.861	<0.001
T_PREM_left	0.331 ± 0.031	0.333 ± 0.032	0.356 ± 0.043	0.363 ± 0.047	0.57 %	2.05 %	-2.648	<0.001	-3.042	<0.001
T_PREM_right	0.344 ± 0.032	0.347 ± 0.034	0.373 ± 0.041	0.381 ± 0.042	0.88 %	2.23 %	-3.029	<0.001	-3.411	<0.001
UF_left	0.311 ± 0.036	0.307 ± 0.035	0.334 ± 0.051	0.334 ± 0.047	-1.09 %	0.18 %	-2.039	0.001*	-2.519	<0.001
UF_right	0.308 ± 0.031	0.305 ± 0.031	0.335 ± 0.035	0.341 ± 0.040	-0.79 %	1.88 %	-2.984	<0.001	-3.842	<0.001

Tables A.14- T-test results for comparisons of the automatically segmented tracts from TractSeg between mTBI and control subjects.

[1]Significant values are marked with an asterisk (*) or <0.001

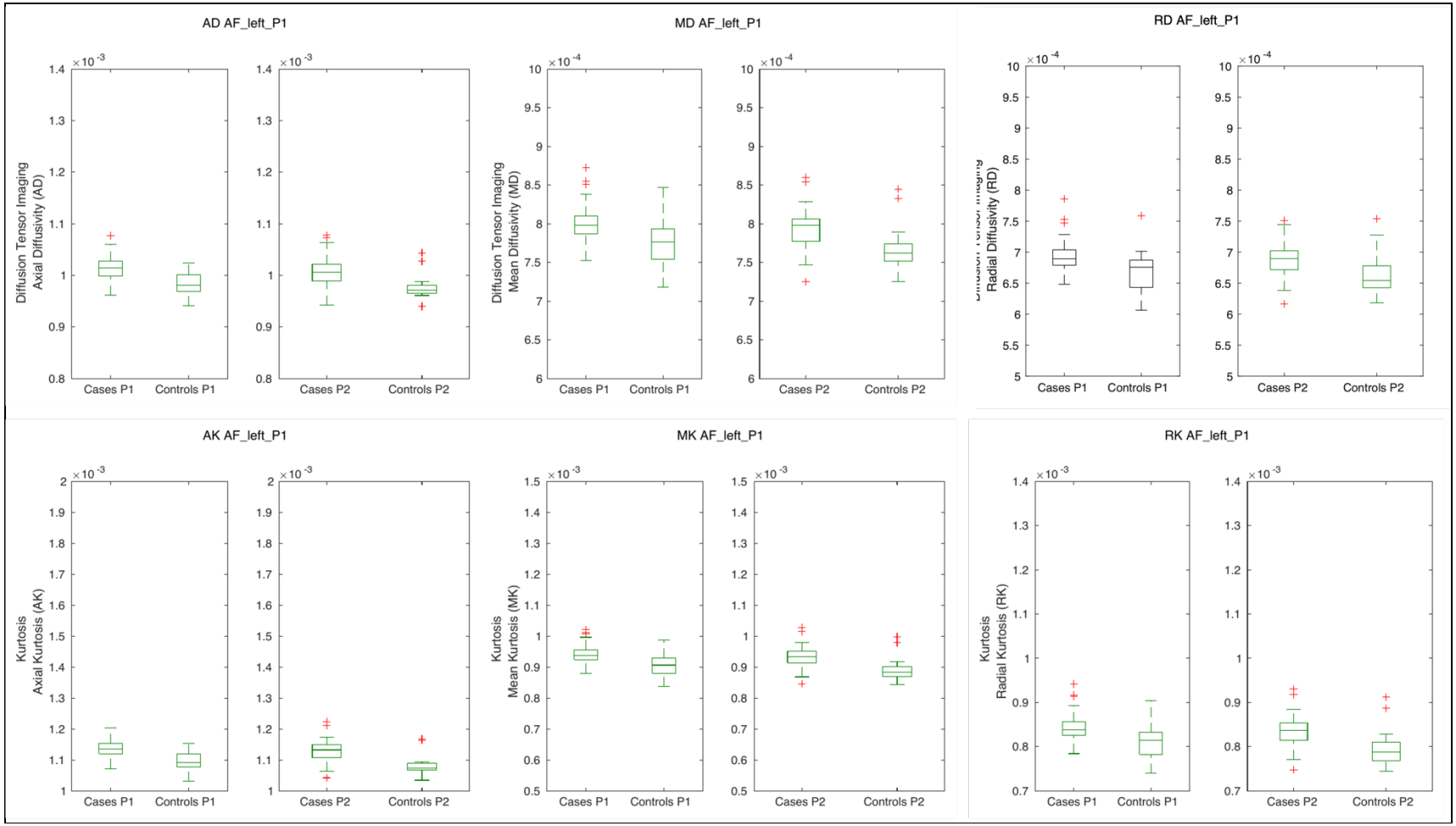

Figure A.1 – Boxplots for t-test results in the Arcuate Fascicle (Left)

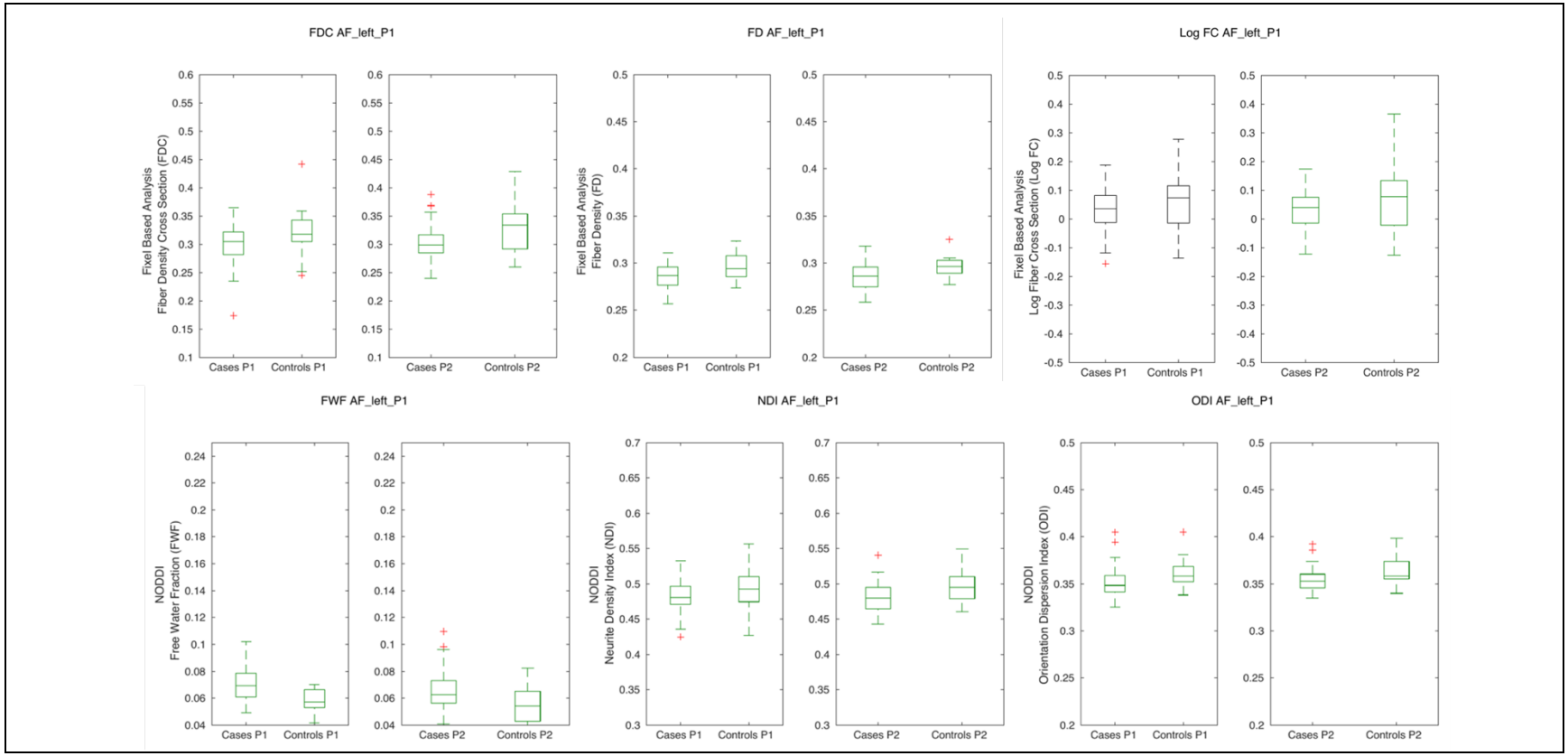

Figure A.2- Boxplots for t-test results in the Arcuate Fascicle (Left)

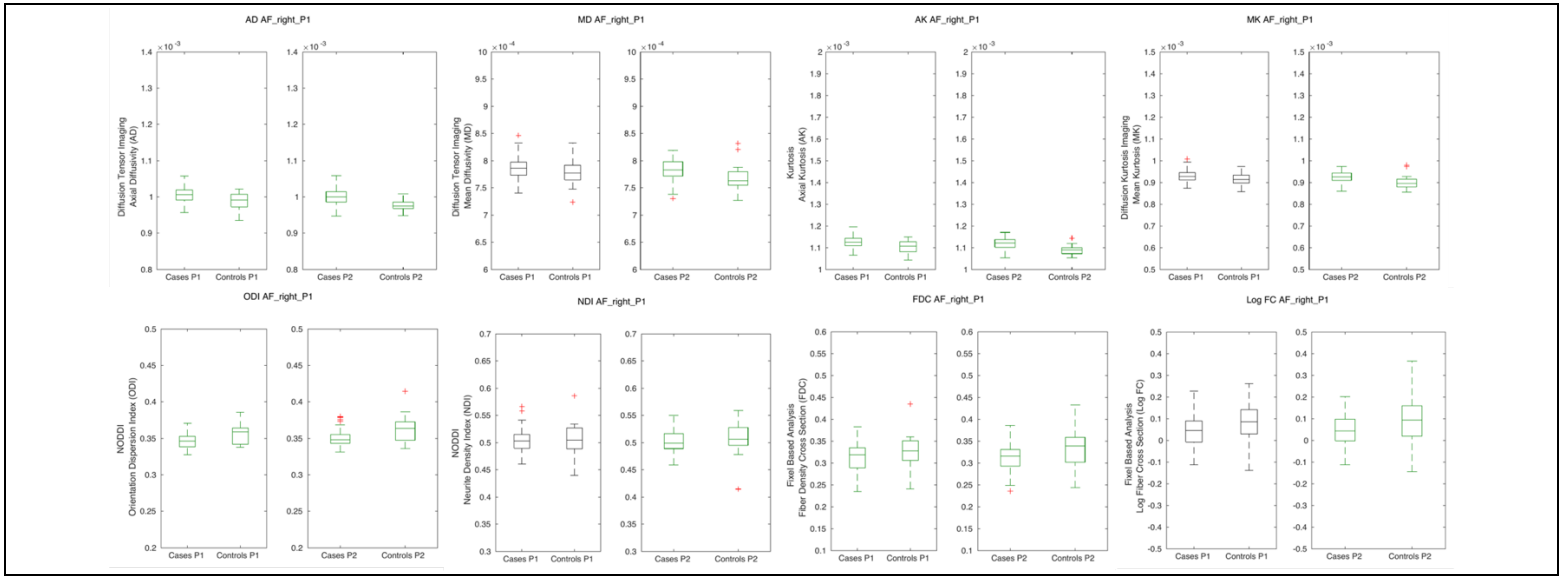

Figure A.3- Boxplots for t-test results in the Arcuate Fascicle (right)

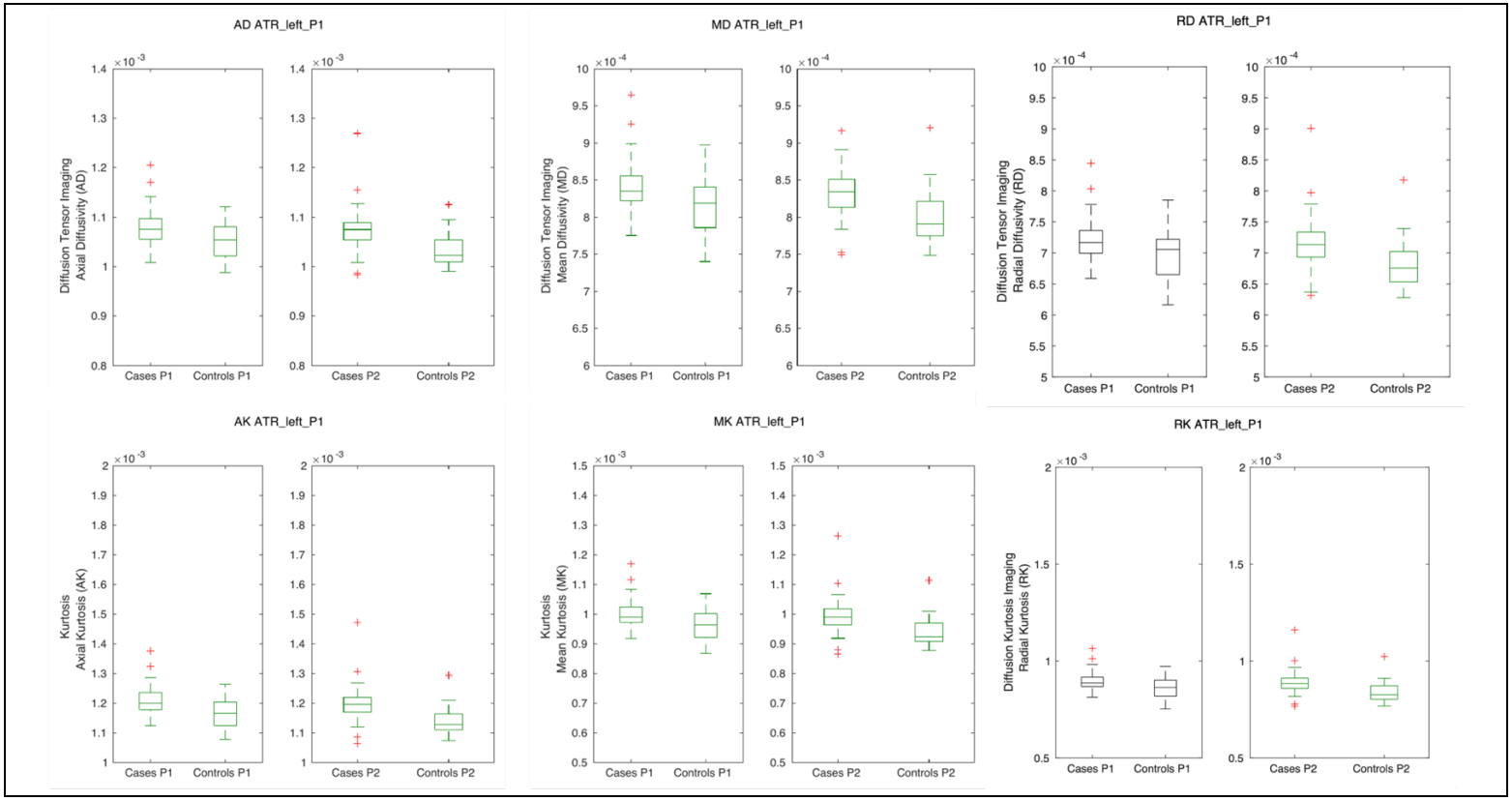

Figure A.4- Boxplots for t-test results in the Anterior Thalamic Radiation (left)

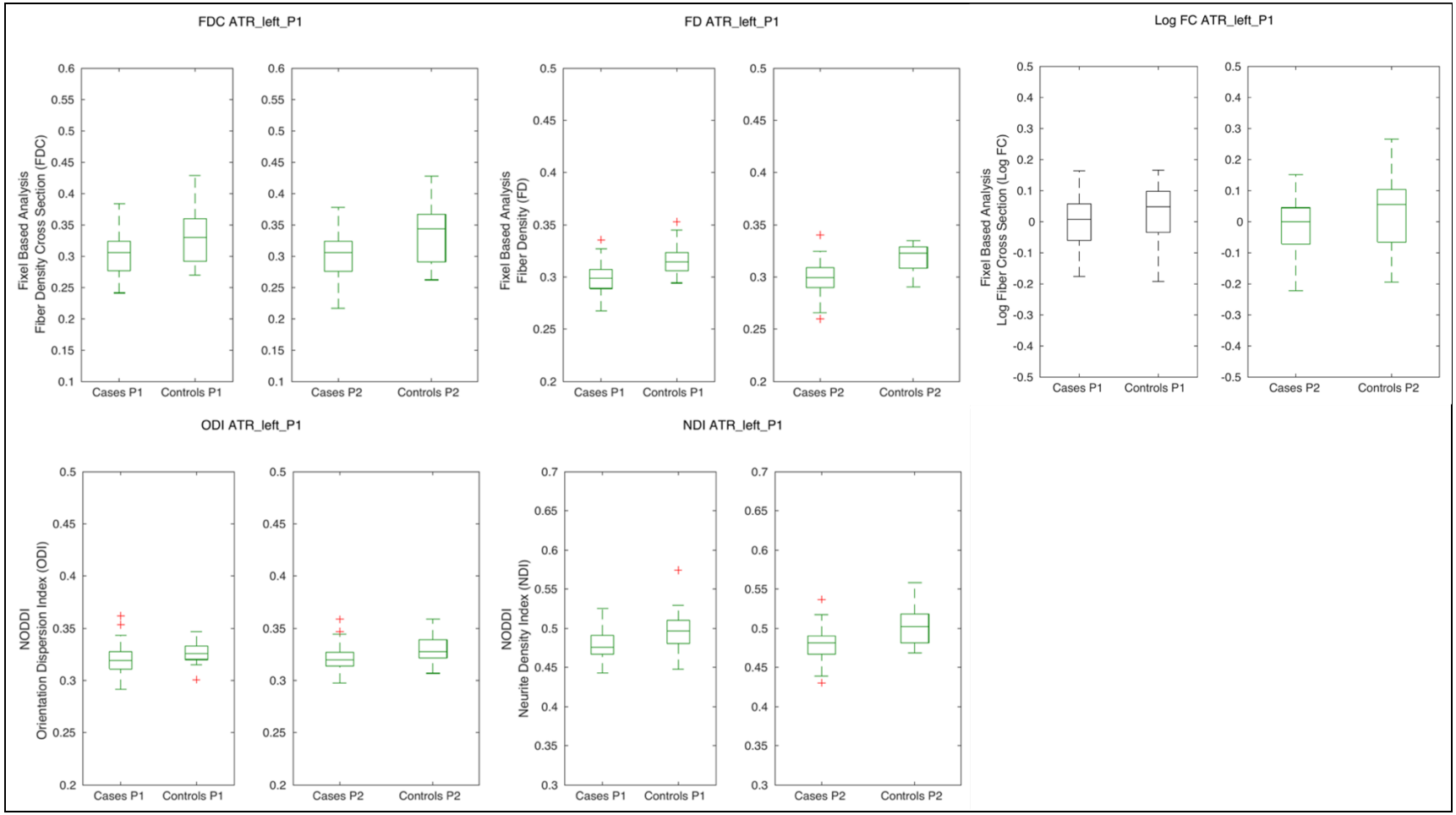

Figure A.5- Boxplots for t-test results in the Anterior Thalamic Radiation (left)

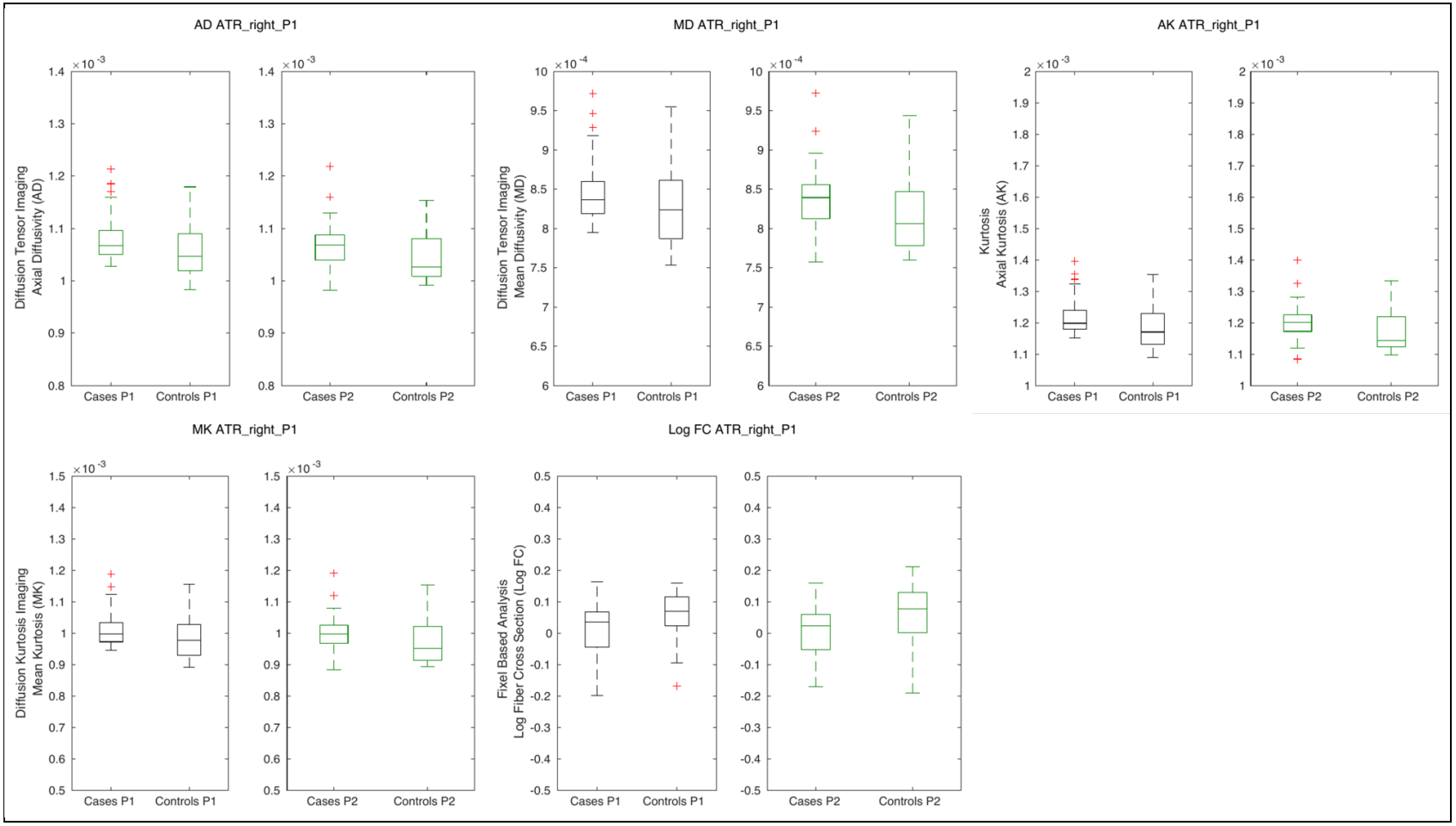

Figure A.6- Boxplots for t-test results in the Anterior Thalamic Radiation (Right)

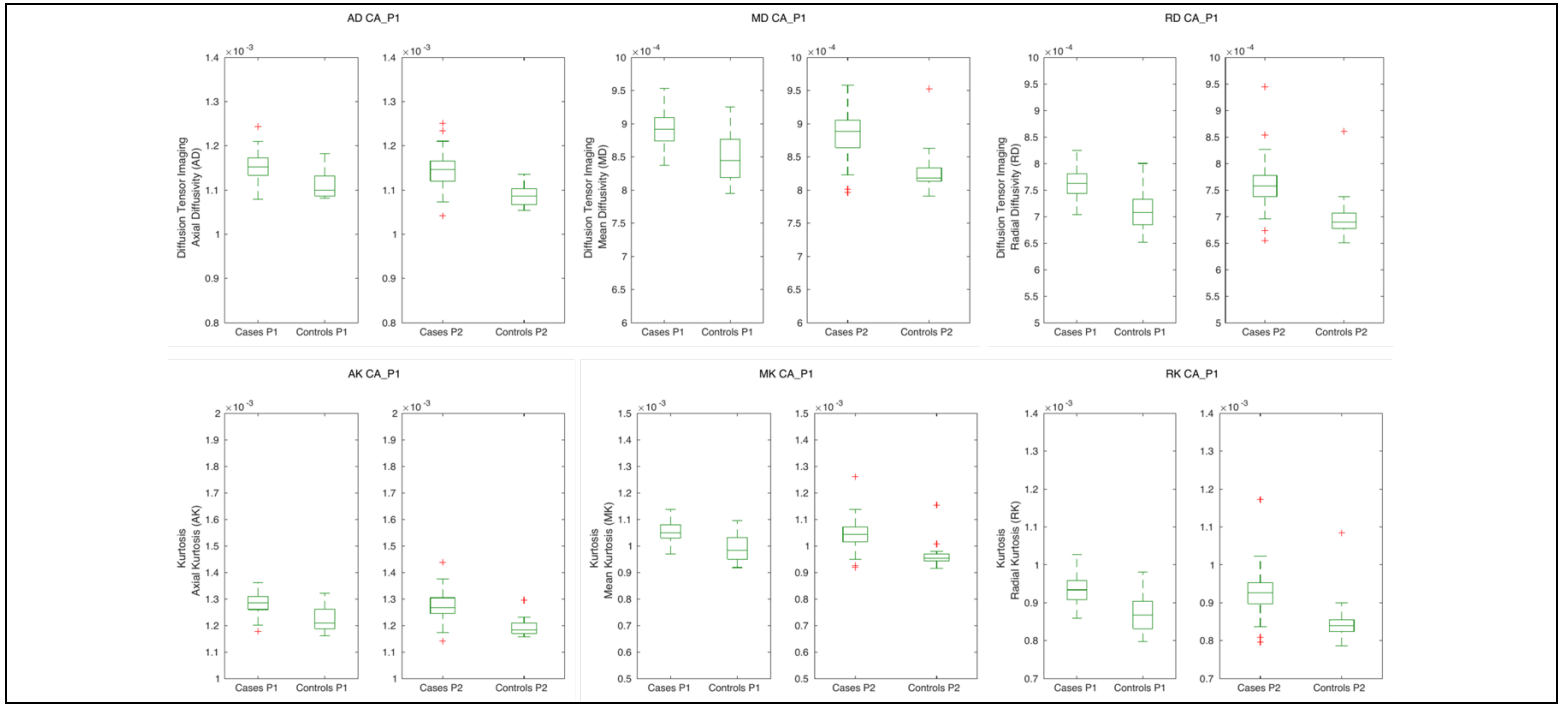

Figure A.7- Boxplots for t-test results in the Anterior Commissure

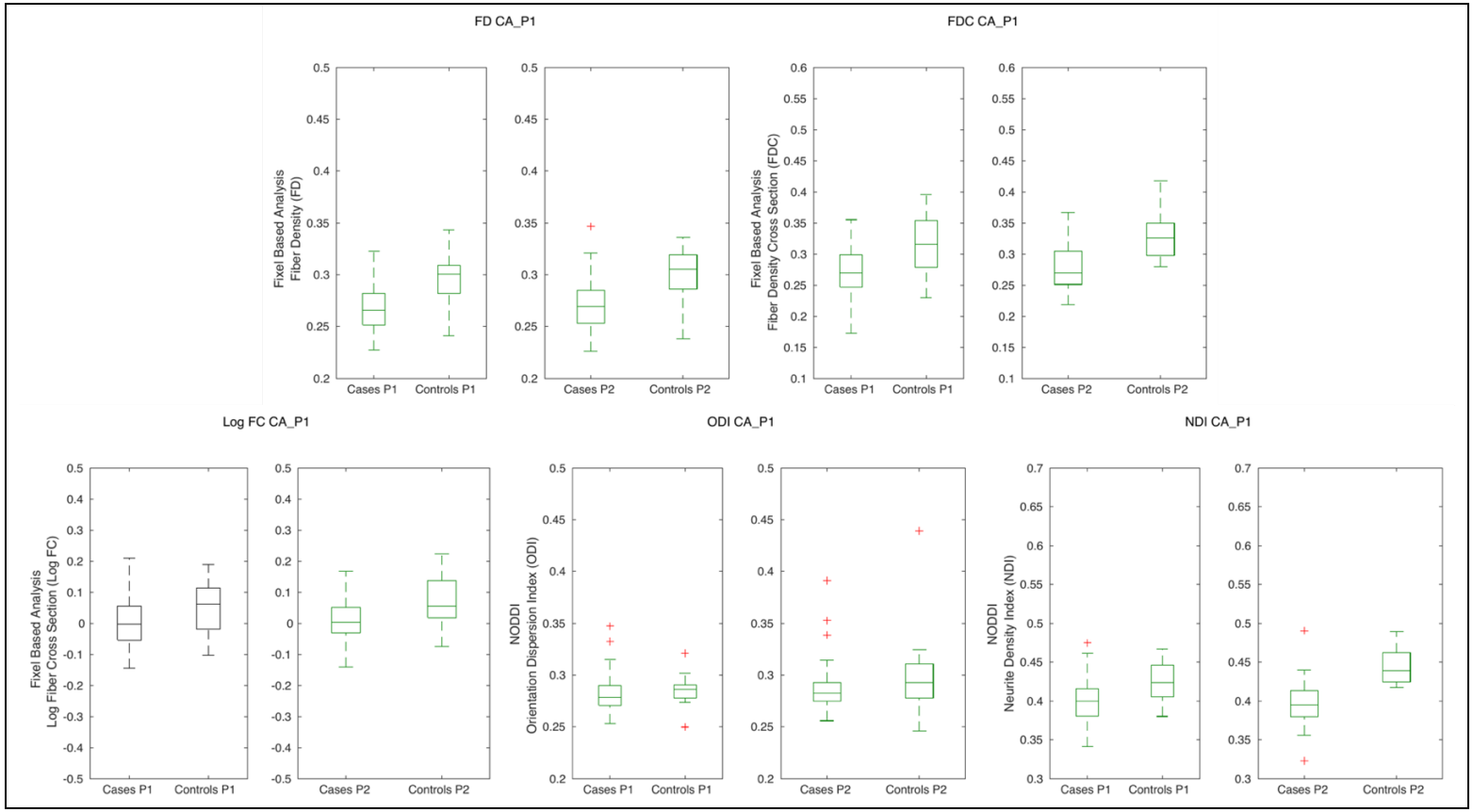

Figure A.8- Boxplots for t-test results in the Anterior Commissure

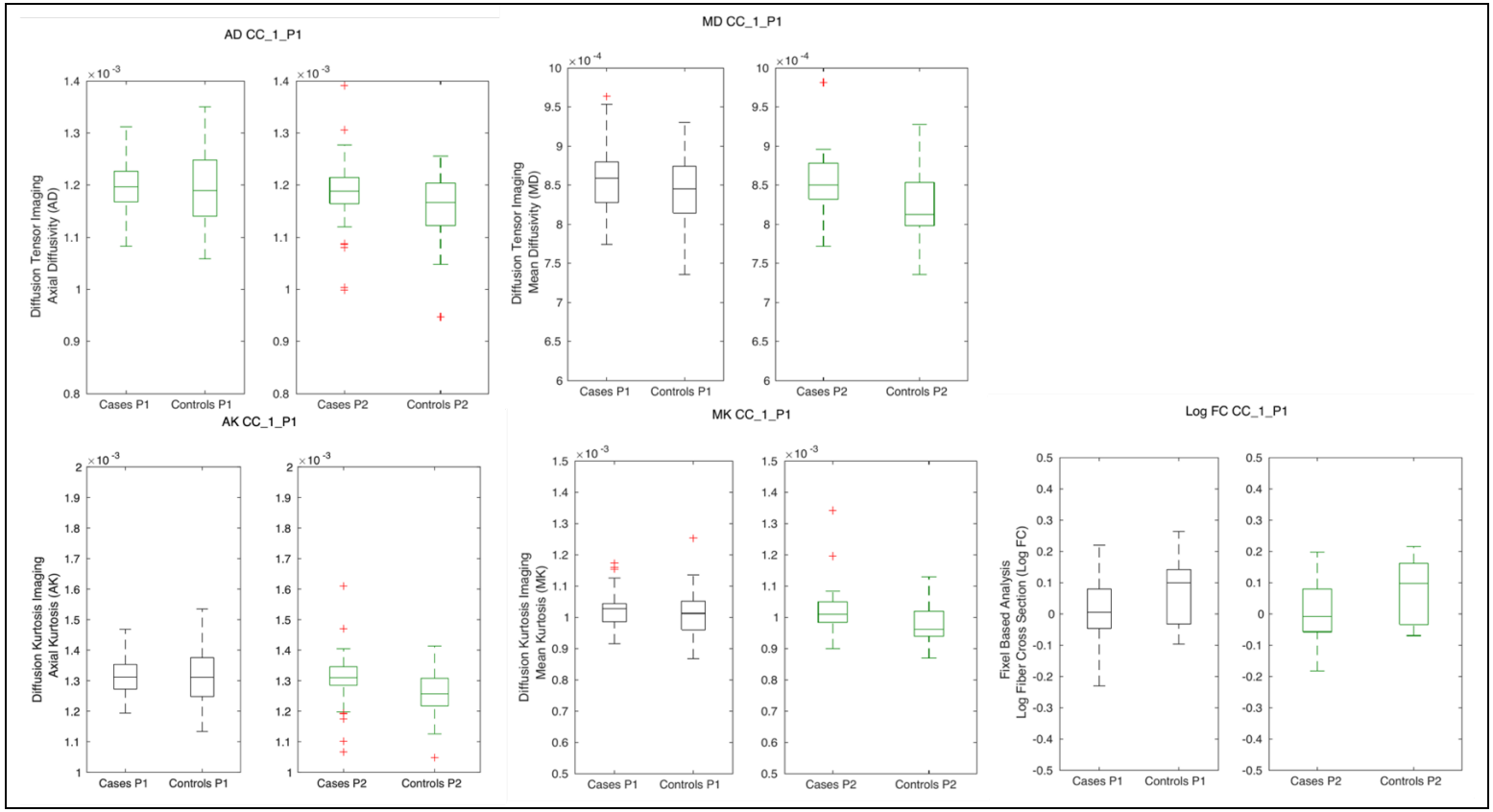

Figure A.9- Boxplots for t-test results in the Corpus Callosum-Rostrum

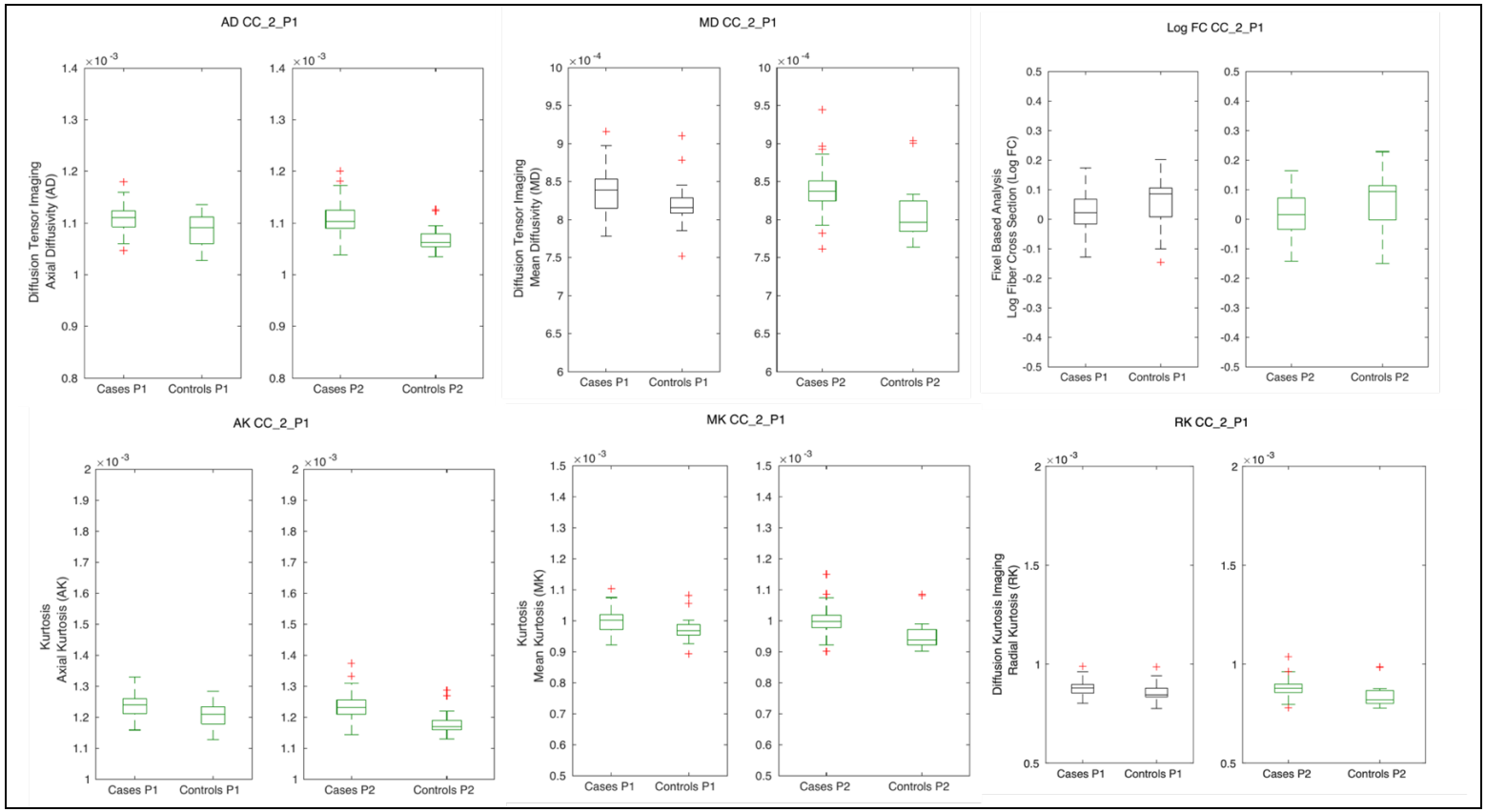

Figure A.10- Boxplots for t-test results in the Corpus Callosum - Genu

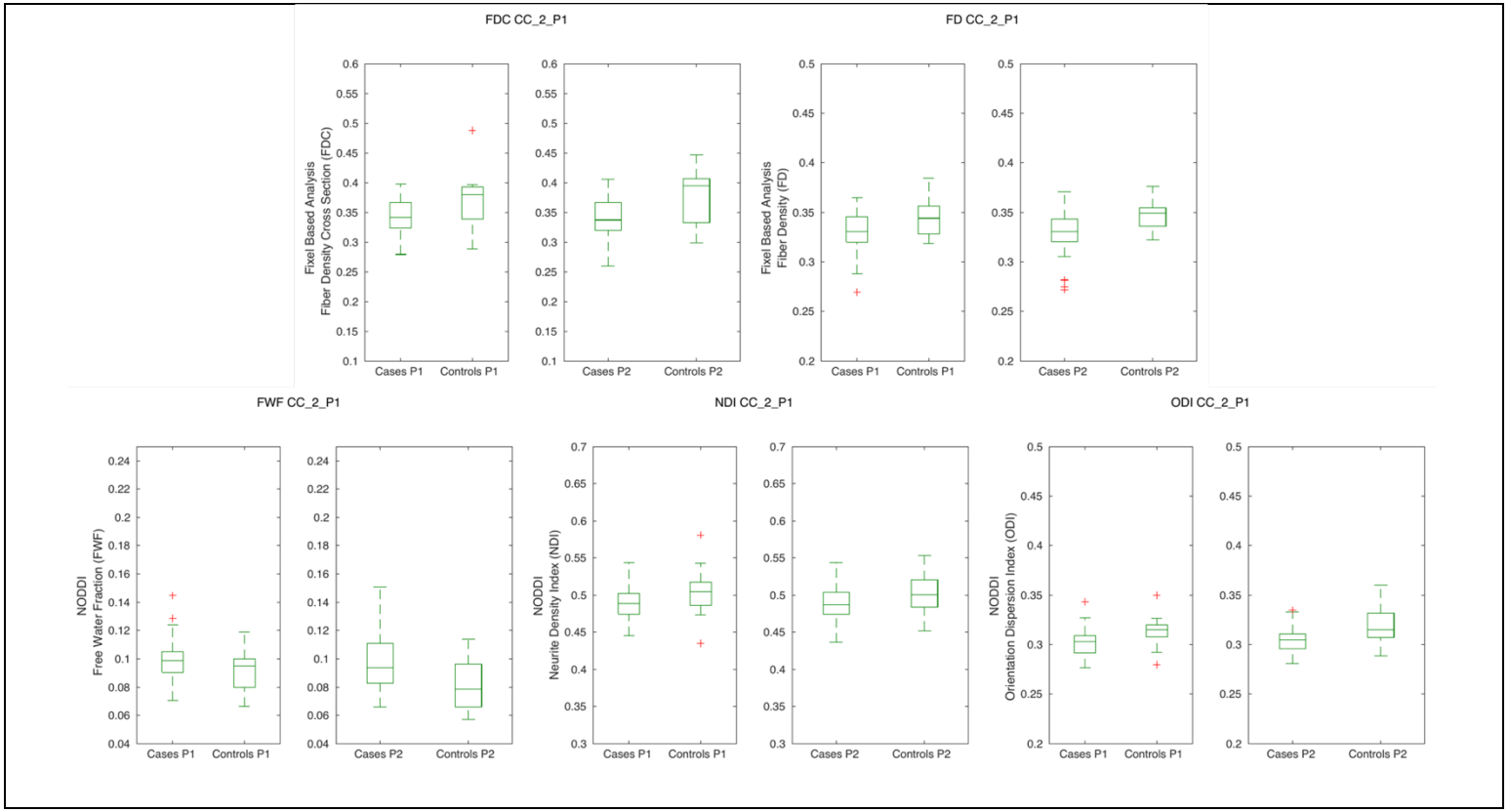

Figure A.11- Boxplots for t-test results in the Corpus Callosum - Genu

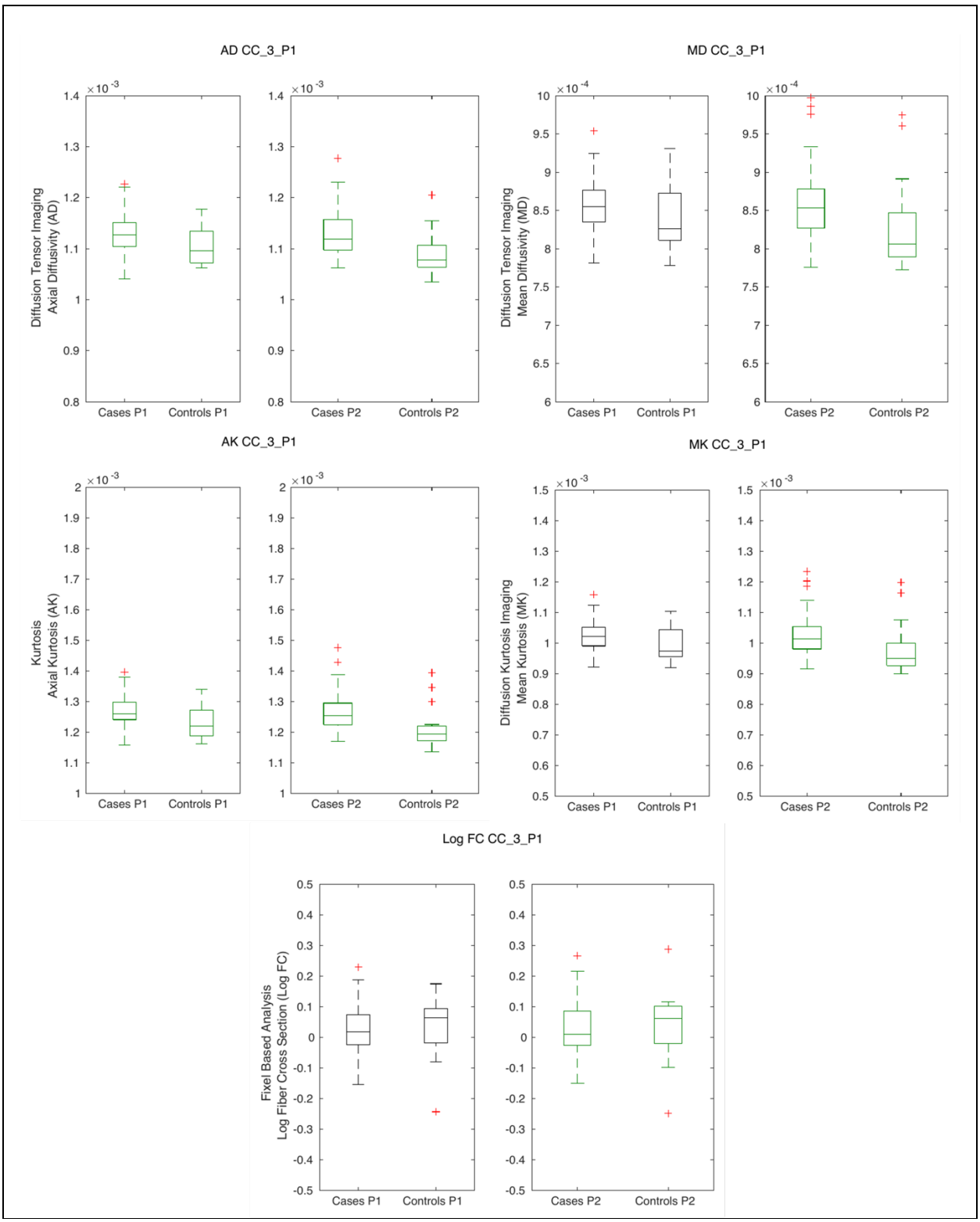

Figure A.12- Boxplots for t-test results in the Corpus Callosum – Rostral Body Premotor

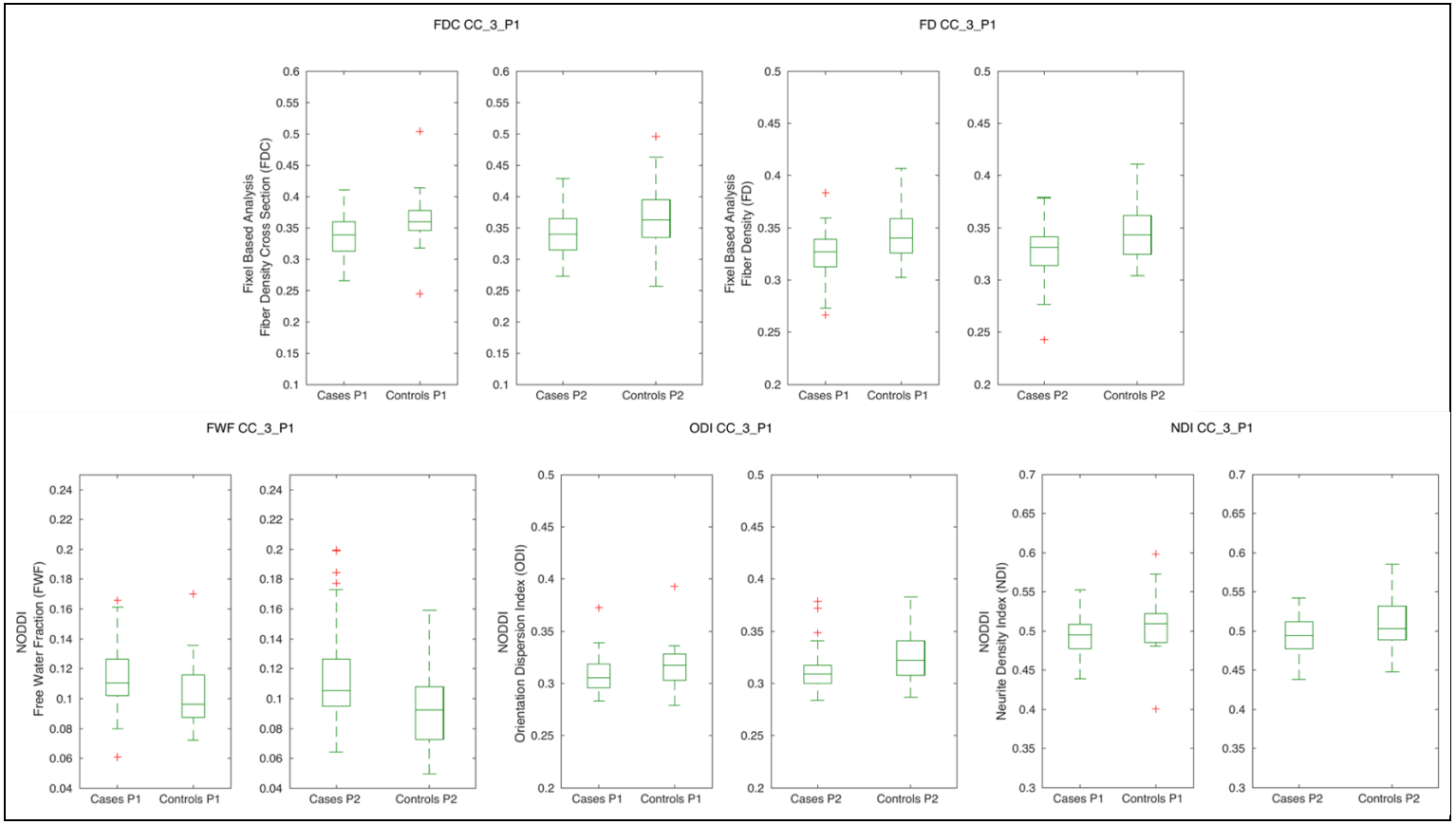

Figure A.13- Boxplots for t-test results in the Corpus Callosum – Rostral

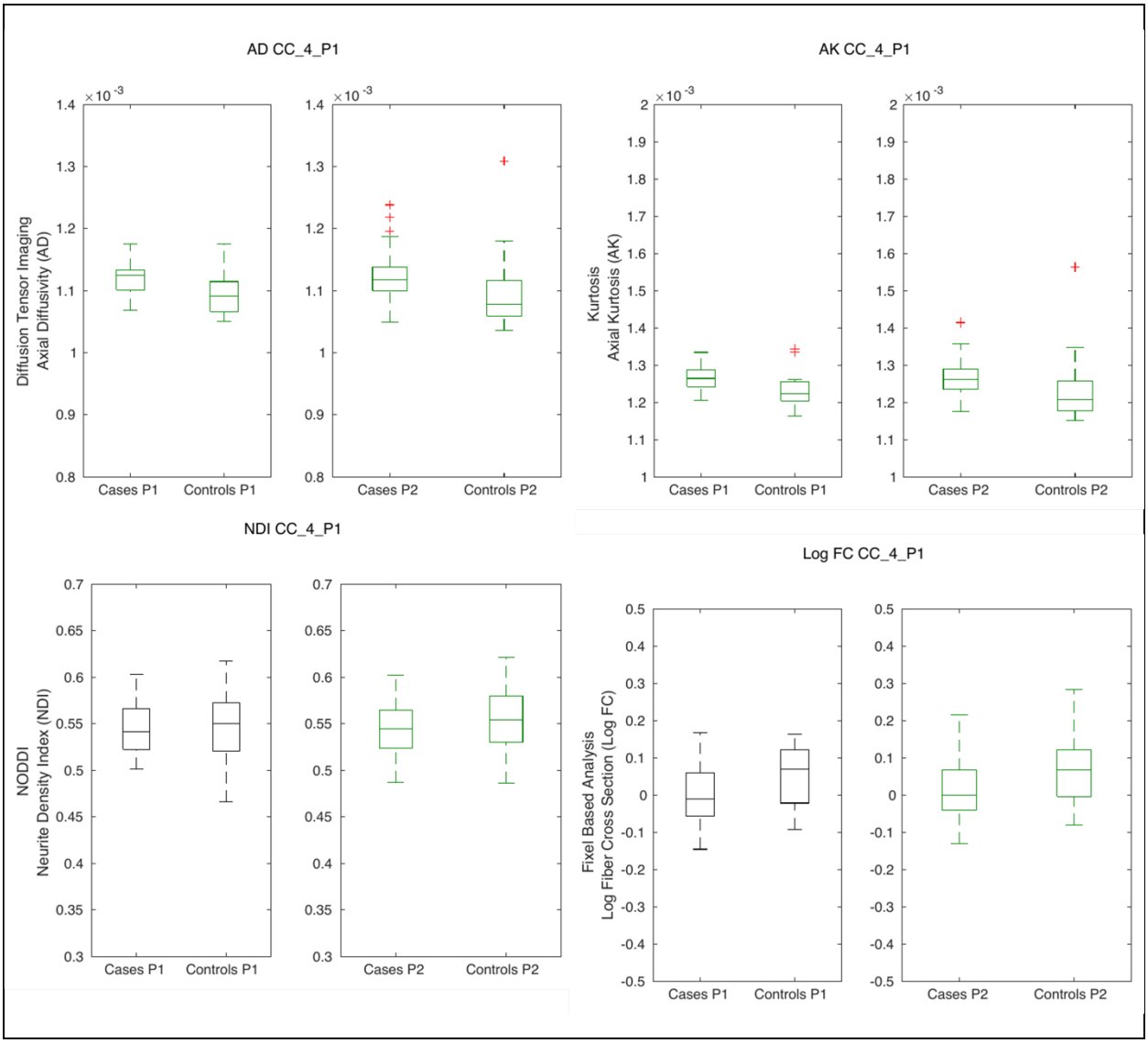

Figure A.14- Boxplots for t-test results in the Corpus Callosum - Anterior midbody (Primary Motor)

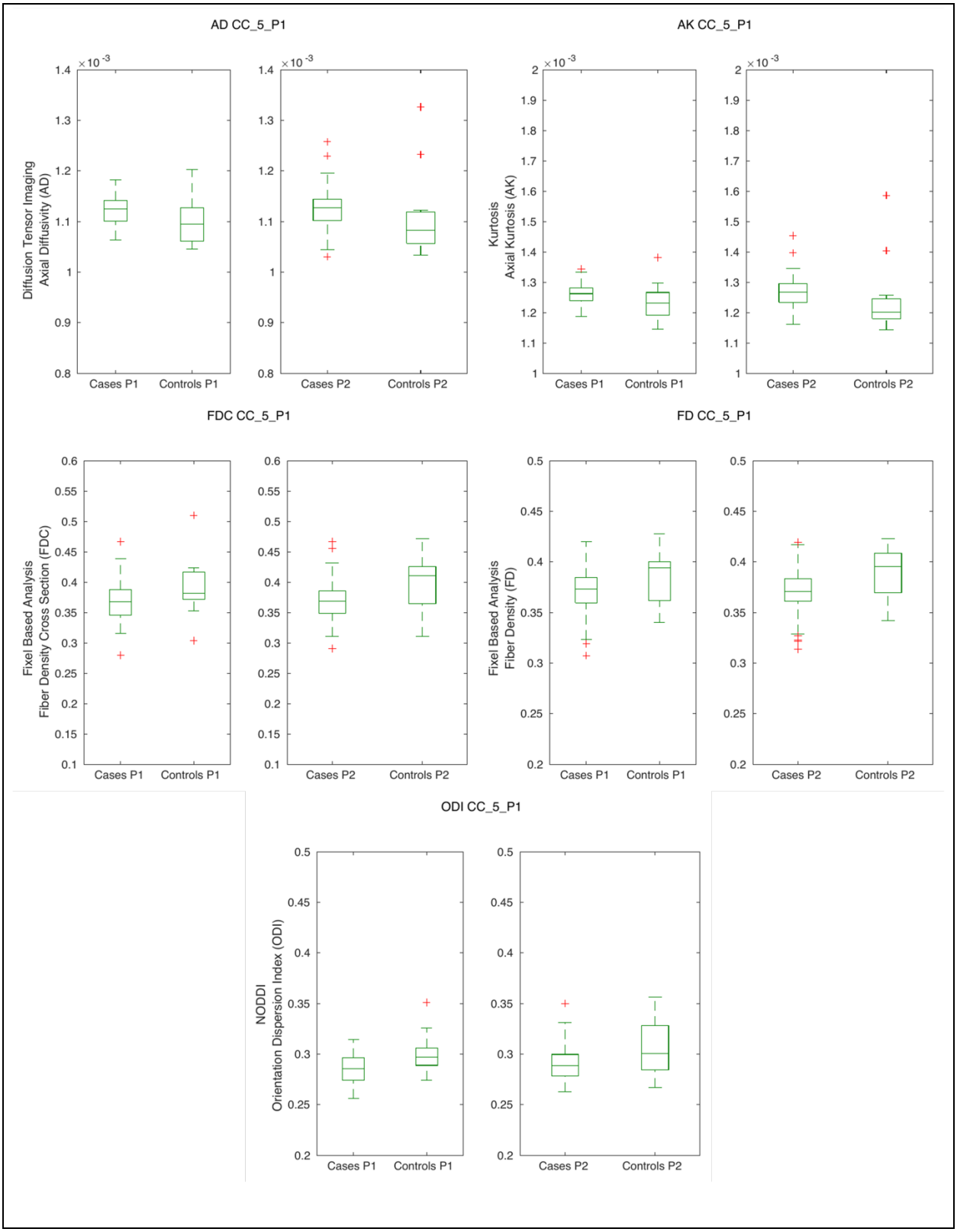

Figure A.15- Boxplots for t-test results in the Corpus Callosum - Posterior midbody (Primary Somatosensory)

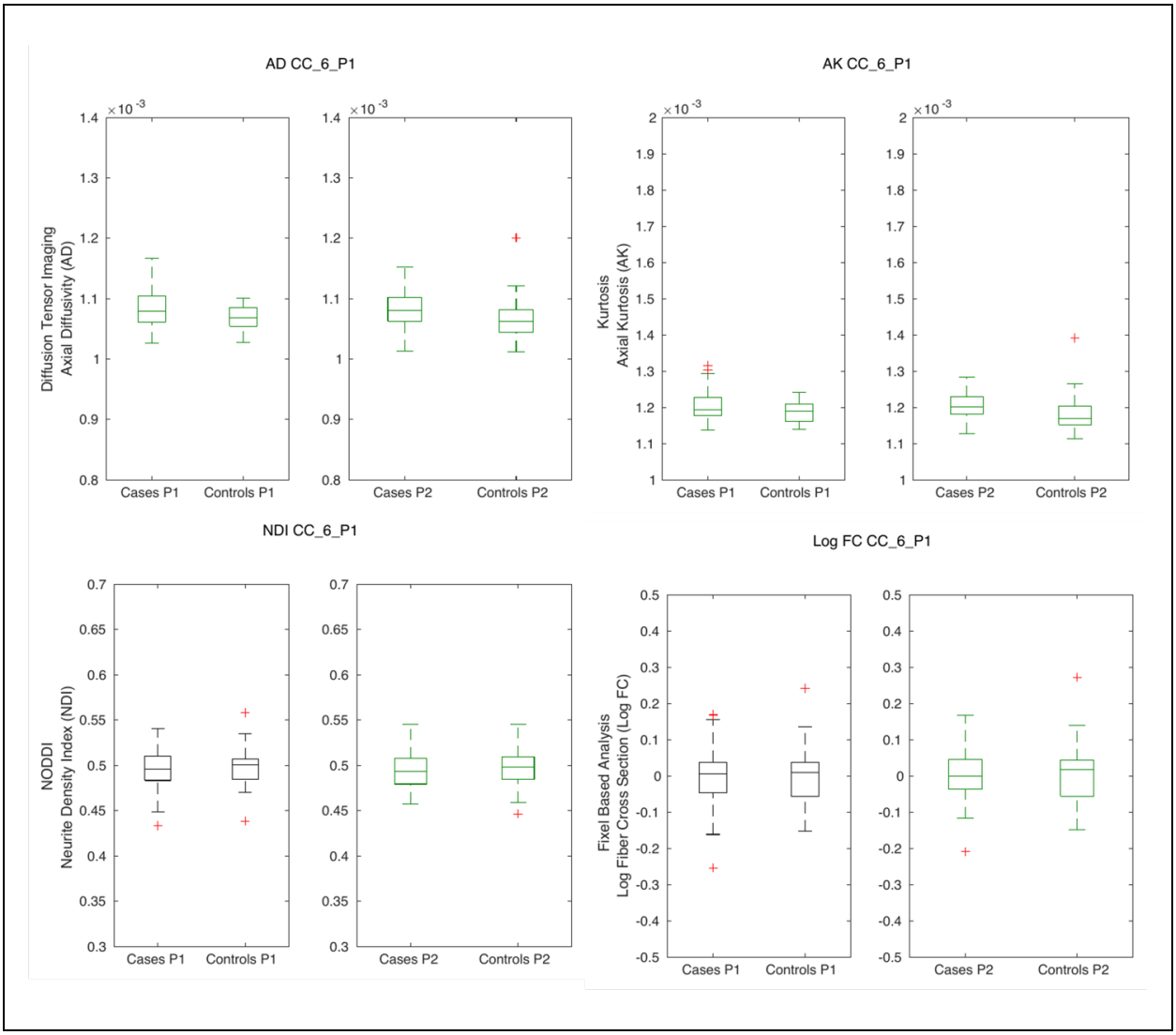

Figure A.16- Boxplots for t-test results in the Corpus Callosum - Isthmus

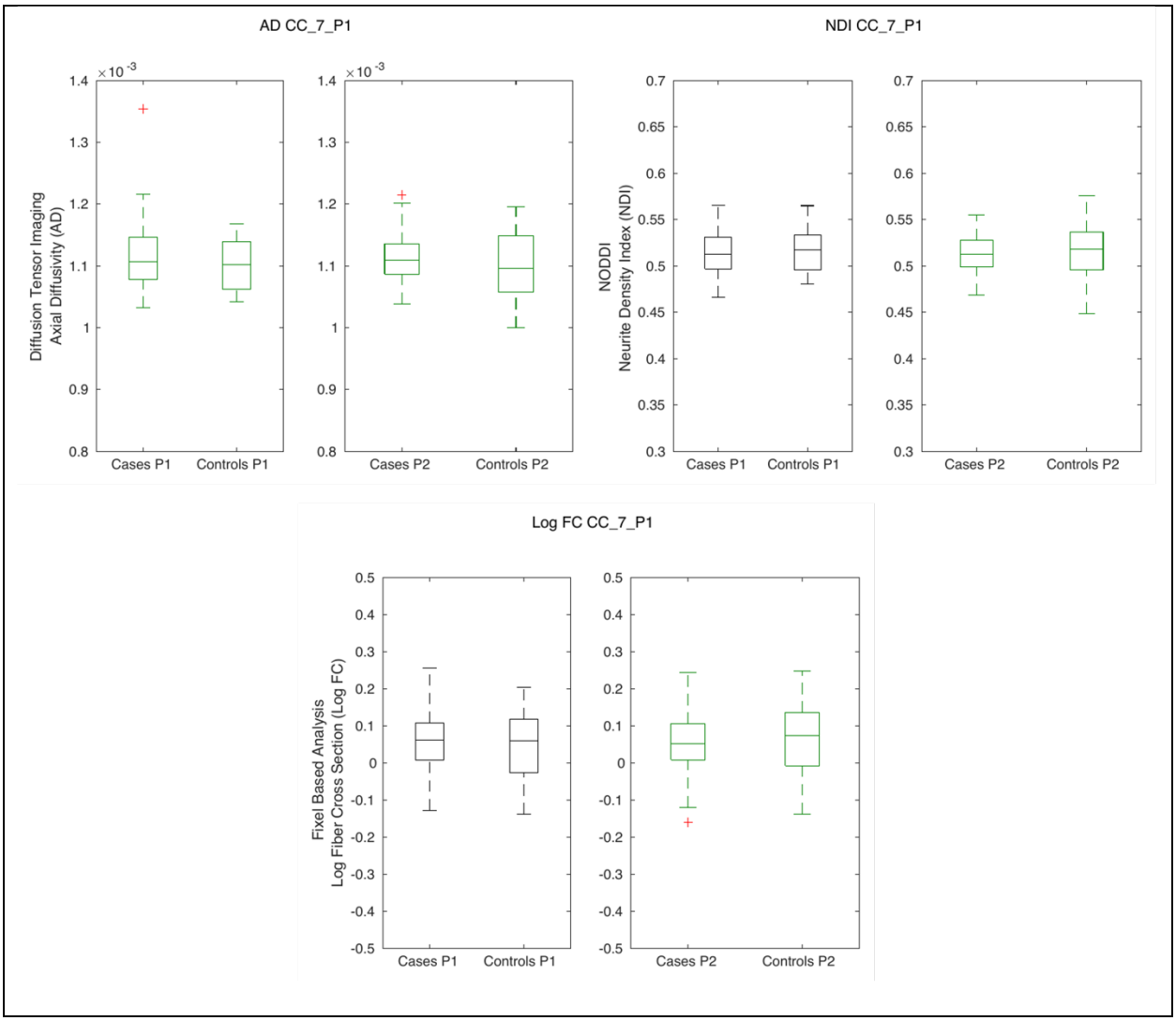

Figure A.17- Boxplots for t-test results in the Corpus Callosum - Splenium

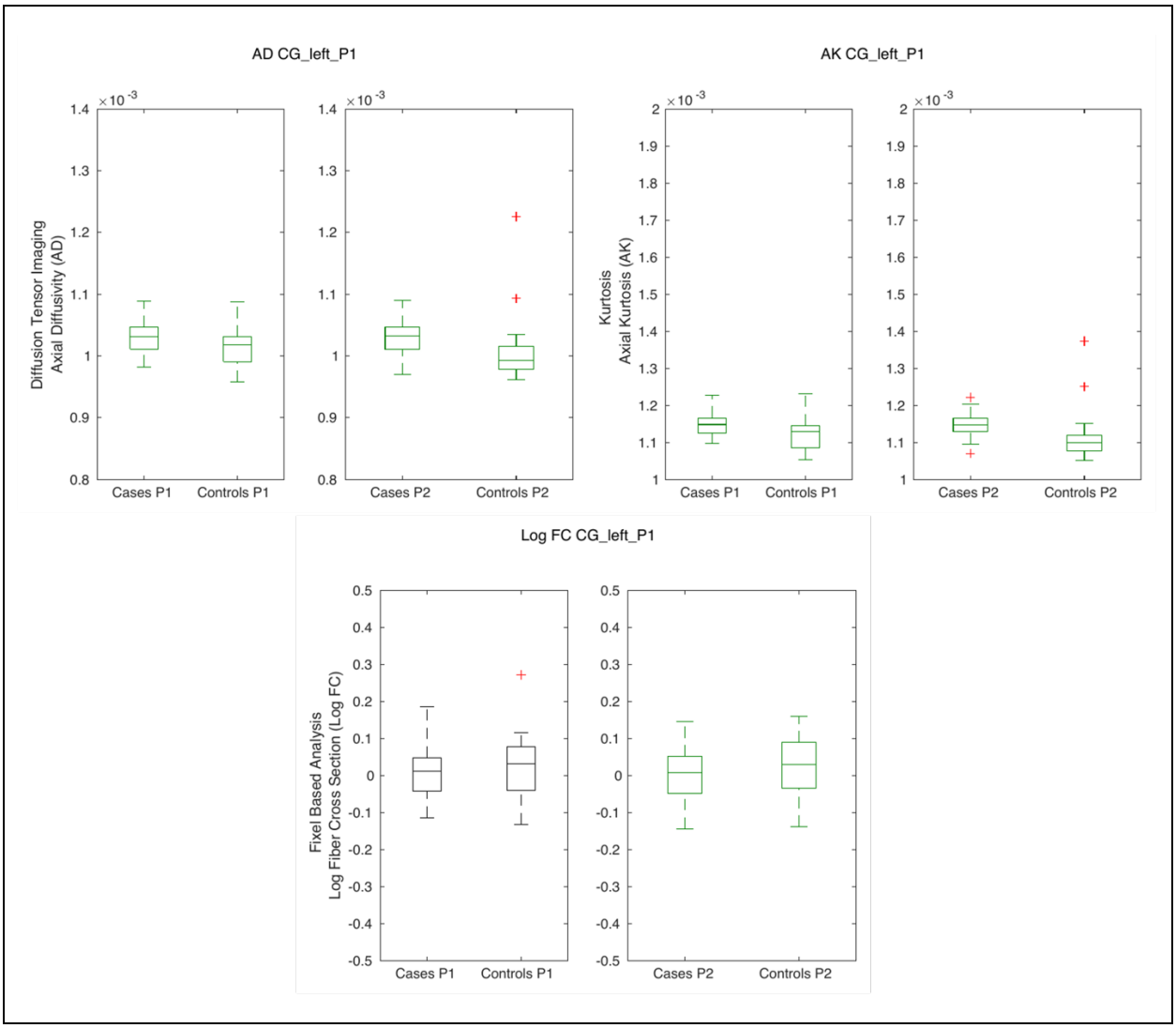

Figure A.18- Boxplots for t-test results in the Cingulum (left)

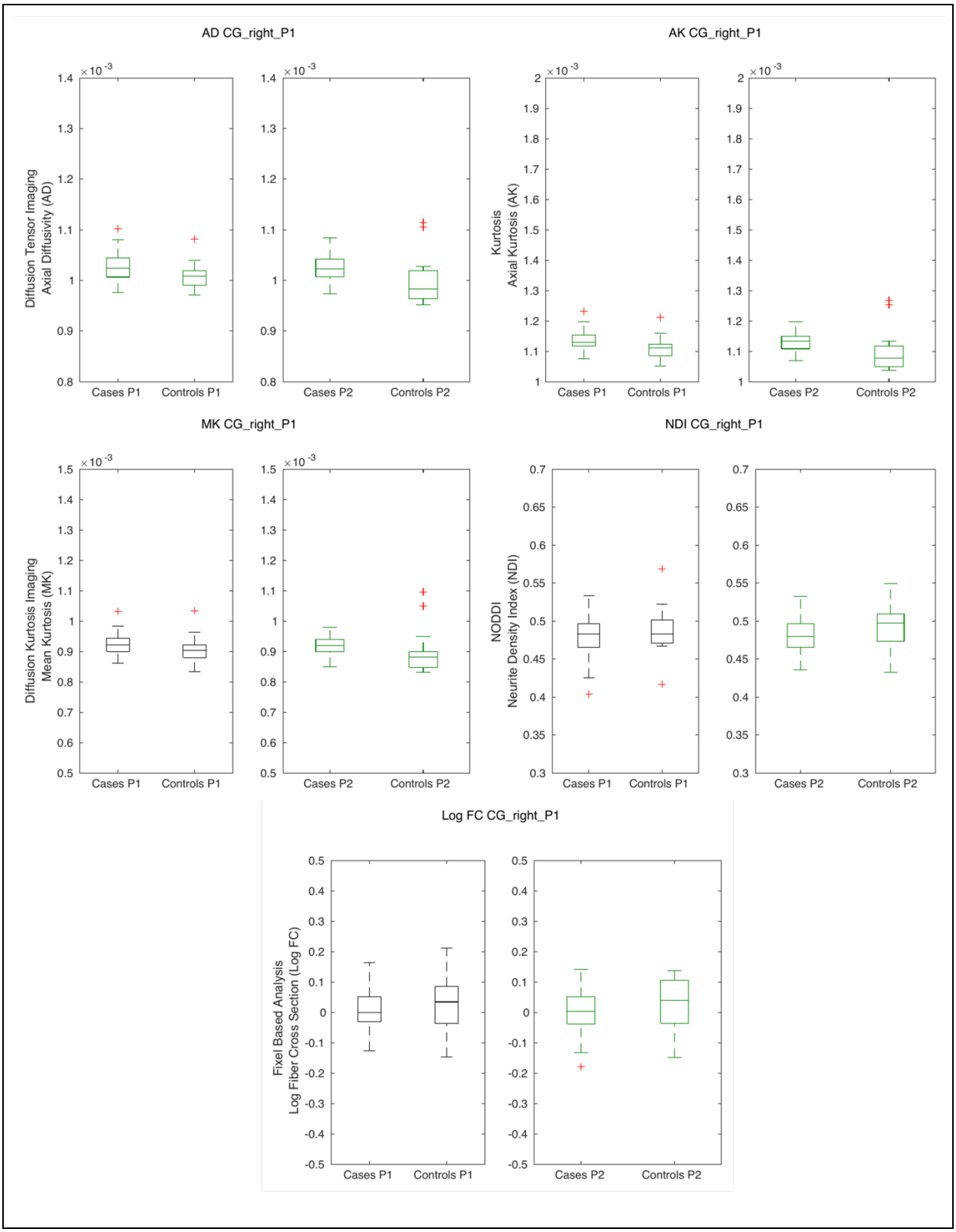

Figure A.19- Boxplots for t-test results in the Cingulum (right)

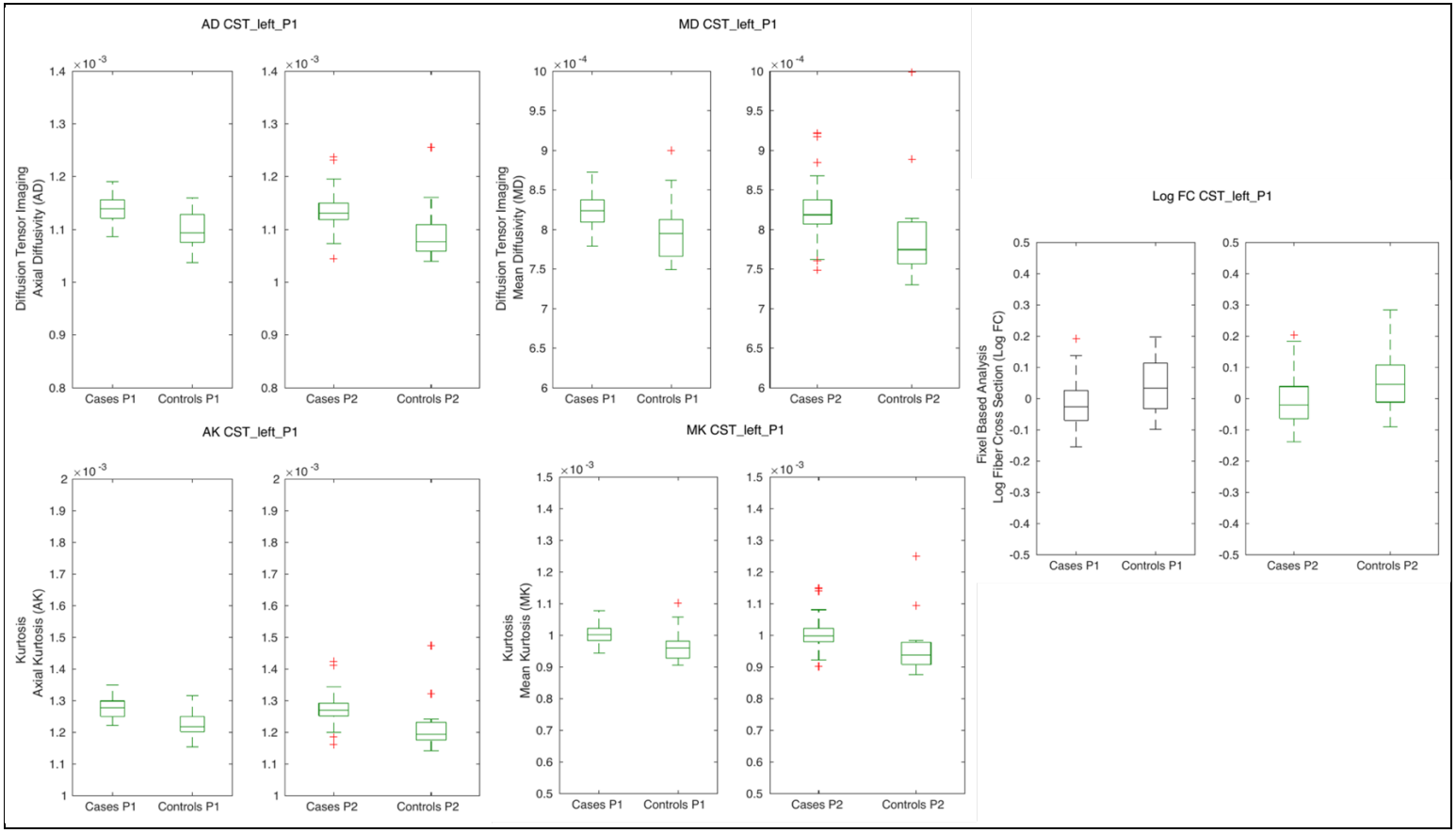

Figure A.20- Boxplots for t-test results in the Corticospinal Tract (Left)

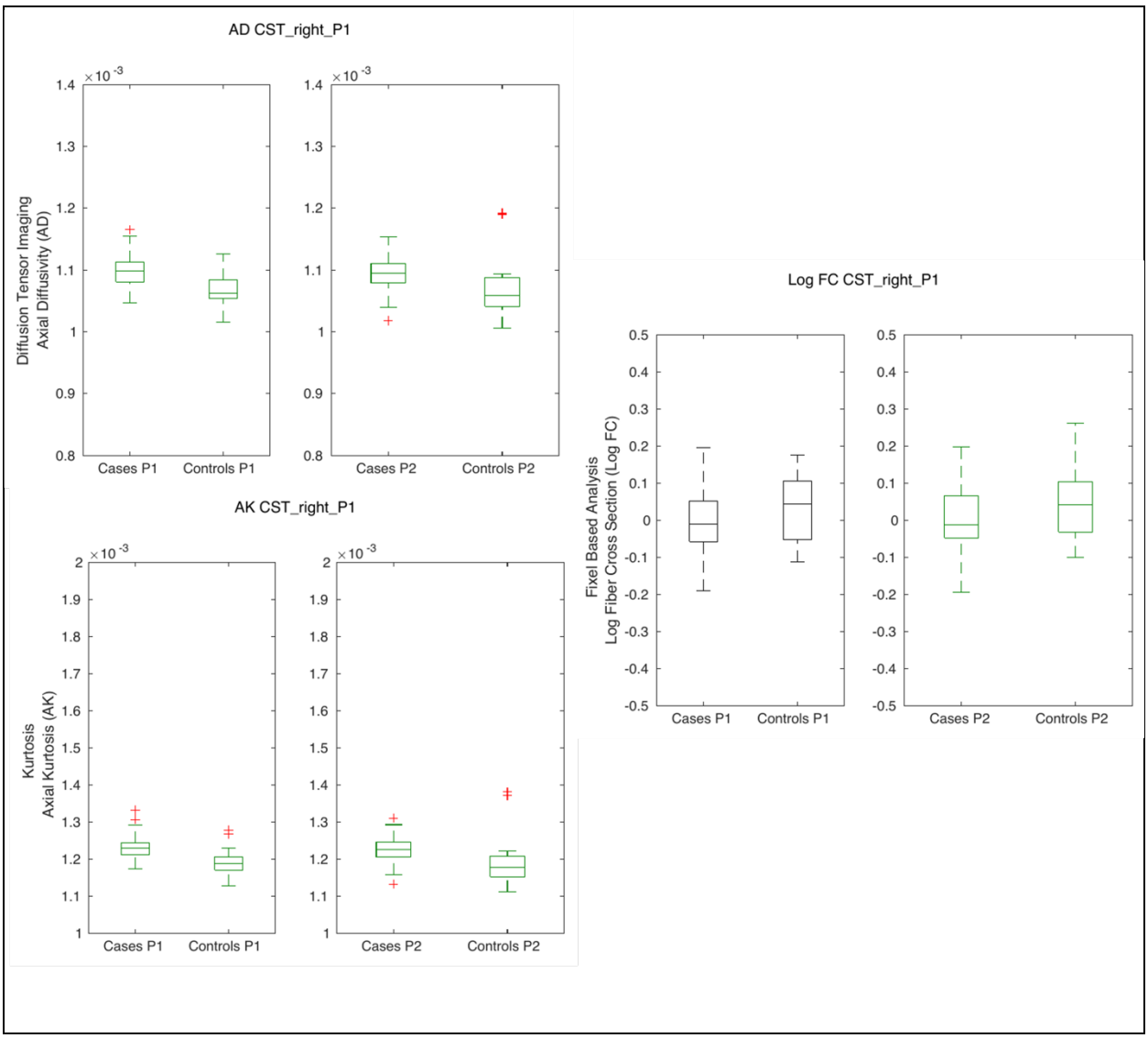

Figure A.22- Boxplots for t-test results in the Corticospinal Tract (Right)

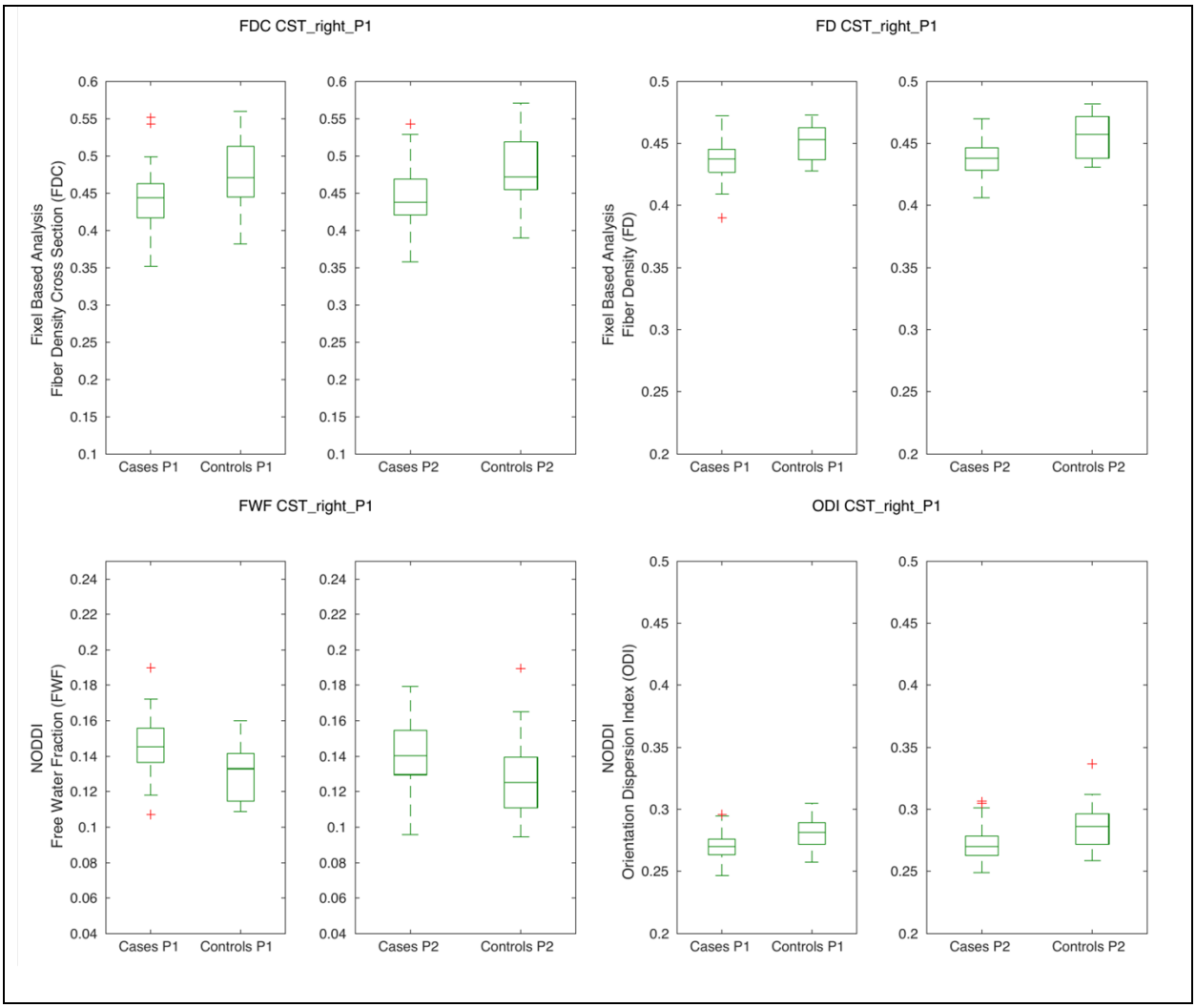

Figure A.23 - Boxplots for t-test results in the Corticospinal tract (right)

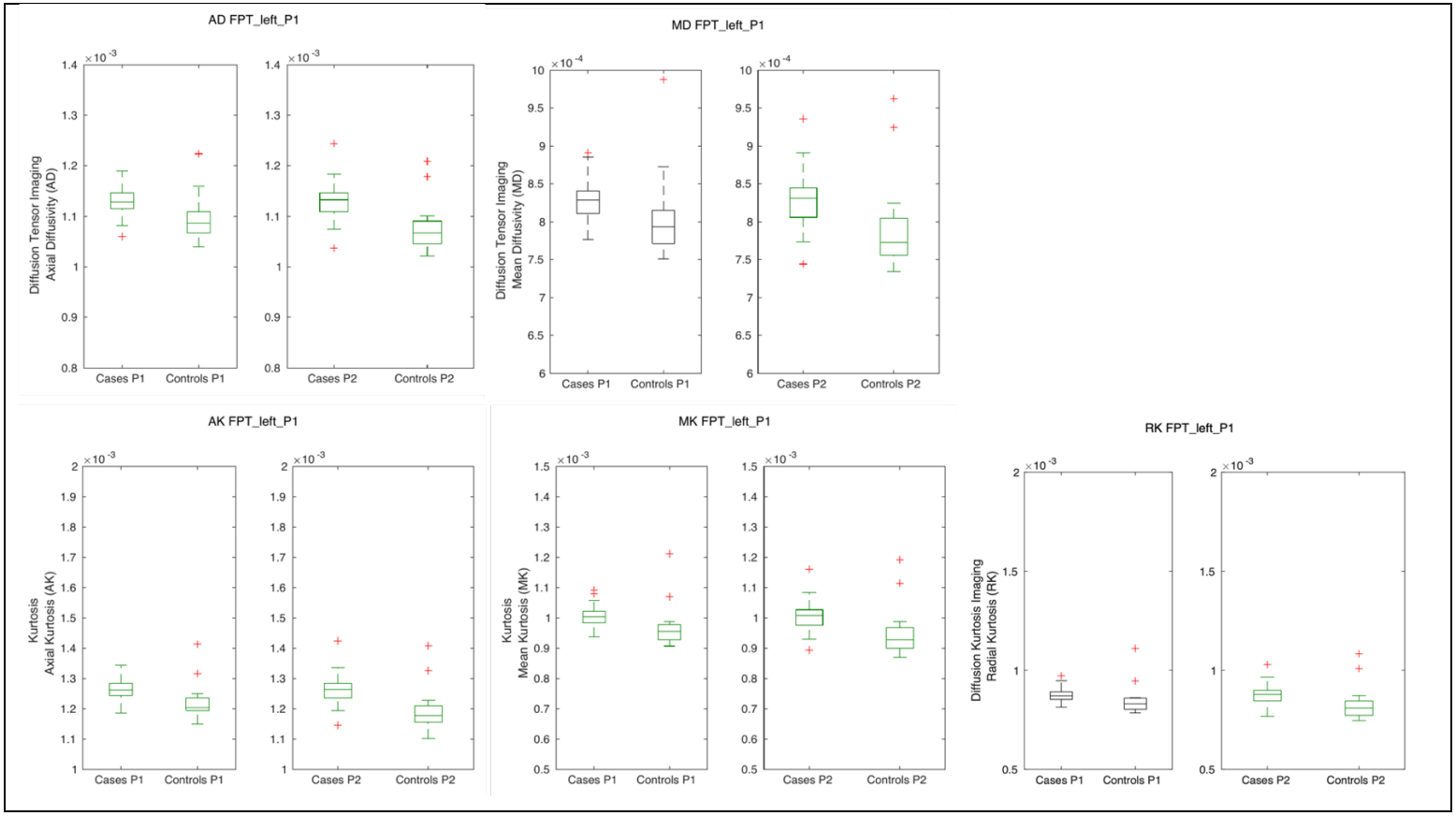

Figure A.24- Boxplots for t-test results in the Fronto-pontine tract (left)

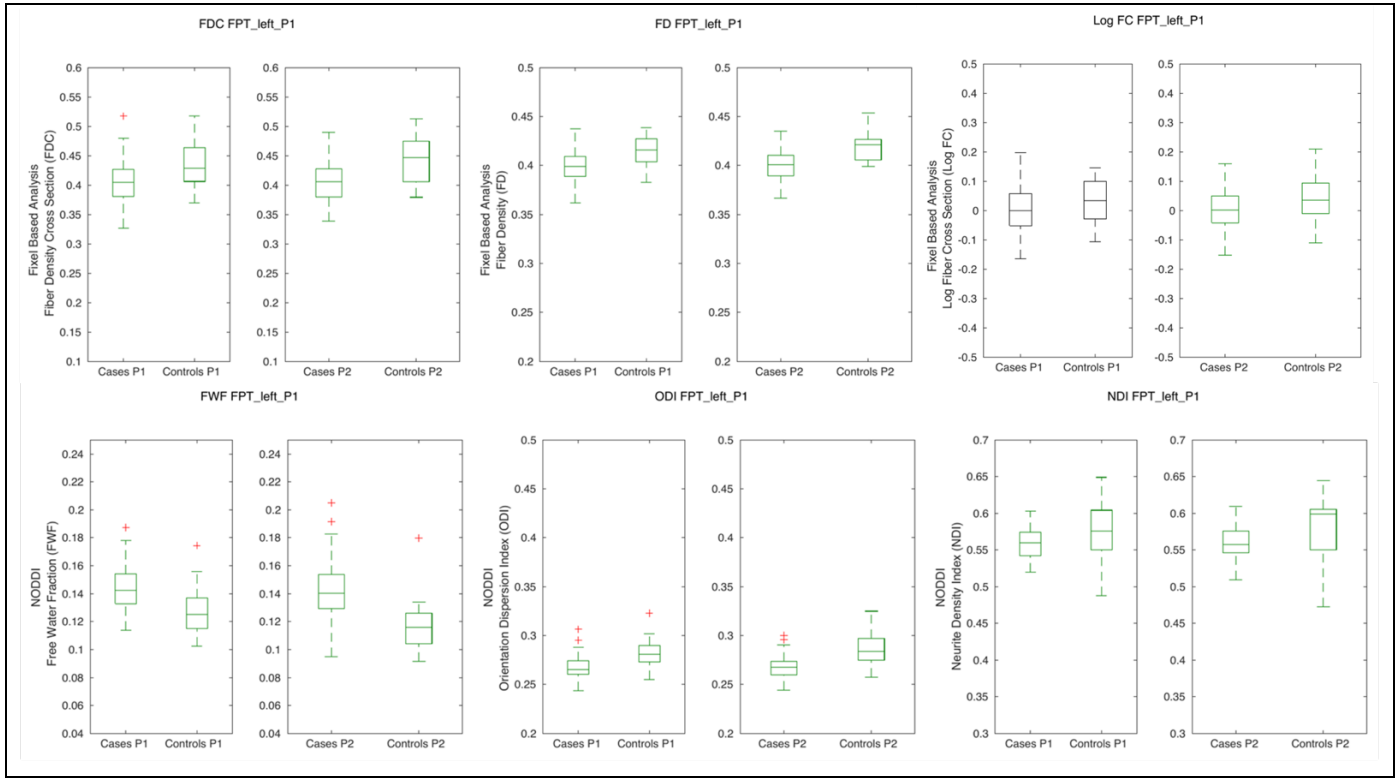

Figure A.25- Boxplots for t-test results in the Fronto-pontine tract (left)

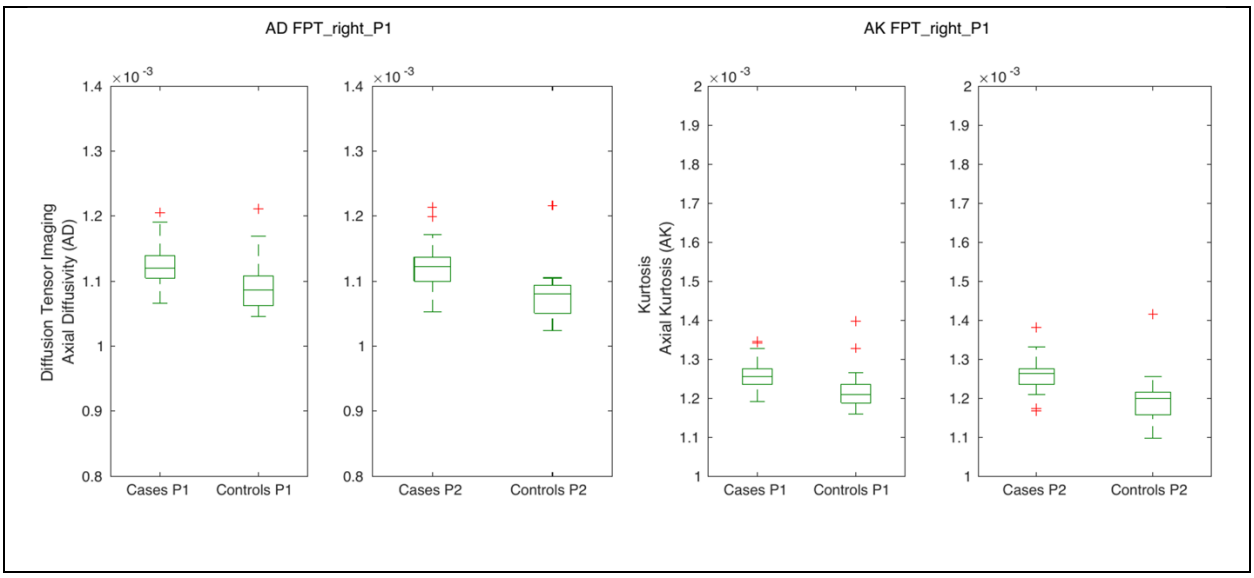

Figure A.26- Boxplots for t-test results in the Fronto-pontine tract (right)

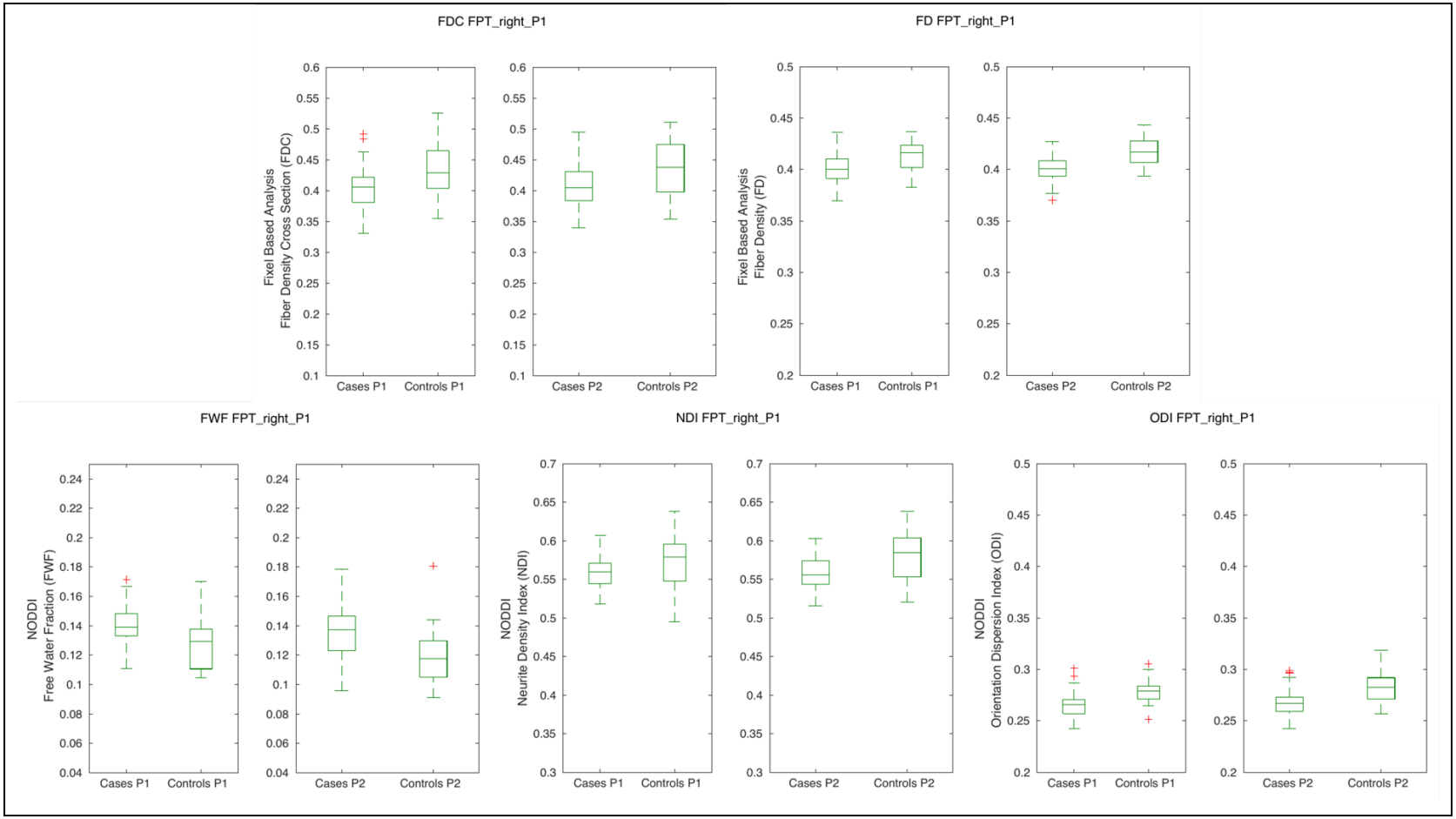

Figure A.27- Boxplots for t-test results in the Frontopontine Tract (Right)

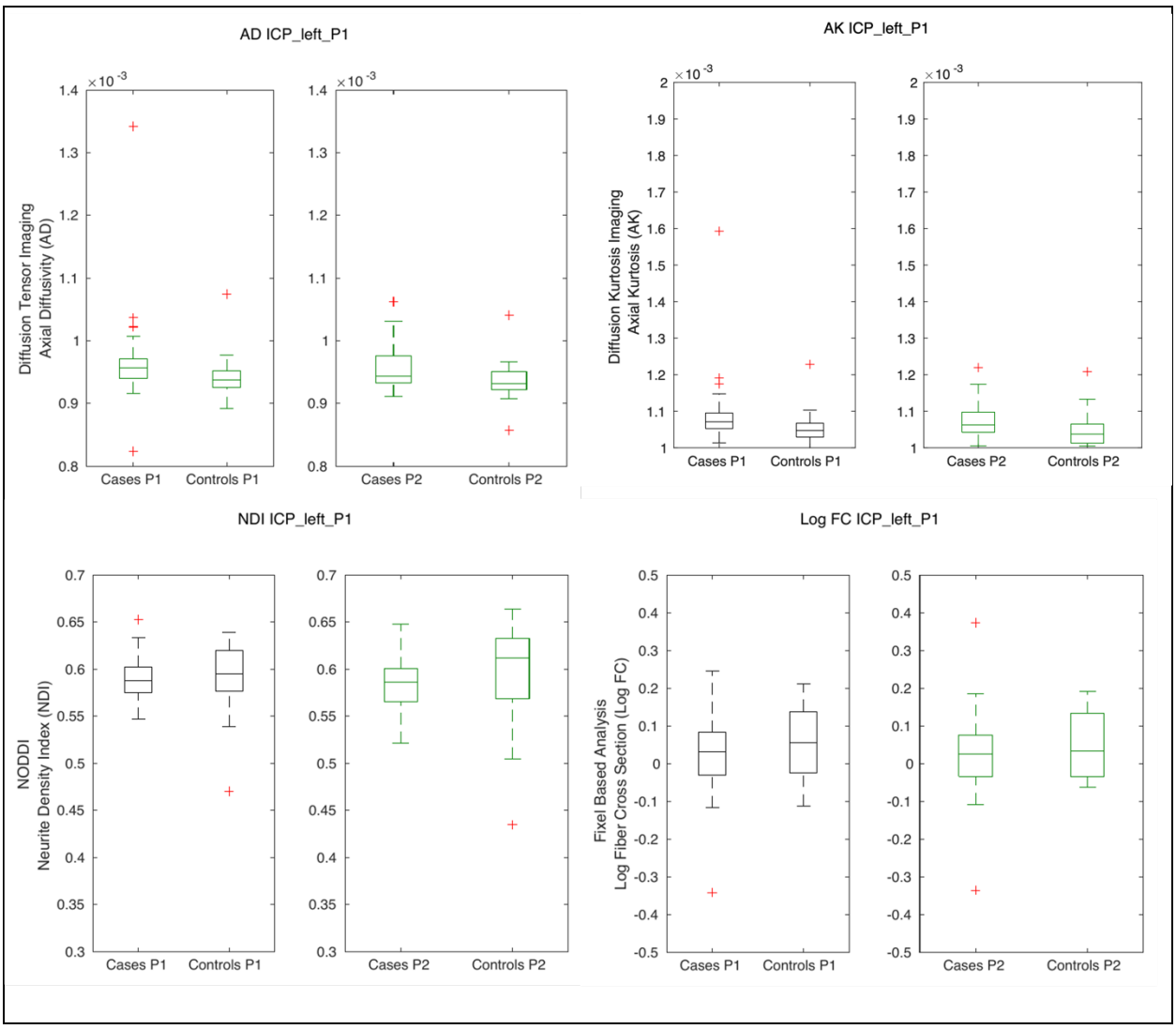

Figure A.28- Boxplots for t-test results in the Inferior cerebellar peduncle (left)

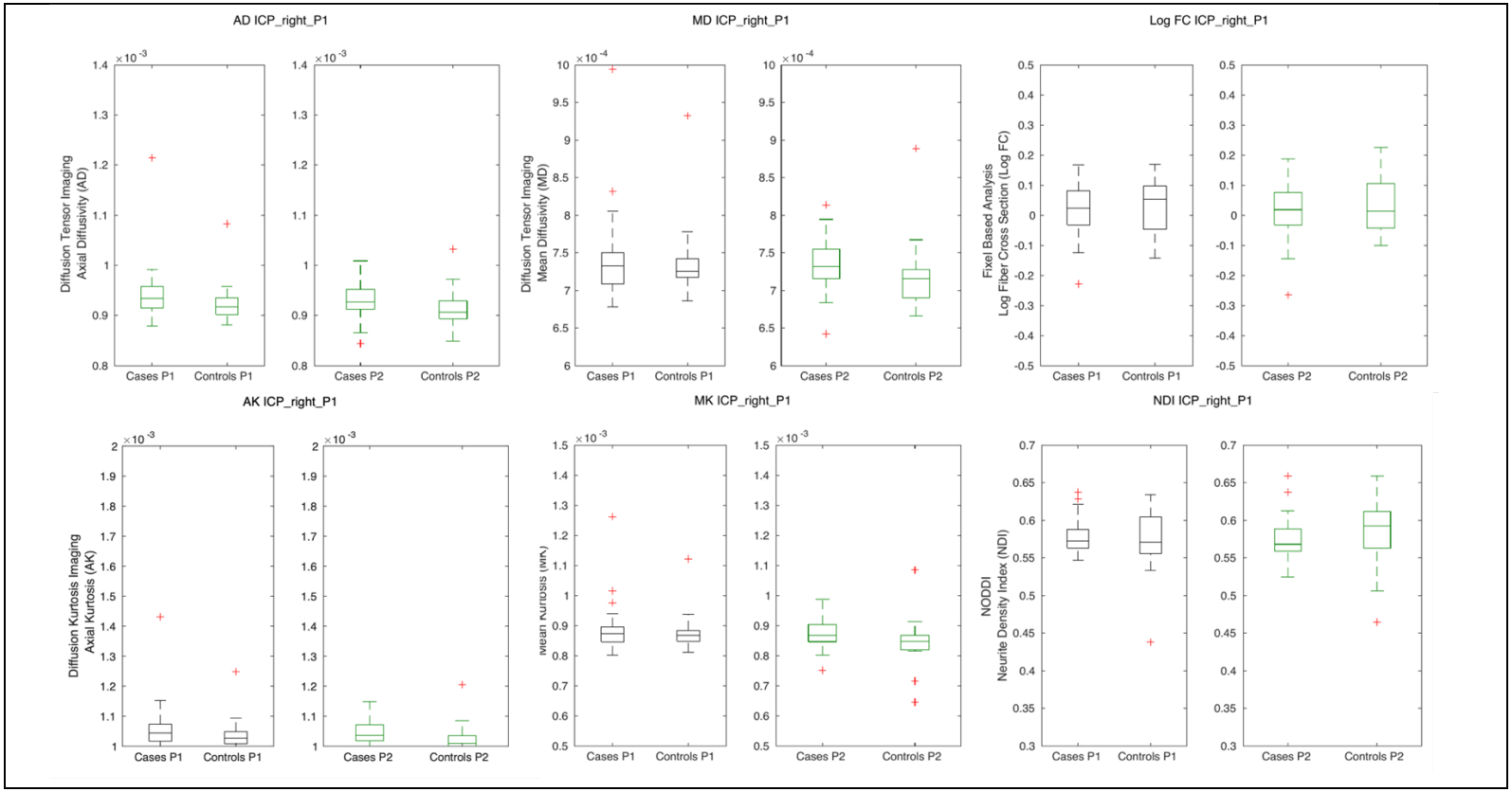

Figure A.29- Boxplots for t-test results in the Inferior cerebellar peduncle (right)

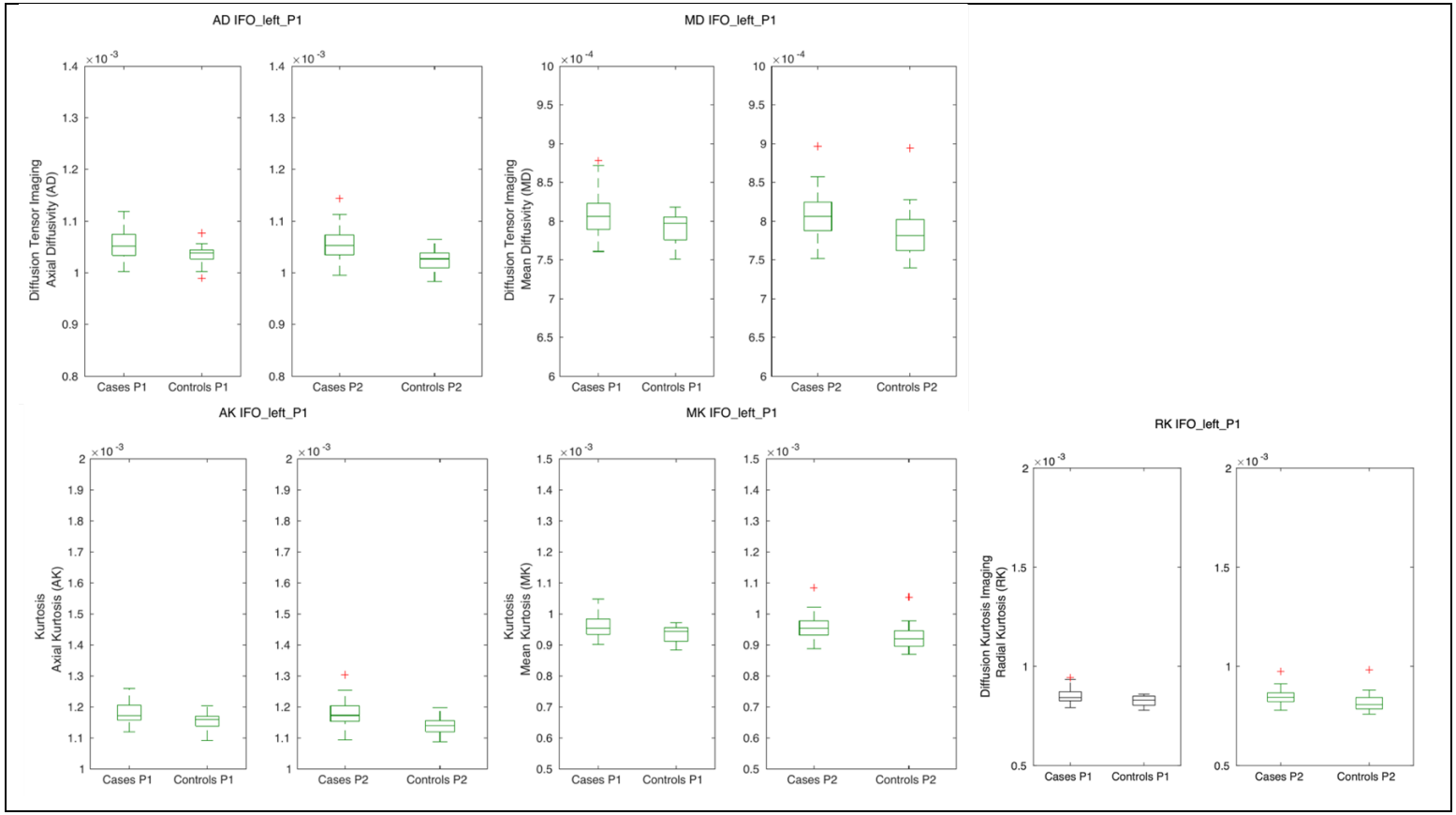

Figure A.30- Boxplots for t-test results in the Inferior occipito-frontal fascicle (left)

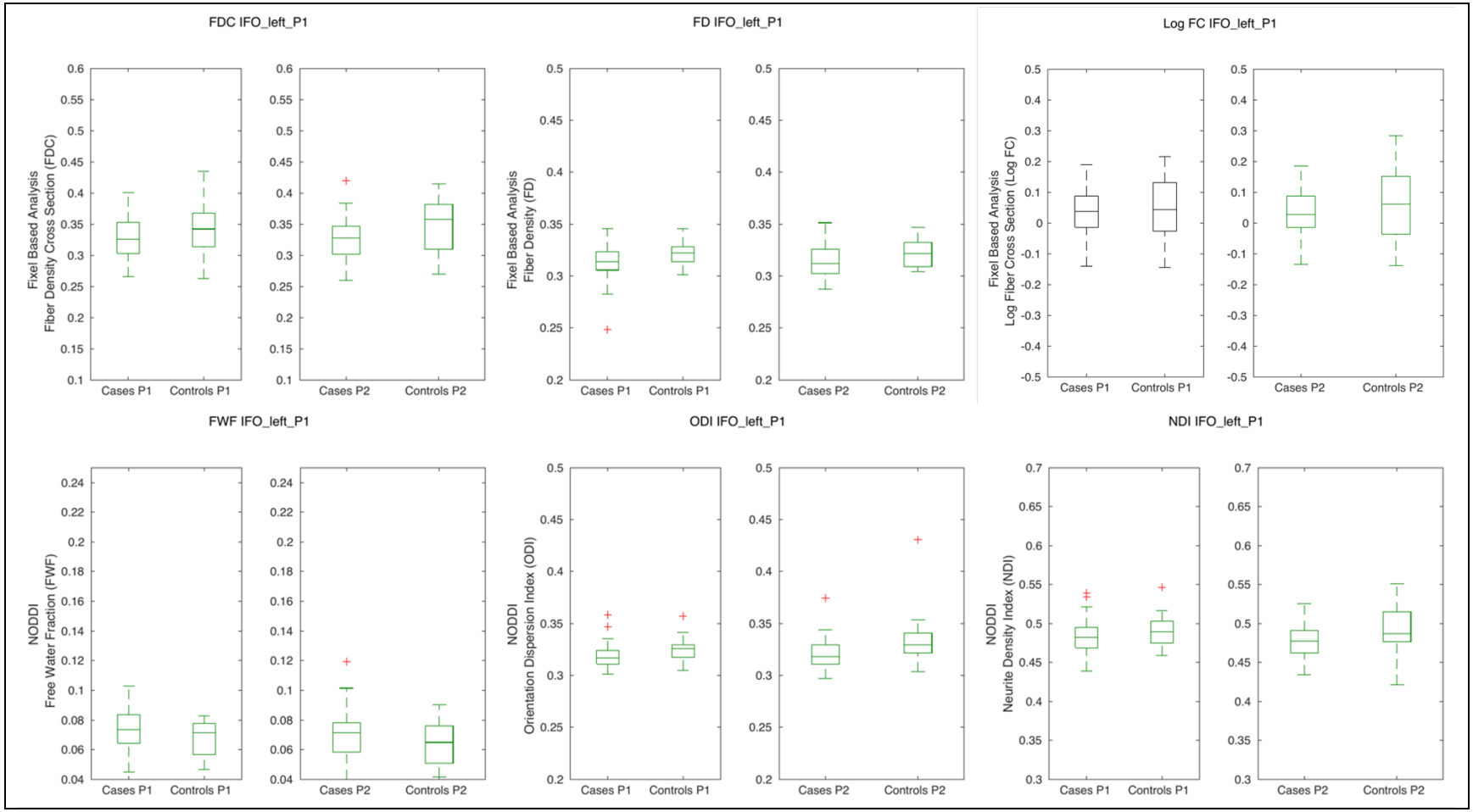

Figure A.31- Boxplots for t-test results in the Inferior occipito-frontal fascicle (left)

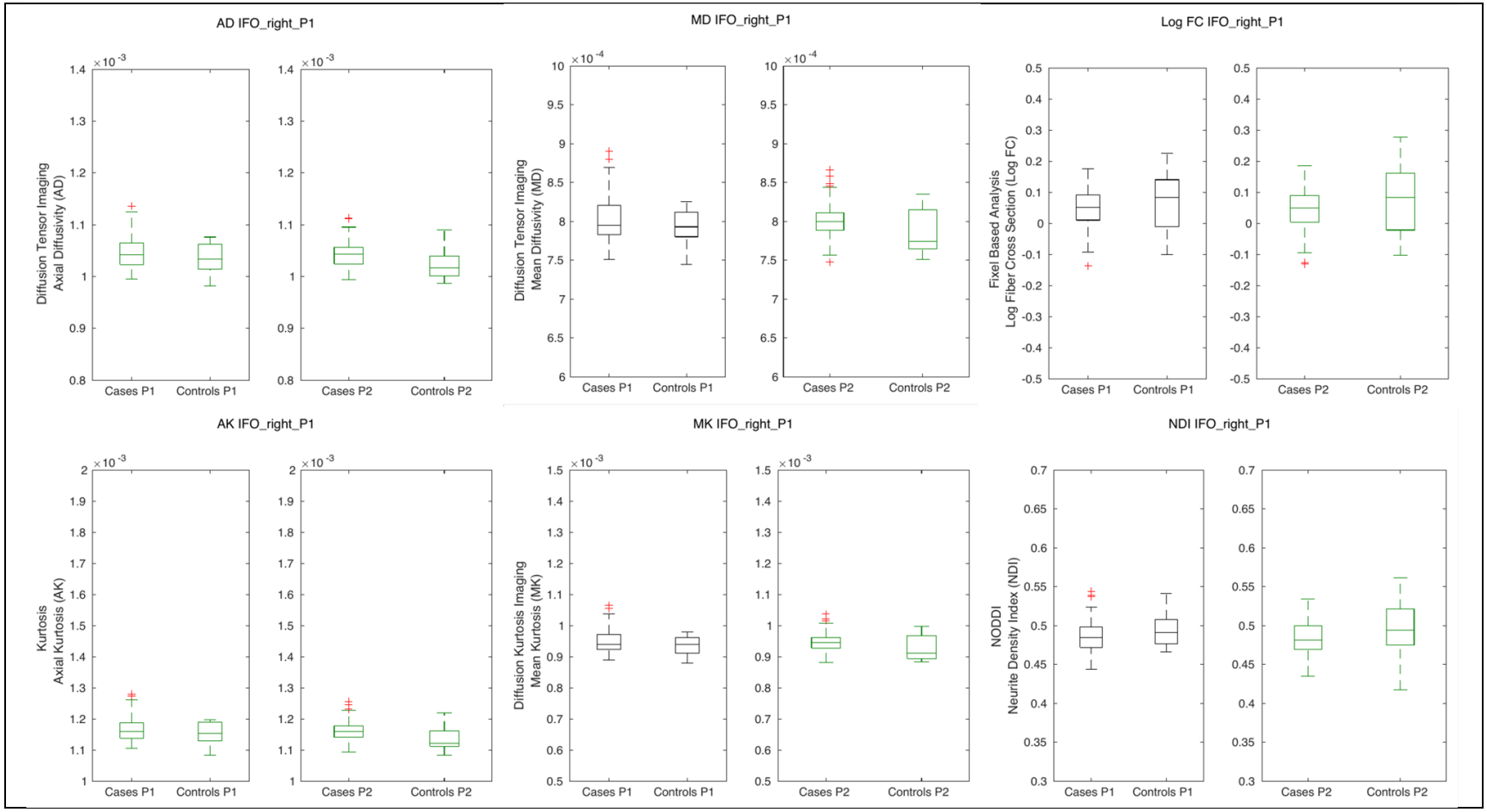

Figure A.32- Boxplots for t-test results in the Inferior occipito-frontal fascicle (right)

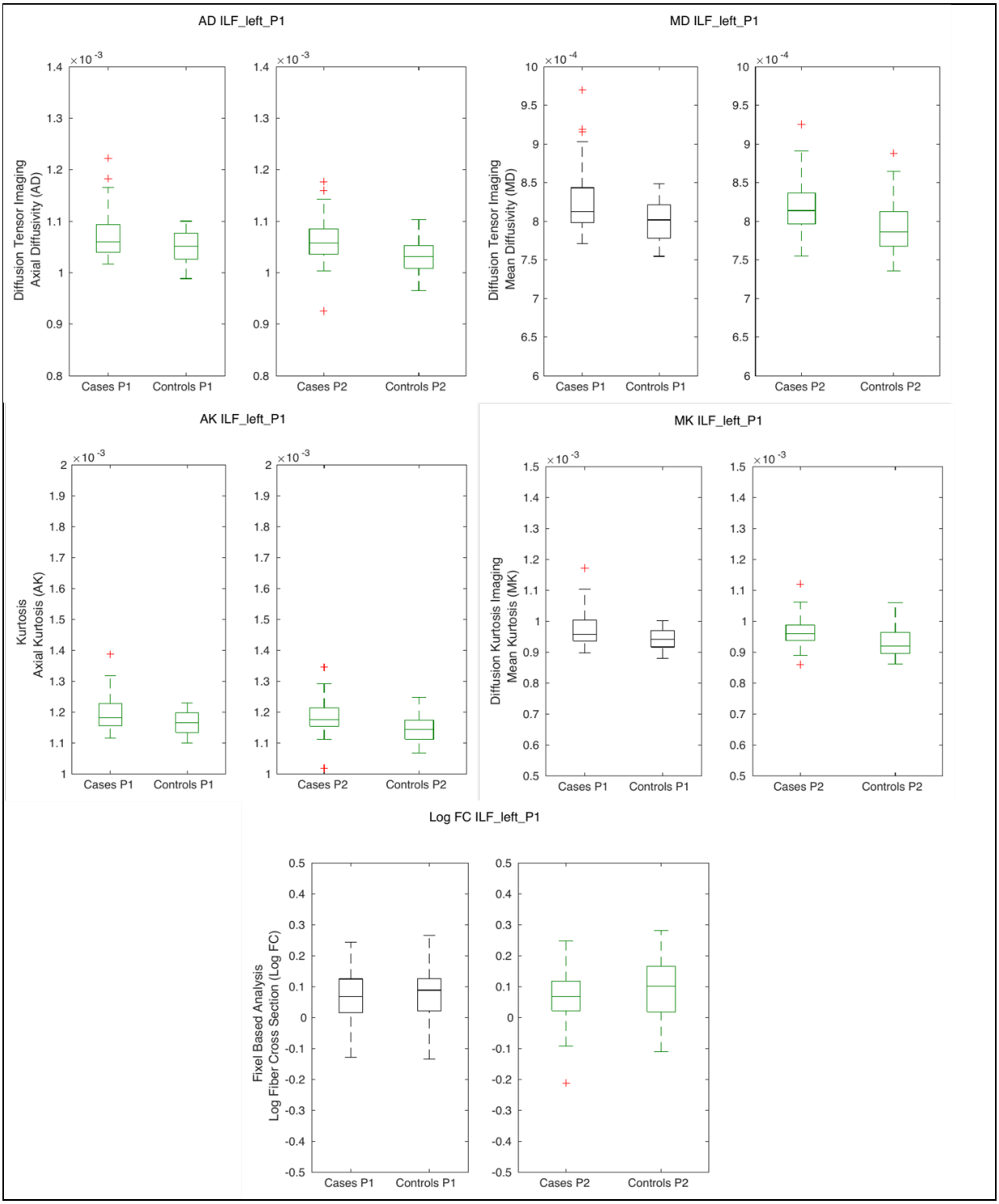

Figure A.33- Boxplots for t-test results in the Inferior longitudinal fascicle (left)

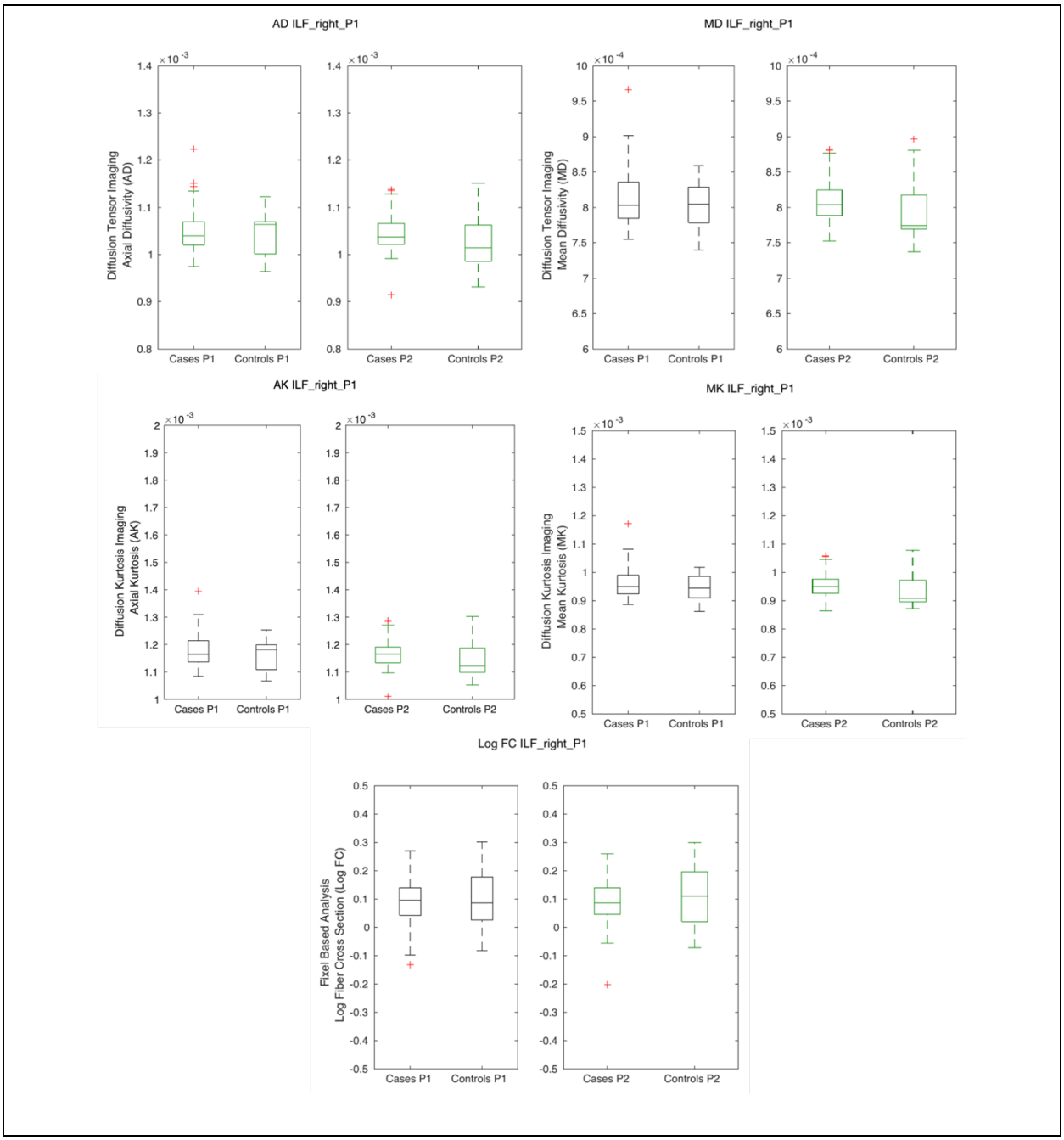

Figure A.34- Boxplots for t-test results in the Inferior longitudinal fascicle (right)

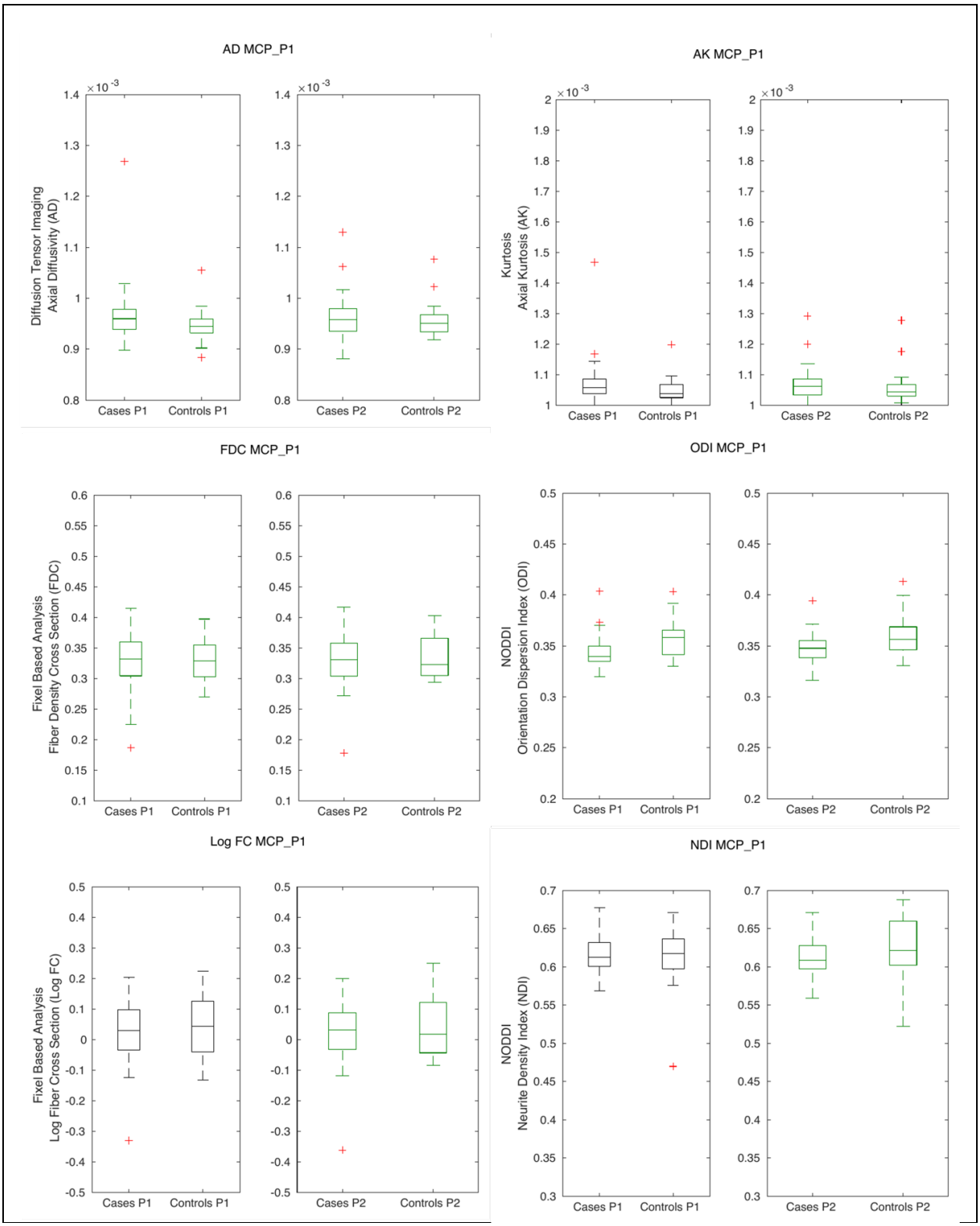

Figure A.35- Boxplots for t-test results in the Middle cerebellar peduncle

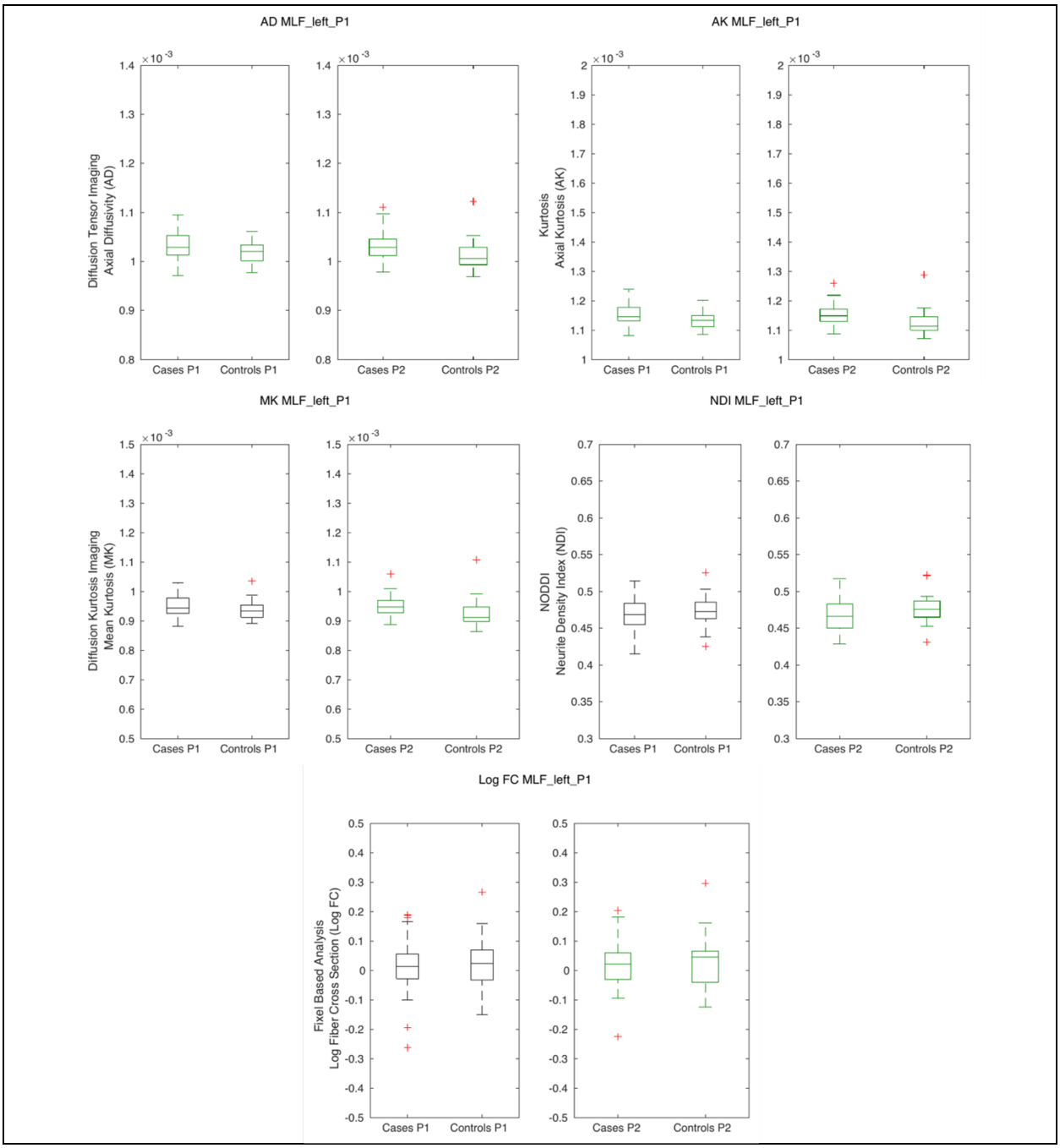

Figure A.36- Boxplots for t-test results in the Middle longitudinal fascicle (left)

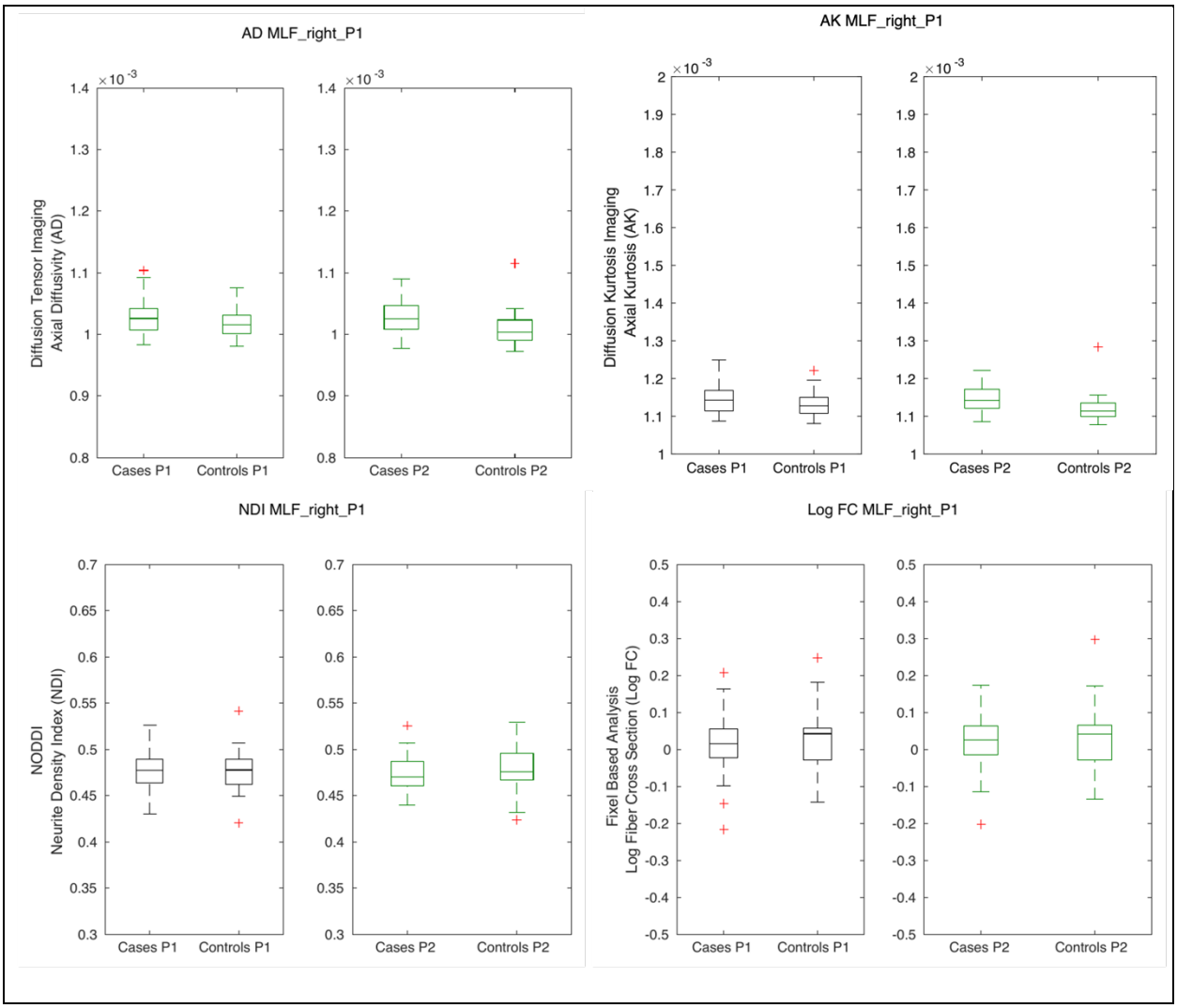

Figure A.37- Boxplots for t-test results in the Middle longitudinal fascicle (right)

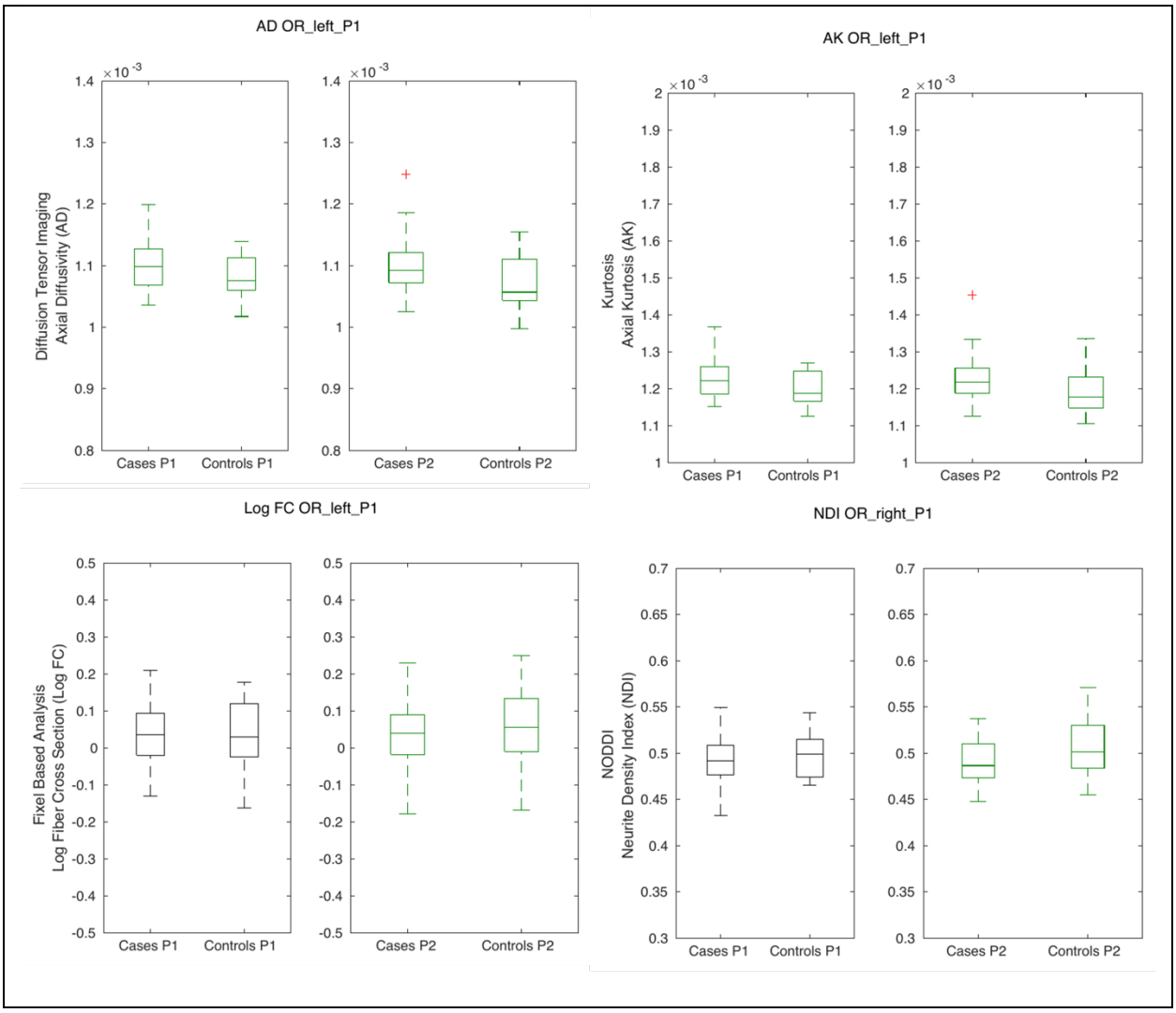

Figure A.38- Boxplots for t-test results in the Optic radiation (left)

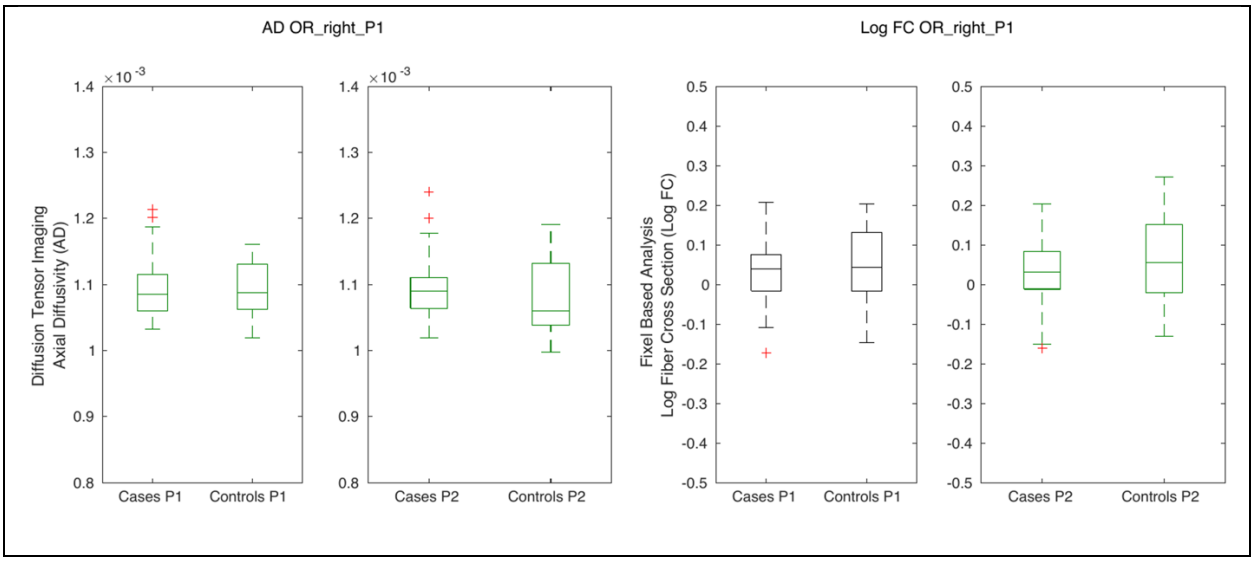

Figure A.39- Boxplots for t-test results in the Optic radiation (right)

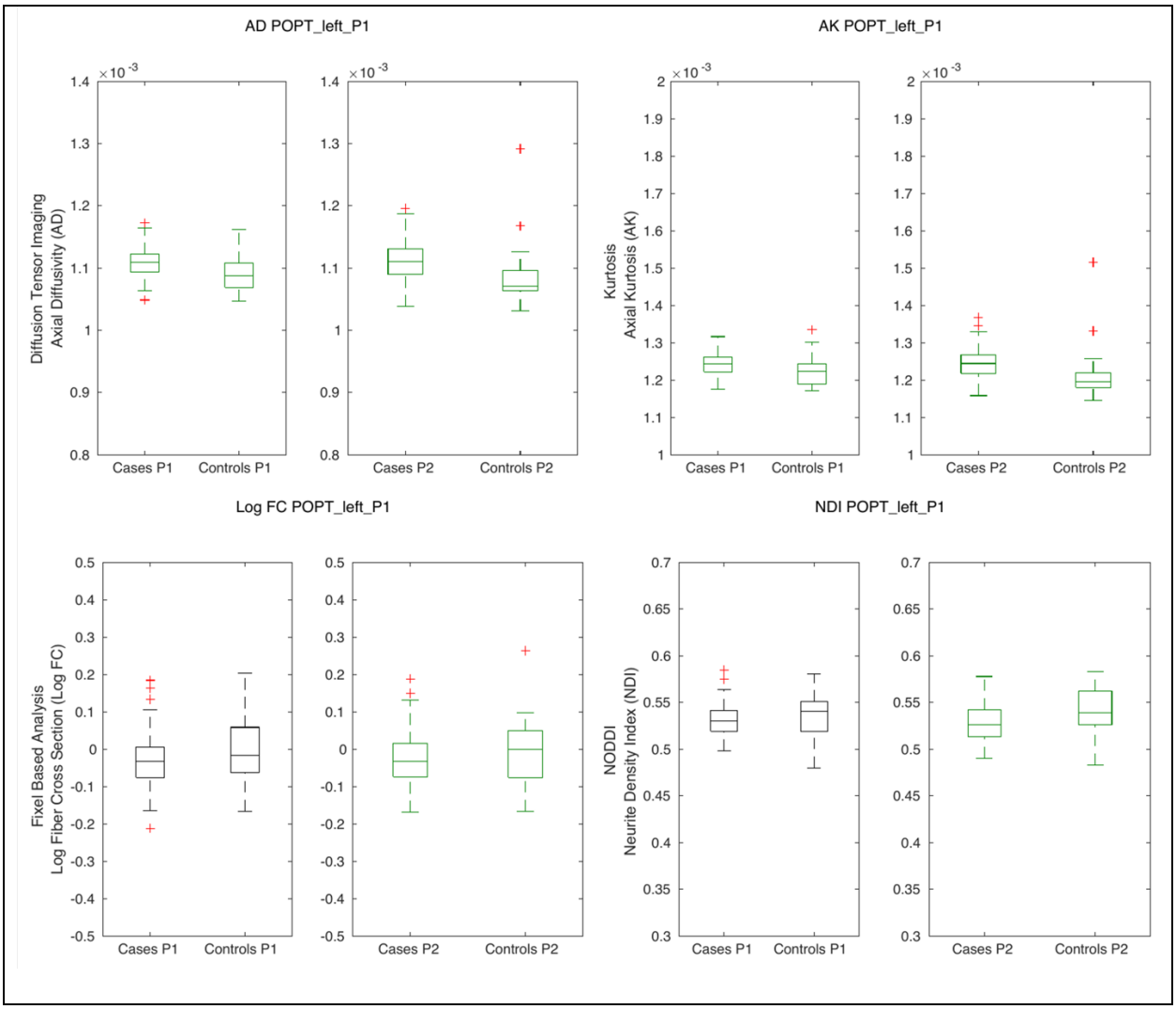

Figure A.40- Boxplots for t-test results in the Parieto-occipital pontine (left)

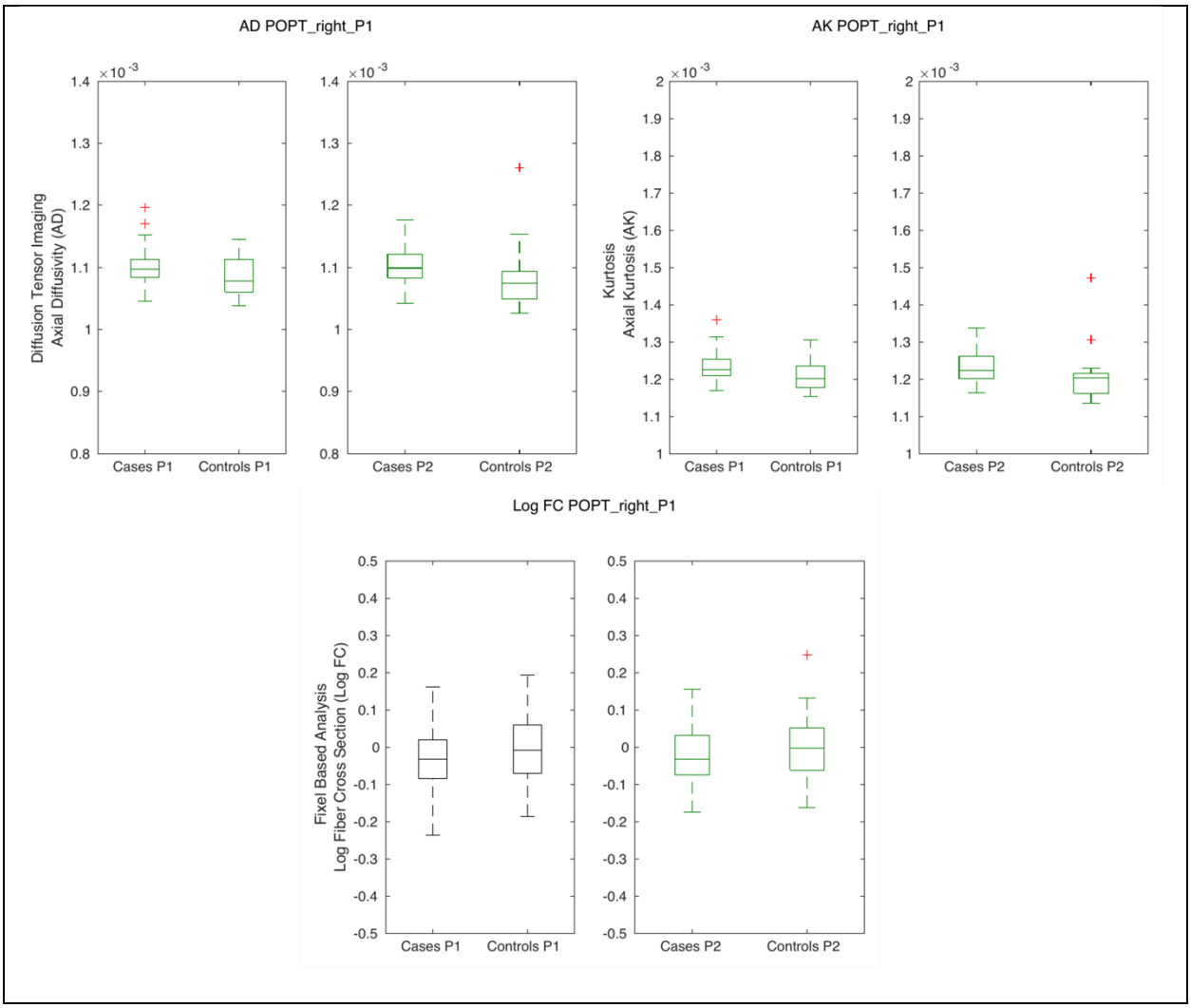

Figure A.41- Boxplots for t-test results in the Parieto-occipital pontine (right)

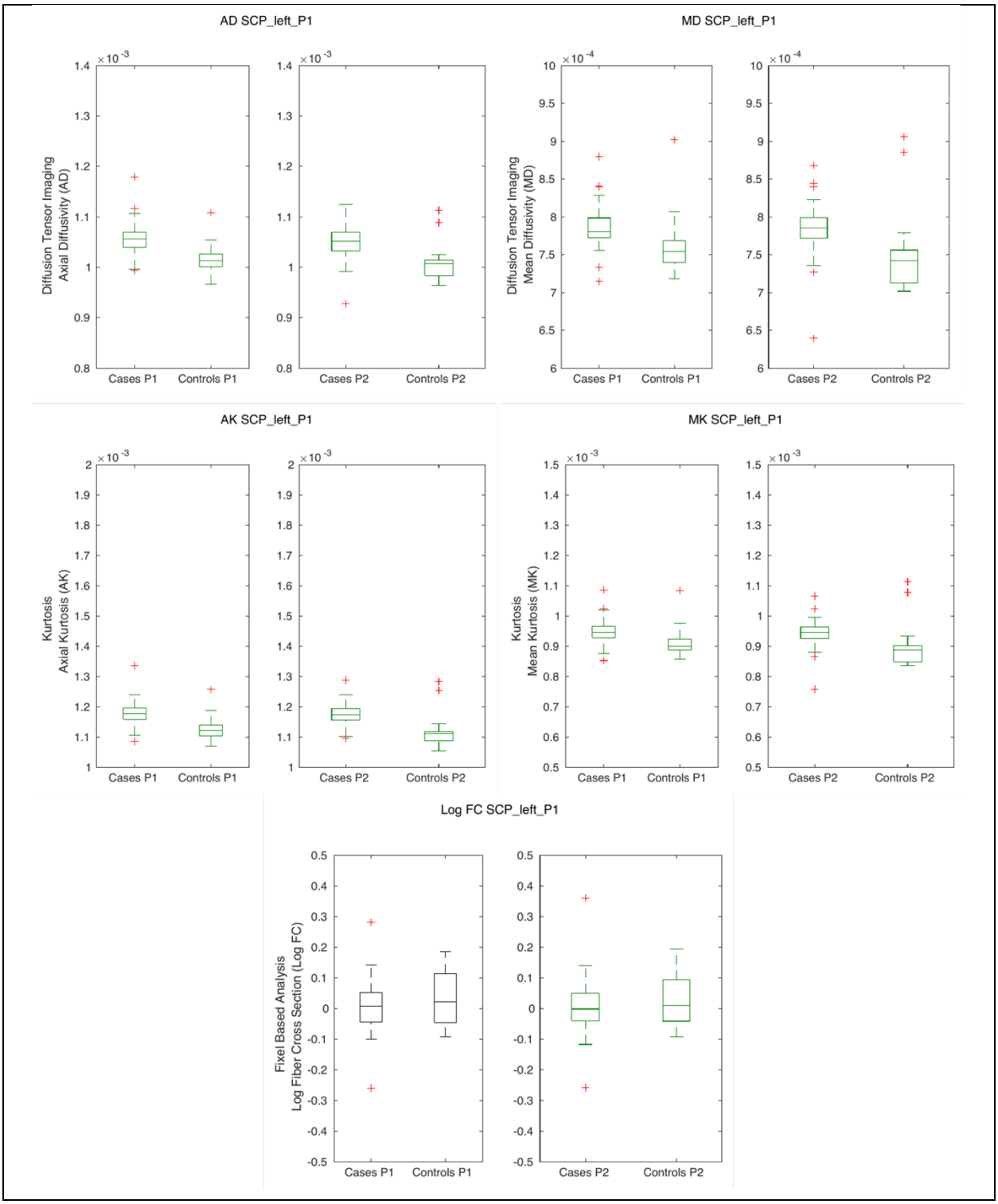

Figure A.42- Boxplots for t-test results in the Superior cerebellar peduncle (left)

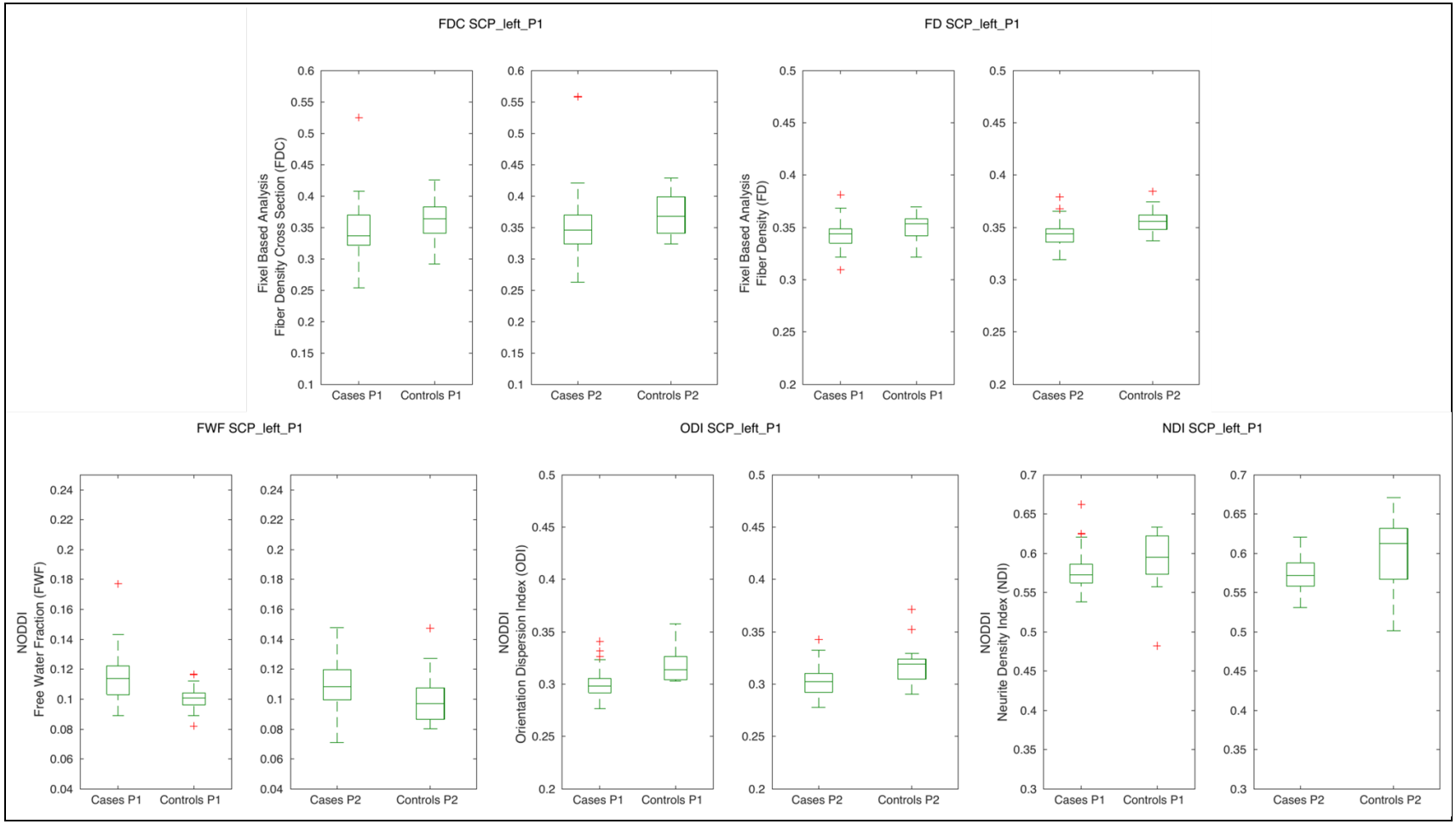

Figure A.43- Boxplots for t-test results in the Superior cerebellar peduncle (left)

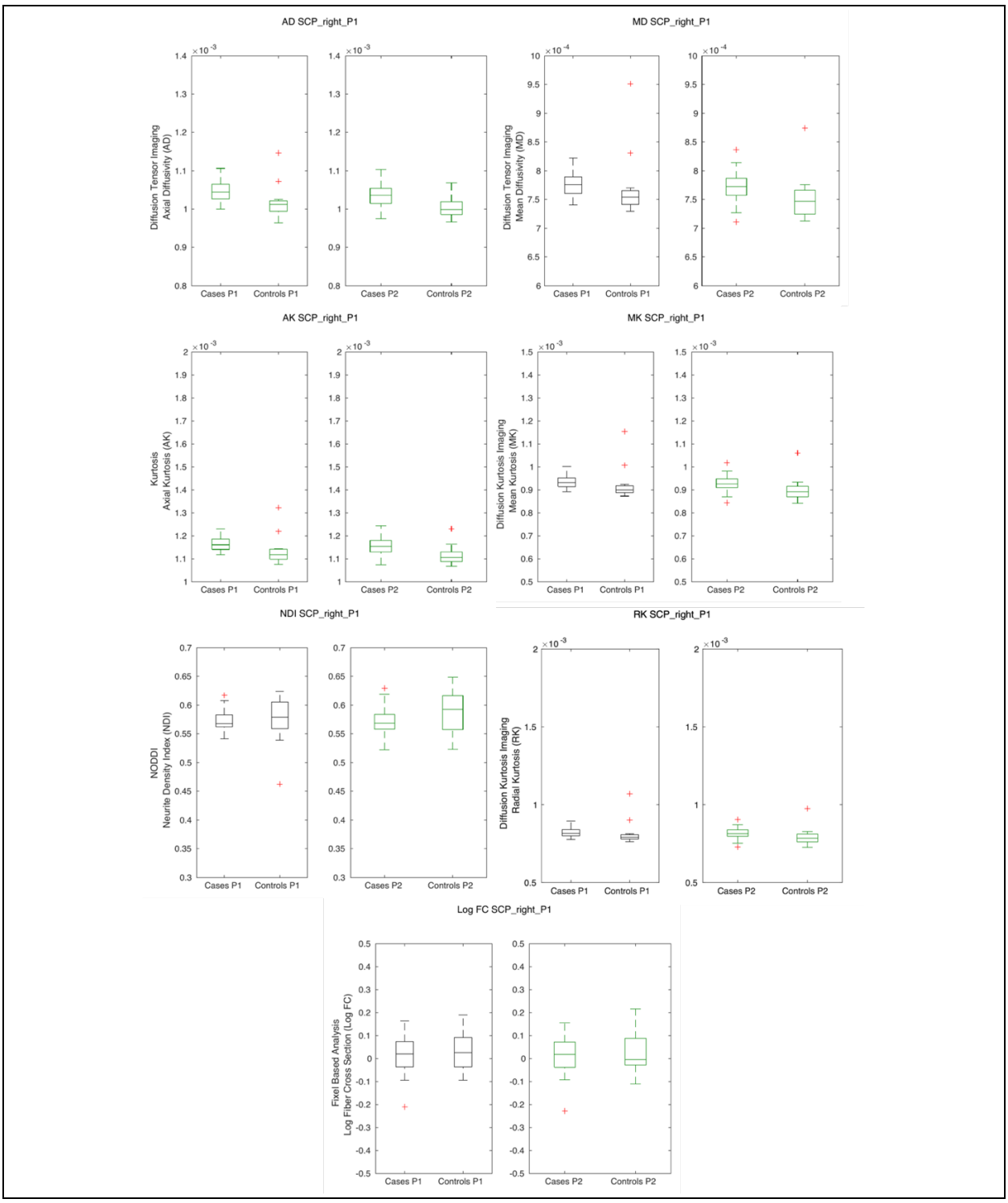

Figure A.44- Boxplots for t-test results in the Superior cerebellar peduncle (right)

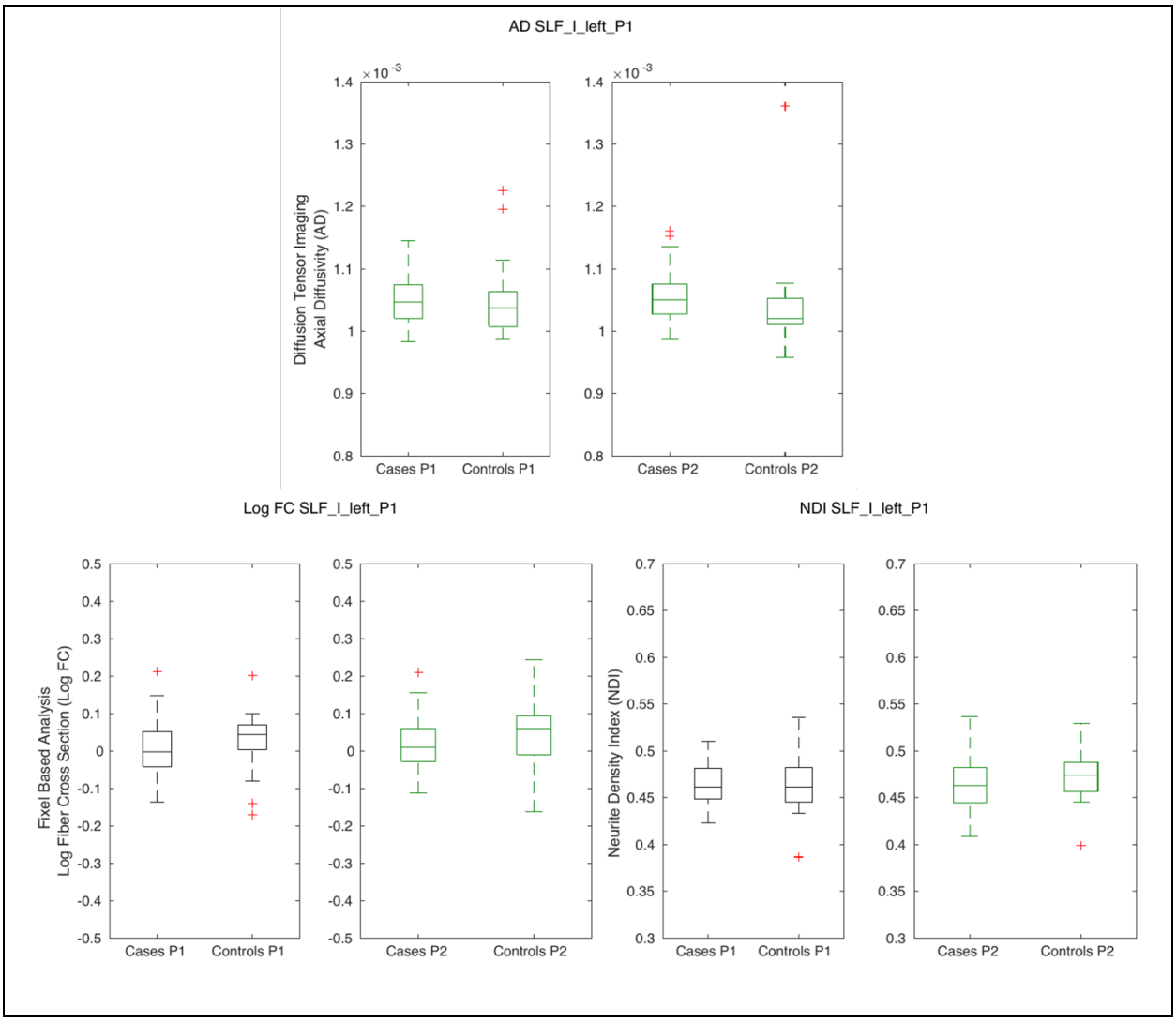

Figure A.45- Boxplots for t-test results in the Superior longitudinal fascicle I (left)

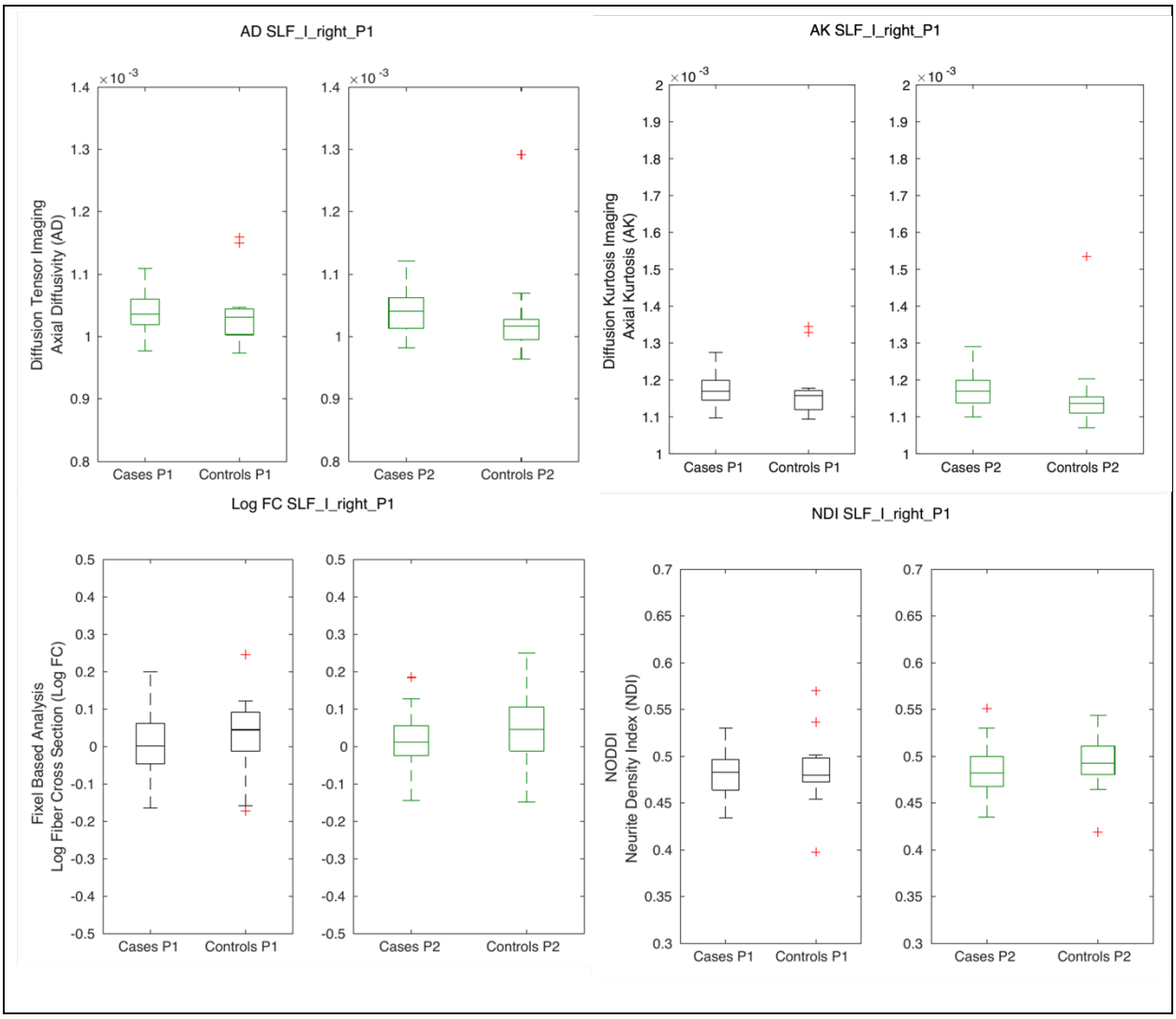

Figure A.46- Boxplots for t-test results in the Superior longitudinal fascicle I (right)

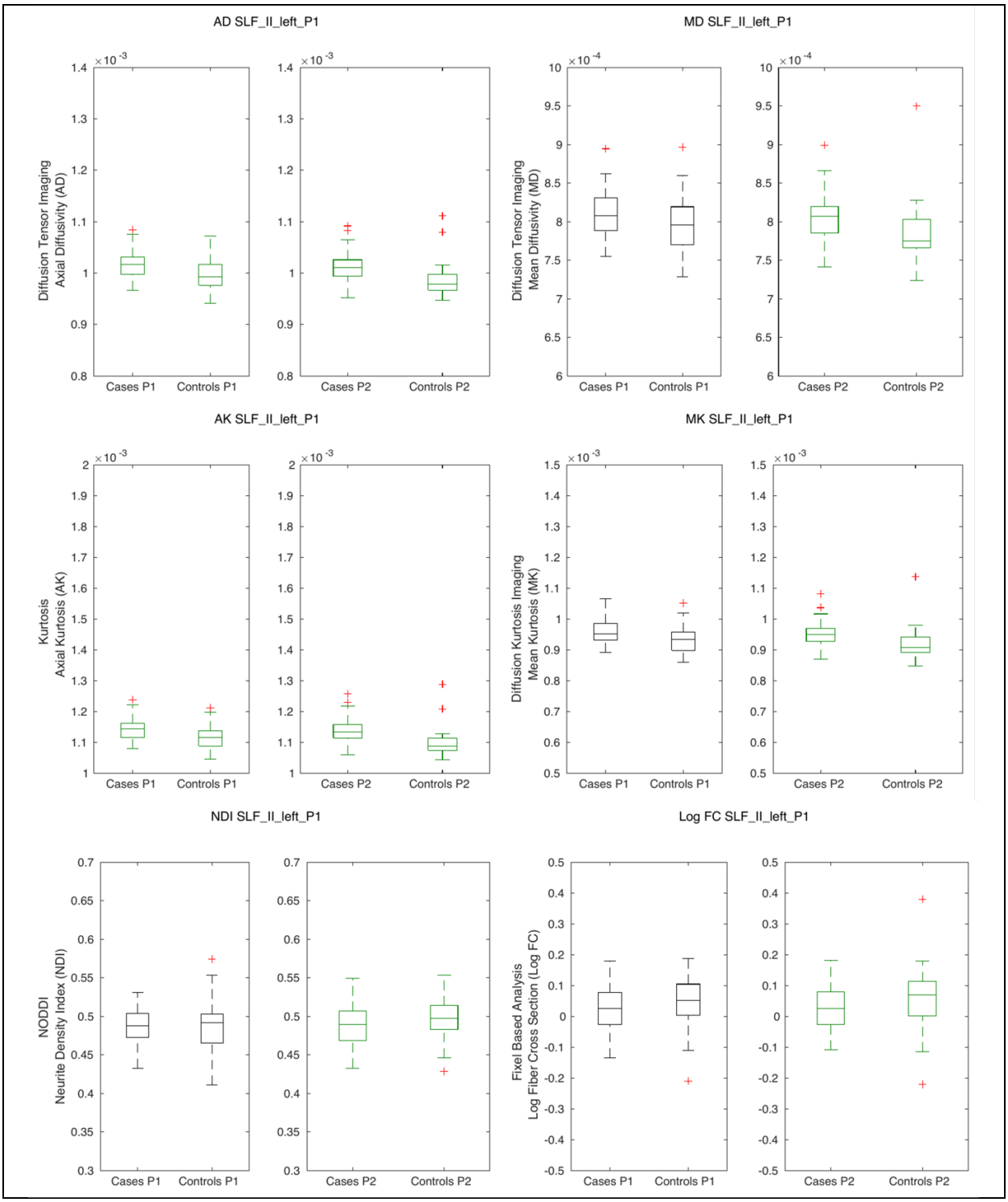

Figure A.47- Boxplots for t-test results in the Superior longitudinal fascicle II (left)

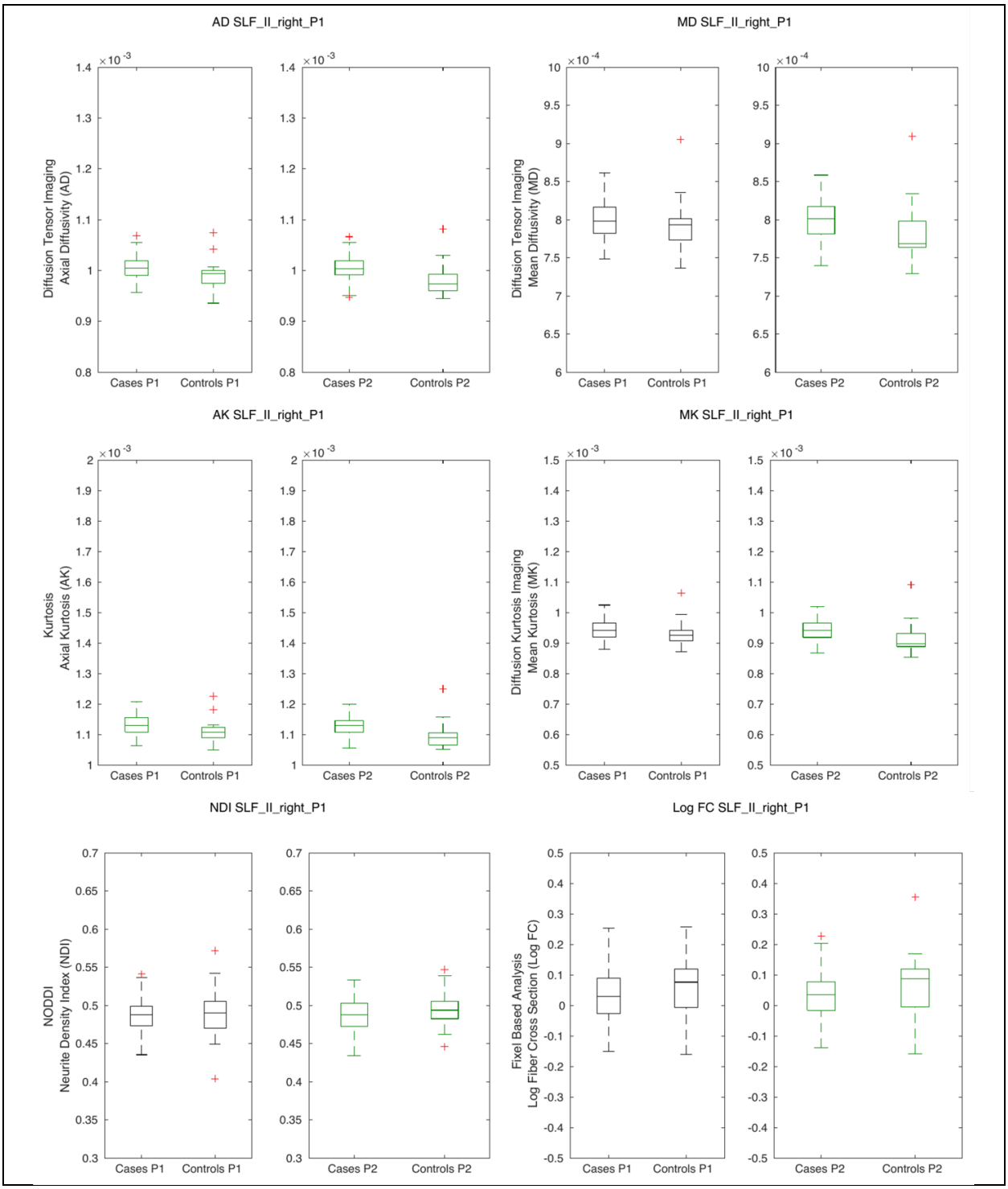

Figure A.48- Boxplots for t-test results in the Superior longitudinal fascicle II (right)

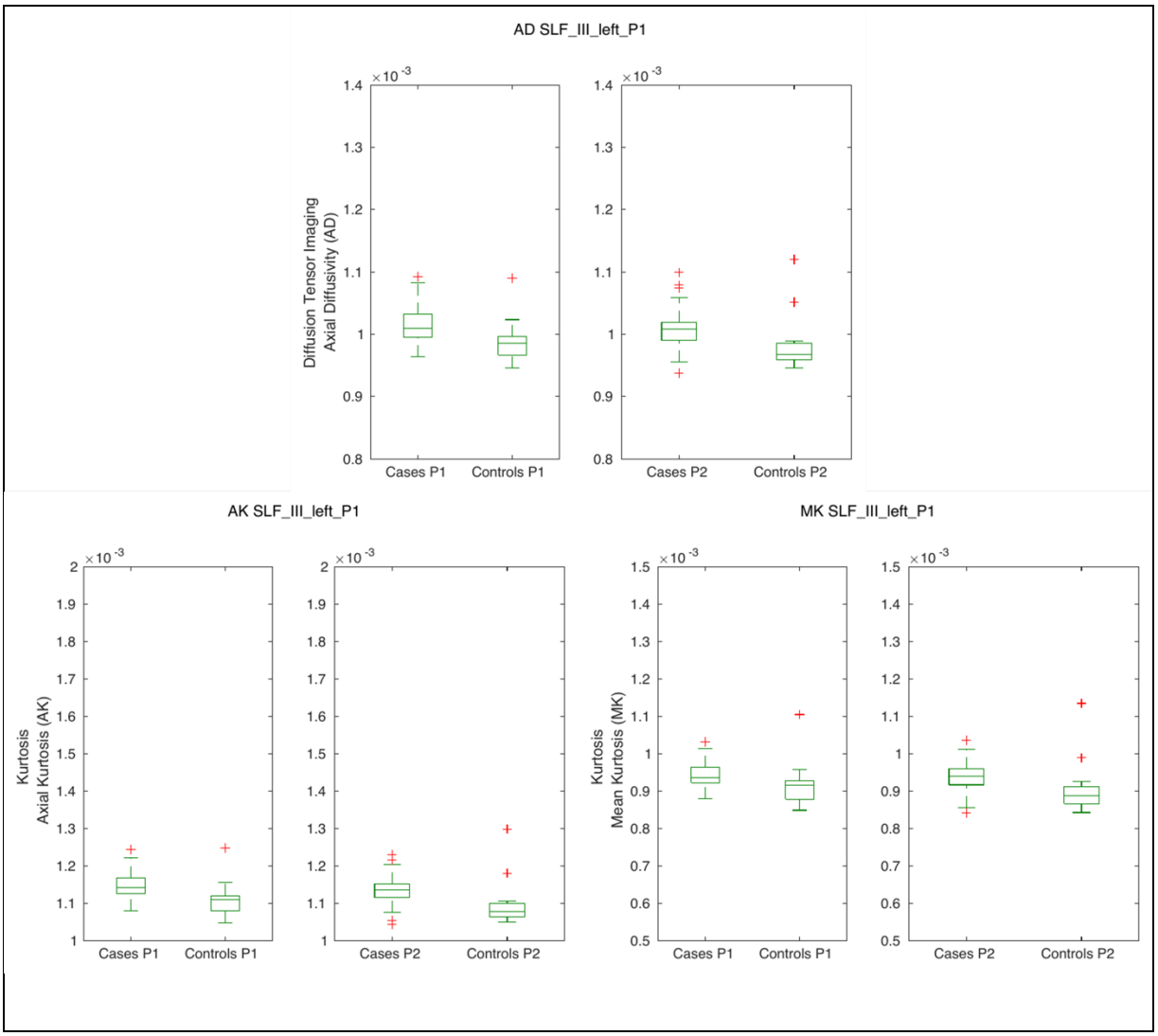

Figure A.49- Boxplots for t-test results in the Superior longitudinal fascicle III (left)

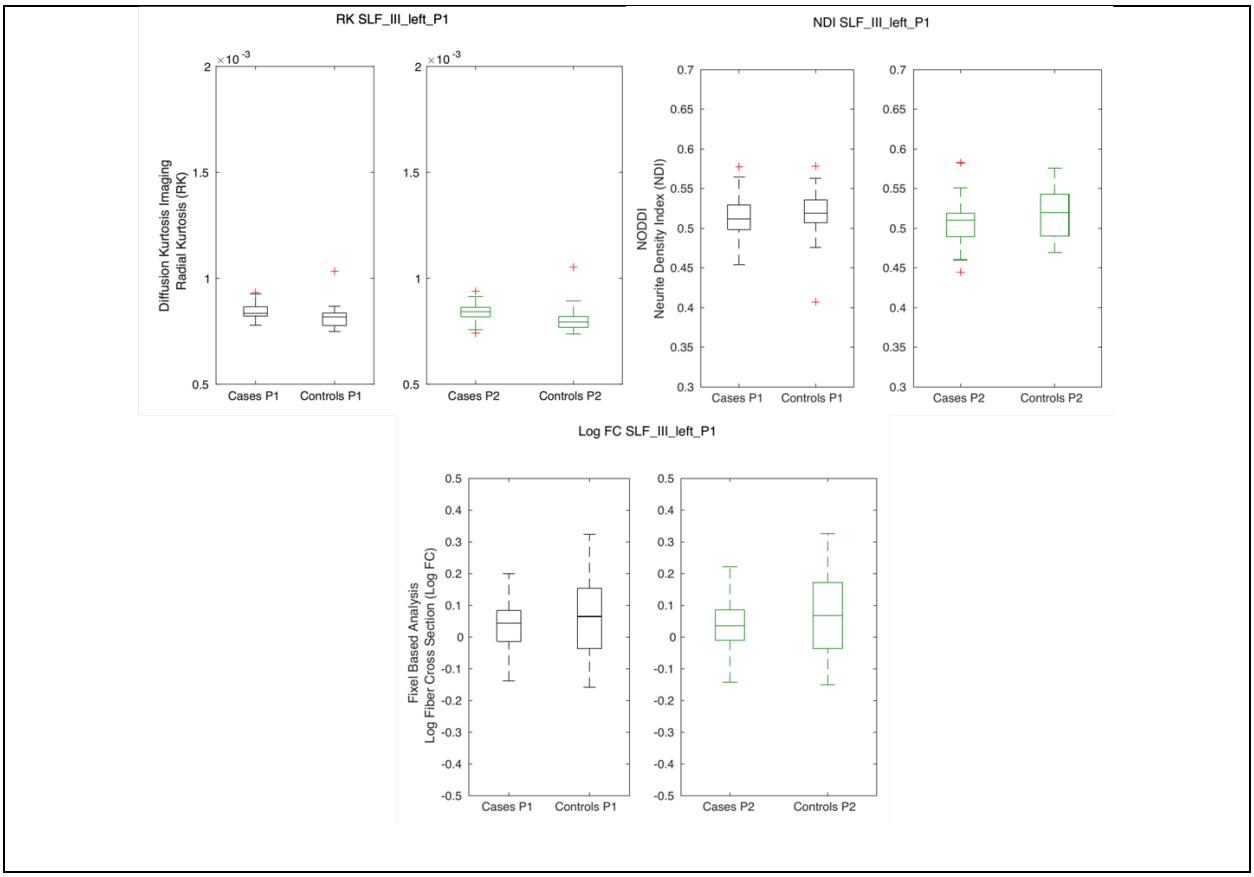

Figure A.50- Boxplots for t-test results in the Superior longitudinal fascicle III (left)

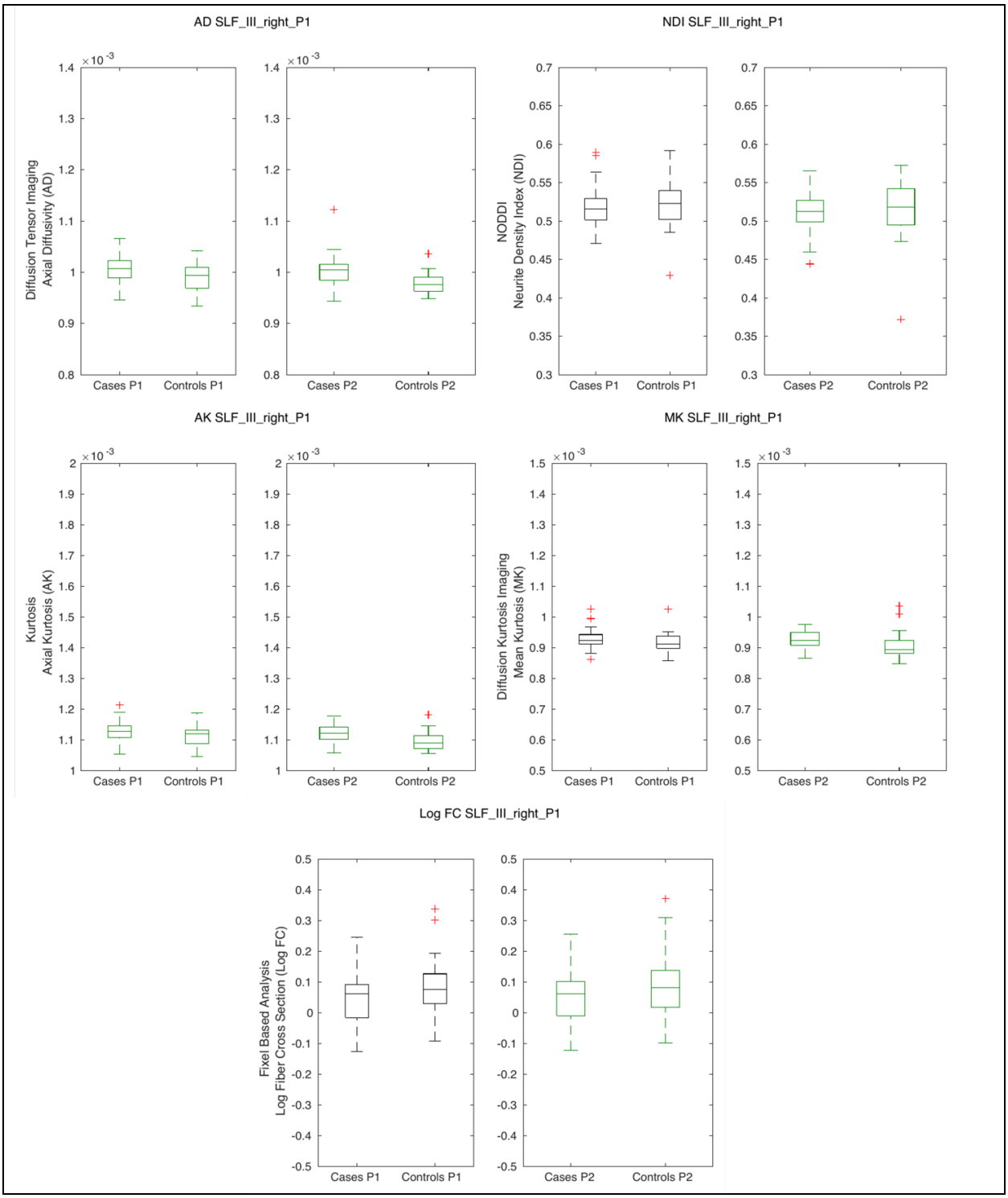

Figure A.51- Boxplots for t-test results in the Superior longitudinal fascicle III (right)

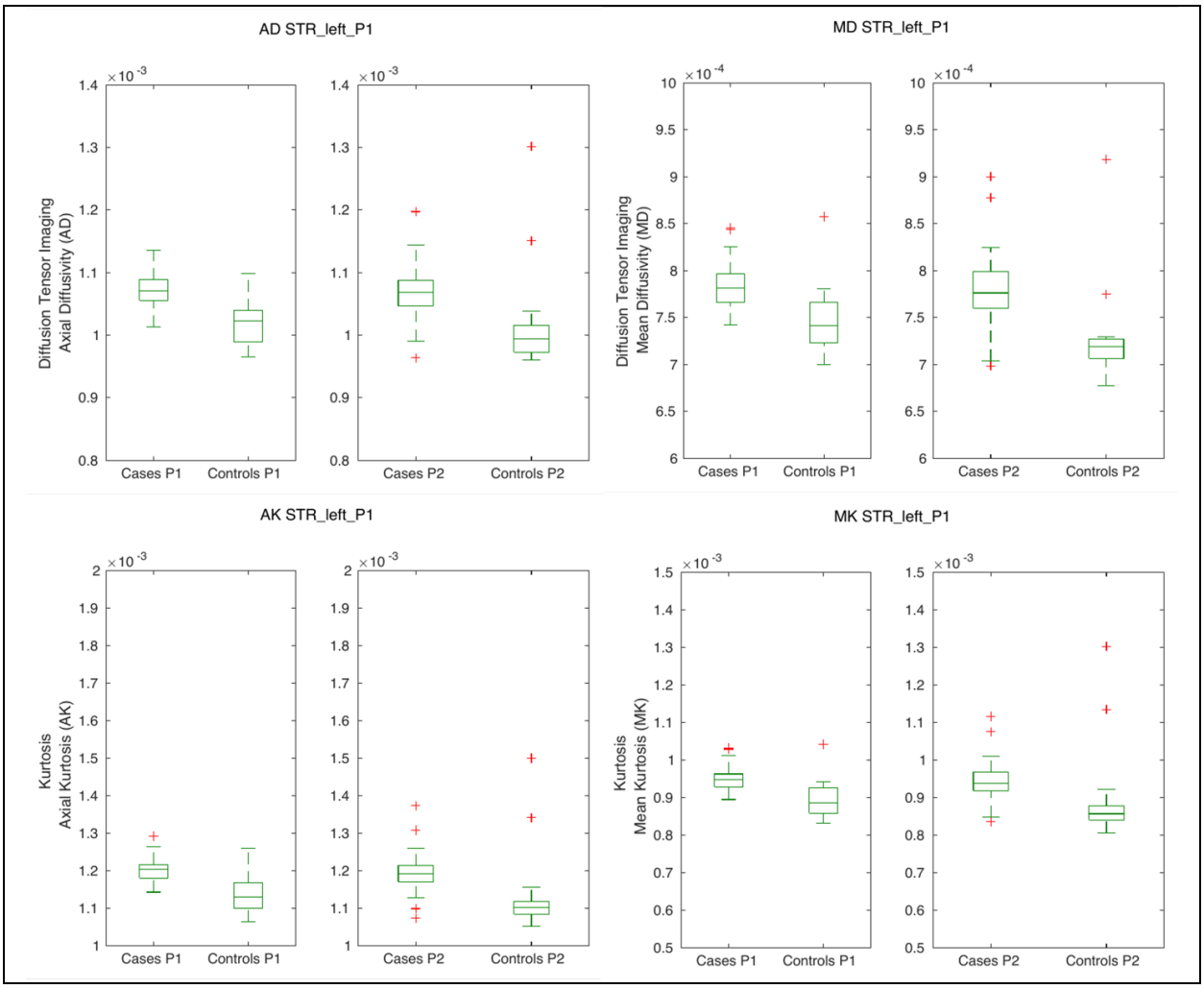

Figure A.52- Boxplots for t-test results in the Superior Thalamic Radiation (left)

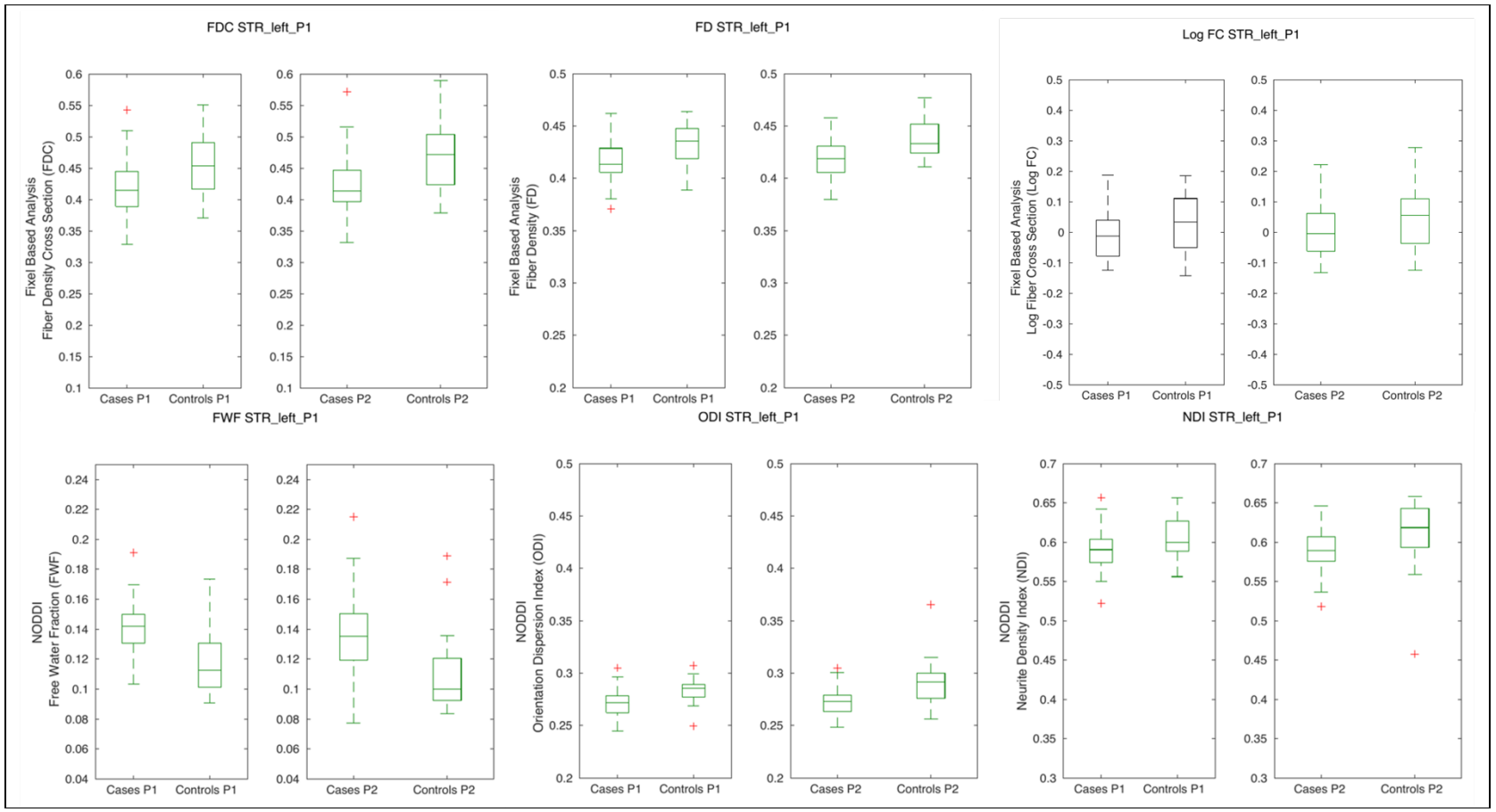

Figure A.53- Boxplots for t-test results in the Superior Thalamic Radiation (left)

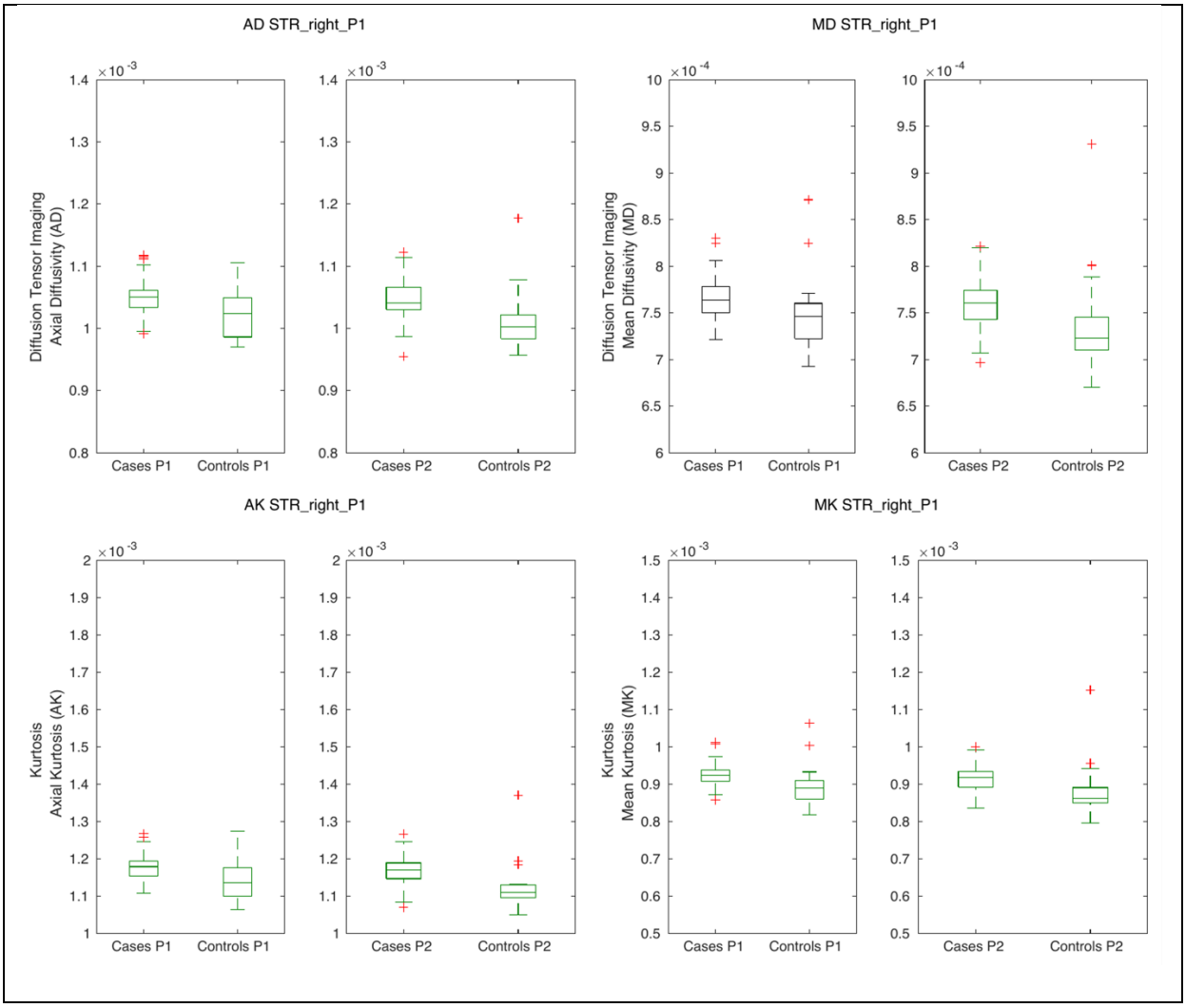

Figure A.54- Boxplots for t-test results in the Superior Thalamic Radiation (right)

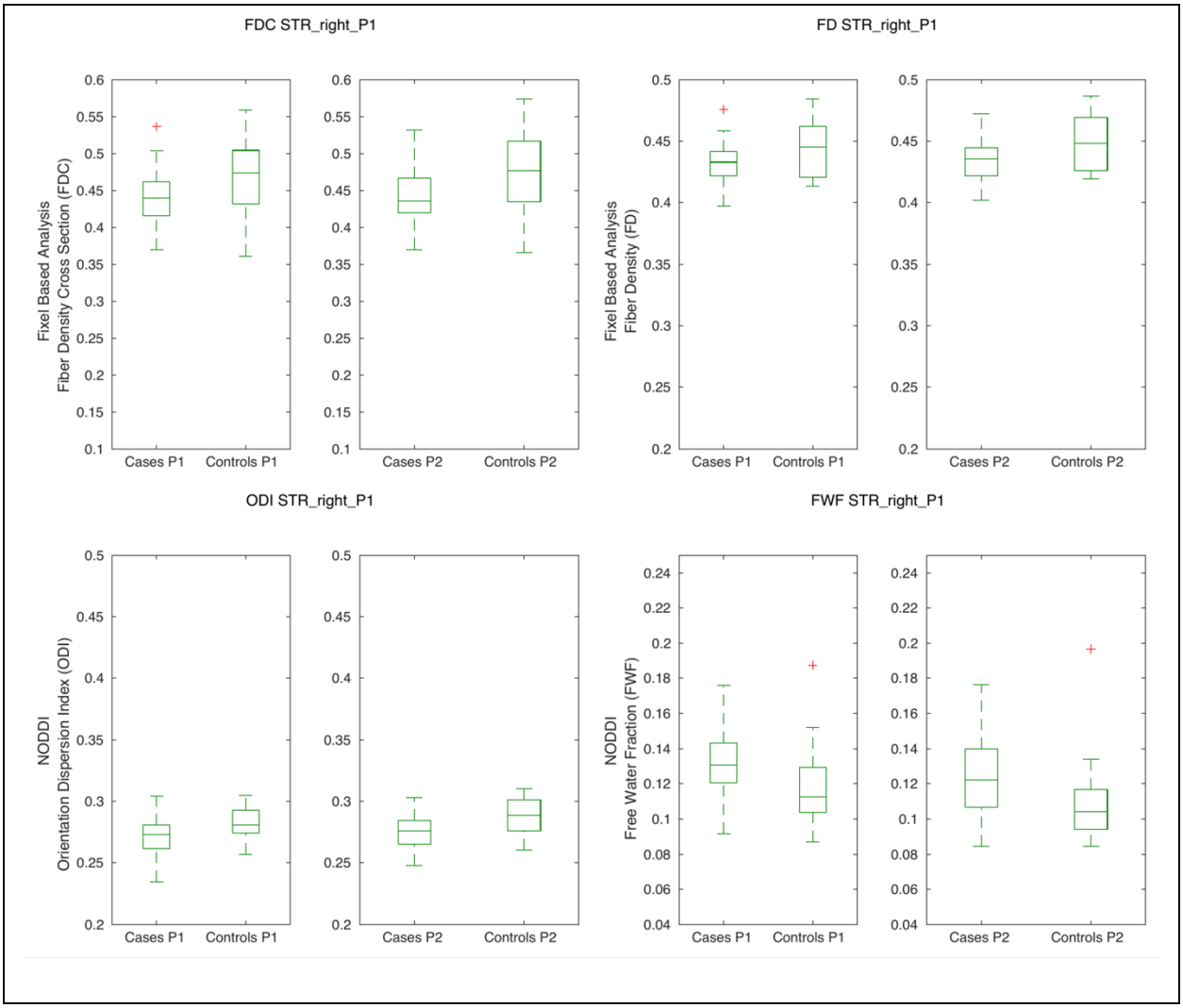

Figure A.55- Boxplots for t-test results in the Superior Thalamic Radiation (right)

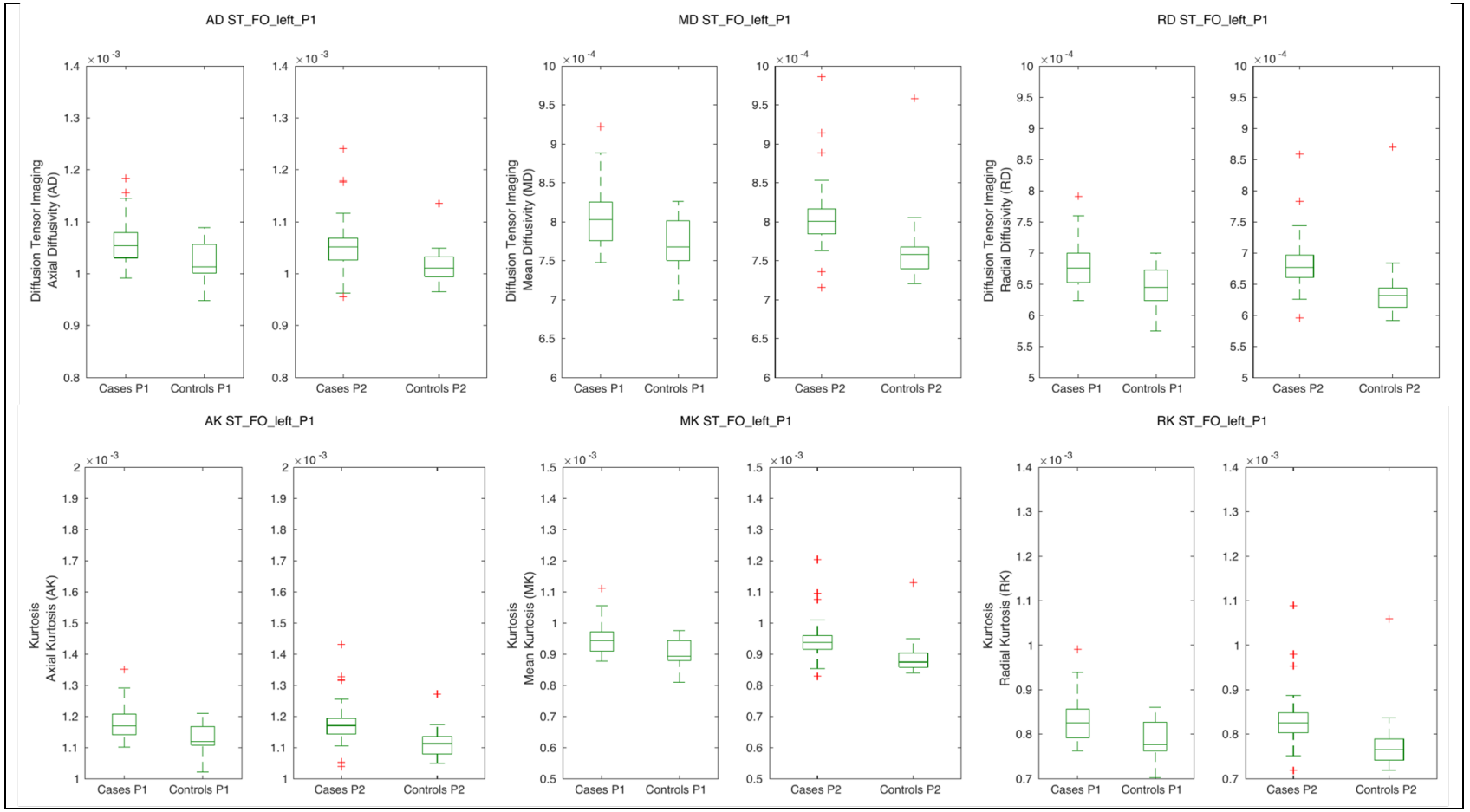

Figure A.56- Boxplots for t-test results in the Striato-fronto-orbital (left)

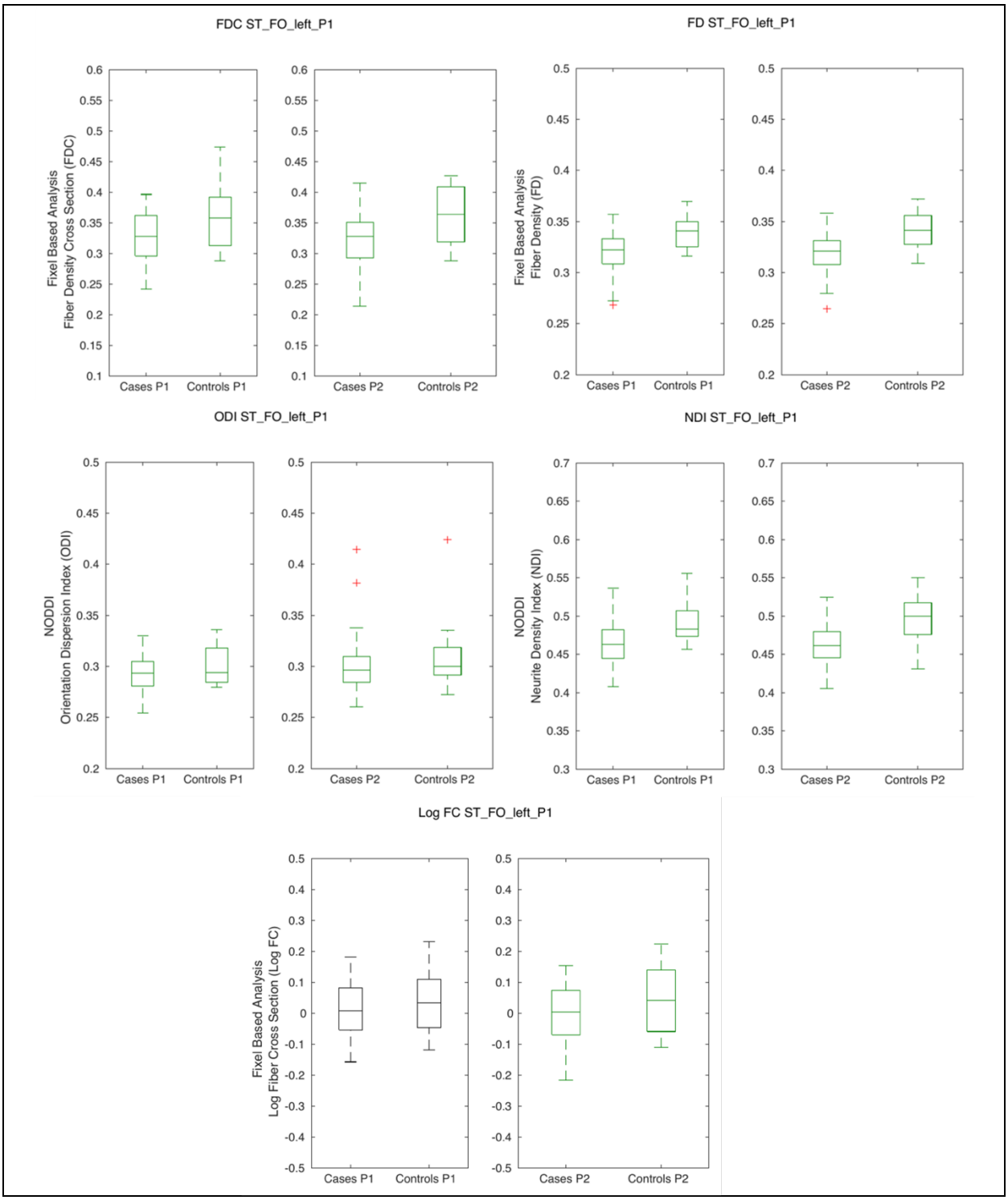

Figure A.57- Boxplots for t-test results in the Striato-fronto-orbital (left)

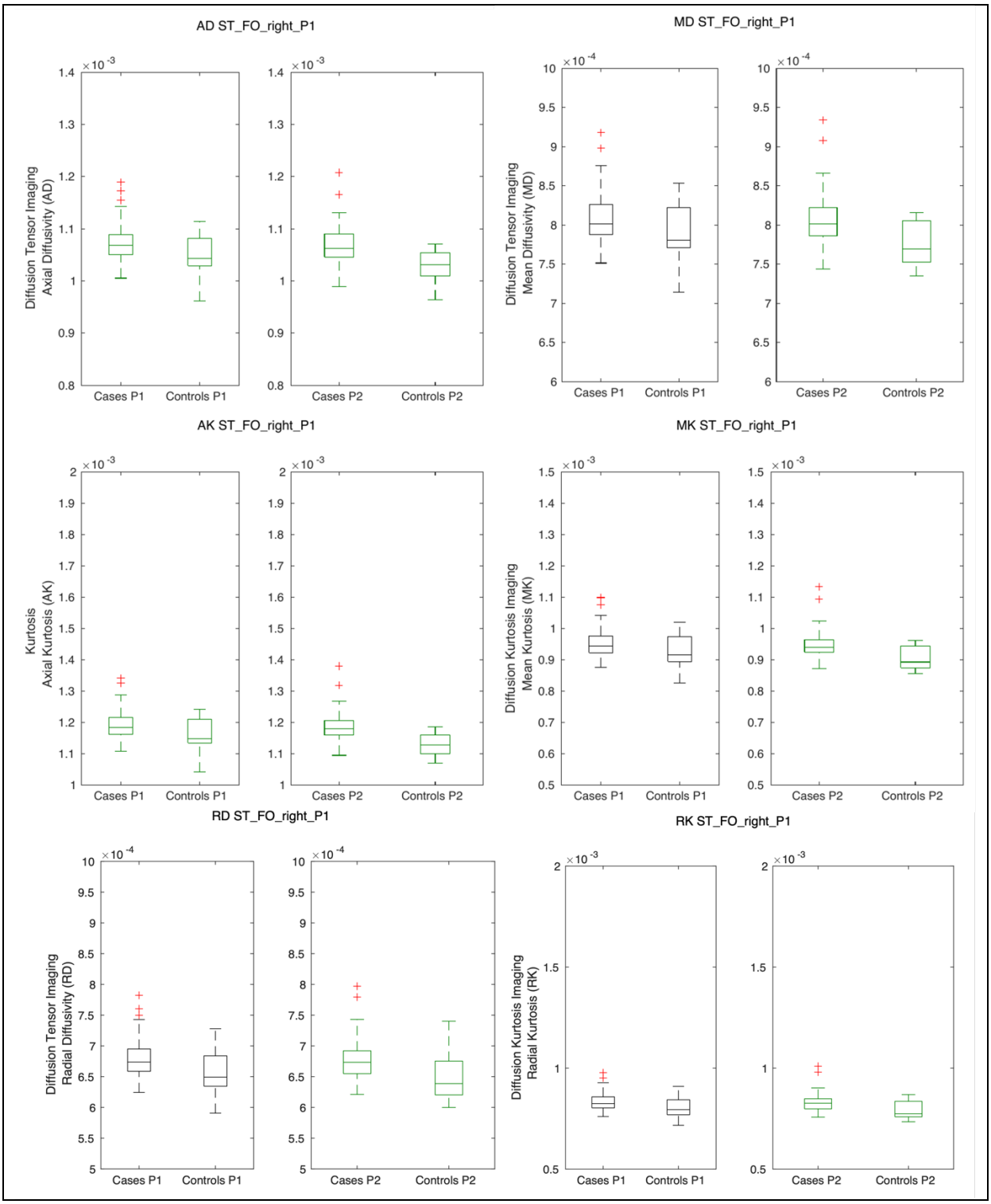

Figure A.58- Boxplots for t-test results in the Striato-fronto-orbital (right)

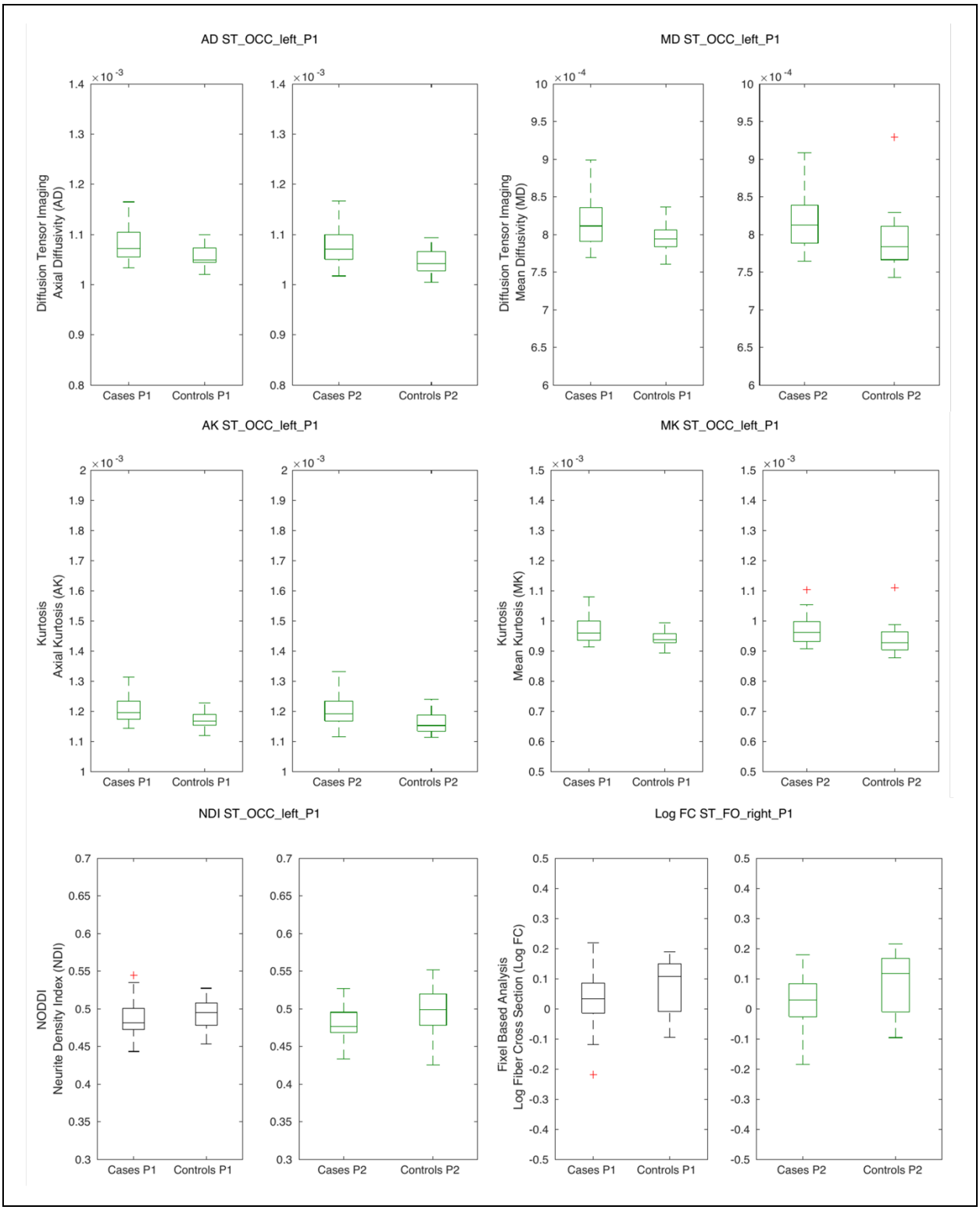

Figure A.59- Boxplots for t-test results in the Striato-occipital (left)

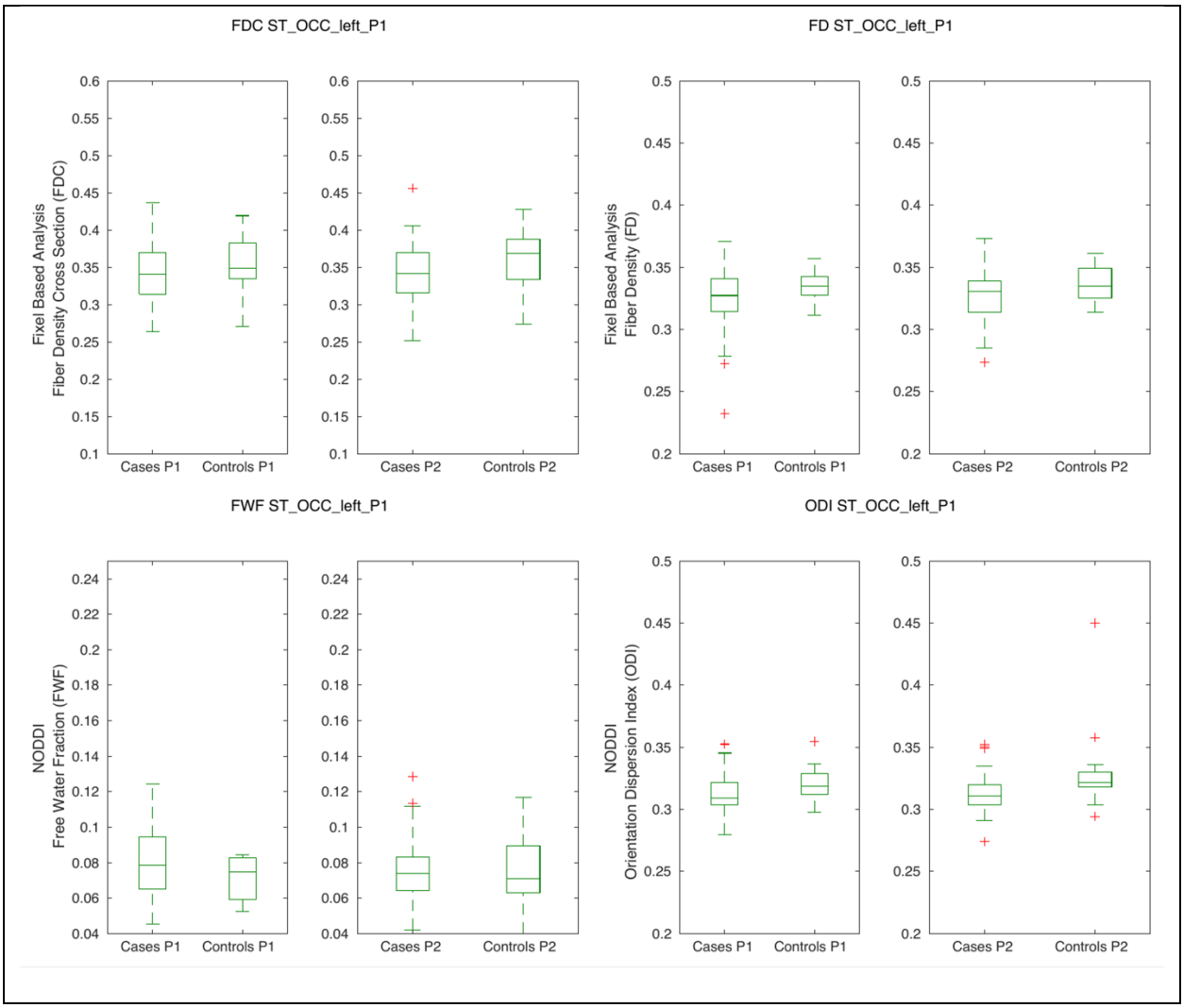

Figure A.60- Boxplots for t-test results in the Striato-occipital (left)

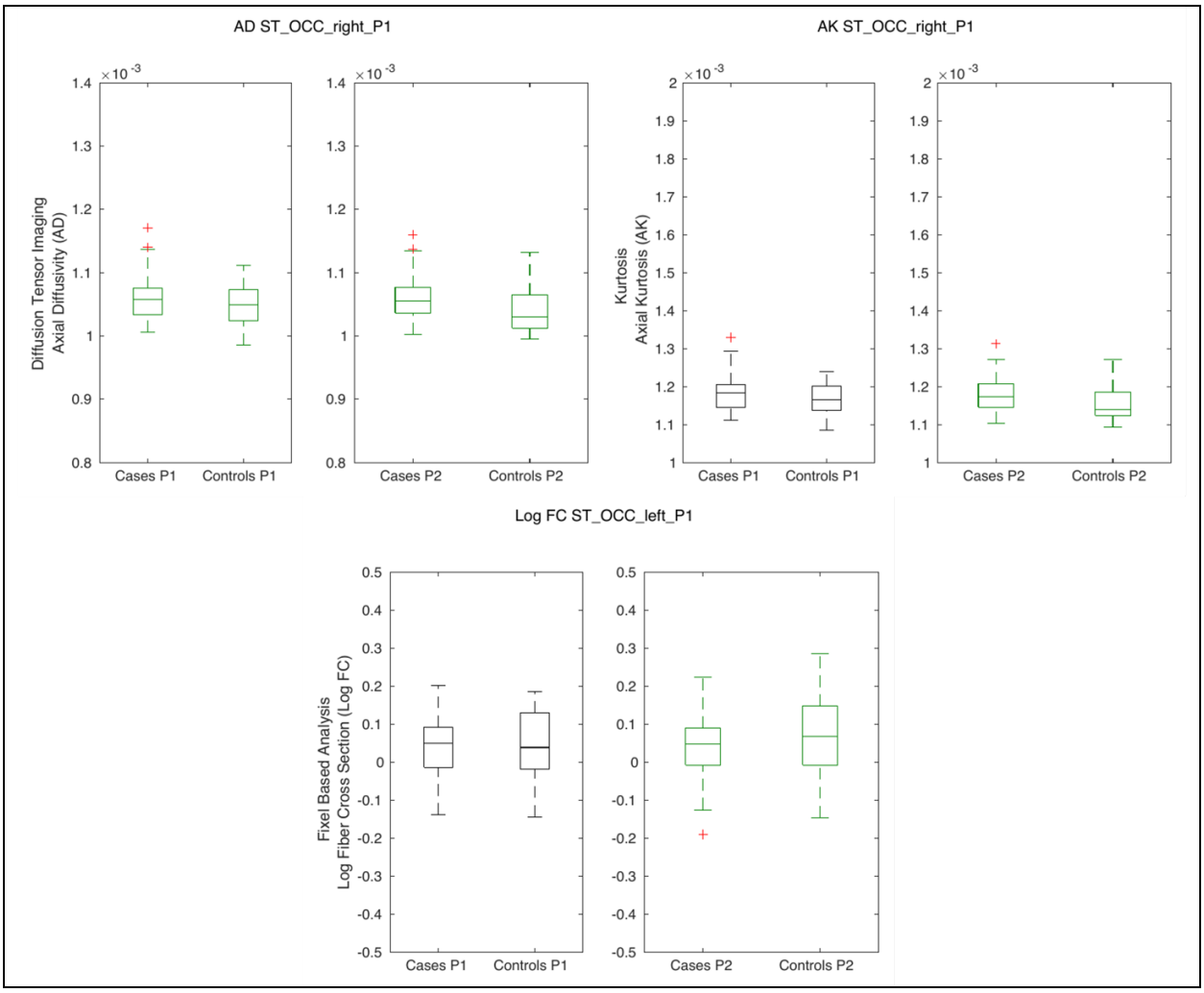

Figure A.61- Boxplots for t-test results in the Striato-occipital (right)

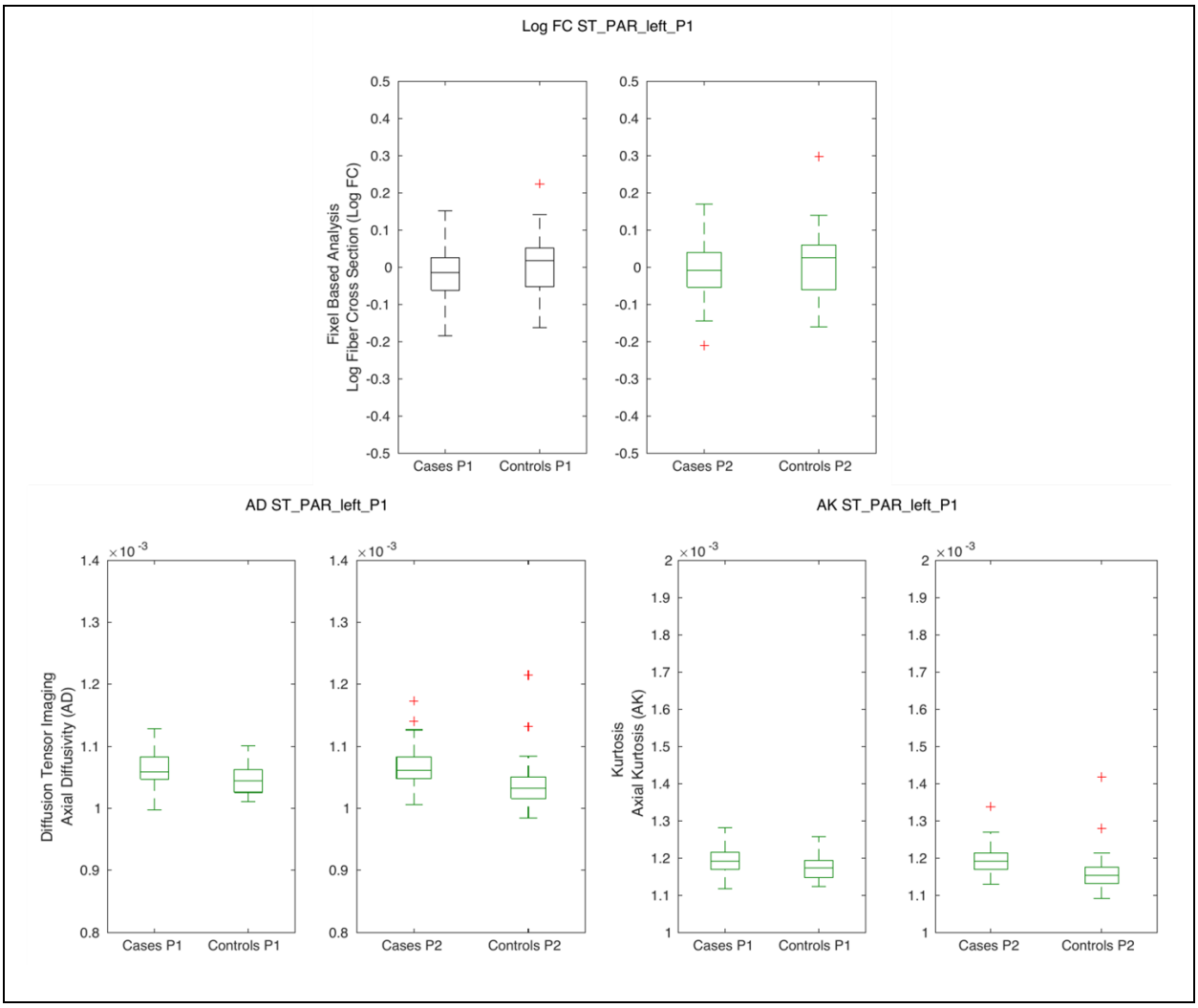

Figure A.62- Boxplots for t-test results in the Striato-parietal (left)

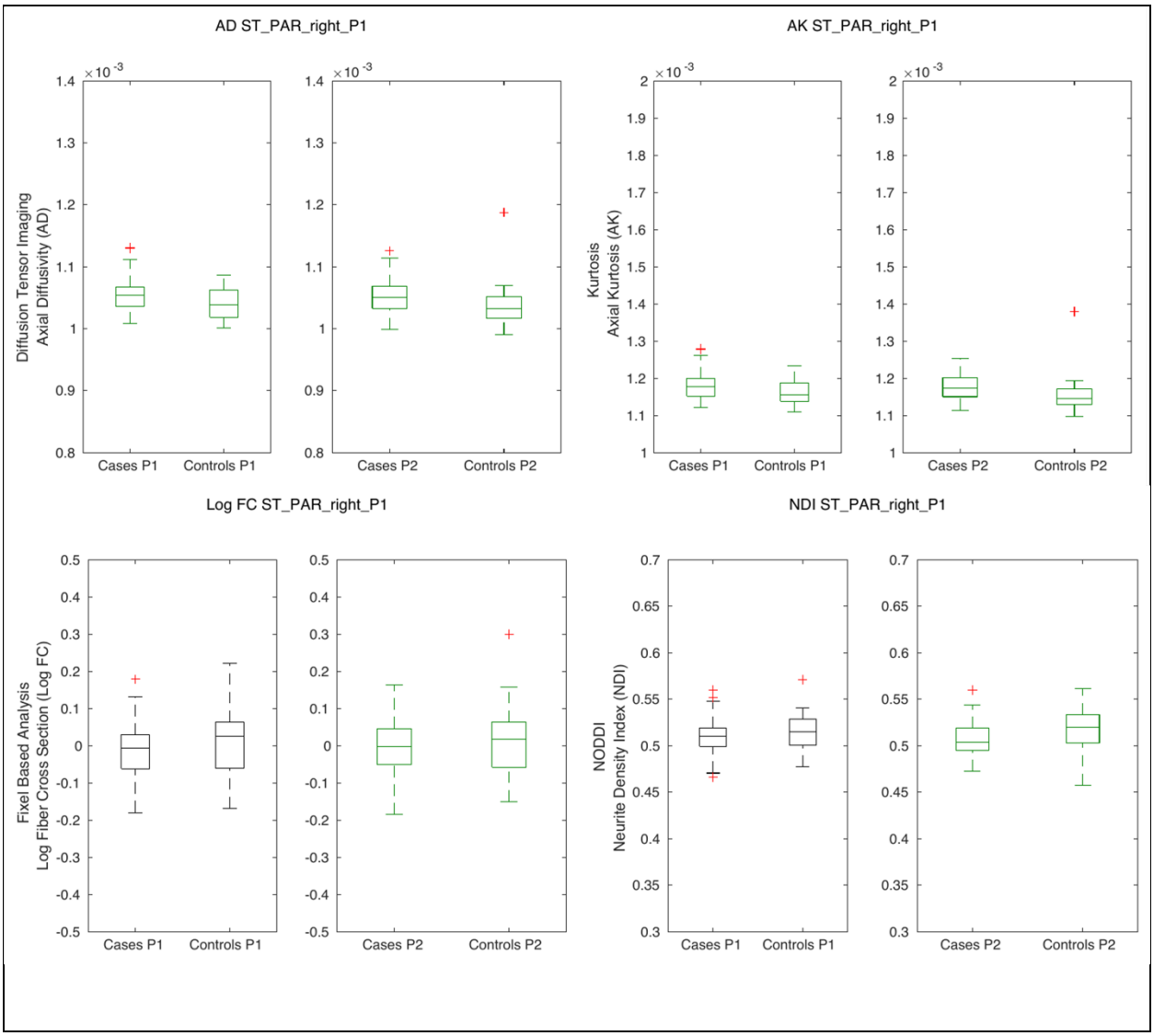

Figure A.63- Boxplots for t-test results in the Striato-parietal (right)

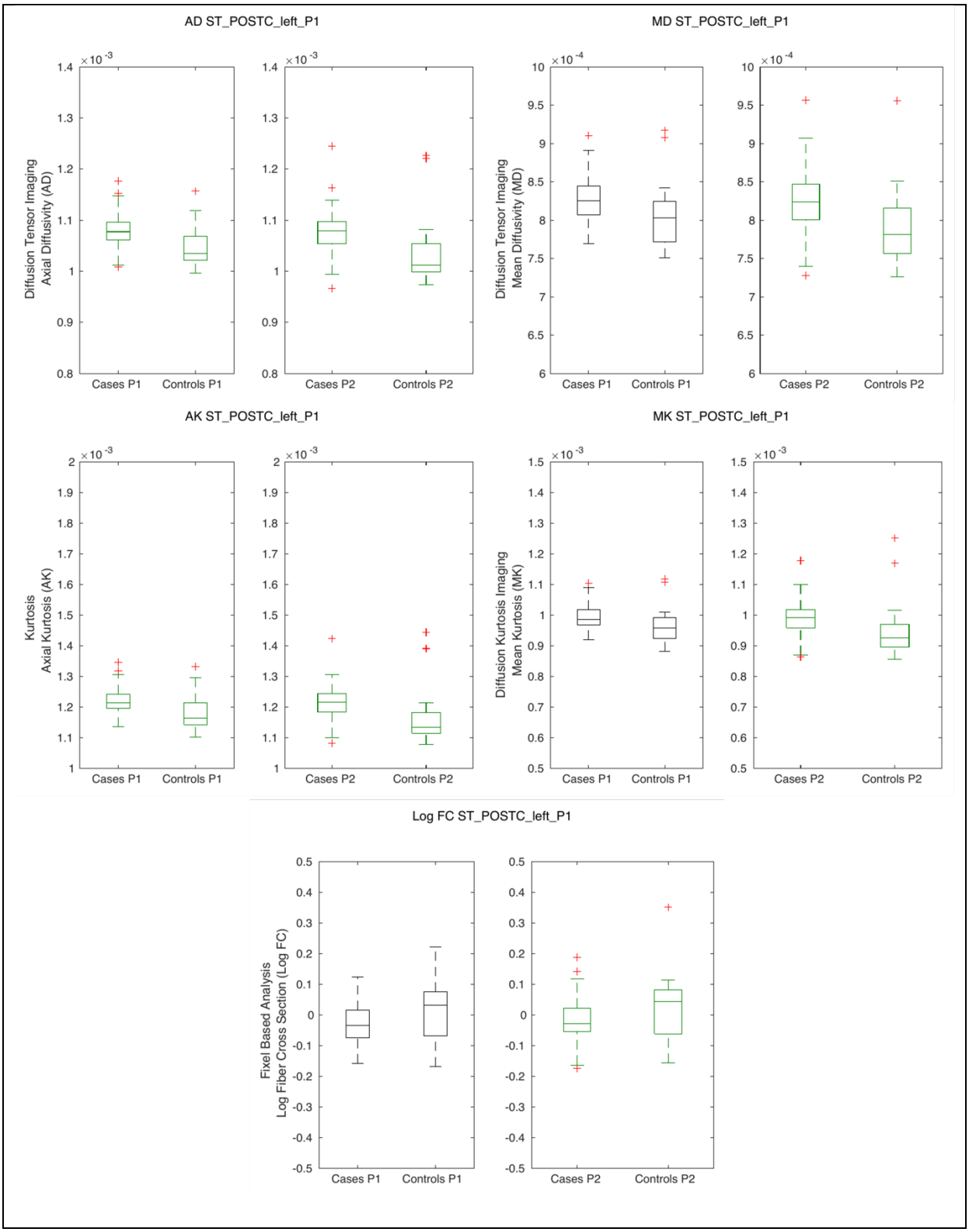

Figure A.64- Boxplots for t-test results in the Striato-postcentral (left)

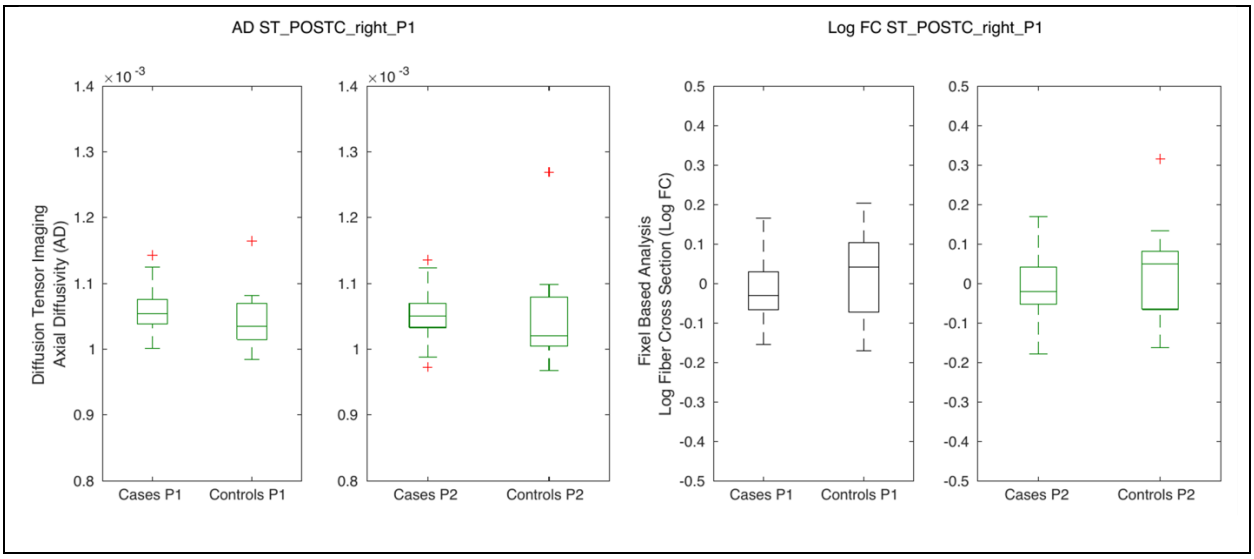

Figure A.65- Boxplots for t-test results in the Striato-postcentral (right)

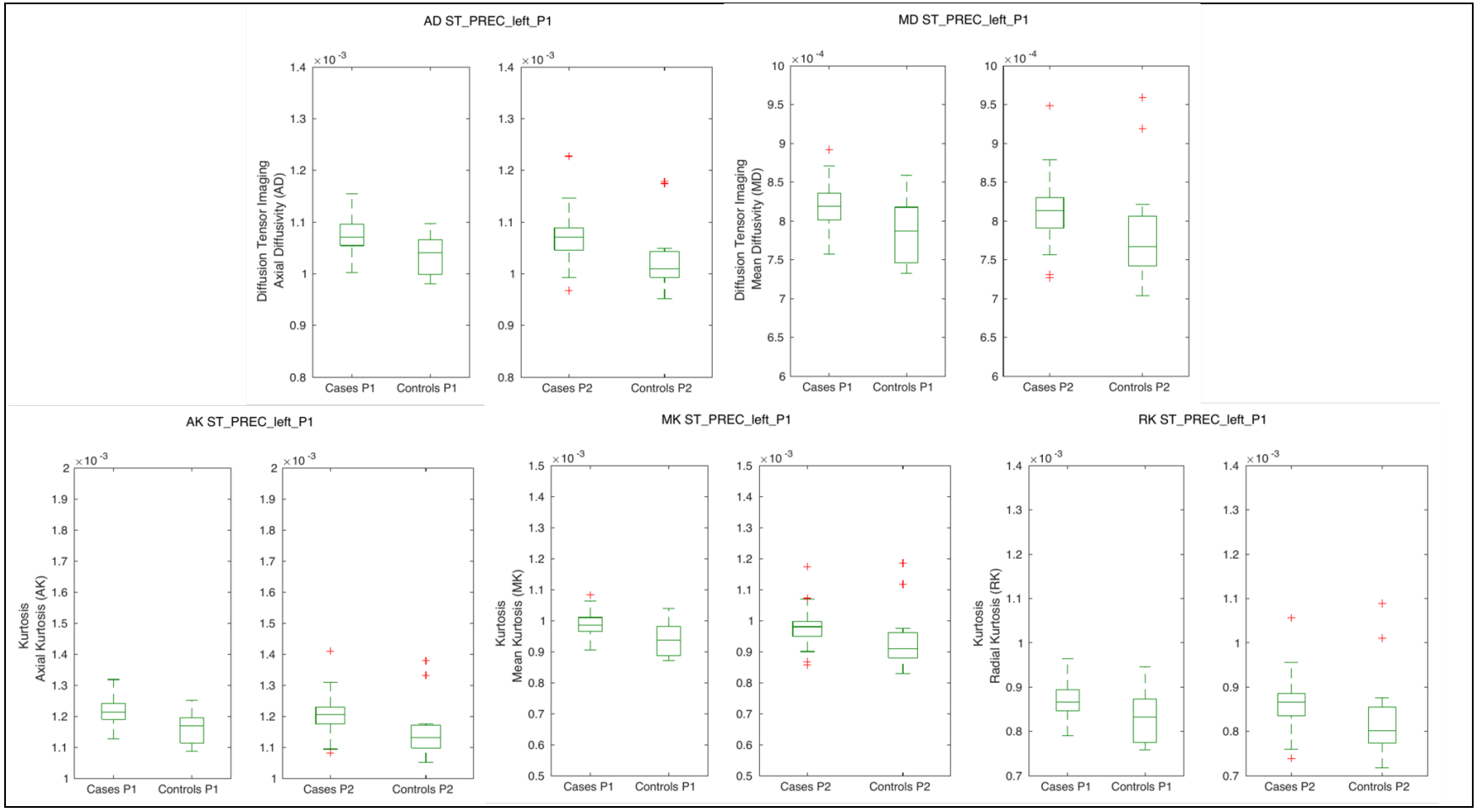

Figure A.66- Boxplots for t-test results in the Striato-precentral (left)

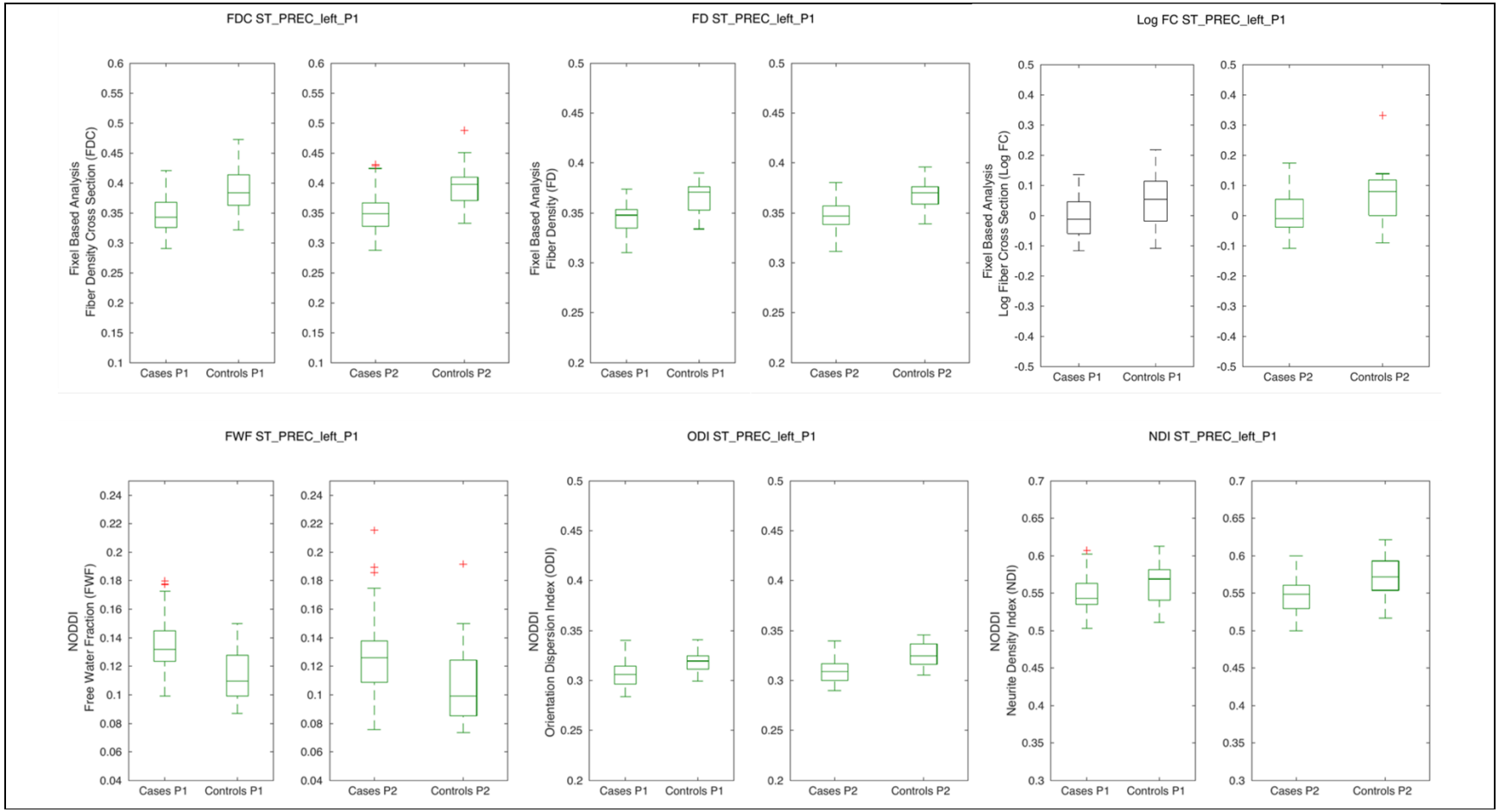

Figure A.67- Boxplots for t-test results in the Striato-precentral (left)

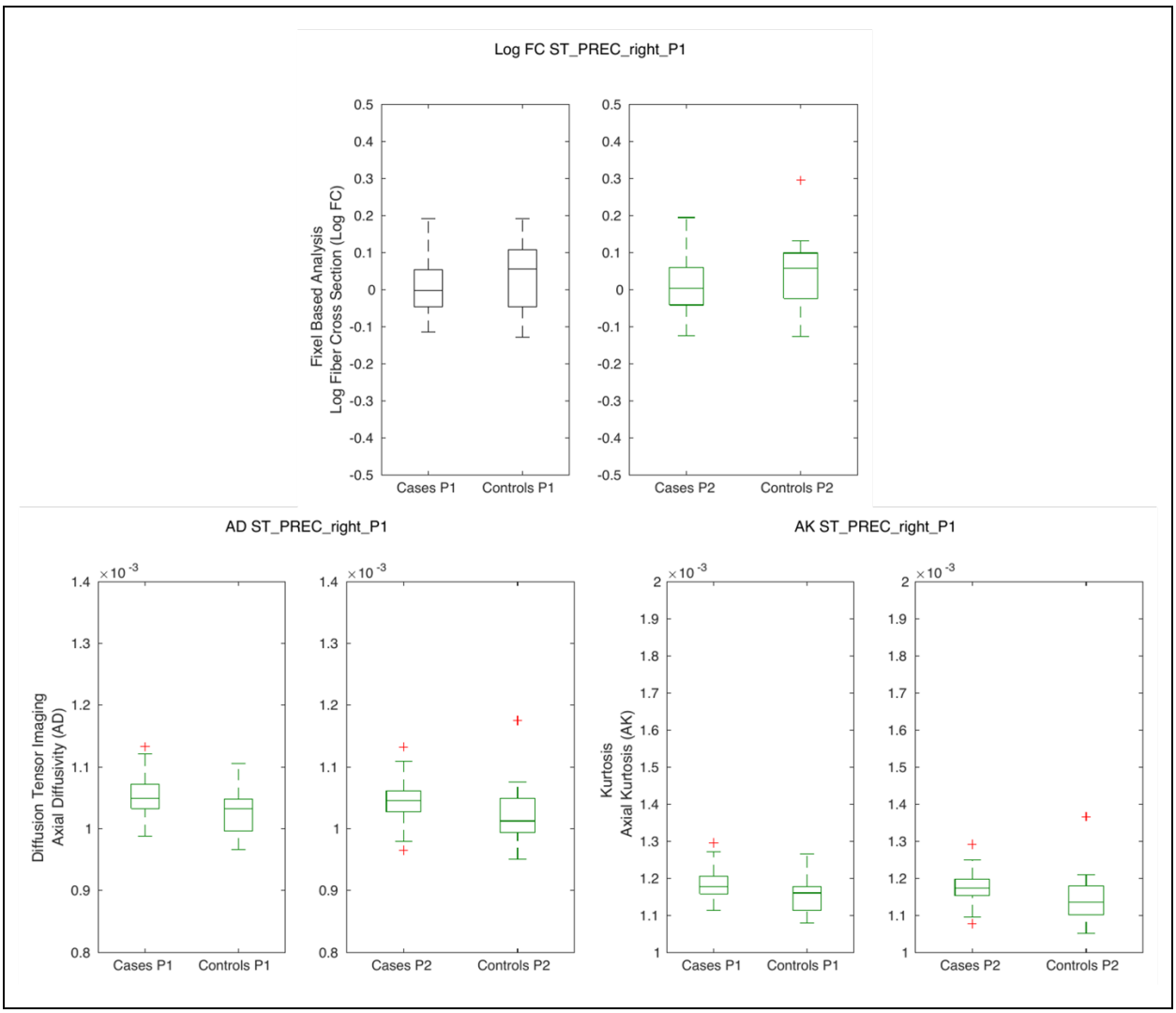

Figure A.68- Boxplots for t-test results in the Striato-precentral (right)

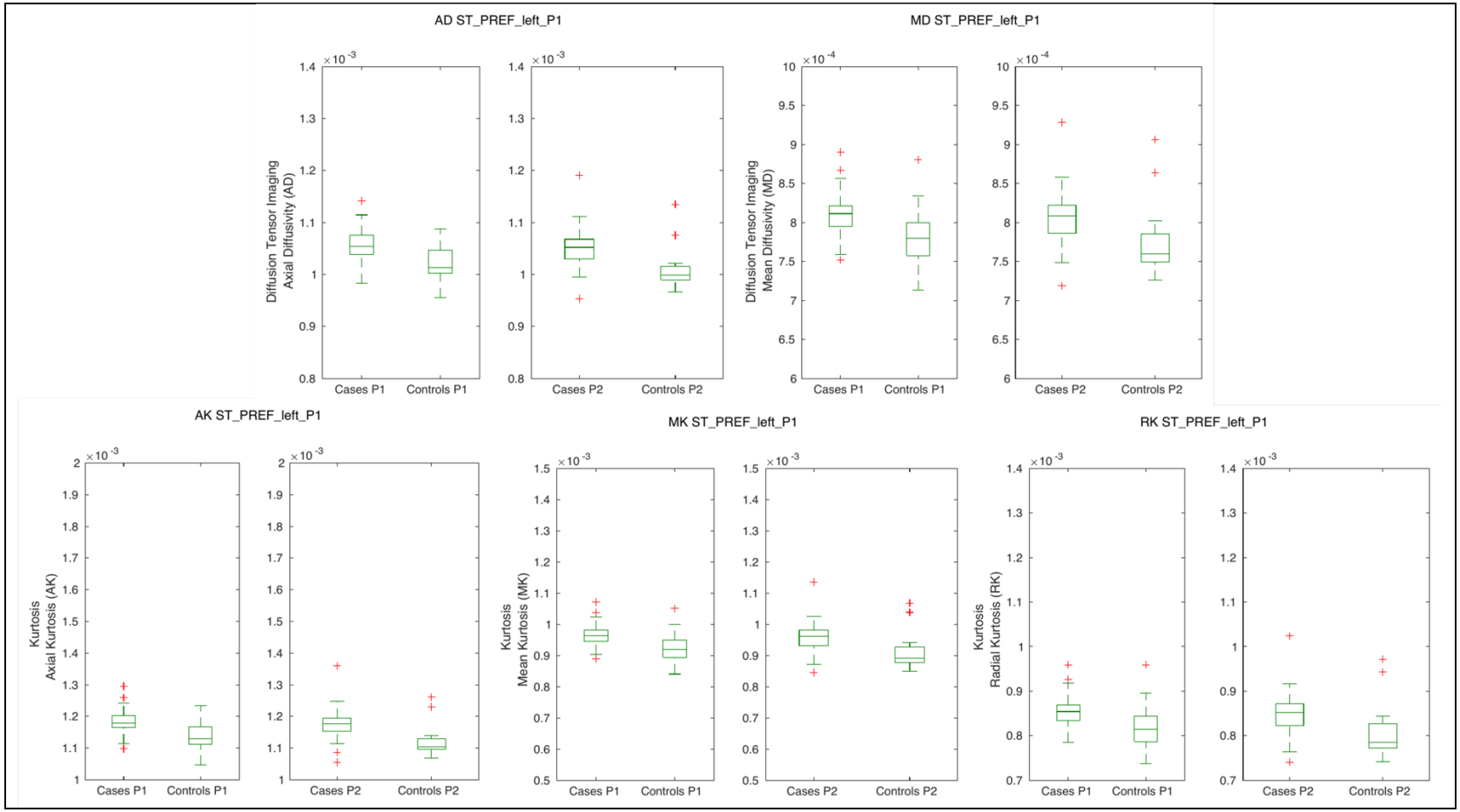

Figure A.69- Boxplots for t-test results in the Striato-prefrontal (left)

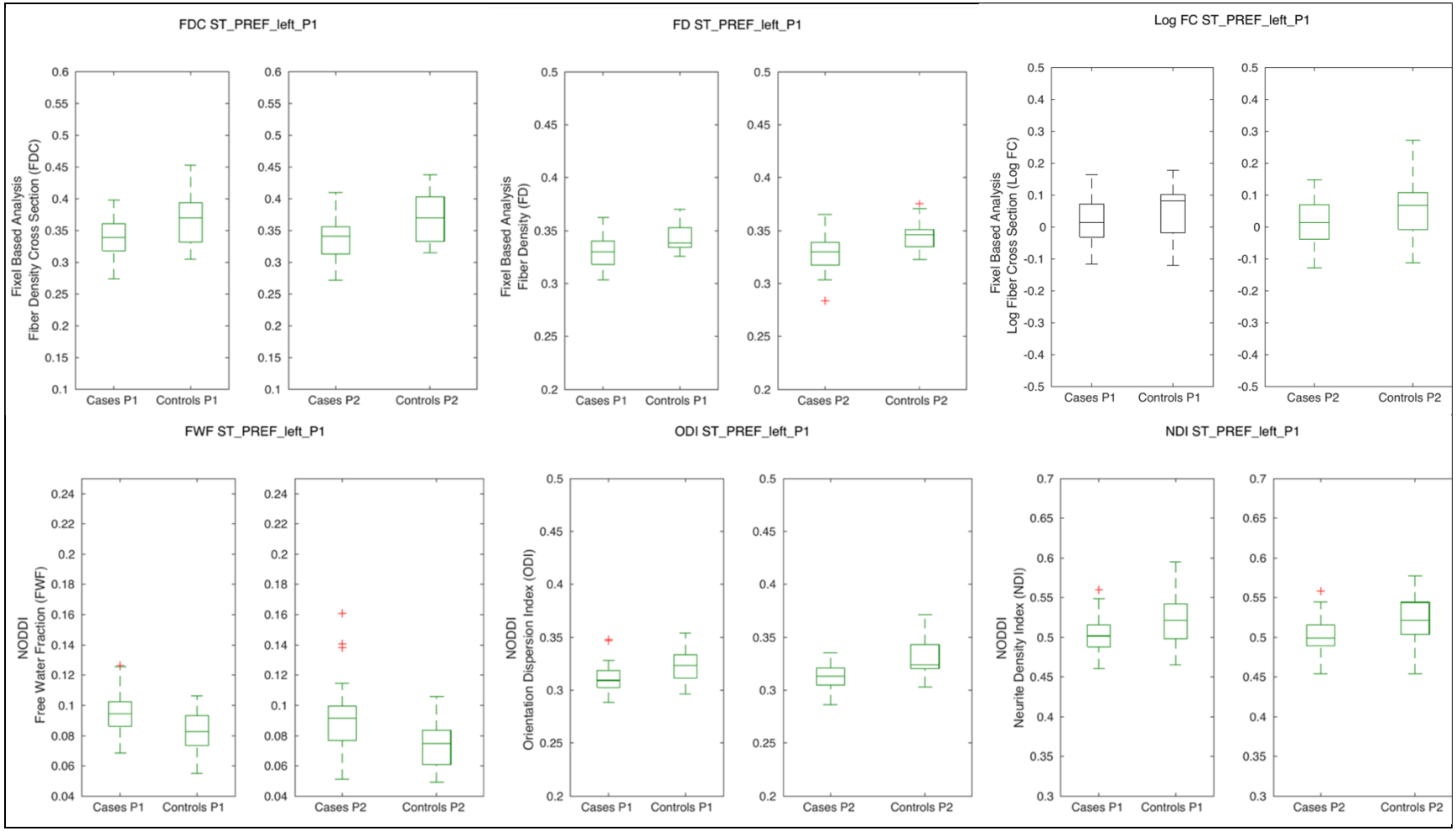

Figure A.70- Boxplots for t-test results in the Striato-prefrontal (left)

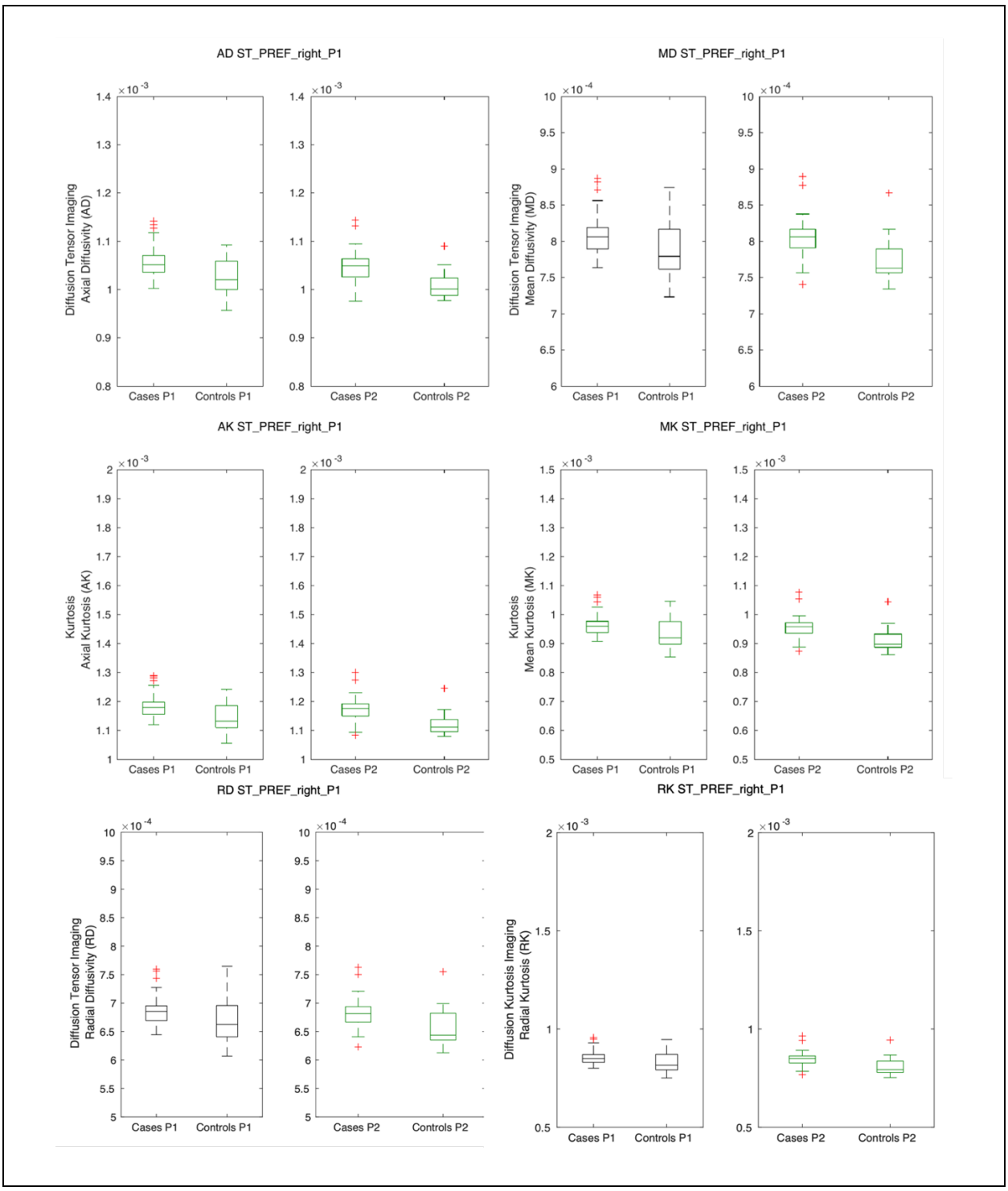

Figure A.71- Boxplots for t-test results in the Striato-prefrontal (right)

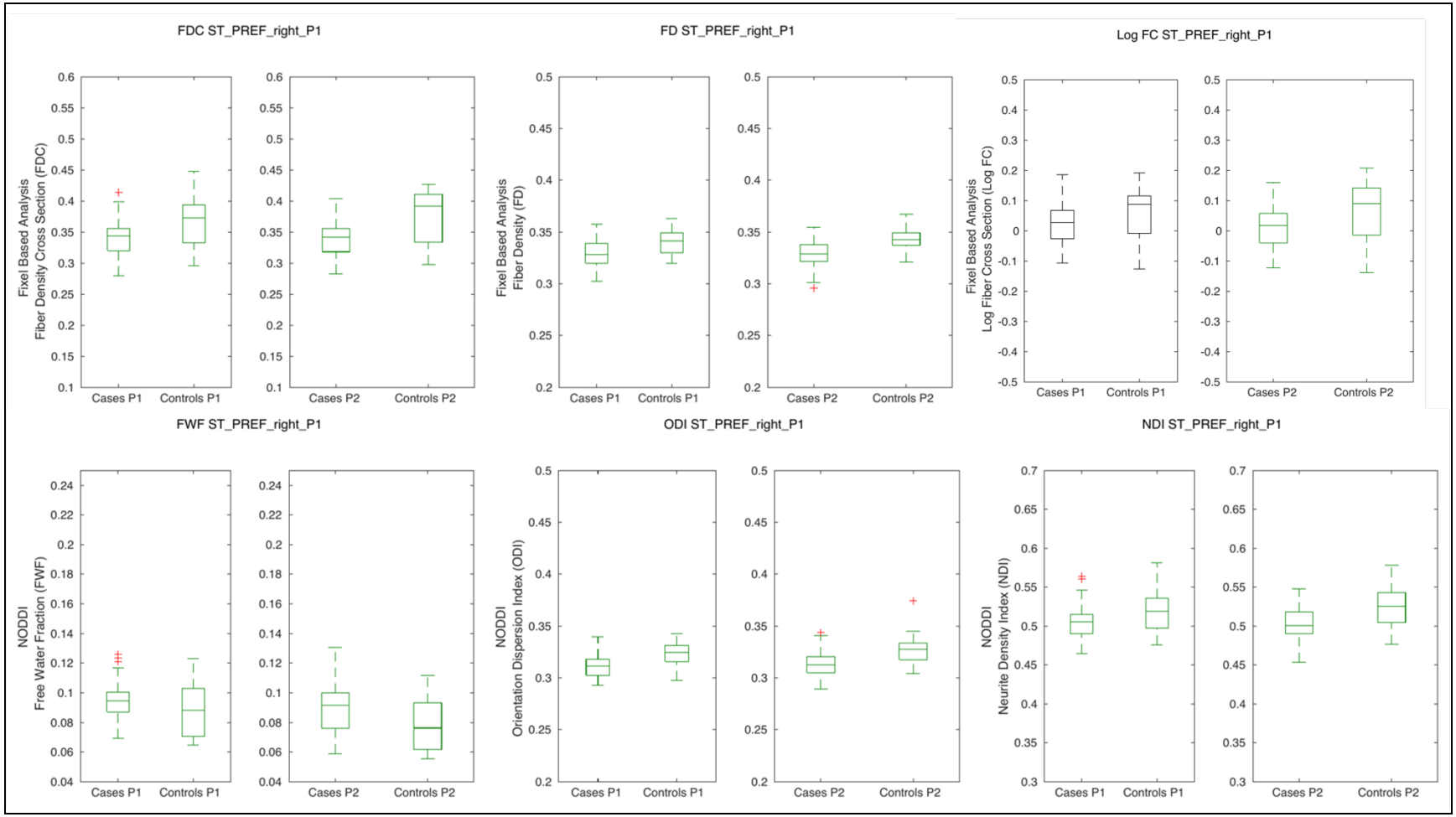

Figure A.72- Boxplots for t-test results in the Striato-prefrontal (right)

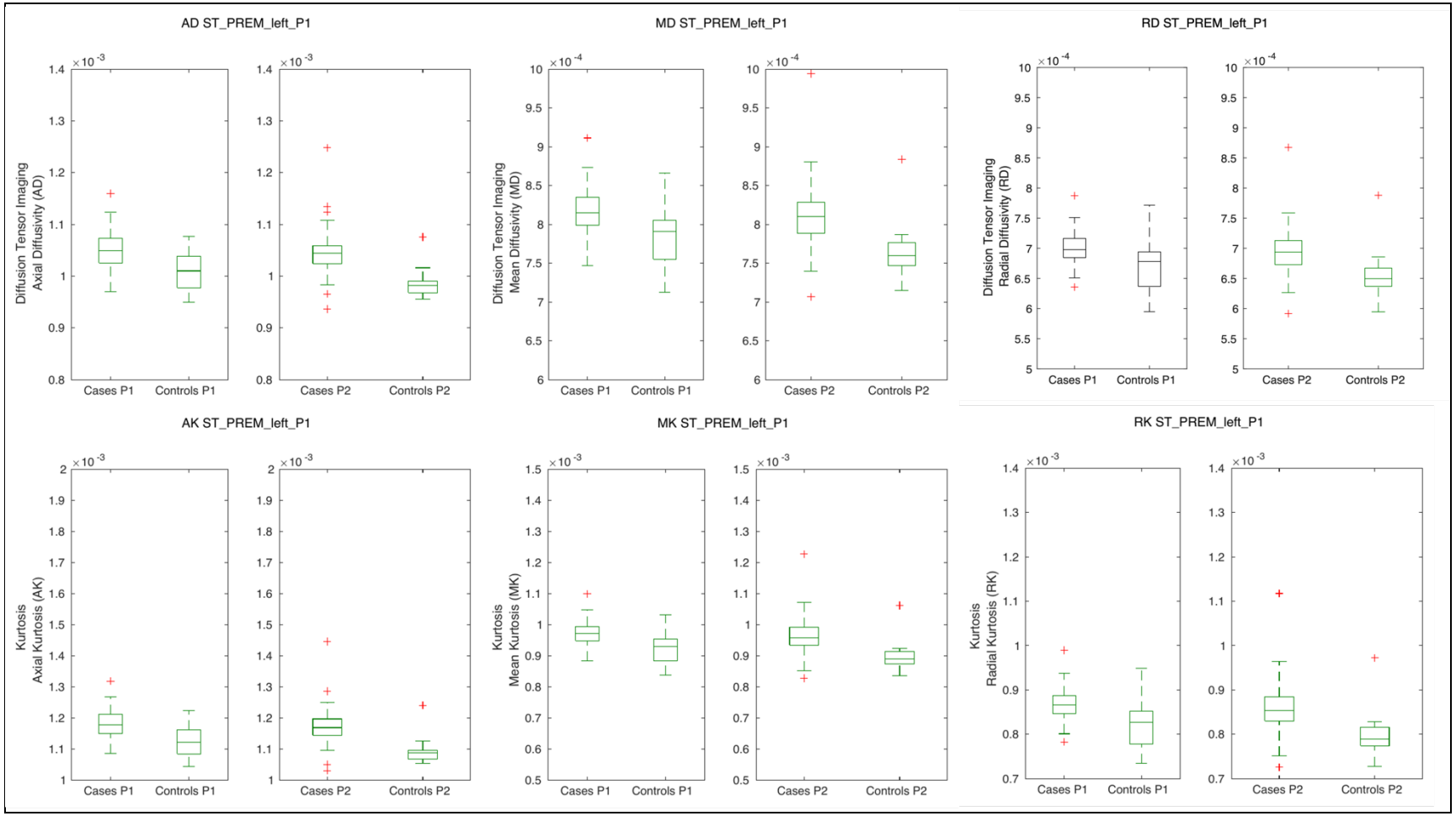

Figure A.73- Boxplots for t-test results in the Striato-premotor (left)

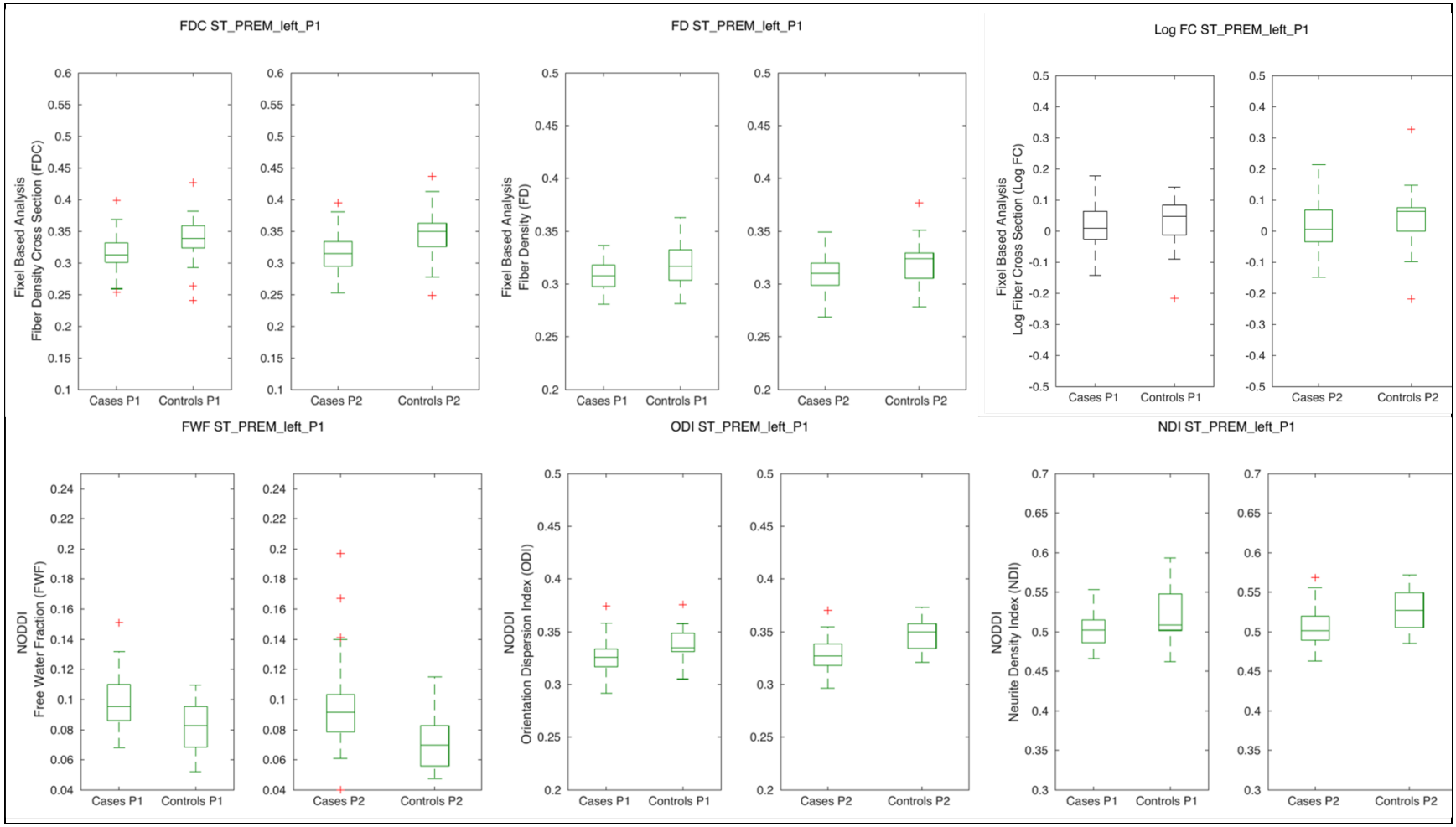

Figure A.74- Boxplots for t-test results in the Striato-premotor (left)

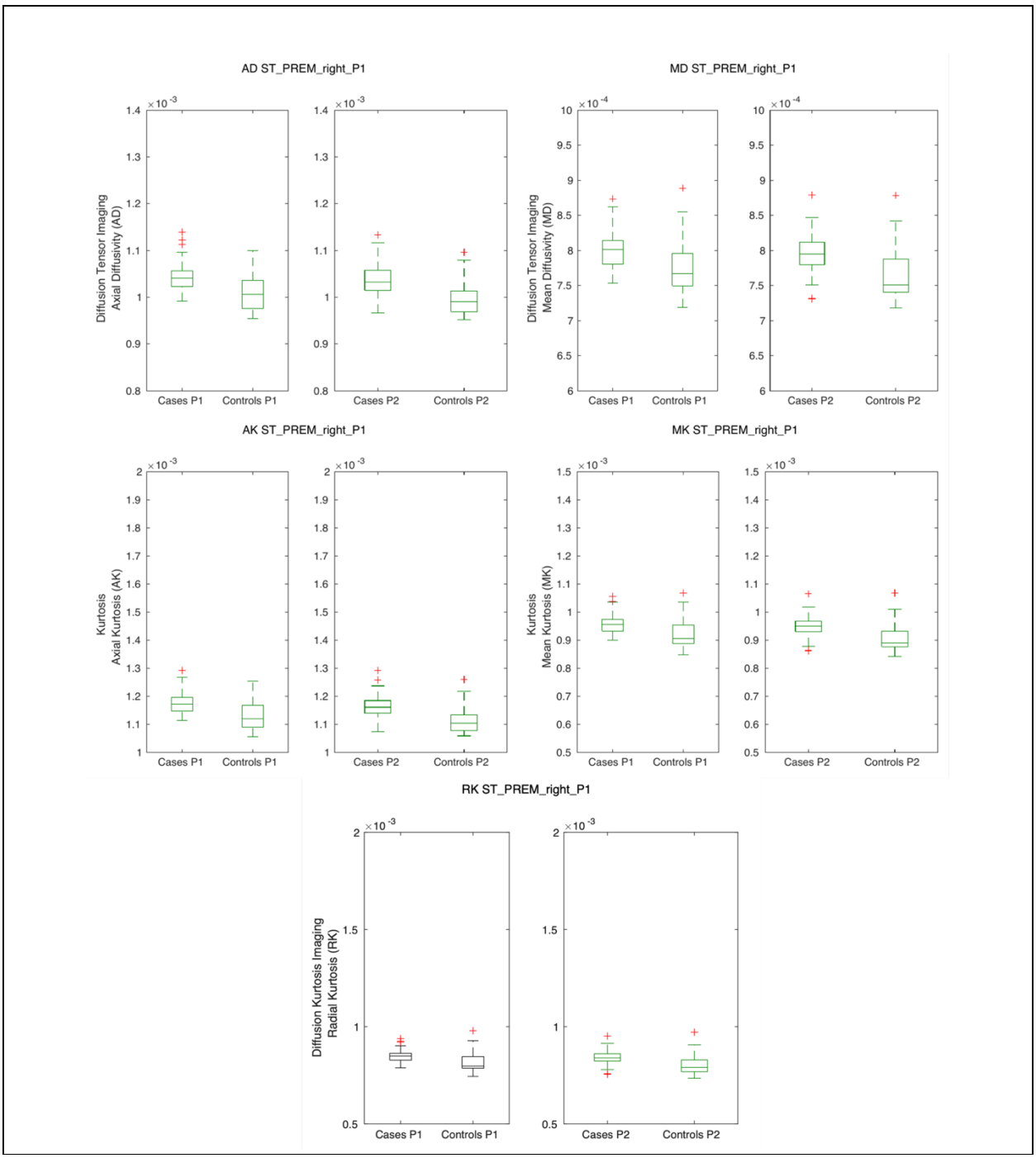

Figure A.75- Boxplots for t-test results in the Striato-premotor (right)

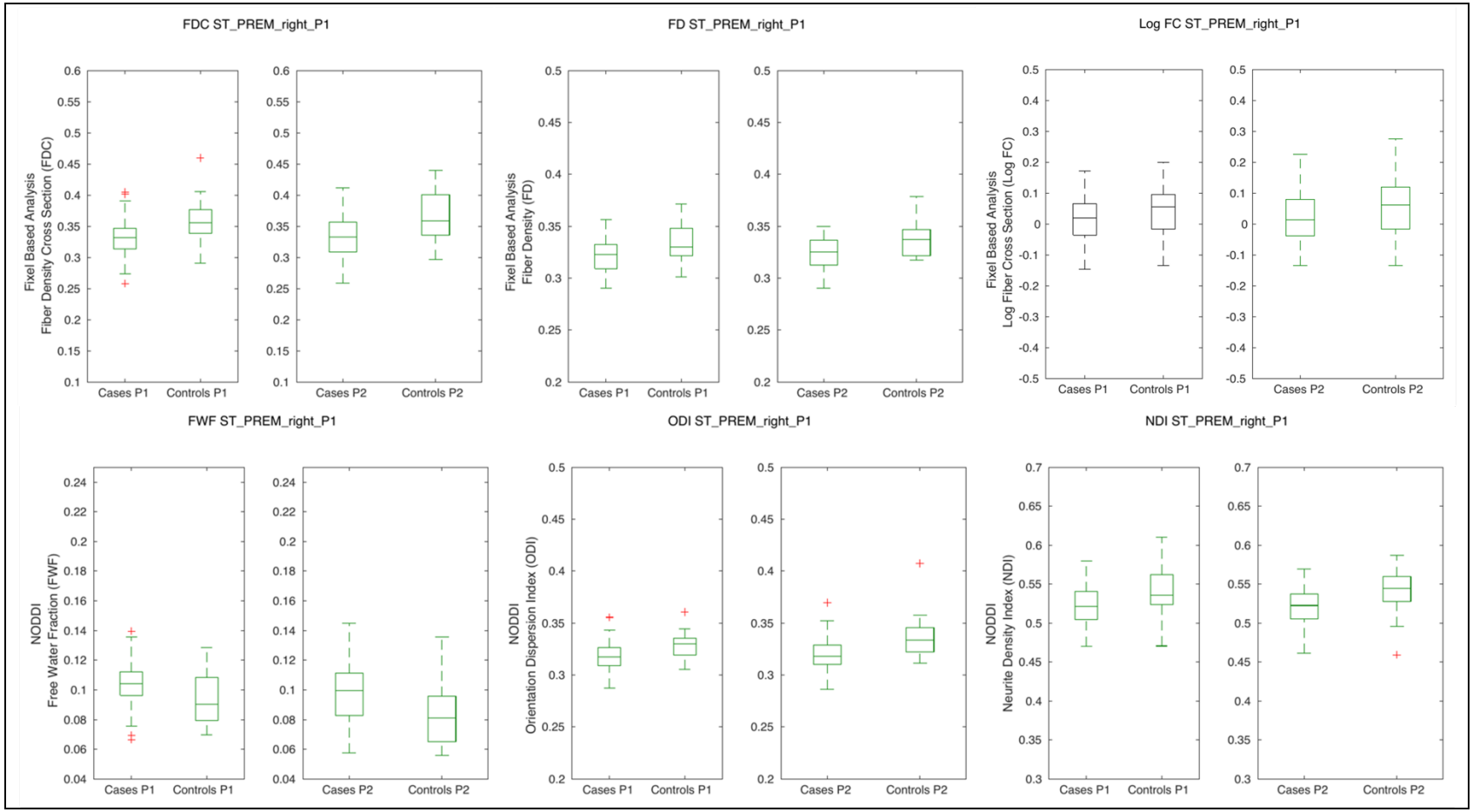

Figure A.76- Boxplots for t-test results in the Striato-premotor (right)

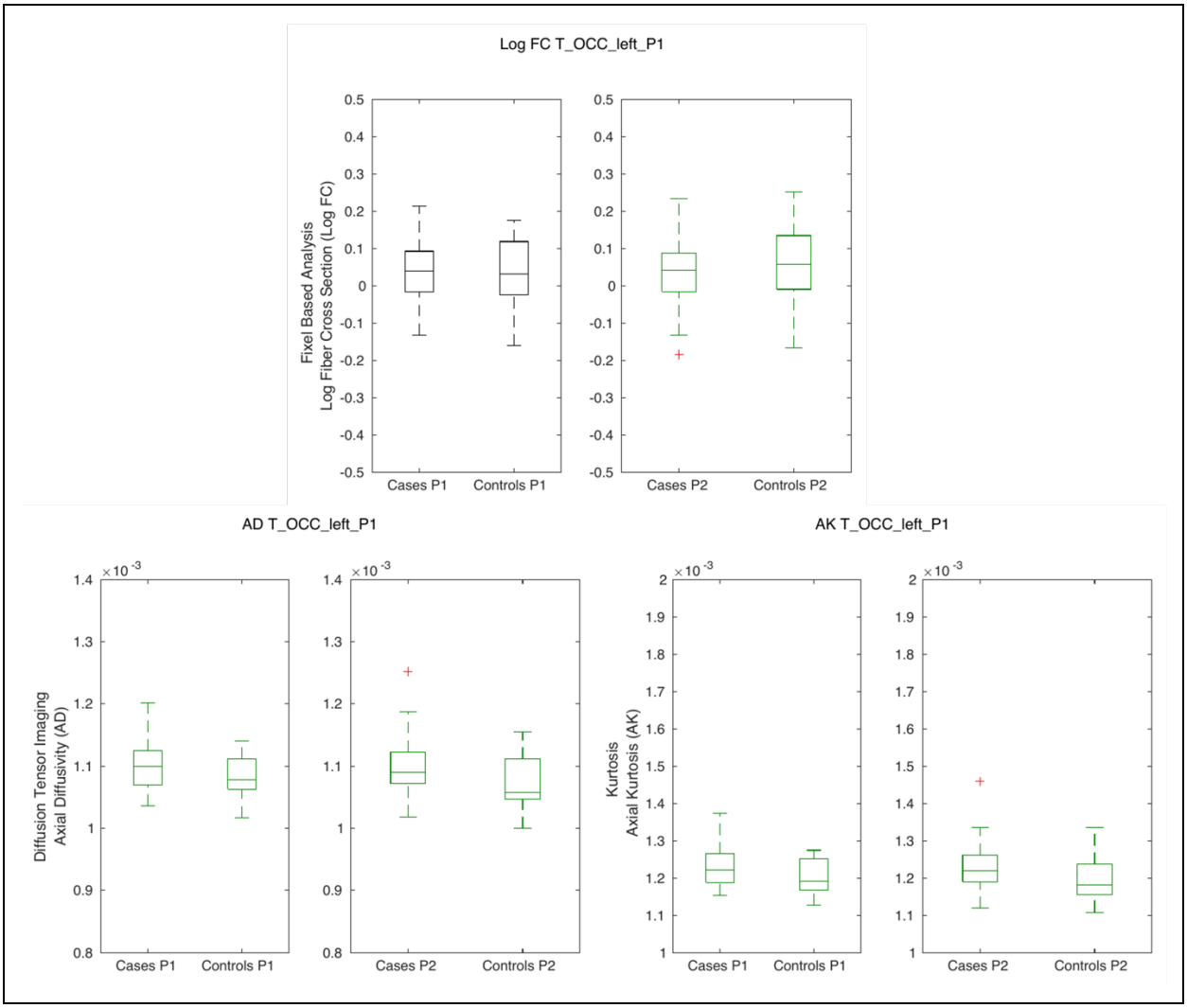

Figure A.77- Boxplots for t-test results in the Thalamo-occipital (left)

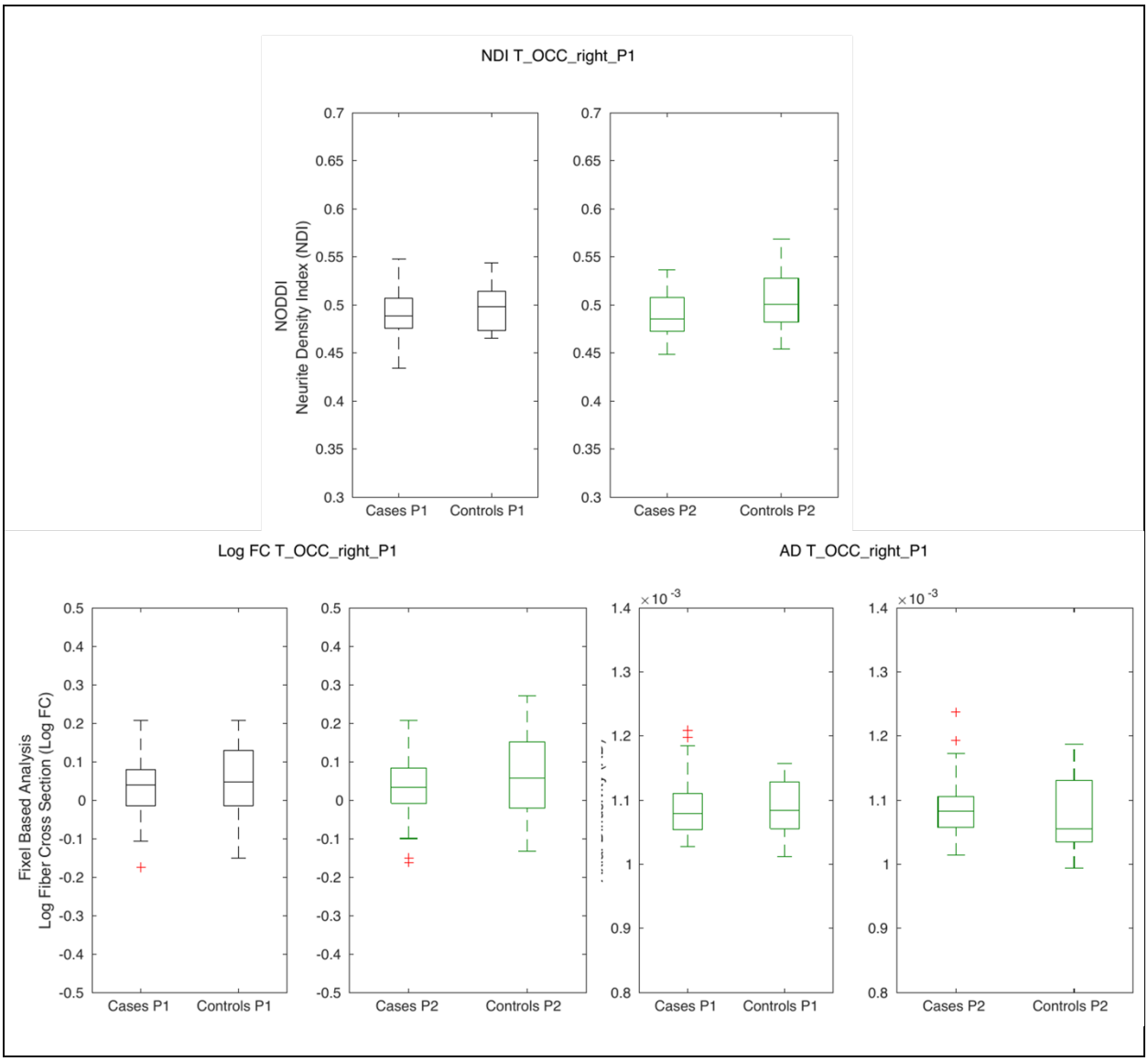

Figure A.78- Boxplots for t-test results in the Thalamo-occipital (right)

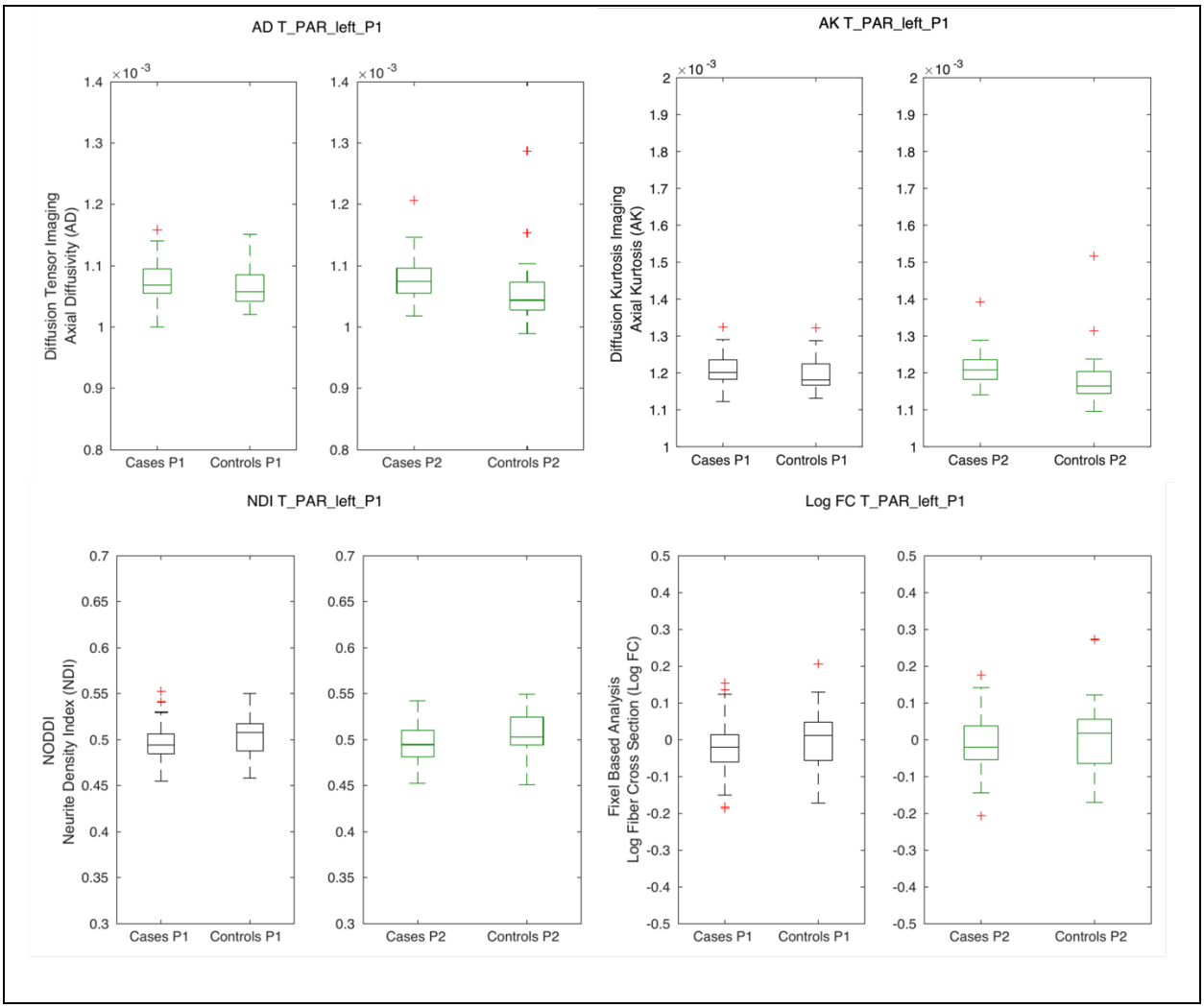

Figure A.79- Boxplots for t-test results in the Thalamo-parietal (left)

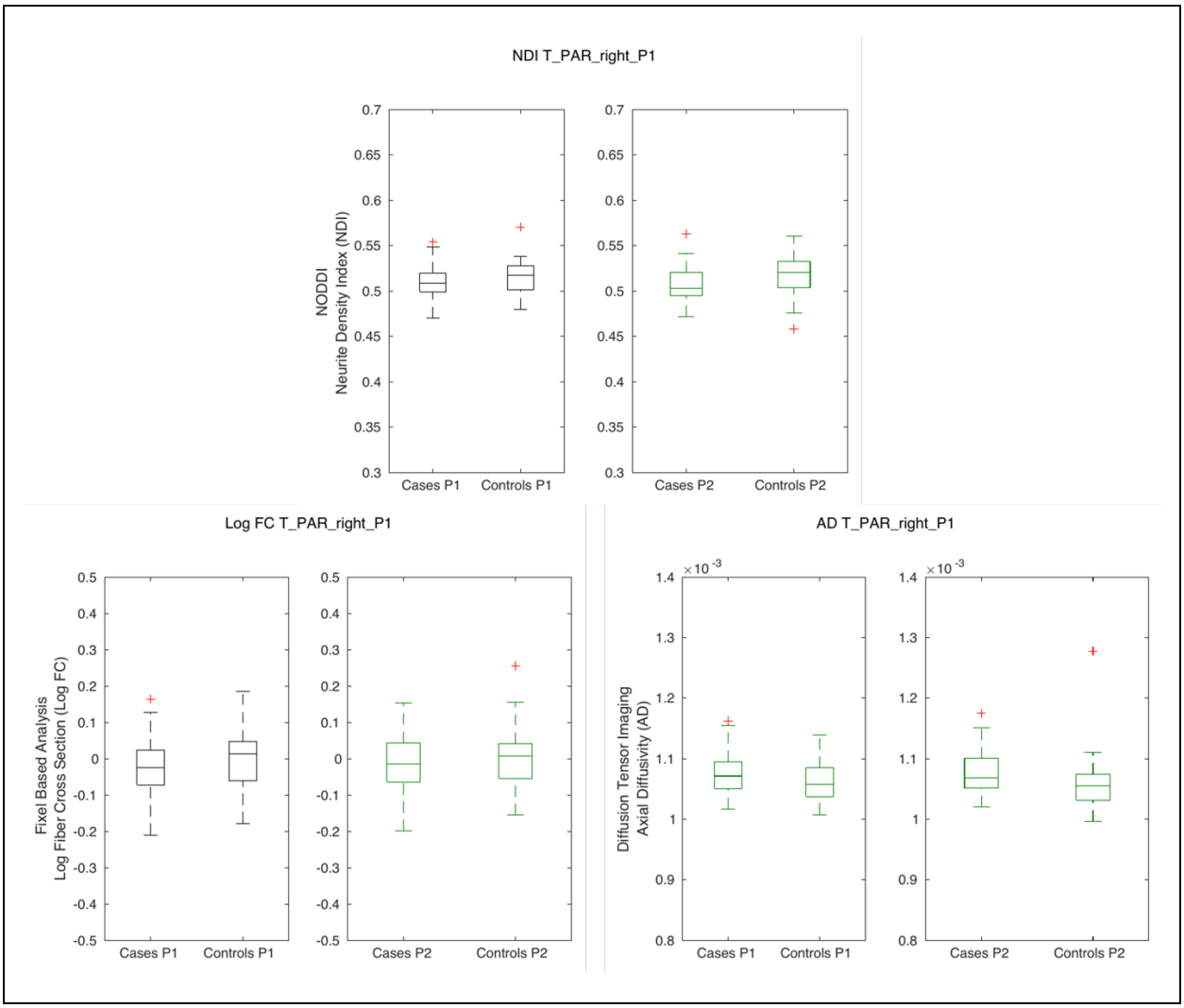

Figure A.80- Boxplots for t-test results in the Thalamo-parietal (right)

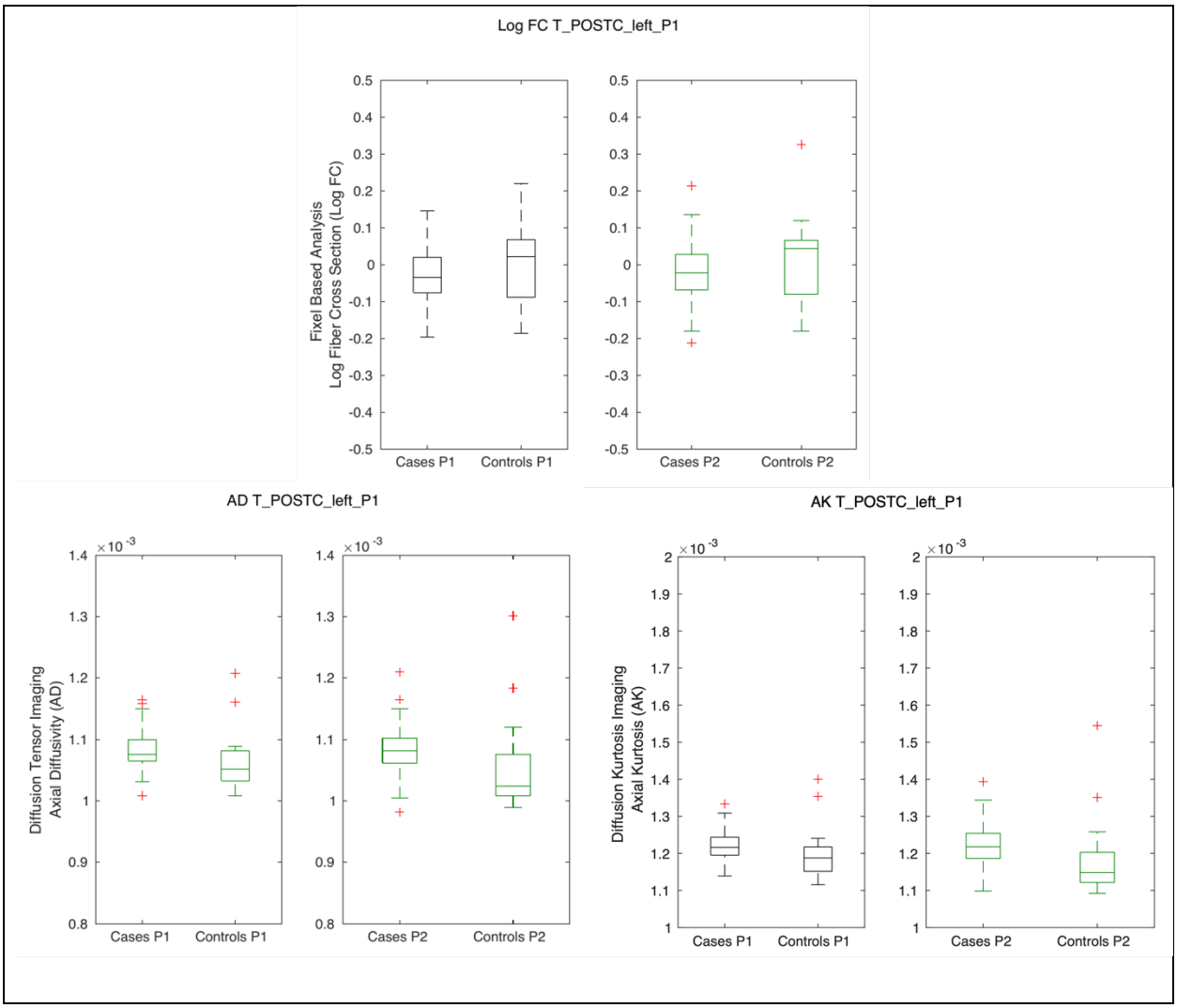

Figure A.81- Boxplots for t-test results in the Thalamo-postcentral (left)

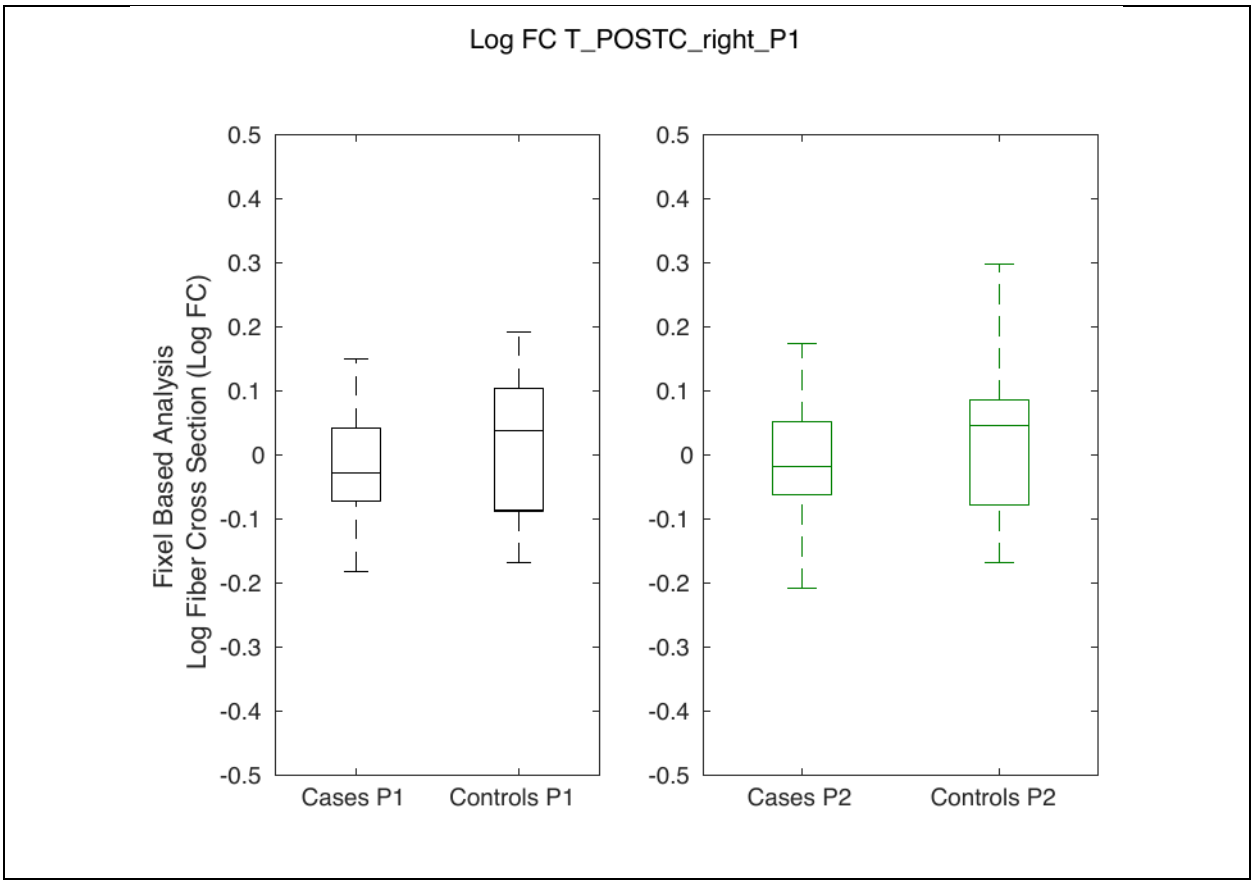

Figure A.82- Boxplots for t-test results in the Thalamo-postcentral (right)

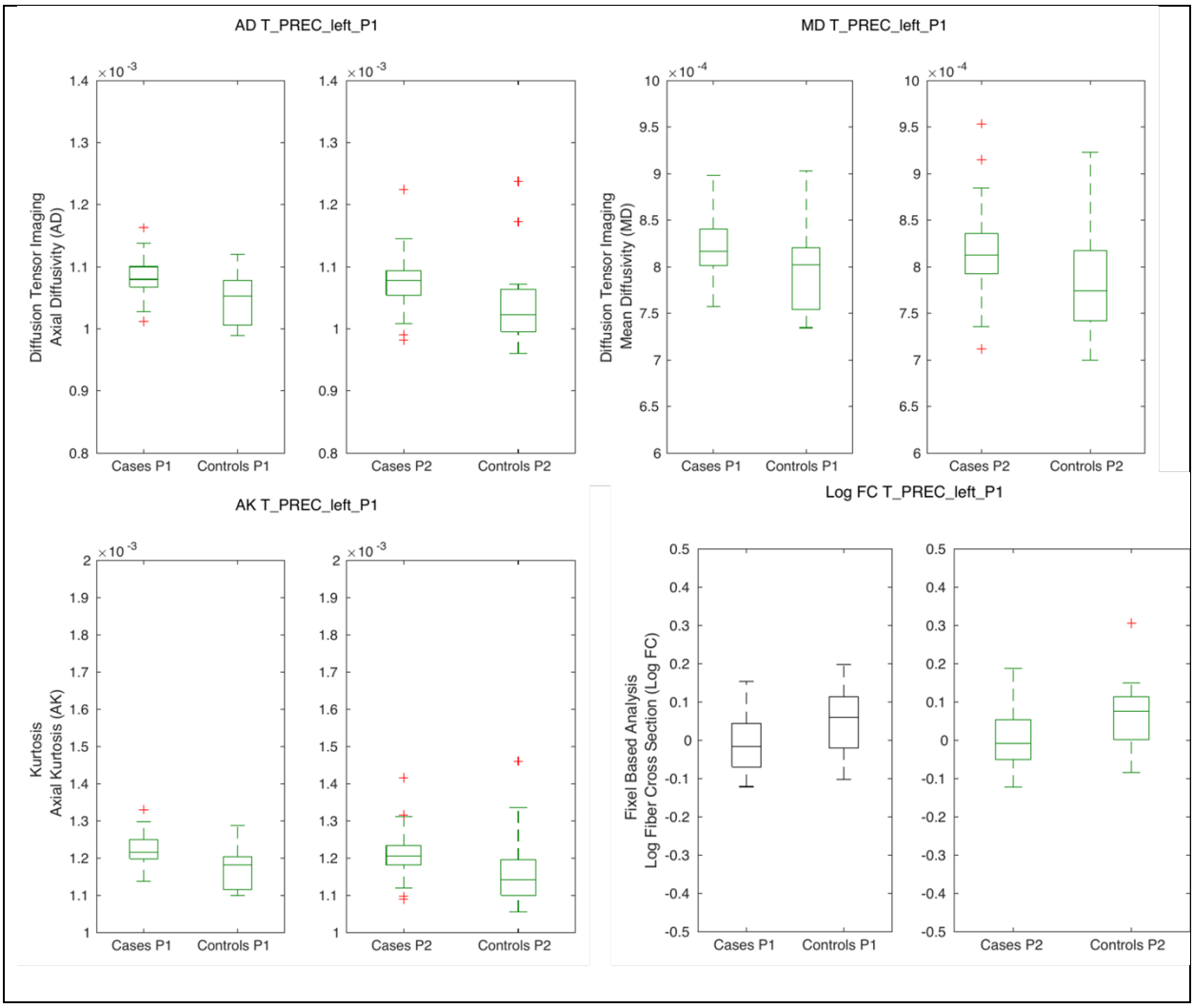

Figure A.83- Boxplots for t-test results in the Thalamo-precentral (left)

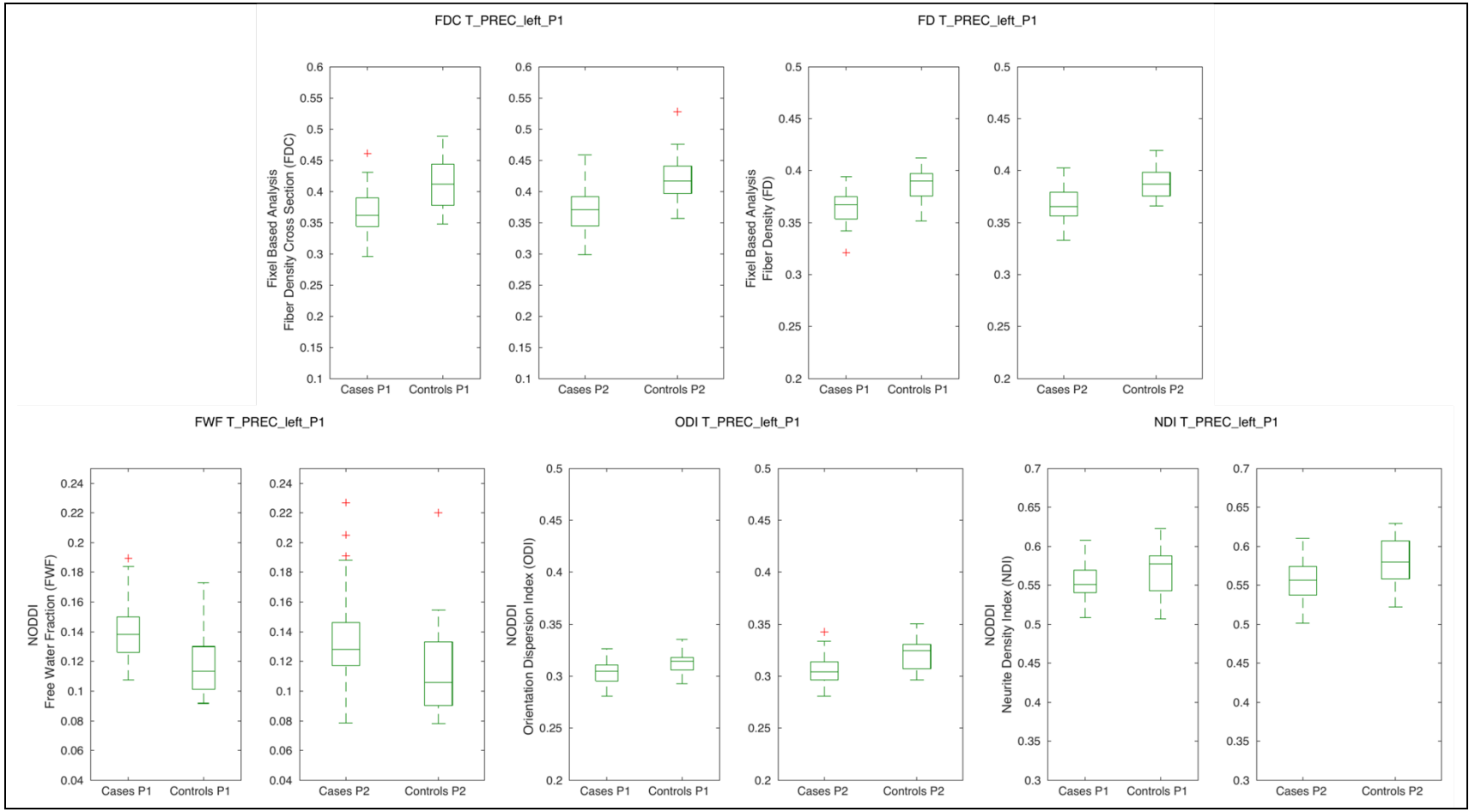

Figure A.84- Boxplots for t-test results in the Thalamo-precentral (left)

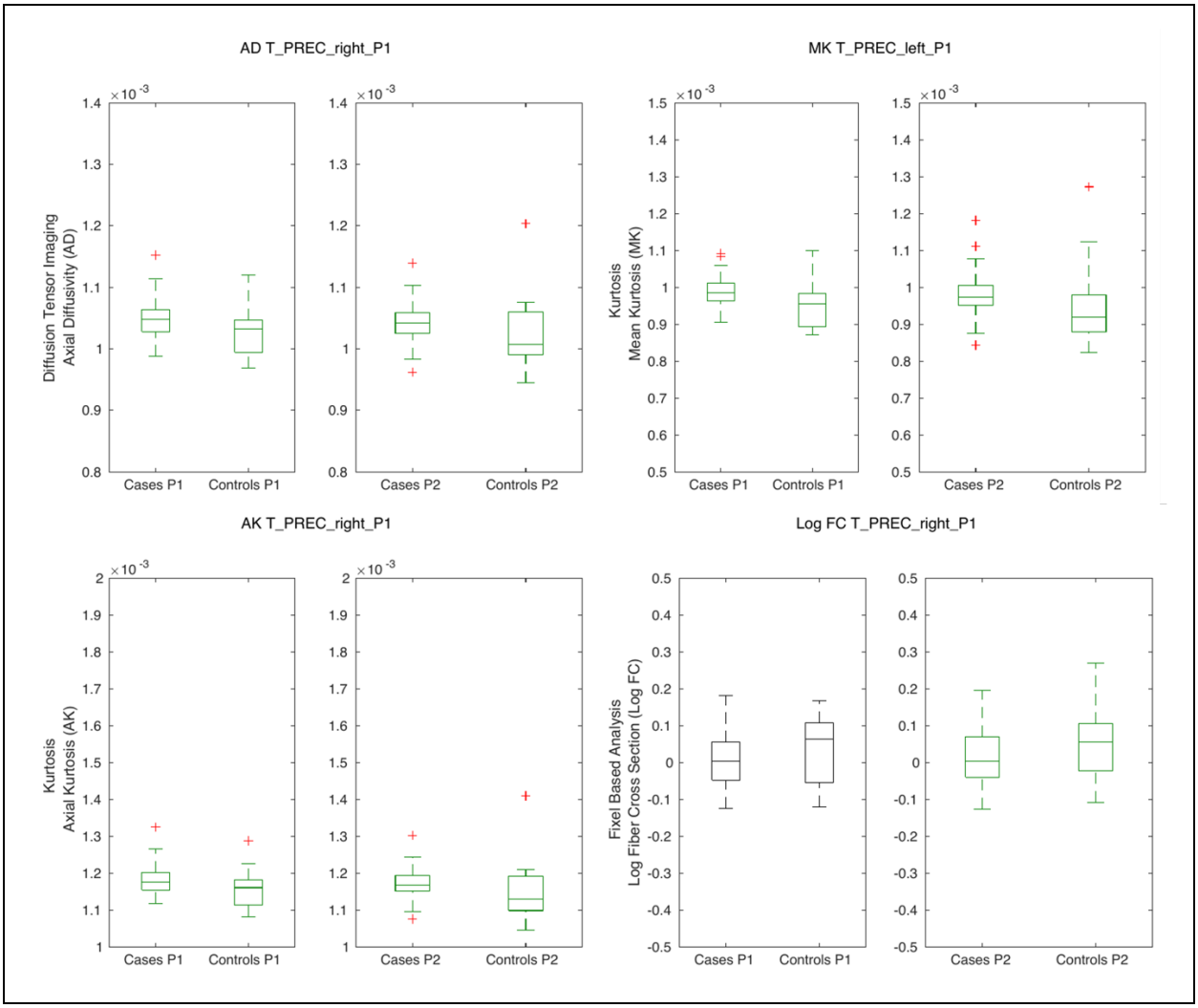

Figure A.85- Boxplots for t-test results in the Thalamo-precentral (right)

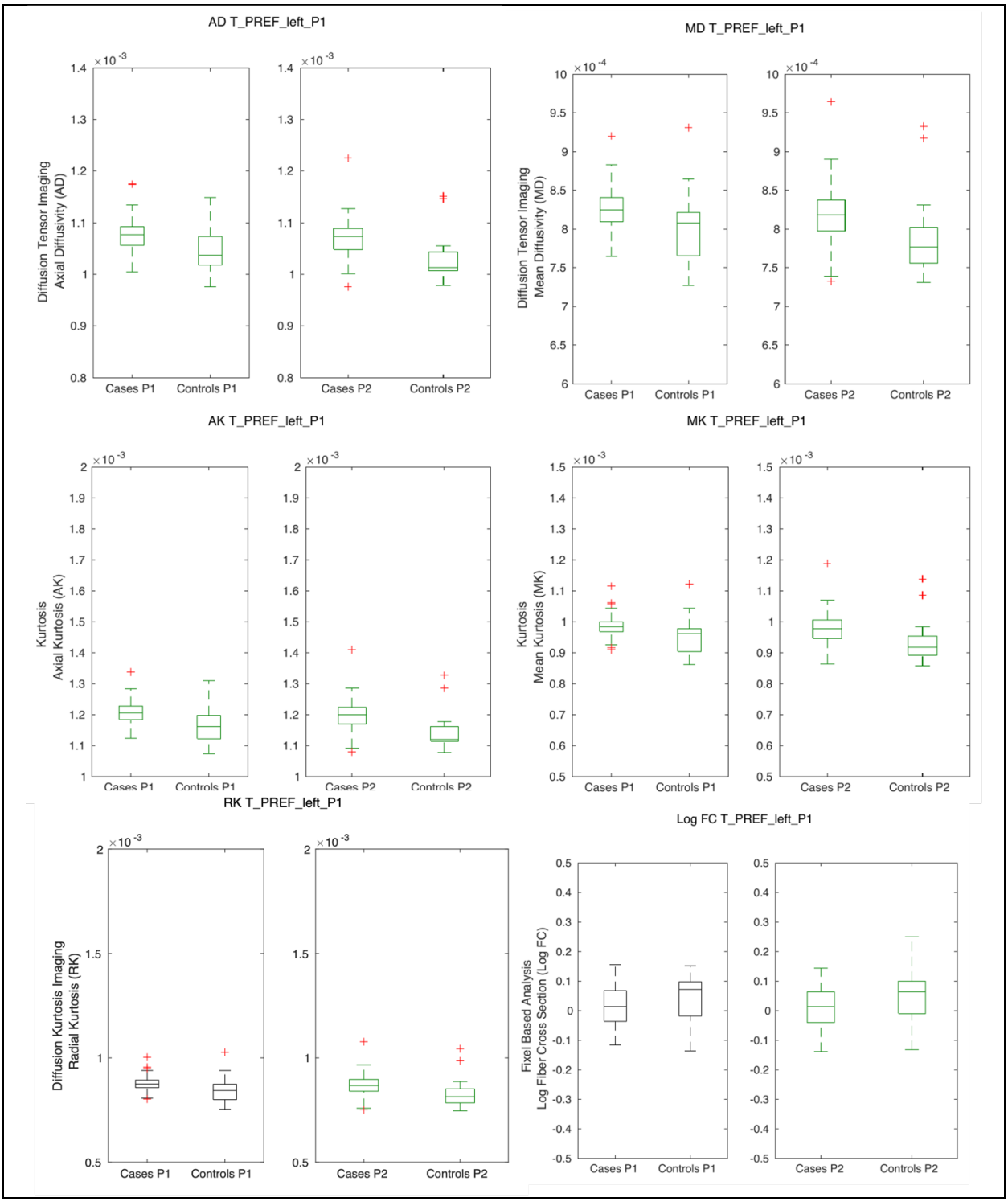

Figure A.86- Boxplots for t-test results in the Thalamo-prefrontal (left)

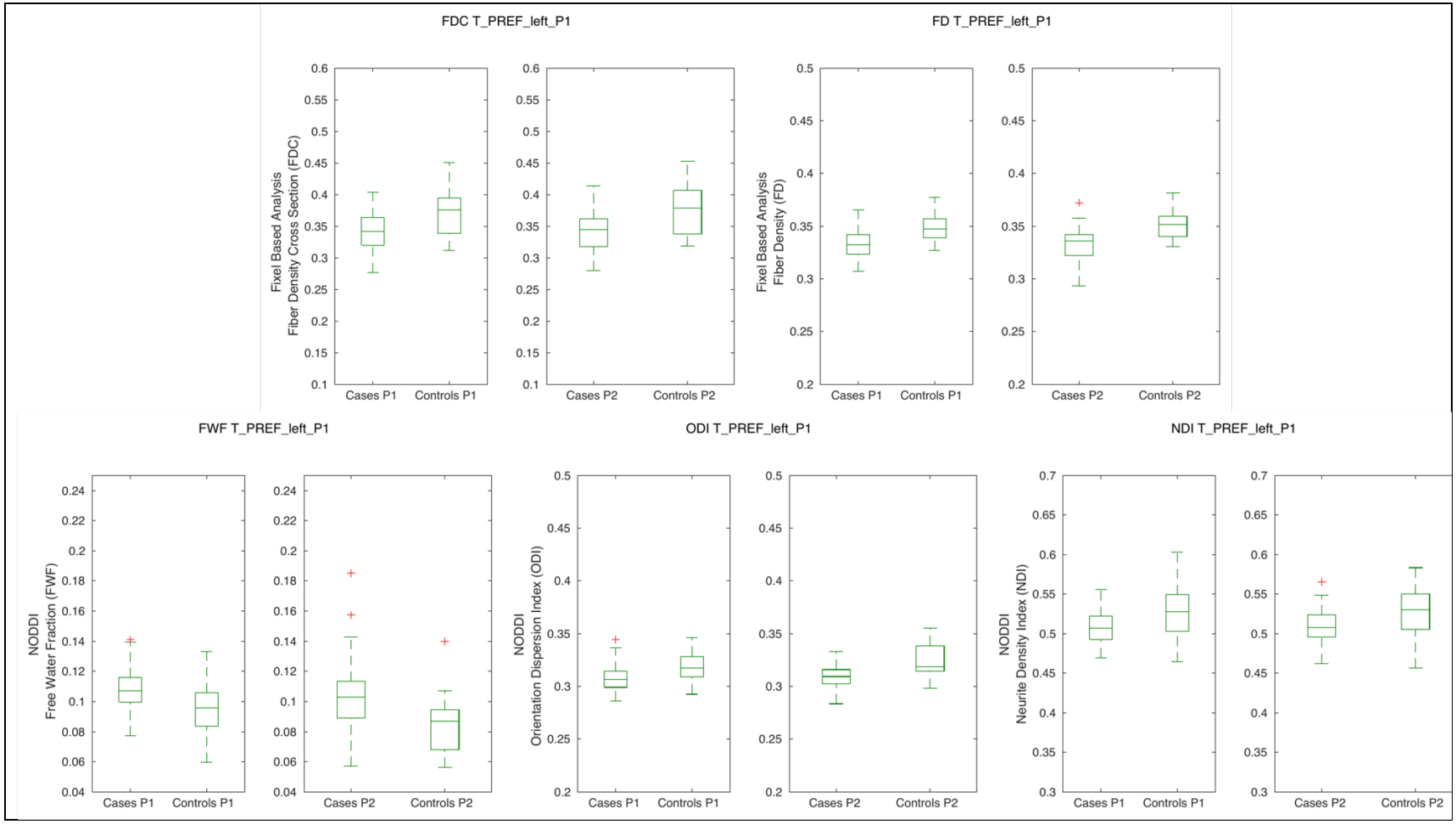

Figure A.87- Boxplots for t-test results in the Thalamo-prefrontal (left)

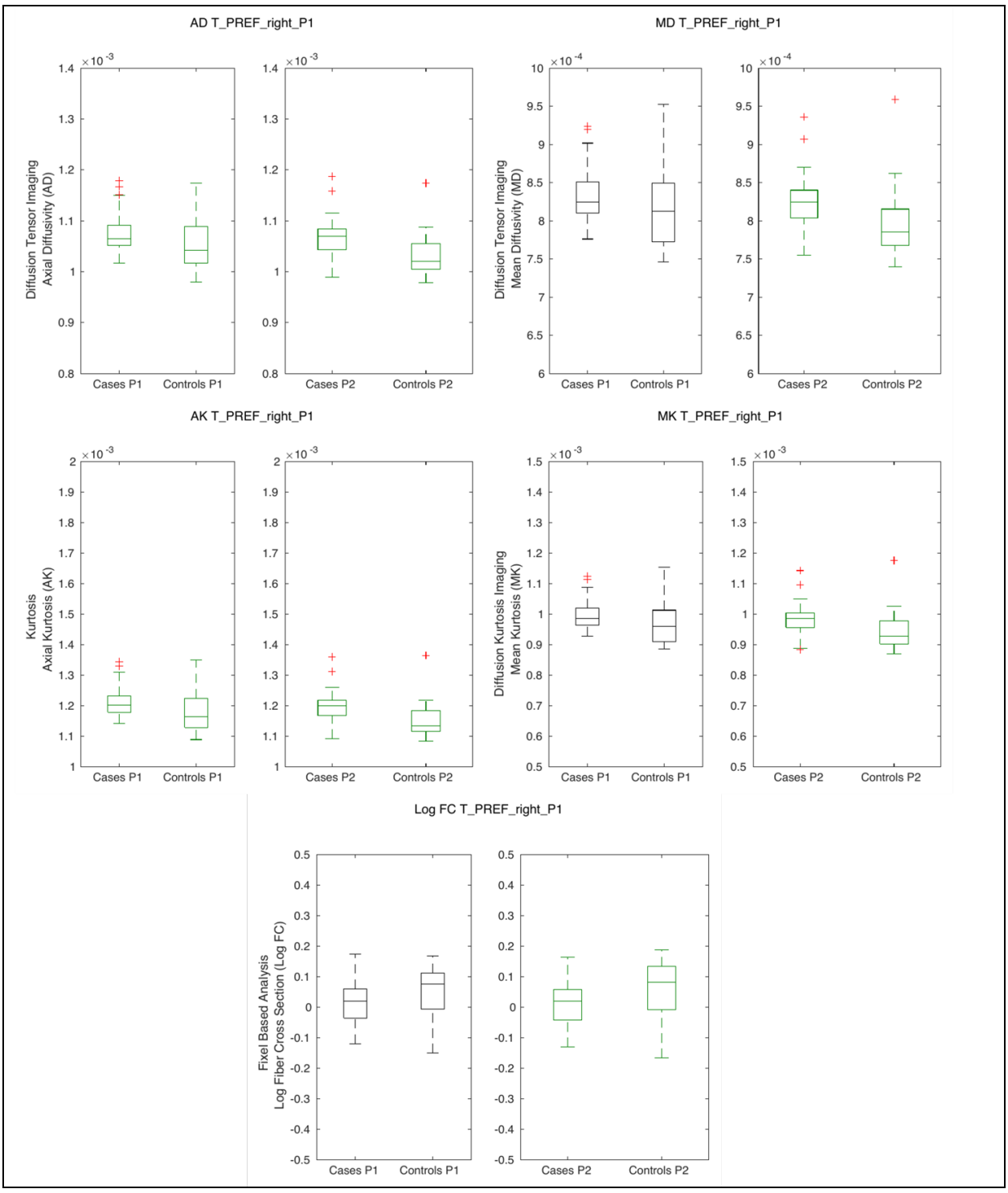

Figure A.88- Boxplots for t-test results in the Thalamo-prefrontal (right)

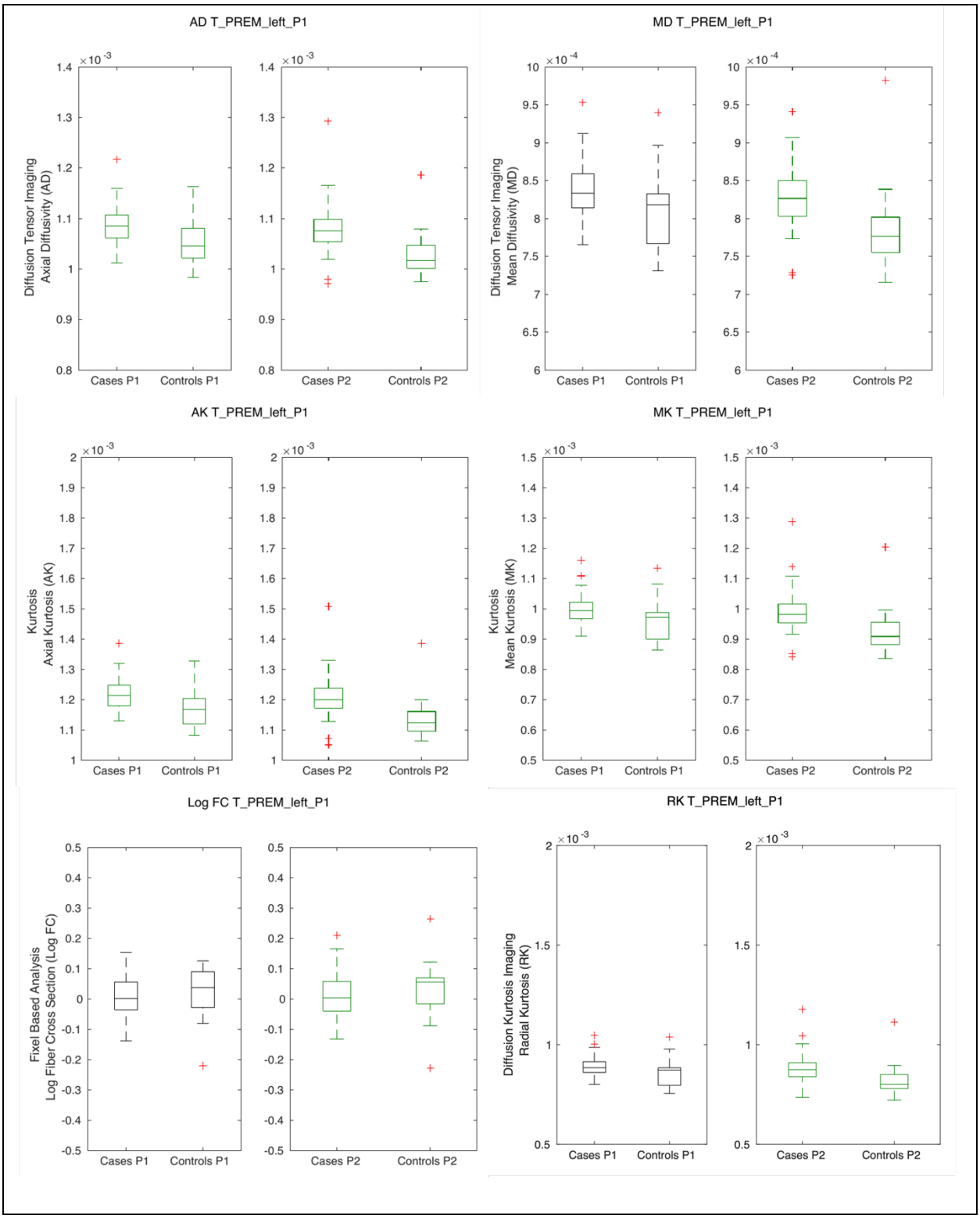

Figure A.89 - Boxplots for t-test results in the Thalamo-premotor (left)

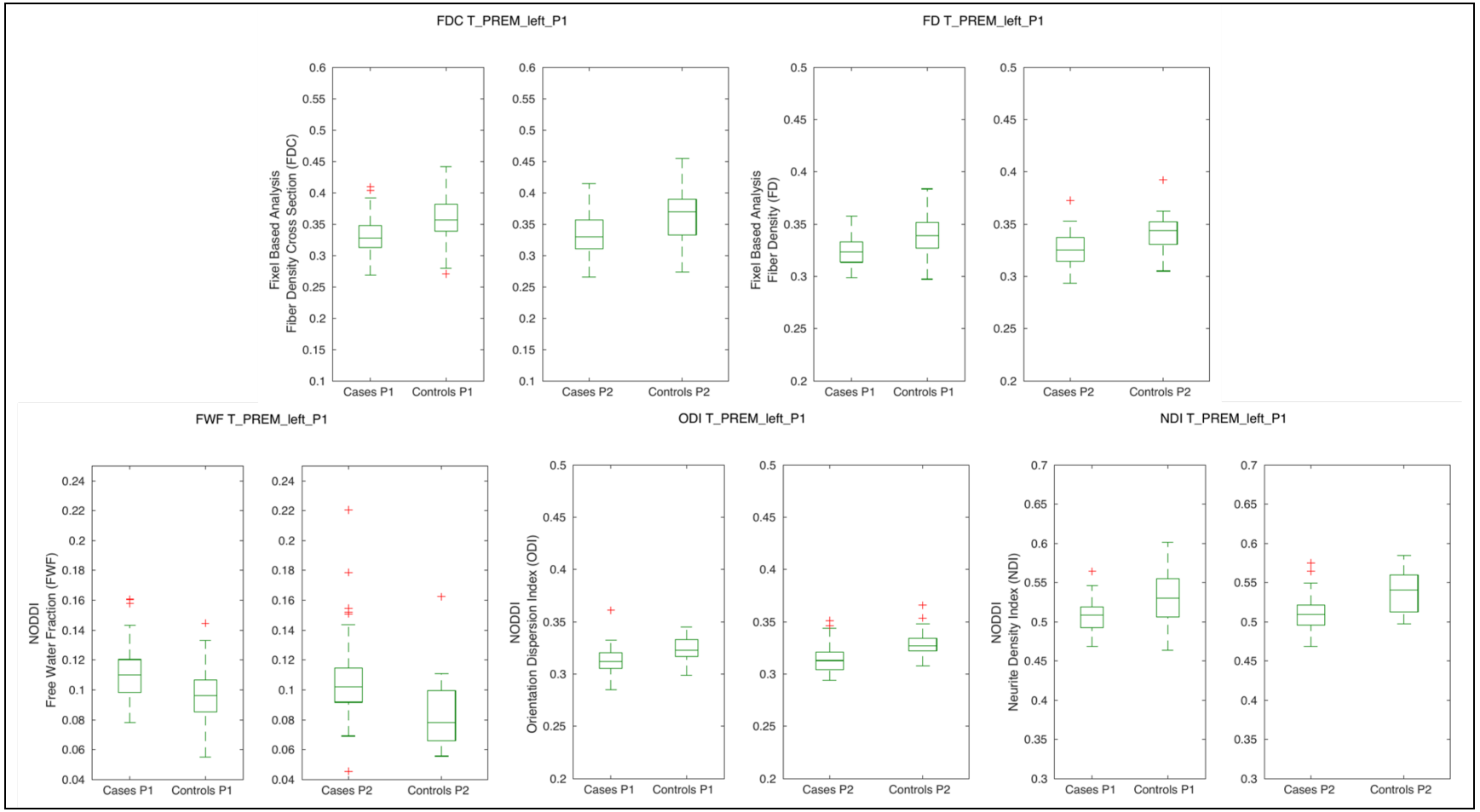

Figure A.90- Boxplots for t-test results in the Thalamo-premotor (left)

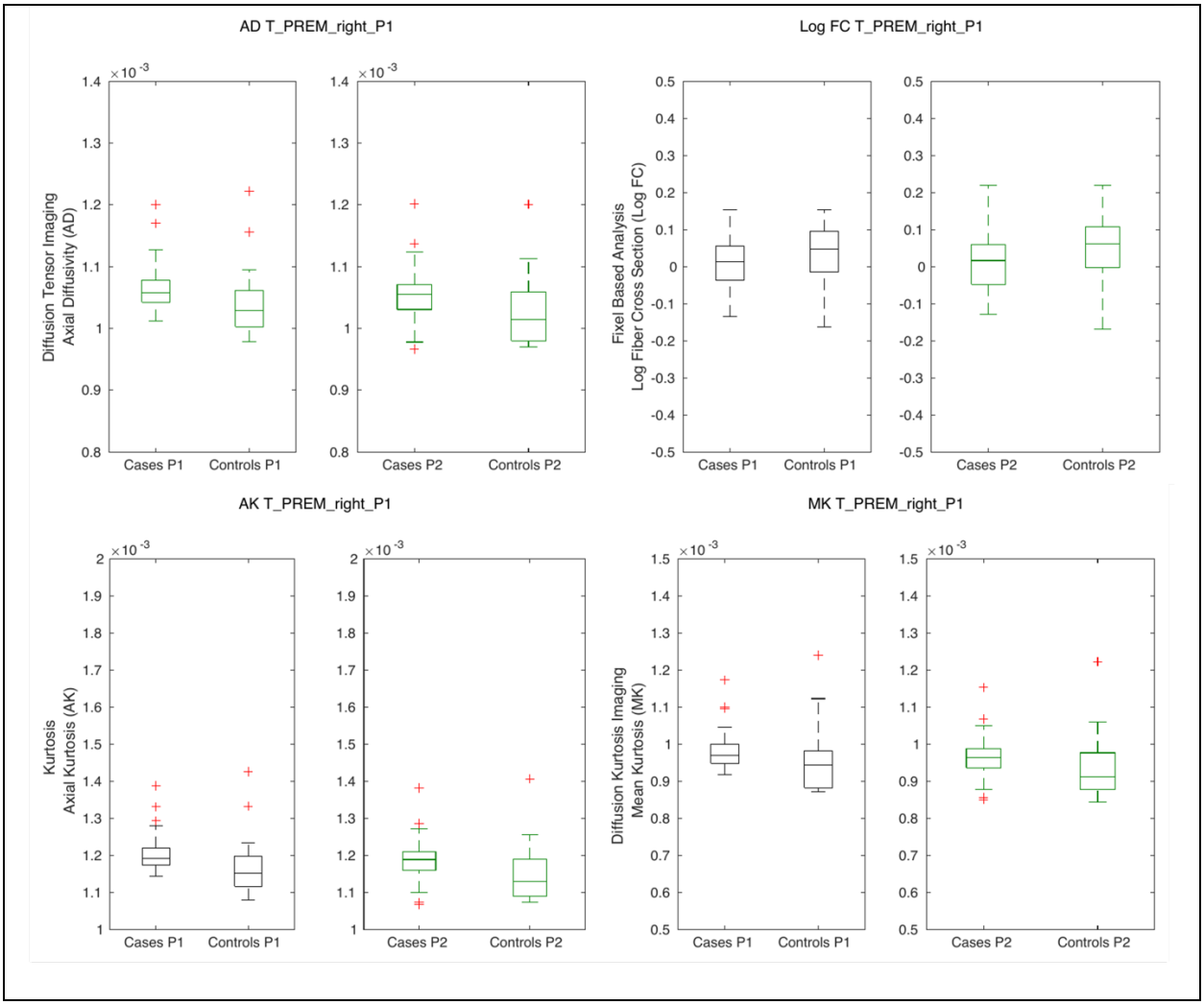

Figure A.91- Boxplots for t-test results in the Thalamo-premotor (right)

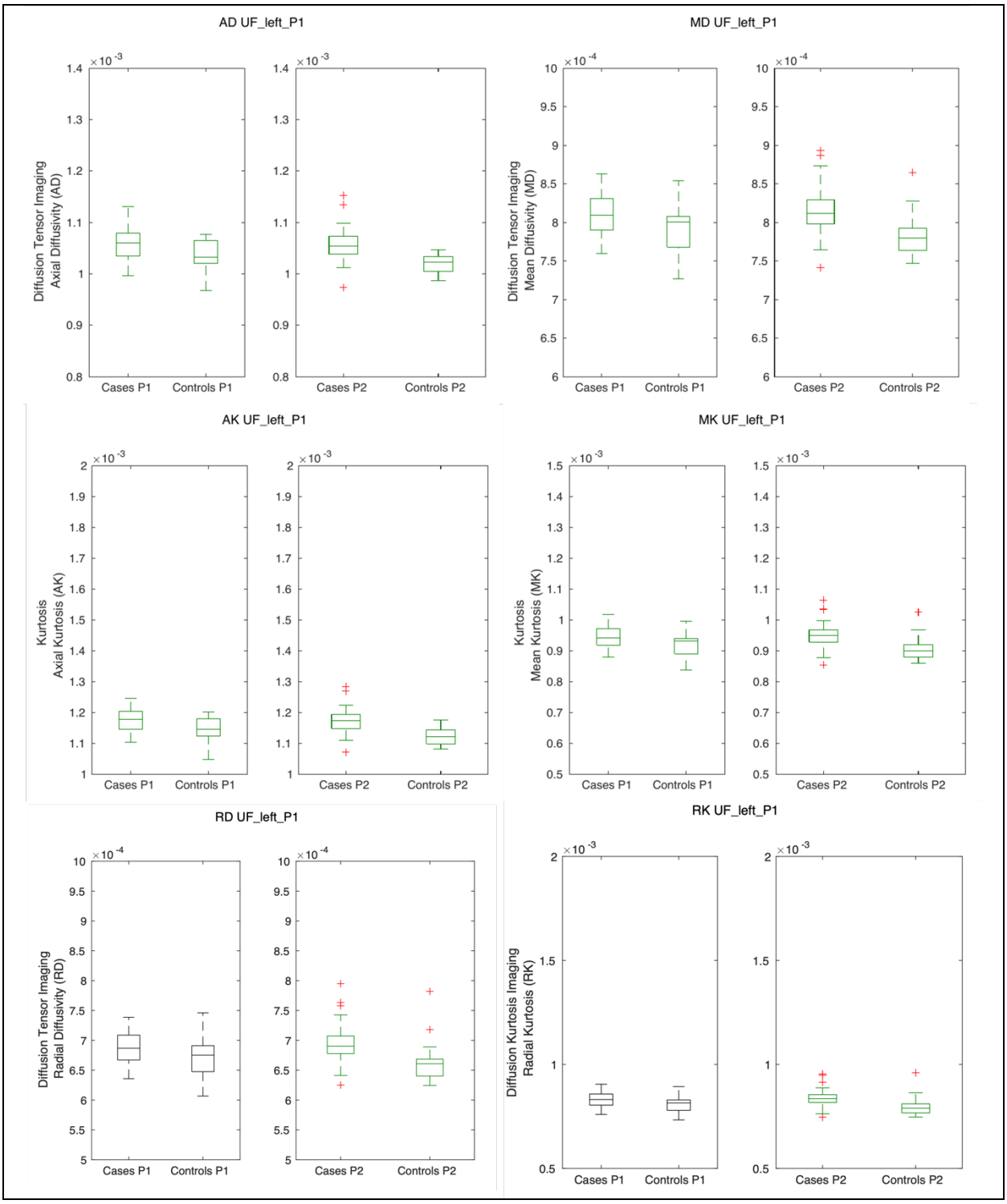

Figure A.92- Boxplots for t-test results in the Uncinate fascicle (left)

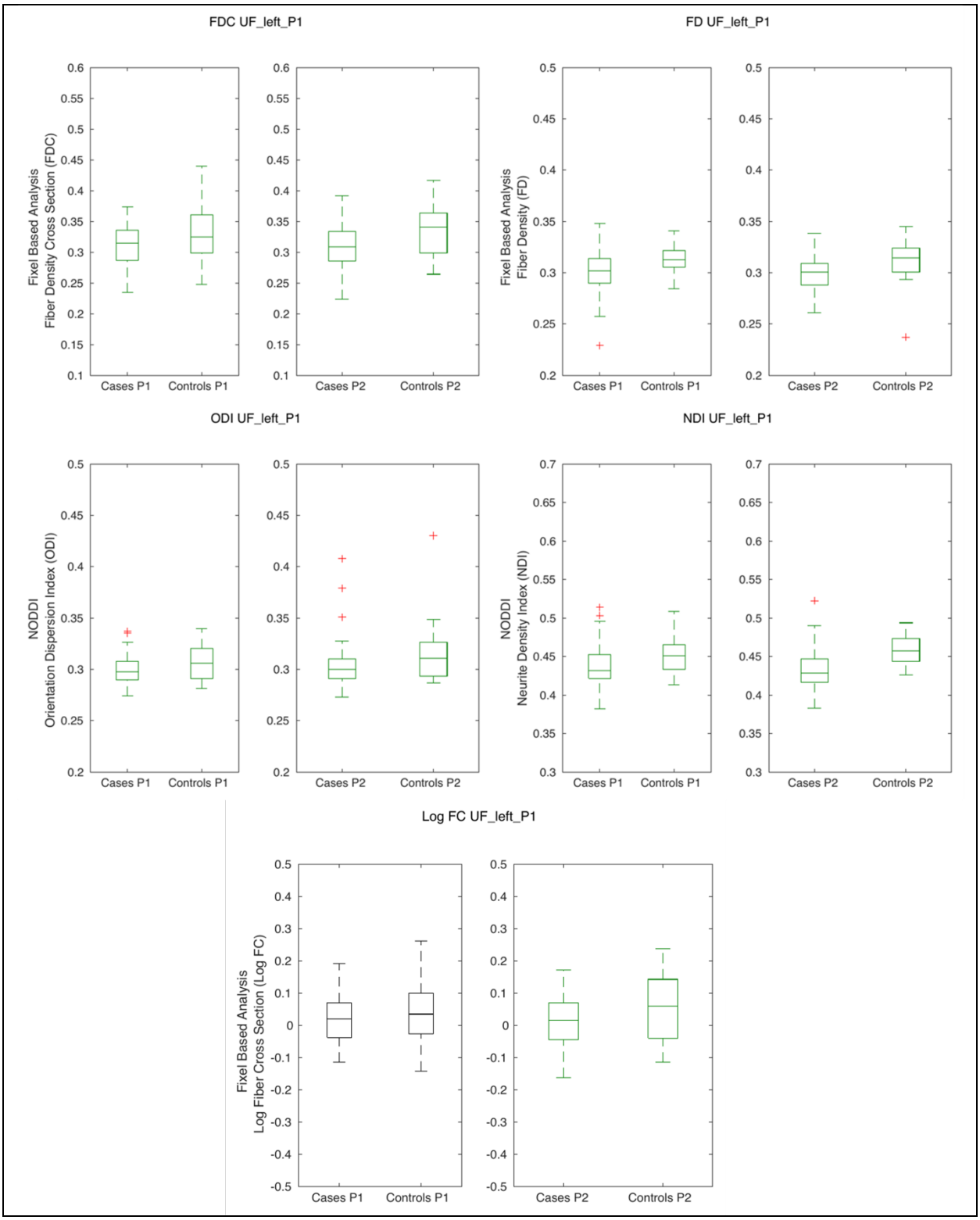

Figure A.93- Boxplots for t-test results in the Uncinate fascicle (left)

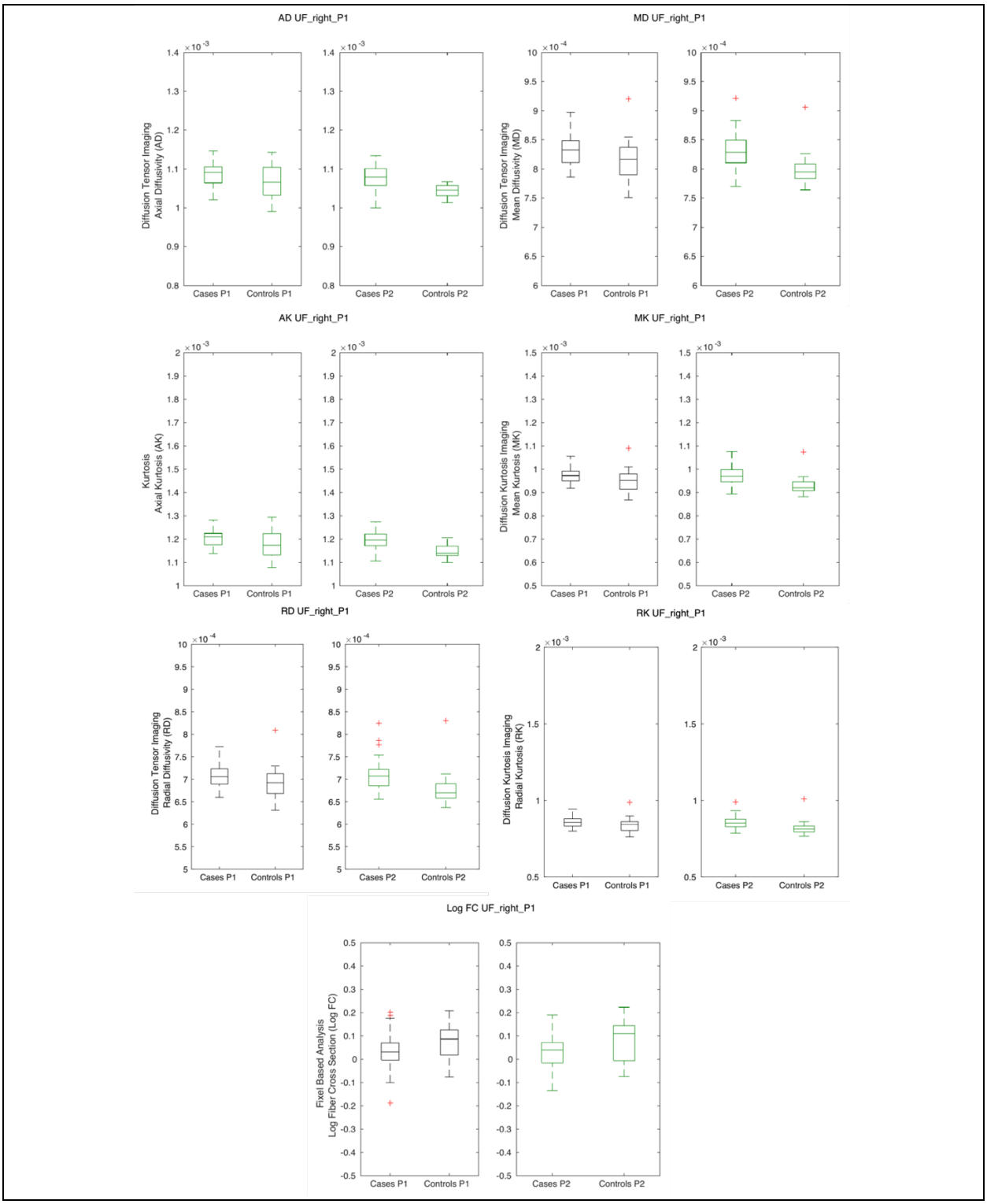

Figure A.94- Boxplots for t-test results in the Uncinate fascicle (right)

Table A.15 Results of Post Hoc Tract Specific Comparison of Diffusion Tensor Metric Fractional Anisotropy

	mTBI		Controls							
TractSeg Name	P1	P2	P1	P2	Percent Change mTBI %	Percent Change Controls %	t-score mTBI	q-value mTBI[1]	t-score controls	q-value controls
AF_left	0.256 ± 0.013	0.256 ± 0.011	0.259 ± 0.019	0.260 ± 0.016	-0.12 %	0.41 %	0.189	0.456	-0.319	0.995
AF_right	0.267 ± 0.011	0.266 ± 0.013	0.263 ± 0.016	0.261 ± 0.026	-0.45 %	-0.64 %	0.958	0.399	0.181	0.995
ATR_left	0.271 ± 0.011	0.271 ± 0.012	0.278 ± 0.020	0.280 ± 0.019	-0.03 %	0.74 %	0.037	0.49	-0.507	0.995
ATR_right	0.263 ± 0.010	0.264 ± 0.012	0.266 ± 0.016	0.269 ± 0.018	0.3 %	1.3 %	-0.466	0.414	-0.760	0.995
CA	0.270 ± 0.017	0.267 ± 0.022	0.287 ± 0.024	0.286 ± 0.030	-1.11 %	-0.4 %	1.164	0.399	0.125	0.995
CC_1	0.343 ± 0.023	0.336 ± 0.032	0.351 ± 0.023	0.343 ± 0.056	-1.88 %	-2.17 %	1.895	0.399	0.443	0.995
CC_2	0.296 ± 0.014	0.295 ± 0.013	0.298 ± 0.023	0.298 ± 0.025	-0.27 %	-0.03 %	0.663	0.402	-0.150	0.995
CC_3	0.291 ± 0.017	0.290 ± 0.021	0.295 ± 0.035	0.295 ± 0.034	-0.47 %	0.16 %	0.511	0.414	-0.199	0.995
CC_4	0.307 ± 0.018	0.305 ± 0.019	0.305 ± 0.032	0.307 ± 0.031	-0.63 %	0.83 %	0.857	0.399	-0.380	0.995
CC_5	0.318 ± 0.017	0.314 ± 0.020	0.313 ± 0.033	0.315 ± 0.035	-1.12 %	0.6 %	1.445	0.399	-0.239	0.995
CC_6	0.301 ± 0.016	0.300 ± 0.015	0.295 ± 0.023	0.293 ± 0.026	-0.25 %	-0.57 %	0.513	0.414	0.167	0.995
CC_7	0.308 ± 0.015	0.306 ± 0.016	0.304 ± 0.014	0.297 ± 0.037	-0.57 %	-2.3 %	1.229	0.399	0.742	0.995
CC	0.298 ± 0.013	0.297 ± 0.013	0.296 ± 0.022	0.294 ± 0.025	-0.27 %	-0.43 %	0.669	0.402	0.061	0.995
CG_left	0.278 ± 0.017	0.281 ± 0.021	0.279 ± 0.023	0.277 ± 0.027	1.02 %	-0.92 %	-0.698	0.402	0.253	0.995
CG_right	0.282 ± 0.019	0.283 ± 0.016	0.280 ± 0.025	0.277 ± 0.025	0.27 %	-1 %	-0.304	0.435	0.059	0.995
CST_left	0.344 ± 0.014	0.345 ± 0.016	0.347 ± 0.025	0.351 ± 0.024	0.46 %	1.16 %	-0.848	0.399	-0.557	0.995
CST_right	0.352 ± 0.013	0.351 ± 0.017	0.350 ± 0.025	0.350 ± 0.031	-0.08 %	-0.01 %	0.287	0.435	0.052	0.995
FPT_left	0.333 ± 0.014	0.335 ± 0.015	0.334 ± 0.027	0.336 ± 0.027	0.52 %	0.65 %	-0.715	0.402	-0.259	0.995
FPT_right	0.333 ± 0.013	0.333 ± 0.014	0.331 ± 0.023	0.335 ± 0.025	0 %	1.01 %	0.192	0.456	-0.445	0.995
FX_left	0.288 ± 0.046	0.281 ± 0.045	0.295 ± 0.047	0.291 ± 0.055	-2.34 %	-1.51 %	1.431	0.399	0.181	0.995
FX_right	0.294 ± 0.045	0.289 ± 0.049	0.294 ± 0.048	0.300 ± 0.052	-1.54 %	1.95 %	1.048	0.399	-1.168	0.995
ICP_left	0.275 ± 0.025	0.273 ± 0.030	0.260 ± 0.029	0.263 ± 0.044	-0.62 %	1.02 %	1.003	0.399	-0.202	0.995
ICP_right	0.258 ± 0.016	0.255 ± 0.017	0.242 ± 0.025	0.248 ± 0.031	-1.4 %	2.42 %	2.396	0.399	-0.555	0.995
IFO_left	0.283 ± 0.011	0.281 ± 0.011	0.285 ± 0.013	0.279 ± 0.029	-0.51 %	-1.94 %	1.292	0.399	0.664	0.995
IFO_right	0.281 ± 0.010	0.279 ± 0.012	0.281 ± 0.011	0.279 ± 0.027	-0.47 %	-0.63 %	1.460	0.399	0.340	0.995
ILF_left	0.277 ± 0.011	0.275 ± 0.017	0.283 ± 0.012	0.274 ± 0.032	-0.7 %	-3.15 %	1.039	0.399	1.151	0.995
ILF_right	0.273 ± 0.011	0.272 ± 0.019	0.278 ± 0.013	0.272 ± 0.033	-0.66 %	-2.31 %	1.266	0.399	0.730	0.995

Table A.15 (cont'd)

	mTBI		Controls							
TractSeg Name	P1	P2	P1	P2	Percent Change mTBI %	Percent Change Controls %	t-score mTBI	q-value mTBI′	t-score controls	q-value controls
MCP	0.301 ± 0.015	0.299 ± 0.016	0.291 ± 0.029	0.291 ± 0.037	-0.87 %	0.02 %	1.749	0.399	0.026	0.995
MLF_left	0.265 ± 0.014	0.266 ± 0.014	0.262 ± 0.018	0.264 ± 0.016	0.39 %	0.57 %	-0.431	0.414	-0.357	0.995
MLF_right	0.272 ± 0.013	0.271 ± 0.014	0.266 ± 0.020	0.264 ± 0.023	-0.35 %	-0.71 %	0.718	0.402	0.166	0.995
OR_left	0.293 ± 0.014	0.292 ± 0.014	0.294 ± 0.009	0.289 ± 0.035	-0.43 %	-1.73 %	0.983	0.399	0.683	0.995
OR_right	0.300 ± 0.013	0.300 ± 0.015	0.300 ± 0.015	0.297 ± 0.026	-0.26 %	-0.99 %	0.895	0.399	0.504	0.995
POPT_left	0.313 ± 0.013	0.313 ± 0.015	0.309 ± 0.022	0.311 ± 0.022	0.14 %	0.84 %	-0.078	0.488	-0.345	0.995
POPT_right	0.327 ± 0.012	0.326 ± 0.016	0.323 ± 0.023	0.325 ± 0.024	-0.16 %	0.52 %	0.463	0.414	-0.104	0.995
SCP_left	0.313 ± 0.019	0.313 ± 0.023	0.308 ± 0.026	0.315 ± 0.034	-0.01 %	2.26 %	0.379	0.423	-0.644	0.995
SCP_right	0.313 ± 0.013	0.311 ± 0.015	0.302 ± 0.029	0.310 ± 0.028	-0.66 %	2.62 %	1.247	0.399	-0.736	0.995
SLF_III_left	0.264 ± 0.015	0.262 ± 0.016	0.263 ± 0.028	0.266 ± 0.022	-0.76 %	1.03 %	0.931	0.399	-0.472	0.995
SLF_III_right	0.273 ± 0.012	0.270 ± 0.020	0.263 ± 0.020	0.259 ± 0.038	-1.15 %	-1.43 %	1.294	0.399	0.351	0.995
SLF_II_left	0.250 ± 0.015	0.253 ± 0.016	0.249 ± 0.022	0.255 ± 0.027	1.16 %	2.16 %	-1.260	0.399	-0.826	0.995
SLF_II_right	0.252 ± 0.014	0.253 ± 0.016	0.247 ± 0.021	0.249 ± 0.018	0.5 %	0.96 %	-0.359	0.424	-0.463	0.995
SLF_I_left	0.243 ± 0.014	0.245 ± 0.018	0.238 ± 0.028	0.239 ± 0.023	1 %	0.68 %	-1.019	0.399	-0.287	0.995
SLF_I_right	0.257 ± 0.014	0.259 ± 0.019	0.252 ± 0.027	0.256 ± 0.022	0.97 %	1.65 %	-0.889	0.399	-0.540	0.995
STR_left	0.335 ± 0.017	0.336 ± 0.019	0.338 ± 0.024	0.338 ± 0.035	0.47 %	0.18 %	-0.636	0.402	-0.007	0.995
STR_right	0.339 ± 0.016	0.339 ± 0.020	0.339 ± 0.027	0.344 ± 0.023	-0.13 %	1.42 %	0.021	0.49	-0.937	0.995
ST_FO_left	0.285 ± 0.017	0.281 ± 0.018	0.295 ± 0.016	0.295 ± 0.033	-1.41 %	0.09 %	1.948	0.399	0.194	0.995
ST_FO_right	0.290 ± 0.017	0.288 ± 0.020	0.294 ± 0.016	0.293 ± 0.037	-0.75 %	-0.36 %	1.050	0.399	0.056	0.995
ST_OCC_left	0.294 ± 0.014	0.293 ± 0.013	0.294 ± 0.013	0.289 ± 0.036	-0.33 %	-1.62 %	0.850	0.399	0.568	0.995
ST_OCC_right	0.295 ± 0.013	0.294 ± 0.014	0.295 ± 0.015	0.292 ± 0.024	-0.33 %	-0.89 %	0.989	0.399	0.445	0.995
ST_PAR_left	0.280 ± 0.012	0.282 ± 0.016	0.278 ± 0.019	0.279 ± 0.018	0.46 %	0.68 %	-0.502	0.414	-0.438	0.995
ST_PAR_right	0.296 ± 0.012	0.295 ± 0.015	0.292 ± 0.019	0.293 ± 0.020	-0.22 %	0.21 %	0.620	0.402	-0.016	0.995
ST_POSTC_left	0.291 ± 0.014	0.292 ± 0.018	0.292 ± 0.019	0.296 ± 0.015	0.42 %	1.2 %	-0.563	0.413	-0.773	0.995
ST_POSTC_right	0.308 ± 0.014	0.306 ± 0.020	0.307 ± 0.022	0.308 ± 0.023	-0.5 %	0.62 %	0.802	0.402	-0.138	0.995
ST_PREC_left	0.295 ± 0.012	0.296 ± 0.015	0.300 ± 0.019	0.301 ± 0.017	0.59 %	0.61 %	-1.127	0.399	-0.522	0.995
ST_PREC_right	0.305 ± 0.012	0.305 ± 0.017	0.305 ± 0.019	0.307 ± 0.019	-0.07 %	0.81 %	0.227	0.453	-0.403	0.995

Table A.15 (cont'd)

	mTBI		Controls							
TractSeg Name	P1	P2	P1	P2	Percent Change mTBI %	Percent Change Controls %	t-score mTBI	q-value mTBI[1]	t-score controls	q-value controls
ST_PREF_left	0.285 ± 0.012	0.286 ± 0.011	0.289 ± 0.020	0.288 ± 0.020	0.38 %	-0.36 %	-0.644	0.402	0.062	0.995
ST_PREF_right	0.283 ± 0.010	0.283 ± 0.011	0.284 ± 0.014	0.286 ± 0.019	-0.05 %	0.68 %	0.382	0.423	-0.465	0.995
ST_PREM_left	0.272 ± 0.011	0.274 ± 0.011	0.275 ± 0.022	0.277 ± 0.018	0.65 %	0.5 %	-1.035	0.399	-0.401	0.995
ST_PREM_right	0.285 ± 0.011	0.285 ± 0.013	0.285 ± 0.021	0.285 ± 0.024	0.24 %	0.16 %	-0.431	0.414	-0.054	0.995
T_OCC_left	0.289 ± 0.013	0.288 ± 0.014	0.291 ± 0.009	0.285 ± 0.034	-0.4 %	-1.79 %	0.971	0.399	0.717	0.995
T_OCC_right	0.295 ± 0.013	0.294 ± 0.014	0.294 ± 0.014	0.291 ± 0.025	-0.18 %	-0.98 %	0.771	0.402	0.508	0.995
T_PAR_left	0.280 ± 0.012	0.282 ± 0.016	0.277 ± 0.019	0.279 ± 0.020	0.45 %	0.71 %	-0.459	0.414	-0.385	0.995
T_PAR_right	0.296 ± 0.013	0.296 ± 0.016	0.292 ± 0.020	0.294 ± 0.020	0.13 %	0.5 %	-0.039	0.49	-0.257	0.995
T_POSTC_left	0.296 ± 0.014	0.297 ± 0.018	0.293 ± 0.025	0.299 ± 0.022	0.22 %	2.07 %	-0.162	0.46	-0.883	0.995
T_POSTC_right	0.311 ± 0.016	0.310 ± 0.023	0.305 ± 0.033	0.307 ± 0.029	-0.27 %	0.64 %	0.288	0.435	-0.193	0.995
T_PREC_left	0.300 ± 0.013	0.302 ± 0.017	0.304 ± 0.023	0.307 ± 0.022	0.66 %	1.05 %	-1.180	0.399	-0.634	0.995
T_PREC_right	0.304 ± 0.013	0.305 ± 0.018	0.302 ± 0.024	0.305 ± 0.020	0.47 %	0.96 %	-0.665	0.402	-0.532	0.995
T_PREF_left	0.287 ± 0.012	0.289 ± 0.013	0.292 ± 0.022	0.292 ± 0.022	0.55 %	0.11 %	-0.909	0.399	-0.147	0.995
T_PREF_right	0.277 ± 0.011	0.278 ± 0.013	0.278 ± 0.017	0.282 ± 0.016	0.4 %	1.23 %	-0.668	0.402	-0.969	0.995
T_PREM_left	0.283 ± 0.013	0.284 ± 0.015	0.287 ± 0.023	0.292 ± 0.021	0.48 %	1.63 %	-0.571	0.413	-0.888	0.995
T_PREM_right	0.286 ± 0.014	0.289 ± 0.016	0.288 ± 0.027	0.291 ± 0.023	0.92 %	1.01 %	-1.308	0.399	-0.542	0.995
UF_left	0.277 ± 0.014	0.273 ± 0.017	0.281 ± 0.019	0.277 ± 0.029	-1.6 %	-1.17 %	2.209	0.399	0.443	0.995
UF_right	0.275 ± 0.013	0.271 ± 0.018	0.277 ± 0.014	0.276 ± 0.033	-1.45 %	-0.37 %	2.048	0.399	0.141	0.995

Tables A.15- T-test results for comparisons of the automatically segmented tracts from TractSeg between timepoints within mTBI and control subjects.

[1]Significant values are marked with an asterisk (*) or <0.001

Table A.16 Results of Post Hoc Tract Specific Comparison of Diffusion Tensor Metric Mean Diffusivity

	mTBI		Controls							
TractSeg Name	P1	P2	P1	P2	Percent Change mTBI %	Percent Change Controls %	t-score mTBI	q-value mTBI[1]	t-score controls	q-value controls
AF_left	7.999e-04 ± 2.322e-05	7.943e-04 ± 2.429e-05	7.756e-04 ± 3.105e-05	7.686e-04 ± 3.164e-05	-0.7 %	-0.91 %	1.973	0.54	0.982	0.601
AF_right	7.868e-04 ± 2.222e-05	7.837e-04 ± 1.881e-05	7.764e-04 ± 2.585e-05	7.686e-04 ± 2.719e-05	-0.4 %	-1.01 %	1.549	0.54	1.250	0.596
ATR_left	8.409e-04 ± 3.346e-05	8.358e-04 ± 3.916e-05	8.161e-04 ± 4.401e-05	8.005e-04 ± 4.388e-05	-0.61 %	-1.91 %	1.193	0.54	1.605	0.596
ATR_right	8.461e-04 ± 3.803e-05	8.380e-04 ± 3.574e-05	8.330e-04 ± 5.677e-05	8.175e-04 ± 5.208e-05	-0.95 %	-1.86 %	2.050	0.54	1.539	0.596
CA	8.916e-04 ± 2.541e-05	8.887e-04 ± 4.040e-05	8.460e-04 ± 3.763e-05	8.296e-04 ± 3.660e-05	-0.33 %	-1.95 %	0.375	0.795	1.312	0.596
CC_1	8.586e-04 ± 4.152e-05	8.545e-04 ± 4.578e-05	8.494e-04 ± 6.718e-05	8.243e-04 ± 4.685e-05	-0.48 %	-2.96 %	0.706	0.722	2.791	0.44
CC_2	8.375e-04 ± 2.624e-05	8.373e-04 ± 2.961e-05	8.216e-04 ± 3.730e-05	8.096e-04 ± 4.104e-05	-0.02 %	-1.45 %	-0.114	0.818	1.151	0.601
CC_3	8.569e-04 ± 3.301e-05	8.594e-04 ± 4.634e-05	8.383e-04 ± 4.583e-05	8.302e-04 ± 6.241e-05	0.29 %	-0.97 %	-0.480	0.782	0.590	0.655
CC_4	8.417e-04 ± 2.701e-05	8.466e-04 ± 3.477e-05	8.317e-04 ± 4.394e-05	8.367e-04 ± 8.721e-05	0.58 %	0.61 %	-1.142	0.548	-0.062	0.664
CC_5	8.335e-04 ± 2.607e-05	8.422e-04 ± 3.891e-05	8.266e-04 ± 4.895e-05	8.317e-04 ± 9.654e-05	1.04 %	0.61 %	-1.887	0.54	-0.106	0.659
CC_6	8.171e-04 ± 3.205e-05	8.205e-04 ± 2.704e-05	8.113e-04 ± 3.214e-05	8.161e-04 ± 6.004e-05	0.41 %	0.59 %	-1.470	0.54	-0.202	0.655
CC_7	8.307e-04 ± 5.528e-05	8.309e-04 ± 3.870e-05	8.254e-04 ± 3.388e-05	8.321e-04 ± 6.310e-05	0.02 %	0.81 %	-0.276	0.804	-0.200	0.655
CC	8.297e-04 ± 2.690e-05	8.312e-04 ± 2.563e-05	8.208e-04 ± 3.323e-05	8.188e-04 ± 5.572e-05	0.19 %	-0.25 %	-0.877	0.653	0.323	0.655
CG_left	7.949e-04 ± 2.359e-05	7.935e-04 ± 2.323e-05	7.818e-04 ± 4.112e-05	7.856e-04 ± 7.225e-05	-0.17 %	0.49 %	0.184	0.818	-0.162	0.655
CG_right	7.884e-04 ± 2.595e-05	7.859e-04 ± 2.197e-05	7.774e-04 ± 4.034e-05	7.734e-04 ± 5.455e-05	-0.32 %	-0.52 %	0.506	0.779	0.346	0.655
CST_left	8.246e-04 ± 2.229e-05	8.226e-04 ± 3.099e-05	7.999e-04 ± 4.135e-05	7.953e-04 ± 6.590e-05	-0.25 %	-0.58 %	0.540	0.779	0.391	0.655
CST_right	7.904e-04 ± 2.320e-05	7.882e-04 ± 2.337e-05	7.718e-04 ± 3.429e-05	7.795e-04 ± 6.850e-05	-0.27 %	0.99 %	0.344	0.795	-0.414	0.655
FPT_left	8.283e-04 ± 2.218e-05	8.271e-04 ± 3.052e-05	8.068e-04 ± 5.824e-05	7.937e-04 ± 6.377e-05	-0.14 %	-1.61 %	0.082	0.818	0.754	0.655
FPT_right	8.233e-04 ± 2.398e-05	8.223e-04 ± 2.555e-05	8.074e-04 ± 5.361e-05	7.924e-04 ± 5.552e-05	-0.13 %	-1.85 %	0.064	0.818	1.147	0.601
FX_left	1.609e-03 ± 2.432e-04	1.590e-03 ± 2.420e-04	1.597e-03 ± 2.552e-04	1.580e-03 ± 2.864e-04	-1.21 %	-1.03 %	1.273	0.54	0.502	0.655
FX_right	1.594e-03 ± 2.327e-04	1.579e-03 ± 2.466e-04	1.585e-03 ± 2.478e-04	1.529e-03 ± 3.021e-04	-0.9 %	-3.5 %	0.615	0.766	1.423	0.596
ICP_left	7.459e-04 ± 5.752e-05	7.398e-04 ± 3.820e-05	7.409e-04 ± 5.451e-05	7.325e-04 ± 5.920e-05	-0.81 %	-1.14 %	0.751	0.717	0.436	0.655
ICP_right	7.377e-04 ± 4.462e-05	7.329e-04 ± 2.946e-05	7.393e-04 ± 5.818e-05	7.150e-04 ± 6.579e-05	-0.64 %	-3.28 %	0.681	0.724	1.396	0.596
IFO_left	8.088e-04 ± 2.674e-05	8.078e-04 ± 2.595e-05	7.904e-04 ± 2.080e-05	7.875e-04 ± 3.704e-05	-0.12 %	-0.37 %	0.146	0.818	0.541	0.655
IFO_right	8.034e-04 ± 3.017e-05	8.009e-04 ± 2.404e-05	7.924e-04 ± 2.364e-05	7.865e-04 ± 2.874e-05	-0.32 %	-0.74 %	0.516	0.779	2.517	0.44
ILF_left	8.232e-04 ± 3.840e-05	8.165e-04 ± 3.108e-05	8.006e-04 ± 2.704e-05	7.935e-04 ± 4.082e-05	-0.8 %	-0.89 %	1.882	0.54	1.041	0.601
ILF_right	8.137e-04 ± 3.955e-05	8.085e-04 ± 2.961e-05	8.014e-04 ± 3.538e-05	7.931e-04 ± 4.544e-05	-0.64 %	-1.04 %	1.299	0.54	2.062	0.474

Table A.16 (cont'd)

	mTBI		Controls							
TractSeg Name	P1	P2	P1	P2	Percent Change mTBI %	Percent Change Controls %	t-score mTBI	q-value mTBI[r]	t-score controls	q-value controls
MCP	7.251e-04 ± 4.452e-05	7.239e-04 ± 3.381e-05	7.178e-04 ± 5.040e-05	7.300e-04 ± 6.087e-05	-0.17 %	1.7 %	0.122	0.818	-0.565	0.655
MLF_left	8.097e-04 ± 2.705e-05	8.088e-04 ± 2.591e-05	8.013e-04 ± 3.068e-05	7.968e-04 ± 4.225e-05	-0.1 %	-0.56 %	-0.066	0.818	0.543	0.655
MLF_right	8.024e-04 ± 2.876e-05	8.033e-04 ± 2.571e-05	7.993e-04 ± 3.606e-05	7.949e-04 ± 4.326e-05	0.12 %	-0.55 %	-0.896	0.653	0.539	0.655
OR_left	8.340e-04 ± 3.934e-05	8.315e-04 ± 3.878e-05	8.193e-04 ± 3.161e-05	8.179e-04 ± 6.352e-05	-0.3 %	-0.17 %	0.429	0.782	0.143	0.655
OR_right	8.257e-04 ± 4.445e-05	8.239e-04 ± 3.876e-05	8.261e-04 ± 3.738e-05	8.206e-04 ± 5.220e-05	-0.22 %	-0.66 %	-0.107	0.818	1.289	0.596
POPT_left	8.315e-04 ± 2.473e-05	8.350e-04 ± 2.884e-05	8.286e-04 ± 4.189e-05	8.256e-04 ± 7.224e-05	0.41 %	-0.36 %	-1.469	0.54	0.275	0.655
POPT_right	8.162e-04 ± 2.751e-05	8.184e-04 ± 2.682e-05	8.094e-04 ± 3.952e-05	8.114e-04 ± 6.759e-05	0.28 %	0.24 %	-1.179	0.54	-0.131	0.655
SCP_left	7.868e-04 ± 2.581e-05	7.823e-04 ± 3.232e-05	7.625e-04 ± 4.451e-05	7.543e-04 ± 5.961e-05	-0.58 %	-1.08 %	1.115	0.548	0.432	0.655
SCP_right	7.779e-04 ± 2.147e-05	7.733e-04 ± 2.205e-05	7.682e-04 ± 5.620e-05	7.523e-04 ± 3.878e-05	-0.6 %	-2.06 %	1.705	0.54	1.324	0.596
SLF_III_left	7.962e-04 ± 2.382e-05	7.944e-04 ± 2.694e-05	7.806e-04 ± 5.033e-05	7.732e-04 ± 5.376e-05	-0.23 %	-0.95 %	0.702	0.722	0.540	0.655
SLF_III_right	7.828e-04 ± 2.264e-05	7.829e-04 ± 2.113e-05	7.793e-04 ± 3.347e-05	7.740e-04 ± 4.087e-05	0.01 %	-0.68 %	-0.056	0.818	0.518	0.655
SLF_II_left	8.100e-04 ± 2.939e-05	8.057e-04 ± 3.014e-05	7.989e-04 ± 4.336e-05	7.891e-04 ± 5.031e-05	-0.54 %	-1.22 %	1.530	0.54	0.979	0.601
SLF_II_right	8.013e-04 ± 2.816e-05	7.979e-04 ± 2.601e-05	7.935e-04 ± 4.066e-05	7.839e-04 ± 4.224e-05	-0.43 %	-1.22 %	1.100	0.548	1.119	0.601
SLF_I_left	8.457e-04 ± 3.854e-05	8.478e-04 ± 4.422e-05	8.576e-04 ± 8.340e-05	8.492e-04 ± 9.782e-05	0.25 %	-0.98 %	-0.461	0.782	0.456	0.655
SLF_I_right	8.284e-04 ± 3.527e-05	8.267e-04 ± 3.849e-05	8.296e-04 ± 6.358e-05	8.219e-04 ± 8.344e-05	-0.21 %	-0.93 %	0.340	0.795	0.525	0.655
STR_left	7.828e-04 ± 2.238e-05	7.788e-04 ± 3.467e-05	7.458e-04 ± 4.054e-05	7.504e-04 ± 9.970e-05	-0.52 %	0.62 %	0.994	0.617	-0.254	0.655
STR_right	7.658e-04 ± 2.186e-05	7.614e-04 ± 2.653e-05	7.499e-04 ± 4.676e-05	7.410e-04 ± 6.010e-05	-0.58 %	-1.19 %	1.209	0.54	0.620	0.655
ST_FO_left	8.061e-04 ± 3.489e-05	8.052e-04 ± 3.935e-05	7.719e-04 ± 3.447e-05	7.685e-04 ± 5.548e-05	-0.11 %	-0.44 %	-0.018	0.823	0.266	0.655
ST_FO_right	8.106e-04 ± 3.320e-05	8.071e-04 ± 3.231e-05	7.906e-04 ± 4.002e-05	7.746e-04 ± 2.859e-05	-0.44 %	-2.03 %	0.979	0.617	2.469	0.44
ST_OCC_left	8.169e-04 ± 3.222e-05	8.147e-04 ± 3.153e-05	7.958e-04 ± 1.883e-05	7.951e-04 ± 4.364e-05	-0.27 %	-0.1 %	0.516	0.779	0.222	0.655
ST_OCC_right	8.034e-04 ± 3.557e-05	8.012e-04 ± 3.058e-05	7.937e-04 ± 2.386e-05	7.912e-04 ± 3.384e-05	-0.28 %	-0.31 %	0.058	0.818	2.300	0.456
ST_PAR_left	8.232e-04 ± 2.826e-05	8.248e-04 ± 2.954e-05	8.176e-04 ± 3.713e-05	8.152e-04 ± 6.397e-05	0.19 %	-0.3 %	-0.901	0.653	0.333	0.655
ST_PAR_right	8.055e-04 ± 2.877e-05	8.060e-04 ± 2.623e-05	7.978e-04 ± 3.132e-05	7.990e-04 ± 5.421e-05	0.07 %	0.15 %	-0.747	0.717	-0.003	0.677
ST_POSTC_left	8.273e-04 ± 2.845e-05	8.256e-04 ± 3.665e-05	8.107e-04 ± 4.887e-05	8.032e-04 ± 7.729e-05	-0.21 %	-0.93 %	0.437	0.782	0.529	0.655
ST_POSTC_right	7.981e-04 ± 2.772e-05	7.965e-04 ± 2.909e-05	7.923e-04 ± 4.763e-05	7.963e-04 ± 7.827e-05	-0.2 %	0.5 %	0.305	0.804	-0.064	0.664
ST_PREC_left	8.188e-04 ± 2.658e-05	8.139e-04 ± 3.580e-05	7.880e-04 ± 4.243e-05	7.863e-04 ± 6.738e-05	-0.6 %	-0.22 %	1.414	0.54	0.261	0.655
ST_PREC_right	7.950e-04 ± 2.800e-05	7.895e-04 ± 2.563e-05	7.793e-04 ± 3.716e-05	7.789e-04 ± 5.685e-05	-0.69 %	-0.05 %	1.364	0.54	0.249	0.655

Table A.16 (cont'd)

	mTBI		Controls							
TractSeg Name	P1	P2	P1	P2	Percent Change mTBI %	Percent Change Controls %	t-score mTBI	q-value mTBI[1]	t-score controls	q-value controls
ST_PREF_left	8.095e-04 ± 2.509e-05	8.057e-04 ± 2.998e-05	7.828e-04 ± 4.072e-05	7.759e-04 ± 4.752e-05	-0.47 %	-0.88 %	1.338	0.54	0.623	0.655
ST_PREF_right	8.088e-04 ± 2.644e-05	8.044e-04 ± 2.507e-05	7.893e-04 ± 4.033e-05	7.747e-04 ± 3.372e-05	-0.55 %	-1.86 %	1.925	0.54	1.909	0.537
ST_PREM_left	8.177e-04 ± 2.850e-05	8.119e-04 ± 3.848e-05	7.848e-04 ± 4.277e-05	7.662e-04 ± 3.664e-05	-0.71 %	-2.38 %	1.669	0.54	2.073	0.474
ST_PREM_right	8.010e-04 ± 2.579e-05	7.946e-04 ± 2.784e-05	7.778e-04 ± 4.761e-05	7.692e-04 ± 4.500e-05	-0.8 %	-1.11 %	2.662	0.54	1.082	0.601
T_OCC_left	8.390e-04 ± 4.054e-05	8.360e-04 ± 3.969e-05	8.243e-04 ± 3.169e-05	8.229e-04 ± 6.250e-05	-0.35 %	-0.17 %	0.557	0.779	0.160	0.655
T_OCC_right	8.269e-04 ± 4.470e-05	8.247e-04 ± 3.885e-05	8.267e-04 ± 3.792e-05	8.218e-04 ± 5.292e-05	-0.26 %	-0.6 %	-0.005	0.823	1.278	0.596
T_PAR_left	8.334e-04 ± 3.315e-05	8.354e-04 ± 3.495e-05	8.344e-04 ± 4.703e-05	8.312e-04 ± 7.984e-05	0.24 %	-0.39 %	-0.767	0.717	0.304	0.655
T_PAR_right	8.233e-04 ± 3.552e-05	8.233e-04 ± 3.270e-05	8.221e-04 ± 4.550e-05	8.210e-04 ± 7.266e-05	0.01 %	-0.13 %	-0.345	0.795	0.170	0.655
T_POSTC_left	8.257e-04 ± 2.980e-05	8.265e-04 ± 3.850e-05	8.250e-04 ± 6.229e-05	8.151e-04 ± 9.048e-05	0.09 %	-1.2 %	-0.128	0.818	0.548	0.655
T_POSTC_right	7.981e-04 ± 3.203e-05	7.993e-04 ± 3.469e-05	8.069e-04 ± 6.816e-05	8.105e-04 ± 1.036e-04	0.15 %	0.45 %	-0.284	0.804	-0.007	0.677
T_PREC_left	8.208e-04 ± 2.865e-05	8.160e-04 ± 3.953e-05	7.968e-04 ± 5.194e-05	7.935e-04 ± 8.025e-05	-0.58 %	-0.41 %	1.258	0.54	0.296	0.655
T_PREC_right	7.933e-04 ± 3.078e-05	7.874e-04 ± 2.872e-05	7.833e-04 ± 4.619e-05	7.813e-04 ± 6.742e-05	-0.74 %	-0.25 %	1.218	0.54	0.296	0.655
T_PREF_left	8.255e-04 ± 2.786e-05	8.209e-04 ± 3.525e-05	8.027e-04 ± 5.094e-05	7.926e-04 ± 5.755e-05	-0.55 %	-1.27 %	1.190	0.54	0.732	0.655
T_PREF_right	8.317e-04 ± 3.290e-05	8.253e-04 ± 3.271e-05	8.185e-04 ± 5.609e-05	8.013e-04 ± 5.377e-05	-0.77 %	-2.1 %	1.805	0.54	1.514	0.596
T_PREM_left	8.370e-04 ± 3.299e-05	8.305e-04 ± 4.623e-05	8.121e-04 ± 5.641e-05	7.900e-04 ± 6.052e-05	-0.78 %	-2.72 %	1.289	0.54	1.551	0.596
T_PREM_right	8.186e-04 ± 3.557e-05	8.100e-04 ± 3.750e-05	8.064e-04 ± 7.571e-05	7.926e-04 ± 6.976e-05	-1.05 %	-1.71 %	1.890	0.54	1.009	0.601
UF_left	8.116e-04 ± 2.571e-05	8.142e-04 ± 2.716e-05	7.926e-04 ± 3.163e-05	7.837e-04 ± 2.922e-05	0.33 %	-1.12 %	-1.175	0.54	0.985	0.601
UF_right	8.327e-04 ± 2.444e-05	8.318e-04 ± 2.798e-05	8.186e-04 ± 4.089e-05	8.018e-04 ± 3.281e-05	-0.11 %	-2.05 %	0.048	0.818	1.435	0.596

Tables A.16- T-test results for comparisons of the automatically segmented tracts from TractSeg between timepoints within mTBI and control subjects.

[1]Significant values are marked with an asterisk (*) or <0.001

Table A.17 Results of Post Hoc Tract Specific Comparison of Diffusion Tensor Metric Axial Diffusivity

TractSeg Name	mTBI		Controls		Percent Change mTBI %	Percent Change Controls %	t-score mTBI	q-value mTBI′	t-score controls	q-value controls
	P1	P2	P1	P2						
AF_left	1.015e-03 ± 2.342e-05	1.007e-03 ± 2.573e-05	9.847e-04 ± 2.329e-05	9.765e-04 ± 2.670e-05	-0.74 %	-0.83 %	2.557	0.106	1.569	0.189
AF_right	1.005e-03 ± 2.231e-05	1.000e-03 ± 2.132e-05	9.878e-04 ± 2.429e-05	9.759e-04 ± 1.501e-05	-0.5 %	-1.2 %	2.287	0.134	2.777	0.139
ATR_left	1.079e-03 ± 3.541e-05	1.073e-03 ± 4.054e-05	1.053e-03 ± 3.877e-05	1.035e-03 ± 3.740e-05	-0.61 %	-1.74 %	1.545	0.186	2.169	0.158
ATR_right	1.077e-03 ± 4.010e-05	1.068e-03 ± 3.867e-05	1.061e-03 ± 5.729e-05	1.044e-03 ± 4.945e-05	-0.85 %	-1.58 %	2.237	0.134	1.727	0.164
CA	1.153e-03 ± 3.106e-05	1.146e-03 ± 3.747e-05	1.113e-03 ± 3.338e-05	1.089e-03 ± 2.505e-05	-0.65 %	-2.19 %	1.287	0.203	2.472	0.139
CC_1	1.198e-03 ± 5.031e-05	1.187e-03 ± 6.398e-05	1.192e-03 ± 7.785e-05	1.152e-03 ± 7.825e-05	-0.95 %	-3.37 %	1.590	0.186	1.825	0.162
CC_2	1.109e-03 ± 2.756e-05	1.107e-03 ± 3.109e-05	1.087e-03 ± 3.036e-05	1.070e-03 ± 2.602e-05	-0.19 %	-1.54 %	0.586	0.33	2.309	0.139
CC_3	1.129e-03 ± 3.908e-05	1.129e-03 ± 4.402e-05	1.105e-03 ± 3.968e-05	1.092e-03 ± 4.430e-05	-0.06 %	-1.16 %	0.102	0.425	1.115	0.275
CC_4	1.121e-03 ± 2.533e-05	1.122e-03 ± 3.542e-05	1.097e-03 ± 3.661e-05	1.101e-03 ± 6.714e-05	0.16 %	0.33 %	-0.444	0.363	-0.064	0.496
CC_5	1.121e-03 ± 2.864e-05	1.126e-03 ± 4.085e-05	1.099e-03 ± 4.358e-05	1.103e-03 ± 7.685e-05	0.47 %	0.36 %	-1.199	0.219	-0.134	0.496
CC_6	1.083e-03 ± 2.908e-05	1.086e-03 ± 3.002e-05	1.068e-03 ± 2.105e-05	1.070e-03 ± 4.447e-05	0.25 %	0.19 %	-1.515	0.188	-0.054	0.496
CC_7	1.116e-03 ± 5.499e-05	1.114e-03 ± 4.317e-05	1.105e-03 ± 4.256e-05	1.104e-03 ± 5.584e-05	-0.15 %	-0.08 %	0.192	0.404	0.985	0.314
CC	1.097e-03 ± 2.436e-05	1.097e-03 ± 2.547e-05	1.080e-03 ± 2.395e-05	1.074e-03 ± 3.965e-05	0.02 %	-0.58 %	-0.389	0.368	1.020	0.307
CG_left	1.031e-03 ± 2.378e-05	1.032e-03 ± 2.771e-05	1.013e-03 ± 3.399e-05	1.013e-03 ± 6.512e-05	0.11 %	0.05 %	-0.560	0.33	-0.038	0.496
CG_right	1.027e-03 ± 2.690e-05	1.024e-03 ± 2.496e-05	1.009e-03 ± 2.887e-05	9.993e-04 ± 4.918e-05	-0.2 %	-0.98 %	0.231	0.396	0.789	0.363
CST_left	1.139e-03 ± 2.442e-05	1.136e-03 ± 3.320e-05	1.098e-03 ± 3.481e-05	1.092e-03 ± 5.409e-05	-0.26 %	-0.57 %	0.809	0.269	0.682	0.388
CST_right	1.100e-03 ± 2.556e-05	1.095e-03 ± 2.623e-05	1.068e-03 ± 3.136e-05	1.072e-03 ± 5.302e-05	-0.4 %	0.41 %	1.031	0.219	-0.248	0.472
FPT_left	1.131e-03 ± 2.590e-05	1.129e-03 ± 3.320e-05	1.095e-03 ± 4.753e-05	1.078e-03 ± 5.047e-05	-0.12 %	-1.49 %	0.280	0.384	1.297	0.245
FPT_right	1.124e-03 ± 2.818e-05	1.121e-03 ± 2.925e-05	1.095e-03 ± 4.575e-05	1.078e-03 ± 4.495e-05	-0.24 %	-1.55 %	0.644	0.319	1.833	0.162
FX_left	2.085e-03 ± 2.114e-04	2.046e-03 ± 2.231e-04	2.066e-03 ± 2.208e-04	2.028e-03 ± 2.725e-04	-1.89 %	-1.85 %	2.755	0.106	0.802	0.363
FX_right	2.077e-03 ± 2.037e-04	2.048e-03 ± 2.239e-04	2.052e-03 ± 2.155e-04	1.990e-03 ± 3.089e-04	-1.4 %	-3.03 %	1.849	0.179	1.194	0.266
ICP_left	9.628e-04 ± 5.867e-05	9.534e-04 ± 3.663e-05	9.448e-04 ± 4.185e-05	9.368e-04 ± 3.789e-05	-0.97 %	-0.84 %	1.186	0.219	0.644	0.388
ICP_right	9.386e-04 ± 4.624e-05	9.298e-04 ± 3.252e-05	9.265e-04 ± 4.801e-05	9.044e-04 ± 7.191e-05	-0.93 %	-2.38 %	1.472	0.195	1.293	0.245
IFO_left	1.056e-03 ± 2.808e-05	1.053e-03 ± 2.968e-05	1.035e-03 ± 2.153e-05	1.024e-03 ± 2.312e-05	-0.26 %	-0.99 %	0.835	0.265	3.486	0.134
IFO_right	1.047e-03 ± 3.094e-05	1.043e-03 ± 2.640e-05	1.033e-03 ± 3.013e-05	1.023e-03 ± 3.073e-05	-0.39 %	-0.98 %	1.302	0.203	2.324	0.139
ILF_left	1.072e-03 ± 4.333e-05	1.061e-03 ± 4.141e-05	1.049e-03 ± 3.176e-05	1.030e-03 ± 3.628e-05	-0.99 %	-1.85 %	2.310	0.134	2.306	0.139
ILF_right	1.053e-03 ± 4.591e-05	1.045e-03 ± 3.940e-05	1.043e-03 ± 4.700e-05	1.025e-03 ± 6.098e-05	-0.75 %	-1.68 %	1.675	0.179	1.883	0.162

Table A.17 (cont'd)

	mTBI		Controls							
TractSeg Name	P1	P2	P1	P2	Percent Change mTBI %	Percent Change Controls %	t-score mTBI	q-value mTBI′	t-score controls	q-value controls
MCP	9.671e-04 ± 4.922e-05	9.626e-04 ± 3.853e-05	9.479e-04 ± 3.816e-05	9.606e-04 ± 4.000e-05	-0.47 %	1.33 %	0.633	0.319	-0.790	0.363
MLF_left	1.033e-03 ± 2.652e-05	1.033e-03 ± 2.832e-05	1.020e-03 ± 2.389e-05	1.015e-03 ± 3.585e-05	-0.05 %	-0.51 %	-0.337	0.374	0.790	0.363
MLF_right	1.029e-03 ± 2.723e-05	1.029e-03 ± 2.783e-05	1.019e-03 ± 2.749e-05	1.011e-03 ± 3.368e-05	0.01 %	-0.8 %	-0.683	0.312	1.284	0.245
OR_left	1.102e-03 ± 3.927e-05	1.097e-03 ± 4.030e-05	1.084e-03 ± 3.617e-05	1.074e-03 ± 4.706e-05	-0.45 %	-0.9 %	1.057	0.219	1.332	0.245
OR_right	1.094e-03 ± 4.333e-05	1.091e-03 ± 3.987e-05	1.093e-03 ± 4.489e-05	1.081e-03 ± 6.077e-05	-0.28 %	-1.09 %	0.313	0.377	1.722	0.164
POPT_left	1.109e-03 ± 2.802e-05	1.112e-03 ± 3.210e-05	1.094e-03 ± 3.411e-05	1.090e-03 ± 6.348e-05	0.28 %	-0.34 %	-1.430	0.196	0.428	0.414
POPT_right	1.100e-03 ± 2.963e-05	1.101e-03 ± 3.086e-05	1.084e-03 ± 3.327e-05	1.085e-03 ± 5.636e-05	0.11 %	0.08 %	-1.000	0.219	-0.040	0.496
SCP_left	1.057e-03 ± 2.989e-05	1.050e-03 ± 3.242e-05	1.016e-03 ± 3.352e-05	1.010e-03 ± 3.981e-05	-0.61 %	-0.58 %	1.567	0.186	0.556	0.4
SCP_right	1.044e-03 ± 2.503e-05	1.035e-03 ± 2.552e-05	1.018e-03 ± 4.347e-05	1.006e-03 ± 2.895e-05	-0.79 %	-1.18 %	3.230	0.066	1.782	0.162
SLF_III_left	1.013e-03 ± 2.510e-05	1.008e-03 ± 2.923e-05	9.897e-04 ± 3.604e-05	9.819e-04 ± 4.455e-05	-0.47 %	-0.79 %	1.828	0.179	0.710	0.384
SLF_III_right	1.006e-03 ± 2.348e-05	1.003e-03 ± 2.646e-05	9.898e-04 ± 2.919e-05	9.790e-04 ± 2.266e-05	-0.31 %	-1.09 %	1.030	0.219	2.007	0.158
SLF_II_left	1.017e-03 ± 2.591e-05	1.014e-03 ± 2.883e-05	1.001e-03 ± 3.330e-05	9.931e-04 ± 4.407e-05	-0.29 %	-0.74 %	1.177	0.219	0.873	0.357
SLF_II_right	1.007e-03 ± 2.589e-05	1.004e-03 ± 2.526e-05	9.925e-04 ± 3.316e-05	9.820e-04 ± 3.410e-05	-0.29 %	-1.06 %	1.045	0.219	1.652	0.171
SLF_I_left	1.051e-03 ± 3.764e-05	1.054e-03 ± 4.073e-05	1.056e-03 ± 7.126e-05	1.045e-03 ± 8.891e-05	0.32 %	-1.01 %	-1.142	0.219	0.632	0.388
SLF_I_right	1.041e-03 ± 3.308e-05	1.041e-03 ± 3.473e-05	1.036e-03 ± 5.265e-05	1.029e-03 ± 7.461e-05	-0.01 %	-0.73 %	-0.063	0.427	0.660	0.388
STR_left	1.071e-03 ± 2.795e-05	1.067e-03 ± 3.761e-05	1.018e-03 ± 3.962e-05	1.019e-03 ± 8.800e-05	-0.42 %	0.09 %	1.108	0.219	-0.114	0.496
STR_right	1.052e-03 ± 2.962e-05	1.045e-03 ± 3.229e-05	1.025e-03 ± 4.226e-05	1.014e-03 ± 5.503e-05	-0.64 %	-1.03 %	1.693	0.179	0.711	0.384
ST_FO_left	1.059e-03 ± 4.021e-05	1.054e-03 ± 4.817e-05	1.025e-03 ± 4.049e-05	1.018e-03 ± 3.978e-05	-0.47 %	-0.7 %	1.015	0.219	1.222	0.262
ST_FO_right	1.073e-03 ± 3.768e-05	1.067e-03 ± 3.943e-05	1.051e-03 ± 4.138e-05	1.029e-03 ± 2.899e-05	-0.6 %	-2.05 %	1.703	0.179	2.067	0.158
ST_OCC_left	1.082e-03 ± 3.268e-05	1.078e-03 ± 3.508e-05	1.055e-03 ± 2.302e-05	1.047e-03 ± 2.724e-05	-0.36 %	-0.73 %	1.005	0.219	2.296	0.139
ST_OCC_right	1.062e-03 ± 3.557e-05	1.058e-03 ± 3.316e-05	1.049e-03 ± 3.533e-05	1.042e-03 ± 3.978e-05	-0.32 %	-0.69 %	0.512	0.342	1.961	0.161
ST_PAR_left	1.064e-03 ± 2.882e-05	1.066e-03 ± 3.255e-05	1.050e-03 ± 2.912e-05	1.047e-03 ± 5.636e-05	0.2 %	-0.31 %	-1.051	0.219	0.441	0.414
ST_PAR_right	1.055e-03 ± 2.873e-05	1.055e-03 ± 2.928e-05	1.040e-03 ± 2.724e-05	1.040e-03 ± 4.490e-05	-0.05 %	-0.05 %	-0.383	0.368	0.190	0.49
ST_POSTC_left	1.081e-03 ± 3.349e-05	1.078e-03 ± 4.209e-05	1.052e-03 ± 4.335e-05	1.043e-03 ± 7.582e-05	-0.23 %	-0.78 %	0.560	0.33	0.565	0.4
ST_POSTC_right	1.058e-03 ± 3.114e-05	1.053e-03 ± 3.115e-05	1.044e-03 ± 4.490e-05	1.046e-03 ± 7.164e-05	-0.43 %	0.22 %	0.924	0.239	0.050	0.496
ST_PREC_left	1.076e-03 ± 2.947e-05	1.070e-03 ± 3.950e-05	1.033e-03 ± 3.791e-05	1.029e-03 ± 6.310e-05	-0.51 %	-0.4 %	1.321	0.203	0.397	0.421
ST_PREC_right	1.053e-03 ± 3.045e-05	1.046e-03 ± 2.879e-05	1.029e-03 ± 3.861e-05	1.026e-03 ± 5.209e-05	-0.72 %	-0.23 %	1.764	0.179	0.491	0.414

Table A.17 (cont'd)

	mTBI		Controls							
TractSeg Name	P1	P2	P1	P2	Percent Change mTBI %	Percent Change Controls %	t-score mTBI	q-value mTBI[1]	t-score controls	q-value controls
ST_PREF_left	1.056e-03 ± 2.776e-05	1.052e-03 ± 3.464e-05	1.022e-03 ± 3.595e-05	1.011e-03 ± 4.110e-05	-0.4 %	-1.1 %	1.363	0.196	1.125	0.275
ST_PREF_right	1.054e-03 ± 3.014e-05	1.048e-03 ± 3.014e-05	1.028e-03 ± 4.096e-05	1.010e-03 ± 3.036e-05	-0.55 %	-1.72 %	2.127	0.15	2.128	0.158
ST_PREM_left	1.053e-03 ± 3.357e-05	1.047e-03 ± 4.465e-05	1.010e-03 ± 3.695e-05	9.868e-04 ± 2.854e-05	-0.57 %	-2.27 %	1.642	0.179	3.129	0.136
ST_PREM_right	1.044e-03 ± 3.148e-05	1.036e-03 ± 3.357e-05	1.011e-03 ± 4.473e-05	9.990e-04 ± 4.066e-05	-0.71 %	-1.21 %	2.621	0.106	1.820	0.162
T_OCC_left	1.103e-03 ± 4.013e-05	1.097e-03 ± 4.116e-05	1.085e-03 ± 3.587e-05	1.076e-03 ± 4.708e-05	-0.48 %	-0.9 %	1.169	0.219	1.346	0.245
T_OCC_right	1.090e-03 ± 4.353e-05	1.086e-03 ± 3.999e-05	1.088e-03 ± 4.596e-05	1.077e-03 ± 6.103e-05	-0.3 %	-1.03 %	0.374	0.368	1.661	0.171
T_PAR_left	1.075e-03 ± 3.197e-05	1.078e-03 ± 3.489e-05	1.069e-03 ± 3.948e-05	1.064e-03 ± 7.090e-05	0.24 %	-0.44 %	-1.041	0.219	0.438	0.414
T_PAR_right	1.076e-03 ± 3.398e-05	1.076e-03 ± 3.320e-05	1.068e-03 ± 3.920e-05	1.066e-03 ± 6.324e-05	-0.02 %	-0.25 %	-0.368	0.368	0.311	0.452
T_POSTC_left	1.083e-03 ± 3.168e-05	1.083e-03 ± 3.916e-05	1.067e-03 ± 5.405e-05	1.058e-03 ± 8.290e-05	-0.02 %	-0.85 %	0.156	0.412	0.599	0.396
T_POSTC_right	1.059e-03 ± 3.156e-05	1.059e-03 ± 3.222e-05	1.057e-03 ± 5.480e-05	1.059e-03 ± 9.134e-05	-0.04 %	0.14 %	-0.040	0.43	0.071	0.496
T_PREC_left	1.083e-03 ± 2.815e-05	1.078e-03 ± 3.880e-05	1.047e-03 ± 4.469e-05	1.042e-03 ± 7.164e-05	-0.49 %	-0.55 %	1.405	0.196	0.462	0.414
T_PREC_right	1.049e-03 ± 3.081e-05	1.042e-03 ± 2.871e-05	1.031e-03 ± 4.103e-05	1.026e-03 ± 6.015e-05	-0.62 %	-0.39 %	1.424	0.196	0.501	0.414
T_PREF_left	1.076e-03 ± 2.889e-05	1.071e-03 ± 3.634e-05	1.047e-03 ± 4.445e-05	1.033e-03 ± 4.993e-05	-0.45 %	-1.37 %	1.370	0.196	1.152	0.275
T_PREF_right	1.074e-03 ± 3.428e-05	1.067e-03 ± 3.426e-05	1.055e-03 ± 5.484e-05	1.035e-03 ± 4.852e-05	-0.67 %	-1.85 %	2.012	0.157	1.799	0.162
T_PREM_left	1.087e-03 ± 3.444e-05	1.079e-03 ± 4.639e-05	1.054e-03 ± 5.017e-05	1.029e-03 ± 5.125e-05	-0.69 %	-2.4 %	1.718	0.179	2.040	0.158
T_PREM_right	1.065e-03 ± 3.573e-05	1.057e-03 ± 3.830e-05	1.047e-03 ± 6.767e-05	1.030e-03 ± 6.163e-05	-0.79 %	-1.6 %	2.079	0.15	1.369	0.245
UF_left	1.057e-03 ± 2.840e-05	1.056e-03 ± 2.995e-05	1.036e-03 ± 3.224e-05	1.020e-03 ± 1.933e-05	-0.12 %	-1.52 %	0.079	0.427	2.707	0.139
UF_right	1.085e-03 ± 2.861e-05	1.080e-03 ± 2.984e-05	1.067e-03 ± 4.207e-05	1.045e-03 ± 1.620e-05	-0.49 %	-2.11 %	1.658	0.179	2.610	0.139

Tables A.17- T-test results for comparisons of the automatically segmented tracts from TractSeg between timepoints within mTBI and control subjects.

[1]Significant values are marked with an asterisk (*) or <0.001

Table A.18 Results of Post Hoc Tract Specific Comparison of Diffusion Tensor Metric Radial Diffusivity

	mTBI		Controls							
TractSeg Name	P1	P2	P1	P2	Percent Change mTBI %	Percent Change Controls %	t-score mTBI	q-value mTBI	t-score controls	q-value controls
AF_left	6.926e-04 ± 2.510e-05	6.880e-04 ± 2.491e-05	6.710e-04 ± 3.590e-05	6.646e-04 ± 3.528e-05	-0.66 %	-0.96 %	1.503	0.963	0.792	0.987
AF_right	6.776e-04 ± 2.346e-05	6.754e-04 ± 1.976e-05	6.708e-04 ± 2.842e-05	6.650e-04 ± 3.511e-05	-0.32 %	-0.87 %	0.827	0.963	0.752	0.987
ATR_left	7.217e-04 ± 3.371e-05	7.173e-04 ± 3.941e-05	6.977e-04 ± 4.747e-05	6.835e-04 ± 4.824e-05	-0.61 %	-2.03 %	0.991	0.963	1.354	0.987
ATR_right	7.305e-04 ± 3.776e-05	7.230e-04 ± 3.543e-05	7.189e-04 ± 5.714e-05	7.041e-04 ± 5.440e-05	-1.02 %	-2.06 %	1.871	0.963	1.417	0.987
CA	7.607e-04 ± 2.680e-05	7.601e-04 ± 4.472e-05	7.125e-04 ± 4.266e-05	7.000e-04 ± 4.786e-05	-0.08 %	-1.75 %	-0.072	0.987	0.856	0.987
CC_1	6.890e-04 ± 4.217e-05	6.885e-04 ± 4.672e-05	6.783e-04 ± 6.571e-05	6.606e-04 ± 5.164e-05	-0.07 %	-2.6 %	-0.144	0.987	1.762	0.987
CC_2	7.017e-04 ± 2.825e-05	7.024e-04 ± 3.106e-05	6.889e-04 ± 4.400e-05	6.794e-04 ± 5.003e-05	0.11 %	-1.39 %	-0.448	0.987	0.806	0.987
CC_3	7.207e-04 ± 3.389e-05	7.247e-04 ± 5.072e-05	7.052e-04 ± 5.606e-05	6.995e-04 ± 7.412e-05	0.55 %	-0.81 %	-0.687	0.987	0.418	0.987
CC_4	7.022e-04 ± 3.236e-05	7.087e-04 ± 3.842e-05	6.990e-04 ± 5.347e-05	7.047e-04 ± 9.832e-05	0.93 %	0.82 %	-1.303	0.963	-0.061	0.987
CC_5	6.899e-04 ± 3.043e-05	7.003e-04 ± 4.238e-05	6.906e-04 ± 5.817e-05	6.961e-04 ± 1.081e-04	1.51 %	0.81 %	-1.989	0.963	-0.094	0.987
CC_6	6.840e-04 ± 3.575e-05	6.876e-04 ± 2.890e-05	6.831e-04 ± 4.045e-05	6.892e-04 ± 6.888e-05	0.53 %	0.89 %	-1.273	0.963	-0.237	0.987
CC_7	6.882e-04 ± 5.660e-05	6.893e-04 ± 3.900e-05	6.858e-04 ± 3.193e-05	6.963e-04 ± 7.274e-05	0.16 %	1.53 %	-0.473	0.987	-0.442	0.987
CC	6.962e-04 ± 3.001e-05	6.984e-04 ± 2.789e-05	6.912e-04 ± 4.055e-05	6.913e-04 ± 6.451e-05	0.31 %	0.01 %	-0.949	0.963	0.150	0.987
CG_left	6.770e-04 ± 2.722e-05	6.744e-04 ± 2.774e-05	6.662e-04 ± 4.741e-05	6.717e-04 ± 7.710e-05	-0.4 %	0.83 %	0.451	0.987	-0.211	0.987
CG_right	6.694e-04 ± 2.930e-05	6.667e-04 ± 2.393e-05	6.615e-04 ± 4.739e-05	6.604e-04 ± 5.967e-05	-0.4 %	-0.17 %	0.534	0.987	0.194	0.987
CST_left	6.676e-04 ± 2.487e-05	6.660e-04 ± 3.272e-05	6.507e-04 ± 4.765e-05	6.469e-04 ± 7.265e-05	-0.24 %	-0.6 %	0.375	0.987	0.288	0.987
CST_right	6.358e-04 ± 2.449e-05	6.347e-04 ± 2.548e-05	6.237e-04 ± 3.943e-05	6.331e-04 ± 7.721e-05	-0.17 %	1.5 %	0.037	0.987	-0.458	0.987
FPT_left	6.770e-04 ± 2.380e-05	6.760e-04 ± 3.174e-05	6.628e-04 ± 6.547e-05	6.514e-04 ± 7.116e-05	-0.15 %	-1.72 %	-0.016	0.987	0.573	0.987
FPT_right	6.729e-04 ± 2.448e-05	6.726e-04 ± 2.664e-05	6.634e-04 ± 5.898e-05	6.495e-04 ± 6.193e-05	-0.04 %	-2.1 %	-0.186	0.987	0.911	0.987
FX_left	1.372e-03 ± 2.615e-04	1.362e-03 ± 2.560e-04	1.362e-03 ± 2.757e-04	1.356e-03 ± 3.019e-04	-0.7 %	-0.4 %	0.530	0.987	0.313	0.987
FX_right	1.352e-03 ± 2.505e-04	1.345e-03 ± 2.628e-04	1.351e-03 ± 2.675e-04	1.299e-03 ± 3.085e-04	-0.51 %	-3.85 %	0.056	0.987	1.528	0.987
ICP_left	6.374e-04 ± 5.814e-05	6.330e-04 ± 4.076e-05	6.390e-04 ± 6.150e-05	6.304e-04 ± 7.152e-05	-0.69 %	-1.35 %	0.480	0.987	0.371	0.987
ICP_right	6.372e-04 ± 4.490e-05	6.344e-04 ± 2.976e-05	6.457e-04 ± 6.380e-05	6.203e-04 ± 6.577e-05	-0.43 %	-3.93 %	0.206	0.987	1.382	0.987
IFO_left	6.853e-04 ± 2.739e-05	6.851e-04 ± 2.548e-05	6.683e-04 ± 2.269e-05	6.691e-04 ± 4.612e-05	-0.02 %	0.11 %	-0.248	0.987	0.016	0.987
IFO_right	6.818e-04 ± 3.044e-05	6.800e-04 ± 2.425e-05	6.720e-04 ± 2.238e-05	6.683e-04 ± 3.391e-05	-0.26 %	-0.54 %	0.072	0.987	1.036	0.987
ILF_left	6.988e-04 ± 3.708e-05	6.941e-04 ± 2.885e-05	6.762e-04 ± 2.638e-05	6.752e-04 ± 4.890e-05	-0.66 %	-0.15 %	1.299	0.963	0.221	0.987
ILF_right	6.943e-04 ± 3.747e-05	6.904e-04 ± 2.834e-05	6.808e-04 ± 3.137e-05	6.771e-04 ± 4.371e-05	-0.56 %	-0.55 %	0.857	0.963	1.387	0.987

Table A.18 (cont'd)

	mTBI		Controls							
TractSeg Name	P1	P2	P1	P2	Percent Change mTBI %	Percent Change Controls %	t-score mTBI	q-value mTBI[f]	t-score controls	q-value controls
MCP	6.041e-04 ± 4.311e-05	6.046e-04 ± 3.286e-05	6.028e-04 ± 5.747e-05	6.147e-04 ± 7.219e-05	0.08 %	1.98 %	-0.163	0.987	-0.491	0.987
MLF_left	6.978e-04 ± 2.931e-05	6.968e-04 ± 2.710e-05	6.920e-04 ± 3.567e-05	6.879e-04 ± 4.632e-05	-0.14 %	-0.6 %	0.069	0.987	0.457	0.987
MLF_right	6.892e-04 ± 3.101e-05	6.905e-04 ± 2.741e-05	6.895e-04 ± 4.188e-05	6.870e-04 ± 4.959e-05	0.19 %	-0.36 %	-0.874	0.963	0.337	0.987
OR_left	7.003e-04 ± 4.076e-05	6.990e-04 ± 3.968e-05	6.871e-04 ± 3.076e-05	6.899e-04 ± 7.430e-05	-0.19 %	0.41 %	0.115	0.987	-0.177	0.987
OR_right	6.915e-04 ± 4.588e-05	6.903e-04 ± 3.964e-05	6.925e-04 ± 3.584e-05	6.903e-04 ± 5.206e-05	-0.18 %	-0.33 %	-0.281	0.987	0.761	0.987
POPT_left	6.928e-04 ± 2.568e-05	6.964e-04 ± 3.043e-05	6.958e-04 ± 4.768e-05	6.931e-04 ± 7.727e-05	0.52 %	-0.38 %	-1.306	0.963	0.219	0.987
POPT_right	6.742e-04 ± 2.835e-05	6.769e-04 ± 2.844e-05	6.720e-04 ± 4.540e-05	6.745e-04 ± 7.402e-05	0.41 %	0.37 %	-1.153	0.963	-0.159	0.987
SCP_left	6.519e-04 ± 2.732e-05	6.483e-04 ± 3.494e-05	6.356e-04 ± 5.143e-05	6.262e-04 ± 7.020e-05	-0.55 %	-1.47 %	0.747	0.987	0.392	0.987
SCP_right	6.451e-04 ± 2.198e-05	6.422e-04 ± 2.353e-05	6.433e-04 ± 6.362e-05	6.256e-04 ± 4.642e-05	-0.44 %	-2.76 %	0.798	0.963	1.152	0.987
SLF_III_left	6.876e-04 ± 2.547e-05	6.873e-04 ± 2.821e-05	6.761e-04 ± 5.829e-05	6.689e-04 ± 5.911e-05	-0.05 %	-1.07 %	0.140	0.987	0.484	0.987
SLF_III_right	6.713e-04 ± 2.392e-05	6.730e-04 ± 2.385e-05	6.741e-04 ± 3.759e-05	6.716e-04 ± 5.256e-05	0.25 %	-0.38 %	-0.618	0.987	0.204	0.987
SLF_II_left	7.067e-04 ± 3.277e-05	7.016e-04 ± 3.297e-05	6.981e-04 ± 4.919e-05	6.871e-04 ± 5.678e-05	-0.72 %	-1.56 %	1.508	0.963	0.954	0.987
SLF_II_right	6.984e-04 ± 3.077e-05	6.947e-04 ± 2.901e-05	6.940e-04 ± 4.574e-05	6.848e-04 ± 4.679e-05	-0.53 %	-1.33 %	0.963	0.963	0.941	0.987
SLF_I_left	7.430e-04 ± 4.054e-05	7.445e-04 ± 4.786e-05	7.586e-04 ± 9.004e-05	7.513e-04 ± 1.027e-04	0.19 %	-0.96 %	-0.223	0.987	0.386	0.987
SLF_I_right	7.220e-04 ± 3.788e-05	7.195e-04 ± 4.255e-05	7.262e-04 ± 7.028e-05	7.184e-04 ± 8.837e-05	-0.35 %	-1.07 %	0.451	0.987	0.476	0.987
STR_left	6.387e-04 ± 2.448e-05	6.349e-04 ± 3.693e-05	6.095e-04 ± 4.429e-05	6.160e-04 ± 1.065e-04	-0.6 %	1.07 %	0.837	0.963	-0.314	0.987
STR_right	6.227e-04 ± 2.252e-05	6.193e-04 ± 2.865e-05	6.126e-04 ± 5.202e-05	6.044e-04 ± 6.454e-05	-0.53 %	-1.33 %	0.894	0.963	0.571	0.987
ST_FO_left	6.794e-04 ± 3.460e-05	6.807e-04 ± 3.755e-05	6.454e-04 ± 3.381e-05	6.439e-04 ± 6.515e-05	0.18 %	-0.23 %	-0.706	0.987	0.027	0.987
ST_FO_right	6.794e-04 ± 3.338e-05	6.773e-04 ± 3.279e-05	6.604e-04 ± 4.087e-05	6.472e-04 ± 3.854e-05	-0.31 %	-2.01 %	0.394	0.987	1.637	0.987
ST_OCC_left	6.844e-04 ± 3.375e-05	6.831e-04 ± 3.157e-05	6.662e-04 ± 2.020e-05	6.689e-04 ± 5.584e-05	-0.2 %	0.41 %	0.179	0.987	-0.164	0.987
ST_OCC_right	6.743e-04 ± 3.673e-05	6.726e-04 ± 3.110e-05	6.658e-04 ± 2.164e-05	6.658e-04 ± 3.611e-05	-0.25 %	-0.01 %	-0.162	0.987	0.772	0.987
ST_PAR_left	7.027e-04 ± 2.979e-05	7.040e-04 ± 3.110e-05	7.013e-04 ± 4.253e-05	6.992e-04 ± 6.829e-05	0.18 %	-0.3 %	-0.660	0.987	0.291	0.987
ST_PAR_right	6.805e-04 ± 3.013e-05	6.816e-04 ± 2.781e-05	6.765e-04 ± 3.588e-05	6.785e-04 ± 5.953e-05	0.16 %	0.3 %	-0.819	0.963	-0.066	0.987
ST_POSTC_left	7.006e-04 ± 2.844e-05	6.993e-04 ± 3.708e-05	6.903e-04 ± 5.255e-05	6.831e-04 ± 7.874e-05	-0.19 %	-1.05 %	0.317	0.987	0.506	0.987
ST_POSTC_right	6.683e-04 ± 2.854e-05	6.682e-04 ± 3.251e-05	6.665e-04 ± 5.109e-05	6.713e-04 ± 8.250e-05	-0.03 %	0.72 %	-0.032	0.987	-0.110	0.987
ST_PREC_left	6.905e-04 ± 2.735e-05	6.859e-04 ± 3.627e-05	6.655e-04 ± 4.600e-05	6.650e-04 ± 7.016e-05	-0.66 %	-0.07 %	1.339	0.963	0.198	0.987
ST_PREC_right	6.658e-04 ± 2.834e-05	6.613e-04 ± 2.734e-05	6.546e-04 ± 3.867e-05	6.551e-04 ± 6.024e-05	-0.68 %	0.08 %	1.044	0.963	0.145	0.987

Table A.18 (cont'd)

	mTBI		Controls							
TractSeg Name	P1	P2	P1	P2	Percent Change mTBI %	Percent Change Controls %	t-score mTBI	q-value mTBI[1]	t-score controls	q-value controls
ST_PREF_left	6.862e-04 ± 2.550e-05	6.826e-04 ± 2.901e-05	6.631e-04 ± 4.479e-05	6.584e-04 ± 5.170e-05	-0.53 %	-0.71 %	1.215	0.963	0.428	0.987
ST_PREF_right	6.861e-04 ± 2.578e-05	6.823e-04 ± 2.420e-05	6.701e-04 ± 4.125e-05	6.570e-04 ± 3.744e-05	-0.55 %	-1.96 %	1.547	0.963	1.664	0.987
ST_PREM_left	7.003e-04 ± 2.757e-05	6.946e-04 ± 3.653e-05	6.724e-04 ± 4.717e-05	6.559e-04 ± 4.144e-05	-0.81 %	-2.45 %	1.588	0.963	1.643	0.987
ST_PREM_right	6.798e-04 ± 2.468e-05	6.738e-04 ± 2.700e-05	6.611e-04 ± 5.068e-05	6.543e-04 ± 4.936e-05	-0.88 %	-1.02 %	2.357	0.963	0.792	0.987
T_OCC_left	7.072e-04 ± 4.198e-05	7.054e-04 ± 4.044e-05	6.937e-04 ± 3.080e-05	6.965e-04 ± 7.268e-05	-0.25 %	0.4 %	0.243	0.987	-0.168	0.987
T_OCC_right	6.955e-04 ± 4.611e-05	6.939e-04 ± 3.958e-05	6.959e-04 ± 3.580e-05	6.940e-04 ± 5.270e-05	-0.23 %	-0.27 %	-0.166	0.987	0.784	0.987
T_PAR_left	7.125e-04 ± 3.498e-05	7.142e-04 ± 3.744e-05	7.171e-04 ± 5.163e-05	7.146e-04 ± 8.467e-05	0.24 %	-0.35 %	-0.595	0.987	0.251	0.987
T_PAR_right	6.970e-04 ± 3.743e-05	6.972e-04 ± 3.505e-05	6.990e-04 ± 4.984e-05	6.988e-04 ± 7.777e-05	0.03 %	-0.04 %	-0.318	0.987	0.118	0.987
T_POSTC_left	6.971e-04 ± 3.117e-05	6.983e-04 ± 4.104e-05	7.039e-04 ± 6.754e-05	6.936e-04 ± 9.480e-05	0.18 %	-1.46 %	-0.242	0.987	0.524	0.987
T_POSTC_right	6.677e-04 ± 3.483e-05	6.697e-04 ± 3.996e-05	6.816e-04 ± 7.665e-05	6.863e-04 ± 1.103e-04	0.3 %	0.68 %	-0.364	0.987	-0.037	0.987
T_PREC_left	6.898e-04 ± 3.095e-05	6.852e-04 ± 4.194e-05	6.714e-04 ± 5.676e-05	6.694e-04 ± 8.506e-05	-0.66 %	-0.31 %	1.137	0.963	0.225	0.987
T_PREC_right	6.655e-04 ± 3.227e-05	6.598e-04 ± 3.168e-05	6.596e-04 ± 5.046e-05	6.588e-04 ± 7.162e-05	-0.84 %	-0.13 %	1.085	0.963	0.213	0.987
T_PREF_left	7.001e-04 ± 2.893e-05	6.957e-04 ± 3.602e-05	6.806e-04 ± 5.524e-05	6.725e-04 ± 6.216e-05	-0.63 %	-1.19 %	1.064	0.963	0.560	0.987
T_PREF_right	7.107e-04 ± 3.313e-05	7.047e-04 ± 3.333e-05	7.004e-04 ± 5.745e-05	6.844e-04 ± 5.691e-05	-0.85 %	-2.29 %	1.625	0.963	1.371	0.987
T_PREM_left	7.121e-04 ± 3.405e-05	7.060e-04 ± 4.735e-05	6.912e-04 ± 6.029e-05	6.707e-04 ± 6.564e-05	-0.85 %	-2.97 %	1.082	0.963	1.337	0.987
T_PREM_right	6.954e-04 ± 3.690e-05	6.867e-04 ± 3.860e-05	6.861e-04 ± 8.031e-05	6.738e-04 ± 7.435e-05	-1.25 %	-1.8 %	1.770	0.963	0.869	0.987
UF_left	6.887e-04 ± 2.637e-05	6.933e-04 ± 2.901e-05	6.710e-04 ± 3.417e-05	6.656e-04 ± 3.905e-05	0.67 %	-0.81 %	-1.624	0.963	0.422	0.987
UF_right	7.064e-04 ± 2.464e-05	7.077e-04 ± 3.061e-05	6.943e-04 ± 4.186e-05	6.804e-04 ± 4.518e-05	0.19 %	-2.01 %	-0.641	0.987	0.938	0.987

Tables A.18- T-test results for comparisons of the automatically segmented tracts from TractSeg between timepoints within mTBI and control subjects.

[1]Significant values are marked with an asterisk (*) or <0.001

Table A.19 Results of Post Hoc Tract Specific Comparison of Diffusion Kurtosis Imaging Kurtosis Fractional Anisotropy

	mTBI		Controls							
TractSeg Name	P1	P2	P1	P2	Percent Change mTBI %	Percent Change Controls %	t-score mTBI	q-value mTBI[1]	t-score controls	q-value controls
AF_left	0.200 ± 0.010	0.200 ± 0.008	0.202 ± 0.014	0.204 ± 0.013	0.02 %	0.77 %	0.046	0.456	-0.557	0.629
AF_right	0.204 ± 0.008	0.203 ± 0.008	0.202 ± 0.011	0.201 ± 0.020	-0.53 %	-0.71 %	1.520	0.422	0.213	0.629
ATR_left	0.204 ± 0.008	0.204 ± 0.009	0.210 ± 0.015	0.213 ± 0.014	0.26 %	1.53 %	-0.365	0.422	-0.987	0.629
ATR_right	0.199 ± 0.008	0.200 ± 0.009	0.203 ± 0.013	0.204 ± 0.016	0.27 %	0.77 %	-0.594	0.422	-0.503	0.629
CA	0.208 ± 0.013	0.207 ± 0.018	0.220 ± 0.016	0.219 ± 0.027	-0.34 %	-0.44 %	0.470	0.422	0.014	0.662
CC_1	0.258 ± 0.016	0.255 ± 0.023	0.264 ± 0.017	0.257 ± 0.041	-0.98 %	-2.65 %	1.215	0.422	0.517	0.629
CC_2	0.224 ± 0.010	0.223 ± 0.010	0.227 ± 0.016	0.228 ± 0.021	-0.34 %	0.43 %	0.874	0.422	-0.350	0.629
CC_3	0.224 ± 0.012	0.223 ± 0.017	0.229 ± 0.025	0.231 ± 0.028	-0.67 %	1.07 %	0.759	0.422	-0.464	0.629
CC_4	0.234 ± 0.013	0.232 ± 0.014	0.235 ± 0.024	0.238 ± 0.025	-0.64 %	1.09 %	0.921	0.422	-0.431	0.629
CC_5	0.243 ± 0.013	0.241 ± 0.015	0.243 ± 0.025	0.245 ± 0.029	-0.98 %	1.06 %	1.382	0.422	-0.362	0.629
CC_6	0.234 ± 0.013	0.234 ± 0.010	0.230 ± 0.017	0.229 ± 0.021	-0.27 %	-0.14 %	0.731	0.422	-0.014	0.662
CC_7	0.236 ± 0.012	0.235 ± 0.012	0.233 ± 0.009	0.229 ± 0.030	-0.33 %	-1.92 %	0.939	0.422	0.555	0.629
CC	0.228 ± 0.010	0.228 ± 0.009	0.228 ± 0.016	0.228 ± 0.021	-0.3 %	0.06 %	0.859	0.422	-0.142	0.649
CG_left	0.215 ± 0.012	0.217 ± 0.014	0.217 ± 0.018	0.216 ± 0.022	0.95 %	-0.37 %	-0.737	0.422	-0.025	0.662
CG_right	0.219 ± 0.013	0.219 ± 0.012	0.218 ± 0.017	0.217 ± 0.019	0.21 %	-0.16 %	-0.217	0.422	-0.218	0.629
CST_left	0.255 ± 0.010	0.257 ± 0.011	0.260 ± 0.019	0.264 ± 0.018	0.45 %	1.47 %	-0.880	0.422	-0.717	0.629
CST_right	0.262 ± 0.010	0.262 ± 0.011	0.263 ± 0.018	0.263 ± 0.024	0.07 %	0.09 %	-0.048	0.456	-0.030	0.662
FPT_left	0.246 ± 0.010	0.247 ± 0.011	0.249 ± 0.020	0.252 ± 0.020	0.44 %	1.2 %	-0.573	0.422	-0.558	0.629
FPT_right	0.248 ± 0.010	0.248 ± 0.010	0.249 ± 0.017	0.251 ± 0.020	0.15 %	1 %	-0.234	0.422	-0.473	0.629
FX_left	0.185 ± 0.037	0.186 ± 0.039	0.192 ± 0.038	0.191 ± 0.046	0.55 %	-0.54 %	-0.221	0.422	-0.212	0.629
FX_right	0.189 ± 0.037	0.190 ± 0.042	0.193 ± 0.039	0.198 ± 0.042	0.56 %	2.1 %	-0.065	0.456	-1.034	0.629
ICP_left	0.200 ± 0.020	0.200 ± 0.022	0.189 ± 0.023	0.189 ± 0.031	-0.15 %	-0.38 %	0.463	0.422	0.090	0.662
ICP_right	0.189 ± 0.013	0.187 ± 0.014	0.178 ± 0.019	0.181 ± 0.024	-1.15 %	1.79 %	1.833	0.422	-0.365	0.629
IFO_left	0.217 ± 0.009	0.216 ± 0.009	0.218 ± 0.010	0.215 ± 0.023	-0.26 %	-1.35 %	0.930	0.422	0.418	0.629
IFO_right	0.216 ± 0.008	0.215 ± 0.009	0.216 ± 0.008	0.215 ± 0.021	-0.37 %	-0.7 %	1.343	0.422	0.358	0.629
ILF_left	0.214 ± 0.009	0.213 ± 0.011	0.217 ± 0.007	0.212 ± 0.027	-0.45 %	-2.37 %	0.807	0.422	0.742	0.629
ILF_right	0.214 ± 0.009	0.213 ± 0.013	0.216 ± 0.009	0.212 ± 0.028	-0.29 %	-1.6 %	0.839	0.422	0.489	0.629
MCP	0.218 ± 0.012	0.217 ± 0.012	0.212 ± 0.023	0.209 ± 0.026	-0.53 %	-1.08 %	1.023	0.422	0.280	0.629
MLF_left	0.207 ± 0.011	0.208 ± 0.008	0.204 ± 0.014	0.206 ± 0.013	0.33 %	0.85 %	-0.362	0.422	-0.552	0.629
MLF_right	0.214 ± 0.010	0.213 ± 0.009	0.209 ± 0.015	0.208 ± 0.019	-0.46 %	-0.05 %	1.247	0.422	-0.061	0.662
OR_left	0.223 ± 0.011	0.223 ± 0.011	0.223 ± 0.007	0.220 ± 0.028	-0.08 %	-1.31 %	0.308	0.422	0.474	0.629
OR_right	0.231 ± 0.011	0.231 ± 0.011	0.230 ± 0.009	0.228 ± 0.020	-0.09 %	-0.66 %	0.644	0.422	0.321	0.629
POPT_left	0.238 ± 0.009	0.238 ± 0.010	0.236 ± 0.017	0.239 ± 0.017	0.12 %	1.2 %	-0.027	0.456	-0.549	0.629
POPT_right	0.249 ± 0.010	0.249 ± 0.010	0.248 ± 0.017	0.250 ± 0.020	-0.06 %	0.78 %	0.469	0.422	-0.236	0.629
SCP_left	0.230 ± 0.013	0.231 ± 0.017	0.229 ± 0.019	0.233 ± 0.023	0.4 %	1.81 %	-0.393	0.422	-0.629	0.629
SCP_right	0.232 ± 0.009	0.231 ± 0.012	0.226 ± 0.020	0.231 ± 0.021	-0.32 %	2.19 %	0.672	0.422	-0.618	0.629
SLF_III_left	0.205 ± 0.011	0.204 ± 0.010	0.205 ± 0.021	0.208 ± 0.017	-0.62 %	1.43 %	0.985	0.422	-0.661	0.629

Table A.19 (cont'd)

	mTBI		Controls							
TractSeg Name	P1	P2	P1	P2	Percent Change mTBI %	Percent Change Controls %	t-score mTBI	q-value mTBI[1]	t-score controls	q-value controls
SLF_III_right	0.209 ± 0.009	0.206 ± 0.011	0.203 ± 0.014	0.200 ± 0.028	-1.33 %	-1.53 %	2.162	0.422	0.388	0.629
SLF_II_left	0.193 ± 0.011	0.194 ± 0.011	0.192 ± 0.015	0.198 ± 0.018	0.69 %	2.71 %	-0.807	0.422	-1.156	0.629
SLF_II_right	0.194 ± 0.010	0.194 ± 0.010	0.191 ± 0.014	0.194 ± 0.015	0.08 %	1.46 %	0.322	0.422	-0.755	0.629
SLF_I_left	0.193 ± 0.010	0.194 ± 0.012	0.190 ± 0.022	0.193 ± 0.018	0.44 %	1.79 %	-0.511	0.422	-0.686	0.629
SLF_I_right	0.201 ± 0.011	0.203 ± 0.012	0.199 ± 0.019	0.203 ± 0.017	0.58 %	2.23 %	-0.511	0.422	-0.775	0.629
STR_left	0.247 ± 0.011	0.249 ± 0.014	0.254 ± 0.019	0.256 ± 0.026	0.53 %	1.05 %	-0.822	0.422	-0.477	0.629
STR_right	0.255 ± 0.012	0.255 ± 0.012	0.257 ± 0.020	0.261 ± 0.018	0.01 %	1.7 %	-0.269	0.422	-0.996	0.629
ST_FO_left	0.225 ± 0.012	0.223 ± 0.013	0.233 ± 0.013	0.231 ± 0.026	-0.77 %	-0.72 %	1.334	0.422	0.355	0.629
ST_FO_right	0.228 ± 0.013	0.227 ± 0.016	0.232 ± 0.014	0.229 ± 0.028	-0.52 %	-1.02 %	0.891	0.422	0.191	0.631
ST_OCC_left	0.225 ± 0.011	0.225 ± 0.011	0.225 ± 0.010	0.221 ± 0.028	0 %	-1.4 %	0.250	0.422	0.447	0.629
ST_OCC_right	0.229 ± 0.011	0.228 ± 0.011	0.227 ± 0.010	0.226 ± 0.020	-0.34 %	-0.46 %	1.063	0.422	0.250	0.629
ST_PAR_left	0.217 ± 0.010	0.218 ± 0.009	0.215 ± 0.016	0.217 ± 0.015	0.42 %	1.09 %	-0.484	0.422	-0.645	0.629
ST_PAR_right	0.228 ± 0.010	0.228 ± 0.009	0.226 ± 0.014	0.228 ± 0.016	-0.25 %	0.76 %	1.006	0.422	-0.265	0.629
ST_POSTC_left	0.222 ± 0.010	0.223 ± 0.011	0.226 ± 0.017	0.230 ± 0.015	0.57 %	1.82 %	-0.816	0.422	-0.983	0.629
ST_POSTC_right	0.234 ± 0.011	0.233 ± 0.012	0.235 ± 0.017	0.238 ± 0.019	-0.22 %	1.24 %	0.606	0.422	-0.434	0.629
ST_PREC_left	0.222 ± 0.009	0.223 ± 0.011	0.229 ± 0.016	0.231 ± 0.014	0.53 %	1.18 %	-1.044	0.422	-0.802	0.629
ST_PREC_right	0.230 ± 0.009	0.230 ± 0.009	0.231 ± 0.015	0.234 ± 0.016	0.18 %	1.25 %	-0.292	0.422	-0.626	0.629
ST_PREF_left	0.215 ± 0.009	0.216 ± 0.008	0.220 ± 0.015	0.221 ± 0.016	0.29 %	0.41 %	-0.323	0.422	-0.391	0.629
ST_PREF_right	0.214 ± 0.008	0.214 ± 0.008	0.217 ± 0.012	0.218 ± 0.016	0.03 %	0.69 %	0.136	0.441	-0.494	0.629
ST_PREM_left	0.207 ± 0.009	0.208 ± 0.009	0.213 ± 0.017	0.215 ± 0.015	0.46 %	1.27 %	-0.554	0.422	-0.813	0.629
ST_PREM_right	0.216 ± 0.008	0.216 ± 0.009	0.218 ± 0.016	0.221 ± 0.018	0.26 %	1.1 %	-0.693	0.422	-0.461	0.629
T_OCC_left	0.220 ± 0.011	0.220 ± 0.011	0.221 ± 0.006	0.218 ± 0.027	-0.02 %	-1.35 %	0.224	0.422	0.491	0.629
T_OCC_right	0.227 ± 0.011	0.227 ± 0.011	0.226 ± 0.009	0.224 ± 0.019	-0.04 %	-0.68 %	0.572	0.422	0.331	0.629
T_PAR_left	0.216 ± 0.010	0.217 ± 0.009	0.214 ± 0.016	0.217 ± 0.017	0.36 %	1.36 %	-0.332	0.422	-0.693	0.629
T_PAR_right	0.228 ± 0.011	0.228 ± 0.010	0.226 ± 0.015	0.228 ± 0.016	0.08 %	1.05 %	0.194	0.425	-0.496	0.629
T_POSTC_left	0.227 ± 0.010	0.228 ± 0.012	0.226 ± 0.021	0.233 ± 0.019	0.32 %	2.76 %	-0.358	0.422	-1.043	0.629
T_POSTC_right	0.239 ± 0.013	0.238 ± 0.015	0.235 ± 0.025	0.238 ± 0.024	-0.28 %	1.38 %	0.425	0.422	-0.442	0.629
T_PREC_left	0.225 ± 0.009	0.226 ± 0.012	0.231 ± 0.019	0.235 ± 0.017	0.56 %	1.79 %	-1.048	0.422	-0.945	0.629
T_PREC_right	0.230 ± 0.010	0.231 ± 0.011	0.231 ± 0.018	0.234 ± 0.016	0.45 %	1.47 %	-0.801	0.422	-0.725	0.629
T_PREF_left	0.215 ± 0.009	0.216 ± 0.010	0.220 ± 0.016	0.223 ± 0.017	0.49 %	1.05 %	-0.751	0.422	-0.693	0.629
T_PREF_right	0.209 ± 0.008	0.210 ± 0.009	0.212 ± 0.013	0.214 ± 0.015	0.39 %	1.22 %	-0.892	0.422	-0.905	0.629
T_PREM_left	0.212 ± 0.009	0.214 ± 0.011	0.219 ± 0.017	0.224 ± 0.016	0.66 %	2.24 %	-0.837	0.422	-1.182	0.629
T_PREM_right	0.217 ± 0.010	0.219 ± 0.011	0.220 ± 0.020	0.224 ± 0.019	0.72 %	1.63 %	-1.279	0.422	-0.771	0.629
UF_left	0.221 ± 0.012	0.219 ± 0.014	0.224 ± 0.014	0.220 ± 0.026	-1.12 %	-1.77 %	1.708	0.422	0.497	0.629
UF_right	0.215 ± 0.010	0.214 ± 0.015	0.218 ± 0.011	0.216 ± 0.028	-0.82 %	-0.92 %	1.328	0.422	0.252	0.629

Tables A.19- T-test results for comparisons of the automatically segmented tracts from TractSeg between timepoints within mTBI and control subjects.

[1]Significant values are marked with an asterisk (*) or <0.001

Table A.20 Results of Post Hoc Tract Specific Comparison of Diffusion Kurtosis Imaging Mean Kurtosis

	mTBI		Controls							
TractSeg Name	P1	P2	P1	P2	Percent Change mTBI %	Percent Change Controls %	t-score mTBI	q-value mTBI[1]	t-score controls	q-value controls
AF_left	9.405e-04 ± 2.940e-05	9.323e-04 ± 3.288e-05	9.049e-04 ± 3.749e-05	8.943e-04 ± 4.150e-05	-0.87 %	-1.18 %	2.102	0.124	1.141	0.741
AF_right	9.296e-04 ± 2.842e-05	9.242e-04 ± 2.501e-05	9.134e-04 ± 3.055e-05	9.025e-04 ± 3.455e-05	-0.58 %	-1.19 %	1.999	0.124	1.390	0.732
ATR_left	9.992e-04 ± 4.547e-05	9.917e-04 ± 5.552e-05	9.651e-04 ± 5.828e-05	9.416e-04 ± 6.102e-05	-0.75 %	-2.43 %	1.195	0.149	1.755	0.732
ATR_right	1.011e-03 ± 5.214e-05	9.990e-04 ± 5.000e-05	9.922e-04 ± 7.752e-05	9.710e-04 ± 7.387e-05	-1.2 %	-2.13 %	2.129	0.124	1.524	0.732
CA	1.051e-03 ± 3.639e-05	1.045e-03 ± 5.522e-05	9.882e-04 ± 4.902e-05	9.673e-04 ± 5.410e-05	-0.58 %	-2.11 %	0.671	0.206	1.173	0.741
CC_1	1.027e-03 ± 5.777e-05	1.019e-03 ± 6.614e-05	1.018e-03 ± 9.343e-05	9.792e-04 ± 6.515e-05	-0.81 %	-3.77 %	1.041	0.172	2.976	0.319
CC_2	9.983e-04 ± 3.397e-05	9.973e-04 ± 4.112e-05	9.747e-04 ± 4.772e-05	9.563e-04 ± 5.529e-05	-0.1 %	-1.89 %	0.067	0.235	1.296	0.732
CC_3	1.023e-03 ± 4.521e-05	1.026e-03 ± 6.617e-05	9.953e-04 ± 6.128e-05	9.825e-04 ± 8.887e-05	0.35 %	-1.29 %	-0.499	0.206	0.617	0.872
CC_4	1.015e-03 ± 3.549e-05	1.021e-03 ± 4.994e-05	9.975e-04 ± 5.900e-05	1.003e-03 ± 1.205e-04	0.61 %	0.6 %	-0.999	0.172	-0.075	0.889
CC_5	1.004e-03 ± 3.478e-05	1.015e-03 ± 5.405e-05	9.915e-04 ± 6.630e-05	9.959e-04 ± 1.314e-04	1.13 %	0.44 %	-1.769	0.145	-0.066	0.889
CC_6	9.667e-04 ± 4.284e-05	9.703e-04 ± 3.623e-05	9.569e-04 ± 3.907e-05	9.626e-04 ± 7.973e-05	0.37 %	0.59 %	-1.251	0.149	-0.190	0.885
CC_7	9.930e-04 ± 7.692e-05	9.924e-04 ± 5.292e-05	9.851e-04 ± 4.702e-05	9.946e-04 ± 8.659e-05	-0.06 %	0.96 %	-0.122	0.232	-0.215	0.884
CC	9.882e-04 ± 3.531e-05	9.895e-04 ± 3.479e-05	9.744e-04 ± 4.187e-05	9.700e-04 ± 7.486e-05	0.13 %	-0.45 %	-0.653	0.206	0.391	0.872
CG_left	9.343e-04 ± 2.881e-05	9.320e-04 ± 2.868e-05	9.146e-04 ± 5.173e-05	9.169e-04 ± 9.080e-05	-0.25 %	0.24 %	0.386	0.206	-0.062	0.889
CG_right	9.228e-04 ± 3.196e-05	9.186e-04 ± 2.781e-05	9.050e-04 ± 4.795e-05	8.982e-04 ± 7.526e-05	-0.46 %	-0.75 %	0.684	0.206	0.357	0.872
CST_left	1.005e-03 ± 3.049e-05	1.002e-03 ± 4.362e-05	9.677e-04 ± 5.499e-05	9.620e-04 ± 9.214e-05	-0.34 %	-0.59 %	0.606	0.206	0.339	0.872
CST_right	9.612e-04 ± 3.090e-05	9.573e-04 ± 3.144e-05	9.326e-04 ± 4.490e-05	9.427e-04 ± 9.243e-05	-0.4 %	1.08 %	0.512	0.206	-0.431	0.872
FPT_left	1.005e-03 ± 2.968e-05	1.003e-03 ± 4.230e-05	9.738e-04 ± 7.679e-05	9.531e-04 ± 8.568e-05	-0.18 %	-2.13 %	0.133	0.232	0.917	0.807
FPT_right	9.983e-04 ± 3.213e-05	9.962e-04 ± 3.487e-05	9.747e-04 ± 7.129e-05	9.528e-04 ± 7.834e-05	-0.21 %	-2.25 %	0.170	0.232	1.219	0.741
FX_left	2.084e-03 ± 3.622e-04	2.053e-03 ± 3.602e-04	2.071e-03 ± 3.822e-04	2.052e-03 ± 4.225e-04	-1.49 %	-0.92 %	1.356	0.149	0.449	0.872
FX_right	2.055e-03 ± 3.465e-04	2.035e-03 ± 3.660e-04	2.050e-03 ± 3.706e-04	1.971e-03 ± 4.431e-04	-1.01 %	-3.89 %	0.563	0.206	1.460	0.732
ICP_left	8.986e-04 ± 8.235e-05	8.888e-04 ± 5.192e-05	8.881e-04 ± 6.794e-05	8.751e-04 ± 8.569e-05	-1.08 %	-1.47 %	0.836	0.194	0.537	0.872
ICP_right	8.806e-04 ± 6.453e-05	8.727e-04 ± 4.092e-05	8.802e-04 ± 7.328e-05	8.455e-04 ± 9.221e-05	-0.9 %	-3.94 %	0.802	0.198	1.528	0.732
IFO_left	9.595e-04 ± 3.503e-05	9.568e-04 ± 3.508e-05	9.338e-04 ± 2.693e-05	9.277e-04 ± 4.550e-05	-0.28 %	-0.66 %	0.598	0.206	0.902	0.807
IFO_right	9.506e-04 ± 4.005e-05	9.457e-04 ± 3.215e-05	9.348e-04 ± 3.207e-05	9.272e-04 ± 3.808e-05	-0.51 %	-0.82 %	1.023	0.172	2.739	0.319
ILF_left	9.724e-04 ± 5.191e-05	9.619e-04 ± 4.314e-05	9.423e-04 ± 3.590e-05	9.315e-04 ± 5.478e-05	-1.07 %	-1.15 %	2.123	0.124	1.104	0.741
ILF_right	9.614e-04 ± 5.392e-05	9.529e-04 ± 4.118e-05	9.451e-04 ± 4.685e-05	9.341e-04 ± 6.133e-05	-0.88 %	-1.16 %	1.570	0.149	2.178	0.512

Table A.20 (cont'd)

	mTBI		Controls							
TractSeg Name	P1	P2	P1	P2	Percent Change mTBI %	Percent Change Controls %	t-score mTBI	q-value mTBI[1]	t-score controls	q-value controls
MCP	8.708e-04 ± 6.393e-05	8.685e-04 ± 4.820e-05	8.572e-04 ± 6.320e-05	8.784e-04 ± 8.677e-05	-0.27 %	2.47 %	0.194	0.232	-0.701	0.872
MLF_left	9.510e-04 ± 3.528e-05	9.494e-04 ± 3.444e-05	9.384e-04 ± 3.773e-05	9.319e-04 ± 5.611e-05	-0.18 %	-0.69 %	0.090	0.234	0.585	0.872
MLF_right	9.415e-04 ± 3.877e-05	9.415e-04 ± 3.484e-05	9.359e-04 ± 4.410e-05	9.289e-04 ± 5.616e-05	0 %	-0.75 %	-0.557	0.206	0.624	0.872
OR_left	9.945e-04 ± 5.449e-05	9.898e-04 ± 5.405e-05	9.744e-04 ± 4.405e-05	9.733e-04 ± 8.667e-05	-0.47 %	-0.12 %	0.643	0.206	0.113	0.889
OR_right	9.831e-04 ± 6.108e-05	9.795e-04 ± 5.414e-05	9.841e-04 ± 5.234e-05	9.772e-04 ± 7.327e-05	-0.37 %	-0.7 %	0.116	0.232	1.280	0.732
POPT_left	9.991e-04 ± 3.297e-05	1.003e-03 ± 3.879e-05	9.932e-04 ± 5.520e-05	9.883e-04 ± 9.957e-05	0.39 %	-0.49 %	-1.218	0.149	0.302	0.872
POPT_right	9.794e-04 ± 3.744e-05	9.816e-04 ± 3.672e-05	9.688e-04 ± 5.193e-05	9.708e-04 ± 9.200e-05	0.22 %	0.2 %	-0.967	0.173	-0.104	0.889
SCP_left	9.493e-04 ± 3.634e-05	9.421e-04 ± 4.372e-05	9.138e-04 ± 5.534e-05	9.047e-04 ± 7.949e-05	-0.75 %	-0.99 %	1.251	0.149	0.379	0.872
SCP_right	9.361e-04 ± 2.950e-05	9.290e-04 ± 3.024e-05	9.207e-04 ± 7.218e-05	9.000e-04 ± 5.096e-05	-0.75 %	-2.25 %	1.880	0.128	1.362	0.732
SLF_III_left	9.434e-04 ± 3.034e-05	9.396e-04 ± 3.632e-05	9.186e-04 ± 6.050e-05	9.067e-04 ± 6.975e-05	-0.4 %	-1.29 %	1.003	0.172	0.644	0.872
SLF_III_right	9.267e-04 ± 2.895e-05	9.254e-04 ± 2.677e-05	9.196e-04 ± 3.960e-05	9.110e-04 ± 5.053e-05	-0.15 %	-0.94 %	0.387	0.206	0.659	0.872
SLF_II_left	9.559e-04 ± 3.748e-05	9.506e-04 ± 3.974e-05	9.367e-04 ± 5.163e-05	9.242e-04 ± 6.602e-05	-0.56 %	-1.33 %	1.444	0.149	0.970	0.807
SLF_II_right	9.449e-04 ± 3.611e-05	9.399e-04 ± 3.350e-05	9.310e-04 ± 4.893e-05	9.181e-04 ± 5.575e-05	-0.54 %	-1.39 %	1.310	0.149	1.189	0.741
SLF_I_left	9.992e-04 ± 5.026e-05	1.002e-03 ± 5.790e-05	1.011e-03 ± 1.104e-04	9.988e-04 ± 1.340e-04	0.29 %	-1.24 %	-0.553	0.206	0.471	0.872
SLF_I_right	9.798e-04 ± 4.602e-05	9.771e-04 ± 5.018e-05	9.788e-04 ± 8.196e-05	9.684e-04 ± 1.147e-04	-0.27 %	-1.06 %	0.427	0.206	0.523	0.872
STR_left	9.481e-04 ± 2.894e-05	9.418e-04 ± 4.814e-05	8.943e-04 ± 5.409e-05	9.001e-04 ± 1.305e-04	-0.66 %	0.65 %	1.102	0.167	-0.242	0.884
STR_right	9.235e-04 ± 2.917e-05	9.162e-04 ± 3.585e-05	8.993e-04 ± 6.302e-05	8.863e-04 ± 8.140e-05	-0.8 %	-1.45 %	1.433	0.149	0.638	0.872
ST_FO_left	9.471e-04 ± 4.708e-05	9.451e-04 ± 5.533e-05	9.020e-04 ± 4.637e-05	8.959e-04 ± 6.989e-05	-0.21 %	-0.67 %	0.172	0.232	0.444	0.872
ST_FO_right	9.540e-04 ± 4.446e-05	9.478e-04 ± 4.387e-05	9.270e-04 ± 5.471e-05	9.033e-04 ± 3.635e-05	-0.65 %	-2.56 %	1.302	0.149	2.638	0.319
ST_OCC_left	9.709e-04 ± 4.304e-05	9.666e-04 ± 4.266e-05	9.416e-04 ± 2.495e-05	9.403e-04 ± 5.582e-05	-0.44 %	-0.14 %	0.878	0.188	0.291	0.872
ST_OCC_right	9.519e-04 ± 4.755e-05	9.476e-04 ± 4.183e-05	9.384e-04 ± 3.310e-05	9.355e-04 ± 4.555e-05	-0.45 %	-0.3 %	0.391	0.206	2.671	0.319
ST_PAR_left	9.781e-04 ± 3.716e-05	9.795e-04 ± 3.927e-05	9.692e-04 ± 4.808e-05	9.649e-04 ± 8.628e-05	0.14 %	-0.45 %	-0.698	0.206	0.371	0.872
ST_PAR_right	9.555e-04 ± 3.860e-05	9.552e-04 ± 3.533e-05	9.441e-04 ± 4.045e-05	9.445e-04 ± 7.279e-05	-0.03 %	0.04 %	-0.463	0.206	0.053	0.889
ST_POSTC_left	9.937e-04 ± 3.872e-05	9.907e-04 ± 5.073e-05	9.698e-04 ± 6.816e-05	9.574e-04 ± 1.078e-04	-0.3 %	-1.27 %	0.514	0.206	0.567	0.872
ST_POSTC_right	9.563e-04 ± 3.757e-05	9.534e-04 ± 3.951e-05	9.484e-04 ± 6.615e-05	9.513e-04 ± 1.081e-04	-0.31 %	0.31 %	0.429	0.206	0.015	0.898
ST_PREC_left	9.860e-04 ± 3.607e-05	9.786e-04 ± 5.040e-05	9.413e-04 ± 5.738e-05	9.381e-04 ± 9.289e-05	-0.75 %	-0.34 %	1.449	0.149	0.276	0.872
ST_PREC_right	9.556e-04 ± 3.735e-05	9.469e-04 ± 3.475e-05	9.327e-04 ± 5.116e-05	9.306e-04 ± 7.729e-05	-0.91 %	-0.22 %	1.549	0.149	0.325	0.872

Table A.20 (cont'd)

	mTBI		Controls							
TractSeg Name	P1	P2	P1	P2	Percent Change mTBI %	Percent Change Controls %	t-score mTBI	q-value mTBI[1]	t-score controls	q-value controls
ST_PREF_left	9.640e-04 ± 3.279e-05	9.582e-04 ± 4.179e-05	9.262e-04 ± 5.308e-05	9.136e-04 ± 6.012e-05	-0.6 %	-1.36 %	1.416	0.149	0.864	0.823
ST_PREF_right	9.622e-04 ± 3.418e-05	9.550e-04 ± 3.441e-05	9.342e-04 ± 5.387e-05	9.133e-04 ± 4.582e-05	-0.75 %	-2.24 %	2.212	0.124	1.962	0.654
ST_PREM_left	9.727e-04 ± 3.862e-05	9.648e-04 ± 5.527e-05	9.254e-04 ± 5.624e-05	8.975e-04 ± 4.967e-05	-0.81 %	-3.02 %	1.538	0.149	2.311	0.479
ST_PREM_right	9.570e-04 ± 3.336e-05	9.475e-04 ± 3.796e-05	9.252e-04 ± 6.306e-05	9.101e-04 ± 5.958e-05	-0.99 %	-1.64 %	2.792	0.124	1.341	0.732
T_OCC_left	1.001e-03 ± 5.633e-05	9.958e-04 ± 5.548e-05	9.813e-04 ± 4.437e-05	9.800e-04 ± 8.538e-05	-0.53 %	-0.14 %	0.757	0.205	0.142	0.889
T_OCC_right	9.842e-04 ± 6.157e-05	9.801e-04 ± 5.434e-05	9.846e-04 ± 5.332e-05	9.783e-04 ± 7.429e-05	-0.41 %	-0.63 %	0.210	0.232	1.273	0.732
T_PAR_left	9.924e-04 ± 4.415e-05	9.945e-04 ± 4.689e-05	9.928e-04 ± 6.218e-05	9.876e-04 ± 1.092e-04	0.21 %	-0.53 %	-0.635	0.206	0.323	0.872
T_PAR_right	9.798e-04 ± 4.823e-05	9.789e-04 ± 4.424e-05	9.773e-04 ± 6.115e-05	9.748e-04 ± 9.990e-05	-0.1 %	-0.26 %	-0.153	0.232	0.210	0.884
T_POSTC_left	9.904e-04 ± 3.971e-05	9.908e-04 ± 5.222e-05	9.876e-04 ± 8.681e-05	9.722e-04 ± 1.256e-04	0.04 %	-1.56 %	-0.034	0.238	0.571	0.872
T_POSTC_right	9.554e-04 ± 4.229e-05	9.565e-04 ± 4.577e-05	9.661e-04 ± 9.372e-05	9.680e-04 ± 1.417e-04	0.12 %	0.19 %	-0.225	0.232	0.045	0.889
T_PREC_left	9.895e-04 ± 3.827e-05	9.824e-04 ± 5.481e-05	9.537e-04 ± 6.981e-05	9.490e-04 ± 1.109e-04	-0.72 %	-0.49 %	1.299	0.149	0.276	0.872
T_PREC_right	9.530e-04 ± 4.062e-05	9.440e-04 ± 3.812e-05	9.369e-04 ± 6.181e-05	9.331e-04 ± 9.125e-05	-0.94 %	-0.41 %	1.354	0.149	0.330	0.872
T_PREF_left	9.875e-04 ± 3.675e-05	9.809e-04 ± 4.894e-05	9.550e-04 ± 6.698e-05	9.383e-04 ± 7.597e-05	-0.67 %	-1.76 %	1.239	0.149	0.904	0.807
T_PREF_right	9.944e-04 ± 4.383e-05	9.846e-04 ± 4.471e-05	9.749e-04 ± 7.562e-05	9.510e-04 ± 7.470e-05	-0.98 %	-2.44 %	1.951	0.124	1.522	0.732
T_PREM_left	9.990e-04 ± 4.493e-05	9.901e-04 ± 6.565e-05	9.630e-04 ± 7.541e-05	9.316e-04 ± 8.453e-05	-0.9 %	-3.26 %	1.242	0.149	1.582	0.732
T_PREM_right	9.810e-04 ± 4.743e-05	9.687e-04 ± 5.084e-05	9.640e-04 ± 1.017e-04	9.429e-04 ± 9.568e-05	-1.26 %	-2.19 %	1.956	0.124	1.089	0.741
UF_left	9.459e-04 ± 3.425e-05	9.485e-04 ± 3.537e-05	9.204e-04 ± 4.060e-05	9.080e-04 ± 4.121e-05	0.28 %	-1.35 %	-0.957	0.173	1.023	0.785
UF_right	9.729e-04 ± 3.170e-05	9.701e-04 ± 3.521e-05	9.535e-04 ± 5.527e-05	9.301e-04 ± 4.556e-05	-0.29 %	-2.46 %	0.485	0.206	1.455	0.732

Tables A.20- T-test results for comparisons of the automatically segmented tracts from TractSeg between timepoints within mTBI and control subjects.

[1]Significant values are marked with an asterisk (*) or <0.001

Table A.21 Results of Post Hoc Tract Specific Comparison of Diffusion Kurtosis Imaging Axial Kurtosis

	mTBI		Controls							
TractSeg Name	P1	P2	P1	P2	Percent Change mTBI %	Percent Change Controls %	t-score mTBI	q-value mTBI[1]	t-score controls	q-value controls
AF_left	1.137e-03 ± 2.870e-05	1.127e-03 ± 3.362e-05	1.095e-03 ± 3.274e-05	1.082e-03 ± 3.656e-05	-0.86 %	-1.15 %	2.577	0.116	1.638	0.173
AF_right	1.126e-03 ± 2.878e-05	1.119e-03 ± 2.558e-05	1.105e-03 ± 3.145e-05	1.089e-03 ± 2.307e-05	-0.68 %	-1.42 %	2.893	0.085	2.740	0.096
ATR_left	1.207e-03 ± 4.550e-05	1.199e-03 ± 5.503e-05	1.169e-03 ± 5.415e-05	1.143e-03 ± 5.492e-05	-0.7 %	-2.24 %	1.423	0.221	2.145	0.151
ATR_right	1.216e-03 ± 5.206e-05	1.203e-03 ± 4.988e-05	1.193e-03 ± 7.617e-05	1.168e-03 ± 6.844e-05	-1.1 %	-2.09 %	2.379	0.132	1.863	0.16
CA	1.285e-03 ± 3.787e-05	1.276e-03 ± 5.025e-05	1.223e-03 ± 4.878e-05	1.194e-03 ± 3.581e-05	-0.69 %	-2.44 %	1.168	0.283	2.154	0.151
CC_1	1.318e-03 ± 6.172e-05	1.306e-03 ± 7.864e-05	1.310e-03 ± 9.903e-05	1.255e-03 ± 8.869e-05	-0.85 %	-4.21 %	1.293	0.244	2.387	0.142
CC_2	1.238e-03 ± 3.436e-05	1.235e-03 ± 4.059e-05	1.207e-03 ± 4.365e-05	1.184e-03 ± 4.207e-05	-0.25 %	-1.97 %	0.621	0.398	2.171	0.151
CC_3	1.267e-03 ± 4.850e-05	1.267e-03 ± 6.164e-05	1.232e-03 ± 5.686e-05	1.214e-03 ± 7.173e-05	0.02 %	-1.48 %	-0.062	0.556	0.967	0.353
CC_4	1.264e-03 ± 3.244e-05	1.267e-03 ± 4.850e-05	1.234e-03 ± 5.206e-05	1.237e-03 ± 1.013e-04	0.23 %	0.19 %	-0.529	0.421	0.014	0.5
CC_5	1.260e-03 ± 3.440e-05	1.268e-03 ± 5.256e-05	1.235e-03 ± 5.934e-05	1.236e-03 ± 1.116e-04	0.63 %	0.08 %	-1.372	0.234	-0.013	0.5
CC_6	1.204e-03 ± 3.913e-05	1.207e-03 ± 3.687e-05	1.185e-03 ± 3.034e-05	1.188e-03 ± 6.570e-05	0.22 %	0.21 %	-1.186	0.283	-0.084	0.5
CC_7	1.240e-03 ± 7.382e-05	1.239e-03 ± 5.439e-05	1.227e-03 ± 5.163e-05	1.229e-03 ± 7.370e-05	-0.13 %	0.18 %	0.049	0.556	0.462	0.412
CC	1.225e-03 ± 3.237e-05	1.225e-03 ± 3.325e-05	1.204e-03 ± 3.478e-05	1.195e-03 ± 6.046e-05	-0.02 %	-0.75 %	-0.244	0.512	0.865	0.379
CG_left	1.148e-03 ± 3.020e-05	1.147e-03 ± 2.997e-05	1.123e-03 ± 4.682e-05	1.121e-03 ± 8.185e-05	-0.06 %	-0.15 %	-0.017	0.556	0.065	0.5
CG_right	1.136e-03 ± 3.228e-05	1.132e-03 ± 2.951e-05	1.112e-03 ± 3.971e-05	1.100e-03 ± 6.918e-05	-0.39 %	-1.08 %	0.668	0.393	0.633	0.398
CST_left	1.278e-03 ± 3.066e-05	1.272e-03 ± 4.403e-05	1.226e-03 ± 4.775e-05	1.218e-03 ± 8.127e-05	-0.4 %	-0.69 %	0.982	0.319	0.566	0.4
CST_right	1.232e-03 ± 3.136e-05	1.226e-03 ± 3.289e-05	1.192e-03 ± 4.279e-05	1.197e-03 ± 7.733e-05	-0.48 %	0.46 %	0.973	0.319	-0.285	0.449
FPT_left	1.265e-03 ± 3.123e-05	1.263e-03 ± 4.285e-05	1.221e-03 ± 6.699e-05	1.197e-03 ± 7.479e-05	-0.23 %	-1.98 %	0.459	0.44	1.311	0.239
FPT_right	1.260e-03 ± 3.421e-05	1.256e-03 ± 3.649e-05	1.224e-03 ± 6.438e-05	1.199e-03 ± 6.964e-05	-0.29 %	-2.09 %	0.569	0.416	1.749	0.169
FX_left	2.431e-03 ± 3.183e-04	2.393e-03 ± 3.217e-04	2.407e-03 ± 3.339e-04	2.369e-03 ± 3.880e-04	-1.57 %	-1.56 %	1.864	0.198	0.644	0.398
FX_right	2.408e-03 ± 3.038e-04	2.381e-03 ± 3.238e-04	2.386e-03 ± 3.260e-04	2.295e-03 ± 4.230e-04	-1.11 %	-3.82 %	1.035	0.317	1.411	0.218
ICP_left	1.081e-03 ± 8.088e-05	1.069e-03 ± 5.278e-05	1.059e-03 ± 5.528e-05	1.043e-03 ± 6.917e-05	-1.1 %	-1.47 %	1.064	0.316	0.831	0.379
ICP_right	1.051e-03 ± 6.341e-05	1.040e-03 ± 4.193e-05	1.039e-03 ± 6.510e-05	1.004e-03 ± 9.658e-05	-1.08 %	-3.33 %	1.324	0.239	1.524	0.194
IFO_left	1.181e-03 ± 3.524e-05	1.177e-03 ± 3.770e-05	1.152e-03 ± 2.899e-05	1.139e-03 ± 3.157e-05	-0.31 %	-1.11 %	0.932	0.331	3.277	0.096
IFO_right	1.168e-03 ± 4.034e-05	1.162e-03 ± 3.385e-05	1.150e-03 ± 3.763e-05	1.137e-03 ± 3.810e-05	-0.54 %	-1.11 %	1.528	0.198	2.962	0.096
ILF_left	1.195e-03 ± 5.468e-05	1.181e-03 ± 5.091e-05	1.163e-03 ± 4.061e-05	1.142e-03 ± 4.550e-05	-1.1 %	-1.82 %	2.338	0.132	2.029	0.155
ILF_right	1.179e-03 ± 5.903e-05	1.169e-03 ± 4.907e-05	1.163e-03 ± 5.609e-05	1.143e-03 ± 7.127e-05	-0.88 %	-1.66 %	1.709	0.198	2.009	0.155

Table A.21 (cont'd)

	mTBI		Controls							
TractSeg Name	P1	P2	P1	P2	Percent Change mTBI %	Percent Change Controls %	t-score mTBI	q-value mTBI[1]	t-score controls	q-value controls
MCP	1.071e-03 ± 6.466e-05	1.066e-03 ± 5.086e-05	1.047e-03 ± 5.328e-05	1.066e-03 ± 6.899e-05	-0.44 %	1.75 %	0.466	0.44	-0.742	0.379
MLF_left	1.155e-03 ± 3.379e-05	1.153e-03 ± 3.526e-05	1.136e-03 ± 3.268e-05	1.128e-03 ± 5.063e-05	-0.15 %	-0.69 %	0.014	0.556	0.795	0.379
MLF_right	1.148e-03 ± 3.761e-05	1.146e-03 ± 3.513e-05	1.136e-03 ± 3.777e-05	1.125e-03 ± 4.764e-05	-0.14 %	-0.91 %	-0.118	0.556	1.115	0.294
OR_left	1.229e-03 ± 5.251e-05	1.223e-03 ± 5.395e-05	1.205e-03 ± 4.734e-05	1.196e-03 ± 6.880e-05	-0.5 %	-0.72 %	0.912	0.333	0.778	0.379
OR_right	1.221e-03 ± 5.889e-05	1.216e-03 ± 5.357e-05	1.219e-03 ± 5.695e-05	1.206e-03 ± 7.741e-05	-0.36 %	-1.06 %	0.296	0.496	1.690	0.171
POPT_left	1.244e-03 ± 3.416e-05	1.247e-03 ± 3.929e-05	1.227e-03 ± 4.715e-05	1.220e-03 ± 9.075e-05	0.23 %	-0.55 %	-1.135	0.29	0.443	0.412
POPT_right	1.231e-03 ± 3.839e-05	1.231e-03 ± 3.888e-05	1.212e-03 ± 4.598e-05	1.212e-03 ± 8.075e-05	0.07 %	0 %	-0.750	0.373	-0.011	0.5
SCP_left	1.179e-03 ± 3.726e-05	1.170e-03 ± 4.364e-05	1.130e-03 ± 4.542e-05	1.120e-03 ± 6.357e-05	-0.75 %	-0.85 %	1.547	0.198	0.562	0.4
SCP_right	1.164e-03 ± 3.064e-05	1.154e-03 ± 3.182e-05	1.134e-03 ± 6.193e-05	1.115e-03 ± 4.157e-05	-0.85 %	-1.74 %	2.834	0.085	1.869	0.16
SLF_III_left	1.143e-03 ± 3.106e-05	1.136e-03 ± 3.644e-05	1.110e-03 ± 4.811e-05	1.097e-03 ± 6.196e-05	-0.58 %	-1.18 %	1.967	0.198	0.819	0.379
SLF_III_right	1.128e-03 ± 2.968e-05	1.123e-03 ± 2.680e-05	1.111e-03 ± 3.722e-05	1.096e-03 ± 3.389e-05	-0.43 %	-1.37 %	1.547	0.198	1.842	0.16
SLF_II_left	1.143e-03 ± 3.460e-05	1.138e-03 ± 3.768e-05	1.118e-03 ± 4.439e-05	1.107e-03 ± 6.121e-05	-0.44 %	-0.95 %	1.522	0.198	0.897	0.378
SLF_II_right	1.131e-03 ± 3.491e-05	1.126e-03 ± 3.241e-05	1.111e-03 ± 4.475e-05	1.098e-03 ± 4.853e-05	-0.5 %	-1.22 %	1.701	0.198	1.492	0.198
SLF_I_left	1.190e-03 ± 4.919e-05	1.192e-03 ± 5.473e-05	1.194e-03 ± 9.878e-05	1.180e-03 ± 1.248e-04	0.23 %	-1.18 %	-0.646	0.393	0.560	0.4
SLF_I_right	1.176e-03 ± 4.418e-05	1.173e-03 ± 4.698e-05	1.168e-03 ± 7.384e-05	1.158e-03 ± 1.053e-04	-0.23 %	-0.89 %	0.553	0.416	0.601	0.4
STR_left	1.201e-03 ± 3.187e-05	1.194e-03 ± 4.787e-05	1.135e-03 ± 5.223e-05	1.137e-03 ± 1.172e-04	-0.63 %	0.16 %	1.437	0.221	-0.142	0.497
STR_right	1.177e-03 ± 3.361e-05	1.168e-03 ± 3.931e-05	1.142e-03 ± 5.843e-05	1.127e-03 ± 7.560e-05	-0.83 %	-1.34 %	1.899	0.198	0.753	0.379
ST_FO_left	1.179e-03 ± 5.018e-05	1.175e-03 ± 6.145e-05	1.132e-03 ± 5.240e-05	1.118e-03 ± 5.352e-05	-0.35 %	-1.2 %	0.652	0.393	1.591	0.18
ST_FO_right	1.192e-03 ± 4.641e-05	1.184e-03 ± 5.045e-05	1.162e-03 ± 5.716e-05	1.130e-03 ± 3.634e-05	-0.69 %	-2.8 %	1.721	0.198	2.665	0.096
ST_OCC_left	1.206e-03 ± 4.186e-05	1.201e-03 ± 4.476e-05	1.171e-03 ± 2.893e-05	1.163e-03 ± 3.766e-05	-0.41 %	-0.71 %	1.026	0.317	1.703	0.171
ST_OCC_right	1.184e-03 ± 4.732e-05	1.179e-03 ± 4.336e-05	1.167e-03 ± 4.299e-05	1.160e-03 ± 4.903e-05	-0.48 %	-0.62 %	0.759	0.373	2.064	0.155
ST_PAR_left	1.196e-03 ± 3.686e-05	1.197e-03 ± 3.992e-05	1.179e-03 ± 3.994e-05	1.173e-03 ± 7.820e-05	0.12 %	-0.51 %	-0.767	0.373	0.488	0.412
ST_PAR_right	1.180e-03 ± 3.836e-05	1.178e-03 ± 3.605e-05	1.161e-03 ± 3.700e-05	1.160e-03 ± 6.385e-05	-0.15 %	-0.1 %	-0.057	0.556	0.181	0.487
ST_POSTC_left	1.221e-03 ± 4.183e-05	1.217e-03 ± 5.251e-05	1.186e-03 ± 6.182e-05	1.172e-03 ± 1.026e-04	-0.33 %	-1.19 %	0.750	0.373	0.644	0.398
ST_POSTC_right	1.188e-03 ± 3.885e-05	1.183e-03 ± 3.930e-05	1.172e-03 ± 6.255e-05	1.173e-03 ± 9.963e-05	-0.43 %	0.1 %	0.817	0.371	0.082	0.5
ST_PREC_left	1.214e-03 ± 3.774e-05	1.206e-03 ± 5.141e-05	1.159e-03 ± 5.239e-05	1.153e-03 ± 8.677e-05	-0.72 %	-0.55 %	1.703	0.198	0.408	0.412
ST_PREC_right	1.185e-03 ± 3.839e-05	1.175e-03 ± 3.579e-05	1.155e-03 ± 5.168e-05	1.150e-03 ± 7.155e-05	-0.87 %	-0.37 %	1.877	0.198	0.519	0.411

Table A.21 (cont'd)

	mTBI		Controls							
TractSeg Name	P1	P2	P1	P2	Percent Change mTBI %	Percent Change Controls %	t-score mTBI	q-value mTBI[1]	t-score controls	q-value controls
ST_PREF_left	1.183e-03 ± 3.438e-05	1.176e-03 ± 4.390e-05	1.138e-03 ± 4.938e-05	1.122e-03 ± 5.255e-05	-0.56 %	-1.46 %	1.670	0.198	1.284	0.242
ST_PREF_right	1.180e-03 ± 3.657e-05	1.172e-03 ± 3.706e-05	1.146e-03 ± 5.420e-05	1.121e-03 ± 4.259e-05	-0.73 %	-2.19 %	2.524	0.116	2.331	0.142
ST_PREM_left	1.182e-03 ± 4.221e-05	1.173e-03 ± 5.867e-05	1.126e-03 ± 5.127e-05	1.094e-03 ± 4.357e-05	-0.75 %	-2.84 %	1.785	0.198	3.145	0.096
ST_PREM_right	1.175e-03 ± 3.808e-05	1.164e-03 ± 4.155e-05	1.135e-03 ± 6.074e-05	1.117e-03 ± 5.415e-05	-0.9 %	-1.59 %	2.970	0.085	1.806	0.16
T_OCC_left	1.233e-03 ± 5.412e-05	1.226e-03 ± 5.529e-05	1.209e-03 ± 4.722e-05	1.200e-03 ± 6.843e-05	-0.54 %	-0.73 %	1.011	0.317	0.807	0.379
T_OCC_right	1.217e-03 ± 5.928e-05	1.212e-03 ± 5.384e-05	1.215e-03 ± 5.855e-05	1.203e-03 ± 7.828e-05	-0.39 %	-0.99 %	0.388	0.465	1.639	0.173
T_PAR_left	1.210e-03 ± 4.214e-05	1.211e-03 ± 4.516e-05	1.202e-03 ± 5.434e-05	1.195e-03 ± 9.944e-05	0.15 %	-0.58 %	-0.703	0.388	0.422	0.412
T_PAR_right	1.205e-03 ± 4.604e-05	1.203e-03 ± 4.326e-05	1.196e-03 ± 5.554e-05	1.192e-03 ± 8.996e-05	-0.16 %	-0.33 %	0.001	0.556	0.296	0.449
T_POSTC_left	1.222e-03 ± 4.028e-05	1.221e-03 ± 5.075e-05	1.205e-03 ± 7.790e-05	1.189e-03 ± 1.154e-04	-0.08 %	-1.33 %	0.231	0.512	0.655	0.398
T_POSTC_right	1.190e-03 ± 4.058e-05	1.189e-03 ± 4.220e-05	1.190e-03 ± 8.110e-05	1.190e-03 ± 1.282e-04	-0.07 %	0.01 %	0.032	0.556	0.082	0.5
T_PREC_left	1.221e-03 ± 3.738e-05	1.213e-03 ± 5.310e-05	1.175e-03 ± 6.239e-05	1.167e-03 ± 1.014e-04	-0.7 %	-0.65 %	1.628	0.198	0.405	0.412
T_PREC_right	1.182e-03 ± 3.977e-05	1.172e-03 ± 3.713e-05	1.157e-03 ± 5.724e-05	1.151e-03 ± 8.315e-05	-0.86 %	-0.51 %	1.627	0.198	0.480	0.412
T_PREF_left	1.208e-03 ± 3.669e-05	1.200e-03 ± 4.826e-05	1.168e-03 ± 6.137e-05	1.148e-03 ± 6.800e-05	-0.61 %	-1.74 %	1.524	0.198	1.193	0.27
T_PREF_right	1.209e-03 ± 4.391e-05	1.198e-03 ± 4.404e-05	1.183e-03 ± 7.357e-05	1.156e-03 ± 6.869e-05	-0.9 %	-2.3 %	2.231	0.149	1.815	0.16
T_PREM_left	1.217e-03 ± 4.501e-05	1.207e-03 ± 6.484e-05	1.173e-03 ± 6.971e-05	1.139e-03 ± 7.681e-05	-0.82 %	-2.97 %	1.533	0.198	1.945	0.16
T_PREM_right	1.202e-03 ± 4.657e-05	1.189e-03 ± 5.014e-05	1.177e-03 ± 9.451e-05	1.153e-03 ± 8.559e-05	-1.08 %	-2.04 %	2.181	0.149	1.333	0.239
UF_left	1.173e-03 ± 3.496e-05	1.173e-03 ± 3.626e-05	1.144e-03 ± 4.304e-05	1.123e-03 ± 2.854e-05	0.02 %	-1.9 %	-0.376	0.465	2.735	0.096
UF_right	1.201e-03 ± 3.376e-05	1.196e-03 ± 3.558e-05	1.178e-03 ± 5.722e-05	1.147e-03 ± 2.801e-05	-0.47 %	-2.66 %	1.337	0.239	2.687	0.096

Tables A.21- T-test results for comparisons of the automatically segmented tracts from TractSeg between timepoints within mTBI and control subjects.

[1]Significant values are marked with an asterisk (*) or <0.001

Table A.22 Results of Post Hoc Tract Specific Comparison of Diffusion Kurtosis Imaging Radial Kurtosis

	mTBI		Controls							
TractSeg Name	P1	P2	P1	P2	Percent Change mTBI %	Percent Change Controls %	t-score mTBI	q-value mTBI[1]	t-score controls	q-value controls
AF_left	8.422e-04 ± 3.098e-05	8.348e-04 ± 3.313e-05	8.099e-04 ± 4.067e-05	8.002e-04 ± 4.466e-05	-0.88 %	-1.19 %	1.807	0.583	0.957	0.994
AF_right	8.312e-04 ± 2.900e-05	8.269e-04 ± 2.550e-05	8.177e-04 ± 3.143e-05	8.092e-04 ± 4.166e-05	-0.52 %	-1.04 %	1.451	0.612	0.934	0.994
ATR_left	8.952e-04 ± 4.606e-05	8.882e-04 ± 5.615e-05	8.629e-04 ± 6.084e-05	8.408e-04 ± 6.470e-05	-0.78 %	-2.56 %	1.078	0.612	1.575	0.994
ATR_right	9.084e-04 ± 5.261e-05	8.970e-04 ± 5.055e-05	8.917e-04 ± 7.865e-05	8.724e-04 ± 7.740e-05	-1.26 %	-2.16 %	1.991	0.583	1.361	0.994
CA	9.338e-04 ± 3.814e-05	9.291e-04 ± 5.964e-05	8.705e-04 ± 5.066e-05	8.542e-04 ± 6.646e-05	-0.5 %	-1.88 %	0.442	0.794	0.818	0.994
CC_1	8.816e-04 ± 5.782e-05	8.747e-04 ± 6.486e-05	8.714e-04 ± 9.258e-05	8.414e-04 ± 6.471e-05	-0.78 %	-3.44 %	0.792	0.753	2.452	0.994
CC_2	8.787e-04 ± 3.511e-05	8.786e-04 ± 4.244e-05	8.584e-04 ± 5.187e-05	8.427e-04 ± 6.318e-05	0 %	-1.83 %	-0.202	0.824	0.996	0.994
CC_3	9.005e-04 ± 4.544e-05	9.058e-04 ± 6.995e-05	8.769e-04 ± 6.721e-05	8.668e-04 ± 9.904e-05	0.59 %	-1.15 %	-0.677	0.753	0.484	0.994
CC_4	8.905e-04 ± 3.930e-05	8.983e-04 ± 5.244e-05	8.790e-04 ± 6.563e-05	8.868e-04 ± 1.308e-04	0.88 %	0.89 %	-1.171	0.612	-0.107	0.994
CC_5	8.753e-04 ± 3.782e-05	8.883e-04 ± 5.664e-05	8.696e-04 ± 7.291e-05	8.757e-04 ± 1.424e-04	1.49 %	0.69 %	-1.890	0.583	-0.086	0.994
CC_6	8.480e-04 ± 4.596e-05	8.520e-04 ± 3.726e-05	8.428e-04 ± 4.536e-05	8.500e-04 ± 8.756e-05	0.48 %	0.85 %	-1.228	0.612	-0.222	0.994
CC_7	8.694e-04 ± 7.903e-05	8.693e-04 ± 5.339e-05	8.642e-04 ± 4.553e-05	8.773e-04 ± 9.609e-05	-0.01 %	1.52 %	-0.198	0.824	-0.371	0.994
CC	8.698e-04 ± 3.778e-05	8.719e-04 ± 3.652e-05	8.597e-04 ± 4.716e-05	8.577e-04 ± 8.279e-05	0.24 %	-0.23 %	-0.793	0.753	0.242	0.994
CG_left	8.276e-04 ± 3.046e-05	8.245e-04 ± 3.115e-05	8.105e-04 ± 5.637e-05	8.148e-04 ± 9.633e-05	-0.38 %	0.52 %	0.516	0.762	-0.113	0.994
CG_right	8.160e-04 ± 3.399e-05	8.119e-04 ± 2.911e-05	8.015e-04 ± 5.317e-05	7.973e-04 ± 7.958e-05	-0.5 %	-0.52 %	0.647	0.753	0.250	0.994
CST_left	8.687e-04 ± 3.196e-05	8.661e-04 ± 4.453e-05	8.385e-04 ± 6.011e-05	8.342e-04 ± 9.824e-05	-0.3 %	-0.52 %	0.429	0.794	0.252	0.994
CST_right	8.258e-04 ± 3.205e-05	8.229e-04 ± 3.218e-05	8.031e-04 ± 4.801e-05	8.154e-04 ± 1.009e-04	-0.34 %	1.54 %	0.303	0.812	-0.478	0.994
FPT_left	8.750e-04 ± 3.036e-05	8.736e-04 ± 4.320e-05	8.500e-04 ± 8.280e-05	8.310e-04 ± 9.193e-05	-0.15 %	-2.23 %	-0.016	0.834	0.769	0.994
FPT_right	8.673e-04 ± 3.241e-05	8.661e-04 ± 3.546e-05	8.499e-04 ± 7.568e-05	8.298e-04 ± 8.381e-05	-0.14 %	-2.37 %	-0.013	0.834	1.015	0.994
FX_left	1.910e-03 ± 3.849e-04	1.883e-03 ± 3.814e-04	1.903e-03 ± 4.074e-04	1.894e-03 ± 4.438e-04	-1.44 %	-0.51 %	1.110	0.612	0.348	0.994
FX_right	1.879e-03 ± 3.690e-04	1.862e-03 ± 3.889e-04	1.882e-03 ± 3.939e-04	1.808e-03 ± 4.573e-04	-0.94 %	-3.94 %	0.350	0.803	1.471	0.994
ICP_left	8.072e-04 ± 8.363e-05	7.985e-04 ± 5.271e-05	8.028e-04 ± 7.506e-05	7.909e-04 ± 9.539e-05	-1.07 %	-1.48 %	0.710	0.753	0.431	0.994
ICP_right	7.954e-04 ± 6.566e-05	7.892e-04 ± 4.163e-05	8.009e-04 ± 7.779e-05	7.661e-04 ± 9.179e-05	-0.78 %	-4.34 %	0.528	0.762	1.496	0.994
IFO_left	8.488e-04 ± 3.565e-05	8.466e-04 ± 3.460e-05	8.250e-04 ± 2.747e-05	8.222e-04 ± 5.424e-05	-0.25 %	-0.35 %	0.400	0.794	0.373	0.994
IFO_right	8.417e-04 ± 4.028e-05	8.375e-04 ± 3.205e-05	8.273e-04 ± 3.026e-05	8.221e-04 ± 4.221e-05	-0.49 %	-0.62 %	0.718	0.753	1.461	0.994
ILF_left	8.612e-04 ± 5.113e-05	8.522e-04 ± 4.061e-05	8.321e-04 ± 3.420e-05	8.265e-04 ± 6.365e-05	-1.05 %	-0.68 %	1.879	0.583	0.558	0.994
ILF_right	8.526e-04 ± 5.201e-05	8.451e-04 ± 3.895e-05	8.363e-04 ± 4.308e-05	8.295e-04 ± 6.147e-05	-0.88 %	-0.82 %	1.405	0.612	1.734	0.994

Table A.22 (cont'd)

	mTBI		Controls							
TractSeg Name	P1	P2	P1	P2	Percent Change mTBI %	Percent Change Controls %	t-score mTBI	q-value mTBI[1]	t-score controls	q-value controls
MCP	7.709e-04 ± 6.400e-05	7.697e-04 ± 4.772e-05	7.622e-04 ± 6.892e-05	7.848e-04 ± 9.616e-05	-0.16 %	2.97 %	0.058	0.834	-0.685	0.994
MLF_left	8.491e-04 ± 3.718e-05	8.474e-04 ± 3.487e-05	8.396e-04 ± 4.156e-05	8.338e-04 ± 5.953e-05	-0.19 %	-0.69 %	0.119	0.824	0.502	0.994
MLF_right	8.383e-04 ± 4.026e-05	8.390e-04 ± 3.575e-05	8.361e-04 ± 4.832e-05	8.307e-04 ± 6.177e-05	0.09 %	-0.65 %	-0.732	0.753	0.462	0.994
OR_left	8.771e-04 ± 5.618e-05	8.731e-04 ± 5.497e-05	8.593e-04 ± 4.323e-05	8.620e-04 ± 9.727e-05	-0.45 %	0.31 %	0.507	0.762	-0.095	0.994
OR_right	8.644e-04 ± 6.271e-05	8.611e-04 ± 5.522e-05	8.667e-04 ± 5.107e-05	8.627e-04 ± 7.361e-05	-0.38 %	-0.45 %	0.033	0.834	0.941	0.994
POPT_left	8.766e-04 ± 3.370e-05	8.809e-04 ± 3.966e-05	8.763e-04 ± 6.043e-05	8.723e-04 ± 1.045e-04	0.5 %	-0.45 %	-1.223	0.612	0.247	0.994
POPT_right	8.538e-04 ± 3.807e-05	8.567e-04 ± 3.692e-05	8.475e-04 ± 5.643e-05	8.504e-04 ± 9.830e-05	0.34 %	0.34 %	-1.041	0.612	-0.137	0.994
SCP_left	8.344e-04 ± 3.701e-05	8.281e-04 ± 4.502e-05	8.059e-04 ± 6.118e-05	7.971e-04 ± 8.812e-05	-0.76 %	-1.09 %	1.052	0.612	0.315	0.994
SCP_right	8.222e-04 ± 2.993e-05	8.166e-04 ± 3.131e-05	8.140e-04 ± 7.787e-05	7.927e-04 ± 5.724e-05	-0.68 %	-2.61 %	1.340	0.612	1.180	0.994
SLF_III_left	8.436e-04 ± 3.142e-05	8.413e-04 ± 3.709e-05	8.230e-04 ± 6.739e-05	8.117e-04 ± 7.424e-05	-0.27 %	-1.37 %	0.554	0.762	0.578	0.994
SLF_III_right	8.262e-04 ± 2.952e-05	8.266e-04 ± 2.818e-05	8.238e-04 ± 4.219e-05	8.184e-04 ± 6.068e-05	0.04 %	-0.65 %	-0.167	0.824	0.346	0.994
SLF_II_left	8.623e-04 ± 3.992e-05	8.568e-04 ± 4.166e-05	8.461e-04 ± 5.588e-05	8.326e-04 ± 7.016e-05	-0.64 %	-1.59 %	1.368	0.612	0.971	0.994
SLF_II_right	8.517e-04 ± 3.760e-05	8.470e-04 ± 3.496e-05	8.409e-04 ± 5.194e-05	8.283e-04 ± 5.991e-05	-0.56 %	-1.5 %	1.080	0.612	1.070	0.994
SLF_I_left	9.040e-04 ± 5.172e-05	9.069e-04 ± 6.034e-05	9.201e-04 ± 1.167e-04	9.083e-04 ± 1.389e-04	0.33 %	-1.29 %	-0.506	0.762	0.433	0.994
SLF_I_right	8.819e-04 ± 4.788e-05	8.793e-04 ± 5.270e-05	8.841e-04 ± 8.675e-05	8.738e-04 ± 1.198e-04	-0.3 %	-1.17 %	0.367	0.803	0.490	0.994
STR_left	8.215e-04 ± 2.976e-05	8.158e-04 ± 4.965e-05	7.739e-04 ± 5.671e-05	7.817e-04 ± 1.379e-04	-0.69 %	1 %	0.926	0.68	-0.286	0.994
STR_right	7.966e-04 ± 2.950e-05	7.905e-04 ± 3.606e-05	7.778e-04 ± 6.669e-05	7.659e-04 ± 8.547e-05	-0.77 %	-1.53 %	1.200	0.612	0.585	0.994
ST_FO_left	8.314e-04 ± 4.660e-05	8.305e-04 ± 5.370e-05	7.872e-04 ± 4.490e-05	7.849e-04 ± 7.971e-05	-0.11 %	-0.29 %	-0.113	0.824	0.132	0.994
ST_FO_right	8.349e-04 ± 4.480e-05	8.297e-04 ± 4.323e-05	8.093e-04 ± 5.486e-05	7.900e-04 ± 4.325e-05	-0.62 %	-2.38 %	0.962	0.666	1.986	0.994
ST_OCC_left	8.532e-04 ± 4.461e-05	8.493e-04 ± 4.268e-05	8.269e-04 ± 2.504e-05	8.290e-04 ± 6.754e-05	-0.46 %	0.26 %	0.761	0.753	-0.042	0.994
ST_OCC_right	8.356e-04 ± 4.836e-05	8.321e-04 ± 4.202e-05	8.240e-04 ± 2.973e-05	8.235e-04 ± 4.740e-05	-0.42 %	-0.07 %	0.192	0.824	1.316	0.994
ST_PAR_left	8.693e-04 ± 3.837e-05	8.707e-04 ± 3.993e-05	8.646e-04 ± 5.316e-05	8.610e-04 ± 9.075e-05	0.16 %	-0.41 %	-0.643	0.753	0.323	0.994
ST_PAR_right	8.433e-04 ± 3.958e-05	8.438e-04 ± 3.587e-05	8.355e-04 ± 4.359e-05	8.366e-04 ± 7.779e-05	0.06 %	0.14 %	-0.636	0.753	0.008	0.994
ST_POSTC_left	8.801e-04 ± 3.850e-05	8.776e-04 ± 5.074e-05	8.617e-04 ± 7.188e-05	8.503e-04 ± 1.108e-04	-0.29 %	-1.32 %	0.396	0.794	0.531	0.994
ST_POSTC_right	8.407e-04 ± 3.839e-05	8.388e-04 ± 4.098e-05	8.364e-04 ± 6.896e-05	8.402e-04 ± 1.130e-04	-0.22 %	0.45 %	0.238	0.824	-0.013	0.994
ST_PREC_left	8.719e-04 ± 3.638e-05	8.652e-04 ± 5.058e-05	8.324e-04 ± 6.067e-05	8.307e-04 ± 9.639e-05	-0.77 %	-0.2 %	1.305	0.612	0.217	0.994
ST_PREC_right	8.407e-04 ± 3.774e-05	8.328e-04 ± 3.523e-05	8.217e-04 ± 5.214e-05	8.208e-04 ± 8.085e-05	-0.94 %	-0.11 %	1.369	0.612	0.243	0.994

Table A.22 (cont'd)

	mTBI		Controls							
TractSeg Name	P1	P2	P1	P2	Percent Change mTBI %	Percent Change Controls %	t-score mTBI	q-value mTBI[1]	t-score controls	q-value controls
ST_PREF_left	8.546e-04 ± 3.296e-05	8.492e-04 ± 4.133e-05	8.202e-04 ± 5.619e-05	8.096e-04 ± 6.461e-05	-0.62 %	-1.28 %	1.260	0.612	0.698	0.994
ST_PREF_right	8.532e-04 ± 3.367e-05	8.467e-04 ± 3.379e-05	8.282e-04 ± 5.459e-05	8.094e-04 ± 4.894e-05	-0.76 %	-2.27 %	1.988	0.583	1.737	0.994
ST_PREM_left	8.681e-04 ± 3.775e-05	8.606e-04 ± 5.403e-05	8.250e-04 ± 5.963e-05	7.990e-04 ± 5.342e-05	-0.86 %	-3.15 %	1.395	0.612	1.973	0.994
ST_PREM_right	8.483e-04 ± 3.205e-05	8.393e-04 ± 3.708e-05	8.203e-04 ± 6.524e-05	8.066e-04 ± 6.358e-05	-1.05 %	-1.67 %	2.629	0.583	1.139	0.994
T_OCC_left	8.854e-04 ± 5.808e-05	8.808e-04 ± 5.635e-05	8.676e-04 ± 4.365e-05	8.699e-04 ± 9.549e-05	-0.52 %	0.27 %	0.627	0.753	-0.071	0.994
T_OCC_right	8.678e-04 ± 6.321e-05	8.642e-04 ± 5.531e-05	8.694e-04 ± 5.158e-05	8.661e-04 ± 7.456e-05	-0.42 %	-0.38 %	0.127	0.824	0.954	0.994
T_PAR_left	8.839e-04 ± 4.589e-05	8.860e-04 ± 4.847e-05	8.881e-04 ± 6.674e-05	8.837e-04 ± 1.144e-04	0.25 %	-0.49 %	-0.601	0.759	0.282	0.994
T_PAR_right	8.672e-04 ± 5.007e-05	8.667e-04 ± 4.562e-05	8.681e-04 ± 6.461e-05	8.663e-04 ± 1.052e-04	-0.06 %	-0.21 %	-0.216	0.824	0.175	0.994
T_POSTC_left	8.748e-04 ± 4.064e-05	8.759e-04 ± 5.389e-05	8.789e-04 ± 9.192e-05	8.638e-04 ± 1.311e-04	0.12 %	-1.72 %	-0.142	0.824	0.535	0.994
T_POSTC_right	8.381e-04 ± 4.468e-05	8.402e-04 ± 4.898e-05	8.543e-04 ± 1.009e-04	8.571e-04 ± 1.489e-04	0.25 %	0.32 %	-0.330	0.805	0.031	0.994
T_PREC_left	8.735e-04 ± 3.971e-05	8.671e-04 ± 5.643e-05	8.432e-04 ± 7.421e-05	8.399e-04 ± 1.161e-04	-0.73 %	-0.38 %	1.143	0.612	0.220	0.994
T_PREC_right	8.384e-04 ± 4.199e-05	8.300e-04 ± 3.974e-05	8.268e-04 ± 6.507e-05	8.240e-04 ± 9.576e-05	-1 %	-0.34 %	1.221	0.612	0.268	0.994
T_PREF_left	8.774e-04 ± 3.761e-05	8.712e-04 ± 4.984e-05	8.484e-04 ± 7.055e-05	8.334e-04 ± 8.054e-05	-0.71 %	-1.77 %	1.098	0.612	0.782	0.994
T_PREF_right	8.873e-04 ± 4.435e-05	8.780e-04 ± 4.565e-05	8.709e-04 ± 7.717e-05	8.488e-04 ± 7.828e-05	-1.04 %	-2.54 %	1.803	0.583	1.388	0.994
T_PREM_left	8.901e-04 ± 4.570e-05	8.816e-04 ± 6.655e-05	8.578e-04 ± 7.861e-05	8.281e-04 ± 8.883e-05	-0.95 %	-3.46 %	1.107	0.612	1.424	0.994
T_PREM_right	8.706e-04 ± 4.872e-05	8.586e-04 ± 5.193e-05	8.573e-04 ± 1.056e-04	8.376e-04 ± 1.012e-04	-1.38 %	-2.3 %	1.843	0.583	0.987	0.994
UF_left	8.323e-04 ± 3.522e-05	8.361e-04 ± 3.717e-05	8.083e-04 ± 4.128e-05	8.006e-04 ± 5.181e-05	0.46 %	-0.95 %	-1.161	0.612	0.498	0.994
UF_right	8.588e-04 ± 3.190e-05	8.573e-04 ± 3.760e-05	8.412e-04 ± 5.533e-05	8.217e-04 ± 5.704e-05	-0.17 %	-2.32 %	0.096	0.824	1.021	0.994

Tables A.22- T-test results for comparisons of the automatically segmented tracts from TractSeg between timepoints within mTBI and control subjects.

[1]Significant values are marked with an asterisk (*) or <0.001

Table A.23 Results of Post Hoc Tract Specific Comparison of Neurite Orientation Dispersion and Density Imaging Orientation Dispersion Index

	mTBI		Controls							
TractSeg Name	P1	P2	P1	P2	Percent Change mTBI %	Percent Change Controls %	t-score mTBI	q-value mTBI′	t-score controls	q-value controls
AF_left	0.351 ± 0.015	0.354 ± 0.012	0.362 ± 0.016	0.365 ± 0.017	0.9 %	0.86 %	-1.495	0.008*	-0.520	0.127
AF_right	0.346 ± 0.010	0.350 ± 0.011	0.356 ± 0.014	0.362 ± 0.020	1.19 %	1.71 %	-2.701	0.005*	-0.970	0.114
ATR_left	0.320 ± 0.013	0.322 ± 0.012	0.327 ± 0.012	0.331 ± 0.015	0.58 %	1.29 %	-1.351	0.008*	-1.084	0.114
ATR_right	0.323 ± 0.011	0.326 ± 0.012	0.332 ± 0.012	0.337 ± 0.018	0.82 %	1.47 %	-1.908	0.007*	-1.139	0.114
CA	0.283 ± 0.018	0.286 ± 0.022	0.286 ± 0.016	0.301 ± 0.042	1.28 %	5.3 %	-1.216	0.008*	-1.406	0.114
CC_1	0.247 ± 0.017	0.252 ± 0.035	0.248 ± 0.022	0.263 ± 0.046	1.96 %	5.9 %	-1.313	0.008*	-0.966	0.114
CC_2	0.303 ± 0.012	0.305 ± 0.012	0.313 ± 0.016	0.319 ± 0.018	0.76 %	2.09 %	-1.469	0.008*	-1.007	0.114
CC_3	0.309 ± 0.017	0.312 ± 0.018	0.319 ± 0.026	0.327 ± 0.026	1.04 %	2.49 %	-1.217	0.008*	-0.814	0.114
CC_4	0.299 ± 0.015	0.302 ± 0.017	0.310 ± 0.019	0.317 ± 0.023	1.16 %	2.33 %	-1.647	0.007*	-1.058	0.114
CC_5	0.285 ± 0.015	0.290 ± 0.016	0.299 ± 0.020	0.305 ± 0.025	1.63 %	1.84 %	-2.083	0.007*	-0.679	0.121
CC_6	0.322 ± 0.015	0.324 ± 0.015	0.333 ± 0.019	0.337 ± 0.021	0.62 %	1.22 %	-0.849	0.012*	-0.521	0.127
CC_7	0.319 ± 0.013	0.322 ± 0.016	0.325 ± 0.015	0.333 ± 0.033	0.65 %	2.34 %	-1.102	0.01*	-0.878	0.114
CC	0.312 ± 0.012	0.315 ± 0.012	0.322 ± 0.015	0.328 ± 0.019	0.73 %	2.03 %	-1.401	0.008*	-0.970	0.114
CG_left	0.327 ± 0.018	0.326 ± 0.020	0.337 ± 0.022	0.344 ± 0.026	-0.28 %	2.16 %	0.128	0.022*	-0.890	0.114
CG_right	0.325 ± 0.021	0.326 ± 0.017	0.337 ± 0.019	0.345 ± 0.024	0.36 %	2.42 %	-0.247	0.02*	-0.691	0.121
CST_left	0.265 ± 0.012	0.266 ± 0.012	0.277 ± 0.014	0.281 ± 0.015	0.52 %	1.67 %	-0.948	0.011*	-1.075	0.114
CST_right	0.270 ± 0.011	0.272 ± 0.012	0.279 ± 0.013	0.287 ± 0.020	0.82 %	2.65 %	-1.545	0.007*	-1.487	0.114
FPT_left	0.267 ± 0.012	0.268 ± 0.012	0.281 ± 0.017	0.287 ± 0.018	0.32 %	1.94 %	-0.889	0.011*	-0.927	0.114
FPT_right	0.265 ± 0.011	0.267 ± 0.012	0.279 ± 0.013	0.283 ± 0.016	0.62 %	1.43 %	-1.411	0.008*	-0.850	0.114
FX_left	0.140 ± 0.043	0.147 ± 0.048	0.154 ± 0.062	0.178 ± 0.079	5.17 %	15.52 %	-2.011	0.007*	-1.518	0.114
FX_right	0.135 ± 0.041	0.142 ± 0.043	0.152 ± 0.058	0.167 ± 0.079	5.24 %	10.19 %	-2.069	0.007*	-0.797	0.114
ICP_left	0.357 ± 0.018	0.359 ± 0.018	0.376 ± 0.023	0.374 ± 0.026	0.82 %	-0.62 %	-1.784	0.007*	0.553	0.127
ICP_right	0.372 ± 0.017	0.376 ± 0.018	0.390 ± 0.018	0.385 ± 0.023	1.28 %	-1.51 %	-2.828	0.005*	0.963	0.114
IFO_left	0.319 ± 0.011	0.321 ± 0.013	0.326 ± 0.013	0.335 ± 0.028	0.67 %	2.96 %	-1.308	0.008*	-1.078	0.114
IFO_right	0.323 ± 0.009	0.326 ± 0.012	0.329 ± 0.014	0.334 ± 0.025	0.85 %	1.63 %	-1.883	0.007*	-0.831	0.114
ILF_left	0.320 ± 0.012	0.324 ± 0.021	0.325 ± 0.011	0.339 ± 0.037	1.36 %	4.52 %	-1.584	0.007*	-1.442	0.114

Table A.23 (cont'd)

	mTBI		Controls							
TractSeg Name	P1	P2	P1	P2	Percent Change mTBI %	Percent Change Controls %	t-score mTBI	q-value mTBI′	t-score controls	q-value controls
ILF_right	0.324 ± 0.015	0.328 ± 0.022	0.326 ± 0.018	0.336 ± 0.032	1.07 %	3.19 %	-1.415	0.008*	-1.157	0.114
MCP	0.344 ± 0.015	0.347 ± 0.015	0.359 ± 0.020	0.359 ± 0.023	0.87 %	0.22 %	-2.284	0.007*	-0.004	0.191
MLF_left	0.348 ± 0.015	0.349 ± 0.014	0.357 ± 0.017	0.359 ± 0.017	0.25 %	0.58 %	-0.230	0.02*	-0.397	0.143
MLF_right	0.344 ± 0.015	0.347 ± 0.015	0.354 ± 0.018	0.359 ± 0.020	0.91 %	1.42 %	-1.623	0.007*	-0.581	0.127
OR_left	0.309 ± 0.013	0.311 ± 0.014	0.316 ± 0.012	0.326 ± 0.032	0.56 %	3.12 %	-0.898	0.011*	-1.214	0.114
OR_right	0.305 ± 0.012	0.306 ± 0.013	0.309 ± 0.018	0.316 ± 0.029	0.38 %	2.38 %	-0.691	0.014*	-0.956	0.114
POPT_left	0.294 ± 0.014	0.296 ± 0.013	0.306 ± 0.015	0.308 ± 0.015	0.5 %	0.73 %	-0.814	0.012*	-0.572	0.127
POPT_right	0.289 ± 0.013	0.291 ± 0.014	0.297 ± 0.015	0.301 ± 0.016	0.67 %	1.33 %	-1.172	0.009*	-0.931	0.114
SCP_left	0.300 ± 0.013	0.303 ± 0.014	0.319 ± 0.016	0.319 ± 0.021	0.86 %	0.06 %	-1.932	0.007*	-0.012	0.191
SCP_right	0.303 ± 0.010	0.307 ± 0.014	0.320 ± 0.016	0.319 ± 0.020	1.3 %	-0.5 %	-2.530	0.006*	0.158	0.172
SLF_III_left	0.340 ± 0.017	0.344 ± 0.015	0.353 ± 0.024	0.356 ± 0.018	1.33 %	0.91 %	-1.916	0.007*	-0.381	0.144
SLF_III_right	0.337 ± 0.012	0.343 ± 0.017	0.352 ± 0.019	0.360 ± 0.029	1.87 %	2.05 %	-2.966	0.005*	-0.784	0.114
SLF_II_left	0.363 ± 0.016	0.362 ± 0.016	0.372 ± 0.017	0.371 ± 0.027	-0.26 %	-0.3 %	0.330	0.019*	0.234	0.163
SLF_II_right	0.364 ± 0.015	0.365 ± 0.015	0.376 ± 0.017	0.379 ± 0.017	0.35 %	0.7 %	-0.860	0.012*	-0.556	0.127
SLF_I_left	0.360 ± 0.017	0.360 ± 0.017	0.371 ± 0.016	0.377 ± 0.017	0 %	1.51 %	0.070	0.023*	-1.096	0.114
SLF_I_right	0.352 ± 0.016	0.353 ± 0.018	0.362 ± 0.016	0.364 ± 0.018	0.12 %	0.66 %	-0.346	0.019*	-0.556	0.127
STR_left	0.270 ± 0.012	0.272 ± 0.012	0.283 ± 0.013	0.292 ± 0.025	0.76 %	3.44 %	-1.690	0.007*	-1.643	0.114
STR_right	0.272 ± 0.014	0.275 ± 0.013	0.283 ± 0.014	0.287 ± 0.016	1.04 %	1.62 %	-2.047	0.007*	-1.155	0.114
ST_FO_left	0.295 ± 0.017	0.299 ± 0.025	0.301 ± 0.018	0.309 ± 0.035	1.52 %	2.47 %	-1.598	0.007*	-0.985	0.114
ST_FO_right	0.287 ± 0.016	0.290 ± 0.026	0.294 ± 0.017	0.302 ± 0.028	1.19 %	2.81 %	-1.212	0.008*	-0.715	0.121
ST_OCC_left	0.312 ± 0.013	0.313 ± 0.015	0.321 ± 0.014	0.330 ± 0.035	0.47 %	2.78 %	-0.710	0.014*	-0.973	0.114

Table A.23 (cont'd)

	mTBI		Controls							
TractSeg Name	P1	P2	P1	P2	Percent Change mTBI %	Percent Change Controls %	t-score mTBI	q-value mTBI[f]	t-score controls	q-value controls
ST_OCC_right	0.315 ± 0.013	0.317 ± 0.014	0.321 ± 0.020	0.326 ± 0.026	0.65 %	1.83 %	-1.007	0.011*	-0.798	0.114
ST_PAR_left	0.327 ± 0.014	0.328 ± 0.014	0.337 ± 0.015	0.341 ± 0.015	0.21 %	0.98 %	-0.341	0.019*	-0.690	0.121
ST_PAR_right	0.319 ± 0.013	0.322 ± 0.013	0.327 ± 0.014	0.331 ± 0.016	0.86 %	1.18 %	-1.672	0.007*	-0.806	0.114
ST_POSTC_left	0.305 ± 0.015	0.308 ± 0.014	0.319 ± 0.012	0.324 ± 0.013	0.87 %	1.51 %	-1.554	0.007*	-0.987	0.114
ST_POSTC_right	0.301 ± 0.014	0.305 ± 0.014	0.310 ± 0.013	0.315 ± 0.018	1.29 %	1.65 %	-2.271	0.007*	-1.322	0.114
ST_PREC_left	0.306 ± 0.013	0.309 ± 0.011	0.318 ± 0.011	0.326 ± 0.013	0.78 %	2.53 %	-1.501	0.008*	-2.009	0.114
ST_PREC_right	0.305 ± 0.010	0.308 ± 0.012	0.314 ± 0.012	0.320 ± 0.015	0.98 %	1.94 %	-2.104	0.007*	-1.782	0.114
ST_PREF_left	0.312 ± 0.012	0.313 ± 0.011	0.322 ± 0.015	0.330 ± 0.017	0.41 %	2.42 %	-1.192	0.009*	-1.380	0.114
ST_PREF_right	0.312 ± 0.010	0.314 ± 0.012	0.323 ± 0.012	0.328 ± 0.016	0.76 %	1.69 %	-2.116	0.007*	-1.274	0.114
ST_PREM_left	0.325 ± 0.015	0.327 ± 0.014	0.339 ± 0.016	0.348 ± 0.016	0.57 %	2.53 %	-1.544	0.007*	-1.637	0.114
ST_PREM_right	0.318 ± 0.014	0.320 ± 0.014	0.330 ± 0.014	0.338 ± 0.023	0.64 %	2.42 %	-1.243	0.008*	-1.293	0.114
T_OCC_left	0.313 ± 0.012	0.314 ± 0.014	0.319 ± 0.011	0.329 ± 0.031	0.56 %	3.07 %	-0.940	0.011*	-1.228	0.114
T_OCC_right	0.311 ± 0.012	0.312 ± 0.013	0.314 ± 0.017	0.322 ± 0.028	0.34 %	2.31 %	-0.621	0.015*	-0.984	0.114
T_PAR_left	0.326 ± 0.013	0.326 ± 0.013	0.335 ± 0.013	0.338 ± 0.016	0.22 %	1.02 %	-0.417	0.018*	-0.779	0.114
T_PAR_right	0.316 ± 0.013	0.317 ± 0.014	0.323 ± 0.012	0.327 ± 0.014	0.51 %	1.19 %	-1.029	0.01*	-0.834	0.114
T_POSTC_left	0.304 ± 0.014	0.307 ± 0.014	0.319 ± 0.015	0.322 ± 0.016	0.95 %	0.84 %	-1.667	0.007*	-0.664	0.121
T_POSTC_right	0.301 ± 0.015	0.304 ± 0.016	0.311 ± 0.018	0.316 ± 0.020	1.13 %	1.64 %	-1.696	0.007*	-0.953	0.114
T_PREC_left	0.303 ± 0.012	0.305 ± 0.012	0.314 ± 0.012	0.321 ± 0.015	0.65 %	2.32 %	-1.348	0.008*	-1.962	0.114
T_PREC_right	0.308 ± 0.011	0.310 ± 0.012	0.316 ± 0.011	0.322 ± 0.014	0.6 %	2.01 %	-1.334	0.008*	-1.932	0.114
T_PREF_left	0.307 ± 0.011	0.308 ± 0.010	0.318 ± 0.014	0.324 ± 0.017	0.32 %	2.13 %	-0.992	0.011*	-1.365	0.114
T_PREF_right	0.314 ± 0.010	0.315 ± 0.011	0.324 ± 0.012	0.329 ± 0.014	0.56 %	1.56 %	-1.552	0.007*	-1.465	0.114
T_PREM_left	0.312 ± 0.013	0.314 ± 0.012	0.324 ± 0.012	0.330 ± 0.015	0.54 %	1.82 %	-1.417	0.008*	-1.442	0.114
T_PREM_right	0.309 ± 0.013	0.310 ± 0.013	0.318 ± 0.012	0.325 ± 0.018	0.28 %	2.21 %	-0.471	0.017*	-1.244	0.114
UF_left	0.300 ± 0.014	0.303 ± 0.022	0.307 ± 0.017	0.319 ± 0.035	1.2 %	3.62 %	-1.373	0.008*	-1.163	0.114
UF_right	0.297 ± 0.014	0.301 ± 0.021	0.305 ± 0.015	0.315 ± 0.032	1.49 %	3.28 %	-1.906	0.007*	-1.016	0.114

Tables A.23- T-test results for comparisons of the automatically segmented tracts from TractSeg between timepoints within mTBI and control subjects.

[f]Significant values are marked with an asterisk (*) or <0.001

Table A.24 Results of Post Hoc Tract Specific Comparison of Neurite Orientation Dispersion and Density Imaging Neurite Density Index

	mTBI		Controls							
TractSeg Name	P1	P2	P1	P2	Percent Change mTBI %	Percent Change Controls %	t-score mTBI	q-value mTBI[1]	t-score controls	q-value controls
AF_left	0.482 ± 0.022	0.481 ± 0.021	0.493 ± 0.030	0.497 ± 0.025	-0.25 %	0.75 %	0.768	0.532	-0.925	0.499
AF_right	0.503 ± 0.023	0.501 ± 0.019	0.507 ± 0.032	0.508 ± 0.034	-0.37 %	0.12 %	1.266	0.33	-0.052	0.588
ATR_left	0.478 ± 0.019	0.479 ± 0.020	0.499 ± 0.029	0.503 ± 0.024	0.13 %	0.73 %	-0.452	0.603	-0.910	0.499
ATR_right	0.480 ± 0.019	0.480 ± 0.018	0.495 ± 0.023	0.500 ± 0.025	0.04 %	1.03 %	-0.009	0.674	-1.316	0.499
CA	0.401 ± 0.026	0.396 ± 0.026	0.426 ± 0.028	0.445 ± 0.024	-1.18 %	4.44 %	2.135	0.13	-2.270	0.499
CC_1	0.485 ± 0.031	0.476 ± 0.037	0.506 ± 0.031	0.496 ± 0.050	-1.73 %	-1.84 %	3.338	0.037*	0.920	0.499
CC_2	0.490 ± 0.023	0.488 ± 0.023	0.502 ± 0.033	0.503 ± 0.029	-0.36 %	0.09 %	1.166	0.338	-0.366	0.56
CC_3	0.493 ± 0.023	0.494 ± 0.024	0.509 ± 0.045	0.511 ± 0.034	0.1 %	0.36 %	-0.191	0.659	-0.478	0.56
CC_4	0.543 ± 0.026	0.544 ± 0.029	0.548 ± 0.041	0.554 ± 0.038	0.03 %	1.05 %	-0.045	0.674	-1.141	0.499
CC_5	0.538 ± 0.024	0.537 ± 0.025	0.546 ± 0.036	0.547 ± 0.035	-0.3 %	0.27 %	0.778	0.532	-0.528	0.56
CC_6	0.497 ± 0.021	0.494 ± 0.020	0.498 ± 0.027	0.497 ± 0.027	-0.62 %	-0.16 %	2.070	0.132	0.079	0.588
CC_7	0.514 ± 0.023	0.512 ± 0.021	0.516 ± 0.023	0.514 ± 0.033	-0.35 %	-0.27 %	1.182	0.338	0.317	0.56
CC	0.501 ± 0.020	0.499 ± 0.020	0.508 ± 0.030	0.508 ± 0.028	-0.38 %	0.08 %	1.480	0.276	-0.327	0.56
CG_left	0.473 ± 0.025	0.473 ± 0.025	0.484 ± 0.033	0.482 ± 0.035	-0.1 %	-0.58 %	0.488	0.602	0.338	0.56
CG_right	0.482 ± 0.025	0.480 ± 0.022	0.488 ± 0.033	0.493 ± 0.030	-0.46 %	1.13 %	1.011	0.408	-1.090	0.499
CST_left	0.598 ± 0.021	0.597 ± 0.023	0.607 ± 0.034	0.619 ± 0.034	-0.03 %	1.96 %	0.137	0.674	-1.876	0.499
CST_right	0.600 ± 0.022	0.599 ± 0.023	0.607 ± 0.033	0.610 ± 0.042	-0.18 %	0.48 %	0.871	0.486	-0.370	0.56
FPT_left	0.559 ± 0.022	0.559 ± 0.024	0.576 ± 0.038	0.580 ± 0.042	0.06 %	0.62 %	0.037	0.674	-0.266	0.56
FPT_right	0.559 ± 0.020	0.558 ± 0.022	0.572 ± 0.034	0.579 ± 0.033	-0.21 %	1.12 %	0.731	0.532	-1.064	0.499
FX_left	0.451 ± 0.053	0.451 ± 0.048	0.463 ± 0.039	0.481 ± 0.052	-0.13 %	3.88 %	0.059	0.674	-1.174	0.499
FX_right	0.447 ± 0.053	0.454 ± 0.056	0.467 ± 0.042	0.471 ± 0.044	1.52 %	0.69 %	-1.339	0.303	0.218	0.56
ICP_left	0.591 ± 0.028	0.589 ± 0.036	0.588 ± 0.042	0.594 ± 0.060	-0.36 %	0.92 %	0.733	0.532	-0.099	0.588
ICP_right	0.577 ± 0.021	0.573 ± 0.026	0.571 ± 0.046	0.584 ± 0.048	-0.64 %	2.26 %	1.432	0.276	-0.658	0.553
IFO_left	0.482 ± 0.022	0.477 ± 0.020	0.491 ± 0.022	0.491 ± 0.032	-1.04 %	-0.01 %	3.550	0.037*	-0.057	0.588
IFO_right	0.486 ± 0.022	0.483 ± 0.020	0.493 ± 0.021	0.497 ± 0.035	-0.69 %	0.76 %	2.500	0.121	-0.431	0.56
ILF_left	0.467 ± 0.022	0.463 ± 0.021	0.478 ± 0.023	0.483 ± 0.029	-0.81 %	1.02 %	2.453	0.121	-1.322	0.499
ILF_right	0.471 ± 0.021	0.469 ± 0.020	0.480 ± 0.026	0.486 ± 0.033	-0.51 %	1.25 %	1.564	0.251	-1.288	0.499
MCP	0.617 ± 0.023	0.615 ± 0.027	0.610 ± 0.046	0.622 ± 0.046	-0.44 %	1.91 %	1.215	0.33	-0.818	0.516
MLF_left	0.470 ± 0.021	0.467 ± 0.020	0.474 ± 0.024	0.477 ± 0.023	-0.56 %	0.79 %	2.286	0.128	-1.012	0.499
MLF_right	0.477 ± 0.020	0.474 ± 0.018	0.477 ± 0.028	0.479 ± 0.030	-0.65 %	0.31 %	2.322	0.128	-0.291	0.56
OR_left	0.487 ± 0.022	0.483 ± 0.022	0.497 ± 0.020	0.501 ± 0.033	-0.77 %	0.86 %	2.041	0.132	-0.632	0.557
OR_right	0.493 ± 0.022	0.490 ± 0.022	0.499 ± 0.026	0.505 ± 0.033	-0.58 %	1.2 %	1.907	0.159	-1.314	0.499
POPT_left	0.531 ± 0.019	0.528 ± 0.019	0.537 ± 0.026	0.541 ± 0.028	-0.67 %	0.88 %	2.226	0.129	-0.757	0.528
POPT_right	0.538 ± 0.017	0.537 ± 0.019	0.545 ± 0.025	0.548 ± 0.032	-0.27 %	0.55 %	1.146	0.34	-0.210	0.56
SCP_left	0.575 ± 0.021	0.575 ± 0.028	0.589 ± 0.039	0.601 ± 0.046	-0.01 %	2.01 %	0.077	0.674	-0.855	0.506
SCP_right	0.572 ± 0.016	0.570 ± 0.022	0.577 ± 0.041	0.591 ± 0.039	-0.26 %	2.32 %	0.652	0.565	-1.228	0.499
SLF_III_left	0.513 ± 0.026	0.508 ± 0.026	0.518 ± 0.040	0.518 ± 0.034	-1.03 %	0.04 %	2.069	0.132	-0.252	0.56
SLF_III_right	0.517 ± 0.025	0.513 ± 0.024	0.519 ± 0.036	0.514 ± 0.048	-0.81 %	-0.99 %	1.708	0.207	0.487	0.56
SLF_II_left	0.488 ± 0.023	0.490 ± 0.026	0.490 ± 0.039	0.498 ± 0.033	0.31 %	1.57 %	-0.491	0.602	-1.073	0.499
SLF_II_right	0.488 ± 0.023	0.488 ± 0.024	0.488 ± 0.038	0.495 ± 0.026	0.02 %	1.28 %	0.204	0.659	-0.992	0.499
SLF_I_left	0.464 ± 0.022	0.465 ± 0.027	0.466 ± 0.036	0.472 ± 0.029	0.22 %	1.25 %	-0.323	0.629	-1.038	0.499
SLF_I_right	0.481 ± 0.023	0.483 ± 0.026	0.485 ± 0.038	0.492 ± 0.028	0.39 %	1.46 %	-0.543	0.601	-0.910	0.499
STR_left	0.590 ± 0.025	0.589 ± 0.025	0.605 ± 0.028	0.609 ± 0.049	-0.06 %	0.57 %	0.309	0.629	-0.214	0.56
STR_right	0.598 ± 0.021	0.593 ± 0.023	0.607 ± 0.025	0.613 ± 0.030	-0.74 %	0.98 %	2.204	0.129	-1.507	0.499
ST_FO_left	0.465 ± 0.026	0.462 ± 0.026	0.492 ± 0.029	0.496 ± 0.030	-0.7 %	0.93 %	1.442	0.276	-0.659	0.553
ST_FO_right	0.467 ± 0.027	0.464 ± 0.029	0.486 ± 0.023	0.486 ± 0.046	-0.64 %	-0.02 %	1.576	0.251	0.030	0.59
ST_OCC_left	0.485 ± 0.022	0.481 ± 0.021	0.493 ± 0.020	0.497 ± 0.033	-0.89 %	0.78 %	2.885	0.068	-0.662	0.553

Table A.24 (cont'd)

	mTBI		Controls							
TractSeg Name	P1	P2	P1	P2	Percent Change mTBI %	Percent Change Controls %	t-score mTBI	q-value mTBI [1]	t-score controls	q-value controls
ST_OCC_right	0.492 ± 0.022	0.489 ± 0.021	0.497 ± 0.023	0.503 ± 0.032	-0.65 %	1.24 %	2.144	0.13	-1.231	0.499
ST_PAR_left	0.494 ± 0.020	0.491 ± 0.019	0.501 ± 0.023	0.504 ± 0.023	-0.61 %	0.67 %	2.310	0.128	-0.931	0.499
ST_PAR_right	0.509 ± 0.019	0.508 ± 0.018	0.515 ± 0.024	0.517 ± 0.029	-0.33 %	0.28 %	1.471	0.276	-0.082	0.588
ST_POSTC_left	0.529 ± 0.019	0.529 ± 0.021	0.547 ± 0.023	0.553 ± 0.023	-0.14 %	1.04 %	0.418	0.603	-1.128	0.499
ST_POSTC_right	0.546 ± 0.021	0.547 ± 0.019	0.560 ± 0.025	0.562 ± 0.033	0.18 %	0.3 %	-0.015	0.674	-0.101	0.588
ST_PREC_left	0.547 ± 0.021	0.547 ± 0.023	0.563 ± 0.028	0.571 ± 0.029	0.04 %	1.52 %	-0.125	0.674	-1.860	0.499
ST_PREC_right	0.558 ± 0.024	0.558 ± 0.022	0.571 ± 0.029	0.573 ± 0.033	-0.04 %	0.41 %	0.543	0.601	-0.347	0.56
ST_PREF_left	0.503 ± 0.022	0.502 ± 0.021	0.521 ± 0.031	0.522 ± 0.031	-0.1 %	0.09 %	0.432	0.603	-0.218	0.56
ST_PREF_right	0.504 ± 0.023	0.503 ± 0.020	0.519 ± 0.026	0.524 ± 0.028	-0.28 %	0.91 %	1.222	0.33	-1.166	0.499
ST_PREM_left	0.502 ± 0.021	0.503 ± 0.021	0.521 ± 0.033	0.527 ± 0.027	0.25 %	1.2 %	-0.647	0.565	-1.478	0.499
ST_PREM_right	0.522 ± 0.023	0.522 ± 0.021	0.542 ± 0.034	0.540 ± 0.033	0.03 %	-0.3 %	-0.063	0.674	0.281	0.56
T_OCC_left	0.486 ± 0.022	0.482 ± 0.022	0.496 ± 0.020	0.499 ± 0.032	-0.71 %	0.7 %	1.960	0.15	-0.526	0.56
T_OCC_right	0.492 ± 0.021	0.489 ± 0.021	0.498 ± 0.025	0.504 ± 0.033	-0.52 %	1.11 %	1.796	0.19	-1.238	0.499
T_PAR_left	0.497 ± 0.019	0.494 ± 0.020	0.503 ± 0.025	0.506 ± 0.025	-0.5 %	0.63 %	1.713	0.207	-0.790	0.52
T_PAR_right	0.510 ± 0.018	0.508 ± 0.019	0.516 ± 0.023	0.517 ± 0.027	-0.35 %	0.35 %	1.386	0.289	-0.248	0.56
T_POSTC_left	0.529 ± 0.020	0.528 ± 0.022	0.541 ± 0.027	0.548 ± 0.026	-0.24 %	1.23 %	0.608	0.58	-1.117	0.499
T_POSTC_right	0.539 ± 0.020	0.539 ± 0.021	0.546 ± 0.027	0.549 ± 0.034	0 %	0.47 %	0.211	0.659	-0.514	0.56
T_PREC_left	0.555 ± 0.021	0.556 ± 0.024	0.569 ± 0.031	0.579 ± 0.031	0.2 %	1.85 %	-0.465	0.603	-2.211	0.499
T_PREC_right	0.559 ± 0.022	0.559 ± 0.023	0.568 ± 0.030	0.571 ± 0.033	-0.03 %	0.61 %	0.335	0.629	-0.873	0.506
T_PREF_left	0.508 ± 0.021	0.509 ± 0.022	0.527 ± 0.032	0.528 ± 0.032	0.17 %	0.21 %	-0.321	0.629	-0.240	0.56
T_PREF_right	0.503 ± 0.020	0.503 ± 0.020	0.517 ± 0.027	0.523 ± 0.025	-0.1 %	1.27 %	0.504	0.602	-1.776	0.499
T_PREM_left	0.507 ± 0.020	0.510 ± 0.022	0.529 ± 0.034	0.537 ± 0.027	0.53 %	1.61 %	-1.224	0.33	-1.856	0.499
T_PREM_right	0.521 ± 0.019	0.521 ± 0.022	0.539 ± 0.033	0.541 ± 0.028	0.07 %	0.37 %	-0.202	0.659	-0.533	0.56
UF_left	0.438 ± 0.026	0.432 ± 0.026	0.452 ± 0.025	0.458 ± 0.019	-1.24 %	1.28 %	2.963	0.068	-1.504	0.499
UF_right	0.430 ± 0.024	0.426 ± 0.023	0.443 ± 0.018	0.451 ± 0.026	-0.96 %	1.74 %	2.680	0.094	-1.334	0.499

Tables A.24- T-test results for comparisons of the automatically segmented tracts from TractSeg between timepoints within mTBI and control subjects.

[1]Significant values are marked with an asterisk (*) or <0.001

Table A.25 Results of Post Hoc Tract Specific Comparison of Neurite Orientation Dispersion and Density Imaging Free Water Fraction

TractSeg Name	mTBI		Controls		Percent Change mTBI %	Percent Change Controls %	t-score mTBI	q-value mTBI[f]	t-score controls	q-value controls
	P1	P2	P1	P2						
AF_left	0.071 ± 0.012	0.066 ± 0.015	0.058 ± 0.009	0.055 ± 0.014	-7.44 %	-5.23 %	2.883	0.027*	1.056	0.501
AF_right	0.076 ± 0.013	0.072 ± 0.013	0.069 ± 0.013	0.065 ± 0.012	-4.97 %	-6.23 %	2.333	0.033*	1.692	0.321
ATR_left	0.090 ± 0.016	0.086 ± 0.022	0.082 ± 0.018	0.072 ± 0.018	-4.3 %	-11.69 %	1.559	0.098	2.417	0.313
ATR_right	0.097 ± 0.019	0.091 ± 0.019	0.092 ± 0.024	0.084 ± 0.025	-5.92 %	-8.32 %	2.462	0.027*	1.662	0.321
CA	0.069 ± 0.026	0.061 ± 0.025	0.054 ± 0.021	0.053 ± 0.029	-10.8 %	-0.49 %	2.015	0.057	0.060	0.606
CC_1	0.100 ± 0.026	0.092 ± 0.031	0.106 ± 0.032	0.087 ± 0.023	-7.51 %	-18.55 %	2.161	0.047*	3.502	0.157
CC_2	0.099 ± 0.013	0.097 ± 0.020	0.092 ± 0.015	0.082 ± 0.018	-2.58 %	-10.93 %	1.056	0.16	2.090	0.313
CC_3	0.114 ± 0.021	0.113 ± 0.031	0.103 ± 0.026	0.095 ± 0.032	-0.46 %	-8.03 %	0.069	0.324	0.935	0.501
CC_4	0.141 ± 0.019	0.142 ± 0.028	0.130 ± 0.023	0.127 ± 0.041	0.37 %	-2.04 %	-0.193	0.306	0.221	0.577
CC_5	0.131 ± 0.019	0.133 ± 0.026	0.126 ± 0.027	0.121 ± 0.044	1.86 %	-3.46 %	-0.876	0.177	0.299	0.562
CC_6	0.081 ± 0.017	0.080 ± 0.015	0.078 ± 0.012	0.077 ± 0.025	-0.65 %	-0.53 %	0.047	0.325	0.196	0.581
CC_7	0.094 ± 0.027	0.093 ± 0.019	0.093 ± 0.019	0.095 ± 0.029	-1.28 %	2.33 %	0.356	0.279	0.039	0.606
CC	0.097 ± 0.014	0.096 ± 0.016	0.093 ± 0.013	0.088 ± 0.023	-1.29 %	-5.23 %	0.579	0.226	0.963	0.501
CG_left	0.060 ± 0.012	0.059 ± 0.014	0.057 ± 0.014	0.053 ± 0.021	-2.33 %	-6.26 %	0.755	0.197	0.667	0.501
CG_right	0.060 ± 0.011	0.056 ± 0.012	0.054 ± 0.009	0.053 ± 0.025	-6.13 %	-2.81 %	2.052	0.055	0.151	0.59
CST_left	0.168 ± 0.017	0.164 ± 0.025	0.143 ± 0.016	0.139 ± 0.027	-2.3 %	-2.3 %	1.210	0.13	0.550	0.501
CST_right	0.145 ± 0.015	0.142 ± 0.017	0.131 ± 0.016	0.130 ± 0.025	-2.41 %	-0.92 %	1.307	0.12	0.129	0.59
FPT_left	0.144 ± 0.015	0.141 ± 0.022	0.128 ± 0.019	0.118 ± 0.021	-1.77 %	-7.88 %	0.874	0.177	1.858	0.313
FPT_right	0.140 ± 0.013	0.136 ± 0.017	0.128 ± 0.019	0.120 ± 0.022	-2.35 %	-6.47 %	1.340	0.116	1.539	0.343
FX_left	0.501 ± 0.108	0.490 ± 0.103	0.485 ± 0.103	0.476 ± 0.123	-2.24 %	-2 %	1.345	0.116	0.541	0.501
FX_right	0.491 ± 0.104	0.483 ± 0.108	0.482 ± 0.104	0.451 ± 0.136	-1.76 %	-6.31 %	0.767	0.197	1.298	0.417
ICP_left	0.095 ± 0.029	0.089 ± 0.016	0.089 ± 0.013	0.092 ± 0.018	-5.86 %	2.98 %	1.257	0.124	-0.233	0.577
ICP_right	0.082 ± 0.026	0.077 ± 0.017	0.081 ± 0.019	0.081 ± 0.025	-5.93 %	-0.41 %	1.201	0.13	0.698	0.501
IFO_left	0.074 ± 0.014	0.069 ± 0.015	0.068 ± 0.012	0.065 ± 0.014	-6.55 %	-4.94 %	2.999	0.027*	1.628	0.321
IFO_right	0.072 ± 0.016	0.067 ± 0.014	0.069 ± 0.014	0.067 ± 0.020	-5.81 %	-2.47 %	2.648	0.027*	1.350	0.417
ILF_left	0.070 ± 0.020	0.063 ± 0.018	0.063 ± 0.015	0.061 ± 0.019	-10.73 %	-2.8 %	3.386	0.027*	0.548	0.501
ILF_right	0.067 ± 0.023	0.061 ± 0.019	0.064 ± 0.018	0.065 ± 0.026	-8.04 %	2.2 %	2.443	0.027*	0.640	0.501
MCP	0.095 ± 0.027	0.092 ± 0.019	0.085 ± 0.012	0.097 ± 0.026	-2.89 %	14.42 %	0.665	0.217	-1.308	0.417
MLF_left	0.064 ± 0.015	0.061 ± 0.014	0.061 ± 0.012	0.060 ± 0.020	-4.84 %	-2.67 %	2.090	0.053	0.516	0.501
MLF_right	0.062 ± 0.017	0.060 ± 0.015	0.061 ± 0.013	0.059 ± 0.019	-2.78 %	-2.82 %	0.754	0.197	0.619	0.501
OR_left	0.090 ± 0.024	0.085 ± 0.022	0.086 ± 0.016	0.087 ± 0.028	-5.8 %	0.89 %	1.946	0.06	0.073	0.606
OR_right	0.086 ± 0.026	0.083 ± 0.022	0.089 ± 0.022	0.088 ± 0.030	-3.77 %	-0.46 %	0.967	0.161	1.088	0.501
POPT_left	0.121 ± 0.017	0.119 ± 0.019	0.117 ± 0.020	0.113 ± 0.033	-1.27 %	-3.2 %	0.641	0.219	0.607	0.501
POPT_right	0.113 ± 0.018	0.113 ± 0.018	0.111 ± 0.020	0.109 ± 0.029	-0.26 %	-1.29 %	-0.140	0.309	0.298	0.562
SCP_left	0.114 ± 0.016	0.109 ± 0.015	0.100 ± 0.009	0.100 ± 0.019	-4.04 %	0.06 %	1.871	0.068	0.296	0.562
SCP_right	0.104 ± 0.013	0.099 ± 0.014	0.097 ± 0.016	0.097 ± 0.017	-4.74 %	-0.8 %	2.750	0.027*	0.798	0.501
SLF_III_left	0.092 ± 0.015	0.086 ± 0.020	0.078 ± 0.012	0.070 ± 0.021	-6.36 %	-10.49 %	2.704	0.027*	1.678	0.321
SLF_III_right	0.083 ± 0.015	0.080 ± 0.015	0.080 ± 0.014	0.072 ± 0.015	-3.91 %	-9.31 %	1.660	0.089	2.353	0.313
SLF_II_left	0.079 ± 0.015	0.077 ± 0.020	0.068 ± 0.011	0.066 ± 0.022	-2.78 %	-4.03 %	1.017	0.161	0.510	0.501
SLF_II_right	0.072 ± 0.014	0.070 ± 0.015	0.065 ± 0.012	0.062 ± 0.017	-2.79 %	-5.41 %	1.003	0.161	1.503	0.346
SLF_I_left	0.083 ± 0.022	0.085 ± 0.025	0.087 ± 0.035	0.083 ± 0.047	1.82 %	-5.55 %	-0.631	0.219	0.454	0.514
SLF_I_right	0.083 ± 0.020	0.084 ± 0.021	0.086 ± 0.027	0.082 ± 0.039	0.49 %	-4.34 %	-0.327	0.28	0.557	0.501

Table A.25 (cont'd)

TractSeg Name	mTBI		Controls		Percent Change mTBI %	Percent Change Controls %	t-score mTBI	q-value mTBI'	t-score controls	q-value controls
	P1	P2	P1	P2						
STR_left	0.141 ± 0.016	0.136 ± 0.026	0.117 ± 0.021	0.113 ± 0.030	-3.47 %	-4.08 %	1.562	0.098	0.509	0.501
STR_right	0.131 ± 0.017	0.123 ± 0.020	0.119 ± 0.025	0.111 ± 0.027	-5.49 %	-7.14 %	2.712	0.027*	0.898	0.501
ST_FO_left	0.061 ± 0.016	0.057 ± 0.023	0.056 ± 0.017	0.053 ± 0.022	-5.49 %	-5.37 %	1.381	0.114	0.671	0.501
ST_FO_right	0.066 ± 0.017	0.060 ± 0.019	0.066 ± 0.021	0.056 ± 0.018	-7.66 %	-14.49 %	2.478	0.027*	2.055	0.313
ST_OCC_left	0.080 ± 0.018	0.074 ± 0.017	0.071 ± 0.012	0.072 ± 0.020	-6.34 %	1.42 %	2.544	0.027*	0.026	0.606
ST_OCC_right	0.073 ± 0.020	0.069 ± 0.018	0.070 ± 0.014	0.071 ± 0.023	-5.05 %	1.85 %	1.527	0.098	0.964	0.501
ST_PAR_left	0.091 ± 0.017	0.089 ± 0.018	0.090 ± 0.020	0.086 ± 0.030	-2.12 %	-4.22 %	0.971	0.161	0.644	0.501
ST_PAR_right	0.087 ± 0.018	0.086 ± 0.016	0.086 ± 0.016	0.083 ± 0.026	-1.01 %	-3.16 %	0.176	0.306	0.600	0.501
ST_POSTC_left	0.124 ± 0.019	0.121 ± 0.025	0.117 ± 0.030	0.109 ± 0.038	-2.35 %	-6.97 %	0.972	0.161	0.802	0.501
ST_POSTC_right	0.111 ± 0.019	0.111 ± 0.021	0.115 ± 0.029	0.110 ± 0.040	-0.23 %	-3.84 %	0.191	0.306	0.467	0.514
ST_PREC_left	0.133 ± 0.019	0.128 ± 0.026	0.113 ± 0.019	0.109 ± 0.031	-3.7 %	-3.51 %	1.619	0.093	0.558	0.501
ST_PREC_right	0.122 ± 0.018	0.117 ± 0.018	0.115 ± 0.022	0.108 ± 0.027	-3.55 %	-5.86 %	1.702	0.085	1.028	0.501
ST_PREF_left	0.094 ± 0.013	0.091 ± 0.020	0.083 ± 0.015	0.074 ± 0.016	-4.1 %	-10.22 %	1.740	0.082	1.974	0.313
ST_PREF_right	0.095 ± 0.013	0.090 ± 0.016	0.088 ± 0.018	0.079 ± 0.017	-4.96 %	-10.48 %	2.735	0.027*	1.950	0.313
ST_PREM_left	0.099 ± 0.018	0.094 ± 0.027	0.083 ± 0.017	0.071 ± 0.017	-4.37 %	-14.08 %	1.393	0.114	2.631	0.313
ST_PREM_right	0.104 ± 0.016	0.099 ± 0.019	0.096 ± 0.019	0.084 ± 0.023	-4.73 %	-12.23 %	2.483	0.027*	2.250	0.313
T_OCC_left	0.092 ± 0.024	0.086 ± 0.022	0.088 ± 0.016	0.088 ± 0.028	-5.71 %	0.41 %	1.952	0.06	0.142	0.59
T_OCC_right	0.085 ± 0.026	0.082 ± 0.022	0.088 ± 0.022	0.087 ± 0.030	-3.74 %	-0.36 %	0.991	0.161	1.139	0.501
T_PAR_left	0.098 ± 0.020	0.096 ± 0.021	0.100 ± 0.024	0.095 ± 0.037	-1.45 %	-4.59 %	0.582	0.226	0.629	0.501
T_PAR_right	0.097 ± 0.021	0.095 ± 0.019	0.098 ± 0.025	0.095 ± 0.034	-1.29 %	-3.7 %	0.325	0.28	0.583	0.501
T_POSTC_left	0.120 ± 0.019	0.119 ± 0.025	0.120 ± 0.038	0.111 ± 0.047	-1.31 %	-7.8 %	0.550	0.229	0.757	0.501
T_POSTC_right	0.105 ± 0.019	0.106 ± 0.022	0.114 ± 0.039	0.110 ± 0.049	0.56 %	-3.25 %	-0.169	0.306	0.282	0.562
T_PREC_left	0.139 ± 0.019	0.135 ± 0.028	0.120 ± 0.023	0.116 ± 0.037	-3.17 %	-3.68 %	1.403	0.114	0.513	0.501
T_PREC_right	0.120 ± 0.018	0.115 ± 0.019	0.114 ± 0.025	0.108 ± 0.031	-4.04 %	-5.42 %	1.755	0.082	0.767	0.501
T_PREF_left	0.107 ± 0.014	0.103 ± 0.022	0.096 ± 0.019	0.086 ± 0.021	-3.38 %	-10.47 %	1.488	0.102	1.866	0.313
T_PREF_right	0.106 ± 0.016	0.101 ± 0.018	0.100 ± 0.023	0.091 ± 0.024	-5.11 %	-9.32 %	2.600	0.027*	1.682	0.321
T_PREM_left	0.110 ± 0.019	0.106 ± 0.029	0.098 ± 0.022	0.086 ± 0.027	-3.74 %	-12.54 %	1.289	0.12	1.917	0.313

Table A.25 (cont'd)

TractSeg Name	mTBI		Controls		Percent Change mTBI %	Percent Change Controls %	t-score mTBI	q-value mTBI[1]	t-score controls	q-value controls
	P1	P2	P1	P2						
T_PREM_right	0.111 ± 0.018	0.105 ± 0.021	0.106 ± 0.029	0.094 ± 0.031	-5.76 %	-10.69 %	2.538	0.027*	1.611	0.321
UF_left	0.043 ± 0.015	0.040 ± 0.016	0.041 ± 0.012	0.039 ± 0.019	-6.96 %	-5.22 %	1.531	0.098	0.317	0.562
UF_right	0.051 ± 0.014	0.046 ± 0.014	0.050 ± 0.019	0.046 ± 0.022	-8.95 %	-8.54 %	2.863	0.027*	0.692	0.501

Tables A.25- T-test results for comparisons of the automatically segmented tracts from TractSeg between timepoints within mTBI and control subjects.

[1]Significant values are marked with an asterisk (*) or <0.001

Table A.26 Results of Post Hoc Tract Specific Comparison of Fixel Based Analysis Fiber Density

	mTBI		Controls							
TractSeg Name	P1	P2	P1	P2	Percent Change mTBI %	Percent Change Controls %	t-score mTBI	q-value mTBI[1]	t-score controls	q-value controls
AF_left	0.285 ± 0.018	0.286 ± 0.014	0.296 ± 0.014	0.296 ± 0.011	0.39 %	-0.12 %	-0.733	0.828	0.107	0.801
AF_right	0.294 ± 0.015	0.293 ± 0.014	0.297 ± 0.015	0.297 ± 0.013	-0.23 %	0.28 %	0.783	0.828	-0.275	0.793
ATR_left	0.298 ± 0.014	0.298 ± 0.016	0.316 ± 0.016	0.318 ± 0.014	0 %	0.57 %	0.011	0.869	-0.514	0.776
ATR_right	0.291 ± 0.014	0.292 ± 0.015	0.306 ± 0.014	0.310 ± 0.014	0.18 %	1.4 %	-0.516	0.828	-1.580	0.776
CA	0.269 ± 0.025	0.271 ± 0.024	0.295 ± 0.027	0.302 ± 0.025	0.81 %	2.26 %	-1.089	0.828	-0.854	0.776
CC_1	0.378 ± 0.024	0.374 ± 0.026	0.392 ± 0.024	0.393 ± 0.023	-1.04 %	0.02 %	1.933	0.828	-0.011	0.824
CC_2	0.331 ± 0.018	0.330 ± 0.019	0.344 ± 0.018	0.346 ± 0.015	-0.21 %	0.55 %	0.624	0.828	-0.544	0.776
CC_3	0.326 ± 0.022	0.328 ± 0.024	0.344 ± 0.029	0.346 ± 0.028	0.6 %	0.55 %	-1.192	0.828	-0.417	0.776
CC_4	0.366 ± 0.023	0.367 ± 0.023	0.386 ± 0.020	0.389 ± 0.019	0.14 %	0.6 %	-0.348	0.832	-0.552	0.776
CC_5	0.370 ± 0.021	0.370 ± 0.021	0.385 ± 0.025	0.389 ± 0.024	-0.11 %	0.8 %	0.294	0.832	-0.579	0.776
CC_6	0.352 ± 0.023	0.352 ± 0.019	0.359 ± 0.015	0.357 ± 0.016	-0.15 %	-0.55 %	0.318	0.832	0.683	0.776
CC_7	0.330 ± 0.029	0.331 ± 0.020	0.333 ± 0.014	0.332 ± 0.016	0.4 %	-0.17 %	-0.513	0.828	0.214	0.797
CC	0.343 ± 0.018	0.343 ± 0.016	0.353 ± 0.016	0.354 ± 0.016	-0.1 %	0.2 %	0.288	0.832	-0.215	0.797
CG_left	0.314 ± 0.016	0.313 ± 0.017	0.324 ± 0.016	0.326 ± 0.013	-0.24 %	0.58 %	0.585	0.828	-0.510	0.776
CG_right	0.314 ± 0.017	0.313 ± 0.018	0.319 ± 0.019	0.322 ± 0.014	-0.33 %	0.95 %	0.994	0.828	-1.021	0.776
CST_left	0.428 ± 0.016	0.431 ± 0.016	0.449 ± 0.017	0.454 ± 0.017	0.67 %	1.04 %	-1.502	0.828	-1.223	0.776
CST_right	0.437 ± 0.016	0.437 ± 0.014	0.451 ± 0.015	0.455 ± 0.018	0.18 %	0.95 %	-0.540	0.828	-1.239	0.776
FPT_left	0.398 ± 0.015	0.400 ± 0.015	0.416 ± 0.015	0.420 ± 0.016	0.51 %	1.06 %	-1.399	0.828	-1.207	0.776
FPT_right	0.400 ± 0.014	0.401 ± 0.013	0.413 ± 0.016	0.418 ± 0.016	0.24 %	1.16 %	-0.812	0.828	-1.592	0.776
FX_left	0.210 ± 0.052	0.213 ± 0.057	0.237 ± 0.051	0.241 ± 0.056	1.45 %	1.87 %	-1.221	0.828	-0.671	0.776
FX_right	0.221 ± 0.054	0.224 ± 0.059	0.236 ± 0.058	0.241 ± 0.055	1.2 %	2.37 %	-0.978	0.828	-0.717	0.776
ICP_left	0.302 ± 0.017	0.302 ± 0.012	0.302 ± 0.014	0.305 ± 0.015	0.1 %	0.95 %	-0.168	0.853	-0.950	0.776
ICP_right	0.277 ± 0.016	0.277 ± 0.015	0.277 ± 0.010	0.278 ± 0.017	-0.2 %	0.25 %	0.281	0.832	-0.218	0.797
IFO_left	0.313 ± 0.017	0.314 ± 0.015	0.323 ± 0.012	0.323 ± 0.013	0.15 %	0.05 %	-0.398	0.828	-0.049	0.817
IFO_right	0.313 ± 0.016	0.313 ± 0.014	0.319 ± 0.011	0.321 ± 0.012	0.03 %	0.57 %	-0.088	0.869	-0.749	0.776
ILF_left	0.288 ± 0.022	0.290 ± 0.015	0.293 ± 0.013	0.295 ± 0.013	0.84 %	0.37 %	-1.323	0.828	-0.404	0.776
ILF_right	0.291 ± 0.019	0.291 ± 0.016	0.296 ± 0.012	0.299 ± 0.013	0.02 %	1.01 %	-0.057	0.869	-1.026	0.776
MCP	0.315 ± 0.014	0.315 ± 0.012	0.315 ± 0.011	0.317 ± 0.010	0.1 %	0.52 %	-0.215	0.843	-0.715	0.776
MLF_left	0.308 ± 0.022	0.308 ± 0.016	0.315 ± 0.016	0.313 ± 0.018	0.3 %	-0.57 %	-0.566	0.828	0.578	0.776
MLF_right	0.325 ± 0.018	0.324 ± 0.017	0.328 ± 0.015	0.325 ± 0.017	-0.46 %	-0.75 %	1.367	0.828	0.807	0.776
OR_left	0.316 ± 0.021	0.318 ± 0.021	0.325 ± 0.014	0.328 ± 0.014	0.49 %	0.92 %	-1.147	0.828	-1.076	0.776

Table A.26 (cont'd)

	mTBI		Controls							
TractSeg Name	P1	P2	P1	P2	Percent Change mTBI %	Percent Change Controls %	t-score mTBI	q-value mTBI[1]	t-score controls	q-value controls
OR_right	0.335 ± 0.022	0.336 ± 0.019	0.338 ± 0.012	0.340 ± 0.014	0.35 %	0.74 %	-0.752	0.828	-1.054	0.776
POPT_left	0.379 ± 0.015	0.380 ± 0.014	0.390 ± 0.018	0.391 ± 0.019	0.2 %	0.4 %	-0.546	0.828	-0.478	0.776
POPT_right	0.402 ± 0.017	0.402 ± 0.016	0.411 ± 0.015	0.412 ± 0.018	0 %	0.29 %	-0.008	0.869	-0.417	0.776
SCP_left	0.342 ± 0.012	0.344 ± 0.012	0.351 ± 0.013	0.356 ± 0.012	0.44 %	1.66 %	-1.511	0.828	-2.619	0.776
SCP_right	0.339 ± 0.011	0.340 ± 0.012	0.344 ± 0.011	0.348 ± 0.013	0.15 %	1.2 %	-0.425	0.828	-1.691	0.776
SLF_III_left	0.304 ± 0.017	0.305 ± 0.015	0.313 ± 0.019	0.314 ± 0.019	0.1 %	0.2 %	-0.228	0.843	-0.173	0.797
SLF_III_right	0.300 ± 0.018	0.299 ± 0.018	0.298 ± 0.017	0.299 ± 0.017	-0.29 %	0.16 %	1.069	0.828	-0.156	0.797
SLF_II_left	0.284 ± 0.017	0.284 ± 0.017	0.288 ± 0.021	0.289 ± 0.020	0.1 %	0.37 %	-0.259	0.836	-0.337	0.779
SLF_II_right	0.281 ± 0.017	0.281 ± 0.018	0.283 ± 0.013	0.283 ± 0.015	-0.19 %	-0.12 %	0.568	0.828	0.146	0.797
SLF_I_left	0.276 ± 0.014	0.275 ± 0.014	0.278 ± 0.016	0.278 ± 0.017	-0.26 %	-0.15 %	0.811	0.828	0.113	0.801
SLF_I_right	0.289 ± 0.015	0.289 ± 0.015	0.295 ± 0.014	0.294 ± 0.015	0 %	-0.39 %	0.010	0.869	0.375	0.779
STR_left	0.416 ± 0.017	0.418 ± 0.018	0.432 ± 0.022	0.439 ± 0.020	0.64 %	1.65 %	-1.996	0.828	-2.003	0.776
STR_right	0.434 ± 0.015	0.433 ± 0.015	0.444 ± 0.023	0.449 ± 0.023	-0.02 %	1.16 %	0.072	0.869	-1.496	0.776
ST_FO_left	0.320 ± 0.019	0.319 ± 0.019	0.339 ± 0.015	0.341 ± 0.018	-0.29 %	0.64 %	0.543	0.828	-0.417	0.776
ST_FO_right	0.335 ± 0.021	0.334 ± 0.019	0.350 ± 0.016	0.355 ± 0.016	-0.52 %	1.24 %	1.006	0.828	-1.223	0.776
ST_OCC_left	0.326 ± 0.023	0.327 ± 0.020	0.335 ± 0.013	0.337 ± 0.015	0.46 %	0.59 %	-0.986	0.828	-0.617	0.776
ST_OCC_right	0.334 ± 0.022	0.335 ± 0.018	0.339 ± 0.013	0.341 ± 0.015	0.32 %	0.45 %	-0.669	0.828	-0.622	0.776
ST_PAR_left	0.335 ± 0.016	0.335 ± 0.015	0.345 ± 0.016	0.345 ± 0.018	0.18 %	0.08 %	-0.497	0.828	-0.084	0.805
ST_PAR_right	0.355 ± 0.017	0.354 ± 0.016	0.361 ± 0.013	0.361 ± 0.016	-0.23 %	0 %	0.741	0.828	-0.002	0.824
ST_POSTC_left	0.338 ± 0.013	0.340 ± 0.014	0.355 ± 0.017	0.358 ± 0.018	0.54 %	0.85 %	-1.536	0.828	-0.728	0.776
ST_POSTC_right	0.361 ± 0.015	0.360 ± 0.014	0.374 ± 0.016	0.376 ± 0.019	-0.2 %	0.53 %	0.667	0.828	-0.492	0.776
ST_PREC_left	0.346 ± 0.013	0.348 ± 0.014	0.365 ± 0.015	0.368 ± 0.016	0.57 %	0.87 %	-1.420	0.828	-0.802	0.776
ST_PREC_right	0.363 ± 0.014	0.363 ± 0.013	0.376 ± 0.015	0.379 ± 0.015	0.13 %	0.75 %	-0.406	0.828	-0.792	0.776
ST_PREF_left	0.329 ± 0.013	0.329 ± 0.015	0.344 ± 0.013	0.345 ± 0.015	0.04 %	0.51 %	-0.120	0.869	-0.452	0.776
ST_PREF_right	0.330 ± 0.013	0.329 ± 0.012	0.340 ± 0.013	0.344 ± 0.013	-0.12 %	1.13 %	0.442	0.828	-1.413	0.776
ST_PREM_left	0.308 ± 0.014	0.309 ± 0.016	0.320 ± 0.024	0.322 ± 0.023	0.38 %	0.64 %	-0.876	0.828	-0.455	0.776
ST_PREM_right	0.322 ± 0.016	0.324 ± 0.016	0.335 ± 0.019	0.337 ± 0.017	0.53 %	0.61 %	-1.384	0.828	-0.507	0.776

Table A.26 (cont'd)

	mTBI		Controls							
TractSeg Name	P1	P2	P1	P2	Percent Change mTBI %	Percent Change Controls %	t-score mTBI	q-value mTBI[1]	t-score controls	q-value controls
T_OCC_left	0.310 ± 0.021	0.312 ± 0.020	0.319 ± 0.013	0.322 ± 0.014	0.46 %	0.96 %	-1.053	0.828	-1.122	0.776
T_OCC_right	0.328 ± 0.021	0.329 ± 0.019	0.331 ± 0.012	0.333 ± 0.014	0.37 %	0.61 %	-0.774	0.828	-0.859	0.776
T_PAR_left	0.335 ± 0.015	0.335 ± 0.015	0.344 ± 0.017	0.345 ± 0.018	0.06 %	0.29 %	-0.169	0.853	-0.329	0.779
T_PAR_right	0.362 ± 0.017	0.361 ± 0.017	0.367 ± 0.015	0.368 ± 0.017	-0.17 %	0.24 %	0.545	0.828	-0.298	0.789
T_POSTC_left	0.357 ± 0.014	0.358 ± 0.015	0.371 ± 0.021	0.374 ± 0.021	0.25 %	1.04 %	-0.735	0.828	-1.154	0.776
T_POSTC_right	0.372 ± 0.017	0.371 ± 0.017	0.383 ± 0.020	0.387 ± 0.021	-0.27 %	0.86 %	0.846	0.828	-0.903	0.776
T_PREC_left	0.365 ± 0.015	0.367 ± 0.015	0.386 ± 0.016	0.390 ± 0.016	0.52 %	1 %	-1.303	0.828	-1.008	0.776
T_PREC_right	0.377 ± 0.015	0.377 ± 0.014	0.390 ± 0.016	0.393 ± 0.016	0.13 %	0.94 %	-0.392	0.828	-1.137	0.776
T_PREF_left	0.333 ± 0.013	0.333 ± 0.014	0.349 ± 0.013	0.352 ± 0.014	0.14 %	0.69 %	-0.430	0.828	-0.673	0.776
T_PREF_right	0.322 ± 0.012	0.322 ± 0.013	0.334 ± 0.013	0.338 ± 0.013	0 %	1.19 %	0.018	0.869	-1.470	0.776
T_PREM_left	0.324 ± 0.013	0.326 ± 0.016	0.340 ± 0.021	0.343 ± 0.020	0.5 %	0.78 %	-1.164	0.828	-0.619	0.776
T_PREM_right	0.335 ± 0.015	0.337 ± 0.017	0.352 ± 0.019	0.356 ± 0.018	0.63 %	0.94 %	-1.532	0.828	-0.896	0.776
UF_left	0.299 ± 0.020	0.299 ± 0.017	0.313 ± 0.015	0.310 ± 0.024	-0.16 %	-0.77 %	0.300	0.832	0.344	0.779
UF_right	0.295 ± 0.016	0.293 ± 0.017	0.307 ± 0.011	0.307 ± 0.020	-0.41 %	0.27 %	0.868	0.828	-0.152	0.797

Tables A.26- T-test results for comparisons of the automatically segmented tracts from TractSeg between timepoints within mTBI and control subjects.

[1]Significant values are marked with an asterisk (*) or <0.001

Table A.27 Results of Post Hoc Tract Specific Comparison of Fixel Based Analysis Fiber Cross Section

	mTBI		Controls							
TractSeg Name	P1	P2	P1	P2	Percent Change mTBI %	Percent Change Controls %	t-score mTBI	q-value mTBI[1]	t-score controls	q-value controls
AF_left	0.035 ± 0.073	0.035 ± 0.070	0.056 ± 0.111	0.068 ± 0.125	-0.26 %	21.44 %	0.021	0.16	-1.356	0.085
AF_right	0.046 ± 0.070	0.045 ± 0.073	0.078 ± 0.101	0.087 ± 0.121	-1.42 %	11.55 %	0.231	0.147	-1.252	0.087
ATR_left	0.003 ± 0.082	-6.888e-03 ± 8.403e-02	0.026 ± 0.102	0.028 ± 0.121	-299.02 %	8.83 %	1.933	0.061	-0.194	0.181
ATR_right	0.014 ± 0.079	0.008 ± 0.080	0.052 ± 0.091	0.056 ± 0.106	-43.33 %	6.57 %	1.259	0.078	-0.610	0.135
CA	0.005 ± 0.083	0.010 ± 0.072	0.056 ± 0.089	0.073 ± 0.085	104.23 %	29.87 %	-0.943	0.108	-1.902	0.06
CC_1	0.013 ± 0.089	0.003 ± 0.092	0.077 ± 0.107	0.081 ± 0.101	-75.6 %	4.94 %	1.615	0.065	-0.522	0.145
CC_2	0.020 ± 0.069	0.015 ± 0.071	0.054 ± 0.093	0.057 ± 0.102	-28.35 %	6.43 %	1.994	0.061	-0.942	0.109
CC_3	0.023 ± 0.080	0.026 ± 0.088	0.028 ± 0.103	0.039 ± 0.119	10.96 %	39.9 %	-0.437	0.142	-1.329	0.086
CC_4	0.003 ± 0.072	0.013 ± 0.075	0.047 ± 0.078	0.064 ± 0.097	286.67 %	37.54 %	-1.944	0.061	-1.859	0.06
CC_5	-1.106e-02 ± 6.943e-02	-2.758e-03 ± 7.171e-02	0.007 ± 0.103	0.017 ± 0.113	-75.08 %	156.28 %	-1.901	0.061	-1.746	0.066
CC_6	8.253e-04 ± 7.889e-02	0.006 ± 0.073	0.006 ± 0.106	0.014 ± 0.110	612 %	122.82 %	-0.844	0.113	-2.446	0.06
CC_7	0.057 ± 0.079	0.053 ± 0.080	0.043 ± 0.103	0.060 ± 0.115	-6.36 %	40.95 %	1.267	0.078	-2.471	0.06
CC	0.013 ± 0.061	0.014 ± 0.063	0.032 ± 0.091	0.040 ± 0.099	8.12 %	25.81 %	-0.333	0.147	-2.404	0.06
CG_left	0.008 ± 0.063	0.006 ± 0.063	0.026 ± 0.101	0.022 ± 0.092	-26.31 %	-14.76 %	0.728	0.128	0.492	0.145
CG_right	0.008 ± 0.063	0.004 ± 0.064	0.024 ± 0.094	0.025 ± 0.090	-47.98 %	5.64 %	1.359	0.078	-0.181	0.181
CST_left	-1.905e-02 ± 7.521e-02	-8.765e-03 ± 7.238e-02	0.039 ± 0.085	0.051 ± 0.095	-53.99 %	29.98 %	-2.866	0.022*	-1.627	0.07
CST_right	-3.508e-03 ± 7.713e-02	0.003 ± 0.076	0.035 ± 0.093	0.041 ± 0.096	-174.57 %	17.98 %	-1.265	0.078	-0.834	0.114
FPT_left	0.004 ± 0.068	0.006 ± 0.065	0.032 ± 0.073	0.039 ± 0.081	52.09 %	23.18 %	-0.679	0.133	-1.465	0.08
FPT_right	0.001 ± 0.064	4.733e-04 ± 6.411e-02	0.030 ± 0.091	0.033 ± 0.090	-65.91 %	11.89 %	0.382	0.142	-1.055	0.099
FX_left	-7.329e-02 ± 1.008e-01	-7.435e-02 ± 1.209e-01	-1.159e-01 ± 1.119e-01	-1.177e-01 ± 1.174e-01	1.44 %	1.52 %	0.210	0.148	0.366	0.163
FX_right	-7.471e-02 ± 1.073e-01	-7.727e-02 ± 1.254e-01	-1.160e-01 ± 1.090e-01	-1.159e-01 ± 1.192e-01	3.42 %	-0.08 %	0.525	0.142	-0.014	0.202
ICP_left	0.025 ± 0.091	0.024 ± 0.097	0.054 ± 0.097	0.049 ± 0.090	-4.04 %	-9.26 %	0.192	0.148	0.489	0.145
ICP_right	0.023 ± 0.081	0.018 ± 0.085	0.036 ± 0.094	0.038 ± 0.103	-24.1 %	7.15 %	1.047	0.098	-0.207	0.181
IFO_left	0.035 ± 0.074	0.028 ± 0.074	0.044 ± 0.105	0.055 ± 0.120	-18.8 %	23 %	1.730	0.065	-1.608	0.07
IFO_right	0.047 ± 0.067	0.042 ± 0.068	0.066 ± 0.099	0.077 ± 0.111	-10.62 %	16.59 %	1.649	0.065	-1.843	0.06
ILF_left	0.069 ± 0.085	0.067 ± 0.087	0.070 ± 0.107	0.091 ± 0.113	-2.51 %	28.83 %	0.397	0.142	-3.214	0.06
ILF_right	0.091 ± 0.082	0.090 ± 0.082	0.091 ± 0.104	0.107 ± 0.107	-1 %	18.01 %	0.263	0.147	-1.738	0.066
MCP	0.028 ± 0.094	0.027 ± 0.097	0.044 ± 0.105	0.045 ± 0.107	-5.45 %	0.86 %	0.289	0.147	-0.037	0.202

Table A.27 (cont'd)

	mTBI		Controls							
TractSeg Name	P1	P2	P1	P2	Percent Change mTBI %	Percent Change Controls %	t-score mTBI	q-value mTBI[1]	t-score controls	q-value controls
MLF_left	0.017 ± 0.082	0.020 ± 0.075	0.026 ± 0.110	0.034 ± 0.113	18.51 %	32.39 %	-0.505	0.142	-2.264	0.06
MLF_right	0.020 ± 0.078	0.025 ± 0.073	0.026 ± 0.102	0.032 ± 0.108	28.69 %	24.39 %	-1.063	0.098	-1.374	0.085
OR_left	0.037 ± 0.080	0.038 ± 0.080	0.036 ± 0.098	0.052 ± 0.114	1.13 %	44.33 %	-0.122	0.153	-2.059	0.06
OR_right	0.035 ± 0.075	0.034 ± 0.074	0.042 ± 0.104	0.055 ± 0.118	-1.84 %	30.6 %	0.255	0.147	-1.947	0.06
POPT_left	-3.043e-02 ± 7.537e-02	-2.240e-02 ± 6.974e-02	-6.398e-03 ± 9.750e-02	-4.521e-04 ± 1.052e-01	-26.39 %	-92.93 %	-1.630	0.065	-1.250	0.087
POPT_right	-2.630e-02 ± 7.626e-02	-1.965e-02 ± 7.247e-02	-4.322e-03 ± 1.042e-01	-9.075e-05 ± 1.045e-01	-25.31 %	-97.9 %	-1.323	0.078	-0.685	0.126
SCP_left	0.007 ± 0.080	0.008 ± 0.085	0.032 ± 0.090	0.029 ± 0.086	28.33 %	-8.05 %	-0.543	0.142	0.332	0.166
SCP_right	0.017 ± 0.072	0.014 ± 0.073	0.033 ± 0.087	0.035 ± 0.093	-15.59 %	4.87 %	0.837	0.113	-0.179	0.181
SLF_III_left	0.036 ± 0.081	0.036 ± 0.082	0.062 ± 0.128	0.067 ± 0.134	-1 %	6.67 %	0.093	0.153	-0.521	0.145
SLF_III_right	0.047 ± 0.074	0.049 ± 0.078	0.089 ± 0.115	0.093 ± 0.124	5.05 %	4.68 %	-0.870	0.113	-1.076	0.098
SLF_II_left	0.027 ± 0.072	0.028 ± 0.073	0.043 ± 0.105	0.058 ± 0.134	4.02 %	37.08 %	-0.393	0.142	-1.245	0.087
SLF_II_right	0.035 ± 0.079	0.033 ± 0.078	0.060 ± 0.104	0.071 ± 0.120	-6.27 %	17.78 %	0.643	0.135	-1.606	0.07
SLF_I_left	0.007 ± 0.069	0.015 ± 0.067	0.025 ± 0.091	0.036 ± 0.099	103.82 %	45.42 %	-1.627	0.065	-2.066	0.06
SLF_I_right	0.006 ± 0.074	0.008 ± 0.072	0.026 ± 0.110	0.035 ± 0.110	34.8 %	36.4 %	-0.512	0.142	-2.073	0.06
STR_left	-7.186e-03 ± 7.695e-02	0.002 ± 0.075	0.029 ± 0.096	0.041 ± 0.110	-127.13 %	40.41 %	-2.528	0.028*	-1.510	0.077
STR_right	0.006 ± 0.065	0.010 ± 0.063	0.030 ± 0.108	0.035 ± 0.106	63.84 %	16.85 %	-0.839	0.113	-0.734	0.122
ST_FO_left	0.010 ± 0.081	5.806e-06 ± 8.671e-02	0.038 ± 0.106	0.043 ± 0.114	-99.94 %	14.79 %	1.625	0.065	-0.733	0.122
ST_FO_right	0.033 ± 0.080	0.026 ± 0.081	0.079 ± 0.092	0.094 ± 0.094	-20.48 %	18.12 %	0.947	0.108	-2.621	0.06
ST_OCC_left	0.042 ± 0.078	0.042 ± 0.079	0.044 ± 0.097	0.062 ± 0.115	-0.72 %	42.71 %	0.100	0.153	-2.449	0.06
ST_OCC_right	0.045 ± 0.074	0.044 ± 0.074	0.050 ± 0.103	0.066 ± 0.117	-3.77 %	30.42 %	0.634	0.135	-2.194	0.06
ST_PAR_left	-1.348e-02 ± 7.252e-02	-6.068e-03 ± 7.133e-02	0.009 ± 0.103	0.018 ± 0.115	-54.99 %	95 %	-1.546	0.068	-1.580	0.071
ST_PAR_right	-1.055e-02 ± 7.394e-02	-4.638e-03 ± 7.093e-02	0.010 ± 0.106	0.018 ± 0.114	-56.06 %	69.63 %	-1.326	0.078	-1.135	0.096
ST_POSTC_left	-2.821e-02 ± 6.992e-02	-1.716e-02 ± 7.083e-02	0.012 ± 0.102	0.024 ± 0.123	-39.16 %	96.42 %	-2.625	0.026*	-1.294	0.087
ST_POSTC_right	-1.800e-02 ± 7.040e-02	-1.046e-02 ± 7.192e-02	0.016 ± 0.113	0.023 ± 0.124	-41.9 %	40.32 %	-2.291	0.043*	-0.744	0.122
ST_PREC_left	-6.573e-03 ± 6.506e-02	0.004 ± 0.066	0.049 ± 0.085	0.064 ± 0.103	-163.74 %	31.1 %	-3.168	0.014*	-1.844	0.06
ST_PREC_right	0.002 ± 0.068	0.008 ± 0.069	0.035 ± 0.096	0.044 ± 0.108	299.6 %	25.28 %	-1.343	0.078	-1.089	0.098

Table A.27 (cont'd)

	mTBI		Controls							
TractSeg Name	P1	P2	P1	P2	Percent Change mTBI %	Percent Change Controls %	t-score mTBI	q-value mTBI[1]	t-score controls	q-value controls
ST_PREF_left	0.016 ± 0.067	0.012 ± 0.067	0.047 ± 0.085	0.054 ± 0.100	-24.73 %	14.88 %	1.240	0.078	-0.922	0.109
ST_PREF_right	0.020 ± 0.065	0.015 ± 0.065	0.060 ± 0.093	0.065 ± 0.102	-24.18 %	8.64 %	1.859	0.061	-1.377	0.085
ST_PREM_left	0.012 ± 0.074	0.015 ± 0.076	0.028 ± 0.094	0.040 ± 0.118	19.98 %	41.08 %	-0.589	0.139	-0.864	0.114
ST_PREM_right	0.016 ± 0.070	0.018 ± 0.074	0.041 ± 0.094	0.050 ± 0.105	12.14 %	24.11 %	-0.447	0.142	-1.644	0.07
T_OCC_left	0.038 ± 0.079	0.039 ± 0.080	0.036 ± 0.098	0.052 ± 0.115	1 %	45.46 %	-0.115	0.153	-2.107	0.06
T_OCC_right	0.037 ± 0.075	0.036 ± 0.075	0.043 ± 0.105	0.056 ± 0.119	-1.82 %	30.71 %	0.258	0.147	-1.976	0.06
T_PAR_left	-1.725e-02 ± 7.338e-02	-9.715e-03 ± 7.206e-02	0.003 ± 0.101	0.010 ± 0.111	-43.68 %	281.16 %	-1.556	0.068	-1.389	0.085
T_PAR_right	-1.994e-02 ± 7.469e-02	-1.372e-02 ± 7.168e-02	-1.538e-03 ± 1.027e-01	0.005 ± 0.106	-31.2 %	-414.66 %	-1.255	0.078	-0.962	0.108
T_POSTC_left	-3.074e-02 ± 7.699e-02	-2.048e-02 ± 7.665e-02	8.301e-04 ± 1.098e-01	0.010 ± 0.126	-33.37 %	1118.82 %	-2.217	0.045*	-1.235	0.087
T_POSTC_right	-1.552e-02 ± 7.574e-02	-7.507e-03 ± 7.689e-02	0.014 ± 0.119	0.021 ± 0.126	-51.62 %	43.72 %	-2.685	0.026*	-0.723	0.122
T_PREC_left	-9.899e-03 ± 6.619e-02	6.543e-04 ± 6.824e-02	0.049 ± 0.083	0.064 ± 0.099	-106.61 %	31.61 %	-3.228	0.014*	-1.879	0.06
T_PREC_right	0.003 ± 0.070	0.009 ± 0.072	0.037 ± 0.094	0.046 ± 0.102	196.31 %	25.4 %	-1.356	0.078	-1.104	0.098
T_PREF_left	0.014 ± 0.067	0.010 ± 0.068	0.041 ± 0.084	0.048 ± 0.097	-25.47 %	16.15 %	1.137	0.09	-0.835	0.114
T_PREF_right	0.016 ± 0.066	0.011 ± 0.067	0.050 ± 0.093	0.054 ± 0.103	-29.73 %	9.28 %	1.707	0.065	-1.174	0.093
T_PREM_left	0.006 ± 0.071	0.008 ± 0.074	0.020 ± 0.090	0.030 ± 0.108	23.69 %	46.58 %	-0.405	0.142	-0.845	0.114
T_PREM_right	0.012 ± 0.070	0.014 ± 0.074	0.033 ± 0.089	0.044 ± 0.096	13.12 %	32.52 %	-0.432	0.142	-2.023	0.06
UF_left	0.025 ± 0.077	0.016 ± 0.079	0.047 ± 0.112	0.057 ± 0.116	-33.31 %	21.04 %	1.480	0.073	-1.037	0.099
UF_right	0.034 ± 0.071	0.033 ± 0.066	0.074 ± 0.086	0.087 ± 0.096	-3.78 %	17.82 %	0.242	0.147	-2.246	0.06

Tables A.27- T-test results for comparisons of the automatically segmented tracts from TractSeg between timepoints within mTBI and control subjects.

[1]Significant values are marked with an asterisk (*) or <0.001

Table A.28 Results of Post Hoc Tract Specific Comparison of Fixel Based Analysis Fiber Density Cross Section

	mTBI		Controls							
TractSeg Name	P1	P2	P1	P2	Percent Change mTBI %	Percent Change Controls %	t-score mTBI	q-value mTBI[1]	t-score controls	q-value controls
AF_left	0.302 ± 0.033	0.302 ± 0.029	0.322 ± 0.045	0.327 ± 0.043	0.27 %	1.51 %	-0.342	0.62	-1.239	0.091
AF_right	0.314 ± 0.031	0.312 ± 0.031	0.327 ± 0.044	0.333 ± 0.046	-0.41 %	1.69 %	0.891	0.47	-1.748	0.059
ATR_left	0.304 ± 0.032	0.301 ± 0.033	0.332 ± 0.044	0.335 ± 0.046	-0.96 %	1.09 %	1.237	0.47	-0.742	0.161
ATR_right	0.300 ± 0.030	0.299 ± 0.031	0.328 ± 0.036	0.335 ± 0.042	-0.38 %	2.22 %	0.595	0.564	-2.107	0.052
CA	0.274 ± 0.040	0.277 ± 0.037	0.316 ± 0.047	0.329 ± 0.040	1.14 %	4.09 %	-1.032	0.47	-1.365	0.08
CC_1	0.388 ± 0.051	0.380 ± 0.051	0.435 ± 0.068	0.437 ± 0.058	-2.08 %	0.44 %	2.296	0.18	-0.171	0.258
CC_2	0.342 ± 0.031	0.340 ± 0.032	0.370 ± 0.045	0.375 ± 0.043	-0.68 %	1.34 %	1.404	0.47	-1.129	0.106
CC_3	0.337 ± 0.032	0.340 ± 0.036	0.363 ± 0.053	0.370 ± 0.056	0.84 %	2.06 %	-1.089	0.47	-1.614	0.067
CC_4	0.371 ± 0.033	0.375 ± 0.034	0.408 ± 0.038	0.420 ± 0.040	1.1 %	2.77 %	-1.603	0.47	-2.255	0.05*
CC_5	0.368 ± 0.032	0.371 ± 0.034	0.392 ± 0.044	0.400 ± 0.041	0.81 %	2.01 %	-1.200	0.47	-1.399	0.078
CC_6	0.360 ± 0.042	0.360 ± 0.036	0.369 ± 0.046	0.370 ± 0.042	0.12 %	0.19 %	-0.141	0.682	-0.219	0.251
CC_7	0.353 ± 0.046	0.353 ± 0.039	0.353 ± 0.042	0.359 ± 0.043	-0.03 %	1.61 %	0.033	0.682	-2.011	0.054
CC	0.352 ± 0.030	0.352 ± 0.029	0.371 ± 0.041	0.376 ± 0.038	-0.04 %	1.25 %	0.073	0.682	-1.346	0.08
CG_left	0.322 ± 0.030	0.320 ± 0.030	0.341 ± 0.051	0.340 ± 0.036	-0.63 %	-0.14 %	1.065	0.47	0.062	0.267
CG_right	0.322 ± 0.031	0.319 ± 0.032	0.333 ± 0.048	0.336 ± 0.038	-0.8 %	0.91 %	1.624	0.47	-0.463	0.202
CST_left	0.424 ± 0.042	0.431 ± 0.040	0.472 ± 0.049	0.483 ± 0.047	1.66 %	2.37 %	-2.420	0.155	-2.307	0.05*
CST_right	0.440 ± 0.041	0.443 ± 0.039	0.473 ± 0.052	0.480 ± 0.050	0.71 %	1.6 %	-1.073	0.47	-1.966	0.055
FPT_left	0.404 ± 0.037	0.406 ± 0.036	0.435 ± 0.042	0.443 ± 0.042	0.64 %	1.96 %	-1.141	0.47	-2.278	0.05*
FPT_right	0.404 ± 0.034	0.405 ± 0.033	0.432 ± 0.048	0.439 ± 0.045	0.21 %	1.63 %	-0.467	0.582	-1.593	0.067
FX_left	0.190 ± 0.044	0.192 ± 0.049	0.207 ± 0.046	0.211 ± 0.051	0.98 %	2.17 %	-0.781	0.496	-0.772	0.158
FX_right	0.199 ± 0.045	0.200 ± 0.049	0.206 ± 0.050	0.211 ± 0.050	0.56 %	2.76 %	-0.454	0.582	-0.806	0.154
ICP_left	0.315 ± 0.040	0.315 ± 0.041	0.321 ± 0.034	0.323 ± 0.029	0.04 %	0.66 %	-0.046	0.682	-0.473	0.202
ICP_right	0.287 ± 0.031	0.285 ± 0.032	0.290 ± 0.031	0.291 ± 0.030	-0.65 %	0.57 %	0.714	0.518	-0.369	0.22
IFO_left	0.328 ± 0.032	0.326 ± 0.032	0.342 ± 0.042	0.347 ± 0.042	-0.44 %	1.32 %	0.725	0.518	-1.400	0.078
IFO_right	0.332 ± 0.030	0.330 ± 0.029	0.345 ± 0.039	0.351 ± 0.042	-0.5 %	1.75 %	0.995	0.47	-2.465	0.048*
ILF_left	0.311 ± 0.038	0.313 ± 0.035	0.320 ± 0.044	0.327 ± 0.040	0.64 %	2.31 %	-0.807	0.493	-2.162	0.052
ILF_right	0.322 ± 0.035	0.322 ± 0.035	0.329 ± 0.042	0.337 ± 0.036	-0.01 %	2.28 %	0.017	0.682	-1.604	0.067
MCP	0.330 ± 0.040	0.330 ± 0.040	0.333 ± 0.039	0.336 ± 0.037	-0.03 %	0.82 %	0.041	0.682	-0.858	0.146
MLF_left	0.319 ± 0.037	0.320 ± 0.031	0.330 ± 0.044	0.330 ± 0.037	0.37 %	0.15 %	-0.417	0.582	-0.130	0.263
MLF_right	0.337 ± 0.036	0.337 ± 0.033	0.342 ± 0.040	0.342 ± 0.037	-0.06 %	-0.06 %	0.091	0.682	0.073	0.267
OR_left	0.330 ± 0.037	0.332 ± 0.038	0.340 ± 0.037	0.350 ± 0.040	0.59 %	2.85 %	-1.030	0.47	-3.376	0.014*
OR_right	0.350 ± 0.037	0.351 ± 0.035	0.356 ± 0.040	0.364 ± 0.045	0.26 %	2.17 %	-0.443	0.582	-3.475	0.014*
POPT_left	0.373 ± 0.036	0.376 ± 0.033	0.394 ± 0.046	0.398 ± 0.042	0.95 %	1 %	-1.334	0.47	-1.387	0.078
POPT_right	0.398 ± 0.039	0.400 ± 0.036	0.418 ± 0.051	0.421 ± 0.050	0.58 %	0.76 %	-0.952	0.47	-1.540	0.07
SCP_left	0.348 ± 0.039	0.350 ± 0.041	0.364 ± 0.038	0.370 ± 0.033	0.71 %	1.61 %	-1.452	0.47	-1.661	0.064
SCP_right	0.349 ± 0.032	0.349 ± 0.032	0.360 ± 0.039	0.365 ± 0.035	0.02 %	1.44 %	-0.033	0.682	-1.394	0.078
SLF_III_left	0.322 ± 0.037	0.322 ± 0.035	0.344 ± 0.063	0.348 ± 0.061	0.03 %	1.08 %	-0.046	0.682	-0.640	0.174
SLF_III_right	0.321 ± 0.038	0.320 ± 0.038	0.334 ± 0.055	0.337 ± 0.054	-0.2 %	1.05 %	0.451	0.582	-0.896	0.142
SLF_II_left	0.298 ± 0.032	0.299 ± 0.032	0.309 ± 0.045	0.316 ± 0.052	0.13 %	2.52 %	-0.282	0.637	-2.782	0.035*
SLF_II_right	0.298 ± 0.036	0.297 ± 0.035	0.309 ± 0.042	0.314 ± 0.045	-0.54 %	1.47 %	0.999	0.47	-2.063	0.052
SLF_I_left	0.283 ± 0.030	0.284 ± 0.029	0.291 ± 0.036	0.294 ± 0.032	0.45 %	1.04 %	-0.669	0.532	-0.698	0.167
SLF_I_right	0.297 ± 0.033	0.297 ± 0.031	0.309 ± 0.043	0.311 ± 0.040	0.12 %	0.82 %	-0.240	0.652	-0.661	0.172
STR_left	0.416 ± 0.041	0.423 ± 0.044	0.453 ± 0.052	0.467 ± 0.055	1.72 %	3.07 %	-2.866	0.107	-2.847	0.035*
STR_right	0.439 ± 0.034	0.441 ± 0.036	0.466 ± 0.057	0.474 ± 0.056	0.45 %	1.69 %	-0.659	0.532	-1.822	0.056
ST_FO_left	0.327 ± 0.039	0.323 ± 0.039	0.358 ± 0.053	0.362 ± 0.050	-1.24 %	1.27 %	1.326	0.47	-0.608	0.177
ST_FO_right	0.351 ± 0.040	0.347 ± 0.038	0.387 ± 0.048	0.397 ± 0.048	-1.32 %	2.76 %	1.307	0.47	-2.003	0.054
ST_OCC_left	0.341 ± 0.037	0.343 ± 0.037	0.353 ± 0.036	0.363 ± 0.039	0.48 %	2.75 %	-0.820	0.493	-3.437	0.014*

Table A.28 (cont'd)

	mTBI		Controls							
TractSeg Name	P1	P2	P1	P2	Percent Change mTBI %	Percent Change Controls %	t-score mTBI	q-value mTBI[1]	t-score controls	q-value controls
ST_OCC_right	0.351 ± 0.036	0.352 ± 0.033	0.360 ± 0.041	0.367 ± 0.045	0.19 %	2 %	-0.303	0.634	-3.482	0.014*
ST_PAR_left	0.334 ± 0.032	0.337 ± 0.031	0.354 ± 0.043	0.358 ± 0.040	0.84 %	1.01 %	-1.248	0.47	-1.247	0.091
ST_PAR_right	0.357 ± 0.035	0.357 ± 0.032	0.372 ± 0.045	0.375 ± 0.045	0.25 %	0.86 %	-0.431	0.582	-1.874	0.056
ST_POSTC_left	0.330 ± 0.030	0.336 ± 0.033	0.364 ± 0.043	0.372 ± 0.041	1.88 %	2.18 %	-2.931	0.107	-2.430	0.048*
ST_POSTC_right	0.357 ± 0.031	0.359 ± 0.031	0.385 ± 0.047	0.390 ± 0.047	0.67 %	1.27 %	-1.208	0.47	-1.770	0.059
ST_PREC_left	0.346 ± 0.029	0.352 ± 0.031	0.388 ± 0.039	0.399 ± 0.038	1.79 %	2.66 %	-2.754	0.107	-2.424	0.048*
ST_PREC_right	0.367 ± 0.030	0.370 ± 0.030	0.395 ± 0.043	0.402 ± 0.044	0.73 %	1.82 %	-1.210	0.47	-2.102	0.052
ST_PREF_left	0.339 ± 0.030	0.338 ± 0.031	0.367 ± 0.039	0.372 ± 0.040	-0.25 %	1.53 %	0.460	0.582	-1.519	0.07
ST_PREF_right	0.340 ± 0.029	0.339 ± 0.028	0.367 ± 0.041	0.374 ± 0.043	-0.56 %	1.96 %	1.296	0.47	-1.897	0.056
ST_PREM_left	0.316 ± 0.030	0.318 ± 0.030	0.336 ± 0.044	0.344 ± 0.048	0.5 %	2.17 %	-0.803	0.493	-2.065	0.052
ST_PREM_right	0.331 ± 0.031	0.334 ± 0.032	0.357 ± 0.041	0.363 ± 0.040	0.78 %	1.85 %	-1.356	0.47	-1.527	0.07
T_OCC_left	0.324 ± 0.036	0.326 ± 0.037	0.334 ± 0.035	0.344 ± 0.039	0.54 %	2.92 %	-0.929	0.47	-3.414	0.014*
T_OCC_right	0.342 ± 0.037	0.343 ± 0.034	0.349 ± 0.040	0.356 ± 0.045	0.28 %	2.03 %	-0.469	0.582	-3.460	0.014*
T_PAR_left	0.334 ± 0.032	0.336 ± 0.031	0.352 ± 0.042	0.356 ± 0.041	0.75 %	1.06 %	-1.119	0.47	-1.497	0.071
T_PAR_right	0.361 ± 0.036	0.362 ± 0.033	0.374 ± 0.044	0.378 ± 0.045	0.34 %	0.98 %	-0.553	0.58	-1.920	0.056
T_POSTC_left	0.347 ± 0.034	0.353 ± 0.036	0.377 ± 0.047	0.385 ± 0.048	1.52 %	2.14 %	-2.419	0.155	-2.468	0.048*
T_POSTC_right	0.368 ± 0.034	0.371 ± 0.034	0.395 ± 0.052	0.401 ± 0.052	0.64 %	1.47 %	-1.178	0.47	-1.840	0.056
T_PREC_left	0.365 ± 0.033	0.371 ± 0.034	0.411 ± 0.041	0.422 ± 0.043	1.71 %	2.83 %	-2.717	0.107	-2.307	0.05*
T_PREC_right	0.382 ± 0.032	0.385 ± 0.032	0.411 ± 0.045	0.419 ± 0.046	0.75 %	2.02 %	-1.186	0.47	-2.159	0.052
T_PREF_left	0.342 ± 0.031	0.342 ± 0.031	0.371 ± 0.039	0.377 ± 0.041	-0.08 %	1.71 %	0.147	0.682	-1.740	0.059
T_PREF_right	0.331 ± 0.028	0.330 ± 0.028	0.357 ± 0.039	0.364 ± 0.042	-0.37 %	1.97 %	0.890	0.47	-1.941	0.055
T_PREM_left	0.331 ± 0.031	0.333 ± 0.032	0.356 ± 0.043	0.363 ± 0.047	0.57 %	2.05 %	-0.954	0.47	-1.711	0.061
T_PREM_right	0.344 ± 0.032	0.347 ± 0.034	0.373 ± 0.041	0.381 ± 0.042	0.88 %	2.23 %	-1.481	0.47	-1.829	0.056
UF_left	0.311 ± 0.036	0.307 ± 0.035	0.334 ± 0.051	0.334 ± 0.047	-1.09 %	0.18 %	1.211	0.47	-0.062	0.267
UF_right	0.308 ± 0.031	0.305 ± 0.031	0.335 ± 0.035	0.341 ± 0.040	-0.79 %	1.88 %	0.918	0.47	-0.942	0.135

Tables A.28- T-test results for comparisons of the automatically segmented tracts from TractSeg between timepoints within mTBI and control subjects.

[1]Significant values are marked with an asterisk (*) or <0.001

Joshua H. Baker, M.S.
3300 Auburn Rd. Ste 406 Auburn Hills MI, 48326
610-442-4695 • bakerj77@msu.edu

Education

Doctor of Osteopathic Medicine Expected May 2026
COMLEX Level 1 & USMLE Step 1 Passed 2021
Michigan State University College of Osteopathic Medicine
East Lansing, MI

Doctor of Philosophy, Neuroscience Expected May 2024
College of Natural Sciences, Michigan State University
East Lansing, MI

Master of Science, **Anatomy** May 2017
The Pennsylvania State University College of Medicine
Hershey, PA

Bachelor of Science, **Psychology** May 2015
Minor in Chemistry
The University of Pittsburgh
Pittsburgh, PA

Professional Positions and Experience

ScholarRx Visual Designer Jan 2023 to Present
Independent Contractor, Visual Bricks Project
Remote

Human Research Technologist II Jul 2017 to May 2018
Department of Psychiatry, Sleep Research and Treatment Center
The Pennsylvania State University College of Medicine
Hershey, PA

Adjunct Faculty Jan 2017 to May 2018
Department of Physical Therapy
Lebanon Valley College
Annville, PA

Certification

Introduction to Interventional Radiology and Minimally Invasive Procedures May 2023
American Medical Student Association Scholars Program: "Racism in Medicine" Dec 2022
ACLS/BCLS Jun 2019 to Present

Translational Science Certificate May 2017
Conceptual Foundation of Medicine Certificate May 2015

Research and Laboratory Experience

Graduate Research Assistant Aug 2018 to Present
Department of Radiology, Cognitive Imaging Research Center
Michigan State University
East Lansing, MI

Human Research Technologist II Jul 2017 to May 2018
Department of Psychiatry, Sleep Research and Treatment Center
The Pennsylvania State University College of Medicine
Hershey, PA

Graduate Student, Master's Thesis Project Jan 2016 to May 2017
Department of Psychiatry, Sleep Research and Treatment Center
The Pennsylvania State University College of Medicine
Hershey, PA

Undergraduate Research Assistant Nov 2011 to May 2015
Western Psychiatric Institute and Clinic
Pittsburgh, PA

Professional Memberships

The American Society of Functional Neuroradiology	2024 to Present
The International Society for Magnetic Resonance in Medicine	2024 to Present
American Osteopathic College of Radiology	2022 to Present
American College of Radiology	2022 to Present
American Society of Neuroradiology	2022 to Present
American Medical Student Association	2019 to Present
American Physician Scientist Association	2018 to Present

Software & Research Tool Competencies

Analysis of Functional Neuroimages (AFNI)
FMRIB Software Library (FSL)
Freesurfer
I2b2
Linux
MATLAB
MRTrix3
R & R Studio
REDCap
SLURM
Statistical Parametric Mapping (SPM)

Publications

Baker JH, Bender A, Scheel N, Zhu DC. A Rapid Review of Signal Modeling Techniques for Diffusion Magnetic Resonance Imaging Beyond DTI: Findings in Mild Traumatic Brain Injury. In preparation.

Baker JH, Bender A, Scheel N, Ding K, Zhu DC, The TRACK-TBI Investigators. A longitudinal Fixel-based analysis of mild traumatic brain injury patients: A TRACK TBI Study. In preparation**.**

Baker JH, Schoppe K, Youmans D, Moriarity A. Scope of Practice Legislation Across the US: Current Trends in Evidence, Advocacy, and Action. Appl Radiol. 2023 Sep 12.

Fernandez Z, Scheel N, **Baker JH**, Zhu DC. Functional connectivity of cortical resting-state networks is differentially affected by rest conditions. Brain Res. 2022 Dec 1;1796:148081. doi: 10.1016/j.brainres.2022.148081. Epub 2022 Sep 12. PMID: 36100086.

Baker JH. 2017. Insomnia Symptoms and Systemic Inflammation in Adolescents: A Population-Based Study. The Pennsylvania State University College of Medicine, Hershey, PA. https://etda.libraries.psu.edu/catalog/13881jxb5933

Fernandez-Mendoza J, **Baker JH**, Gaines J, Liao D, Vgontzas A, Bixler E. Insomnia Symptoms with Objective Short Sleep Duration is Associated with Systemic Inflammation in Adolescents. Brain Behavior Immunity. 2017. 61: 110-116.

Baker JH, Rothenberger S, Kline C, Okun M (2016): Exercise During Early Pregnancy is Associated With Greater Sleep Continuity. Behavioral Sleep Medicine. 2016. 14:1-14.

Posters/Oral Presentations

Scheel N, Hubert J, **Baker JH**, Fernandez Z, Vongpatanasin W, Zhang R, Zhu DC. Comparison of T2 FLAIR WM Hyperintensity Segmentation Algorithms in Clinical Trials. Michigan Alzheimer's Disease Research Center Beyond Amyloid Research Symposium. 2023. Poster Presentation.

Baker JH, Bender A, Scheel N, Hubert J, Fernandez Z, Zhu, DC. A Pilot Longitudinal Diffusion-Weighted Magnetic Resonance Imaging Fixel-Based Analysis in a Sample of Mild Traumatic Brain Injury Patients: A TRACK-TBI Study. Michigan State University College of Osteopathic Medicine Research Day. 2023. Poster Presentation

Fernandez Z, Scheel N, **Baker JH**, Zhu DC. Functional connectivity of cortical resting-state networks is differentially affected by rest conditions. AAP/ASCI/APSA JM. Chicago, Illinois on April 21-23. Poster Presentation.

Baker JH (host & presenter), Gadde JA (mentor & article author). American College of Radiology Medical Student Journal Club "Imaging of Hypoxic-Ischemic Injury in the Era of Cooling". January 6, 2023. Virtual National Oral Presentation.

Baker JH, Brauman S, Tilden SE, Sadasivan M. Piloting Undergraduate Medical Student Participation in Curricular Change: A Lilly Fellowship Project. Michigan Osteopathic Association Autumn Scientific Research Exposition. 2022. Poster presentation.

Fernandez Z, **Baker JH**, Scheel N, Zhu D. Functional Connectivity of Resting-State Networks is Affected by Excess Environmental Stimuli. Abstract submitted to the 26th Annual Meeting of the OHBM, June 26-30 2020, Montreal Canada.

Baker JH, Vgontzas A, Fernandez-Mendoza J, Krishnamurthy B, Gaines J, Basta M, Criley C, Bixler EO. Effects of Trazodone on Blood Pressure: A Longitudinal, Observational Study of Patients Presenting to a Sleep Disorder Clinic. 32nd Annual Meeting of the Associated Professional Sleep Societies. Baltimore, Maryland on June 3-6, 2018. Associated Professional Sleep Societies. Poster presentation. SLEEP 2018; 41 (Abstract Supplement): A157.

Vgontzas A, Fernandez-Mendoza J, **Baker JH**, Krishnamurthy B, Gaines J, Calhoun S, Basta M, Bixler EO. *Trazodone vs. Cognitive Behavioral Therapy in Insomnia with Short Sleep Duration: Effects on Total Sleep Time and Cortisol Levels*. 32nd Annual Meeting of the Associated Professional Sleep Societies. Baltimore, Maryland on June 3-6, 2018. Associated Professional Sleep Societies. Oral presentation. SLEEP 2018; 41 (Abstract Supplement): A142-A143.

Fernandez-Mendoza J, Gaines J, **Baker JH**, Calhoun S, Liao D, Bixler E, Vgontzas A. Insomnia is Associated with Increased C-reactive Protein levels in Adolescents: Role of Objective Short Sleep Duration. 23rd Congress of the European Sleep Research Society. Bologna, Italy, September 13-16 2016. European Sleep Research Society. Oral presentation. J Sleep Res. 2016; (abstract supplement).

Okun M, **Baker JH**, Rothenberger S, Kline C The Effect of Exercise on Sleep During Pregnancy Paternal Maternal Stress and Child Outcome: Exploring Novel Underlying Mechanisms Symposium. Society for Research in Child Development Oral Presentation. Philadelphia, Pennsylvania SRCD 2015

Awards and Scholarships

2024 Medical Student Scholarship Jan 2024
American College of Radiology
Reston, VA

Dissertation Completion Fellowship May 2023
College of Natural Sciences, Michigan State University
East Lansing, MI

Second Place Poster Competition Award Winner May 2023
Michigan State University College of Osteopathic Medicine Research Day
Novi, MI

Graduate Teaching Assistant Scholarship May 2016
The Pennsylvania State University College of Medicine
Hershey, PA

Peer-Review

Early Career Section of Editorial Advisory Board Aug 2023 to Present
Applied Radiology

Peer-Reviewer Jan 2022 to Present
Spartan Medical Journal

Peer-Reviewer May 2022
ScholarRx Bricks Create Grant

Peer-Reviewer, supervised by Dr. David Zhu Mar 2019
British Journal of Sports Medicine

Peer-Reviewer, supervised by Dr. Fernandez-Mendoza Mar 2017
Pediatrics

Peer-Reviewer, supervised by Dr. Fernandez-Mendoza Jan 2017
Brain Behavior and Immunity

Peer-Reviewer, supervised by Dr. Fernandez-Mendoza Oct 2017
Journal of Sleep Research

Educational Activities

ScholarRx Visual Designer March 2023 to Jan 2024
Independent Contractor, Video Bricks Project
-"The Electrocardiogram Leads and Localization"
-"Cardiac Cycle: Pressure-Volume Loop"
-"Pathophysiology of Aortic Stenosis"

Lilly Fellowship Contributor Aug 2021 to May 2022
Michigan State University
-Autonomic control of bronchial smooth muscle
-Introduction to the arachidonic acid pathway
-Introduction to catecholamine synthesis

Adjunct Faculty, Department of Physical Therapy Jan 2017 to May 2018
Lebanon Valley College
-Physiology Laboratory Instructor
-Kinesiology Laboratory Instructor
-Exercise Physiology Laboratory Instructor

Graduate Teaching Assistant, MSDR Block Oct 2016 to Dec 2016
The Pennsylvania State University College of Medicine
-Cadaveric Dissection Lab Instructor
-Lecture, Anatomy of the Vertebral Column and Spinal Cord

Graduate Teaching Assistant, Neurology Residency Program Oct 2016
The Pennsylvania State University College of Medicine
-Lecture, Cerebellum and Cerebellar Vasculature
-Lecture**,** Cerebral Vasculature

Graduate Teaching Assistant, GI/GU Block Aug 2016
The Pennsylvania State University College of Medicine
-Cadaveric Dissection Lab Instructor
-Lecture, Anatomy of the Retroperitoneum

Graduate Teaching Assistant, Physician Assistant Program May 2016 to Sep 2016
The Pennsylvania State University College of Medicine
-Cadaveric Prosection Lab Instructor
-Lecture, Anatomy of the Pelvis

Social Media

Twitter: @DO_Radiology
Instagram: @do_radiology

Service & Leadership activities

ACR Medical Student Journal Club Moderator May 2023 to Present
American College of Radiology

Michigan Radiologic Society Class of 2026 School Liaison Sept 2023 to Present
Michigan Radiologic Society

Education Lead, Medical Student Section May 2023 to Present
American College of Radiology

Co-Founder and Member Jan 2023 to Present
MSUCOM Radiology Interest Group
Michigan State University College of Osteopathic Medicine

Student Mentor Sept 2022
Summer Research Opportunity Program
Michigan State University

Rad Reserves Volunteer July 2022 to Present
The Radiology Room
American College of Radiology

Council Member Aug 2021 to Present
Student Advisory Council
ScholarRx, First Aid for the USMLE

Committee Member May 2019 to Apr 2020
DO/PhD Student Advisory Committee
Michigan State University DO/PhD Program

Volunteer Lecturer Mar 2019 to Present
Brain Awareness Week
Metro Detroit Public Schools

Volunteer Instructor Oct 2018 to
Present
Physiology PhUn Day
Impression 5 Science Center, Lansing MI

Co-Founder and Member Aug 2016 to May 2017
Society for Applied Anatomy
The Pennsylvania State University College of Medicine

Secretary and Member Aug 2016 to May 2017
Pathology Interest Group
The Pennsylvania State University College of Medicine

Volunteer Nov 2016 to May 2018
Ronald McDonald House
The Pennsylvania State University College of Medicine

Volunteer Lab Instructor Aug 2016 to May 2018
Healthcare Career Exploration Pre-College Program
The Pennsylvania State University College of Medicine

Volunteer Lab Instructor Feb
2016
Central Pennsylvania Brain Bee
The Pennsylvania State University College of Medicine

Volunteer Lab Instructor Feb
2015
Central Pennsylvania Brain Bee
The Pennsylvania State University College of Medicine